UNIVERSITY OF LONDON THESIS

Degree PhD. Year 2007 Name of Author AMANDA DALY

Mechanisms of Smad regulation that determine the specificity of TGF-β responses during tumorigenesis

Amanda Daly

This thesis is submitted in fulfilment of the requirements for the degree of Doctor of Philosophy

University College London

University of London

October 2006

Supervisor: Dr Caroline Hill (Cancer Research UK)

Developmental Signalling Laboratory

ProQuest LLC
789 East Eisenhower Parkway
P.O. Box 1346
Ann Arbor, MI 48106-1346

I, Amanda Daly, confirm that the work presented in this thesis is my own. Where information has been derived from other sources, this has been clearly indicated.

Amanda Daly

Abstract

Transforming growth factor beta (TGF-β) regulates many diverse biological processes including proliferation, motility, differentiation and survival. Aberrant TGF-β signalling is also involved in tumour development. TGF-β signals predominantly through a receptor complex, comprising of ALK5 and TβRII, to activate the R-Smads, Smad2 and Smad3. These activated R-Smads form complexes with Smad4 to regulate the transcription of TGF-β inducible genes, which results in a huge array of biological responses. This has raised the question of the mechanism by which signalling specificity and diversity is generated.

To address this question, I have used a model tumour cell system developed in Hartmut Beug's laboratory. The parental cell line, EpH4, is a non-tumorigenic, mouse mammary epithelial cell line that undergoes growth inhibition and apoptosis in response to TGF-β. However, EpH4 cells that have been transformed by stable expression of oncogenic Ras (EpRas cells) undergo an Epithelial-to-Mesenchymal Transition (EMT) in response to TGF-β and form rapidly growing tumours in mice.

Initially, I established the TAP-tagging purification system to identify new Smad-interacting partners in EpH4 and EpRas cells. Unfortunately, despite great efforts, no novel Smad partners were found using this method. I then went on to characterise the components of the TGF-β pathway in this model tumour system. This work revealed that Smad3 is downregulated in EpRas cells compared with EpH4 cells and also that Smad3 expression is cell cycle regulated. Both transcriptional regulation and stability play a role in determining Smad3 expression. Low Smad3 levels in EpRas cells may account for their inability to growth arrest in response to TGF-β.

I have also observed C-terminal phosphorylation of Smad1/5 as a result of autocrine Bone Morphogenetic Protein (BMP) signalling and also upon TGF-β stimulation. Again, this is regulated at the cell cycle level. The Smad complexs formed as a result of Smad1 phosphorylation by TGF-β are distinct from those formed by Smad1 activated by BMP. Molecular analysis of these signalling pathways has led to a model whereby TGF-β induced Smad1 acts in concert with Smad2 and Smad3 to induce transcription of a unique set of genes, which adds a level of complexity and specificity to the TGF-β signalling pathway.

Dedicated to my twin sister, Helen

Acknowledgements

The long and winding journey of my pHD studies have come to an end. It was not an easy road, but it would have been much more difficult without the love and support of all those around me. Firstly I would like to convey my sincere gratitude to Caroline, my supervisor, for her constant support and encouragement throughout the years. Without her guidance and supervision, I would not be the scientist I am today. I would also like to thank the wonderful group of people that make up the Hill lab, including past and present members. The laughs and tears shared brightened everyday life in the lab and opened my eyes to new cultural experiences. Special thanks to Karel and Gareth who introduced me to London nightlife, and Laurence, my tissue culture partner and confidant, who picked me when times were tough. And thanks to Mike, a great listener and advisor, who helped me from start to finish. Not least forgetting Becky (my teacher), Debi, Sarah, Julie, Mary, Sean, Berni, Thedoras, for scientific discussion and advice and great laughs. I would also like to thanks all of the staff at Cancer Research UK and my collaborators who provided reagents, technical support and advice.

To all my friends and family back home, whose constant encouragement lifted me when times were hard. Special thanks to mom and dad who went through these years with me and never gave up on me. Friends and flatmates in London, especially Niamh, Alexia, Anna and Liz who provided constant entertainment, laughter and fun to keep all your troubles away. And importantly, I would to thank Diarmuid for embarking on this great adventure with me four years ago. Without you, I would not be here. Thank you for being so understanding and putting up with all the demands of pHD life. Above all, I would like to thank my twin sister, Helen. There are no words to describe the strength and support you have been to me over these years and I will never forget that.

Table of Contents

List of Figures

List of Tables

List of Abbreviations

™	trademark
®	registered trademark
A	alanine
aa	amino acid residue
ALK	activin receptor-like kinase
APC	anaphase-promoting complex
ARE	activin-responsive element
ARF	activin-responsive factor
APS	ammonium persulphate
ATP	adenosine 5'-triphosphate
Babo	baboon
BAMBI	bmp and activin membrane-bound inhibitor
Bisacrylamide	NN'-Methylenebisacrylamide
BMP	bone morphogenetic protein
BRE	bmp-responsive element
BSA	bovine serum albumin
C-	carboxy
C.elegans	Caenorhabditis elegans
CAM	calmodulin
CBP	calmodulin binding peptide
CDK	cyclin dependent kinase
CDKI	cyclin dependent kinase inhibitor
CFC	cripto, frl-1 and cryptic domain
cpm	counts per mintute
CRE	cAMP response element
CREB	cre-binding protein
CRM1	chromosomal region maintenance 1
CRUK	cancer research uk
dATP	deoxyadenosine 5'-triphosphate
dCTP	deoxycytosine 5'-triphosphate

dGTP	deoxyguanosine 5′-triphosphate
dTTP	deoxythymidine 5′-triphosphate
Dpp	decapentaplegic
DNA	deoxyribonucleic acid
DEPC	diethylpyrocarbonate
DT	dual-tagged
DTT	1,4-dithiothreitol
EC	endothelial cells
ECM	extracellular matrix
EDTA	ethylene-diamine-tetraacetic acid
EGF	epidermal growth factor
EMT	epithelial-mesenchymal transition
ER	oestrogen receptor
ERK	extracellular signal-related kinase
FAST	forkhead activin signal transducer
FHA	forkhead associated
GFP	green fluorescent protein
Grb2	growth factor receptor-bound protein 2
GPI	glycosylphosphatidylinositol
GS domain	glycine-serine domain
HDAC	histone deacetylase
HGF	hepatocyte growth factor
HHT	hereditary hemorrhagic telangiectasia
HNPCC	hereditary non-polyposis colorectal cancer
HRP	horse radish peroxidase
I-Smad	Inhibitory Smad
Ig	immunoglobulin
JNK	jun n-terminal kinase
JP	juvenile polyposis
kDa	kilodalton
LAP	latency-associated protein
LB	luria-bertani medium
LMB	leptomycin B

LTBP	latent TGF-β binding protein
M	molar
MAPK	mitogen-activated protein kinase
MDCK	Madin-Darby canine kidney
MEK	MAPK/ERK kinase
MEKK	MEK kinase
mg	milligram
MH	mad homology
Mix	mesoderm-induced homeobox
ml	millilitre
mM	millimolar
MMP-2	matrix matalloprotease 2
MMP-9	matrix metalloprotease 9
MO	morpholino oligonucleotide
N-CoR	nuclear transcriptional corepressor
NES	nuclear export signal
ng	nanogram
NLS	nuclear localisation signal
NP-40	nonidet P40
NPC	nuclear pore complex
OAZ	olf-1/ebf-associated zinc finger
OD	optical density
Oep	one-eyed pinhead
P-Smad	C-terminal phosphorylated form of Smad
PAI-1	plasminogen activator inhibitor-1
PCR	polymerase chain reaction
PFA	Paraformaldehyde
PI3K	phosphoinositide 3-kinase
PKA	Protein Kinase A
PKB	Protein Kinase B
PKC	Protein Kinase C
Ponceau S	3-hydroxy-4-[2-sulfo-4-(4-sulfo-phenylazo)phenylazo]-2,7-naphthalenedisulfonic acid

PP2A	phosphatase 2A
pMoles	picomoles
R-Smad	receptor-regulated Smad
Rb	retinoblastoma protein
rpm	revolutions per minute
RTK	receptor tyrosine kinase
SAD	smad4 activation domain
SARA	smad anchor for receptor activation
Sax	saxophone
SBD	smad-binding domain
SBE	smad-binding element
SDS	sodium dodecyl sulphate
SIP1	smad-interacting protein 1
Shn	Schnurri
Smurf1/2	smad ubiquitin regulatory factor 1/2
SnoN	ski-related novel gene
STRAP	serine-threonine kinase receptor-associated protein
TAP	tandem affinity purification
TEMED	N,N,N',N'-tetramethylethylenediamine
TEV	Tobacco Etch Virus
TGF-β	transforming growth factor β
Tkv	thickveins
TSP	thrombospondin
Ubx	ultrabithorax
UV	ultra violet
Vg	vestigial
v/v	volume per volume
w/v	weight per volume
µg	microgram
µl	microlitre

1 Introduction

1.1 Signal transduction

Cellular communication is a critical process for all multicellular organisms, whereby transmission of signals between cells is required for proper embryonic development and adult physiology. Cell interactions with the extracellular matrix and surrounding cells allows them to sense their environment and respond to signals that regulate most aspects of cell behaviour, including survival, proliferation, and differentiation. For coordinated biological processes, messengers usually take the form of proteins or peptides and bind to receptors on the surface of neighbouring cells. Ligand binding can induce many cellular activities including cytoskeletal remodelling, adhesion, motility and apoptosis. In addition, many receptors invoke gene expression responses, a subset of which has been shown to be independent of new proteins synthesis (Gomperts, B. D. et al., 2003). This revealed the existence of transcytoplasmic signalling pathways that regulate the activity of transcription factors which ultimately affects gene expression. In order to activate or repress transcription, transcription factors must be located in the nucleus, bind to DNA and interact with the basal transcription apparatus. An emerging theme is that extracellular signals, which regulate transcription factor activity, can affect one or more of these processes. Furthermore, a central principle in the regulation of transcription factors is the key role of phosphorylation, which can alter the activity of enzymes through the combined action of a protein kinase and a protein phosphatase. To date, phosphorylation by protein kinases is the most widespread mechanism of regulation in eukaryotic cells and forms the basis of many cell signalling networks (Karin, M. et al., 1995).

One of the simplest mechanisms of nuclear signalling is mediated downstream of the largest receptor family, the G protein-coupled receptors. In response to hormonal stimulation, these seven transmembrane receptors activate heteromeric G proteins via GTP exchange, which then directly interact with and activate enzymes such as adenyl or guanylyl cyclase leading to the accumulation of second messengers, namely cAMP and cGMP (Gomperts, B. D. et al., 2003). Downstream events leading to the initiation of transcription was first identified for the PKA/CREB system (Karin,

M. et al., 1995). In this case, elevated cAMP activates the tetrameric protein kinase A (PKA) by binding to the regulatory subunits, thus liberating the catalytic subunit which then translocates to the nucleus. Therefore, the signalling cascade downstream of G-protein-coupled receptors leads to the activation of a kinase by virtue of its translocation from the cytoplasm to the nucleus. The nuclear targets for PKA are the CREB transcription factors, which bind to DNA sequences known as cAMP-response elements (CREs). Once in the nucleus, the PKA catalytic subunit phosphorylates CREB on a serine residue, thereby stimulating its ability to activate transcription (Karin, M. et al., 1995). In addition to the cyclic nucleotides cGMP and cAMP, molecules other than proteins can act as second messengers. Phosphatidylinositol 3-Kinase (PI3 Kinase), which is recruited to the membrane by various stimuli, phosphorylates membrane-bound inositol phospholipids to produce PI(4,5)P2 or PI(3,4,5)P3, which are potent second messengers (Gomperts, B. D. et al., 2003). These phospholipids then recruit signalling proteins via PIP3-binding plectrin homology (PH) domains to the membrane where they are activated. In addition, phospholipase action on PI(4,5)P2 by phospholipase C (PLC) generates a series of potent, phospholipid-derived second messengers, including diacylglycerol (DAG), IP3, PI(3,4,5)P3, IP4 and IP5. DAG is required for the activity of protein kinase C (PKC), whereas IP3 acts to release Ca^{2+} from intracellular stores, thus triggering a program of Ca^{2+}-activated events. These include a Ca^{2+} sensing protein, called Calmodulin, which then targets a family of Ca^{2+}/calmodulin activated protein kinases (Cam Kinases) (Gomperts, B. D. et al., 2003). In essence, the ultimate role of second messengers is to activate kinases such as PKA, PKB, PKC and Cam Kinase, which can then phosphorylate downstream targets to initiate transcription.

A more complex mechanism involving the activation of protein kinase cascades is used to transmit growth-factor signals from via receptor tyrosine kinases (RTKs) to the nucleus (Waskiewicz, A. J. et al., 1995). This cascade, however, results in the translocation of an active kinase to the nucleus. Receptor tyrosine kinases (RTKs) are single pass transmembrane receptors with intrinsic kinase activity that is activated upon ligand binding. Consequently, the receptor phosphorylates tyrosine residues on the cytoplasmic domains of the receptors themselves, which creates recruitment centres for effector proteins at the membrane (Schlessinger, J., 2000). Once recruited and activated, effector proteins initiate a mitogen activated protein

kinase (MAPK) cascade, which involves three serine/threonine protein kinases, named MAP kinase kinase kinase (MAPKKK), MAP kinase kinase (MAPKK) and MAP kinase (MAPK). These protein kinases are activated in series, such that the MAPKKK phosphorylates the MAPKK at serines in its activation loop, which is thereby activated and phosphorylates the MAPK at a threonine and tyrosine in its activation loop, leading to its activation. The terminal MAPK, once activated, can migrate into the nucleus, and there phosphorylate and activate transcription factors (Waskiewicz, A. J. et al., 1995). A well characterised MAPK cascade is mediated downstream of the proto-oncogene Ras, consisting of Raf, MEK (MAPK and extracellular signal-regulated kinase (ERK) kinase) and ERK/MAPK proteins, which will be discussed in Section 1.6.1.3.

Another fundamental principle that has emerged in signal transduction pathways is the translocation of latent cytoplasmic transcription factors into the nucleus upon receptor stimulation. In some instances, a transcription factor can be sequestered in the cytoplasm through the binding of an inhibitory protein. An example of such a transcription factor is NF-κB. In this case, NF-κB is held in the cytoplasm through the binding to an inhibitor protein, IκB, which masks the nuclear localisation signal in the NF-κB heterodimer. Activating stimuli induce phosphorylation of IκB, at specific sites, which targets it for degradation, thus releasing active NF-κB to migrate into the nucleus (Gomperts, B. D. et al., 2003). A second family of transcription factors whose activity is regulated by their compartmentalisation are the STATs. In response to a variety of interferons and cytokines, members of the Janus kinase (JAK) family, which are associated with cytokine receptors, are activated. This results in tyrosine phosphorylation of receptor subunits and specific STAT transcription factors, which leads to the dimerisation of STATs, which then migrate to the nucleus and activate transcription (Gomperts, B. D. et al., 2003). This type of regulation allows for rapid information transfer from the cell surface to the nucleus. A third family of transcription factors whose subcellular localisation is regulated by extracellular signals is the Smads, which is the subject of this thesis. Activation of the TGF-β receptors by ligand binding induces the phosphorylation of the downstream transcription factors, the Smads, which leads to their complex formation. Monomeric Smads are continuously shuttling in and out of the nucleus, however complex formation allows accumulation in the nucleus, which results in the initiation of transcription (ten Dijke,

P. et al., 2006). The regulation of Smad activation will be discussed in much greater detail in the Section 1.5

Stabilisation of transcription factors is another mechanism by which growth factors, such as Wnt elicit their respsones. β-catenin is a component of adherens junctions at the cell membrane where it is associated with the cytoplasmic domains of cadherins. Under normal conditions, the cytoplasmic β-catenin levels are tightly regulated by association pf β-catenin with the adenomatous polyposis coli (APC) complex. The APC complex which also includes the scaffold proteins axin or conductin/axin2, casein kinase I (CKI) and glycogen synthase kinase3β (GSK-3β), facilitates the sequential phosphorylation of β-catenin by CKI and GSK-3β, leading to its degradation through the ubiquitin-proteasome pathway (Peifer, M. et al., 2000). Upon Wnt binding to its receptors, the cytoplasmic phosphoprotein, Dishevelled, is activated at the plasma membrane, which then interferes with the degradation of the cytoplasmic protein β-catenin. Stabilization of β-catenin, allows it to enter the nucleus and form complexes with high motility group box transcription factors of the LEF (lymphoid enhancer factor)/TCF (T-cell factor) family to initiate transcription of Wnt target genes (Peifer, M. et al., 2000).

A novel mode of signalling was demonstrated by the Notch family of receptors, which utilises the principle of ligand-induced proteolytic cleavage (Louvi, A. et al., 2006). Upon ligand binding, Notch undergoes a series of proteolytic events which results in cleavage of the Notch intracellular domain of the receptor, (NICD), which carries nuclear localization signals and can therefore translocate into the nucleus. Once in the nucleus, NICD interacts with the DNA-binding protein CSL, resulting in transcriptional activation of Notch target genes (Louvi, A. et al., 2006).

Finally, some ligands override the need for surface receptors such as the lipid-soluble retinoic acid, estrogen and other homones. These hormones traverse the plasma membrane and bind to these so-called nuclear receptors. These complexes then move into the nucleus and induce cellular responses by binding to and activating members of a family of zinc finger transcription factors (Gomperts, B. D. et al., 2003).

1.2 An overview of the TGF-β pathway

The transforming growth factor beta (TGF-β) superfamily is a large family of secreted cytokines involved in the regulation of diverse biological processes including proliferation, motility, differentiation and survival. Members of the TGF-β superfamily are present in vertebrates and metazoans including the fruit fly *Drosophila melanogaster* (Padgett, R. W. et al., 1987) as well as the nematode *Caenorhabditis elgans (C.elegans)* (Estevez, M. et al., 1993). The founding member of the family, TGF-β, was originally named as a factor produced by virus-transformed cells which could promote anchorage-independent growth of fibroblasts in culture (Roberts, A. B. et al., 1981). Since its discovery, however, subsequent studies have revealed a wide range of cellular responses elicited by TGF-β, including its role as a potent growth inhibitor (Polyak, K., 1996).

The basic mechanism of signal transduction by the TGF-β superfamily is conserved from *C.elegans*, *Drosophila* and *Xenopus* to higher vertebrate organisms (Miyazono, K. et al., 2001). Ligands in all of these species signal via a complex of type I and type II serine/threonine kinase receptors. As depicted in Figure 1.1, signalling is initiated by ligand binding at the cell surface and this allows the assembly of the type I and type II receptors into heteromeric complexes. The type II receptor is constitutively active and the ligand-induced receptor complex formation, permits the type II receptor to phosphorylate the juxtamembrane region of the type I receptor, which is rich in glycine and serine residues (Massagué, J., 1998). This phosphorylation event results in the activation of the type I receptor, which can then signal downstream to the intracellular mediators of the TGF-β superfamily, the Smad protein family. The Smads are divided into three distinct subfamilies, which include the receptor regulated Smads (R-Smads), Smad4, a common partner for R-Smads and the inhibitory Smads (I-Smads). Interestingly, phosphorylation of the type I receptor creates a binding site for the R-Smads, which is essential and sufficient for TGF-β signalling. Access of the R-Smads to this binding site on the type I receptors is facilitated by auxiliary proteins, such as Smad anchor for receptor activation (SARA) (Tsukazaki, T. et al., 1998). The type I receptor then phosphorylates the R-Smads at their conserved C-terminal SSXS motif, which results in dissociation from the receptor and heteromeric complex formation

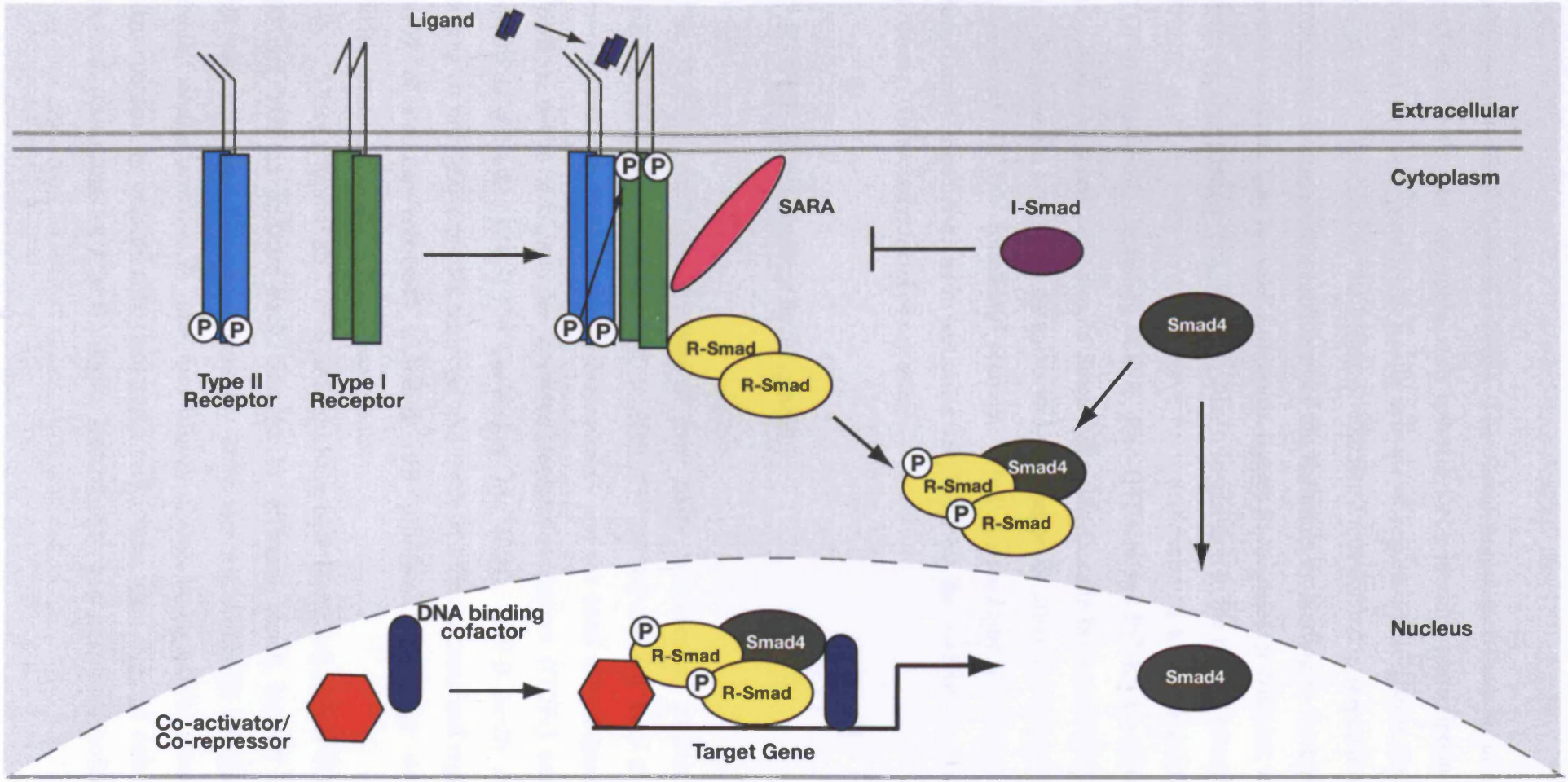

Figure 1.1. Overview of the TGF-β Signalling Pathway

The black arrows indicate the flow of signal. Phosphate groups are shown as a 'P' in a circle. R-Smad, receptor-regulated Smad, I-Smad, inhibitory Smad. For discussion, see text.

with Smad4 (Shi, Y. et al., 2003). The Smad complexes then accumulate in the nucleus, where they assemble with specific DNA-binding transcription factors, co-activators and co-repressors to finally activate or repress transcription. Termination of the signal is regulated by the I-Smads, which are upregulated in response to TGF-β. I-Smads act as competitive inhibitors of the R-Smads by binding to the type I receptor and in addition, they recruit E3 ubiquitin ligases to the receptor complex which targets them for degradation (Shi, Y. et al., 2003). In addition to the critical role played by the Smads, multiple other pathways have been demonstrated to act downstream of the TGF-β superfamily, including MAPK, Rho-GTPases and PI3 Kinase (Derynck, R. et al., 2003). This relatively simple Smad signalling cascade becomes highly complex if all the potential regulatory elements and integration of other signalling pathways are considered. In the following sections I will discuss the regulation of TGF-β superfamily signalling, with particular emphasis on the role of the Smads in this pathway, which is the focus of my thesis.

1.3 TGF-β superfamily ligands

The TGF-β superfamily consists of over thirty members of structurally related polypeptide growth factors. The superfamily can be divided into three distinct subfamilies: The TGF-βs, the Activins/Nodals and the bone morphogenetic proteins (BMPs), which also includes growth/differentation factors (GDFs) and Mullerian inhibiting substance (MIS) (de Caestecker, M., 2004). TGF-β family members are expressed in highly complex temporal and tissue-specific patterns and regulate a wide array of cellular processes including cell proliferation, lineage determination, differentiation, motility, adhesion and death.

Three mammalian TGF-β isoforms have been identified, named TGF-β1, TGF-β2 and TGF-β3 and are each encoded by different genes, located on different chromosomes and share approximately 80% identity. Although all three isoforms exhibit similar activities *in vitro*, they display distinct biological functions *in vivo*, as demonstrated by considerable phenotypic differences upon targeted deletion of each isoform (Goumans, M. J. et al., 2000). Interestingly, two additional isoforms exist in

both chicken and Xenopus. Whereas TGF-β1 was named for its transforming activities in *in vitro* assays, bone morphogenetic proteins (BMPs) were originally named for their ability to induce ectopic bone formation (Wozney, J. M. et al., 1988). To date, the BMP family represent the largest TGF-β subfamily, with over 20 members identified, of which can be classified into multiple groups of highly related proteins (Mehler, M. F. et al., 1997). *Drosophila melanogaster* Dpp, a homologue of BMP2 and BMP4, together with the vertebrate proteins BMP2 and BMP4 form one BMP subgroup, the DPP/BMP group. The functional conservation of these ligands within this subgroup was demonstrated by the ability of Dpp to induce endochondral bone formation in mammals (Sampath, T. K. et al., 1993). The third TGF-β subfamily includes Activins, Inhibins, Nodals, Lefty/Antivin and Derriere. Activin was first discovered as a local regulator of pituitary follicle-stimulating hormone (FSH) release, whereas Inhibin was found to attenuate Activin effects at the pituitary (Gaddy-Kurten, D. et al., 1995). It was subsequently discovered that Inhibin, which is structurally related to Activin, acts as an endogenous antagonist of Activin signalling, by acting as a competitive inhibitor of the receptor complex (Lebrun, J. J. et al., 1997). In addition, Lefty, a divergent member of this subfamily, has been shown to antagonise Nodal signalling, and the balance between Lefty and Nodal activity underlies the proper execution of many developmental processes (Solnica-Krezel, L., 2003).

The high number of ligands in this superfamily is presumably due to the need for finely tuned developmental patterns of receptor activation. This is achieved in part by differential regulation of ligand expression and activation from latent complexes. TGF-β superfamily members are synthesized as large inactive precursor molecules that undergo proteolytic cleavage, releasing the prodomain from the active, receptor binding, carboxy-teminal region of the molecules. These cleavage events are regulated in the Golgi apparatus by endoproteases of the convertase family including SPC1/Furin and SPC4/PACE4 (Dubois, C. M. et al., 1995). For members of the superfamily such as TGF-β, GDF8 and possibly others, the N-terminal cleavage product, also known as latency associated peptide (LAP), binds non-covalently to the mature ligands, preventing binding to their respective receptors (de Caestecker, M., 2004). A variety of molecules release the mature ligand from its latent state, which includes a number of proteases such as plasmin, and the metalloproteases MMP-2 and MMP-9, and also thrombospondin, integrins and even reactive oxygen species

(Annes, J. P. et al., 2003). Activation of mature lignad is achieved by either proteolytic cleavage of LAP or through disruption of non-covalent interactions between LAP and TGF-β (Crawford, S. E. et al., 1998; Lyons, R. M. et al., 1988).

Table 1.1 Members of the TGF- β superfamily of ligands

Ligand	*Alternative names*	*Subgroup*
TGF-β		
TGF-β1		TGF-β s
TGF-β2		
TGF-β3		
Activin/Nodal		
Activin A	Activin β_A-β_A sub-units	Activins
Activin B	β_B-β_B	
Activin AB	β_A-β_B	
Inhibin A	Inhibin α-Activin β_A subunits	Inhibins
Inhibin B	α-β_B	
Nodal	Ndr	Nodal
Lefty1	Lefty A/EBAF	Lefty
Lefty2	Lefty B	
BMP/GDF		
BMP2	BMP2A	BMP2/4
BMP4	BMP2B	
BMP5		BMP5/6/7
BMP6	Vgr1/DVR6	
BMP7	OP1	
BMP8A	OP2	
BMP8B	OP3/PC8	
GDF1		GDF1
GDF3	Vgr2	
GDF5	CDMP1	GDF5/6/7
GDF6	CDMP2/BMP13	
GDF7	BMP12	
BMP9	GDF2	BMP9/10
BMP10		
BMP3	Osteogenin	BMP3
BMP3b	GDF10/Sumitomo-BIP	
GDF9		GDF9
GDF9b	BMP15	
GDF15	MIC1/PLAB/PTGFB/PDF	
GFD8	Myostatin	GDF8
GDF11	BMP11	
MIS	MIF/AMH	MIS

The active domains of the TGF-β ligands have six intra-strand disulfide bonds that form a characteristic "cystine knot" folding motif (Shi, Y. et al., 2003). Each protein then dimerises, in an anti-parallel fashion, to form the active ligand, which is stabilised by hydrophobic interactions. With the exception of GDF3 and GDF9, all TGF-β superfamily members have an additional conserved cysteine residue that is required to form an intersubunit disulfide bridge, which further stabilises the homodimers (Mittl, P. R. et al., 1996). Although homodimers represent the predominant form of these ligands, heterodimers, such as that between BMP7 and GDF7, have been generated *in vitro* and these proteins display greater biological activity than their corresponding homodimers. *In vivo*, heterodimers might also function as competitive inhibitors of the homodimers, and thereby act to modulate signalling during development (ten Dijke, P. et al., 2003). Upon dimerisation, the TGF-β superfamily ligands are secreted from the cell into the interstitial milieu where they initiate autocrine or paracrine signalling.

1.4 TGF-β receptors

The cellular effects of the TGF-β superfamily members are mediated by a complex of transmembrane receptors with cytoplasmic serine-threonine kinase activity (Massague, J., 1998). Initial investigations using affinity labelling of TGF-β identified two types of receptors found to be indispensable for signal transduction (Laiho, M. et al., 1990; Wrana, J. L. et al., 1992b). This led to the rapid identification of many other members of this receptor family. To date, the receptor serine/threonine kinase family in the human genome comprises of 12 members, all of which are TGF-β receptors (Manning, G. et al., 2002). Based on structural and functional properties, the serine-threonine kinase receptors fall into two families called the type I and type II receptors. Type I receptors have a higher level of sequence similarity than type II receptors and also contain a highly conserved region rich in glycine and serine residues called the GS domain (or type I box) located just N-terminal to the kinase domain. The nomenclature for the types I and II receptors is somewhat confusing. For simplicity, I have referred to the type I receptors by a common nomenclature, the Activin-receptor like kinases

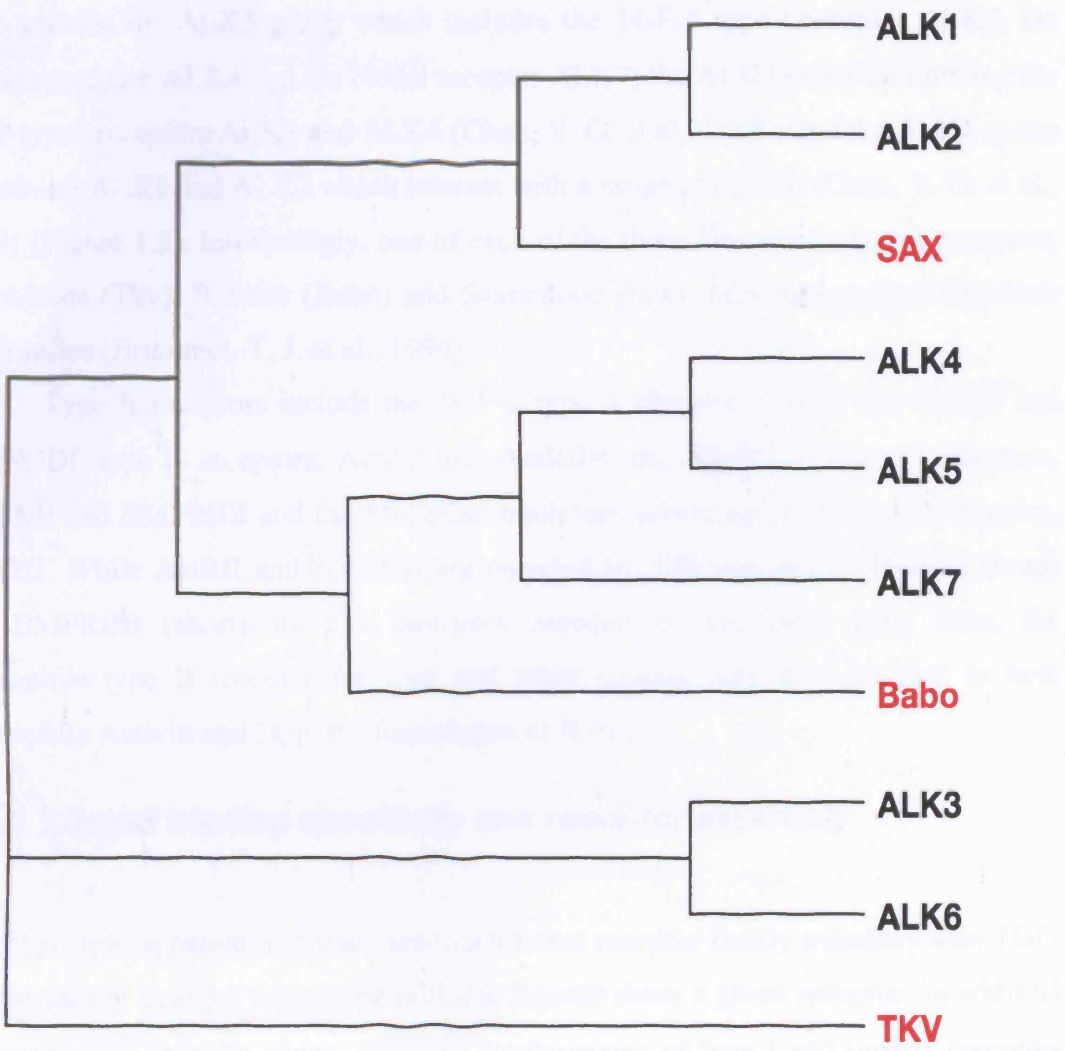

Figure 1.2. Dendrogram of the type I receptors

The dendrogram indicates the relative level of amino acid sequence similarity of the type I receptors. The tree was produced by using the ClustalX alignment package (bootstrapping method) and was viewed in TreeView. ALKs 1-7 are mammalian (blck type) and Saxophone (Sax), Baboon (Babo) and Thickveins (Tkv) are *Drosophila* (red type).

(ALKs) (ten Dijke, P. et al., 1993; ten Dijke, P. et al., 1994a), and the type II receptors according to their dominant ligand interactions (de Caestecker, M., 2004).

Type I receptors are classified according to sequence similarities into three main groups: the ALK5 group which includes the TGF-β type I receptor ALK5, the Activin receptor ALK4 and the Nodal receptor ALK7; the ALK3 group comprising the BMP typeI receptors ALK3 and ALK6 (Chen, Y. G. et al., 1998); and the ALK1 group containing ALK1 and ALK2 which interact with a range of ligands (Chen, Y. G. et al., 1999) (Figure 1.2). Interestingly, one of each of the three *Drosophila* type I receptors, Thickveins (Tkv), Baboon (Babo) and Saxophone (Sax), falls into each of the three subfamilies (Brummel, T. J. et al., 1994).

Type II receptors include the TGF-β type II receptor, TβRII, the Activin and BMP/GDF type II receptors, ActRII and ActRIIB, the BMP/GDP type II receptors, BMPRII and BMPRIIB and the Mullerian inhibitory substance (MIS) type II receptor, MISRII. While ActRII and ActRIIB are encoded by different genes, BMPRII (long) and BMPRIIB (short) are two isoforms encoded by the same gene. Punt, the Drosophila type II receptor for Dpp and other ligands, acts as a receptor to both Drosophila Activin and Dpp, the homologue of BMP2/4.

1.4.1 Ligand binding specificity and receptor assembly

It is strikingly apparent that there are much fewer receptor family members than TGF-β superfamily ligands, suggesting multiple ligands share a given receptor. In addition to overlapping receptor usage, different combinations of type I and type II receptors pair with different ligands (Feng, X. H. et al., 2005) (Figure 1.3). The BMP ligands exhibit the greatest potential in receptor combinations, which is due in part to their ability to bind not only the "classical" BMPRII but also with ActRII/ActRIIB (Macias-Silva, M. et al., 1998; Nishitoh, H. et al., 1996) (Figure 1.3). However, subgroups of the BMP ligands form specific receptor configurations. For example, the closely related BMP2 and BMP4 can both bind either ALK3 or ALK6, in concert with BMPRII, ActRII or ActRIIB (Macias-Silva, M. et al., 1998; ten Dijke, P. et al., 1994b). In addition, BMP6/7 can also form complexes with ALK2 together with the type II receptors (Macias-Silva, M. et al., 1998). ALK2 has been implicated as a dual receptor, demonstrated by its ability to also bind activin as well as BMP6/7, in concert

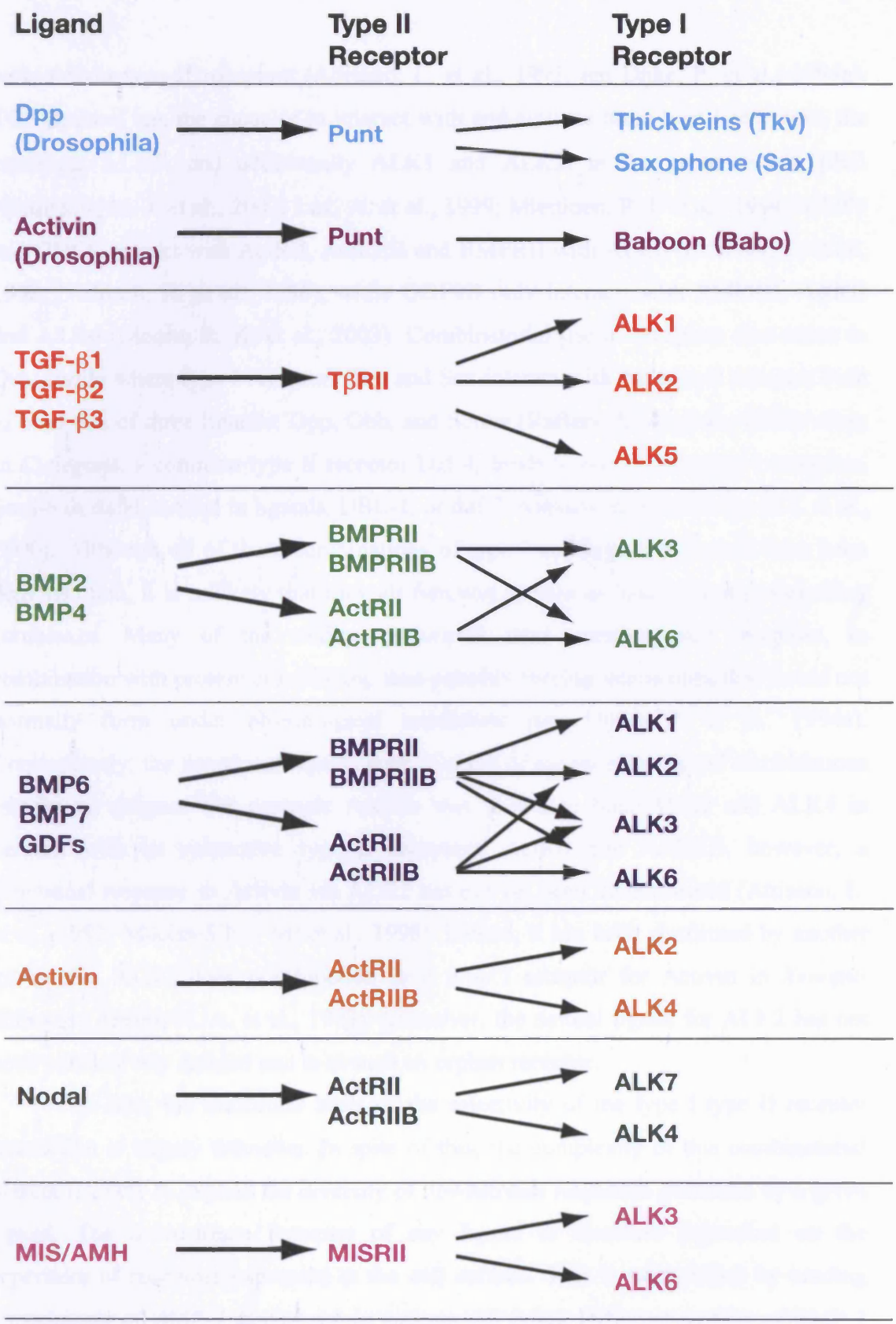

Figure 1.3. Heteromeric combinations of TGF-β superfamily receptors.

TGF-β ligands bind to specific combinations of RII-RI heterotetramers at the cell surface. Ligands, type I and type II receptors are colorcoded for each pathway. (Adapted from Feng and Derynck, 2005)

with activin type II receptors (Attisano, L. et al., 1993; ten Dijke, P. et al., 1994a). TGF-β, itself has the capacity to interact with and activate three type I receptors, the canonical ALK5, and additionally ALK1 and ALK2, in the presence of TβRII (Goumans, M. J. et al., 2002; Lux, A. et al., 1999; Miettinen, P. J. et al., 1994). GDF5 and GDF6 interact with ActRII, ActRIIB and BMPRII with ALK6 (Erlacher, L. et al., 1998; Nishitoh, H. et al., 1996), while GDF9B only interacts with BMPRII, ActRII and ALK6 (Moore, R. K. et al., 2003). Combinatorial use of receptors also occur in *Drosophila* where type I receptors Tkv and Sax interact with the type II receptor Punt to bind one of three ligands: Dpp, Gbb, and Screw (Raftery, L. A. et al., 1999). Also, in *C.elegans*, a common type II receptor Daf-4, binds to one of two type I receptors, Sma-6 or daf-1 to bind to ligands, DBL-1, or daf-7, respectively (Patterson, G. I. et al., 2000). Although all of these combinations of type I and type II receptors have been demonstrated, it is unlikely that they all function *in vivo* as ligand-binding signalling complexes. Many of the studies performed used overexpressed receptors, in combination with protein crosslinking thus possibly forcing interactions that would not normally form under physiological conditions (ten Dijke, P. et al., 1994a). Consequently, the functional significance of some of the receptor-ligand combinations remain an enigma. For example Activin was shown to bind ALK2 and ALK4 in concert with its respective type II receptors, ActRII and ActRIIB, however, a functional response to Activin via ALK2 has not yet been demonstrated (Attisano, L. et al., 1993; Macias-Silva, M. et al., 1998). Indeed, it has been confirmed by another group that ALK2 does not function as a type I receptor for Activin in *Xenopus* embryos (Armes, N. A. et al., 1997). Moreover, the natural ligand for ALK2 has not been conclusively defined and is as such an orphan receptor.

To date, the molecular basis of the selectivity of the type I-type II receptor interaction is largely unknown. In spite of this, the complexity of this combinatorial system is likely to explain the diversity of downstream responses generated by a given ligand. The downstream response of any ligand is therefore dependent on the repertoire of receptors expressed at the cell surface. This is exemplified by binding experiments of BMP-7 carried out in various cell types. Different profiles of BMP-7 receptors complexes were observed in different cells types examined. In some cases, BMP-7 formed complexes with either ALK2, 3 or 6, and combinations of all three, each with different affinities (Yamashita, H. et al., 1995). Consistent with this idea, the

signalling response by individual ligands would depend on the nature of the activated receptor complex. Indeed, differential signalling responses were observed by the BMP type I receptors in specification of mesenchymal precursor cells, whereby ALK3 is able to promote adipogenic differentiation, and ALK6 may be more potent in osteoblast differentiation (Chen, D. et al., 1998). In addition, endothelial cell migration and proliferation is attributed to TGF-β signalling via ALK1, whereas growth inhibition and differentiation activities functions through ALK5 during angiogenesis (Goumans, M. J. et al., 2003b; Goumans, M. J. et al., 2002) (see Section 1.6.2). In conclusion, the association of different type I and type II receptors generates a diverse repertoire of receptor complexes possessing distinct signalling potentials.

1.4.2 Structural features

Type I and Type II receptors are glycoproteins of approximately 55 kDa and 70 kDa, respectively. Both types of the receptor serine/threonine kinases consist of about 500 amino acids, with an N-terminal extracellular ligand binding domain, a transmembrane region, and a C-terminal serine/threonine kinase domain. The extracellular domain is relatively short (approximately 150 amino acids), and contains either one or two N-glycosylation sites in type I and type II receptors, respectively (Franzen, P. et al., 1993). A characteristic structural feature of all TGF-β receptors is the three-finger toxin fold in the ligand binding domain, which has a common pattern of eight cysteines forming four disulfide bonds (Greenwald, J. et al., 1999)(Figure 1.4). A number of snake venom neurotoxins also share this structural fold, however, sequence identities between the TGF-β receptors and the toxins are low and no functional similarities between the two groups are known (Kirsch, T. et al., 2000). A highly conserved region of approximately thirty amino acids, known as the GS region is found only in the type I receptor family and is named for the ^{185}TTSGSGSG^{192} sequence at its core. It is essential for the ligand-induced activation of the type I receptor, whereby at least three, and perhaps four to five of the serines and threonines in the GS region, must be phosphorylated to fully activate the type I receptor (Wieser, R. et al., 1995; Willis, S. A. et al., 1996). In addition to the GS region, the intracellular region of the type I and type II receptors contains the canonical serine/threonine kinase

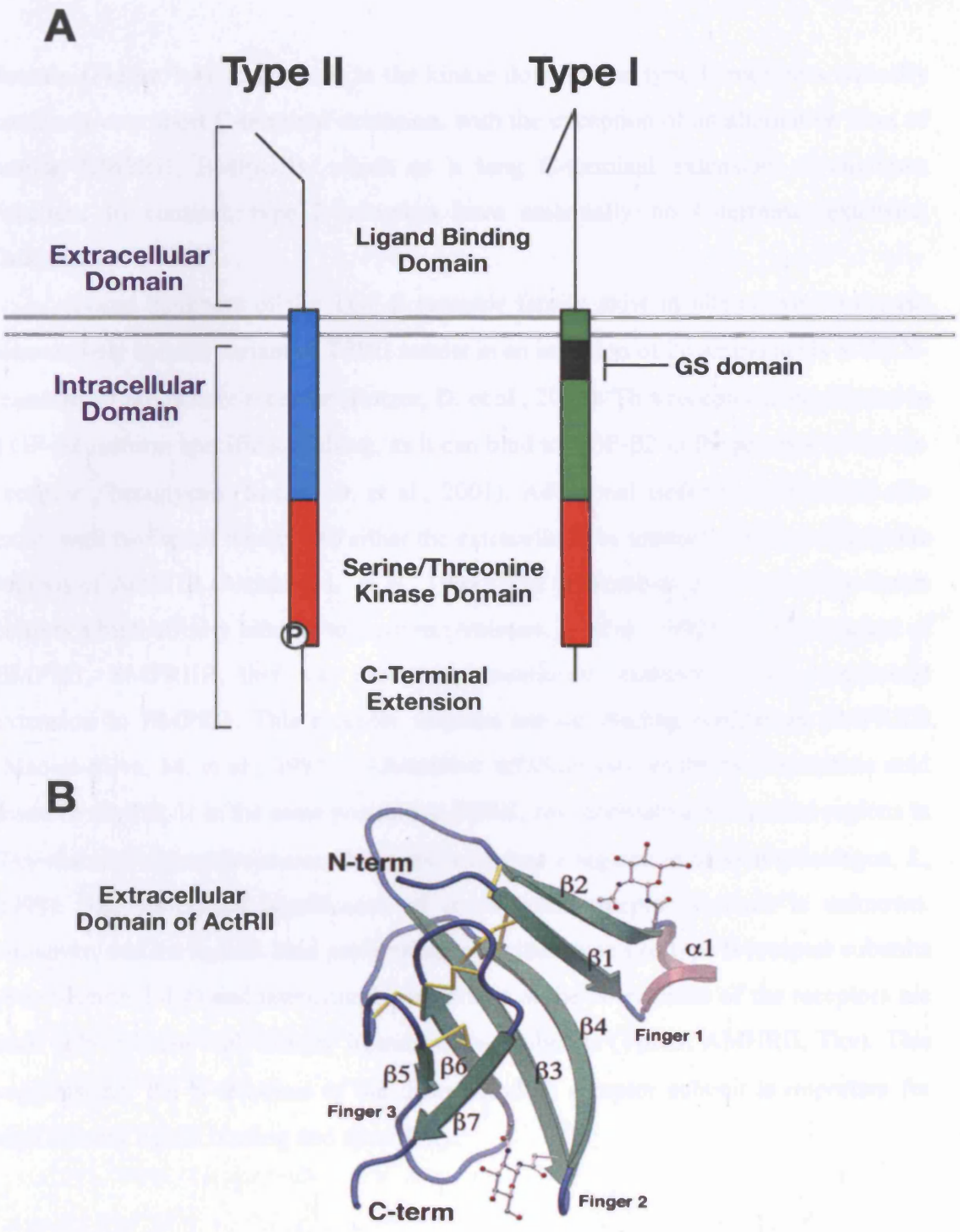

Figure 1.4. Structure of the TGF-β family receptors

A) Schematic diagram of the structural features of the Type I and Type II receptors.The P represents the consitutive serine/threonine phosphorylations of the type II receptor. The GS region is rich in glycine and serine residues and contains the characteristic TTSGSGSG sequence at its core.
B) Stereo ribbon diagram of the extracellular ligand binding domain of the type II Activin receptor (ActRII). The strands are numbered in the order that they occur in the sequence. The structure resembles the so-called three-finger toxin fold. (Taken from Greenwald, et al., 1999)

domain (Figure 1.4). C-terminal to the kinase domain, the type II receptors typically contain a very short C-terminal extension, with the exception of an alternative form of human BMPRII, BMPRIIB, which as a long C-terminal extension of unknown function. In contrast, type I receptors have essentially no C-terminal extension (Massague, J., 1998).

Some members of the TGF-β receptor family exist in alternative forms. An alternatively spliced variant of TβRII results in an insertion of 26 amino acids at the N-terminus of the mature receptor (Rotzer, D. et al., 2001). This receptor is implicated in TGF-β2 isoform specific signalling, as it can bind to TGF-β2 in the absence of the co-receptor , betaglycan (Rotzer, D. et al., 2001). Additional isoforms of ActRIIB also exist, with two small inserts into either the extracellular or intracellular juxtamembrane regions of ActRIIB (Attisano, L. et al., 1992). The presence of the extracellular insert confers a high affinity binding to Activin (Attisano, L. et al., 1992). A splice variant of BMPRII, BMPRIIB, that was previously mentioned, contains a long C-terminal extension in BMPRII. This receptor displays similar binding profiles as BMPRIIB (Macias-Silva, M. et al., 1998). Alternative splicing also results in a 61-amino acid insert in AMHR-II in the same position as TβRII, two alternative N-terminal regions in Tkv and two alternative extracellular juxtamembrane regions in baboon (Massague, J., 1998). The functional significance of these latter receptor variants is unknown. However, certain ligands bind preferentially to either type I or type II receptor subunits (See Section 1.4.4) and interestingly, insertions at the N-terminus of the receptors are seen only in these high affinity ligand binding subunits (TβRII, AMHRII, Tkv). This suggests that the N-terminus of the ligand binding receptor subunit is important for high affinity ligand binding and specificity.

1.4.3 Receptor Complex formation

The basic paradigm by which TGF-β family ligands interact with their receptors has been largely established from studies of TGF-β (Wrana, J. L. et al., 1992b). The initial observation that stable expression of the type II receptor in mutant mink lung (Mv1Lu) cells which lacked functional type II receptors, restored the interaction of the type I receptor with TGF-β, prompted investigation into the possibility of a ligand induced

complex formation (Wrana, J. L. et al., 1992a). Subsequently it was shown that the type I and type II receptors physically associate to form a stable complex (Franzen, P. et al., 1993; Moustakas, A. et al., 1993; Wrana, J. L. et al., 1992a) and furthermore, chimeric receptor systems established that this complex is required for signalling (Luo, K. et al., 1996; Vivien, D. et al., 1995). Kinase dead mutants of the type II receptor still restored ligand binding to type I receptor, suggesting that the kinase domain is not required for heteromeric complex formation (Wrana, J. L. et al., 1992a). In addition, truncated versions of the receptors, which lacked their entire intracellular domain, were still found to crosslink to ligand, indicating that the cytoplasmic domains of the receptors are not required for complex assembly (Greenwald, J. et al., 2003).

The exact stoichiometry of the active receptor complex has slowly been unravelled. Type I and type II receptors were shown to form homodimers in the absence of ligand (Gilboa, L. et al., 1998; Henis, Y. I. et al., 1994). These homomeric complexes are not sufficient to propagate TGF-β responses but are proposed to be functionally important for regulating receptor kinase activity (Luo, K. et al., 1996; Luo, K. et al., 1997). In addition, complementation studies between kinase-defective ALK5 and activation-defective ALK5 indicated a cooperative interaction between multiple ALK5 molecules that is essential for signal transduction (Weis-Garcia, F. et al., 1996). These studies raised the possibility that the active receptor signalling complex could be a large multimeric complex consisting of a minimum of two copies of each receptor. Indeed, early studies indicated that a single dimeric ligand interacts with two type I and two type II receptors to form a hetero-tetrameric signalling complex, based on either velocity centrifugation or electrophorectic mobility of receptor complexes crosslinked to [^{125}I]TGF-β (Wells, R. G. et al., 1999; Yamashita, H. et al., 1994). To date, structural data confirms the proposed model of the four-receptor signalling complex (Greenwald, J. et al., 2003). The elucidation of the cocrystal structure of ActRII ectodomain (EC) with BMP7 indicated that the complex consists of the BMP-7 dimer and two ActRII receptor ECs, and its structure exhibits a perfect twofold axis of symmetry (Greenwald, J. et al., 2003). When crystal structure of the ALK3 EC in complex BMP2 complex, is superimposed on the ActRII-BMP2 structure, a symmetrical complex with four receptors bound to the BMP-7 dimer was formed (Greenwald, J. et al., 2003; Kirsch, T. et al., 2000). Taken together, this

evidence strongly suggests the existence of active hetero-tetrameric signalling complexes, however, this does not rule out the possibility for higher order structures.

In addition, the receptors have been shown to have an intrinsic affinity for each other. As demonstrated by co-immunopreciptitation and antibody-mediated copatching experiments, a small, but detectable proportion of ALK5 and TβRII heteromeric receptor complexes exists already in unstimulated cells (Chen, R. H. et al., 1995; Vivien, D. et al., 1995; Wells, R. G. et al., 1999). The dramatic induction of complex formation upon ligand binding, however, suggests that the majority of the receptors are unoccupied at the cell surface. This is further substantiated by the ability of type I and type II receptors to bind in different combinations, depending on the ligand present (de Caestecker, M., 2004; Wrana, J. L. et al., 1994).

1.4.4 Ligand Binding

Surprisingly, individual members of the TGF-β superfamily bind to their respective receptors in a distinct fashion, despite sharing similar patterns of downstream signalling events. In general, there are two modes by which TGF-β ligands recognise their receptors, either by high affinity binding to the type I or the type II receptor (Shi, Y. et al., 2003). TGF-β1, TGF-β3 and Activins initiate receptor assembly by binding with high affinity to the type II receptor. The type I receptor is subsequently recruited by the type II-ligand complex to stablilise the type II-type I receptor complex (Boesen, C. C. et al., 2002; Hart, P. J. et al., 2002). This binding mode is characterised in the TGF-β system, whereby the type I receptor has the ability to recognise TβRII-bound TGF-β but is unable to bind TGF-β free in solution (Laiho, M. et al., 1990; Wrana, J. L. et al., 1992a). The elucidation of the structure of the TβRII ectodomain-TGF-β3-complex has revealed insights into the mechanism of receptor binding. The TβRII ectodomain (EC) interacts with the homodimeric, antiparallel TGF-β3, by binding identical regions at opposite ends of the ligand, called the 'fingertips' (Hart, P. J. et al., 2002) (Figure 1.5). Each receptor binds to one monomer of the dimeric TGF-β3. The receptor assembly model predicts that ALK5 binds TβRII-TGF-β adjacent to TβRII on the concave surface of the ligand, which stabilises the complex (Hart, P. J. et al., 2002)

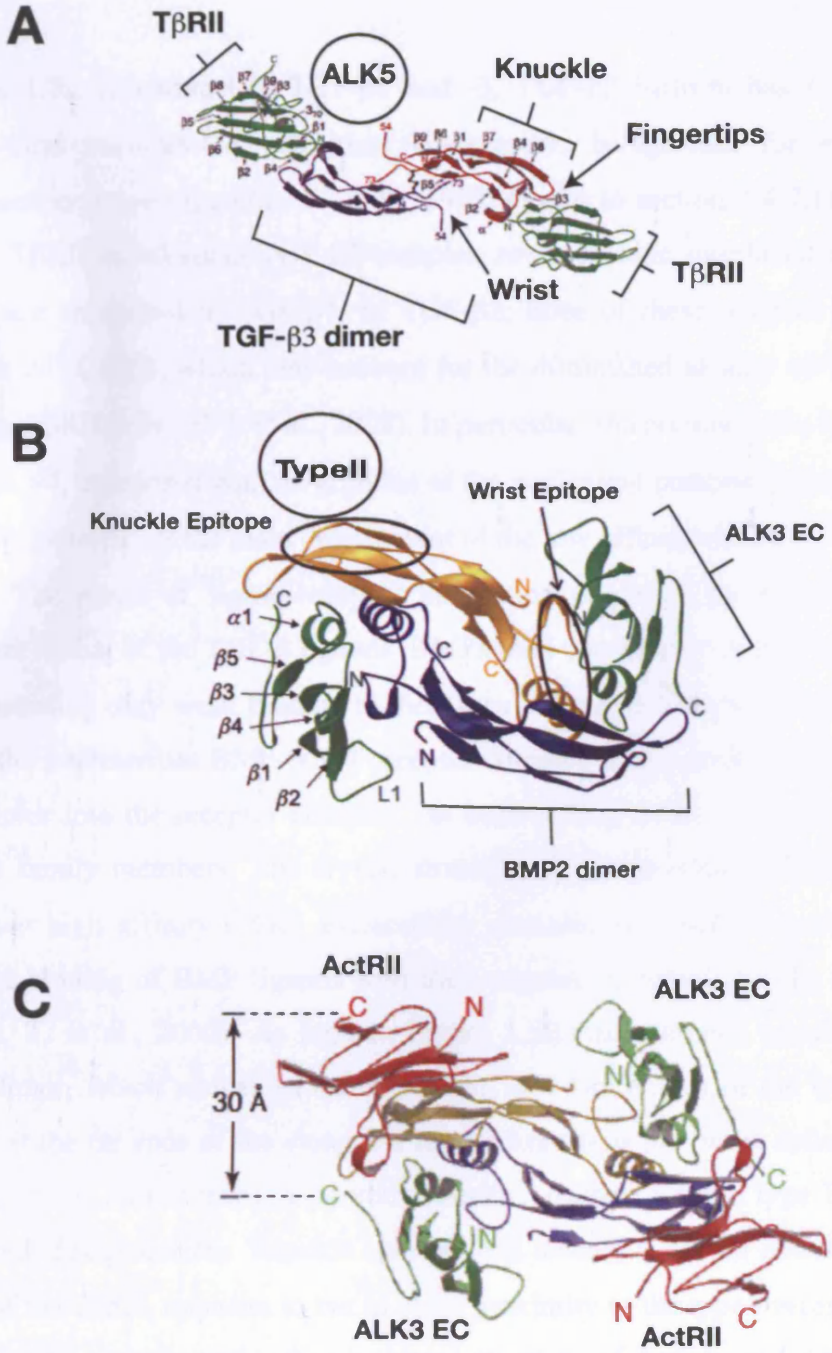

Figure 1.5. Ligand-Receptor Interactions

(A) Side view of the human TβRII extracellular (ec) domain -TGF-β3 complex, with two ecTβRII molecules (green) and the two TGF-β3 monomers (blue and red). The TGF-β3 interchain disulfide bond is shown in black.The predicted positioning of ALK5 in the complex is shown by a black circle. (Adapted from Hart et al., 2002)

(B) The structure of the BMP2-ALK3ec complex. The BMP monomers are coloured gold and blue, the two ALK3ec molecules are green. Secondary structure elements, chain termini and receptor loops 1 and 3 are labeled. The 'wrist' and the putative 'knuckle' epitopes on BMP-2 are highlighted and the positioning of the type II receptor at the knuckle epitope is represented by a black circle. (Adapted from Kirsch et al., 2000)

(C) The heterohexameric complex of BMP7–ALK3–ActRII consisting of one ligand dimer bound to four receptor extracellular (ec) domains. The components are shown in blue and yellow (BMP7), green (ecs of ALK3) and red (ecs of ActRII). The ALK3 ecs were docked to the BMP7–ActRII complex by superposition with the BMP2–ALK3 complex. (Taken from Sebald and Mueller, 2003)

(Figure 1.5). In contrast to TGF-β1 and -3, TGF-β2 isoform has a low affinity to TβRII and requires an additional co-receptor, betaglycan, for efficient signal transduction (Lopez-Casillas, F. et al., 1993) (Refer to section 1.4.7.1). The structure of the TβRII ectodomain-TGF-β3-complex revealed nine interfacial residues, all of which are conserved in TGF-β1. In TGF-β2, three of these residues are substituted relative to TGF-β3, which may account for the diminished affinity of TGF-β2 toward binding TβRII (Hart, P. J. et al., 2002). In particular, the presence of a lysine residue at position 94, compared with an arginine at the equivalent position in both TGF-β1 and TGF-β3 isoforms, is the main determinant of the low affinity observed.

The mode of ligand-receptor interaction exhibited by the BMP ligands is different to that of the TGF-β ligands. BMPs bind specifically to their type I receptors, demonstrating only weak binding to their type II receptors alone (Liu, F. et al., 1995). Thus, the intermediate BMP-type I receptor complex then recruits the low affinity type II receptor into the receptor complex, an order which is the reverse from most other TGF-β family members. The crystal structure of human dimeric BMP2 in complex with two high affinity ALK3 extracellular domains (BRIAec) has revealed insights into the binding of BMP ligands with their cognate receptors (Keller, S. et al., 2004; Kirsch, T. et al., 2000). As seen in Figure 1.5B, the complex consists of a BMP2 homodimer, which adopts an extended fold, and two copies of the type I receptors, bound at the far ends of the elongated ligand, known as the 'wrist epitope' (Kirsch, T. et al., 2000). Furthermore, a potential binding epitope for the type II receptor was proposed, designated the 'knuckle epitope' and located at the far end of the central β-sheet of the dimer, opposite to but in close proximity to the type I receptor (Kirsch, T. et al., 2000). Subsequently, the elucidated structure of Activin and ActRIIB complex revealed that Activin type II receptor shares a similar binding site to the BMP type II receptor on its respective ligand (Thompson, T. B. et al., 2003). Activin A binds ActRIIB along the 'knuckle' region of the monomer structure, similarly to the proposed binding epitope of BMP2 (Thompson, T. B. et al., 2003). This binding mode is significantly different from TGF-β3 binding to TβRII, where TGF-β binds TβRII at the tips of the monomer fingers (Hart, P. J. et al., 2002). These structural data reveal that the binding epitopes of the type II receptors differs greatly between the TGF-β ligands compared with those of Activin and BMP ligands (Compare Figure 1.6A and

B), supporting the idea that the type II receptors play a dominant role in determining the specificity of ligand. Also, these different binding modes may have consequences in downstream signalling, through differential or cooperative recruitment of type I and type II receptors in the holo complex.

As previously mentioned, BMP ligands have a higher affinity for their type I receptors than their type II receptors, however, BMP-7 differs in this respect in that it retains the TGF-β/Activin-like preference for its type II receptor. As a result, the structure of BMP7 type II receptor complex was elucidated, which revealed additional insights into the assembly of the TGF-β receptor complex. Because of the high sequence homology of BMP2 and BMP7, the model of the BMP7-ActRII structure could be confidently combined with the BMP2-ALK3ec complex to assemble a six-chain complex. The most striking observation of the predicted model was the lack of a direct physical interaction between any of the receptor extracellular domains, which were connected only through ligand (Greenwald, J. et al., 2003). This is in contrast to the current paradigm in which the type II receptor recruits the type I receptors. Yet the two receptors cooperatively bind to the BMP7 ligand, whereby the high affinity interaction of the type II receptor with the ligand, allows the cooperative recruitment of the low affinity type I receptor. Thus, this represents a new mode of cooperative ligand-mediated receptor assembly without receptor-receptor contacts (Sebald, W. et al., 2003). Furthermore, it has been proposed that cooperativity is achieved by immobilisation of the ligand at the membrane surface by the initial binding of the high affinity binding (ActRII in the case of BMP7), thus enhancing the affinity for the second receptor (Greenwald, J. et al., 2004).

1.4.5 Receptor activation

The basic mechanism of receptor activation was first established with TGF-β receptors (Chen, F. et al., 1995; Wrana, J. L. et al., 1994) and subsequently similar mechanisms were also revealed for the activin receptors (Attisano, L. et al., 1996) (Figure 1.6). The notion that ALK5 acts downstream of TβR-II was supported by the inability of the type II receptors to signal in the absence of type I receptors, in spite of their ability bind TGF-β (Boyd, F. T. et al., 1989; Laiho, M. et al., 1990; Wrana, J. L. et al.,

1992a). This was further substantiated by studies showing that a mutation in TβR-II which inactivates its ability to recognize ALK5 as a substrate does not signal (Carcamo, J. et al., 1994), and that a constitutively active ALK5 mutant (threonine residue at 204 replaced by an aspartic acid residue) can signal in the absence of ligand and TβR-II (Wieser, R. et al., 1995). The TGF-β type II receptor is constitutively active. Autophosphorylation occurs on four residues and ligand occupancy causes no appreciable change in this activity (Wrana, J. L. et al., 1994). The regulation of this remains elusive, however autophosphorylation of three of these residues, S213, S409 and S416, were shown to positively and negatively affect receptor function (Luo, K. et al., 1997). Upon ligand binding, formation of the heteromeric complex between the type I and type II receptors rapidly leads to phosphorylation of the type I receptor (Wrana, J. L. et al., 1994). Phosphorylation occurs on one threonine and three serines in the GS domain, adjacent to the N-terminus of the kinase domain in all type I receptors (Weis-Garcia, F. et al., 1996). This phosphorylaion is catalysed by the type II receptor, as shown by coexpression of wild-type and kinase-defective mutants of type I and II receptors in various combinations (Wrana, J. L. et al., 1994). These multiple phosphorylation events activate the type I receptor kinase, which transduces the signal by phosphorylating and activating downstream mediators of the pathway, the Smads (Figure 1.6). To date, members of the Smad family of transcription factors are the only direct substrates of the type I receptors (See Section 1.5). Phosphorylation in the GS domain is essential for signal propagation since mutations in two or more of the serine residues impairs signalling (Franzen, P. et al., 1995). In an additional study, Huse *et al.*, used an elegant chemical ligation method to produce a homogenous, tetra-phosphorylated GS region in ALK5. By use of this semisynthetic protein, it was shown that the primary effect of GS phosphorylation is the creation of a binding site for one of ALK5's downstream target, Smad2, and that the unphosphorylated GS region is inhibitory only through binding of the immunophilin FKBP12 (Huse, M. et al., 2001) (Figure 1.6). Thus the receptor activation is not due to an increase of the actual kinase activity, but rather is based on the creation of a substrate binding site. In line with this idea, constitutively active (ca) type I receptors, mentioned earlier, function by maintaining this open conformation, to which the Smads can bind and are activated (Wieser, R. et al., 1995).

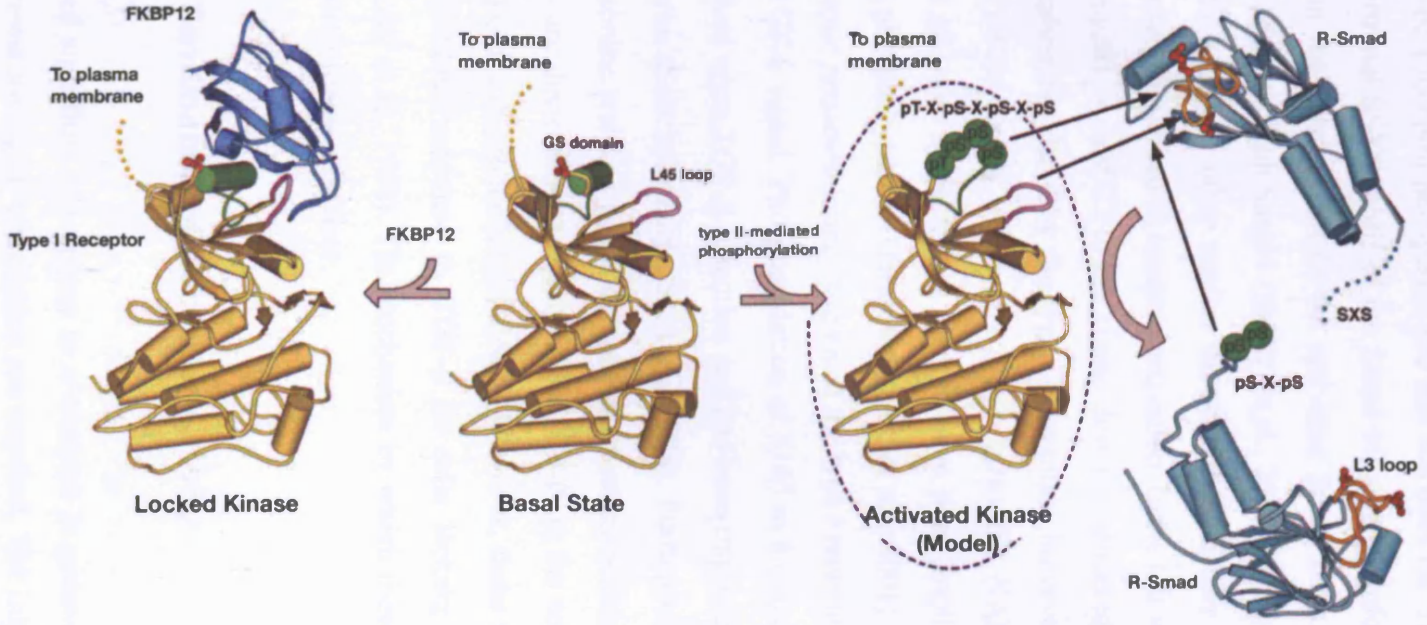

Figure 1.6. Receptor Activation

In the absence of ligand (basal state), the type I receptor is stabilised in an inactive conformation by the presence of FKBP12, which organises the flexible GS loop into an inhibitory wedge generating a 'locked' conformation. This prevents spurious receptor complex formation and subsequent signalling. Upon ligand binding, the type II receptor recruits the type I receptor into a hetermeric receptor complex. The close proximity of the receptors allows the constitutively active type II receptor to phosphorylate the GS domain of the type I receptor. Phosphorylation of the GS domain eliminates a binding site FKBP12 and simultaneously creates a binding site for the Smad substrate. The GS domain in conjunction with the L45 loop of the type I receptor mediates the interaction with the L3 loop of an R-Smad, resulting in phosphorylation of its C-terminal SSXS motif. The green circles represent the putative phosphorylation sites of the type I receptor and the R-Smads. (Taken from Shi and Massague, 2003).

The specificity of the interaction is determined by a nine amino acid sequence in the type I receptor, known as the L45 loop and a complementary region in the Smad C-terminal domain, the L3 loop (Chen, Y. G. et al., 1998; Chen, Y. G. et al., 1999)(See Secion 1.5.4.2). Once the Smad-receptor interaction is established, the kinase domain of the type I receptor phosphorylates and activates the Smads. The phosphorylation of the C-terminal SSXS motif of the Smad triggers a conformational change which then results in the dissociation of the activated Smad from the receptor and subsequent heteromerisation with Smad4 (Shi, Y. et al., 2003).

In addition, other studies investigated whether other residues of the type I receptor were involved in receptor activation. Indeed, it was observed that mutations in either Gly261 or Gly322 in the kinase domain, rendered the type I receptor unable to be transphosphorylated by the type II receptors, however they still maintained kinase activity (Weis-Garcia, F. et al., 1996). Also the NANDOR box, which refers to residues 482-491 in the kinase domain have been implicated in the regulation of GS domain phosphorylation (Garamszegi, N. et al., 2001). Furthermore, residues in the cytoplasmic juxtamembrane domain of the type I receptor are required for transduction of the TGF-β signal. Phosphorylation of S165 in the juxtamembrane domain of type I is observed upon TGF-β induction and has been implicated in modulation of the TGF-β response (Souchelnytskyi, S. et al., 1996). Furthermore, mutagenesis of the serine and threonine residues in the cytoplasmic juxtamembrane domain, revealed that these residues are dispensable for binding to TGF-β on the cell surface, forming a complex with TβR-II and production of PAI-1. However, these mutants could not restore the antiproliferative response to TGF-β in cells lacking endogenous type I receptor (Saitoh, M. et al., 1996). The mechanism by which these residues contribute to signal propagation remains unclear.

1.4.6 Termination of Receptor Activity

Sustained signalling in response to a stimulus is generally undesirable, and therefore mechanisms for signal termination are required. The inhibitory Smads (I-Smads) play a pivitol role in this regard. Initial evidence indicated that they could act as competitor inhibitors of the receptor regulated Smads (R-Smads), by binding directly to the type I

receptors and thereby blocking access to the receptor (Izzi, L. et al., 2004) (See section 1.5.2.3). More importantly, it has been shown that ubiquitination of the TGF-β receptor family, leading to the proteasomal degradation, is a major route for turning off the signal mediated by TGF-β superfamily ligands (ten Dijke, P. et al., 2006). The I-Smads are key players in this process, whereby both Smad6 and Smad7 initiate degradation of the receptors by recruitment of E3 ubiquitin ligases (Smurf1 and Smurf2) to the activated receptors (See section 1.5.2.3) (ten Dijke, P. et al., 2004). The expression of I-Smads is quickly induced upon stimulation by members of the TGF-β family, thereby creating a negative feedback loop to regulate the duration of downstream signalling. In addition, an emerging theme in the regulation of the TGF-β signal is the action of phosphatases for terminating the activity of the receptors. It was recently reported that the TGF-β-induced Smad7 can interact with the growth arrest and DNA damage protein 34 (GADD34), which acts a regulatory subunit of the serine/threonine protein phosphatase, PP1. The Smad7- GADD34 complex was shown to recruit the PP1 catalytic subunit (PP1c) to ALK5, and thereby dephosphorylate and inactivate it (Shi, W. et al., 2004).

Recent work has revealed that the trafficking of the TGF-β receptor family is also tightly regulated (ten Dijke, P. et al., 2004). This work has been demonstrated for TGF-β receptors but similar mechanisms are inferred for the other family members. TGF-β receptors can be internalised via two distinct routes, a clathrin- and a lipid raft/caveolar-dependent pathway, each of which has a distinct outcome (ten Dijke, P. et al., 2004). Receptors that are internalised via the clathrin pathway enter early endosomes where SARA is also enriched and thus promote Smad signalling (Di Guglielmo, G. M. et al., 2003). These receptors can recycle back to the plasma membrane, where once again binding of TGF-β is initiated (ten Dijke, P. et al., 2004). Termination of receptor activity in this case is likely to be via dephosphorylation of the receptors. In contrast, internalisation of the receptor complex via caveolin-positive lipid-raft domains results in association with the Smad7/Smurf2 complex. This ultimately leads to accelerated degradation of the receptors via the ubiquitin-proteasome pathway (Di Guglielmo, G. M. et al., 2003). The mechanism underlying the segregation of the receptors between these two routes is unclear, however the internalisation pathway has dramatic implications for the specificity of the TGF-β

response, in terms of receptor availability and signal duration (ten Dijke, P. et al., 2004).

1.4.7 Regulation of Ligand-Receptor Interaction

The regulation of ligand-receptor binding is highly complex, and this is underscored by additional requirements for other cell surface proteins. Initial experiments using affinity labelled TGF-β to search for cell surface receptors isolated three complexes (Cheifetz, S. et al., 1987), which corresponded to receptors type I, II and III. Receptor types I and II have been discussed in detail (Section 1.4). The type III receptor, which has been identified as betaglycan, is now classified as a TGF-β co-receptor. Other co-receptors for different family members have been identified and the significance of these regulatory interactions will be discussed next.

1.4.7.1 Betaglycan

Betaglycan, originally identified as a type III receptor, is a highly glycosylated trans-membrane protein with a large extracellular domain and short cytoplasmic tail that lacks kinase activity (Lopez-Casillas, F. et al., 1991; Wang, X. F. et al., 1991). In addition to independently binding all three TGF-β isoforms (Cheifetz, S. et al., 1990), betaglycan acts to faciliate TGF-β binding to its type II receptor (Lopez-Casillas, F. et al., 1993; Wang, X. F. et al., 1991), leading to the formation of a ternary complex containing TGF-β, TβRII and betaglycan (Lopez-Casillas, F. et al., 1993; Moustakas, A. et al., 1993). The TGFβ2 isoform differs from TGF-βs 1 and 3, in that it binds TβRII with a much lower affinity (1000-fold weaker) than TGF-βs 1 and 3 (Cheifetz, S. et al., 1990; De Crescenzo, G. et al., 2006). However, betaglycan has been shown to enhance TGF-β2 binding to TβRII (Lopez-Casillas, F. et al., 1993). In addition, betaglycan seems to increase TGF-β2 signalling, leaving unaffected the TGF-β1 response in myoblasts (Letamendia, A. et al., 1998b; Lopez-Casillas, F. et al., 1993). Moreover, betaglycan null cells exhibited significantly reduced sensitivity to TGF-β2 in terms of Smad2 nuclear accumulation and transcriptional responses, effects not

observed with other isoforms (Stenvers, K. L. et al., 2003). In light of these findings, a model has been proposed in which betaglycan acts to present TGF-β to its type II receptors, ultimately leading to an increase in signalling (Lopez-Casillas, F. et al., 1993). The physiological relevance of betaglycan in TGF-β2 mediated signalling was elegantly demonstrated in the chick heart. TGF-β2 is essential for endocardial epithelial-to-mesenchymal transition (EMT) during development of the heart valves (Camenisch, T. D. et al., 2002)(Section 1.6.3.2). Incubation of chick heart explant with neutralising antibodies against betaglycan, which blocked its ability to bind TGF-β2, disrupted TGF-β2-induced endocardial EMT (Brown, C. B. et al., 1999). In conclusion, these studies establish betaglycan as a high affinity receptor for TGF-β, especially for TGF-β2, and indicate a requirement for betaglycan in mediating some of TGF-β responses.

Additional roles for betaglycan in modulation of TGF-β signalling have recently been proposed (Gray, P. C. et al., 2002). It was also demonstrated that betaglycan can act as a co-receptor for inhibin, increasing the affinity of inhibin for type II receptors, primarily the activin type II receptors, ActRII and ActRIIB, and the BMP type II receptor BMPRII (Lewis, K. A. et al., 2000; Wiater, E. et al., 2003). Inhibin binding to betaglycan promotes interactions wtih the type II receptors, thereby sequestering them, which leads to a competitive blockade in BMP and Activin signalling (Lewis, K. A. et al., 2000; Wiater, E. et al., 2003). Betaglycan appears to behave similarly with respect to both TGF-β and inhibin, enhancing binding of these ligands to type II receptors. However, whereas betaglycan acts to increase TGF-β signalling, it appears to enhance the ability of inhibin to antagonise Activin and BMP signalling. Hence, betaglycan provides a regulatory network that has the capacity to modify diverse TGF-β signalling pathways.

1.4.7.2 Endoglin

Endoglin is a 180-kDa homodimeric transmembrane glycoprotein that is predominantly expressed in vascular endothelial cells (Gougos, A. et al., 1988). Other sites of expression include syncytiotrophoblasts of full-term placenta, stromal cell and certain haemopoietic cells (Gougos, A. et al., 1992; Lastres, P. et al., 1992). The first

indication that endoglin was involved in TGF-β signalling was revealed upon the molecular cloning of betaglycan (Gougos, A. et al., 1990). The high sequence similarity between these two proteins, in particular in the cytoplasmic tail where these two proteins are 71% identical, indicated they could have similar functions (Cheifetz, S. et al., 1992). Subsequently, endoglin was found to act as an accessory receptor for TGF-β (Cheifetz, S. et al., 1992). In sharp contrast to betaglycan, endoglin only binds ligand while in association with the TGF-β type II receptor (TβRII) and can bind TGF-β1 and TGF-β3 efficiently but not TGF-β2 (Barbara, N. P. et al., 1999; Letamendia, A. et al., 1998a). In addition, endoglin has been shown to bind other members of the TGF-β superfamily, including activin and BMPs, and in that case interacts with activin type II receptors (Barbara, N. P. et al., 1999). However, the physiological role of endoglin in signalling by activin and BMP is unclear. Futhermore, endoglin can bind to type I and II receptors even in the absence of ligand (Guerrero-Esteo, M. et al., 2002; Lux, A. et al., 1999). Multiple sites of interaction in both the extracellular and intracellular domains of endoglin interact with ALK5 and TβRII (Guerrero-Esteo, M. et al., 2002).

Endoglin has been shown to modulate TGF-β signalling (Goumans, M. J. et al., 2003a). Ectopic expression of endoglin has been shown to inhibit TGF-β induced growth inhibition and PAI-1 expression (Letamendia, A. et al., 1998b). Depletion of endoglin by use of antisense oligonucleotides enhances the ability of TGF-β to suppress growth and migration in endothelial cells (Li, C. et al., 2000). These data suggest a role for endoglin in negatively regulating TGF-β signalling. In a recent study, light was shed on the molecular mechanism by which endoglin inhibits TGF-β responses (Lebrin, F. et al., 2004). This study presents data to suggest that endoglin acts predominantly to promote ALK1 signalling in response to TGF-β, which in turn antagonises the canonical ALK5 signalling. In addition, endoglin is upregulated in response to ALK1, suggesting the existence of a positive feedback loop (Ota, T. et al., 2002). Furthermore, mutations of the Endoglin and ALK1 genes are linked to the vascular disorder hereditary hemorrhagic telangiectasia (HHT), which firmly places these two proteins in a common pathway (Johnson, D. W. et al., 1996; McAllister, K. A. et al., 1994). The highly similar TGF-β1, TβRII, ALK1, ALK5 , Smad5 and Endoglin knockout phenotypes provide additional evidence for a role of Endoglin in

modulating TGF-β signalling and indicate that these different components of the TGF-β pathway work together during blood formation *in vivo* (Goumans, M. J. et al., 2000).

Furthermore, another study has suggested that a sequential mechanism of serine and threonine phosphorylation by TβRII and ALK1, respectively, is involved in the regulation of endoglin activity (Koleva, R. I. et al., 2006). Taken together, this evidence suggests that the expression, activity and the protein-protein interactions of endoglin are under tight regulation, which suggest important physiological roles for endoglin in TGF-β signalling. The contribution of endoglin to the process of angiogenesis will be discussed in more detail in latter sections (Section 1.6.2).

1.4.7.3 BAMBI

BAMBI (BMP and Activin membrane-bound inhibitor) is the *Xenopus* and *Zebrafish* orthologue of the mammalian gene NMA, which was first identified from differential mRNA screen in melanoma cell lines (Degen, W. G. et al., 1996). BAMBI/NMA is structurally related to type I serine/threonine kinase receptors in the extracellular domain, but it lacks the intracellular serine/threonine kinase domain (Onichtchouk, D. et al., 1999). Functional and biochemical evidence suggest that these proteins act as pseudoreceptors and antagonize the effects of TGF-β, Activin, and BMPs. BAMBI interacts with all of the type I receptors except for ALK2, as well as TβRII and ActRII, thus preventing the formation of active receptor complexes (Onichtchouk, D. et al., 1999; Tsang, M. et al., 2000). Expression of BAMBI appears to be regulated by both BMP and TGF-β signalling, indicating mechanisms for negative feedback (Onichtchouk, D. et al., 1999; Sekiya, T. et al., 2004b). Also, a recent study demonstrated an elevated level of BAMBI in colorectal and hepatocellular carcinomas and which may act to interfere with the growth inhibitory response to TGF-β (Sekiya, T. et al., 2004a). This suggests that the use of this decoy receptor may be employed by tumours to actively inhibit signalling by TGF-β family members.

1.4.7.4 EGC-CFC family

The membrane-bound EGF-CFC family are defined by four founding members: mammalian Cripto and Criptic (Dono, R. et al., 1993), zebrafish one-eyed pinhead (Oep) (Zhang, J. et al., 1998) and *Xenopus* FRL1 (FGF-Related Ligand) (Kinoshita, K. et al., 1995). To date, there are three known family members in Xenopus, FRL1 (now called XCR1) and XCR2 and XCR3. All family members contain an N-terminal signal peptide, a modified EGF-like region, a conserved cysteine-rich domain named CFC (Cripto, FRL-1, Criptic) motif and a short hydrophobic C-terminus bearing a glycosylphosphatidylinositol (GPI)-anchor signal (Minchiotti, G. et al., 2000). Genetic studies in zebrafish and mouse have defined an essential role for the EGF-CFC family in Nodal signalling. Mutations in oep result in cyclopia, impaired gastrulation, loss of anterioposterior positioning and defects in left–right asymmetry, processes in which Nodal signalling has been implicated (Gritsman, K. et al., 1999; Zhang, J. et al., 1998). In mouse, *cripto*, like *nodal*, is necessary for establishing the anterioposterior axis (Whitman, M., 2001) and targeted disruption of *cryptic* results in defects in left-right asymmetry (Yan, Y. T. et al., 1999). More recent biochemical studies in *Xenopus* have revealed that members of the EGF-CFC are required for Nodal-related ligands to signal during early *Xenopus* development. This is demonstrated by the inhibition of nodal-dependent developmental processes, gastrulation and mesendoderm formation, upon knockdown of XCR1 and XCR3 (Dorey, K. et al., 2006).

Biochemical data indicates a direct interaction between mouse Critpo and ALK4 in Xenopus oocytes and this interaction is necessary for Nodal to bind to the ALK4/ActRIIB receptor complex (Bianco, C. et al., 2002; Yeo, C. et al., 2001). In addition to functioning as a co receptor to Nodal, Cripto and other members of the EGF-CFC family mediate the binding of Activin, Xenopus Vg1 and GDF1 to Activin receptors (Cheng, S. K. et al., 2003). These results establish that multiple TGF-β signals converge on Activin receptor/EGF-CFC complexes and suggest a widespread requirement for Cripto in TGF-β signalling. Furthermore, Cripto is overexpressed in several cancers and its overexpression is associated with the development of mammary tumours in mice (Strizzi, L. et al., 2005).

Table 1.2 Requirements of Co-receptors in TGF-β signalling

Ligand	Type I Receptor	Type II Receptor	Co-receptor Required
TGF-β2	ALK5	TβRII	Betaglycan
TGF-β1, 3	ALK1	TβRII	Endoglin
Nodal, VgI, GDF1,Activin	ALK4/7	ActRII/B	Cripto

The TGF-β signalling pathways are subjected to delicate regulation at multiple levels. This is exemplified by the extracellular regulation of a subset of ligands, which require the co-expresssion of additional partners for signal propagation. Table 1.2 summarises these ligands and their absolute requirement of a co-receptor for efficient signal transduction. The biological relevance of two of these receptors, Betaglycan and Endoglin, will be discussed in more detail in the following sections (1.6.2 and 1.6.3.2).

1.4.7.5 FKBP12

In addition to the co-receptors involved in TGF-β signalling, other intracellular proteins also act to regulate downstream signalling events. The immunophilin, FKBP12, which is known to play a crucial role in mediating the effects of the immunosuppressant drugs FK506 and rapamycin (Schreiber, S. L., 1991), also functions in TGF-β signal regulation. FKBP12 has been shown to interact strongly with the cytoplasmic regions of several different type I receptors (Okadome, T. et al., 1996; Wang, T. et al., 1994). In addition, FKBP12 binding has been shown to inhibit TGF-β receptor-mediated signalling (Chen, Y. G. et al., 1997; Stockwell, B. R. et al., 1998; Wang, T. et al., 1996), and it has been proposed that FKBP12 serves to eliminate spurious signalling caused by receptor oligomerisation in the absence of ligand by occluding the type II receptor phosphorylation sites in the GS region (Chen, Y. G. et al., 1997). The structure of FKBP12 with a cytoplasmic fragment of TβRI supports these arguments. The 3-D structure reveals that FKBP12 binds to the GS region of the receptor, so that it is positioned to impede the approach of a TβRII kinase domain (Huse, M. et al., 1999). Further molecular investigation using a homogenously tetra-phosphorylated GS form of TβRI, revealed that FKBP12 stabilises the inactive

conformation of the TβRI and also organises the flexible GS loop into an inhibitory wedge generating a 'locked' conformation. Phosphorylation of the GS domain eliminates a binding site FKBP12 and simultaneously creates a binding site for the Smad substrate (Huse, M. et al., 2001) (Figure 1.6). FKBP12 null mice exhibit no apparent defects in TGF-β signalling (Shou, W. et al., 1998), however, numerous studies have shown that FKBP12 dissociation, while not sufficient, is required for TβRI activation (Chen, Y. G. et al., 1997; Stockwell, B. R. et al., 1998; Wang, T. et al., 1996). In light of this, FKBP12 appears to act as a buffer, rather than an antagonist of the TGF-β system, stabilising and prolonging the lifetime of downregulated TβRI.

1.4.8 Evolution of TGF-β receptors: A comparison with Receptor Tyrosine Kinases

Many of the cell surface receptors that bind to and are activated by polypeptide ligands possess intrinsic protein kinase activity in their cytoplasmic domains. The largest family of this type is the receptor tyrosine kinases (RTKs), single pass transmembrane receptors whose cytoplasmic residues catalyze phosphorylation of tyrosine residues in the receptors themselves and in downstream signalling proteins (Schlessinger, J., 2000). In contrast, the TGF-β receptor family mediate phosphoryl transfer on serine and threonine (Ser/Thr) residues. Sequence comparisions have shown that while the catalytic domains of the TGF-β receptor kinases contain sequence motifs that are characteristic of Ser/Thr kinases, this family clusters close to the tyrosine kinases in terms of overall sequence similarity (Hanks, S. K. et al., 1995). This raises the possibility that the TGF-β receptor family represents a link in the evolution of tyrosine kinases. Indeed, sequence similarities as well as conserved mechanisms between the two families support this theory. Interestingly, the protein kinase of known structure most closely related to ALK5 in terms of overall sequence identity is the tyrosine kinase IRK, which shares 30% identity with ALK5, over ~250 aligned residues (Huse, M. et al., 1999). The sequence identity between ALK5 and Ser/Thr kinases is lower (e.g., ~22% versus PKA, ERK2, and Cdk2). Also, structural analysis reveals that the location of the catalytic segment of TGF-β receptor and, by implication, the bound

nucleotide, resembles that seen in tyrosine kinases rather than serine/threonine kinases. Also, the active site configuration of ALK5 appears to be consistent with binding both tyrosine as well as the smaller serine and threonine side chains, as suggested by previous biochemical analyses for the related type II receptor (Lawler, S. et al., 1997). These similarities between TGF-β family receptors and tyrosine kinases, suggest that an ancestor of the former may represent a branch point in the evolution of tyrosine kinases from cytoplasmic serine/threonine kinases (Manning, G. et al., 2002).

Naturally, stark differences also exist between the two families of transmembance kinases. Many receptor tyrosine kinases are activated by phosphorylation of the activation loop or segment, a central structural element within the kinase domain (Johnson, L. N. et al., 1996). The mechanism of activation by multiple phosphorylations upstream of the catalytic domain, in the GS region of the type I receptor, is unique to the TGF-β receptor family. The downstream signalling events also vary in that the signalling events of the tyrosine kinase receptors are largely dictated by cytoplasmic sequences outside kinase domains, including Src Homology (SH) domains, which are not present in the TGF-β receptors. In contrast, the type I receptors specify their signalling largely through a nine amino acid sequence, the L45 loop, located within the kinase domain, as previously mentioned.

1.5 The Smads

1.5.1 Discovery of the Smads as downstream mediators of the TGF-β pathway

While work was underway to uncover mechanisms governing TGF-β receptor regulation, the downstream mediators of the signal transduction pathway were as yet unknown. In 1995, a genetic approach was used to identify genes involved in *dpp* signalling in *Drosophila melanogaster*. The screen was designed to identify dominant mutations which could enhance a weak dpp mutant phenotype (Raftery, L. A. et al., 1995). These efforts resulted in the genetic identification of mutations in *Mothers against dpp* (Mad) and *Medea*. Mutations in both genes resulted in embryonic

lethality, and implicated these gene products as integral components of the dpp signalling pathway (Sekelsky, J. J. et al., 1995). Furthermore, homozygous Mad mutant flies exhibited phenotypes reminiscent of dpp mutants. Three Mad homologues were identified in C. elegans and called sma-2,-3, and -4 because their mutant phenotype results in reduced body size (Savage, C. et al., 1996). These mutants are phenotypically similiar to daf-4 mutants in *C.elegans*, where daf-4 encodes a serine/threonine kinase receptor (Savage, C. et al., 1996). Following the identification of these proteins in Drosophila and C. elegans, several vertebrate homologues were cloned in *Xenopus*, mouse and humans and all were shown to function as principal effectors downstream of the TGF-β family of serine/threonine kinase receptors (Eppert, K. et al., 1996; Graff, J. M. et al., 1996; Hoodless, P. A. et al., 1996; Liu, F. et al., 1996). A simplified nomenclature has been adopted for the vertebrate genes and their products to avoid confusion, by referring to them as Smad, a merge of the sma- and Mad gene names (Derynck, R. et al., 1996). The human genome encodes eight Smad family members (Mad-homologues (*MADH*)), and related proteins are now known in the rat, mouse, *Xenopus*, zebrafish, the helminth *Schistosoma mansoni*, *Drosophila* and *C. elegans* (Manning, G. et al., 2002)(Figure 1.7).

1.5.2 Smad Subfamilies

Smads are now well documented as integral components in the TGF-β superfamily signalling pathways. Based on structure and function, the Smads are classified into three subfamilies, as illustrated in the phylogenetic tree (Figure 1.7). The receptor-regulated Smads (R-Smads) are the direct substrates of the type I receptors, whereas the second group, common-partner Smads (Co-Smads), function by forming complexes with the R-Smads which then accumulate in the nucleus. The third group, the inhibitory Smads (I-Smads), function to antagonise the signalling mediated by the R-Smads and Co-Smads. Each group will be discussed below.

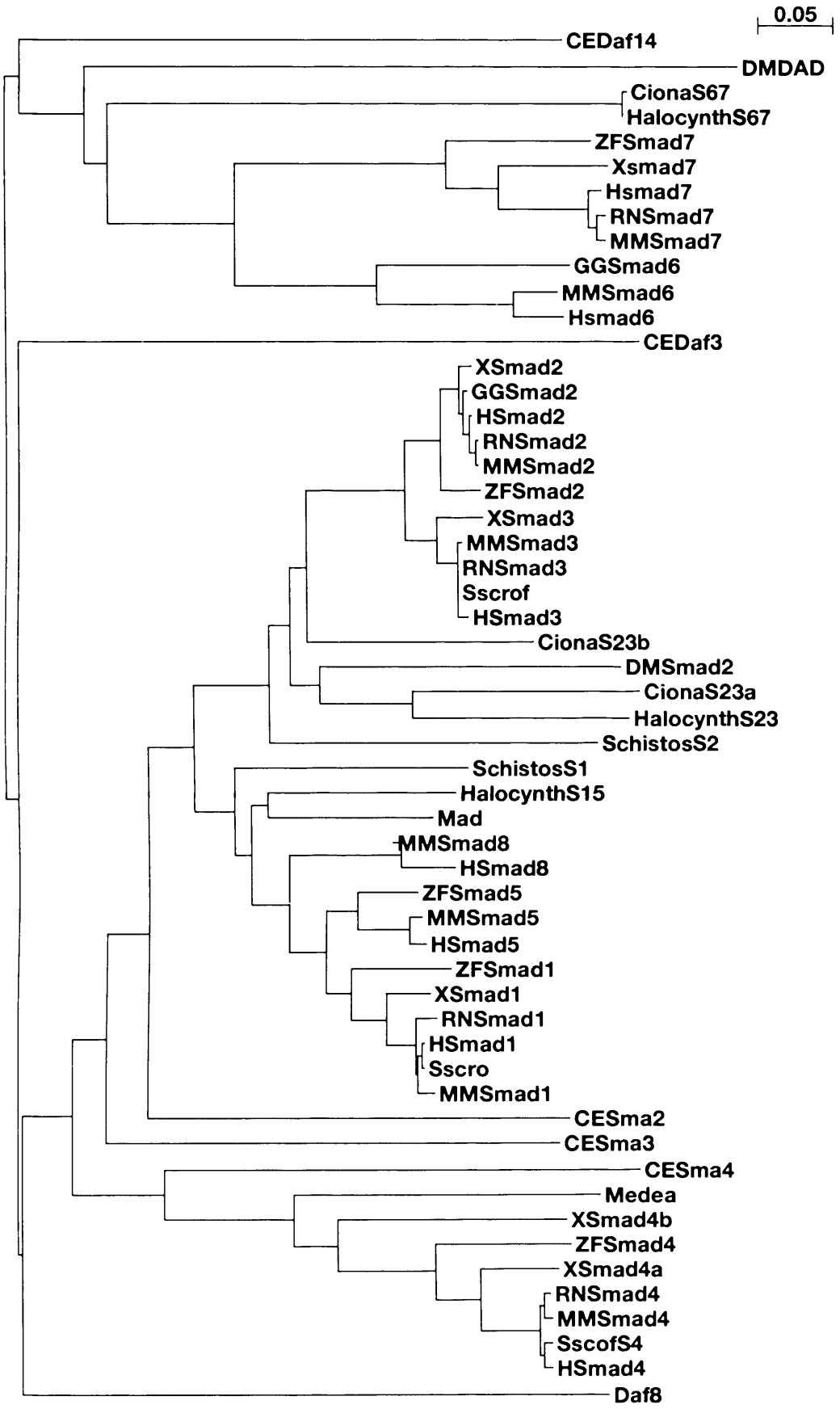

Figure 1.7 Phylogenetic analysis of the Smad family

This tree shows the relationship of Smads from the following species; Ciona intestinalis (Ciona);Drosophila Melanogaster (DM); Halocynthia (H); Homosapiens (H); Mus musculus (MM); Rattus norvegicus (RN); Schistosoma mansoni (Schisto); Sus scrofa (Sscrof);Xenopus laevis (X); Zebrafish (ZB).

1.5.2.1 R-Smads

To date, the R-Smads are the only known substrates for type I receptor kinases known to have a signalling function. These include the vertebrate Smad1, Smad2, Smad3, Smad5 and Smad8 and their invertebrate homologues, *Drosophila Mad* and *dSmad2* and *C.elegans Sma-2, Sma-3, daf8 and daf14* (ten Dijke, P. et al., 2006). An indication that R-Smads could mimic TGF-β superfamily signals came from overexpression studies in *Xenopus*. Indeed, expression of either of Smad2, mimics the dorsal mesoderm induction and axis formation by Activin (Baker, J. C. et al., 1996; Graff, J. M. et al., 1996), whereas Smad1 or Smad5 overexpression mimic the ability of BMP4 to ventralise mesoderm (Graff, J. M. et al., 1996; Suzuki, A. et al., 1997). These observations not only firmly placed the Smads as downstream components of pathway, but also suggested that different Smads might transduce distinct TGF-β superfamily signals. Concomitant observations that BMP4 stimulates Smad1 phosphorylation and nuclear accumulation (Hoodless, P. A. et al., 1996; Liu, F. et al., 1996), whereas activin or TGF-β induces Smad2 activation (Baker, J. C. et al., 1996; Eppert, K. et al., 1996; Graff, J. M. et al., 1996) confirmed that these Smads participate in distinct TGF-β superfamily signalling pathways. This evidence has led to a model whereby TGF-β superfamily ligands signal via two distinct Smad pathways; the TGF-β/Activin R-Smads, or the BMP R-Smads (ten Dijke, P. et al., 2006). In vertebrates, BMP signalling is mediated by Smad1, and its close homologues Smad5 and Smad8, whereas in *Drosophila* the sole BMP-specific Smad is *Mad*. In addition, *C.elegans Sma-2* and *Sma-3* have been demonstrated to function downstream of BMP-like signals. In contrast, Smad2 and Smad3 propagate signals from TGF-β and Activin-like ligands as they act as specific substrates for the receptor kinases of these ligands (ten Dijke, P. et al., 2006). The molecular mechanisms underlying this specificity are explained in Section 1.5.4.2. For the most part this model holds true, however this proposed view of two distinct and segregated pathways appears to be oversimplified and increasing evidence suggests that a certain degree of overlap exists (Goumans, M. J. et al., 2003b; Goumans, M. J. et al., 2002). This will be discussed in much more detail in Section 1.6.2 and Chapter 6.

1.5.2.2 Co-Smads

Smad4, which was originally isolated as the product of the tumour suppressor gene DPC4 (Hahn, S. A. et al., 1996), serves as the co-Smad in mammals. Additional co-Smads include *Xenopus* XSmad4α and XSmad4β (Howell, M. et al., 1999), *Drosophila* Medea and *C.elegans Sma-4* and daf-3(ten Dijke, P. et al., 2006). Unlike the R-Smads, the Co-Smads are not phosphorylated in response to TGF-β family members, but engage in signalling by forming complexes with R-Smads which then accumulate in the nucleus to activate transcription. Co-Smads are shared among multiple signalling pathways, whereby BMP stimulation leads to complex formation of Smad4 with Smad1, 5 and/or 8, and TGF-β/Activin signalling recruits Co-Smads to partner Smad2 or Smad3 (Whitman, M., 1998). The importance of Co-Smads in TGF-β family signalling is highlighted by the fact that human Smad4 is mutated or deleted in about 50% of pancreatic and in about 15% of colorectal cancers, which results in the loss of growth inhibitory responses to TGF-β (Levy, L. et al., 2006). Still, the absolute requirement for Smad4 in TGF-β family signalling pathway is under much debate (Deckers, M. et al., 2006; Levy, L. et al., 2005). Indeed, cells with little or no Smad4 can still respond to TGF-β family ligands and mediate downstream responses (Levy, L. et al., 2005) (See Chapter 6).

1.5.2.3 I-Smads

Vertebrate Smad6 and Smad7 and *Drosophila* Dad represent members of the I-Smad subfamily, whose function to inhibit TGF-β family signalling (Feng, X. H. et al., 2005). The I-Smads lack the C-terminal phosphorylation motif and have a highly divergent MH1 domain (Whitman, M., 1998). Whereas Smad7 acts as an inhibitor of TGF-β family signalling, Smad6 preferentially blocks BMP signalling (Hata, A. et al., 1998). Ectopic expression of dad, the Drosophilal-Smad in the Drosphila wing disc inhibits signalling by Dpp and can also block BMP signalling when expressed in Xenopus embryos.Whether Dad is a selective inhibitor of BMP signalling or might also inhibit activin/TGF-β has not been examined (Whitman, M., 1998).

Several mechanisms have been proposed for the action by which the I-Smads elicit their antagonistic effects. Firstly, it has been demonstrated that the I-Smads interact stably with the type I receptor, suggesting that they act as competitive inhibitors of receptor-mediated activation of R-Smads (Nakao, A. et al., 1997). In addition, Smad6 has been shown to compete with Smad4 for complex formation with the phosphorylated Smad1, thus sequestering Smad1 in inactive complexes which inhibits BMP signalling (Hata, A. et al., 1998). Another mechanism by which I-Smads inhibit Smad signalling is via receptor degradation. Smad7 constitutively interacts with with E3 ubiquitin ligases, Smurf1 and Smurf2 (Ebisawa, T. et al., 2001). Upon recruitment of the Smad7/Smurf complex to the activated receptor, Smurf1 or Smurf2 induces receptor degradation via proteosomal and lysosomal pathways. In the basal state, I-Smads reside in the nucleus, and upon ligand stimulation, they translocate to the plasma membrane, whereupon they mediate inhibition. Since Smad7 does not contain a known nuclear export signal (NES), it has been proposed that it interacts with Smurf1/2 in the nucleus (Suzuki, C. et al., 2002; Tajima, Y. et al., 2003). Using their N-terminal C2 domain, Smurf1 and Smuf2 target the Smurf-Smad7 complex to the plasma membrane, where they target the receptors for degradation (Tajima, Y. et al., 2003). Finally, I-Smad expression is potently induced by TGF-β family members and thus these proteins participate in a negative feedback loop to control the intensity and duration of TGF-β signalling (Nakao, A. et al., 1997). It is important to note that much of the data on both the function and mechanism of I-Smads have come from overexpression studies, due to the poor availability of antibodies. Thus, studies on endogenous proteins will yield insight into the regulatory mechanisms governing the I-Smads and determine the extent of specificity of inhibition of different TGF-β family members.

1.5.3 Structure of the Smads

The primary sequence of all Smads revealed extensive sequence homology among Smads in two distinct regions: an amino-terminal domain designated Mad homology 1 (MH1) and a carboxy-terminal domain termed MH2 domain. The region between the MH1 and MH2 domains is referred to as the linker region and is less well conserved

among Smads. The MH1 domain of Smad4 and most R-Smads (except the full length form of Smad2) is responsible for sequence specific DNA binding. The structure of the MH1 domain, as exemplified by Smad3, adopts a globular fold, with two small β-sheets and one protruding β-hairpin that mediates the DNA binding through direct contact with residues of Smad binding element (SBE) (Shi, Y. et al., 1997) (See section 1.5.6.1). This β-hairpin is located next to a positively charged H2 helix, which contains a nuclear localisation sequence. The MH1 domain has also been reported to inhibit the activity of the MH2 domain (Baker, J. C. et al., 1996; Hata, A. et al., 1997; Liu, F. et al., 1996), however upon receptor mediated phosphorylation of the C-terminal serine residues, this inhibitory effect is relieved (Kretzschmar, M. et al., 1997; Macias-Silva, M. et al., 1996). The amino-terminus of the I-Smads is highly divergent from the MH1 domain, as exhibited by their inability to bind DNA.

In contrast the MH2 domain is highly conserved among all Smads. It has been termed the 'effector' domain as it mediates multiple interactions required for the function of the Smads, including binding with transcription factors, coactivators and corepressors (Massague, J. et al., 2005). The MH2 domain is also responsible for interactions with the receptor, SARA, formation of homomeric as well as heteromeric Smad complexes, and directly contacting the nuclear pore complex for nucleocytoplasmic shuttling (Lo, R. S. et al., 1998; Randall, R. A. et al., 2002; Tsukazaki, T. et al., 1998; Xu, L. et al., 2003; Xu, L. et al., 2002). The MH2 domain of the R-Smads, but not the Co-Smads nor I-Smads, contain a characteristic SSXS motif at their extreme C-termini(Hoodless, P. A. et al., 1996; Macias-Silva, M. et al., 1996). The two C-terminal serine residues in the motif are phosphorylated by the type I receptor during signalling. Interestingly, the linker region contains multiple phosphorylation sites, which have been shown be phosphorylated by MAPK, calcium-dependent kinases and cyclin dependent kinases (Kretzschmar, M. et al., 1997; Kretzschmar, M. et al., 1999; Matsuura, I. et al., 2004) (See Sections 1.5.7. and 1.6.1.4) Thus, the linker region allows specific crosstalk with a spectrum of other signalling pathways. In addition, the linker region contains a PY motif, which mediates specific interaction with the Smad ubiquitination regulatory factors (Smurfs). Smurf1 and Smurf2 are HECT-domain-containing E3 ubiquitin ligases that target the Smads as well as the TGF-β receptors for degradation by the proteasome.

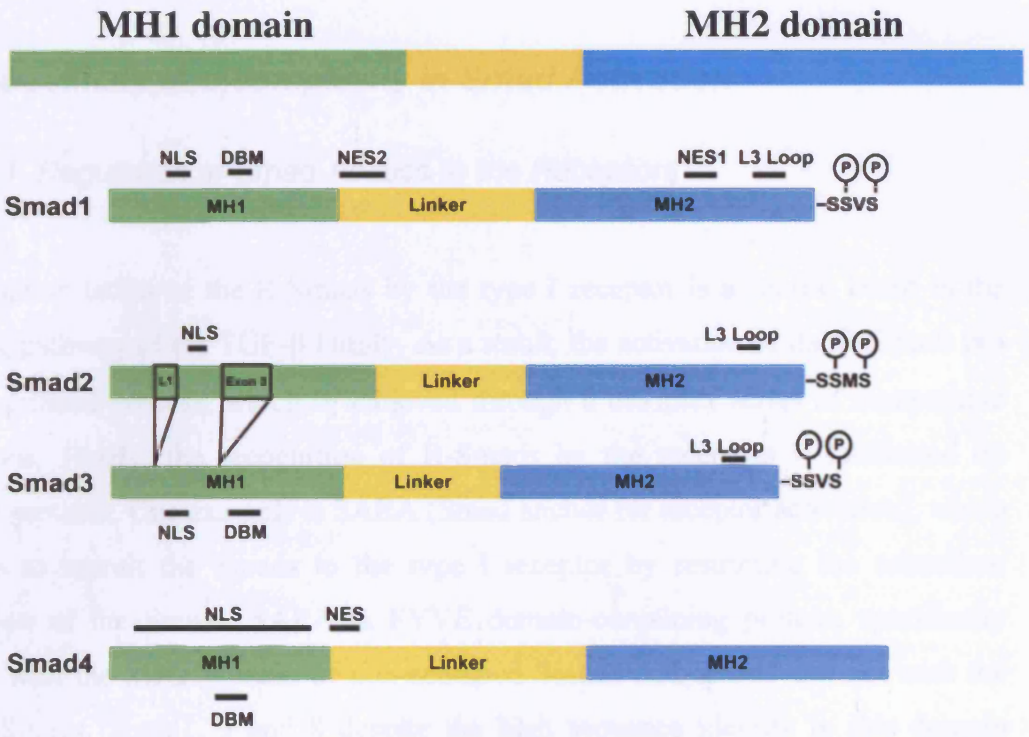

Figure 1.8. Structure of the Smads

Diagrammatic representation of the structure of the Smads, indicating Mad Homology Domains (MH1 and MH2), structural motifs and C-terminal phosphorylation sites. DNA binding domain (DBM), Nuclear Export Signal (NES), Nuclear Localisation signal (NLS).

1.5.4 Specificity and complexity in Smad Activation

1.5.4.1 Regulation of Smad Access to the Receptors

The phosphorylation of the R-Smads by the type I receptor is a central event in the signalling pathway of the TGF-β family. As a result, the activation of the R-Smads is a highly regulated process, which is achieved through a complex series of competitive interactions. Firstly, the recognition of R-Smads by the receptors is facilitated by auxiliary proteins. One example is SARA (Smad anchor for receptor activation), which functions to recruit the Smads to the type I receptor by restricting the subcelluar localisation of the Smads. SARA, a FYVE domain-containing protein, specifically interacts with the MH2 domain of non-activated Smad2 and Smad3 but not with the BMP R-Smads, Smad1, 5 and 8 despite the high sequence identity in this domain (Tsukazaki, T. et al., 1998). By interacting with both Smad2/Smad3 and the receptor complex, SARA forms a bridge, which assists in the specific phosphorylation of Smad2/Smad3 by the type I receptor (Tsukazaki, T. et al., 1998). The crystal structure of the Smad2 MH2 domain in complex with the Smad-binding domain (SBD) of SARA has been elucidated. This has revealed that the SBD, which comprises a rigid coil, an α-helix and a β strand, interacts with an extended hydrophobic surface area on Smad2/Smad3 (Wu, G. et al., 2000). Interestingly the rigid coil domain of the SARA SBD is similar to a Smad interaction motif (SIM) found in transcription factor partners of the Smads, the Mixer and FoxH1 family members. Mutagenesis studies combined with molecular modelling, revealed that the rigid coil of the SARA SBD binds to the MH2 domains of Smad2 and Smad3 in the same way that Mixer and FoxH1 proteins bind to these domains through the SIM (Randall, R. A. et al., 2002). Structural analysis also reveals that SARA promotes R-Smad-kinase recognition by precisely positioning the phosphorylation site of the R-Smad in the kinase catalytic centre (Qin, B. Y. et al., 2002). Upon phosphorylation of Smad2/Smad3 by the type I receptor, SARA can no longer bind the R-Smads efficiently, which results in activated Smad being released from SARA and the type I receptor. Furthermore, the interaction of SARA with ALK5 has been proposed to trigger internalisation of the SARA-receptor complexes via

clathrin-coated pits, resulting in the formation of endosomes where Smad2 and Smad3 can be activated (Di Guglielmo, G. M. et al., 2003) (See Section 1.4.6).

A second FYVE-containing protein, Hgs (Hrs) was also found to cooperate with SARA to facilitate Smad2 signalling (Miura, S. et al., 2000). Other adaptor proteins, including disabled 2 (Dab2), 14-3-3ε, the negative regulator of Wnt signalling Axin and the ELF β-spectrin have been reported to facilitate TGF-β signalling by linking Smad2/Smad3 to the receptor complex (Moustakas, A. et al., 2001). However, the molecular mechanisms behind these observations remain unclear. More recently, another modulator of the pathway was identified as a receptor associated protein, TLP (TRAP-1-like protein) (Felici, A. et al., 2003). The data reveals that TLP binds to Smad4 upon TGF-β signalling and appears to influence the balance of activated Smad2 versus Smad3, which may be important for generating distinct TGF-β responses in different cell types.

1.5.4.2 Smad-Receptor Interactions

A crucial determinant of specificity in TGF-β superfamily signalling is the differential recruitment and subsequent activation of Smad family members by the type I receptors (Huse, M. et al., 2001; Shi, Y. et al., 2003). As previously mentioned, receptors for the TGF-β and Activin ligands recruit and activate Smad2 and Smad3, whereas those for the BMPs phosphorylate Smad1, 5 and 8 (Shi, Y. et al., 2003). On the one hand, there is a high level of structural similarity between the receptors of these ligands, and on the other hand there is high sequence homology between the corresponding R-Smads. This led to an intense interest in elucidating the basis for this specificity. As the C-terminal phosphorylation motif is almost identical for all R-Smads, it was unlikely that this sequence could determine the specificity of the activated Smad. Interestingly, removal of the C-tail actually increases the interaction between the type I receptor and R-Smad, suggesting that this region does not contribute to the Smad-receptor interaction, but may be inhibitory particularly when these sites are phosphorylated (Lo, R. S. et al., 1998). Instead, biochemical and structural studies have revealed that the specificity of the R-Smad activation arises from two discrete structural elements: the L45 loop in the kinase domain of the type I receptor, and a corresponding region in the

L3 loop of the MH2 domain of the R-Smads (Chen, Y. G. et al., 1998; Lo, R. S. et al., 1998; Wu, G. et al., 2000).

The L45 loop is a nine-amino acid sequence, which connects the β strands 4 and 5 in the kinase domain of the type I receptor, but is not part of the catalytic centre (Feng, X. H. et al., 1997; Huse, M. et al., 1999). Sequence analysis reveals that receptors with different signalling specificities have distinct L45 sequences, whereas similar signalling receptors share highly conserved L45 loops. The L45 sequences of ALK4 and ALK5, which activate Smad2 and Smad3, are identical, whereas they differ in four amino acids from the L45 sequences in ALK3 and ALK6, whose substrates consist of Smad1, 5, and 8 (Chen, Y. G. et al., 1998)(Figure 1.9). The third group of type I receptors, which include ALK1, ALK2 and *Drosophila* Saxaphone exhibits a more divergent L45 loop, which differs in seven residues from the L45 of the ALK3/ALK6 group, yet they both activate Smad1, 5 and 8 (Chen, Y. G. et al., 1999) (Figure 1.9). The replacement of all but the L45 loop in the kinase domain of ALK5 with the corresponding regions from ALK2, yielded a construct that still mediated TGF-β responses, which first signified the importance of this element in dictating specific responses (Feng, X. H. et al., 1997). Similarly, the L45 loop of ALK6 substituted with that of ALK5, caused a switch in the specificity to induce a TGF-β/Activin-like response, including phosphorylation of Smad2/3, transcription from TGF-β/Activin-responsive elements, and induction of dorsal mesoderm in *Xenopus* embryo explants (Chen, Y. G. et al., 1998). Consistent with this, ALK5 with an ALK6 L45 loop, also demonstrated a clear switch in substrate specificity, however this was incomplete with respect to induction of ventral mesoderm, which is definitive of a TGF-β/Activin response (Chen, Y. G. et al., 1998).

The L45 loop interacts directly with the L3 loop in the MH2 domain of an R-Smad (Chen, Y. G. et al., 1998; Lo, R. S. et al., 1998). As inferred from the crystal structure of the Smad4 MH2 domain, the L3 loop protrudes from the β-sandwich core structure of the MH2 domain, and that it is exposed to solvent in the trimeric Smad complexes (Shi, Y. et al., 2003). Analogous to the L45 loop, only a few amino acids in the L3 loop define receptor binding specificity. The sequence of the L3 loop is invariant among TGF-β Smads R-Smads and BMP R-Smads, but differs at two positions between these two groups (Lo, R. S. et al., 1998). Consequently, Smad1 with an L3 loop of Smad2 interacts with and is phosphorylated by ALK5, while Smad2

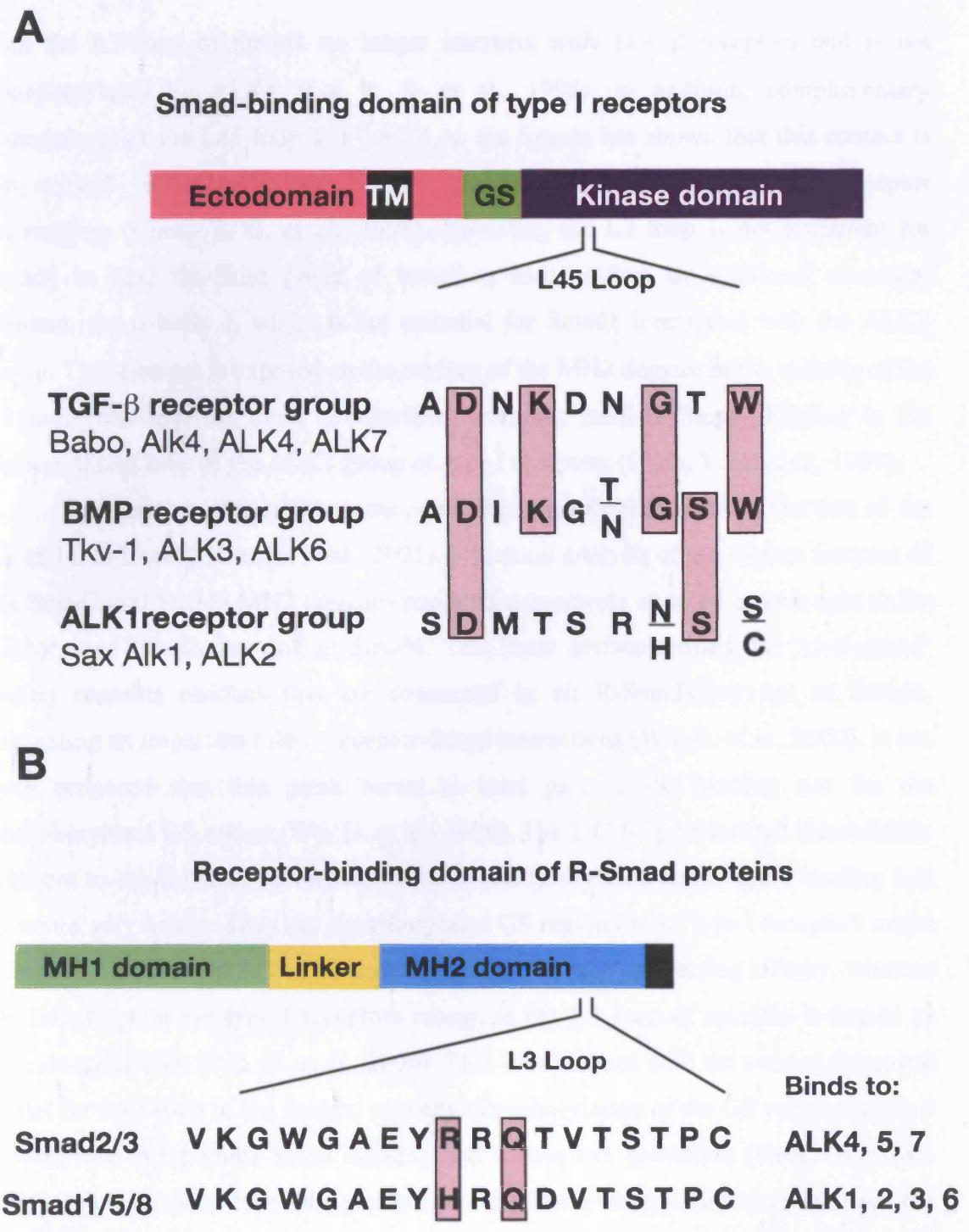

Figure 1.9 Specificity of Smad-Receptor Interactions

The specificity of the Smad-Receptor interaction is determined by the sequence of the L45 loop on the receptor kinase domain and the sequence of the L3 loop in the Smad MH2 domain.

with the L3 loop of Smad1 no longer interacts with TGF-β receptors and is not phosphorylated by ALK5 (Lo, R. S. et al., 1998). In addition, complimentary mutagenesis of the L45 loop and the L3 on the Smads has shown that this contact is the critical determinant that dictates specificity between Smads and receptor interactions (Chen, Y. G. et al., 1998). However, the L3 loop is not sufficient for Smad1 to bind the third group of receptors and requires an additional structural element, the α-helix 1, which is not essential for Smad1 interaction with the ALK3 group. This element is exposed on the surface of the MH2 domain in the vicinity of the L3 loop, and together these two surface structures mediate Smad1 binding to the divergent L45 loop of the ALK1 group of type I receptors (Chen, Y. G. et al., 1999).

Furthermore, adjacent sequences are thought to stabilise the interaction of the L3 and L45 loops (Huse, M. et al., 2001). Structural analysis of the surface features of the Smad2 and Smad4 MH2 domains revealed a positively charged groove next to the L3 loop on Smad2, but not on Smad4. This basic surface termed the 'loop-strand' pocket contains residues that are conserved in all R-Smads but not in Smad4, suggesting an important role in receptor-Smad interactions (Wu, G. et al., 2000). It has been proposed that this patch forms at least part of the binding site for the phosphorylated GS region (Wu, G. et al., 2000). The L45 loop, is located immediately adjacent to the flexible GS region, which is phosphorylated upon ligand binding and becomes very acidic. Thus the phosphorylated GS region on the type I receptors might interact with the 'loop-strand' pocket on R-Smads to provide binding affinity, whereas the L45 loop on the type I receptors recognise the L3 loop of specific R-Smads to provide specificity (Wu, G. et al., 2000). This is consistent with the current structural model for activation of the Smads, whereby phosphorylation of the GS region creates a binding site that permits Smad docking and subsequent activation (Huse, M. et al., 2001). In conclusion, these data provide evidence for a complex interface between the type I receptors and their substrates, the R-Smads, that includes the phosphorylated GS region and the L45 loop of the receptor and the basic loop-strand' pocket and L3 loop of the R-Smads and possibly other components in the kinase (ten Dijke, P. et al., 2006). The precise details of the receptor/Smad interaction, however, await structural analysis of a receptor/Smad2 interaction.

1.5.4.3 Smad Activation and Complex formation

Upon R-Smad binding to the type I receptor, the second and third serine residues of an SSXS motif, located at the extreme C-terminus of the R-Smad is phosphorylated (Shi, Y. et al., 2003) (Figure 1.7). Receptor mediated phosphorylation is proposed to relieve the MH1 and MH2 domains from a mutually inhibitory interaction (Hata, A. et al., 1997), thus allowing complex formation and nuclear accumulation. Phosphorylation of R-Smads results in their dissociation from both SARA and the type I receptor, which is likely to occur via a series of competitive interactions (ten Dijke, P. et al., 2004). As previously mentioned, the loop-strand pocket in the L3 loop region of the Smad MH2 domain is required for R-Smad interaction with the phosphorylated GS domain of the type I receptor. Interestingly, the loop-strand pocket coincides with the surface that interacts with the C-terminal phosphoserines in the homotrimer (Shi, Y. et al., 1998). Therefore, upon phosphorylation of the R-Smads, the phosphorylated serine residues at the C-terminus of an R-Smad compete with the phosphorylated GS domain for the loop-strand pocket, thus facilitating dissociation from the receptor (Wu, J. W. et al., 2001b). In addition, as the type I receptors are proposed to form heterodimers , and are likely to bind two Smad molecules simultaneously, the phosphorylated R-Smad molecules might assist each other in their release from the receptor (Qin, B. Y. et al., 2001; Wu, J. W. et al., 2001b).

Upon dissociation from the receptor, Smad proteins form complexes with other Smads. The stoichiometry (and composition) of these complexes has been a subject of much debate. Studies of Smad complexes in solution have revealed that in the uninduced state Smad2 exists as a monomer (Jayaraman, L. et al., 2000; Kawabata, M. et al., 1998; Wu, J. W. et al., 2001a; Wu, J. W. et al., 2001b), whereas similar biochemical analysis indicates that Smad3 can exist in multiple oligomeric states (Jayaraman, L. et al., 2000). Similarly Smad4 can exist as monomers, dimers or trimers (Jayaraman, L. et al., 2000; Kawabata, M. et al., 1998; Shi, Y. et al., 1997). Following ligand stimulation size exclusion chromatography analysis of endogenous Smad2/Smad4 from TGF-β-induced cells or biochemical analysis of purified Smad2 and Smad4 suggested that these complexes were heterodimers (Jayaraman, L. et al., 2000; Kawabata, M. et al., 1998; Shi, Y. et al., 1997). However, studies of purified phosphorylated Smad2 and Smad3 have demonstrated that activated Smad2 and

Smad3 preferentially form heterotrimers (Wu, J. W. et al., 2001b). Recently, the crystal structure of the complexes consisting of the MH2 domains of phosphorylated-Smad2-Smad4 and phosphorylated Smad3-Smad4 revealed that both complexes are heterotimers, comprising two phosphorylated R-Smad subunits and one Smad4 (Chacko, B. M. et al., 2004). X-ray crystallography analysis of trimeric Smad complexes has revealed that these trimers are stabilised by interactions within an extensive protein-protein interface between MH2 domains as well as the binding of the pS-X-pS motif into the the loop-strand pocket in the L3 loop region of the Smad MH2 domain (Wu, J. W. et al., 2001b). From a structural standpoint, it is feasible that the heterotrimeric Smad complex could include two different R-Smad molecules, as the trimer interface among the R-Smads is highly conserved. Such combinatorial mechanism could greatly increase the number of distinct signalling species, each with a different Smad constitution. Indeed, Smad2/3 mixed oligomers have also been observed in cell on TGF-β stimulation (Chacko, B. M. et al., 2004; Wu, J. W. et al., 2001b) (see also Chapter 6).

Studies on endogenous Smads *in vivo* have suggested a more complex scenario. Analysis of nuclear extracts of cells transiently cotransfected with differentially tagged Smads suggested that the DNA-bound Smad3/Smad4 complex was a heterodimer. In this case, Smad3 and Smad4 bind as a heterodimer in association with as yet unknown cofactors to the c-jun promoter to initiate transcription (Inman, G. J. et al., 2002a). In addition, this study supported the formation of heterotrimeric complex of Smad2 and Smad4, which is recruited to DNA by the FoxH1 transciption factor (Inman, G. J. et al., 2002a). These data suggest that both heterodimers and heterotrimers may be formed depending on the target gene and the other factors present. In view of the stability of the trimeric complex, it is unclear how these heterodimeric complexes form *in vivo*. However, one possibility is that Smad cofactors, upon binding the R-Smad/Smad4 complex can disrupt the core heterotrimer in such a way that one of the R-Smad subunits is replaced by a cofactor, resulting in a Smad heterodimer. Interestingly, IRF-3, a member of the interferon regulatory factor (IRF) family of transcription factors aswell as the forkhead-associated (FHA) domain, found in many signalling proteins including the forkhead transcription factors, exhibit marked structural similarity to the MH2 domain of the Smad protein family (Qin, B. Y. et al., 2003).

1.5.5 Nucleocytoplasmic shuttling of Smad proteins

Once the Smad complexes are formed, they accumulate in the nucleus where they modulate gene transcription. This dual role of the Smads in transmitting the signal from the nucleus and the regulating transcription demands strict regulation of the subcellular localisation of the Smads. Early studies on Smad regulation established that in the basal state, R-Smads are predominantly cytoplasmic, whereas Smad4 is distributed throughout the cytoplasm and nucleus. Upon ligand stimulation, Smad complexes rapidly accumulate in the nucleus, where they appear to remain for several hours (Baker, J. C. et al., 1996; Hoodless, P. A. et al., 1996; Liu, F. et al., 1996). However, it has now become clear that the Smads are not stationary but are constantly shuttling between both compartments in the uninduced and induced state and that this activity is highly regulated (Inman, G. J. et al., 2002c). This was first observed through transport studies of Smad4. Treatment of cells with leptomycin B (LMB), a specific inhibitor of the prototypic export receptor CRM1 or exportin 1 led to a rapid accumulation of Smad4 in the nucleus (Pierreux, C. E. et al., 2000; Watanabe, M. et al., 2000). This demonstrated that Smad4 must be rapidly shuttling between both compartments in the absence of signal and that CRM1 activity is required for nuclear export (Pierreux, C. E. et al., 2000; Watanabe, M. et al., 2000). Subsequently, it has been shown that the R-Smads also engage in nucleocytoplasmic shuttling in the absence and presence of TGF-β (ten Dijke, P. et al., 2004).

The detailed molecular mechanisms governing Smad nucleocytoplasmic shuttling remain limited. Smad4 has been shown to contain a basic bipartite nuclear localisation signal (NLS) motif in its MH1 domain, which is generally conserved in R-Smads and in addition it contains a nuclear export signal (NES) in the linker region. The NLS of Smad4 binds importin-α, which can then bind to importin-β to mediate import (Xiao, Z. et al., 2003b). As previously mentioned, the NES, mediates CRM1-dependent export of Smad4. Smad1, the BMP-regulated R-Smad, also has a NLS in its MH1 domain and, like Smad4 also possesses an NES although this is located in its C-terminal domain (Xiao, Z. et al., 2003a; Xiao, Z. et al., 2001). It has been demonstrated that Smad1 also accumulates in the nucleus upon treatment with LMB, suggesting that it is also shuttling via CRM1-dependent export, however the import mechanism is not yet clear (Xiao, Z. et al., 2001). The transport mechanism for Smad2

and Smad3 is less evident, although, a nuclear localisation signal has been identified in the MH1 domain of Smad3, which is thought to bind directly to importin-β (Kurisaki, A. et al., 2001). An NLS is also present in Smad2 but in the full length protein, its function appears to be masked by a 20-amino acid insert encoded by exon3 (Kurisaki, A. et al., 2001). It has been proposed that the Smads (Smad2, 3 and 4) bind directly to components of the nuclear pore and it is through this interaction that nuclear transport is driven (Xu, L. et al., 2003; Xu, L. et al., 2002). It may be the case that shuttling of Smads between compartments is controlled by the NLS and NES motifs as well as by non-classical pathways involving interactions between the MH2 domain and the nuclear pore complex. The mechanism remains to be clarified.

Another question which arises from this work is what mediates the strong nuclear accumulation of Smad4 upon induction of TGF-β signalling? (Inman, G. J. et al., 2002c). A variety of mechanisms have been proposed to explain the switch in the balance of cytoplasmic to nuclear Smad that accounts for nuclear accumulation of Smad complexes in response to TGF-β. One such mechanism involves the existence of cytoplasmic and nuclear anchoring proteins (Xu, L. et al., 2002). SARA was suggested as a candidate for a cytoplasmic retention protein as overexpression of SARA sequestered Smad2 in clusters in the cytoplasm (Tsukazaki, T. et al., 1998; Xu, L. et al., 2000). A candidate nuclear retention factor was the Smad2 transcription partner, FoxH1. Consistent with this, expression of FoxH1 trapped Smad2 in the nucleus even in the absence of ligand (Xu, L. et al., 2002). This model was supported by the fact that both proteins interact with a common binding pocket in Smad2, and that phosphorylation dependent disruption of Smad2-SARA interaction allowed Smad2 to move into the nucleus where it could be retained by interaction with FoxH1 or related proteins (Xu, L. et al., 2002). However, a Smad2 mutant (W368) which cannot interact with several transcription factors, including FoxH1, accumulates in the nucleus in response to TGF-β as efficiently as wild type Smad2 (Schmierer, B. et al., 2005). Thus it is unlikely that transcription factor complexes play a role in nuclear retention. Nonetheless, kinetic analysis of Smad2 and Smad4 reveal that decreased nuclear mobility in the presence of TGF-β stimulation supports a role for trapping of active Smad complexes in the nucleus (Schmierer, B. et al., 2005). In addition, this study revealed that TGF-β-induced nuclear accumulation of Smad2 is a reflection of its decreased nuclear export rate, associated with this observed decrease in nuclear

mobility (Schmierer, B. et al., 2005). These data suggest that the import rate does not play an important role in nuclear accumulation of Smads, but more importantly, the decreased rate of export results in a shift in the localisation of the active Smad pool. Therefore, it has been proposed that mechanisms are in place to selectively trap active Smad complexes in the nucleus, possibly by masking binding sites for the export machinery, as has already been shown for Smad4 (Chen, H. B. et al., 2005).

Nucleocytoplasmic shuttling has been proposed to function as a mechanism whereby Smads can monitor receptor activity in response to ligand (Inman, G. J. et al., 2002c). It has been shown that continuous activity of the receptors is required to maintain active Smads in the nucleus and that artificial abrogation of receptor activity by use of the ALK5 kinase inhibitor SB-431542, caused redistribution of the Smads into the cytoplasm (Inman, G. J. et al., 2002c). In addition, the shuttling of Smads in the presence of TGF-β appears to require cycles of Smad phosphorylation and dephosphorylation (Inman, G. J. et al., 2002c; Xu, L. et al., 2002). Dephosphorylation of R-Smads results in their dissociation from Smad4 and recycling back to the cytoplasm, which allows active receptors to rephosphorylate the R-Smads (Inman, G. J. et al., 2002c). Duration of signalling is a critical determinant in TGF-β signalling (Nicolas, F. J. et al., 2003a). To this end, the Smads employ a rapid mechanism to actively 'sense' when the receptors have been turned on or off, through the process of nucleocytoplasmic shuttling (ten Dijke, P. et al., 2004).

Termination of activated Smad signalling is also a highly regulated process. As previously mentioned, the activity of the receptors is terminated by either dephosphorylation or ubiquitin-mediated degradation (Shi, Y. et al., 2003). However, elucidation of the mechanims by which the TGF-β signal is terminated at the level of the R-Smads is only just emerging. It was initially suggested that the nuclear R-Smads are ubiquitinated and subsequently degraded by the proteosome, thus terminating TGF-β superfamily signalling (Lo, R. S. et al., 1999). However, in light of the nucleoplasmic shuttling of Smads, a more favoured model for the termination of Smad signalling is the dephosphorylation of the R-Smads (ten Dijke, P. et al., 2004). Indeed, the identification of these phosphatases has proved a difficult task, perhaps due to the redundancy of catalytic subunits of these enzymes. Several studies have been reported which identify phosphatases capable of dephosphorylating BMP/dpp R-Smads have been proposed, including a small C-terminal domain phosphatase (SCP) (Knockaert,

M. et al., 2006) and pyruvate dehydrogenase phosphatase (PDP) (Chen, H. B. et al., 2006). In addition, PPM1A has been proposed as the phosphatase that regulates termination of Smad2/3 signalling through dephosphorylation (Lin, X. et al., 2006). These data suggest that specific phosphatases target the BMP R-Smads and the TGF-β R-Smads. However, future work is required to investigate the role of these phosphatases and the mechanisms that govern them.

1.5.6 The Smads as Transcriptional Regulators

1.5.6.1 DNA binding ability

The Smad proteins direct transcriptional responses through both activation and repression of genes. Smad4 and all R-Smads (except the full length Smad2) have an intrinsic, site specific DNA-binding activity. This was first demonstrated for the MH1 domain of Mad, which binds a site in a Dpp-responsive element in the gene vestigal (vg) *in vitro* (Kim, J. et al., 1997). The DNA binding specificity of the Smads has been determined through a site selection strategy as a 5'-GTCT-3', or its compliment 5'-AGAC-5' and has been termed the Smad binding element (SBE) (Yingling, J. M. et al., 1997; Zawel, L. et al., 1998). Many Smad-responsive promoter regions contain one or more SBEs, and in many cases it contains an extra base, as 5'-CAGAC-3' hence termed the CAGA motif. By crystal structure analysis of Smad3, it was revealed that a conserved 11-residue β-hairpin motif in the MH1 domain mediates DNA binding, through specific contact with three of the four bases of the SBE (Shi, Y. et al., 1998). The β-hairpin element is conserved in all Smads regardless of whether they function in the BMP, TGF-β or activin pathways Therefore, the Smad-DNA interaction is unlikely to provide selectivity in the gene targets of individual Smads (Shi, Y. et al., 1998).

Individual Smad2 and Smad3 genes are thought to result from a gene duplication in chordates of the single Smad2/3 gene found in flies and worm (Newfeld, S. J. et al., 1999) and this duplication event has resulted in a difference in the DNA binding ability of these R-Smads (Yagi, K. et al., 1999). Exon 3 of Smad2, a 30 amino acid insert, is not found in Smad3 and precludes the DNA-binding of Smad2.

However, a naturally occurring Smad2 splice variant/form of Smad2 lacking exon 3 can bind interchangeably with Smad3 to the SBE in DNA (Yagi, K. et al., 1999).

In addition to the SBE, Smads have also been reported to bind to G/C rich sequences. Mad (*Drosophila* Smad1) was shown to interact with a 5 -GCCGNCGC motif in the promoters of *Vestigal* (Kim, J. et al., 1997) and *Tinman* (Xu, X. et al., 1998). Similar Smad1consensus sequences have also been found in *Drosophila Ultrabithorax* (Ubx) (Szuts, D. et al., 1998), Smad6 (Ishida, W. et al., 2000) and Smad7 (Benchabane, H. et al., 2003). In addition, the Bcl-2 promoter region contains three overlapping copies of a GC-rich repeat, which is identical to the Drosophila Mad binding element, GCCGnCGc, and has been shown to bind Smad3 *in vivo* (Yang, Y. A. et al., 2006). This suggests that both TGF-β and BMP R-Smads can bind GC-rich elements although it is possible that Smad3 may be bound to the Bcl-2 promoter by association with Smad1 (See Chapter 7). Furthermore, a second DNA binding consensus site has been proposed for Smad1/4 complexes which recruit the transcription factor Schnurri (Yao, L. C. et al., 2006). This site includes a Mad/Smad1 binding GC-rich motif and a canonical Smad4 SBE motif, which is separated by 5 bp and is found in many BMP responsive genes such as the *Id1*, *Vent2* and *Drosophila brinker*, *bag of marbles* (*bam*) and *gooseberry* (*gsb*) (see below) (Yao, L. C. et al., 2006). These data suggest that Smad1 and *Drosophila* Mad preferentially bind to GC rich sequences however, it cannot be ruled that Smad1 can also bind an SBE. Cooperation of SBE and GC rich motifs is also required for binding of Smad3-Smad4 complexes to promoter elements, such as the *Id1* promoter (Kang, Y. et al., 2003; Korchynskyi, O. et al., 2002). The *Id1* promoter contains both BMP and TGF-β responsive elements, where binding of Smad3-Smad4 complexes to the Id1 promoter results in transcriptional repression and the binding of Smad1/4 complexes results in the transcriptional activation promoter (Kang, Y. et al., 2003; Korchynskyi, O. et al., 2002). However, it is not clear in the case of Smad3-Smad4 complexes, which Smad binds the individual motifs and whether the spacing of these sites are critical for binding of the cooperating transcription factor, ATF3 (Kang, Y. et al., 2003). As no crystal structure for Smad binding to a GC-rich motif has been reported, it is not clear how the Smads bind to this GC-rich motif, but it has been proposed that the region of the MH1 domain that binds to GC-rich sequences may be distinct from the β-hairpin loop which binds to the SBE (Shi, Y. et al., 2003).

Smads bind to these low complexity sites with weak affinity and thus it is generally assumed that the Smad-DNA interactions are enhanced by interactions with other transcription partners that are also crucial for promoter selectivity. The role of these factors is discussed below.

1.5.6.2 Transcription Factors

To date, at least 60 regulatory transcription factors, corepressors and coactivators have been reported to physically and/or functionally interact with the Smads (Massague, J. et al., 2005). These include factors from almost every structural family and a wide range of functional classes and these interactions allow the Smads to mediate transcriptional activation or repression in response to TGF-β superfamily ligands. This may reflect the functional diversity of the Smads themselves but it is important to note that the majority of these reports have relied on data derived from studies carried out *in vitro* or by protein overexpression. Indeed many of the interaction motifs have not been characterised. Many of these interactions await confirmation by immunoprecipitation of endogenous proteins, chromatin immunoprecipitation (ChIP) and siRNA depletion to verify a functional role in TGF-β signalling (Massague, J. et al., 2005). For the purpose of this thesis, I will focus on some of the Smad-interaction factor interactions that have been extensively characterised.

The first identified Smad transcription partner was *Xenopus* forkhead Activin signal transducer (FAST-1, now renamed XFoxH1a), which directly binds Smad2. FoxH1 contains an N-terminal forkhead/winged helix DNA binding domain and forms a transcriptionally competent complex with activated Smad2 and Smad4 in response to Activin, when bound to the Activin response element (ARE) in the *Mix.2* promoter (Chen, X. et al., 1996; Chen, X. et al., 1997). The TGF-β R-Smads, Smad2 and Smad3, also interact with the paired-like homeodomain proteins, Mixer and Milk (Germain, S. et al., 2000). Sequence analysis of the Mixer and FoxH1 family of transcription factors revealed that these transcription factors bind active Smad complexes through a common, proline rich, 25 amino acid Smad interaction motif (SIM), characterised by a core PPNK sequence, present in their C-terminal regions (Germain, S. et al., 2000). The SIM is necessary and sufficient to interact with both

monomeric Smad2 and Smad3, and activated Smad complexes, which can then subsequently recruit these complexes to DNA (Germain, S. et al., 2000). In addition, FoxH1 family members have a second conserved interaction motif named the FoxH1 motif (FM) (Randall, R. A. et al., 2004). Unlike the SIM, the FM only interacts with activated complexes of Smad2 and Smad4, and homomeric Smad2 complexes. The binding sites for the SIM and FM motifs in Smad2 have been investigated by site directed mutagenesis in combination with structural modelling. The binding sites of these two motifs partially overlap on a target Smad2, and thus it has been suggested that a FoxH1 monomer can interact with both subunits of Smad2 in a Smad2-Smad4 heterotrimer (Randall, R. A. et al., 2004) (Figure 1.10). The interaction between the FM motif and Smad2 discriminates Smad2 with Smad3, thus conferring on FoxH1 specificity for Smad2 binding. Although there were some report that FoxH1 can bind Smad3, this was using overexpressed protein (Randall, R. A. et al., 2002; Randall, R. A. et al., 2004).

Much less is known about the Smad interacting transcripton factors which determine the specificity of gene targets in response to BMP. However, recently progress has been made in revealing a crucial component of the nuclear Smad/Mad complex in dpp/BMP signalling. *Drosophila* Schnurri (Shn) is a large DNA-binding transcription factor with multiple, widely separated zinc finger domains, and was one of the first partners identified for BMP-specific R-Smads (Dai, H. et al., 2000; Udagawa, Y. et al., 2000). Genetic studies in *Drosophila* revealed that Shn plays an important role in Dpp signalling, downstream of the receptors and is essential for Dpp signalling at many developmental stages. Interestingly, the early function of dpp, which is to pattern the developing embryo, is not affected in shn mutants, suggesting that Shn is not an essential component of dpp signalling but it might act as a tissue-specific cofactor (Affolter, M. et al., 2001). It was subsequently uncovered that Schnurri can interact directly with Mad, the Smad1 homologue, to engage in transcriptional activation, but more often repression (Affolter, M. et al., 2001). A major target of Shn is the transcriptional repressor brinker, and inhibition mediated by Shn, relieves repression of a plethora of Dpp target genes. Shn represses brinker via the formation of a Shn/Mad/Med complex on defined elements in the brinker promoter (Muller, B. et al., 2003; Pyrowolakis, G. et al., 2004). In addition to the founding member in *Drosophila*, Schnurri homologues exist in other phyla, namely Sma-9 in *C.*

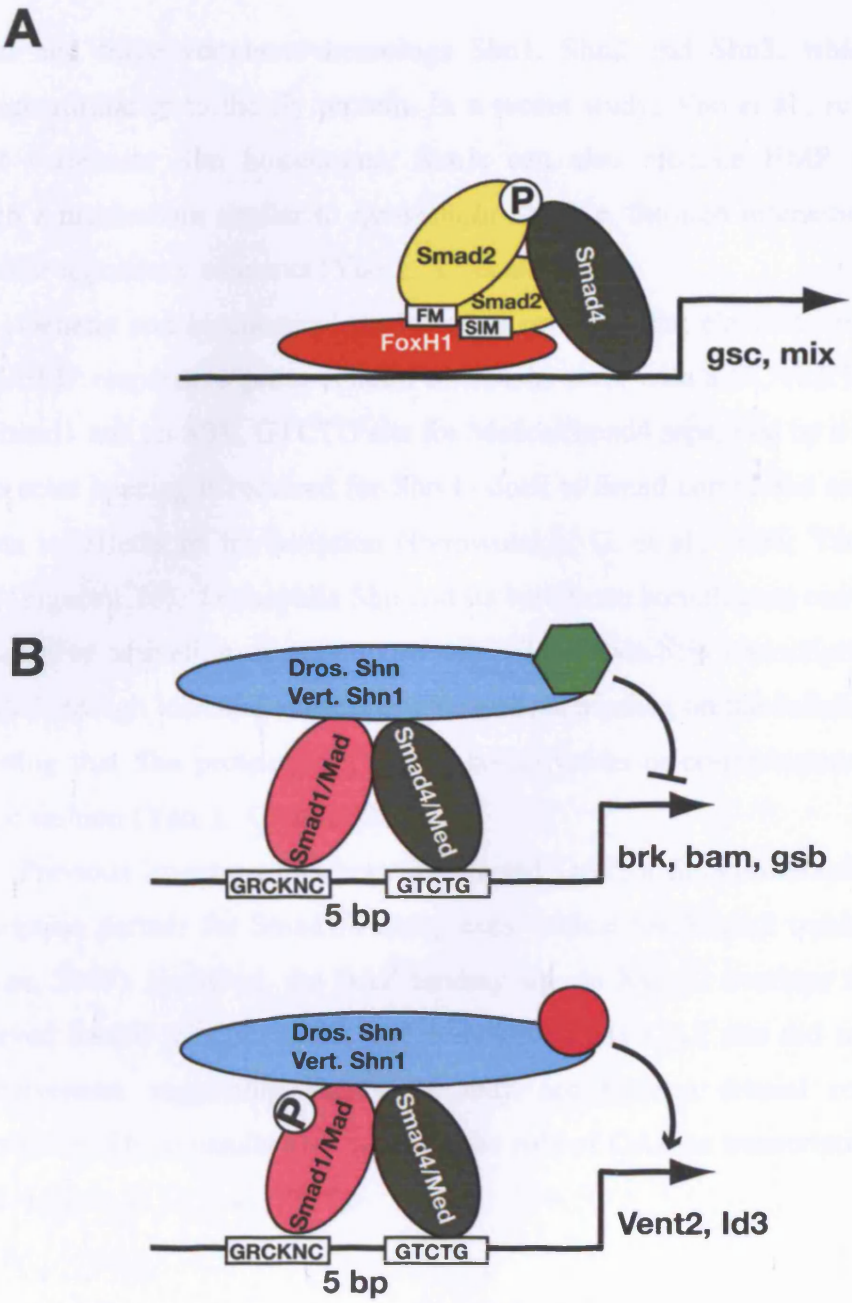

Figure 1.10 Transcription Factor Interactions

(A) FoxH1 binds to each monomer of a Smad2 subunit in a heterotrimeric complex through a Smad-interacting (SIM) motfi and an FoxH1 motif (FM). This interaction recruits Smad2-Smad4 complexes to site specific DNA sequences and stabilises the complex on DNA. Based on model from Randall, et. al., 2004.

(B) Schnurri as a scaffolding platform for Smad1-Smad4 complexes. Smad1/Mad and Smad4/Med bind to GRCKNC and GTCT sites, probably as a heterotrimeric complex (not represented in this figure). Shn/Shn1 interacts with the MH2 domains of Smads and acts to stabilise the complex and provide docking sites for cell specific co-repressors and coactivators. (Taken from Yao, 2006).

elegans and three vertebrate homologs Shn1, Shn2 and Shn3, which exibit high sequence similarity to the fly protein. In a recent study, Yao et al., revealed that the closest vertebrate Shn homologue, Shn1, can also mediate BMP responsiveness through a mechanism similar to *Drosophila* Shn, i.e. through interaction with Smads on similar regulatory elements (Yao, L. C. et al., 2006).

Genetic and biochemical analysis has revealed that elements in the promoters of dpp/BMP responsive genes contain consensus sites, with a GC-rich binding site for Mad/Smad1 and an SBE, GTCTG site for Medea/Smad4 separated by a spacer of 5 bp. This precise spacing is required for Shn to dock to Smad complexes on the DNA and mediate its effects on transcription (Pyrowolakis, G. et al., 2004; Yao, L. C. et al., 2006) (Figure 1.10). Drosophila Shn and its vertebrate homologues can mediate either repression or activation of gene expression. This switch in transcriptional output is mediated through identical consensus elements, depending on the cellular context, thus suggesting that Shn proteins can recruit co-activators or co-repressors in a cell-type specific fashion (Yao, L. C. et al., 2006).

Previous investigations have implicated OAZ, a Smad-interacting factor as a transcription partner for Smad1/4 complexes, critical for Xvent2 transcription (Hata, A. et al., 2000). However, the OAZ binding site on Xvent2 overlaps with the highly conserved Smad1 binding motif and mutation of this OAZ site did not affect BMP responsiveness, suggesting that OAZ may not have a crucial role in Xvent2 transcription. These results also question the role of OAZ as transcriptional partner to Smad1/4 (Yao, L. C. et al., 2006).

1.5.7 Crosstalk with other Signalling Pathways

The response elicited by cells upon TGF-β superfamily ligand stimulation is not an isolated event. The cell type and context specific response is a net result of contributing environmental cues, which is dictated by the signalling pathways that are activated in the cell (Massague, J., 2000). Thus, TGF-β superfamily signalling is a constituent of an integrated network, by which the activation of other pathways often defines cellular responses of TGF-β family members. Communication can be achieved at different levels of the TGF-β superfamily pathway, either through direct activation

of signalling components or through integration by targeting the activity of the Smads (Massague, J., 2000).

1.5.7.1 Smad-independent Signalling

Although the Smads represent the major and most direct route of communication of the TGF-β ligands, alternative signalling cascades may also be activated by TGF-β family members (Derynck, R. et al., 2003). These include a diverse array of signalling pathways involved in many aspects of cellular regulation. For example, TGF-β can activate the ERK, JNK and p38 MAPK kinase pathways. Activation with slow kinetics in some cases may result from Smad-dependent transcriptional respsonses, but the rapid activation (5-15 min) in other cases suggests independence from transcription (Javelaud, D. et al., 2005). Studies using mutated ALK5 receptors, defective in Smad activation demonstrated that activation of p38 in mouse mammary epithelial cells did not require activation of the Smads (Yu, L. et al., 2002). The mechanism of receptor coupling however is poorly understood. It is likely that TGF-β can activate upstream regulators of these kinases, such as MAPKK or MAPKKK. Indeed, both TGF-β and BMP4 can activate TGF-β-activated kinase 1 (TAK1), a MAPKKK family member (Lutz, M. et al., 2002), which in turn can trigger p38 and JNK pathways. Because TAK1 can phosphorylate and activate IκB kinase, thus stimulating NF-κB signalling, TAK1 represents a point of convergence with TGF-β/BMP signalling and other signalling pathways (Lutz, M. et al., 2002).

In addition, rapid activation of small Rho-like GTPases, including RhoA, Rac and Cdc42 has also been demonstrated upon stimulation of TGF-β in a subset of cell lines (Bakin, A. V. et al., 2002; Bhowmick, N. A. et al., 2001). A delayed activation of RhoA and Cdc42 has also been observed, which is dependent on protein synthesis. The activity of these Rho-like GTPases have been implicated in TGF-β-induced cytoskeletal reorganisation, such as membrane ruffling, stress fibre formation and epithelial-to-mesenchymal transition (EMT) (Bakin, A. V. et al., 2002; Bhowmick, N. A. et al., 2001). Furthemore, Ras activation in response to TGF-β may also contribute to the induction of Rho-like GTPase activity (Yue, J. et al., 2000). In addition, a recent study also revealed that a member of the p21-activated kinases (PAKs), PAK2, was

activated by TGF-β specifically in fibroblasts but not in epithelial cells (Wilkes, M. C. et al., 2003). PAK2 activation was found to be Smad-independent but required Rac1 and Cdc42 GTPase activity, to mediate cell proliferation and morphological transformation (Wilkes, M. C. et al., 2003).

TGF-β has also been shown to activate the phosphatidylinositol-3-kinase (PI3K) pathway, as indicated by phosphorylation of its effector Akt (Bakin, A. V. et al., 2000; Vinals, F. et al., 2001). This activation can be direct, with possible involvement of RhoA (Bakin, A. V. et al., 2000), but can also be mediated through a Smad-dependent pathway, whereby induction of TGF-α expression leads to Epidermal Growth Factor (EGF) receptor activation (Vinals, F. et al., 2001). The role of PI3K activity in promoting EMT is under debate due to conflicting results (Bakin, A. V. et al., 2000; Piek, E. et al., 1999), but accumulating evidence has implicated a role in modulating TGF-β-induced apoptosis (Bakin, A. V. et al., 2000; Janda, E. et al., 2002; Piek, E. et al., 1999). Two recent studies investigated the molecular mechanism into how the PI3K/Akt pathway can regulate Smad (Conery, A. R. et al., 2004; Remy, I. et al., 2004). They propose that in some epithelial and hematopietic cell lines, Akt can physically interact with Smad3 and sequester it at the plasma membrane, thus preventing nuclear accumulation and transcriptional activity and ultimately, protection from TGF-β induced apoptosis (Conery, A. R. et al., 2004; Remy, I. et al., 2004). Therefore a balance between Akt activity and Smad3 level will determine the sensitivity of a cell to TGF-β-induced apoptosis.

Also, an additional substrate for the TGF-β type II receptor has been uncovered. PAR6, a component of junction complexes in epithelial cells is phosphorylated in response to TGF-β signalling and contributes to loss of epithelial polarity (Ozdamar, B. et al., 2005). This will be discussed in more detail in Section 1.6.3.1.

1.5.7.2 Signal Integration with signalling pathways

In addition to the Smad independent signalling responses, the Smads can also act as nodes for signal integration. Many signalling pathways have been shown to affect Smad activity through a number of mechanisms including nuclear accumulation and

transcriptional activity. One of the first pathways to be implicated in modulating Smad activity was the Ras/Raf/ERK MAPK pathway (Kretzschmar, M. et al., 1997; Kretzschmar, M. et al., 1999). The linker region of the R-Smads contains multiple Ser-Pro and Thr-Pro residues that are phosphorylated by ERK1/2, downstream targets of the Ras MAPK pathway. ERK phosphorylation of the linker sites of Smad1, 2 and 3 has been proposed to inhibit nuclear accumulation of R-Smads and thus dampen down the transcriptional response (Kretzschmar, M. et al., 1997; Kretzschmar, M. et al., 1999). It has also been shown that Smad2 signalling is abrogated in mid-gastrula *Xenopus* explants due to increased Ras/ERK activity, whereby phosphorylation of Smad2 sites by ERK1/2 was shown to prevent Smad2 accumulation in the nucleus (Grimm, O. H. et al., 2002). In addition, activation of Ras/MAPK that is required for neuralization in dissociated Xenopus embryonic ectodermal cells, which acts to inhibit BMP signaling by phosphorylation of Smad1 in the linker (Kuroda, H. et al., 2005).

However, extensive variability has been observed on the activity of ERK on Smad responses in different cell types and moreover, contradictory results have also been reported. Inducible activation of ERK1/2 in canine kidney epithelial cells (MDCK cells) with a constitutively active form of Raf did not significantly influence the function of Smad2 or Smad3 at the level of nuclear accumulation, DNA binding or transcriptional activation (Lehmann, K. et al., 2000). In another study, the activity of H-Ras in squamous carcinoma cells was shown to promote the transcriptional activity of Smad2 and Smad3, which resulted in a synergistic TGF-β response (Oft, M. et al., 2002). In addition, Smad2-dependent formation of mesoderm in the blastula stage of *Xenopus* embryos appears to occur in regions of peak MAPK activation (Schohl, A. et al., 2002). The paradox that Ras/MAPK and Smad signalling may cooperate in some instances (Lehmann, K. et al., 2000; Oft, M. et al., 2002) while acting in opposition in others (Kretzschmar, M. et al., 1997; Kretzschmar, M. et al., 1999) requires further investigation. Uncovering the mechanism by which phosphorylation of the Smad linker region exerts its effects will hopefully gain insight into the contradictory results obtained.

In addition, the JAK/STAT pathways activated by cytokines and growth factors also mediate crosstalk with both BMP and TGF-β Smad pathways. Cooperation between STAT3 and Smad1 has been reported to mediate BMP-2 and Leukamia inhibitory factor (LIF)-induced differentiation of primary fetal neural progenitor cells

to astrocytes (Nakashima, K. et al., 1999). The formation of a complex between STAT3 and Smad1, bridged by p300, is required for the synergistic activation of astrocyte-specific gene encoding the glial fibrillary acidic protein (GFAP). The JAK/STAT pathway has also been implicated in modulation of the TGF-β signallling. Interferon-γ (INFγ) signalling via the JAK/STAT pathway has been shown to indirectly regulate Smad3 activity through upregulation of the inhibitory Smad7 (Ulloa, L. et al., 1999).

Notch signalling has also proven to be a key player in the regulation of both TGF-β and BMP signalling. Here both synergistic and antagonistic effects on Smad signalling have been observed (Kluppel, M. et al., 2005). Furthermore, the TGF-β signalling cascade is also influenced by cross-talk with other pathways such as NF-kB and β-catenin/LEF signalling. A more in depth discussion on the integration of these signalling pathways with TGF-β signalling during EMT can be found in Section 1.6.3.1.

1.6 Biological Functions of TGF-β superfamily members in development and in adult homeostasis

The biological actions of TGF-β superfamily members are diverse and sometimes opposing effects can be observed dependent on cell type and environmental cues. In this section many of the multifunctional actions of TGF-β and related factors will be discussed.

1.6.1 Cell Cycle Control during G1

TGF-β has been shown to be a potent inducer of growth inhibition in many cell types. To appreciate the molecular mechanisms by which TGF-β affects cell proliferation, a brief outline of the regulation of the cell cycle is given below.

1.6.1.1 The Cell cycle

All vertebrate embryos begin their existence as a single cell entity, which then divides over time by a process of DNA duplication and cell division to form the entire

organism. The development of the cell cycle is clearly illustrated in *Xenopus* embryos. These early divisions in the embryo occur rapidly, with continuous cycles of DNA replication and nuclear division, which are completed in approximately thirty minutes. However, as the embryo reaches gastrulation, environmental cues need to be interpreted to direct the fate of the cells. Hence, the cell cycle adapts by incorporation of two distinct gaps whereby these signals can influence progression of the cell cycle and the fidelity of DNA replication can be checked (Blagosklonny, M. V. et al., 2002). The first, called G1 phase occurs between nuclear division (M phase) and DNA synthesis (S-phase), and a second gap called G2 phase between S and M phases (Massague, J., 2004) (Figure 1.11). During the G1 phase, growth factors play a prominent role in the initiation and maintenance of the transition through G1 phase leading to S-phase. Cell cycle progression requires growth factor stimulation up to a stage late in G1 phase known as the restriction point, at which point commitment occurs. Once past this point, cells are refractory to both mitogenic and anti-mitogenic signals until the next G1 phase. After a successful completion of DNA synthesis, cells enter G2 phase in preparation for mitosis. During the G2 phase, the accuracy of DNA replication is scrutinised, whereby replication errors are corrected and the integrity of the microtubule function is assessed, to ensure efficient chromosome segregation. Most mammalian cells are diploid and therefore after DNA duplication, a cell must divide (Blagosklonny, M. V. et al., 2002). As cells exit mitosis, the cell cycle is reset, allowing the whole cycle to start again.

At the molecular level, cell cycle progression through G1 is driven by the activities of cyclin-dependent kinases (CDKs), in association their regulatory subunits, cyclins (Sherr, C. J. et al., 1999). The D-type cyclins (cyclin D1, D2, D3) bind to and activate CDK4, as well as the homologous CDK6, at early to mid G1. As the cells progress to late G1, cyclins E1 and E2 form active complexes with CDK2. For complete activation of the CDKs a critical threonine is phosphorylated by CAK (CDK-activating kinase) and an inhibitory phosphorylation is removed by the phosphatase CDC25 (Massague, J., 2004). After mitogenic stimuli active cyclin-CDK complexes accumulate and assemble in the nucleus where they phosphorylate a set of substrates to initiate cell cycle progression. In addition, the activity of these kinases is also constrained by two classes of CDK inhibitors, (CDIs), which function to suppress inappropriate cell cycle progression (Sherr, C. J. et al., 1999).

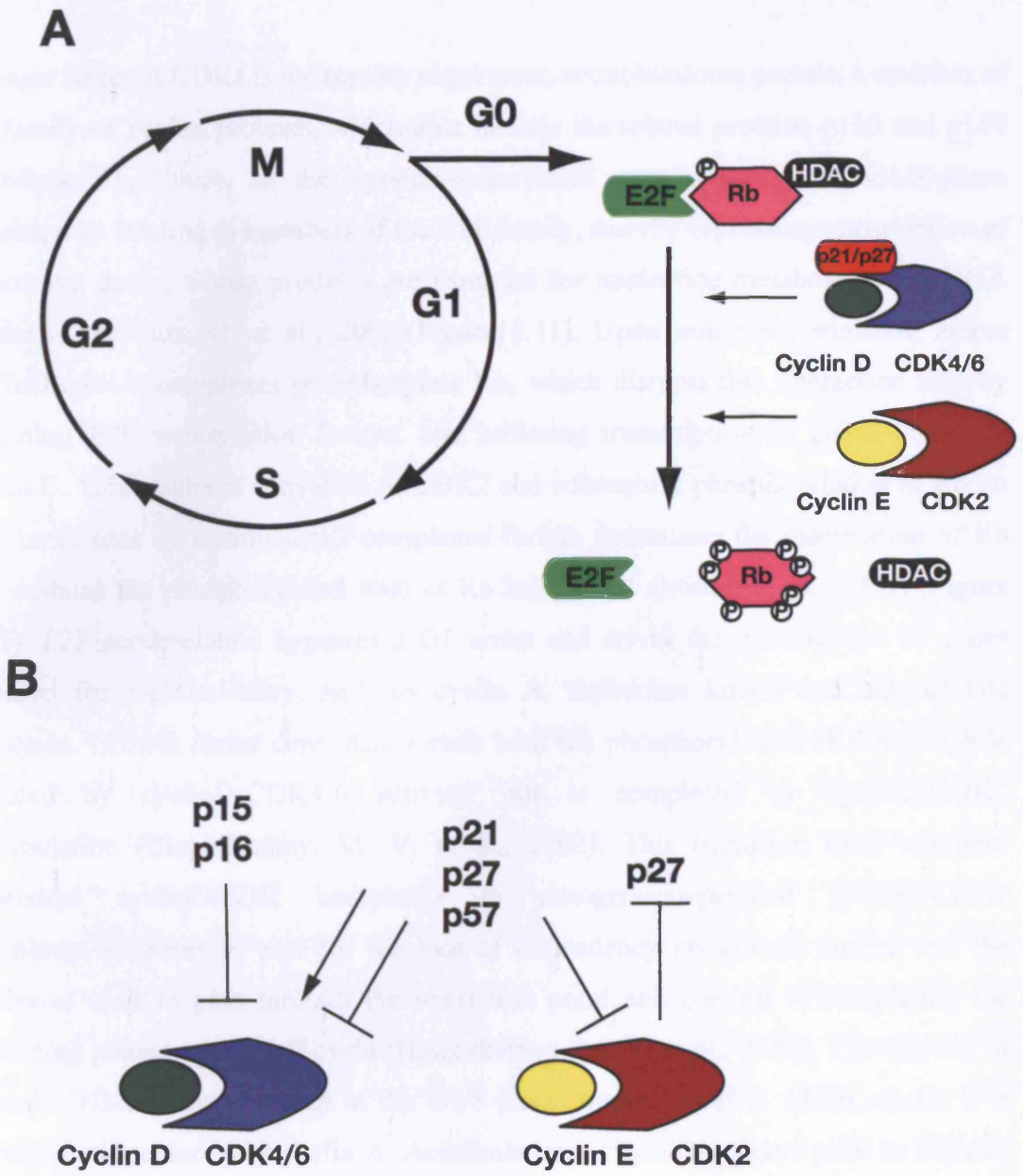

Figure 1.11 Regulation of the cell cycle by CDKs

(A) CDK activity regulates G1 entry and cell cycle progression.The activation of cyclinD-CDK4/6 and cyclinE-CDK2 in turn promotes hyperphosphorylation of Rb, leading to the release of histone deacytyases (HDAC) and activation of E2F allowing E2F-dependent transcription. Along with cyclin E, the E2Fs activate transcription of a large set of components that support DNA replication (ORCs, MCMs, DNA polymerase) and subsequent events (cyclin B, Cdk1 and various DNA quality-control components).
(B) Effects of CDK Inhibitors. p21, p27, and p57 can either activate or inactivate CDK4/6. In addition, phosphorylation of p27 by CDK2 targets it for degradation. The INK family of CDKIs target cyclinD-dependent kinases only.(Adapted from Blagoslonny and Pardee, 2002).

A major target of CDKs is the tumour suppressor, retinoblastoma protein, a member of the family of pocket proteins, which also include the related proteins p130 and p107 (Cobrinik, D., 2005). In the hypophosphorylated state, pRb blocks G1/S-phase transition by binding to members of the E2F family, thereby repressing transcription of responsive genes, whose products are essential for nucleotide metabolism and DNA synthesis (Stevaux, O. et al., 2002)(Figure 1.11). Upon mitogenic stimulus, active cyclinD-cdk4/6 complexes phosphorylate Rb, which disrupts this interaction thereby liberating E2F transcription factors, and initiating transcription of genes including cyclin E. This results in activation of CDK2 and subsequent phosphorylation of Rb on additional sites by cyclinE-cdk2 complexes further potentiates the inactivation of Rb and sustains the phosphorylated state of Rb beyond G1 (Mittnacht, S., 1998) (Figure 1.11). E2F accumulation bypasses a G1 arrest and drives the transcription of genes required for S-phase entry, such as cyclin A, thymidine kinase and dihyrofolate reductase. Growth factor dependency ends with the phosphorylation of Rb, which is initiated by cyclinD-CDK4/6 activity, but is completed by cyclinE-CDK2 accumulation (Blagosklonny, M. V. et al., 2002). This transition from mitogen-dependent cyclinD/CDK complexes to mitogen-independent cyclinE/CDK2 complexes accounts in part for the loss of dependency on growth factors and the ability of cells to pass through the restriction point and commit to completing the remaining phases of the cell cycle (Blagosklonny, M. V. et al., 2002). The activity of cyclinE/CDK2 complex peaks at the G1/S-phase transition, after which, cyclin E is degraded and replaced by cyclin A. Accumulation of cyclinA occurs prior to S-phase entry and cyclinA associated kinase activity is required for completion of S-phase and entry into M-phase.

Many studies have supported the general scheme outlined above, however, it would be a gross oversimplification to suggest that a linear scheme of activation of CDKs occur. Positive and negative feedback loops exist throughout the G1 phase and act to attenuate or perpetuate the signals (Massague, J., 2004). In addition, the knockout mouse studies have revealed that not all of the components are absolutely essential for cell proliferation. Cyclin E, Cyclin D, CDK4 and CDK6 deletions suggest that these components are only required in certain tissues, whereas most organogenesis and development are unaffected. Furthermore, it is generally viewed that the activity of CDK2 is the engine that drives progression through the G1/S transition, yet strikingly,

mice lacking CDK2 are viable. This adds to the growing suspicion that different mammalian CDKs are redundant, either in the absence of a family member or in certain abnormal circumstances (Massague, J., 2004).

1.6.1.2 CDK inhibitors (CKIs)

The activities of cyclin-CDK complexes are also modulated by CDK inhibitors (CKIs). These inhibitory proteins are major targets for regulation by many growth factors including TGF-β. CDKIs can be divided into two families based on their structures and CDK targets; the INK4 family and the family of CIP/KIP proteins. The INK4 proteins (inhibitors of CDK4) specifically inhibit the catalytic subunits of CDK4 and CDK6 through direct 1:1 interactions with, and sequesteration of, CDKs. In contrast, members of the Cip/KIP inhibitor family (CDK interacting protein/kinase inhibitor protein), $p21^{Cip1/WAF1}$, $p27^{Kip1}$ and $p57^{Kip2}$, bind to CDKs and disrupt their catalytic centre. These proteins share a homologous CDK binding region in their amino terminus and act as inhibitors for CDK2 compelxes *in vivo* but they have been found to bind and inhibit all cyclin/CDK complexes *in vitro* (Sherr, C. J. et al., 1999). At high levels, p21 and p27 function as integral brakes of the cell cycle, in that they silence cyclin-CDK2 activity resulting in growth arrest. Mitogenic stimuli release CDK2 from inhibition by suppressing the transcription, translation, stability or nuclear localisation of either p21 or p27. Once CDK2 is activated, it bites back by phosphorylating p27 on a C-terminal threonine, thus targeting it for degradation (Sheaff, R. J. et al., 1997). In addition to their inhibitory role, the Cip/KIP proteins can positively affect cyclinD-dependent kinases (Sherr, C. J. et al., 1999). At low levels, p21 and p27 actually promote the assembly, stability and nuclear retention of cyclin D-CDK4 and cyclinD-CDK6 complexes. In proliferating cells, p27 is predominantly bound to cyclinD-CDK4 without inhibiting this kinase, and allowing the assembly of cyclinD/CDK4 complexes (Soos, T. J. et al., 1996). Also, a non catalytic function of the cyclinD-CDK4 complexes is to sequester p21 and p27 from CDK2, relieving its inhibition and promoting cell cycle progression (Sherr, C. J. et al., 1995). Mitogen withdrawal results in rapid cyclinD degradation and the previously sequestered

Cip/Kip proteins are released, inhibiting cyclinE/CDK2 activity and thus leading to cell cycle arrest (Reynisdottir, I. et al., 1997).

The members of the INK4 proteins, p16, p15, p18 and p19 contain multiple ankyrin repeats, allowing them to specifically inhibit the kinase activity of the cyclin D associated CDKs, CDK4 and CDK6. The signals which lead to the synthesis of INK4 proteins are poorly understood, but it is clear that $p15^{INK4b}$ is induced by TGF-β which participates in G1 arrest (Reynisdottir, I. et al., 1997). In general, the INK4 proteins act as competitive inhibitors of D-type cyclins for binding to their CDKs, preventing formation of the active cyclin-CDK complex (Pruitt, K. et al., 2001). It has also been demonstrated that INK4 activity is dependent on the displacment of Cip/Kip proteins from complexes containing cyclinD-CDK4, releasing free Cip/Kip proteins that then bind to and inactivate cyclinE-CDK2 complexes, resulting in growth arrest (Reynisdottir, I. et al., 1997). In conclusion, it is clear that the relative levels of cyclin, CDK and CDKI proteins determine the activity of Rb and the proliferative state of the cell. The effects of growth factors on the relative levels of these components and the progression through the G1 phase are discussed below.

1.6.1.3 Cell cycle control by Ras

In contrast to TGF-β, many growth factor signalling pathways contribute to the progression of the cell cycle through the G1/S phase transition. Of these, the Ras pathway has been implicated as a major player in this respect (Coleman, M. L. et al., 2004). As the two pathways are integrated on many levels, it is important to understand the opposing actions of Ras in the control of the cell cycle and a brief outline of the role of Ras signalling is discussed below. Diverse extracellular stimuli signal through many different receptor tyrosine kinases (RTKs), which transduce their signal by activation of Ras proteins. Once activated, Ras in turn interacts with a diverse spectrum of effectors and initiates a multitiude of cytoplasmic signalling cascades (Schlessinger, J., 2000). Hence Ras proteins act as a nodal point, whereby multiple signals converge to elicit their responses. The importance of Ras signalling in cell cycle progression is underscored by the fact that the prototypical Ras proteins, H-Ras, N-Ras and K-Ras were first identified as the products of active oncogenes in

human tumours. Aberrant cell cycle regulation due to inappropriate activation of Ras proteins leads to uncontrolled proliferation and cancer, however these GTPases also contribute to cell-cycle regulation in normal, non-transformed cells. The Ras GTPase proteins are positioned at the inner face of the plasma membrane, where they serve to transmit signals via receptor tyrosine kinases to the cytoplasm (Malumbres, M. et al., 1998). The RTKs initiate signalling by creating docking sites that are recognised by adaptor proteins such as Grb2 and Sos, which subsequently recruit effectors (Figure 1.12A). Upon recruitment, Ras proteins are activated by GTP-GDP exchange, catalysed by GTP exchange factors (GEFs), to form an active GTP-bound state, which can then engage a complex network of effectors. Among these, the Ras-MEK-ERK kinase cascade and the PI3Kinase pathways have key roles in promoting cell cycle progression.

Early studies established a central role for Ras in G1/S progression as demonstrated by blocking the entry of cells into S-phase upon microinjection of Ras-neutralising antibodies or use of a dominant negative RasN17 (Mulcahy, L. S. et al., 1985; Stacey, D. W. et al., 1991). It was later revealed that the principal function of Ras in G1/S-phase progression is to increase levels of cyclin D and ultimately inactivate Rb (Mittnacht, S. et al., 1997). In the absence of mitogenic growth factors, levels of cyclin D remain low, due to its highly labile state. However, accumulation of cyclin D is essential for mitogen-dependent progression through the G1 phase. Upon mitogen activation, the Ras/Raf/ERK pathway induces cyclin D1 transcription, which leads to the inactivation of Rb (Coleman, M. L. et al., 2004). Ectopic expression of cyclin D1 was shown to rescue cell cycle inhibition by dominant negative ras (Peeper, D. S. et al., 1997) and also cells derived from p16 null mice, were found to be less sensitive to the inhibitory effects of the anti-Ras antibody (Mittnacht, S. et al., 1997). This establishes that the function of D-type cyclins is to link extracellular signals to the cell cycle machinery, and thereby act as growth factor sensors. The regulation of Cyclin D stability is also modulated by downstream effectors of Ras, the PI3 kinase pathway (Massague, J., 2004) (Figure 1.12A). Cyclin D turnover is governed by ubiquitination and proteasomal degradation, which are stimulated by cyclin D1 phosphorylation on threonine 286 by glycogen synthase kinase-3β (Diehl, J. A. et al., 1998; Diehl, J. A. et al., 1997). PI3 kinase signalling to Akt/protein kinase B (PKB) results in inhibition of GSK-3β, thereby enhancing cyclinD1 stability (Massague, J.,

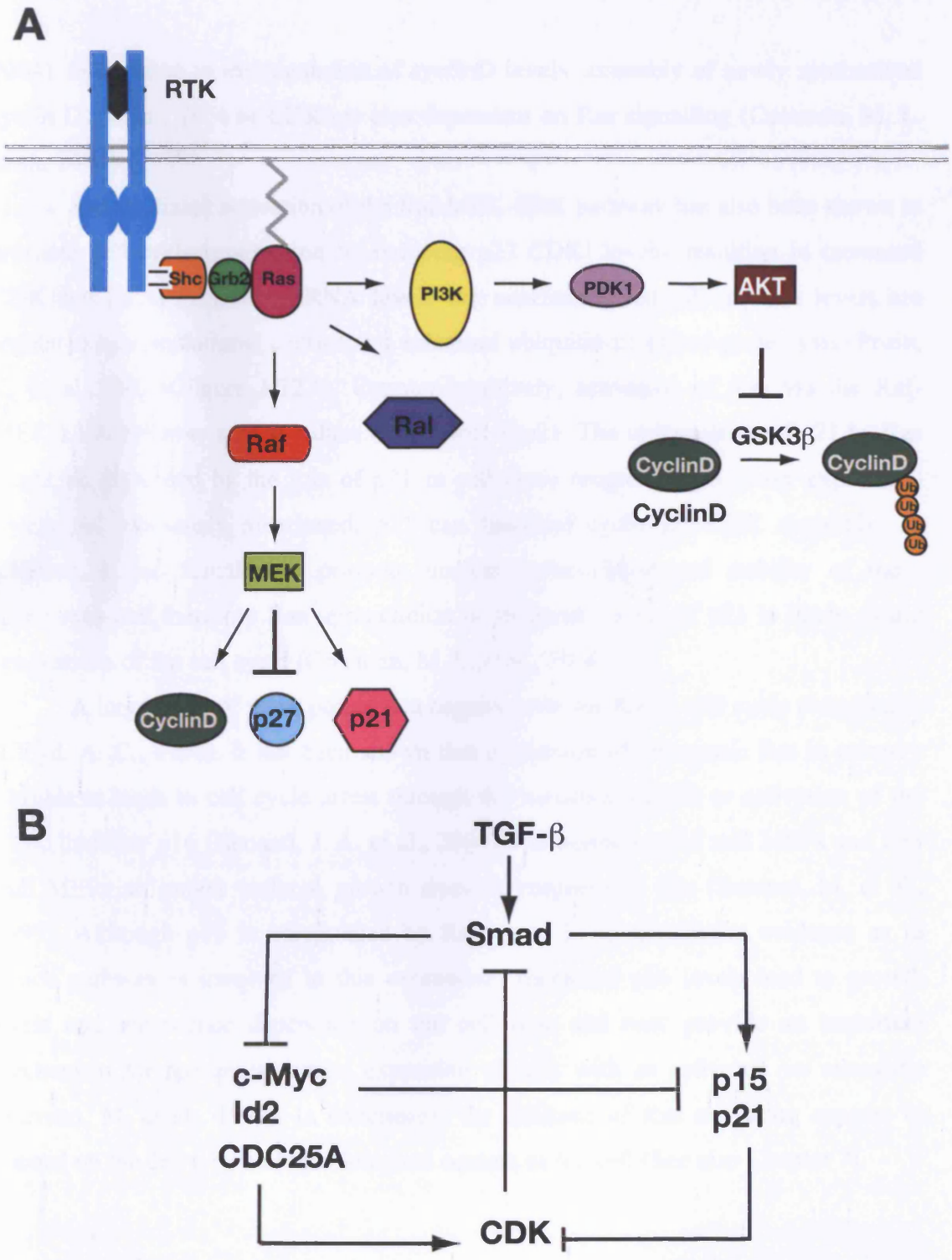

Figure 1.12. Regulation of the Cell Cycle by Ras and TGF-β pathways

(A)Ras signalling in cell cycle control. Activation of Ras initiates a cascade of events leading to cell cycle progression. These include increased expression and stabilisation of Cyclin D, downregulation of p27 and induction of p21.
(B) Cell cycle control by TGF-β through transcriptional regulation. TGF-β signalling leads to the inhibition of CDK4/6 and CDK2 activities by downregulating expression of c-Myc, Id, CDC25A and upregulation of p15 and p21.(Adapted from Liu and Matsuura, 2005).

2004). In addition to the regulation of cyclinD levels, assembly of newly synthesized cyclin D1 with CDK4 or CDK6 is also dependent on Ras signalling (Coleman, M. L. et al., 2004).

Ras mediated activation of the Raf-MEK-ERK pathway has also been shown to promote cell-cycle progression by reducing p27 CDKI levels, resulting in increased CDK activity. P27 levels mRNA levels are unaffected, but p27 protein levels are regulated by translational control and enhanced ubiquitin-mediated proteolysis (Pruitt, K. et al., 2001)(Figure 1.12A). Counter-intuitively, activation of Ras via the Raf-MEK-ERK pathway acts to induce expression of p21. The upregulation of p21 by Ras might be explained by the role of p21 in cell cycle progression at lower expression levels. As previously mentioned, p21 can facilitate cyclin-D1–CDK assembly. In addition, it can function to promote nuclear accumulation and stability of these complexes and therefore Ras upregulation of moderate levels of p21 is likely to aid progression of the cell cycle (Coleman, M. L. et al., 2004).

A large body of work points to a negative role for Ras in cell cycle progression (Lloyd, A. C., 1998). It has been shown that expression of oncogenic Ras in primary fibroblasts leads to cell cycle arrest through the induction of p53 or activation of the CDK inhibitor p16 (Benanti, J. A. et al., 2004). Furthermore, p16 null MEFs and P53 null MEFs no longer undergo growth arrest in response to Ras (Serrano, M. et al., 1997). Although p16 is upregulated by Ras, there is no conclusive evidence as to which pathway is involved in this expression. Increased p16 levels lead to growth arrest and senescence depending on the cell type and may provide an important mechanism for preventing clonal expansion of cells with an activated *ras* oncogene (Serrano, M. et al., 1997). In conclusion, the outcome of Ras activation appears to depend on the cell type and the biological context of the cell (See also Chapter 7).

1.6.1.4 TGF-β-induced growth inhibition

In most systems TGF-β is a potent physiological inhibitor of cell growth (Polyak, K., 1996). The majority of nontransformed mammalian cell types are growth inhibited by TGF-β, but its growth inhibitory effect is most pronounced on epithelial, endothelial, lymphohematopoietic cells, and some cells of neuroectodermal origin, where TGF-β

treatment leads to complete growth arrest (Polyak, K., 1996). TGF-β exerts its potent growth-inhibitory effects through inhibition of CDK activity. This is achieved by several mechanisms, the most characterised of which, is the transcriptional regulation of key targets by the Smads (Massague, J. et al., 2006).

The primary mediators of the cytostatic transcriptional programme in response to TGF-β are Smad3 and Smad4. The key role of Smad3 in the antiproliferative effects of TGF-β was revealed from studies in knockout mice. Smad3 deficient mice show increased re-epithelialization due to impaired TGF-β growth inhibition (Ashcroft, G. S. et al., 1999), and a variety of primary cells from Smad3 null mice, such as fibroblasts, keratinocytes, astrocytes and T cells are largely resistant to the TGF-β cytostatic response (ten Dijke, P. et al., 2006). It has also been convincingly demonstrated by two independent groups that Smad4 is essential for the antiproliferative effects of TGF-β. Knockdown of Smad4 in either transformed human keratinocyte cells or mouse mammary epithelial cells, completely abolished TGF-β-induced cell cycle arrest and responses were restored upon re-expression of Smad4 levels into these cell lines (Deckers, M. et al., 2006; Levy, L. et al., 2005). The role of Smad2 in TGF-β induced growth arrest is less well defined. Interestingly, it was shown that the depletion of Smad2 by siRNA markedly enhanced the TGF-β cytostatic response (Kim, S. G. et al., 2005). Moreover, depletion of Smad2, in cancer cell lines, which exhibit resistance to the antiproliferative effects of TGF-β, was sufficient to restore TGF-β-induced G1 cell cycle arrest (Kim, S. G. et al., 2005). These observations have led to a model whereby the intensity of the TGF-β cytostatic signal depends on the endogenous ratio of Smad3 to the ratio of Smad3 to Smad2 (Kim, S. G. et al., 2005). These data are not conclusive for a negative role for Smad2 in TGF-β induced growth inhibition, in particular regarding its role as a tumour suppressor. Thus the role of Smad2 in TGF-β induced growth inhibition requires further investigation.

Molecular basis of G1 arrest by TGF-β

The antiproliferative effect of TGF-β generally results from growth arrest at the G1 phase of the cell cycle. It has been shown that a critical set of TGF-β cytostatic gene responses result in the inhibition of G1 Cdk activities and the subsequent accumulation

of hypo-phosphorylated retinoblastoma protein (pRB) (Massague, J. et al., 2000a). These gene responses by TGF-β cooperatively mediate cell cycle arrest at the G1 phase (Figure 1.12B). A major target of the cytostatic programme is the protooncogene, *c-myc*, whereby TGF-β causes a rapid inhibition *of c-myc* transcription (Massague, J. et al., 2000a). Conversely overexpression of c-Myc abrogates the growth inhibition of keratinocytes by TGF-β (Claassen, G. F. et al., 2000). c-Myc plays a major role as a transcriptional activator of growth and proliferation, and additionally acts as a direct transcriptional repressor of p15 and p21Cip1/Waf1 (Claassen, G. F. et al., 2000; Feng, X. H. et al., 2002). Therefore, targeting c-Myc for downregulation by TGF-β, renders p21 and p15 competent for activation. Repression of *c-Myc* occurs in cooperation with E2F4/5 and the Rb family member p107 (Chen, C. R. et al., 2002). TGF-β induces a repressor complex containing Smad3, Smad4, together with E2F4/5 and p107 which binds to the TGF-β inhibitory element (TIE) of the c-Myc promoter and repress its transcription (Chen, C. R. et al., 2002; Yagi, K. et al., 2002).

Furthermore, TGF-β has been found to directly alter components of the cell cycle, whereby TGF-β upregulates expression of the CDIs, p15 and p21. c-Myc expression plays a key role in coordinating the expression levels of p15 and p21 (Massague, J. et al., 2006) (Figure 1.12B). Firstly, c-myc actively represses the transcription of *p15* and *p21* in complex with Miz-1 (Myc-interacting zinc finger 1), which binds to *p15* initiator and the proximal region of *p21* (Liu, F. et al., 2005). Repression mediated by c-myc inhibits the transcriptional activation of these genes by TGF-β, p53 and other signals. In addition, high levels of c-myc persistant in the initial hours of TGF-β treatment also inhibit TGF-β induction of *p15* and *p21* by directly binding to Smad3 and Smad4 and suppressing their function (Liu, F. et al., 2005). Once Myc repression is relieved upon downregulation of myc levels by TGF-β, *p15* and *p21* are rendered competent for activation by the Smads. Smad-mediated induction of $p21^{Cip1/Waf1}$ occurs in cooperation with FoxO, p53 and possibly other factors whereas induction of $p15^{INK4B}$ has been reported to occur in cooperation with Sp1 (Massague, J. et al., 2006). It was demonstrated that accumulation of p15 in the cytoplasm prevents p27 from binding to Cdk4/6-Cyclin D complexes, and is therefore released from these complexes and redistributes to bind to and inactivate Cdk2-Cyclin E complexes

(Reynisdottir, I. et al., 1997; Reynisdottir, I. et al., 1995). p21 also acts to inhibit cyclin E-CDK2 activity (ten Dijke, P. et al., 2006).

In addition, TGF-β targets the inhibitor of differentiation (Id) proteins for repression. The Id proteins (Id1, Id2, and Id3) are Helix-Loop-Helix (HLH) proteins that promote cell cycle progression by releasing E2F from the effects of Rb as well as by inhibiting differentiation (Perk, J. et al., 2005). For downregulation of Id1, Smad3 activates ATF3, a transcriptional repressor, and together with Smad4 repress the transcription of the Id1 promoter (Kang, Y. et al., 2003). Downregulation of CDC25A is also important for the growth-inhibitory response of TGF-β. CDC25A promotes cell cycle progression from G1 to S phase by dephosphorylating and activating CDK2 and CDK2/4. Downregulation of CDC25A can be achieved by multiple mechanisms including transcriptional repression, inhibition of enzymatic activity or enhanced ubiquitin-mediated degradation (ten Dijke, P. et al., 2006). Along with induction of CKIs, downregulation of all the cell cycle promoting factors by TGF-β contributes to its negative effect on G1 progression (Figure 1.12B).

Interestingly, in addition to the effect of TGF-β on components of the cell cycle, recent evidence suggests that this regulation is bidirectional. A recent study has implicated Smad3 as a target for CDK2 and CDK4 activity (Matsuura, I. et al., 2004). Phosphorylation of Smad3 at three sites including two serine/proline rich sites in the linker region, decreases the transcriptional activity of Smad3 (Matsuura, I. et al., 2004). Mutation of these sites increases the transcriptional activity of Smad3, leading to an increase in p15 expression and decreased c-Myc levels. Furthermore, mutation of the CDK phosphorylation sites increases Smad3 ability to inhibit cell cycle progression from G1 to S phase (Matsuura, I. et al., 2004). Taken together, these data suggest that negative feedback control of Smad3 by CDK is achieved by inhibition of its transcriptional activity and antiproliferative function (Figure 1.12B).

1.6.2 Angiogenesis

Another function of TGF-β signalling is the critical role it plays in normal vascular development and physiology. The vasculature is the first functional organ system to develop in vertebrate embryos, and is vital for the distribution of nutrients and oxygen as well as the removal of waste products (Bohnsack, B. L. et al., 2004). Two processes are responsible for the formation of new blood vessels, both of which result in the formation of endothelial-lined tubes (Figure 1.13). The first, vasculogenesis, is the primary *in situ* differentiation of endothelial cell precursors (angioblasts) which then form the primary capillary plexus (Figure 1.13). This non-functional plexus is subsequently remodelled to form a mature vascular network consisting of large vitelline vessels and capillary networks during angiogenesis (Pepper, M. S., 1997). Angiogenesis, which involves the differential growth and sprouting of endothelial tubes, is a multistep process that can be divided into two phases (Table 1.3). In the activation phase, endothelial cells degrade the perivascular basement membrane, migrate into the extracellular space, proliferate, and form capillary sprouts and tubular structures. In the resolution phase, endothelial cells cease migration and proliferation, reconstitute a basement membrane and recruit smooth muscle cells permitting the maintenance of vessel wall integrity. A key regulatory step during this process is the control of endothelial cell proliferation. To this end, both mitogenic and anti-proliferative signals are required for appropriate vessel formation and remodelling.

Table 1.3 Phases of angiogenesis

Activation: initiation and progression
Increased vascular permeability and extravascular fibrin deposition
Basement membrane degradation
Cell migration/matrix invasion
Cell division
Lumen Formation
Resolution: termination and maturation
Cessation of migration
Inhibition of cell division
Basement membrane reconstitution
Junctional complex maturation

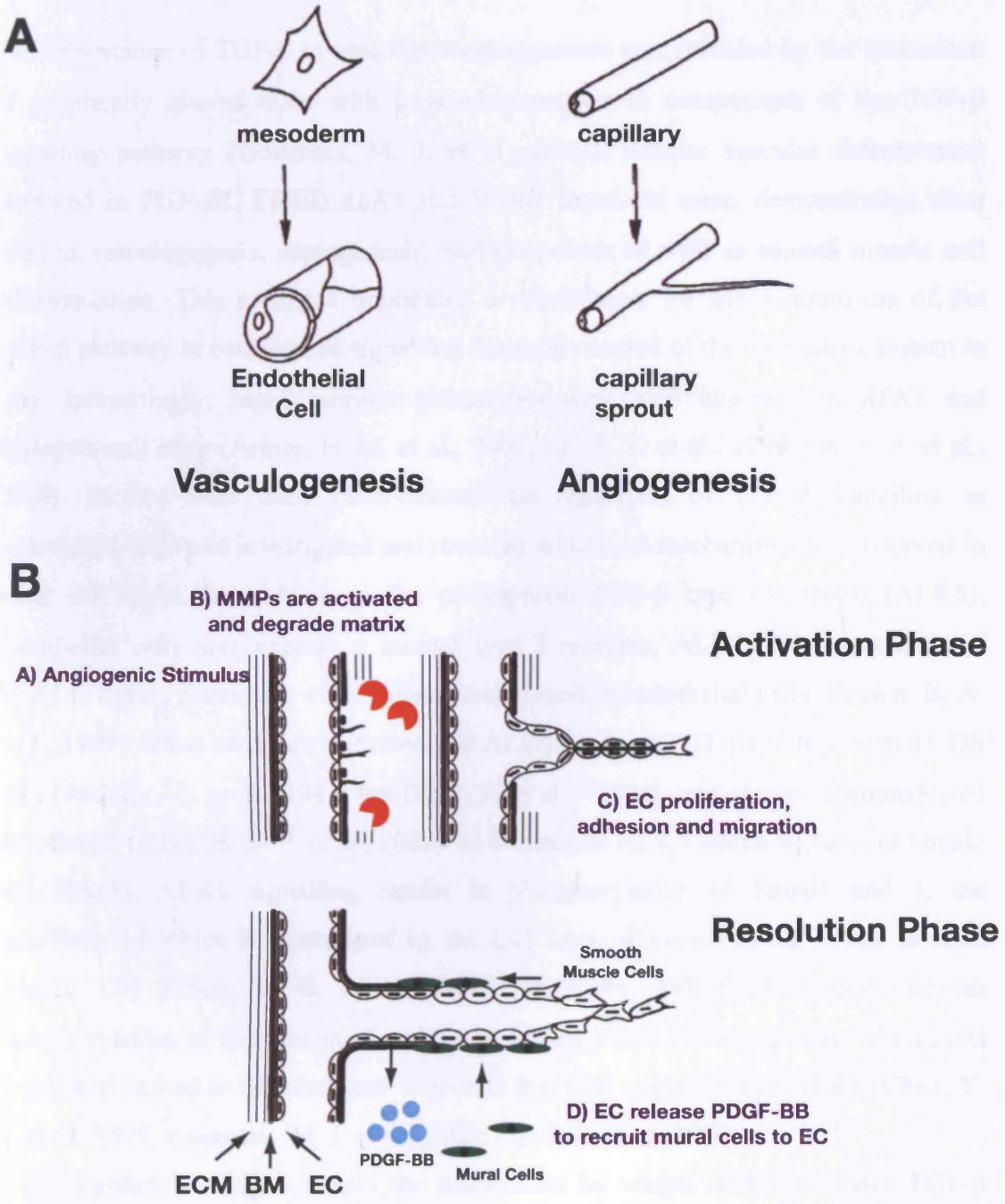

Figure 1.13. Vasculogenesis and Angiogenesis

A) Capillary blood vessels are formed by two processes. Endothelial precursors (angioblasts) in the embryo assemble in a primitive network during the process of vasculogenesis. Angiogenesis is the formation of new capillaries by a process of sprouting from pre-existing networks, such as the primary vascular plexus in the yolk sac or the vasculature in injured tissues during wound healing. (Taken from Pepper, 1997)

B) Schematic representation of the angiogenic process. Endothelial cell activation is triggered by an angiogenic stimulus (A), which results in the degradation of the basement membrane by matrix metalloproteinases (B), which allows the extension of thin cytoplasmic processes in the direction of the stimulus (C). This is followed by cell migration into the surrounding matrix and the formation of a capillary sprout. The maturation phase occurs by reconstitution of the basement membrane and recruitment of pericytes and smooth muscle cells (SMCs), which protect the bare endothelial cells and function to inhibit proliferation and migration of the endothelial cells (D). (Adapted from Pepper, 1997 and Goumans et al., 2003).

The importance of TGF-β in vascular morphogenesis was revealed by the generation of genetically altered mice with targeted mutations in components of the TGF-β signalling pathway (Goumans, M. J. et al., 2000). Similar vascular defects were observed in *TGF-β1*, *TβRII*, *ALK5* and *Smad5* knockout mice, demonstrating clear roles in vasculogenesis, angiogenesis, haematopoiesis as well as smooth muscle cell differentiation. This evidence implicated a requirement for the components of the TGF-β pathway in coordinated signalling during formation of the circulatory system *in vivo*. Interestingly, highly similar phenotypes were also observed in *ALK1* and *Endoglin* null mice (Arthur, H. M. et al., 2000; Li, D. Y. et al., 1999; Oh, S. P. et al., 2000). In line with these observations, the regulation of TGF-β signalling in endothelial cells was investigated and revealed additional mechanisms not observed in other cell types. In addition to the prototypical TGF-β type I receptor (ALK5), endothelial cells also express a second type I receptor, ALK1. The expression of ALK1 is tightly restricted, with highest levels found in endothelial cells (Roelen, B. A. et al., 1997). It has been demonstrated that ALK1 can bind TGF-β1 in transfected COS cells (Attisano, L. et al., 1993; ten Dijke, P. et al., 1994a), and also in nontransfected endothelial cells (Oh, S. P. et al., 2000). In contrast to ALK5 which signals via Smad2 and Smad3, ALK1 signalling results in phosphorylation of Smad1 and 5, the specificity of which is determined by the L45 Loop sequence in the kinase domain (Figure 1.9) (Chen, Y. G. et al., 1999). Therefore, TGF-β stimulation induces phosphorylation of both Smads 2 and 3 and Smads 1 and 5 in these cells, whereas its targets are limited to Smads 2 and 3 in cells that lack expression of ALK1 (Chen, Y. G. et al., 1999; Goumans, M. J. et al., 2002; Oh, S. P. et al., 2000).

Further investigation into the mechanism by which ALK1 mediates TGF-β signalling revealed that ALK1-induced phosphorylation of Smad1 and -5 is inhibited in mouse embryonic endothelial cells deficient in ALK5 (Goumans, M. J. et al., 2003b). Moreover, biochemical studies demonstrated that ALK5 is required to recruit ALK1 into the TGF-β receptor complex in a TGF-β dependent manner (Goumans, M. J. et al., 2003b), presumably due to its higher affinity for TGF-β ligand than ALK1 (ten Dijke, P. et al., 1994a). In addition, the kinase activity of both ALK5 and TβRII is required for optimal TGF-β/ALK1-induced responses (Goumans, M. J. et al., 2003b).

The mechanism by which TGF-β signalling regulates angiogenesis has not been clearly defined. However, these biochemical studies prompted investigations as to how the individual type I receptors contribute to TGFβ signalling during angiogenesis. Both ALK1 and ALK5, are clearly required for embryonic angiogenesis, as demonstrated by the defect in vessel formation in mouse embryos lacking either one of them (Larsson, J. et al., 2001; Oh, S. P. et al., 2000; Urness, L. D. et al., 2000). To determine the individual roles of each receptor, investigators used constitutively active (ca) forms of ALK1 and ALK5, thereby circumventing dual receptor activation by stimulation with TGF-β. In embryonic endothelial cells, ALK5 induced transcription of the Smad3/4-dependent reporter construct, $(CAGA)_{12}$-luciferase, however, it was unable to activate the Smad5/4-dependent BRE-luciferase reporter (Goumans, M. J. et al., 2003b; Goumans, M. J. et al., 2002). In contrast, ALK1 specifically induced transcription of the BRE-luciferase reporter and not the $(CAGA)_{12}$-luciferase reporter. Both receptors stimulated the $(SBE)_4$-luciferase, which is responsive to all TGF-β family members (Jonk, L. J. et al., 1998). In agreement with this data, microarray analysis of ALK1 and ALK5 activity, revealed remarkable differences in their transcriptional gene targets (Ota, T. et al., 2002). Thus, ALK1 and ALK5 mediate TGF-β signalling through distinct transcriptional regulation of target genes, thereby increasing the diversity of responses.

The two phases of angiogenesis clearly require opposing actions (Table 1.3). In light of this and other accumulating evidence, a hypothesis has been proposed whereby TGF-β exerts differential responses via the individual type I receptors (Goumans, M. J. et al., 2003b; Goumans, M. J. et al., 2002; Lamouille, S. et al., 2002; Ota, T. et al., 2002). Plasminogen activator inhibitor type I (PAI-1) and fibronectin are induced specifically by ALK5 (Goumans, M. J. et al., 2002; Ota, T. et al., 2002), resulting in increased ECM deposition. PAI-1 is a potent inhibiter of EC migration *in vitro* and angiogenesis *in vivo* indicating that ALK5 may be involved in the antiangiogenic properties of TGF-β (Goumans, M. J. et al., 2003a). In addition, ALK5 specifically induced SM22α and other smooth muscle-related genes in HUVECs (Ota, T. et al., 2002), suggesting that TGF-β stimulates the differentiation of periendothelial cells. These data implicate a role for ALK5 in the resolution phase in angiogenesis. In contrast, ALK1 induced expression of Inhibitor of DNA binding 1 (Id1) and Id2

proteins (Goumans, M. J. et al., 2002; Ota, T. et al., 2002). Id proteins, helix-loop-helix proteins, act dominantly to inhibit other transcription factors such as Ets family members from promoting cell-cycle exit into a differentiated fate (Perk, J. et al., 2005). Interleukin 1 receptor like 1 (IL1RL1), which plays a role in cell growth, was also identified as a specific target for ALK1.These target genes suggest that ALK1 has a mitogenic effect on endothelial cells. In agreement with a role for ALK5 in the maturation stage, caALK5 activity has been shown to inhibit endothelial cell proliferation (Goumans, M. J. et al., 2002; Ota, T. et al., 2002) and migration (Goumans, M. J. et al., 2002). Conversely, ALK1 stimulates EC proliferation and migration in mouse embryonic endothelial cells. Ota and colleagues also showed that caALK5 clearly inhibits the formation of a tube-like network of HUVECs in 3-D collagen gels (Ota, T. et al., 2002), whereas caALK1 shad no significant effect.

The emerging scheme whereby ALK1 and ALK5 elicit distinct transcriptional programmes, and therefore biological actions helps to explain the multitude of TGF-β-induced effects during angiogenesis. However, in this model the regulation of the individual receptor activities is a critical factor for normal angiogenesis. Interestingly, it was shown that ALK1 not only induced biological responses distinct from those of ALK5, but also antagonised ALK5 transcriptional responses (Goumans, M. J. et al., 2003b). The mechanism by which this antagonism is achieved has not yet been elucidated but it is thought to act downstream of the receptors (Byfield, S. D. et al., 2004; Goumans, M. J. et al., 2003a) (Figure 1.14). In addition to the requirement for ALK5 in efficient ALK1 activation, the antagonistic effect of ALK1 on ALK5 activity provides an endothelial cell with a regulated TGF-β-controlled switch, which would then determine the fate of the cell, whether it is quiescence or active migration and proliferation. In addition, it has been revealed that endoglin, an accessory receptor of TGF-β, acts as a modulator of the balance between TGF-β/ALK1 and TGF-β/ALK5 signalling pathways (Lebrin, F. et al., 2004). Previous investigations have shown that mutations of the Endoglin and ALK1 genes are linked to the autosomal dominant disorder human hereditary hemorrhagic telangiectasia (HHT) type I and type II, respectively (Johnson, D. W. et al., 1996; McAllister, K. A. et al., 1994), a heterogenous disease which is characterised by bleeding through haemorrhage from vascular malformations (van den Driesche, S. et al., 2003). These data suggest that endoglin and ALK1 may act in the same pathway *in vivo*. Indeed, inhibition of

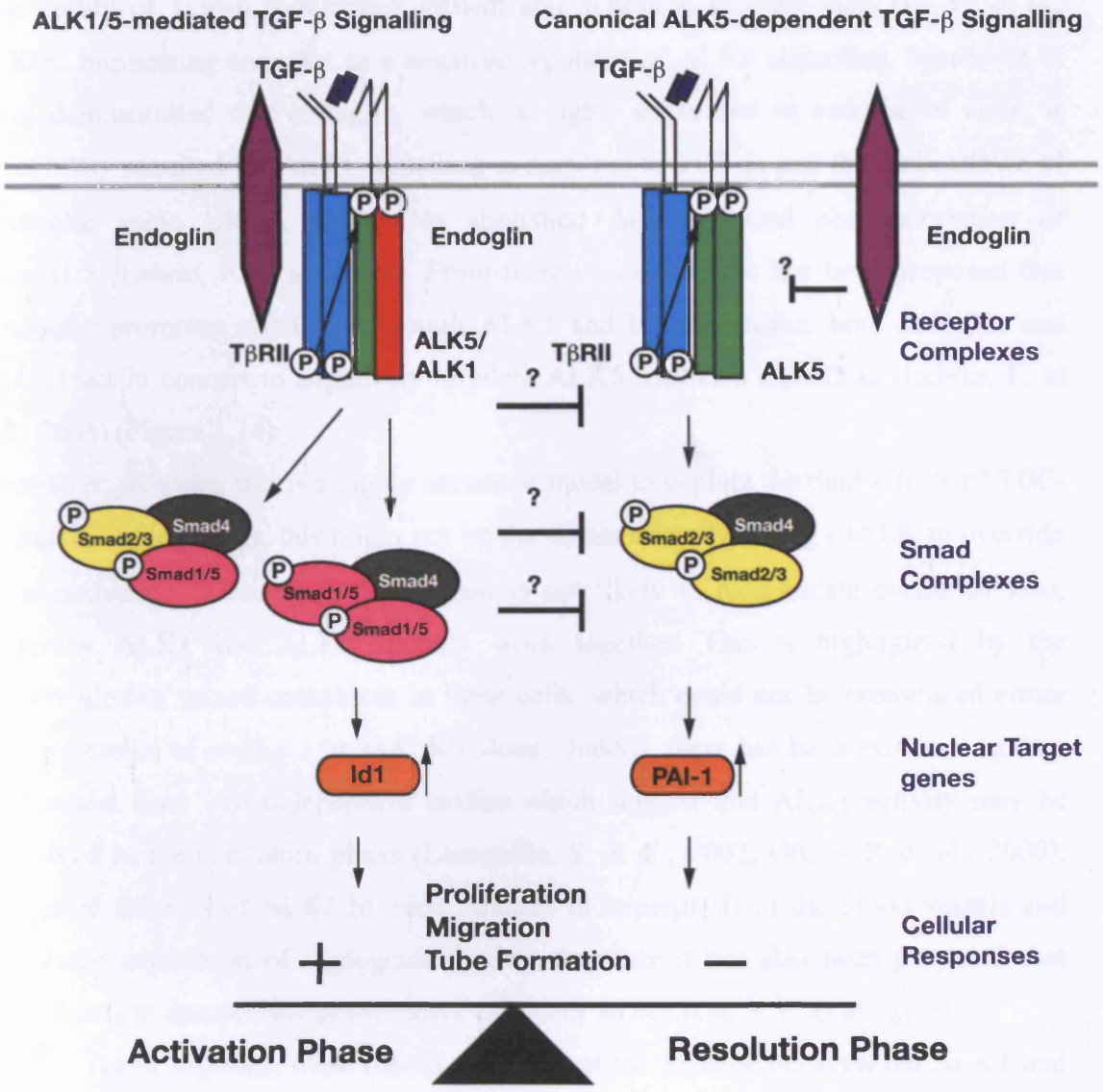

Figure 1.14. A model of the regulation of TGF-β signalling during Angiogenesis

TGF-β can stimulate two distinct type I receptor/Smad signalling pathwasy with opposite effects in endothelial cells. The TGF-β/ALK5 pathway induces transciption of PAI-1 and fibronectin which ultimately leads to inhibition of cell proliferation and migration, whereas, the TGF-β/ALK1 pathway induces Id1 expression and thus promotes enothelial cell proliferation and migration. Endoglin, an accessory TGF-β receptor, is essential for ALK1 signalling. In the absence of endoglin, the TGF-β/ALK5 signalling is predominant and maintains quiscence resulting in the resolution phase of angiogenesis. High endoglin expression stimulates the ALK1 pathway and indirectly inhibits ALK5 signalling, thus promoting the activation state of angiogenesis. Smad complexes downstream of ALK1/ALK5 receptor complexes are thought to mediate the antagonism of ALK5 activity by ALK1. (Adapted from Byfield and Roberts, 2004 and Goumans et al., 2003b).

endoglin translation in human umbilical vein endothelial cells (HUVECs), enhances the ability of TGF-β to suppress growth and migration in these cells (Li, C. et al., 2000), implicating endoglin as a negative regulator of ALK5 signalling. Moreover, it was demonstrated that endoglin, which is highly expressed in endothelial cells, is absolutely required for ALK1 signalling in response to TGF-β, and that knockdown of endoglin using siRNA completely abolished ALK1-induced phosphorylation of Smad1/5 (Lebrin, F. et al., 2004). From these observations it has been proposed that endoglin promotes signalling through ALK1 and by this means, both endoglin and ALK1 act in concert to negatively regulate ALK5 mediated signalling (Lebrin, F. et al., 2004) (Figure 1.14).

However, although this is a highly attractive model to explain the dual effects of TGF-β during angiogenesis, this might not be the whole story. By using caALK to override dual activation of receptor, this system is not likely to recapitulate events *in vivo*, whereby ALK1 and ALK5 actually work together. This is highlighted by the observation of mixed complexes in these cells, which could not be reproduced either by expression of caALK1 or caALK5 alone. Indeed, there has been evidence against the model from two independent studies which suggest that ALK1 activity may be involved in the resolution phase (Lamouille, S. et al., 2002; Oh, S. P. et al., 2000). Targeted deletion of ALK1 in mice, resulted in hyperplasis of the blood vessels and increased expression of angiogenic factors, therefore it has also been proposed that ALK1 acts to dampen the proliferative effects of ALK5 (Oh, S. P. et al., 2000).

Taken together, these results suggest that the balance between the ALK1 and ALK5 signaling pathways in endothelial cells plays a crucial role in determining vascular endothelial properties during angiogenesis. The specific expression of two TGF-β type I receptors on the surface of endothelial cells, allows the formation of two distinct receptor complexes, which signal via different Smad complexes to elicit opposing effects (Figure 1.14). The selective use of each complex by TGF-β is regulated on several levels, such as the requirement for a co-receptor, endoglin, and the antagonistic activity elicited by ALK1 signalling. These mechanisms are in place to ensure the correct signal is received during the highly complex process of angiogenesis.

1.6.3 Epithelial-Mesenchymal Transition (EMT)

Epithelium is the earliest tissue formed during embryogenesis by compaction of loosely adherent cells at the blastula stage or by cellularisation of the syncytial blastoderm. Epithelial cells form layers of cells that are closely adjoined by specialised membrane structures with distinct apical-basal polarity. This polarity manifests itself through the localised distribution of adhesion molecules and cell-cell junctions and the presence of a basement membrane or basal lamina (Schock, F. et al., 2002). The structures which mediate cell-cell and cell-matrix contact in epithelia include adherens junctions, tight junctions, desmosomes and gap junctions. The adherens junction is generally a circumferential junction located just basal to the apical-basolateral boundary (Figure 1.15). Adherens junctions are mediated by homotypic interactions of the extracellular domains of E-cadherin (cad for calcium dependent). Its major function is to link the actin cytoskeleton of neighbouring cells, which is mediated through interactions via α- and β-catenin. Tight junctions are located in the most apical lateral regions and seal the space between adjacent cells to prevent transport of molecules through the intercellular space. At a molecular level, tight junctions are mediated by transmembrane claudins, occludins and scaffold proteins such as ZO1 (TJP1), which associate with the intracellular actin cytoskeleton and various signalling systems. Epithelial cells under tension develop very strong adherenes junctions called desmosomes. Desmosomes support the integrity of the epithelial unit and cell–cell adhesions through cadherin molecules (desmoglein and desmocollin) and link the cell–cell adhesion molecules with cytoskeletal keratin fibers by desmosomal plaque proteins such as desmoplakin and plakoglobin (Getsios, S. et al., 2004).

Epithelial cells are motile and can move away from neighbouring cells, while remaining within the epithelial layer. Epithelia migrate either as a sheet, as during would closure, or as a tube. However, cells do not detach and move away from the epithelial layer under normal conditions. Most epithelia are single-layered, but a few adult epithelia are multilayered such as the stratified skin of mammals. Epithelial cell plasticity has been conserved in all metazoans. Epithelial sheets can undergo remodelling by various processes, including cell intercalation (the basis of body-plan formation in many species), invagination, evagination, branching and multilayering

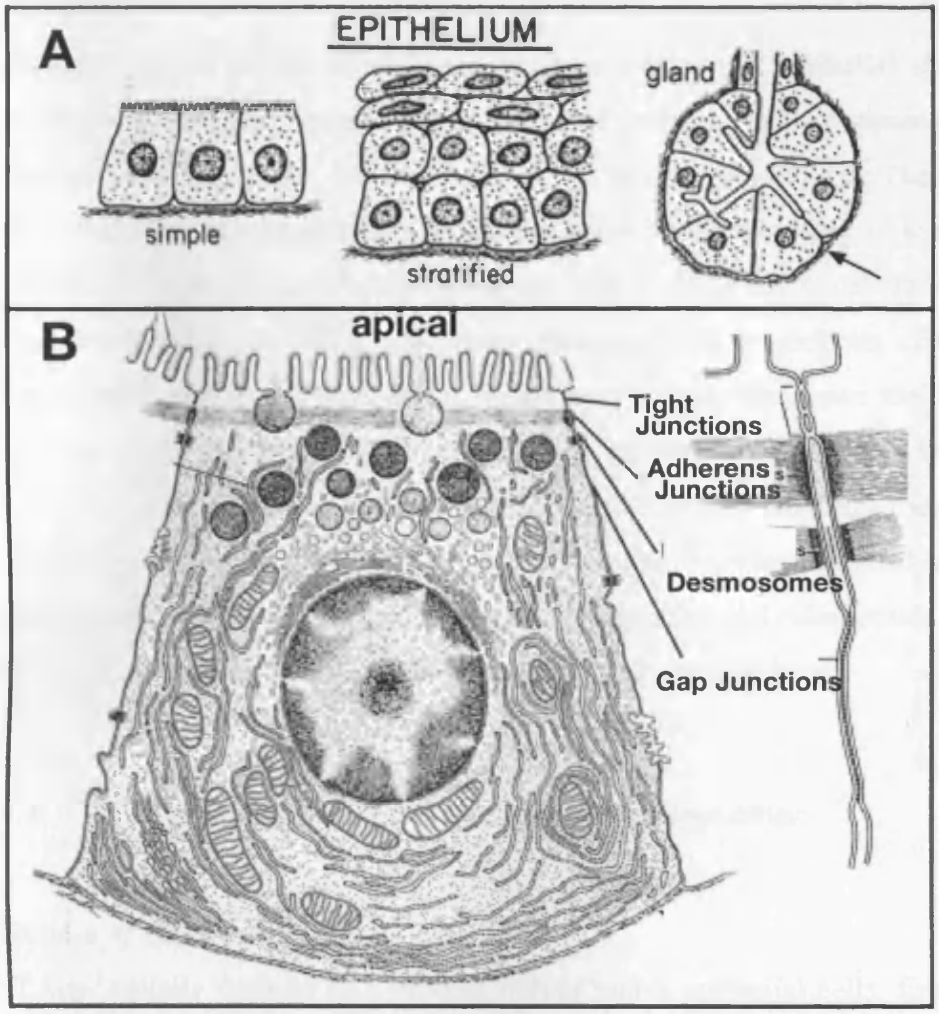

Figure 1.15. The structure of Epithelial and Mesechymal Cells

A) Organisation of epithelium. Most epithelium form a compact, single cell layer, however different packing arrangements of cells are also found, such as the multilayered skin of mammals.
B) Epithelial cells have apical-basal polarity. The apical (free) side may have microvilli. The basal actin cortex attaches the cytoskeleton to the underlysing basal lamina that contains collagen and laminin. They often secret glandular products from the apical surface and some also secrete ECM from the basal surface. Epithelial cells form tight contact with neighboring cells through numerous structures, including tight junctions, adherens junctions, desmosomes and gap junctions. (Adapted from Hay, 2005).

(Schock, F. et al., 2002). In addition, in most metazoans, epithelial sheets can be reversibly or irreversibly converted into mesenchymal cells by a process known as epithelial-to–mesenchymal transition (EMT) (Hay, E. D., 2005). The term EMT describes a series of events during which epithelial cells lose many of their epithelial characteristics and take on properties that are typical of mesenchymal cells. Epithelial and mesenchymal cells differ in various functions and phenotypic characteristics. Mesenchymal cells do not form an organised layer, nor do they have the same apical-basolateral organisation and polarisation of the cell-surface molecules and the actin cytoskeleton as epithelial cells. They contact neighbouring cells only focally, and are not typically associated with a basal lamina. In culture, mesenchymal cells have a spindle shaped, fibroblast-like morphology, whereas epithelial cells grow as clusters of cells that maintain complete cell-cell adhesion with their neighbours.

1.6.3.1 Mechanisms of EMT: Pathways and Regulation

Definition of EMT

EMT was initially defined as a process during which epithelial cells: first, acquire a fibroblastoid, invasive phenotype; second downregulate epithelial-specific proteins (for example, tight- and adherens-junction proteins) and induce various mesenchymal proteins (for example, vimentin); and third, digest and migrate through the extracellular matrix (ECM) (Grunert, S. et al., 2003). These criteria for EMT processes have been ascribed to three major physiological and pathophysiologcal contexts, including embryonic development and morphogenesis, cancer progression and metastasis, and chronic degenerative, fibrotic disorders of mature organs. Early embryonic events such as mesoderm formation during gastrulation, palate fusion and emigration of neural-crest cells from the neural tube involve EMT, including transcriptional loss of epithelial markers (E-cadherin) and induction of vimentin (See section 1.6.3.2). Significantly, a similar variety of epithelial-plasticity changes occur during pathological processes. It is increasingly appreciated that inflammatory mediators that are produced in response to injury of epithelial cells, can trigger EMT, which can lead to fibrosis. For example, EMT is a major contributor to the pathogenesis of renal fibrosis, as it leads to a substantial increase in the number of

myofibroblasts, leading to tubular atropy (Zeisberg, M. et al., 2003a). In addition, EMT can also contribute to lung fibrosis, chronic obstructive pulmonary disease and chronic asthma. The phenotypic changes observed in EMT events, are also reminiscent of a progressive metastatic carcinomas, such as conversion from a sessile to a migratory phenotype and proteolytic degradation of the basement membrane (Thiery, J. P., 2002). Over the past ten years, EMT has gained recognition as a central mechanism for carcinoma progression and metastasis (See section 1.6.3.4).

Molecular mechanisms of EMT

Early work on the regulation of EMT focused on embryonic development. However, the observation that a polarised epithelial line, Madin-Darby canine kidney (MDCK) cells, could be induced to scatter into individual, migratory cells by incubation with conditioned medium from cultured fibroblasts, opened up new avenues for *in vitro* experimental investigations (Stoker, M. et al., 1985). The factor involved in this transition was designated scatter factor (SF) and was later identified as hepatocyte growth factor (HGF) (Nakamura, T. et al., 1989; Naldini, L. et al., 1991). Over the last twenty years, EMT has received much attention and many *in vitro* and *in vivo* model systems have been established to investigate the signalling mechanisms involved in its regulation. Accumulating evidence from these studies show that a common set of molecular events occurs during the process of EMT. Primarily, the delocalisation and downregulation of adherens junction proteins, such E-cadherin has become a widespread marker for the progression of EMT and is associated with the loss of a polarised phenotype. Dramatic remodelling of the actin cytoskeleton and upregulation of mesenchymal proteins such as vimentin are also frequent events during EMT, which allows epithelial cells to become more migratory (Thiery, J. P., 2002). In addition, these systems have provided many insights into the molecular mechanisms governing EMT in both development and cancer progression and it has become clear that many parallels are being found between these two processes. In each model system, inducers of EMT signal via a specific set of downstream effectors to elicit the transition of polarised epithelial cells to a mesenchymal phenotype (Figure 1.16). Many signalling proteins, including TGF-β family members, receptor tyrosine kinases (RTKs), small GTPases, MAP kinases, integrins as well as matrix-metalloproteinases and extracellular matrix components have been implicated in the regulation of EMT

(Thiery, J. P. et al., 2006). These studies also show that extensive crosstalk exists between the signalling pathways that activate and repress EMT, and that EMT-inducing signalling pathways have many common endpoints, including downregulation of E-cadherin and expression of EMT-associated genes. In contrast, however, developmental EMT events are regulated by a particular subset of EMT activators and repressors. This is highlighted by the discriminatory ability of specific isoforms of TGF-β to elicit developmental EMT *in vivo*. For example, TGF-β2 regulates EMT in the atrioventricular canal, whereas TGF-β3 regulates EMT during palatal fusion (See section 1.6.3.2).

Epithelial plasticity is triggered by an interplay of extracellular signals, including components of the extracellular matrix (ECM), such as collagen and hyaluronic acid, as well as soluble growth factors such as members of the TGF-β and fibroblast growth factor (FGF) families, epidermal growth factor (EGF) and SF/HGF (Thiery, J. P. et al., 2006) (Figure 1.16). Studies using *in vitro* models of EMT have revealed that these growth factors can induce alterations in epithelial plasticity termed 'scattering' or else a complete EMT, depending on the specific cell system analysed (Grunert, S. et al., 2003). The common denominator of these processes is a morphological change to a spindle-like phenotype. Scattering occurs by exposure of cells to growth factors or inducible oncogenes for 48 hours or less, which induces a fibroblastoid, migratory phenotype concomitant with a loss of epithelial polarity, characterised by a downregulation of epithelial markers (Miettinen, P. J. et al., 1994; Piek, E. et al., 1999). However, these cells fail to turn on mesechymal gene-expression programmes (Janda, E. et al., 2002). In contrast to scattering, full EMT is completed only after 4-6 days of exposure to several signals and occurs only in certain cell types. One critical difference is the persistence of a mesenchymal phenotype, even after removal of the inducing agent, which can be achieved through the induction of an autocrine loop (Oft, M. et al., 1996). The differences observed *in vitro* can be explained by the observation that different signals can cause qualitatively different alterations of epithelial plasticity in the same cell type (Janda, E. et al., 2002). Therefore, the precise spectrum of changes that occur during EMT is probably determined by the integration of extracellular signals the cell receives. Another critical parameter for inducing scattering or EMT appears to be acute versus chronic signal exposure (Grunert, S. et al., 2003). Due to these differences observed, it has been

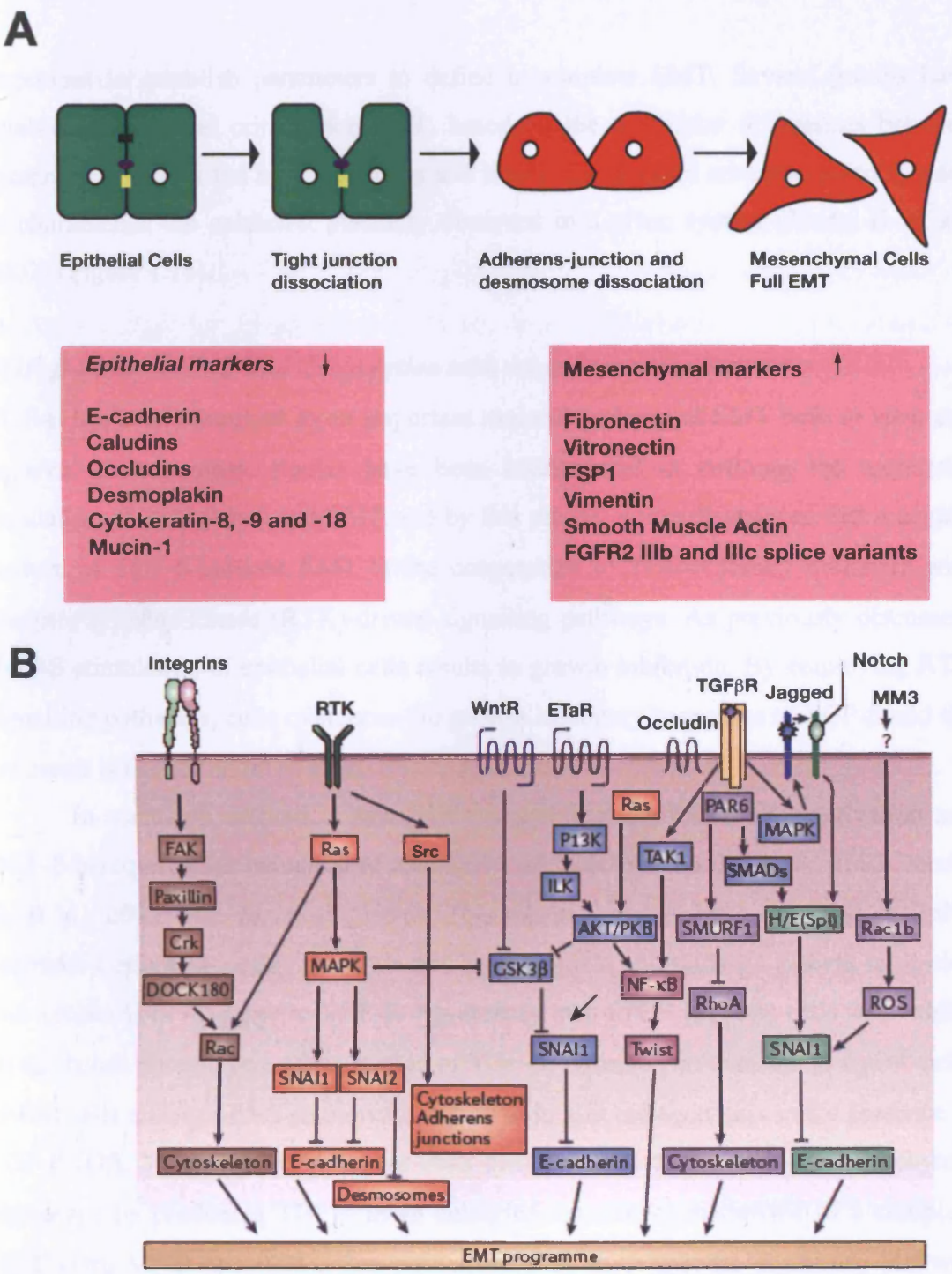

Figure 1.16. Overview of the signalling networks that regulate EMT events

A) Schematic diagram of the cycle of events duing EMT. The different stages during which epithelial cells are transformed into mesenchymal cells is shown. For a complete EMT process to occur epithelial junction proteins are delocalised and donwregulated, resulting in a loss of epithelial polarity. In addition, mesenchymal proteins are upregulated. A number of markers have been identified that are characteristic of either epithelial cells or mesenchymal cells, which are listed here.
B) Overview of the signalling pathways that are involved in the regualtion of EMT. ETaR, endothelin-A receptor; FAK, focal adhesion kinase; GSK3β, glycogen-synthase kinase-3β; H/E(Spl), hairy/enhancer of split; ILK, integrin-linked kinase; MAPK, mitogen-activated protein kinase; NF-κB, nuclear factor-κB; PAR6, partitioning-defective protein-6; PI3K, phosphatidylinositol 3-kinase; PKB, protein kinase-B; ROS, reactive oxygen species; TAK1, TGF-β-activated kinase-1; TGFβR, TGF-β receptor; WntR, Wnt receptor. (Adaptated from Thiery and Sleeman 2006).

important to establish parameters to define a complete EMT. Several groups have established essential criteria for EMT, based on the molecular differences between mesenchymal cells and epithelial cells and molecular markers are now routinely used to characterise the epithelial plasticity observed in a given system (Janda, E. et al., 2002) (Figure 1.16).

TGF-β-induced EMT and Cooperation with other Signalling Pathways

TGF-β has been identified as an important molecular player of EMT both *in vitro* and *in vivo*. Tissue-culture studies have been instrumental in defining the molecular regulation of TGF-β-induced EMT and by this means, it was discovered that a central feature of TGF-β-induced EMT is the cooperation of TGF-β family members with receptor tyrosine kinase (RTK)-driven signalling pathways. As previously discussed, TGF-β stimulation of epithelial cells results in growth inhibition. By employing RTK signalling pathways, cells overcome the growth inhibitory responses to TGF-β and the net result is the induction of EMT.

In some cell systems, a synergistic cooperation between H-Ras activation and TGF-β is required for induction of a complete EMT (Gotzmann, J. et al., 2002; Janda, E. et al., 2002; Oft, M. et al., 1996). This mechanism has been explored in EpH4 mammary epithelial cells, which are non-tumourigenic and undergo growth inhibition and apoptosis in response to TGF-β. Ras-transformed EpH4 (EpRas) cells still exhibit an epithelial phenotype in the absence of TGF-β, however, in contrast to EpH4 cells, EpRas cells undergo EMT and invasive growth in 3-D collagen gels in the presence of TGF-β (Oft, M. et al., 1996). These cells then continue to maintain a mesenchymal phenotype by producing TGF-β in an autocrine manner, characteristic of a complete EMT (Oft, M. et al., 1996). The participation of each specific signalling pathway activated by TGF-β and/or H-Ras to induce EMT has also been elucidated (Janda, E. et al., 2002). In this study, Beug and colleagues implicate the requirement of MAPK activity for TGF-β-induced EMT, tumourigenesis and metastasis, whereas they show that Ras-induced PI3K activity promotes cell scattering and rescues cells from TGF-β-induced cell-cycle arrest and apoptosis (Janda, E. et al., 2002). Similarly, the cooperation between Ras and TGF-β signalling pathways are involved in

hepatocarcinogenesis, where PI3K signalling is important in maintaining the fibroblastoid phenotype of hepatocytes (Gotzmann, J. et al., 2002).

The synergism between Ras and TGF-β signalling has also been observed in models of tumour progression. Tumour cell lines derived from sequential stages of mouse skin carcinogenesis, show elevated TGF-β signalling and an increase in mutated H-Ras during progression to the metastatic phenotype, from squamous carcinoma cells to spindle-cell carcinomas (Buchmann, A. et al., 1991; Oft, M. et al., 2002). In an elegant study by Oft and colleagues using this model, they showed that squamous carcinoma cells cannot undergo EMT by TGF-β alone, but require a cooperation between TGF-β signalling and H-Ras, which mimics the *in vivo* progression towards the spindle-cell carcinoma stage (Oft, M. et al., 2002). Activated Smad2 or Smad3, co-expressed with H-ras induce upregulation of mesenchymal markers such as vimentin and α-smooth muscle actin, whereas expression of either Smad or H-Ras alone, cannot induce a full EMT. Here, it has been claimed that H-Ras induces nuclear accumulation of P-Smad2 and consequent upregulation of transcription, whereas Smad2 is required for maintaining the mesenchymal phenotype (Oft, M. et al., 2002). Furthermore, it has been proposed that a high threshold of H-Ras activity is needed for PI(3)K activation, which is required for protection against TGF-β-induced apoptosis, a model which is consistent with the EpRas model (Janda, E. et al., 2002; Oft, M. et al., 2002). In addition, constitutive Raf signalling in an immortalized dog kidney epithelial line, MDCK cells, is able to induce EMT, leading to the establishment of an autocrine TGF-β loop that promotes invasive behavior of the cells in collagen gels *in vitro* (Lehmann, K. et al., 2000). In this model strong activation of Raf, and, consequently, the ERK MAP kinases, protects the cells from the growth inhibitory and apoptotic effects of TGF-β, while enhancing the invasive responses (Lehmann, K. et al., 2000). It is now essential to further analyse at which levels these two pathways cooperate to abrogate the classical functions of TGF-β in growth arrest and induction of apoptosis (See Chapter 5 and Chapter 6).

NF-κB, a transcriptional regulator of inflammatory and innate immune responses, has also been implicated in the progression of EMT (Huber, M. A. et al., 2004b). A recent study using the EpRas EMT model, revealed the NF-κB signalling pathway as a modulator of TGF-β-induced EMT (Huber, M. A. et al., 2004a). TGF-β

stimulation leads to induction of a functionally active NF-κB in EpRas cells, which is required in combination with oncogenic Ras for efficient protection of EpRas cells from TGF-β induced apoptosis (Huber, M. A. et al., 2004a). Interestingly, activation of NF-κB activity by a constitutively active (ca) IKK-2/β mutant promoted EMT and induced a partial EMT-phenotype even in the absence of TGF-β (Huber, M. A. et al., 2004a). This observation suggests that NF-κB can partly substitute for the essential role of TGF-β in the collaboration with Ras, leading to EMT. Also, inhibition of NF-κB activity reverses the TGF-β-induced EMT in mesenchymal cells, which suggests that NF-κB is essential for both induction and maintenance of EMT (Huber, M. A. et al., 2004b). TGF-β activates TGF-β-activated kinase 1(TAK1), which has been shown to induce NF-κB activation by phosphorylation of the IKK complex in response to TGF-β, thus providing a potential mechanism of crosstalk between the two signalling pathways (Arsura, M. et al., 2003) (Figure 1.16). In addition, the Ras-activated PI3K-Akt/PKB pathway has also been implicated in NF-κB activation, suggesting the possibility of crosstalk between all three pathways (Huber, M. A. et al., 2004b). Downstream targets of NF-κB activation may include the transcription factors twist and snail, which are induced by NF-κB and act to repress E-cadherin expression (Bachelder, R. E. et al., 2005; Sosic, D. et al., 2003).

Accumulating evidence also implicates cooperative signalling between β-catenin/LEF and TGF-β during EMT (Eger, A. et al., 2004; Eger, A. et al., 2000; Liebner, S. et al., 2004; Nawshad, A. et al., 2003). β-catenin is an integral component of E-cadherin-type adherens junctions in epithelial cells (Eger, A. et al., 2000). It also functions as a downstream effector of the wnt/wingless signalling cascade and interacts with transcription factors of the LEF/TCF family, regulating gene expression and cell-fate decisions during embryonic development (Peifer, M. et al., 2000). Aberrant nuclear expression of β-catenin is a frequent event during tumour progression, occurring through loss of E-cadherin or mutations in β-catenin or APC (Bienz, M. et al., 2000). It was previously shown that long-term stimulation of an inducible c-fos estrogen receptor (c-FosER) in mouse mammary epithelial cells induces EMT (Reichmann, E. et al., 1992), and this process was accompanied by a dramatic reduction in E-cadherin expression, resulting in β-catenin nuclear translocation and upregulation of β-catenin/lymphoid enhancer binding factor-1

(LEF1) transcriptional activity (Eger, A. et al., 2000). Further investigation revealed that autocrine production of TGF-β is induced at late stages of EMT, which cooperates with β-catenin to maintain an undifferentiated mesenchymal phenotype (Eger, A. et al., 2004). This cooperation was convincingly demonstrated by simultaneous inhibition of both pathways, which reverted mesechymal FosER cells to a polarized epithelial phenotype, whereas inhibition of a single pathway caused only partial rescue of epithelial features (Eger, A. et al., 2004). In addition, TGF-β2 induction of EMT of endocardial cells in the developing heart is accompanied by activation of β-catenin activity *in vivo* (Liebner, S. et al., 2004). Indeed, targeted deletion of β-catenin in endothelial cells severely impaired formation of the heart cushion and AV explants from β-catenin deficient mice failed to undergo TGF-β2-induced EMT *in vitro* (Liebner, S. et al., 2004). Insights into the molecular mechanism for the cooperation of the β-catenin/LEF and TGF-β pathways were uncovered with the demonstration that the Smad2, 3 and 4 can physically interact with members of the LEF/TCF family of HMG-box proteins to activate transcription of LEF/TCF target genes (Labbe, E. et al., 2000; Nishita, M. et al., 2000). However, it has also been shown that TGF-β can activate LEF1/TCF target genes in the absence of β-catenin. During palatogenesis, TGF-β stimulates Smad2/4-dependent induction of LEF1, a downstream target of Wnt/β-catenin signalling independently of β-catenin (Nawshad, A. et al., 2003). It was also demonstrated that while LEF1 and Smad4 were required for TGF-β-induced palatal EMT, β-catenin was not (Nawshad, A. et al., 2003).

Role of the Smads

The role of Smad3 and Smad4 in TGF-β-induced EMT was initially established in the mouse mammary epithelial line, NMuMG cells (Piek, E. et al., 1999). Cells, infected with retroviruses expressing a combination of Smad3 and Smad4, together with a low dose of caALK5, resulted in a differentiation of these cells to a mesenchymal phenotype. The transdifferentiation was less well pronounced when Smad3 was replaced with Smad2, suggesting a more prominent role for Smad3 in TGF-β-mediated EMT. Further investigations in this model system, eliminated a role for Smads of the BMP branch in eliciting EMT, and implicated only the (Valcourt, U. et al., 2005). In addition to these *in vitro* studies, Smad3 null mice were employed in numerous studies

to ascertain the role of Smad3 in EMT and fibrosis *in vivo* (Saika, S. et al., 2004b; Saika, S. et al., 2004c; Sato, M. et al., 2003). In a model of renal fibrosis, injury was induced by unilateral uretal obstruction (UUO), which led to the progression of EMT wild type renal tubular cells, resulting in fibrosis of the kidney, which was absent in Smad3 null mice (Sato, M. et al., 2003). In this model, Smad3 induced upregulation of Snail and α-SMA and autocrine signalling of TGF-β, however these EMT associated events were abrogated in Smad3 null mice, indicating that the transition of renal tubular epithelial cells to myofibroblasts is mediated by a Smad3-specific mechansim (Sato, M. et al., 2003). Similar results for the requirement of Smad3 were demonstrated in models of EMT induced injury in the eye, including a lens injury model and partial detachment of the retina to model proliferative vitreoretinopathy (PVR) (Saika, S. et al., 2004b; Saika, S. et al., 2004c).Consistent with these observations, TGF-β fails to induce EMT in primary tubular epithelial cells derived form kidneys of *Smad3* knockout mice (Zavadil, J. et al., 2004).

In addition, hepatocytes isolated from liver-specific Smad3 knockout mice failed to undergo EMT, whereas the *Smad2* knockout hepatocytes spontaneously transition to a mesenchymal phenotype in the absence of TGF-β (Ju, W. et al., 2006). This suggests that Smad2 may function to maintain an epithelial phenotype, whereas Smad3 is required for induction of EMT. However, although Smad3 appears to play a more prominent role in EMT than Smad2, this is not always the case. In squamous carcinoma cells, where TGF-β signalling in concert with H-Ras activation, is required for a full EMT, expression of an activated form of either Smad2 or Smad3 with H-Ras was sufficient to induce a full EMT (Oft, M. et al., 2002). Also, Smad2 activity was convincingly shown to act downstream of TGF-β, to enhance the invasive and metastatic properties of spindle tumour cells (Oft, M. et al., 2002). In addition, Smad2 mediates TGF-β induced EMT during palatal fusion (Cui, X. M. et al., 2003; Nawshad, A. et al., 2003). Formation of the secondary palate (palatogenesis) in Smad3 null mice is unimpaired (Yang, X. et al., 1999), further supporting the role for Smad2 in EMT during palatal fusion (Nawshad, A. et al., 2005).

Although Smad3 is often an essential component of the signalling pathway during EMT, a recent study revealed that the level of Smad3 is gradually downregulated during EMT in MDCK cells (Nicolas, F. J. et al., 2003b). In this study, the Smad3 levels were decreased to low levels but they never completely disappeared.

The activation of the Raf/ERK MAPK pathway in these cells induces autocrine TGF-β production, which then synergises with ERK/MAPK to induce EMT. By this means, MDCK cells are protected from the growth inhibitory and apoptotic effects of TGF-β (Lehmann, K. et al., 2000). Strong evidence supports an essential role for Smad3 in TGF-β-induced growth arrest, and it was demonstrated that the gradual loss of Smad3 during EMT is sufficient for these cells to lose their ability to undergo growth arrest in respone to TGF-β (Nicolas, F. J. et al., 2003b). Ectopic expression of Smad3 restores the growth inhibitory response to TGF-β, however the cells do not revert to an epithelial phenotype. The loss of Smad3 during EMT provides a mechanism by which cells overcome the growth inhibitory responses to TGF-β, whereas the low Smad3 level is still sufficient to transduce the invasive effects of TGF-β.

Critical roles for the inhibitory Smads, Smad6 and Smad7 in EMT processes have also been suggested. Several studies have implicated Smad6 as a negative regulator of EMT in the atrioventricular (AV) cushion of the developing heart (Desgrosellier, J. S. et al., 2005; Galvin, K. M. et al., 2000; Yamada, M. et al., 1999) (Figure 1.21). In support of this, Smad6 mRNA exhibits a highly restrictive pattern, with high levels expressed during endocardial EMT in both mouse and chick (Galvin, K. M. et al., 2000; Yamada, M. et al., 1999). Hyperplasia of the cardiac valves in Smad6 null mice, due to excess mesenchymal cells, further supports an inhibitory role for Smad6 in EMT in the developing heart (Galvin, K. M. et al., 2000). The type I receptor, ALK2, is sufficient to induce EMT in the chick heart and it has been suggested that Smad6 may act to inhibit ALK2 signalling, since Smad6 is a selective antagonist of BMP signalling (Desgrosellier, J. S. et al., 2005; Hata, A. et al., 1998) (See section 1.6.3.2 and Figure 1.21). Indeed, overexpression of Smad6 in AV cushion chick explants resulted in decreased EMT, supporting a role for Smad6 as a negative regulator of EMT (Desgrosellier, J. S. et al., 2005). In contrast, Smad7 acts specifically in Smad3 mediated EMT, as its overexpression consistently inhibits Smad3-dependent EMT progression (Zavadil, J. et al., 2005). For example, adenoviral infection of NMuMG cells with Smad7, abrogated the robust TGF-β-induced EMT *in vitro* (Valcourt, U. et al., 2005). In addition, injury-induced EMT of lens epithelial cells (Saika, S. et al., 2004a) and UUO model of EMT (Lan, H. Y. et al., 2003) were blocked *in vivo* by ectopic expression of Smad7, providing strong evidence for the inhibitory role of Smad7 in Smad3-dependent EMT.

The role of Smad4 has been more difficult to define. Conflicting data suggest either a requirement for Smad4 or Smad4 independency during TGF-β mediated EMT in NMuMG cells or Colo-357 cells, respectively (Deckers, M. et al., 2006; Levy, L. et al., 2005). This contradiction may be explained by differences in cell type, with particular reference to the contributing signalling pathways for TGF-β induction of EMT. In Colo-357 cells, TGF-β cooperates with K-Ras to elicit a transition from an epithelial cell to a fibroblastoid phenotype, whereas NMuMG cells signals through Smad-dependent and independent pathways, including PI3 kinase and p38-MAPK, to achieve a mesenchymal state (Bakin, A. V. et al., 2002; Bakin, A. V. et al., 2000). These differences may underlie the controversial data obtained. In addition, it is important to note that the use of NMuMG cells as a model system for EMT is somewhat controversial. These cells exhibit an epithelial polarity but also express the mesenchymal marker vimentin. Furthermore, EMT is achieved within a short time frame of approximately 36 hrs and after this time, the cells cease to proliferate but grow in size. Thus, requirement of EMT effectors in this system might differ dramatically from other systems and as a result, observations in these cells should be confirmed elsewhere.

Smad Independent Signalling During EMT Pathways

Tight junctions help establish polarity in mammalian epithelia by forming a physical barrier that separates apical and basolateral membranes. During EMT, tight junctions dissolve and their essential components are downregulated. A recent study by Wrana and colleagues revealed a direct link between the components of tight junctions and the TGF-β receptors. In NMuMG cells, a major component of tight junctions, occludin, was found to bind directly to ALK5 and promote its recruitment (Ozdamar, B. et al., 2005). In addition, a component of an epithelial polarity complex, Par6 was also identified as an interacting protein of ALK5. Upon stimulation with TGF-β, Par6 located in the occuldin-ALK5 complex, is phosphorylated on Ser345 by TβRII. This protein interaction is direct and independent of Smad proteins (Ozdamar, B. et al., 2005). Interestingly, expression of a Par6 mutant, which cannot be phosphorylated by the type II receptor, completely abrogated downregulation of Zona-Occludins 1 (Z0-1), without affecting Smad activation. This resulted in a partial progression of TGF-β-induced EMT. Phosphorylation of Par6 allows it to recruit Smurf1, which in turn

mediates ubiquitination of RhoA, a small GTPase family member involved in cytoskeletal reorganisation. This leads to local disassembly of the actin cytoskeleton and dissolution of tight junctions (Ozdamar, B. et al., 2005). Depletion of Smurf1 or use of RhoA mutants lacking ubiquitination sites, inhibited the downregulation of tight junction components. This work revealed not only a Smad-independent pathway, but also the first example of a non-TGF-β receptor substrate for the type II receptor, which acts to alter a cell surface protein complex structure, independently of transcription.

Transcriptional Programmes of TGF-β in EMT

Expression profiling by microarray analysis has identified genes specifically regulated during TGF-β-induced EMT, including genes with defined roles in cell proliferation, epithelial polarity, cell-matrix interaction, cell motility and survival (Jechlinger, M. et al., 2003; Xie, L. et al., 2003; Zavadil, J. et al., 2001). In addition, profiling of polysome-bound mRNA revealed that a substantial number of these genes were regulated at the translational level including ILEI and Tenascin C (Jechlinger, M. et al., 2003; Waerner, T. et al., 2006). A phlethora of transcriptional regulators have also been identified as downstream targets of TGF-β at the onset of EMT (Zavadil, J. et al., 2005). Interestingly, it has been revealed that a major target of these transcription factors is the transcriptional repression of the E-cadherin gene, which leads to a downregulation of E-cadherin expression, a hallmark of EMT (Thiery, J. P. et al., 2006). This discovery has prompted extensive studies to define the role of these transcriptional repressors in EMT during embryonic development and during the acquisition of invasive properties in epithelial cells.

E-cadherin, a homophilic Ca^{2+}-dependent transmembrane adhesion protein, and and its associated catenins are among the major constituents of the epithelial cell junction system (Schock, F. et al., 2002). Epithelial-specific expression of E-cadherin is governed by regulatory elements in the E-cadherin promoter, namely two E2 boxes (CACCTG) (Peinado, H. et al., 2004). Subsequently, it has been revealed that transcriptional repressors can downregulate E-cadherin by binding to proximal E-boxes, particularly in the E-pal element in the mouse promoter (Cano, A. et al., 2000). The first transcriptional repressor of E-cadherin to be identified was the zinc finger protein, Snail1, whereby its stable expression led to the loss of E-cadherin expression and induction of EMT (Batlle, E. et al., 2000; Cano, A. et al., 2000). Snail repression

of E-cadherin was also observed during mesoderm formation in early embryonic development and in neural crest cells which undergo EMT (Carver, E. A. et al., 2001). In vertebrates, three members of the Snail family of zinc-finger transcription factors have been identified, Snail1 (Snail), Snail2 (also known as Slug) and the most recent family member, Snail3 (Barrallo-Gimeno, A. et al., 2005). Snail2 is also a strong repressor of E-cadherin, however it binds with a lower affinity than Snail1 to the proximal E-boxes (Bolos, V. et al., 2003). Ectopic expression of Snail2 results in repression of E-cadherin and is sufficient to induce complete EMT in MDCK cells (Bolos, V. et al., 2003; Hajra, K. M. et al., 2002). The central role of Snail1 in EMT was highlighted by the complex regulation of Snail1 stability, subcellular localisation and function by the activity of glycogen-synthase kinase-3β (GSK-3β) (Zhou, B. P. et al., 2004). It was recently discovered that Snail is highly unstable, which is governed by dual phosphorylation events mediated by GSK-3β. GSK-3β phosphorylates two serine residues on Snail1, one which targets Snail1 for ubiquitination and degradation, whereas the other promotes its nuclear export (Zhou, B. P. et al., 2004). Mutations in Snail1 that prevent GSK-3β phosphorylation result in a stabilised form of Snail1 that localizes in the nucleus and induces EMT. Thus, GSK-3β activity maintains the integrity of adherens junctions and of epithelial phenotype by inhibition of Snail1 activity. Consistent with a role in EMT, Snail is expressed in high-grade human breast carcinoma tissues and also in lymph-node-positive tumours (Blanco, M. J. et al., 2002). Moreover, an inverse correlation has been shown between E-cadherin and Snail levels in breast carcinoma and oral squamous-cell carcinoma (Blanco, M. J. et al., 2002; Yokoyama, K. et al., 2001).

TGF-β has also been shown to regulate Snail, by inducing expression of Snail in epithelial cells (Peinado, H. et al., 2003). This induction was abrogated using the MEK1/2 inhibitor suggesting that it requires MEK1/2 activity. However, expression of a dominant negative Smad4 mutant had no effect, and it was proposed that the effects of TGF-β on Snail reporter are Smad4-independent. The dominant negative Smad4 mutant was been found to be highly unstable compared with wild type Smad4 and as such, its use is not representative of inactivating Smad4 signalling (Maurice, D. et al., 2001). It has also been shown that TGF-β synergistically cooperates with either FGF or H-Ras to induce Snail1 transcription and use of the well characterised Ras mutants, which selectively signal along either the MAPK pathway, the PI3K pathway or the

Ral-GDP pathway, revealed that both MAPK and PI3K pathways are required for the H-Ras /TGF-β mediated induction of the Snail promoter (Peinado, H. et al., 2003). Futhermore, TGF-β activation of Snail1 and Snail2 in primary mouse kidney epithelial cells was found to be mediated via Smad3, since Smad3 null cells are unable to induce transcription of either Snail genes (Zavadil, J. et al., 2004). This evidence strongly argues in favour of Smad3 requirement for Snail induction. In addition, different members of the Snail family members can be regulated by different TGF-β isoforms, for example, TGF-β3 regulates transcription of Snail1 during EMT of palate fusion (Martinez-Alvarez, C. et al., 2004), whereas TGF-β2 induces Snail2 expression in endocardial cells to initiate cushion formation during heart development (Romano, L. A. et al., 2000). Snail1 and Snail2 have been shown to be key components in initiating EMT of the neural crest cells, however the inductive signals for expression, vary for different species (Tucker, R. P., 2004). In chick, BMP signalling is crucial for Snail2 expression and inhibition of BMP activity by implanting noggin by the neural folds *in vivo* or *in vitro* abolishes Snail2 expression (Selleck, M. A. et al., 1998).

Increasing investigation into the mechanisms that repress E-cadherin has uncovered numerous transcription factors that function similarly to the Snail family such as the prototypical vertebrate members of the two-handed zinc finger/homeodomain protein family, ZEB-1 (δEF1) and ZEB-2 (SIP1) (Comijn, J. et al., 2001; Eger, A. et al., 2005) (Figure 1.17). ZEB-2 was originally identified as a Smad interacting, binding to the MH2 domain of Smad1 and has subsequently been found to interact with Smad2, Smad3 and Smad5, although the significance of this is not clear (Verschueren, K. et al., 1999). ZEB-2 can be induced by TGF-β and its stable expression in MDCK cells significantly downregulates E-cadherin, resulting in loss of cell-cell adhesion, activation of invasion and migration (Comijn, J. et al., 2001). Similarly, ZEB-1 has been shown to interact with the E-cadherin promoter and its expression in mammary epithelial cells causes these cells to undergo EMT resulting in an invasive phenotype (Comijn, J. et al., 2001; Eger, A. et al., 2005). A more recent finding has revealed that Twist, the basic Helix-Loop-Helix (bHLH) transcription factor that is important in developmental events, is also involved in the downregulation of E-cadherin (Yang, J. et al., 2004). Ectopic expression of Twist in MDCK cells causes transcriptional repression of E-cadherin, α-, β- and γ- catenins, and expression of mesenchymal markers including fibronectin, vimentin, smooth muscle actin and N-

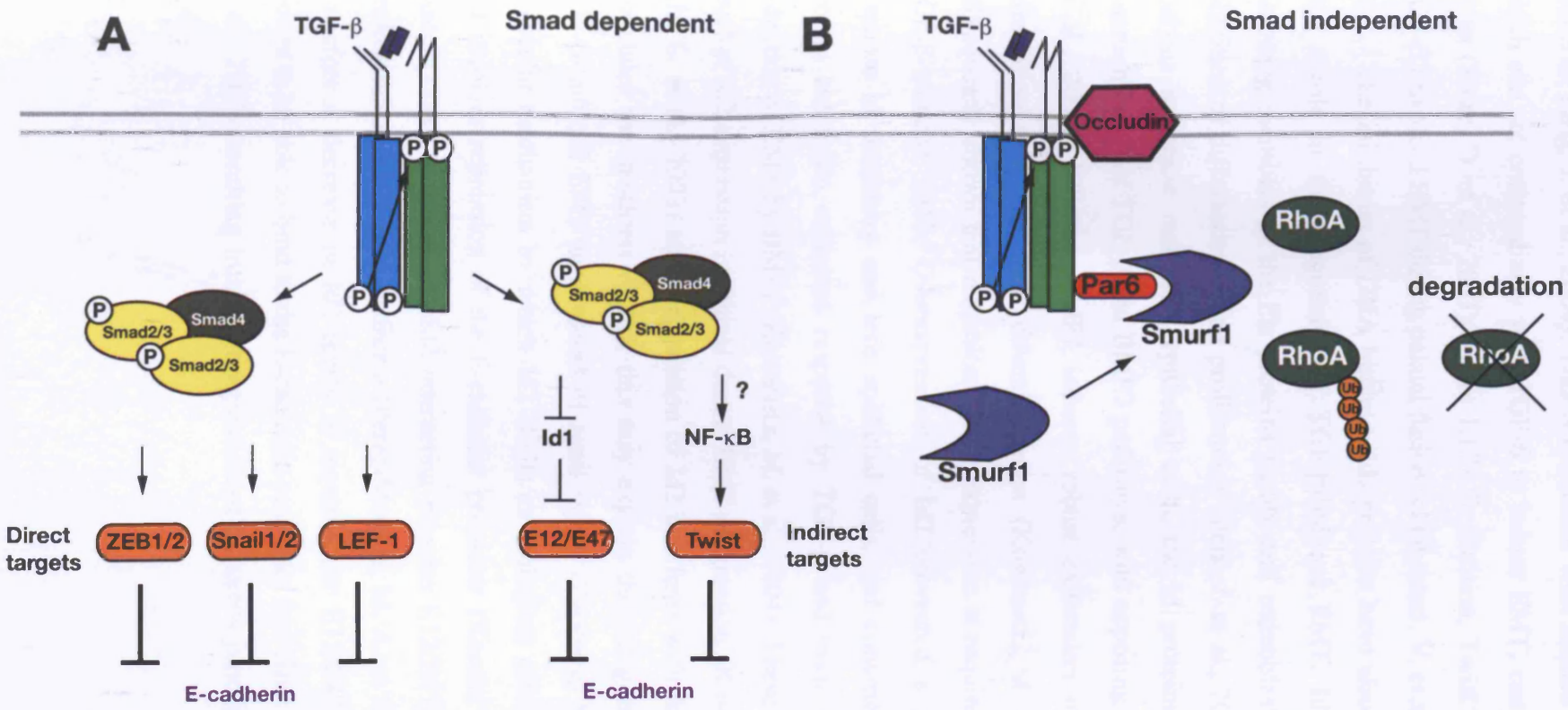

Figure 1.17. Mediators of TGF-β signalling during EMT

TGF-β signals via Smad-dependent and Smad-independent mechansims to elicit downstream responses which mediate.
A)TGF-β signalling via Smad2/3 complexes with Smad4 leads to activation of multiple transcription factors which function by repressing of the E-cadherin promoter. Downregulation of E-cadherin results in loss of E-cadherin-dependent intercellular epithelial junctional complexes, and E-cadherin-mediated sequestering of β-catenin in the cyoplasm is abolished. As a result, β-catenin localises to the nucleus and feeds into the Wnt signalling pathway by activating transcriptional regulation through LEF1/TCF4.
B) TGF-β induces the recruitment of TβRII to the preexisting ALK5-Occludin-Par6 Complex.TβRII phosphorylates Par6, which then binds to Smurf1. Smurf ubiquitinates RhoA, which is degraded in the proteasome. Subsequent loss of the actin network leads to the disassembly of tight junctions, possibly followed by adherens junction dissolution. However, adherens junction disintegration likely occurs through a Smad-dependent pathway after transcriptional repression of the E-cadherin gene. (Adapted from Thiery and Huang, 2005).

cadherin(Yang, J. et al., 2004). This is consistent with studies indicating that NF-κB, which can act cooperatively with TGF-β to induce EMT, can activate expression of Twist (Sosic, D. et al., 2003)(Figure 1.17). In addition, Twist has been implicated in TGF-β3-induced EMT during palatal fusion (el Ghouzzi, V. et al., 1997).

The inhibitors of DNA binding (Id) proteins have also been demonstrated to play a role in the progression of TGF-β-induced EMT. Id proteins function by inhibiting members of the Ets proteins family and retinoblastoma, which results in inhibition of differentiation and proliferation (Perk, J. et al., 2005). Using microarray analysis in mouse mammary epithelial cells, the Id proteins were identified as a common target of TGF-β and BMP7 pathways, with opposing effects (Kowanetz, M. et al., 2004). Whereas BMP7 induces robust expression of Id proteins, TGF-β stimulation results in their downregulation (Kowanetz, M. et al., 2004). It was subsequently shown that reduction of Id2 expression is required for cells to undergo TGF-β-induced EMT. Overexpression of Id2 prevented a TGF-β induced EMT response in mammary and lens epithelial cells, and consistently, depletion of the protein led to an enhanced response by TGF-β and even sensitised the cells to induction of EMT by BMP7 (Kowanetz, M. et al., 2004). These data suggest that a low level of Id2 expression is critical during EMT progression (Kowanetz, M. et al., 2004; Xie, L. et al., 2003) and upregulation of Id2 interferes with this process. As BMP-7 stimulates the synthesis of Id2, this may explain the antagonistic role of BMP7 in TGF-β-induced EMT in a model of renal injury (Zeisberg, M. et al., 2003b). The molecular mechanism by which Id2 elicits its biological effect has been elucidated, and involves repression of the E-cadherin promoter (Kondo, M. et al., 2004). The transcriptional mediator and Id2 interacting proteins E12/E47, have previously been demonstrated to repress E-cadherin (Perez-Moreno, M. A. et al., 2001) (Figure 1.17). Therefore a decrease in Id2 levels is required for E12/E47 bHLH transcriptional factors to be able to bind to the E-cadherin promoter and elicit repression (Kondo, M. et al., 2004), resulting in a downregulation of adherens junctions and progression of EMT.

1.6.3.2 The role of TGF-β superfamily members in EMT throughout Development

EMT is a fundamental process during embryonic development. The formation of mesenchymal cells from a primitive epithelium is an essential feature of most metazoans. Structural epithelial units disaggregate and during this transition, mesenchymal cells exhibit a morphology, which allows them to migrate in an extracellular environment to areas involved in organ formation. During embryonic development, these transitions are highly coordinated in a spatial and temporal manner, resulting in a synchronised process. Events such as gastrulation, neural crest cell formation, heart valve formation, somite differentiation, Mullerian duct regression and palate fusion rely upon the formation of mesechymal cells from an epithelial sheet (Thiery, J. P., 2003). In the absence of EMT, development cannot proceed past the blastula stage. Eventually these mesenchymal cells may regain a fully differentiated epithelial phenotype via a mesenchyme-to-epithelium transition (MET) and thus participate in the formation of epithelial organs (Thiery, J. P., 2003). MET occurs during somitogenesis, kidney development, and coelomic-cavity formation (Thiery, J. P. et al., 2006). Individual developmental EMT events are governed by different strategies and are species-dependent. Members of the TGF-β superfamily have been implicated in many developmental EMT processes such as gastrulation, heart valve formation, Mullerian duct regression and palate formation.

The aberrant signalling mediating EMT during tumourigenesis is in sharp contrast to the tightly controlled signalling mechanisms governing EMT events in development. A focus of my thesis is the role of TGF-β in EMT during tumorigenesis. However, it is also important to understand the integration of TGF-β and other pathways in naturally occurring EMT. This is likely to shed light on the main players involved in EMT events during tumour progression. To this end, I discuss three EMT events in development and the role of TGF-β superfamily members in these processes.

EMT during Palate Fusion

The formation of the secondary palate (palatogenesis) in mammals involves the orchestration of several processes to produce the correct separation of the oral and nasal cavities. It is a complex process, involving fine-tuned interactions between the epithelial and mesenchymal cells (Nawshad, A. et al., 2004). Failure of palatogenesis results in cleft palate, one of the most common birth defects in humans (Ferguson, M. W., 1988). During mammalian development, bilateral palatal shelves arise from the maxillary process and grow vertically down the sides of the tongue. The palatal shelves elevate rapidly into a horizontal position above the tongue, adhere in the midline, followed by fusion of the paired shelves (Figure 1.18). A critical step in mammalian palatal fusion is the removal of the tip of the prefusion palatal shelves, the medial edge epithelial (MEE) cells, from the midline seam and formation of continuous mesenchyme (Figure 1.18). The cellular mechanisms underlying seam degeneration and the fate of the MEE seam cells have been a major focus of investigation for more than a decade, yet still, controversies remain on this issue. Three major models have been postulated to explain the midline epithelial seam degeneration: epithelial-mesenchymal transdifferentation (Nawshad, A. et al., 2004; Shuler, C. F. et al., 1992); MEE cell apoptosis (Cuervo, R. et al., 2004; Cuervo, R. et al., 2002); and lateral migration of MEE cells (Carette, M. J. et al., 1992). Recently, however, a comprehensive study was performed to assess the contribution of each mechanism to palatal fusion (Jin, J. Z. et al., 2006). To assess the fate of the MEE cells, a Cre lox labelling system was employed to genetically mark Keratin-14-expressing palatal epithelial cells, which allowed the investigaters to follow their fate during palatal fusion *in vivo*. Strikingly, a significant number of mesenchymal cells stained positively for β-Gal during and after palate fusion, revealing conclusive evidence for the occurrence of EMT during palate fusion (Jin, J. Z. et al., 2006). In addition, a non-essential role for apoptosis was demonstrated, whereby palatal fusion was unimpaired *in vivo* using *Apaf1* mutant mouse embryos that cannot activate Caspase 3, a key effector caspase (Jin, J. Z. et al., 2006).

The first evidence to reveal an essential role of TGF-β in palatal development was the observation of cleft palate formation in TGF-β3 null mice (Kaartinen, V. et al., 1995; Proetzel, G. et al., 1995). Unlike other null mutants with cleft palate, TGF-β3 null mice did not exhibit other concomitant craniofacial abnormalities. Cleft palate can

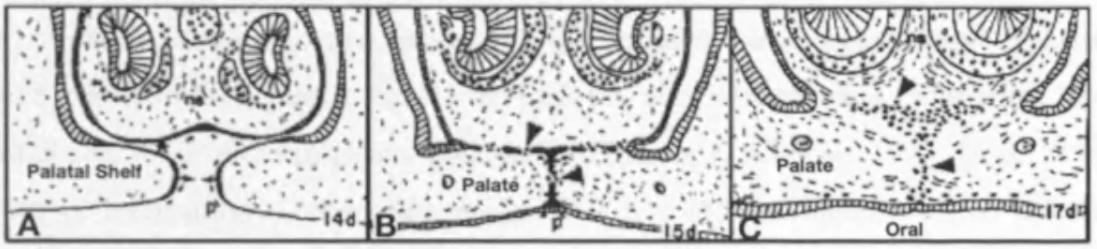

Figure 1.18. Diagrams of palate development in the mouse

The development of the mammalian secondary palate involves multiple steps.The anterior palate (shown) of the mouse fuses with the nasal septum (ns), but the posterior palate does not, because there is no nasal septum posteriorly.
(A) Between 13 and 14 dpc, the palatal shelves grow out from the inner face of the maxillary processes and move across the roof of the mouth.
(B) Sloughing of the outer epithelial layer promotes adherence of the basal epithelial cells that form the midline palatal seam.
(C) The medial edge epithelia that form the seam then undergo EMT (arrowheads, B and C) between 15 and 17 dpc. This results in connective tissue confluence and fusion of the palate shelves with the nasal septum. The dark cells (arrowheads) show diagramatically the relative contribution to mesenchyme made by these epithelial seams. (Taken from Hay, E., 2003).

occur at several stages during palatal development, but the mechanism underlying this defect in the TGF-β3 null mouse is a failure of palatal shelf fusion (Taya, Y. et al., 1999). Indeed, addition of exogenous TGF-β3 in an *in vitro* organ culture system rescued the defective palatal fusion in TGF-β3 null mutant mice, supporting an essential role for TGF-β3 in palatal shelf fusion (Brunet, C. L. et al., 1995; Taya, Y. et al., 1999). Interestingly, other isoforms of TGF-β could not induce normal palatal fusion (Taya, Y. et al., 1999), suggesting that this process discriminates between isoforms of TGF-β. In addition, inhibition of normal TGF-β3 activity either by antisense oligonucleotide or neutralising antibody, resulted in a failure of palate fusion *in vitro* (Brunet, C. L. et al., 1995). The spatial and temporal expression of TGF-β3 is consistent with its role in mediating palatal fusion, as it is abundantly expressed in the tips of prefusion palatal shelves, the medial edge epithelium.

TGF-β3 serves several functions in seam degeneration during palatal fusion, including initiating cell adhesion (Gato, A. et al., 2002; Sun, D. et al., 1998), inducing EMT (Kaartinen, V. et al., 1997; Sun, D. et al., 1998), and by this means promoting basement membrane and cell matrix degeneration (Blavier, L. et al., 2001). Although the role of TGF-β3 in EMT during palatal fusion has been well documented, the downstream events remain somewhat elusive. Investigation of the TGF-β receptors involved in this process, revealed that ALK1, -2 and -5 are all endogenously expressed in the palatal epithelium (Dudas, M. et al., 2004). *In vitro* analysis further demonstrated that constitutively active (ca) ALK5 could rescue the failed induction of palatal fusion of *TGF-β3* null palatal shelves (Dudas, M. et al., 2004). caALK2 could also rescue the TGF-β3 deficient fusion although less efficiently than ALK5, but ALK1, although highly homologous to ALK2, could not. In addition, incubation with the specific ALK5 inhibitor, SB-4131542 (Inman, G. J. et al., 2002b), prevented mesenchymal confluence in the anterior palate (Dudas, M. et al., 2006). Moreover, specific deletion of ALK5 in the ectodermal epithelial and neural crest lineages, resulted in impaired palatal fusion (Dudas, M. et al., 2006), further supporting a role for ALK5 in TGF-β3-induced palatal EMT (Dudas, M. et al., 2006; Dudas, M. et al., 2004). In contrast, however, these palatal defects observed in ALK5 conditional knockouts are not present in corresponding TβRII knockout mice, arguing against a role for this type II receptor and furthermore, for TGF-β in this process, as TGF-β3

binding to alternative type II receptors has not, as yet, been described (Ito, Y. et al., 2003; Xu, X. et al., 2006). However, as ALK5 mutant mice have far more severe facial phenotypes than TβRII, it has been proposed that another type II receptor, other than the conventional TβRII may function to transduce the TGF-β3 signal during palatal fusion (Dudas, M. et al., 2006). Evidence was provided to show that ALK5 can interact with ActRII, the dual specificity type II receptor for BMP and Activin, using a heterodimerisation model system. However, as previous data suggests that this is not the case, a more detailed investigation *in vivo* is required to confirm this hypothesis (Dudas, M. et al., 2006).

Activation of ALK5 results in the phosphorylation of Smad2 and/or 3. Smad2 null cells die during or immediately after gastrulation, preventing the use of these mice in palatal studies (Nomura, M. et al., 1998). However, palate formation is unimpaired in the Smad3 null mice (Datto, M. B. et al., 1999; Yang, X. et al., 1999; Zhu, Y. et al., 1998), suggesting that the role of Smad3 in palatogenesis, if any, is redundant and that it can be functionally compensated by Smad2. Indeed, Smad2 signalling has been implicated in the process of TGF-β3-induced EMT during palate fusion (Dudas, M. et al., 2004; Nawshad, A. et al., 2003). Immunohistochemical data demonstrate that *in vivo* P-Smad2 activation is abolished in TGF-β3 null palate shelves, whereas P-Smad1/5/8 is unaffected (Dudas, M. et al., 2004). Furthermore, Smad2/4 signalling has been implicated in up-regulation of the LEF-1 gene during palatal EMT (Nawshad, A. et al., 2003), but the full details of this mechanism remain to be established. It is noteworthy that the role of Smad2 versus Smad3 is complicated by the existence of an alternative splice variant of Smad2, Smad2Δexon3, which has DNA binding ability (Shi, Y. et al., 1997) and the fact that Smad3 can functionally compsenate for Smad2 loss (Dunn, N. R. et al., 2004).

Downstream effectors of the pathway are being uncovered, including the transcriptional repressor, Snail, which is involved in triggering the MEE cells to undergo EMT in mouse (Martinez-Alvarez, C. et al., 2004). It has been proposed that Snail1 confers the MEE cells, resistance to cell death thus enabling them to differentiate. *Snail1* expression is detected at the time of fusion in a subset of cells, which correlates with low E-cadherin staining, suggesting it is involved in TGF-β3 mediated EMT of MEE cells. Interestingly, Snail2 is the Snail family member expressed in the chick MEE, providing another example of the interchange of Snail1

and Snail2 expression between avian and mammalian embryos (Martinez-Alvarez, C. et al., 2004). Finally, the basic Helix-Loop-Helix (bHLH) transcription factor, Twist, has also been implicated in palatogenesis. Mutations of the gene are associated with an autosomal-dominant craniosynostosis (Saethre-Chotzen syndrome) characterised by cleft palate, and may contribute to the inhibition of palatal EMT (el Ghouzzi, V. et al., 1997).

Neural Crest Formation

In addition to the role of TGF-β in EMT, other members of the superfamily have also been implicated in EMT. During the neural crest, BMP signalling is important to mediate this EMT event as discussed below.

The neural crest is a unique and highly specialised population of cells found in all vertebrate embryos. The appearance of this tissue was likely a turning point in vertebrate evolution, since many of the structures which define the vertebrates are derived from neural crest cells (Meulemans, D. et al., 2004). During embryogenesis, the neural crest develops at the border between the neural plate and embryonic ectoderm and once specified the neural crest cells undergo an EMT, which confers on them the ability to migrate (Figure 1.19). When the EMT is complete, the neural crest cells delaminate from the neural folds dorsal neural tube and migrate along characteristic pathways to differentiate into a wide variety of derivatives including bone, smooth muscle, peripheral neurons and glia, and melanocytes (Tucker, R. P., 2004).

Most of the studies on the signalling pathways governing neural crest induction and subsequent EMT have been performed using Xenopus and avian embryological models. As a result, analysis of neural crest gene-regulatory relationships have largely been restricted to gain- or loss-of-function studies using injected mRNA, cDNA, or antisense oligonucleotides. Hierarchial relationship of these genes have not been fully elucidated, however most of the main players in the pathway have been identified (Meulemans, D. et al., 2004). Though different species seem to use different combinations of factors, members of the Wnt and fibroblast growth factor (FGF) families are frequently implicated as working together with BMP to drive neural crest induction (Tucker, R. P., 2004). The spatial and temporal integration of these signals, which originate from the non-neural ectoderm, the neural plate and/or the paraxial

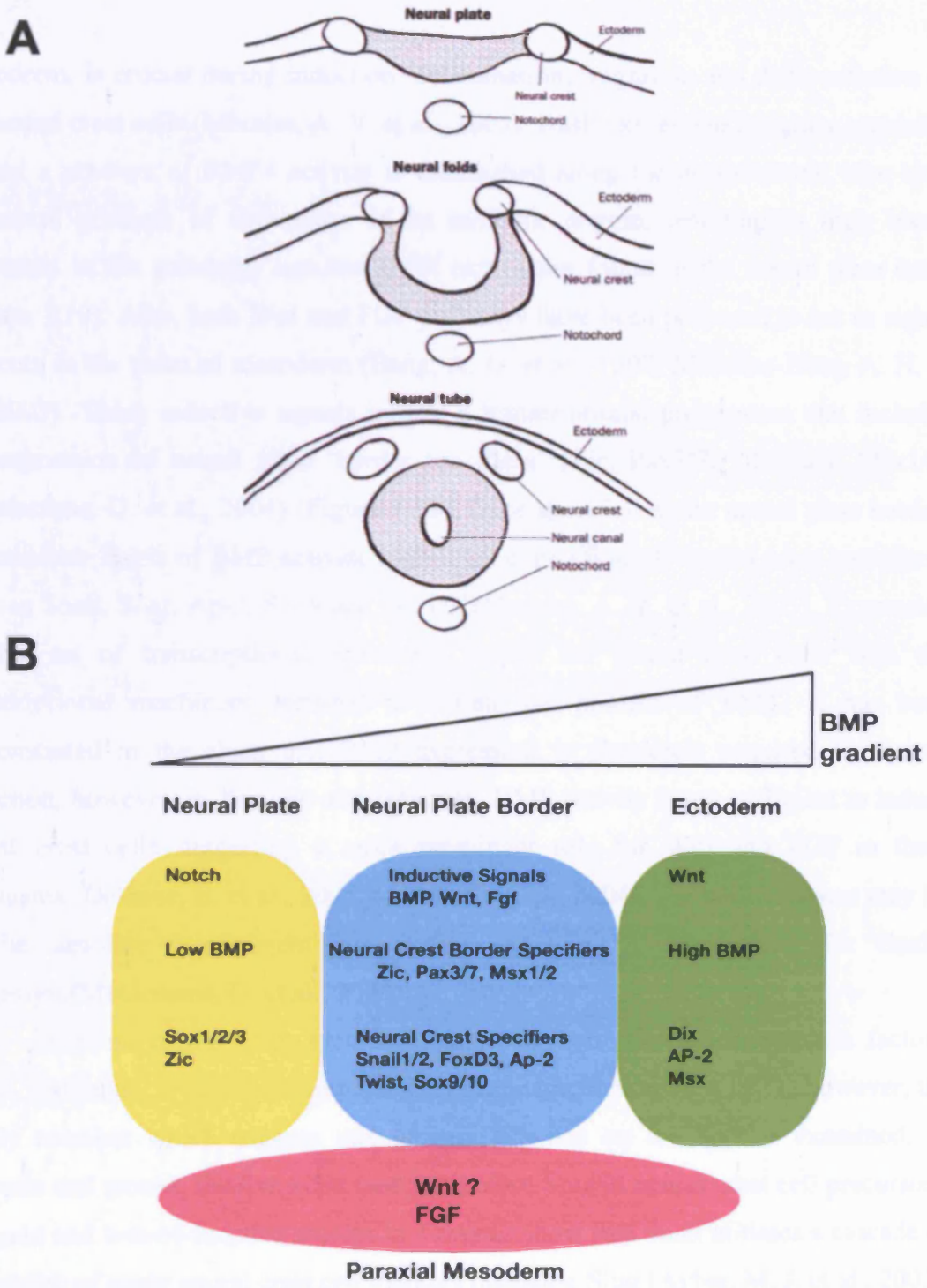

Figure1.19. Neural Crest Cell Formation

A) Schematic diagram of the developmental events during neural induction. The central nervous system forms during the process of neuralation, as the neural plate bends and folds into the neural tube. Presumptive neural crest cells are initally localised at the edges of the neural plate at its border with the non-neural ectoderm. During the folding process, neural crest precursors are contained within the neural folds and subsequently localised within the dorsal portion of the neural tube when closure is complete. Shortly thereafter, these cells undergo an EMT, delaminate from the neuroepithelium, and migrate away from the neural tube to various embryonic sites.
(Taken from http://www.med.umich.edu/lrc/coursepages/M1/embryology/embryo/08nervoussystem.htm)
B) Schematic summary of signalling events at the neural plate border during neural crest induction using data from several organsims. (Adapted from Meulemans and Bronner-Fraser, 2004).

mesoderm, is crucial during induction, delamination, migration and differentiation of the neural crest cells (Morales, A. V. et al., 2005). BMP expression is tightly regulated so that a gradient of BMP4 activity is established along the dorsal neural tube by a reciprocal gradient of expression of its inhibitor noggin, resulting in high levels expressed in the ectoderm and low BMP expression found in the neural plate itself (Figure 1.19). Also, both Wnt and FGF pathways have been proposed to act as signal inducers in the paraxial mesoderm (Bang, A. G. et al., 1997; Monsoro-Burq, A. H. et al., 2003). These inductive signals initiate a transcriptional programme that includes the expression of neural plate 'border specifiers' (Zic, Pax3 7, Dlx5 and Msx1 2) (Meulemans, D. et al., 2004) (Figure 1.19). Once specified at the neural plate border, intermediate levels of BMP activate high-level expression of "neural crest specifiers" such as Snail, Slug, Ap-2, Sox9 and FoxD3 (Morales, A. V. et al., 2005). Expression of this set of transcriptional activators, equips the neural crest cells with the transcriptional machinery required to initiate the process of EMT. It has been demonstrated in the chick that BMP expression is absolutely required for neural induction, however, in *Xenopus* and *zebrafish*, BMP activity is not sufficient to induce neural crest cells suggesting a more prominant role for Wnt and FGF in these organisms (Delaune, E. et al., 2005; Linker, C. et al., 2004). These differences may lie in the absolute requirement for BMP2 signalling in the chick for Snail2 expression(Meulemans, D. et al., 2004).

Of these neural crest specifier genes, the two related transcription factors, Snail1 and Snail2 are crucial components in regulating neural crest EMT, however, the family member which triggers this process depends on the species examined. In *Xenopus* and mouse, Snail is expressed just before Slug in neural crest cell precursors, and gain and loss-of-function studies in *Xenopus* show that Snail initiates a cascade of expression of many neural crest cell markers including Slug (Aybar, M. J. et al., 2003). In contrast, in the chick Snail2 expression precedes Snail (Sefton, M. et al., 1998), and was first shown to initiate EMT of the chick neural crest in functional interference studies. Incubation of early chick blastomeres with antisense oligonucleotides to Snail2, inhibited neural crest delamination from the neural tube (Nieto, M. A. et al., 1994). Subsequently, defects in crest migration and lack of specific derivatives were demonstrated in the neural crest of *Xenopus* embryos after inhibition of Snail2 function (Nieto, M. A., 2002). Overexpression of Snail2 in *Xenopus* resulted in

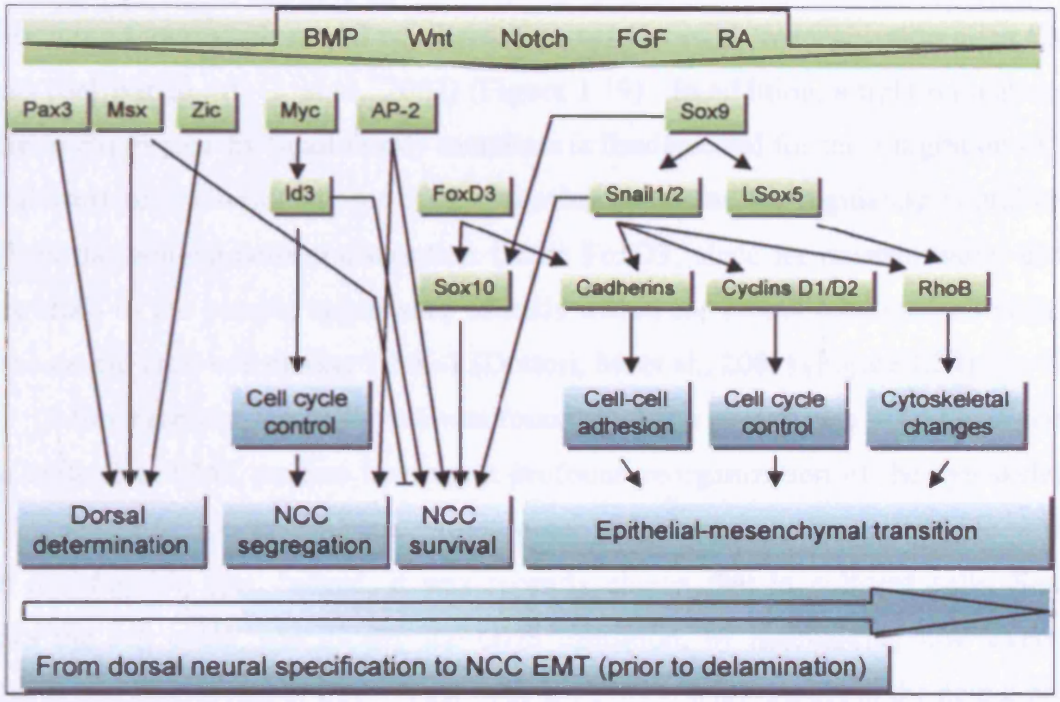

Figure 1.20. Overview of the Neural Crest Genetic network.

The steps represented in the figure run from the induction of dorsal properties to the neural plate/neural tube up to the completion of the EMT prior to delamination. Multiple factors signal in a coodinated fashion to trigger the induction of "neural crest specifiers", which leads to the acquisition of the properties of the neural crest cells. Neural crest cells require an integrated network of interactions among factors with differential coordinated functions to achieve their specific fate. The arrows indicate the flow of the pathway, not the direct transcriptional regulation. The different players are shown in light green and their effects are shown in turquoise. (Taken from Morales et al., 2005).

increased levels of RhoB, concomitant with an increase of neural crest production, highlighting their role in neural cell induction and a possible mechanism to elicit EMT events (del Barrio, M. G. et al., 2002) (Figure 1.19). In addition, a tight regulation of cadherin expression by Snail family members is fundamental for the emigration of the neural-crest cells (Nieto, M. A., 2002). Another candidate for regulating neural crest EMT is the winged-helix transcription factor FoxD3, since its misexpression in the chick leads to the ectopic appearance of cells within the neural tube that are positive for the neural crest cell marker HNK-1 (Dottori, M. et al., 2001) (Figure 1.20).

More recently, the cell cycle was found to play a pivotal role in EMT of neural crest cells. The EMT process involves a profound reorganization of the cytoskeleton and induction of a transcriptional programme, which may not be compatible with a high proliferation rate. Indeed, it was recently shown that in cultured cells, Snail1 blocks the cell cycle, specifically the G1 S transition, by maintaining low levels of cyclin D and high levels of p21 (Vega, S. et al., 2004). With respect to the neural crest, cell proliferation is very low in Snail-expressing cells (Snail1 in the mouse and Snail2 in the chick, undergoing EMT), which in turn express very low levels of Cyclins D1 and D2 (Morales, A. V. et al., 2005). However, it has also been shown that transition from G1 to S is necessary for the epithelial to mesenchymal conversion of premigratory neural crest cells (Burstyn-Cohen, T. et al., 2002). It was demonstrated that trunk level avian neural crest cells synchronously emigrate in the S-phase of the cell cycle. Specific inhibition with G1 S blockers in explants and *in ovo*, but not with S or G2 blockers, prevents mesenchymalization of premigratory neural crest cells (Burstyn-Cohen, T. et al., 2002). This suggests that synchronization of the neural crest cells in G1 may occur during EMT, however progression to S-phase is required for the full acquisition of migratory properties of these cells. Moreover, BMP signalling drives the onset of neural crest migration in the trunk neural tube though the control of G1 S transition, which is controlled upstream by Wnt signalling (Burstyn-Cohen, T. et al., 2004).

The programme of EMT during neural crest formation is a highly integrated, complex interplay of genes in a coordinated manner. Although many effectors of EMT have been identified, the precise spatio-temporal expression and activity of all of these factors and the complex pattern of interactions and crossregulations requires further investigations. In addition, despite the plethora of growth factors and transcription

factors identified, none of these genes have proven to be the master regulator of EMT and important regulatory mechanisms remain to be discovered.

Regulation of EMT in the development of the heart

A classical example of developmentally regulated EMT occurs during the initial stages of cardiac morphogenesis. At embryonic day 8.5 (E8.5), the mouse heart tube is composed of an outer myocardial layer lined by a monolayer of specialised endothelium, the endocardium, separated by a thick extracellular matrix, the cardiac jelly (Figure 1.21). In response to regionalized myocardial signals, a subset of endocardial cells that overlies the atrio-ventricular (AV) canal and out(Azhar, M. et al., 2003)flow tract regions undergoes E. These cells delaminate from the endocardial sheet and invade the cardiac jelly to form the endocardial cushions, which will contribute to cardiac valve development and heart septation. However adjacent endothelial cells in the atrium and ventricle remain epithelial (Azhar, M. et al., 2003). The localised nature of the EMT suggests a mechanism to molecularly distinguish the myocardium and or endocardium of the AV canal from the rest of the non-cushion-forming heart. The signals that induce EMT have been investigated in chick embryos using a 3-D collagen gel assay (Runyan, R. B. et al., 1983). Data from these co-culture experiments show that signals from both the adjacent myocardium and from the extracellular matrix of the cardiac jelly play a critical role in the endocardial cell EMT (Eisenberg, L. M. et al., 1995) (Figure 1.21). In addition, these studies revealed that TGF-β2 and TGF-β3 perform crucial and sequential functions in cushion morphogenesis. TGF-β2 is thought to mediate the activation of the endocardium, while TGF-β3 functions in mesenchymal invasion of the cardiac jelly (Boyer, A. S. et al., 1999; Brown, C. B. et al., 1996; Camenisch, T. D. et al., 2002). It is noteworthy that TGF-β1 mRNA is absent in the developing chick heart.

Further studies using neutralising antibodies in the chick explant model have suggested that the prototypical TGFβ receptor, ALK5, is not involved in the cushion EMT, whereas inhibition of ALK2 prevents transdifferentiaion (Lai, Y. T. et al., 2000). Subsequently it was shown that constitutively active ALK2 is sufficient to stimulate EMT (Desgrosellier, J. S. et al., 2005). The type III TGF-β receptor (betaglcan) has also been shown to play a critical role in endocardial EMT as antibodies against the receptor were found to inhibt EMT and migration in AV cushion

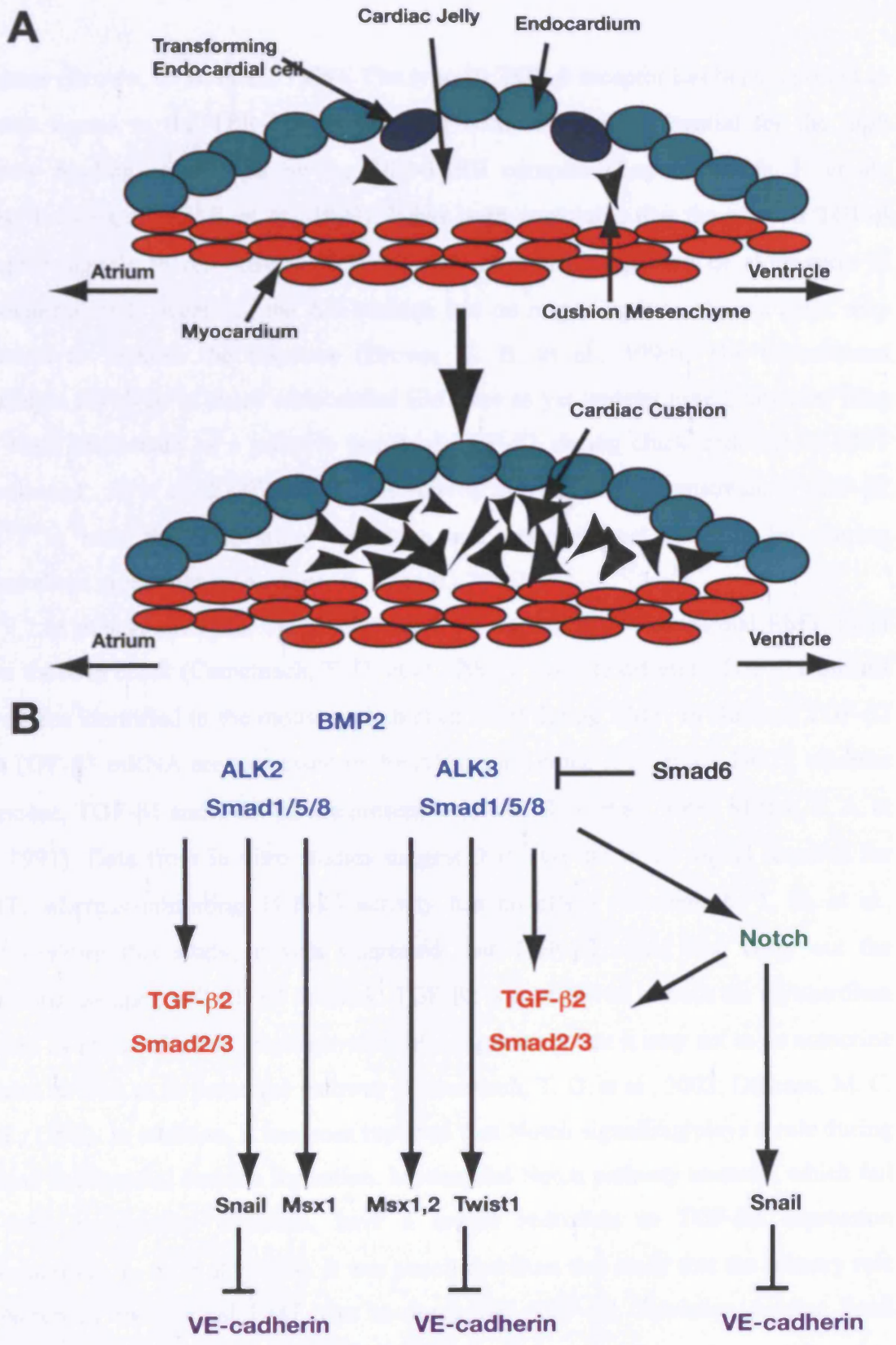

Figure 1.21. Endocardial EMT to form heart cushions

A) Schematic representation of the atrioventricular (AV) canal during heart development. (Adapted from Azhar et al., 2003).
B) Summary of the signalling pathways that function in the AV canal in mouse.

explants (Brown, C. B. et al., 1999). The type III TGF-β receptor has been reported to present ligand to the TβR-TβRII signalling complex and is essential for the high affinity binding of TGF-β2 by the TβR-TβRII complex (Lopez-Casillas, F. et al., 1994; Lopez-Casillas, F. et al., 1993). It has been postulated that the type III TGF-β receptor signals in response to TGF-β2 and its restricted pattern of expression in endocardial cells overlying the AV cushion and on migrating mesechymal cells, may function to localise the response (Brown, C. B. et al., 1999). The downstream mediators involved in chick endocardial EMT are as yet undetermined, however Slug has been implicated as a putative target of TGF-β2 during chick endocaridal EMT (Romano, L. A. et al., 2000). Also RhoA activity may function downstream of TGF-β2 and 3 in both the endocardial activation and mesenchymal invasion by altering cytoskeletal components (Tavares, A. L. et al., 2006).

In mouse embryos, the requirements for induction of endocardial EMT differ from those in chick (Camenisch, T. D. et al., 2002). To date different TGF-β isoforms have been identified in the mouse and chicken heart during EMT. In chicken, TGF-β2 and TGF-β3 mRNA are expressed in the AV canal (Potts, J. D. et al., 1992), whereas in mouse, TGF-β1 and TGF-β2 are present (Akhurst, R. J. et al., 1990; Millan, F. A. et al., 1991). Data from in-vitro studies suggest that TGF-β2 is the signal required for EMT, whereas inhibiting TGF-β3 activity has no effect (Camenisch, T. D. et al., 2002). From this study, it was suggested that TGF-β2 could also carry out the functions assigned to TGF-β3 in chick. TGF-β2 was observed in both the myocardium as well as in transformed mesenchymal cells suggesting that it may act in an autocrine fashion as well as its paracrine pathway (Camenisch, T. D. et al., 2002; Dickson, M. C. et al., 1993). In addition, it has been reported that Notch signalling plays a role during murine endocardial cushion formation. Myocardial Notch pathway mutants, which fail to form endocardial cushions, have a severe reduction in TGF-β2 expression (Timmerman, L. A. et al., 2004). It was concluded from this study that the primary role of Notch in endocardial EMT was to upregulate TGF-β2. However, cardiac Snail expression was also dramatically affected in these mice and this may have attributed to the defects observed. Increasing evidence suggests that other signals are required in vivo to induce EMT in mammals. This is highlighted by the fact that mice

homozygous for a null allele of TGF-β2 still make cushions (Sanford, L. P. et al., 1997).

More recent data has implicated the BMP ligands in playing a critical role in endocardial EMT. It was shown that *Bmp2* is expressed in the AV myocardium at 9.5 and 10.5 days (Sugi, Y. et al., 2004). Experiments using the collagen gel assay showed that BMP2 could substitute for myocardium to induce EMT in mouse embryos (Sugi, Y. et al., 2004). In accordance with this hypothesis, gene inactivation studies in mice revealed that *Bmp2* was necessary for myocardial development (Zhang, H. et al., 1996). Moreover, specific deletion of Bmp2 in the AV myocardium resulted in failure of the AV endothelial cells to form cushions, implicating BMP2 signalling in endothelial EMT (Ma, L. et al., 2005).

The relationship between BMP2 and TGF-β2 signalling, and the requirements of each ligand to induce EMT has not yet been fully established. It was reported that a tissue specific deletion of the BMP type I receptor ALK3 in myocardial cells resulted in downregulation of TGF-β2 expression specifically in myocardium adjacent to the AV canal (Gaussin, V. et al., 2002). This suggests that BMP ligands act to regulate myocardial TGF-β2 expression in a cell autonomous manner, which is importatant for later aspects of AV cushion development (Ma, L. et al., 2005). Furthermore, BMP2 induces TGF-β2 expression in explants cultured in collagen gel (Sugi, Y. et al., 2004), and TGF-β2 expression is dramatically reduced in the AV cushions of BMP2 conditional knockout mutant embryos (Ma, L. et al., 2005). Additional work is required to firmly establish the genetic relationship between BMP signalling and TGF-β transcriptional regulation and its role in mouse endocardial EMT.

The type I receptors which transduce the BMP signal have also been investigated. Conditional inactivation of ALK3 in the myocardium resulted in normal AV cushions in mutant embryos (Gaussin, V. et al., 2002), whereas targeted deletion of ALK3 in the AV endocardium disrupted EMT in most mutants (Ma, L. et al., 2005). This indicates that endocardial ALK3 tranduces the BMP signal required for EMT. However, one third of conditional mutants lacking endocardial ALK3, still made cushions. In addition, the level of P-Smad1/5/8 in the endothelial cells was only reduced by 50% in the absence of ALK3. This evidence suggested the possibility that other type I receptors function in the cushion endocardium.

ALK2 has also been shown to be required for endocardial EMT in the mouse as well as in chick embryo as discussed previously (Desgrosellier, J. S. et al., 2005; Wang, J. et al., 2005). Mouse embryos deficient for ALK2 in cushion endocardium had a severe defect in AV cushion morphogenesis (Wang, J. et al., 2005). Although ligands signalling via ALK2 in vivo are currently unknown, it is likely that they include the BMPs. ALK2 interacts with BMPRII as well as TGF-β and activin type I receptors in the presence of their respective ligands (Attisano, L. et al., 1993; Ebner, R. et al., 1993; Yamashita, H. et al., 1995). Despite potentially signalling through TGF-β, activin and BMP ligands, ALK2 activation has thus far only been demonstrated for BMP7 in conjugation with the activin type II receptors (Macias-Silva, M. et al., 1998). However, there is evidence that ALK2 signals downstream of ligands other than BMP7 since alk2 null mice die early in gastrulation (Gu, Z. et al., 1999), while BMP7 null mice survive until soon after birth (Dudley, A. T. et al., 1995; Luo, G. et al., 1995). Furthermore, ALK2 has been proposed to mediate MIS-induced EMT of coelomic epithelium during Mullerian duct regression (Zhan, Y. et al., 2006). ALK2 has also been implicated in TGF-β mediated EMT in cultured mammary epithelial cells (Miettinen, P. J. et al., 1994).

In the AV tract ALK2 signalling has also been implicated in regulating TGF-β signalling. Activation of both BMP Smads and TGF-β Smads is affected in ALK2 mutant mice. However, EMT cannot be rescued by exogenous addition of TGFβ (Wang, J. et al., 2005), suggesting that the role of BMP/ALK2 signalling is not solely the induction of TGF-β expression. These data suggest that ALK2 and ALK3 may both function as BMP type I receptors in regulating EMT in mouse endocardium. Distinct but overlapping target pathways have been suggested for the type I receptors by comparision of downstream signalling pathways in knockout mice (Ma, L. et al., 2005; Wang, J. et al., 2005).

In accordance with a crucial requirement for BMP signalling for endocardial EMT, Smad6 has been implicated as a regulator of the process. A specific role for Smad6 in endocardial EMT was first revealed by the targeted deletion of Smad6 in mouse (Galvin, K. M. et al., 2000), which revealed the presence of excess mesenchymal cells in the cardiac valves of Smad6 mutant mice. Since Smad6 has been shown to have a preferential inhibitory role in BMP signalling (Hata, A. et al., 1998; Imamura, T. et al., 1997), it is possible that Smad6 acts by limiting the response to the

inductive BMP signal. Whether Smad6 functions to antagonise ALK2 and ALK3 signalling, or an individual type I receptor, has yet to be uncovered.

In conclusion, strong evidence has accumulated to demonstrate the role of BMP signalling in mouse endocardial EMT. Furthermore, this process displays the finely tuned interplay of signalling components and pathways to implement morphogenetic events that are crucial to the development of an embryo.

1.6.3.3 Conclusions

The most striking property of the EMT process is the use of a plethora of growth factors and transcription factors in a coordinated and cooperative fashion to elicit distinct changes in the structural morphology of epithelial cells. In the TGF-β superfamily, all three TGF-β isoforms induce various developmental EMTs, whereas BMP ligands function as both inductive and inhibitory signals during EMT. In addition to the inhibitory roles of BMPs during EMT, BMP-7 has been identified as a key regulator during MET in kidney ontogenesis (Dudley, A. T. et al., 1995). Furthermore, intricate requirements for receptors by the TGF-β family members in different developmental and cell systems have been implied, suggesting that although a similar endpoint is reached in many cases, specific pathways are required to elicit these signals. This is true also of the discriminatory use of TGF-β isoforms throughout development, which is not based on the expression profiles of these ligands. Similarly, a wide variety of transcription factors are employed to mediate an EMT signal, however it is clear that many of these signalling pathways converge to elicit transcriptional repression of the E-cadherin promoter. Moreover, as the mechanisms underlying EMT are gradually unravelled, it is apparent that developmental and metastatic EMTs seem to be governed by common signalling pathways, thus raising the hypothesis that tumour metastasis could be regarded as a reactivation of at least some aspects of the embryonic programme of EMT (Thiery, J. P., 2002). As TGF-β family members are major players in developmental EMT events, it is not surprisingly that they are also involved in tumourigenesis.

1.6.3.4 EMT during Tumour Progression

Tumours associated with metastasis formation account for 90% of cancer deaths, and represent one of the prime causes of human mortality (Sporn, M. B., 1996). The release of tumour cells from organised tissue structures and invasion to more distal sites requires phenotypic changes and alterations in gene expression profiles, common to EMT-associated changes (Thiery, J. P., 2003). For a long time, however, the relevance of EMT during tumour progression in was questioned, due to the difficulty in distinguishing an EMT process in progressing human tumours. However, tumour cells that have undergone EMT co-express mesenchymal markers such as vimetin (which is also present in stromal fibroblasts) together with epithelial cytokeratines (laking in stromal fibroblasts). More recently, *in vivo* imaging techniques have been developed which allow the identification of such dedifferentiated cells in human tumours (Ahmed, F. et al., 2002).

To date, numerous observations support a central role for EMT in tumour progression. Detailed immunocytochemical analysis of adenocarcinomas of the colon, revealed the release of single-cells from an epithelial island. These solitary cells stained E-cadherin-negative and were found at the sites of tumour invasion, implicating a mechanism of EMT. In addition, the metastatic potential of carcinoma cells correlates with the mesenchymal gene expression patterns and the loss of epithelial markers such as E-cadherin (Thiery, J. P., 2002). For example in breast cancers, the loss of E-cadherin expression has been shown to positively correlate with advanced grade, metastasis and decreased survival (Peinado, H. et al., 2004). It has also been observed that Snail1 promotes the recurrence of mammary tumours in mice and high levels of Snail1 act as a marker for poor prognosis in human cancer (Moody, S. E. et al., 2005).

In addition, it is also clear that induction of EMT in many carcinoma cell lines results in the acquisition of metastatic properties *in vivo*. In a microarray analysis to identify genes involved in metastasis, Twist, a transcription factor important in development, was found to be essential in the metastatic process (Yang, J. et al., 2004). It was subsequently shown that suppression of Twist expression in highly metastatic carcinoma cells reduces their ability to metastasize from the mammary gland to lung (Yang, J. et al., 2004). Ectopic expression of Twist, however, promotes

EMT, expression of mesenchymal markers, increased motility and loss of E-cadherin expression, thus, clearly establishing a mechanistic link between EMT and metastasis.

The role of TGF-β induced EMT *in vivo* also strengthens the argument for EMT in tumour cells. *In vivo* mouse models of skin carcinogenesis have shown a dual role of TGF-β, whereby TGF-β inhibits formation of benign papillomas, but promotes proliferation and dedifferentiation during the squamous-cell carcinoma stages, leading to the formation of spindle-cell carcinoma, the most aggressive from skin cancer (Cui, W. et al., 1996). These spindle cell carcinomas also upregulate TGF-β3 expression, which may be required in maintenance of the aggressive phenotype. Also, the stable expression of dominant negative TβRII in a squamous carcinoma cell line prevented the spontaneous progression of these cells to a spindle cell phenotype *in vivo*, clearly demonstrating that the EMT event is mediated directly via the TGF-β signalling pathway (Portella, G. et al., 1998). In the EpRas mammary carcinoma model, it was demonstrated that after injection into mice, these polarized cells formed tumours consisting of depolarised, spindle shaped cells capable of invasive growth. These tumours displayed autocrine production of TGF-β, which is required to maintain the mesenchymal, spindle-like phenotype (Oft, M. et al., 1996). Administration of TGF-β in the vicinity of the injected EpRas cells dramatically accelerated the conversion of these cells into a fibroblastoid phenotype, indicating a key role of TGF-β in regulating EMT during tumourigenesis (Oft, M. et al., 1996). In addition, expression of a dominant negative TβRII in EpRas cells was employed to block TGF-β signalling, which resulted in delayed tumour formation and prevention of EMT and metastasis *in vivo* (Oft, M. et al., 1998). Thus, it was proposed that autocrine TGF-β signalling is required for both induction and maintenance of invasiveness and metastasis during late-stage tumourigenesis. Furthermore, NF-kB, has been shown to be essential for TGF-β-induced EMT in EpRas cells, and inhibtion of NF-kB activity reverses the TGF-β-induced EMT and also abrogates the metastatic potential of these cells *in vivo* (Huber, M. A. et al., 2004a).

Finally, a secreted interleukin-related protein (ILEI), which is upregulated during TGF-β-induced EMT in EpRas cells, has been shown to induce tumour growth, EMT and lung metastasis *in vivo* when stably expressed in non-tumourigenic EpH4 cells

(Waerner, T. et al., 2006). Taken together, these studies suggest a role for TGF-β signalling in the progression of tumours to late stages, associated with EMT.

1.7 TGF-β and Cancer

TGF-β was originally discovered by its ability to induce malignant behaviour of normal fibroblasts in culture, a property which led to the notion that TGF-β was an effector of transformation, and hence named 'transforming' growth factor (Roberts, A. B. et al., 1981). However, it later emerged that TGF-β has profound growth suppressive effects on many cells, thus uncovering the role of TGF-β as a tumour suppressor (Roberts, A. B. et al., 2003). Over the last twenty years it has been demonstrated that TGF-β plays a complex, biphasic role in cancer, exhibiting opposing effects at either early or late states of tumour progression. In the initial phases of cancer, it acts as a tumour suppressor primarily through its growth inhibitory effects on epithelial and lymphoid cells from which the majority of human tumours are derived. However, in advanced stages of cancer TGFβ appears to act as a tumour promoter, typically when the growth inhibitory response of cells to TGF-β has been lost (Wakefield, L. M. et al., 2002).

The dual role of TGF-β in cancer was first demonstrated in transgenic mouse models. In a model of chemical carcinogenesis in the skin, targeted expression of TGF-β1 inhibited the formation of benign papillomas but led to an enhanced rate of aggressive and highly malignant tumours which expressed high levels of endogenous TGF-β3 (Cui, W. et al., 1996). It was also observed that TGF-β1 heterozygous mice exhibit increased cell turnover in liver and lung (Tang, B. et al., 1998). However, treatment of these mice with chemical carcinogens resulted in an increase in tumor incidence. Moreover, these tumours retained the remaining TGF-β1 allele, suggesting that haploid loss of TGF-β is insufficient for the tumour suppressive function of TGF-β (Tang, B. et al., 1998). In addition, introduction of dominant negative TβRII into mice enhanced tumorigenesis in the mammary gland and lung in response to a carcinogen (Bottinger, E. P. et al., 1997). Furthermore, it has also been demonstrated that the pro-oncogenic activities of TGF-β in the progressive stages of cancer, is

associated with the requirement of many tumours for TGF-β activity to form metastases (Akhurst, R. J. et al., 2001). Indeed, two independent studies revealed that administration of soluble TGF-β antagonists selectively inhibits metastatic disease without affecting normal physiology or tumorigenesis at the primary site in metastatic mammary mouse models (Muraoka, R. S. et al., 2002; Yang, Y. A. et al., 2002). Furthermore, using a series of breast cancer cell lines that differ in degrees of malignancy, it was shown that Smad2 and Smad3 exerted tumour suppressive activity in premalignant and well-differentiated tumour cells but enhanced lung metastases of more aggressive carcinoma cells (Tian, F. et al., 2003). In addition, a high percentage of human tumors overexpress TGF-β1, and this excess production of TGF-β1 appears to be associated with poor prognosis (Tsushima, H. et al., 1996; Wikstrom, P. et al., 1998). These date clearly establish a role for TGF-β in mediating both tumour suppressive and tumour promoting activities *in vivo*.

1.7.1 Genetic Alterations in TGF-β signalling components

The importance of TGF-β signalling in the suppression of tumourigenesis is supported by the presence of deletions and mutations in genes encoding both TGF-β receptors and downstream components of the signalling pathway in cancer (Levy, L. et al., 2006). Smad4 was originally identified as a tumour suppressor gene lost in pancreatic cancers, deleted in pancreatic cancer locus 4 (DPC4) (Hahn, S. A. et al., 1996). Smad4, located in 18q21, follows the classic Knudsonian paradigm for a tumour suppressor, in that the second allele is disrupted by loss of heterozygosity (LOH) in about 90% of pancreatic cancers (Levy, L. et al., 2006). Indeed, Smad4 has now been shown to be mutated or deleted in about 50% pancreatic cancers, 15% of colorectal tumours and less frequently in a number of other cancers including breast, prostate and cervical cancer. Germ line mutations in *Smad4* also occur in a subset of patients with juvenile polyposis (JP), an autosomal dominant gastrointestinal polyposis syndrome (Howe, J. R. et al., 1998). Smad2, also located on 18q21, is mutated at a low frequency in a small proportion of colorectal cancers (Eppert, K. et al., 1996; Uchida, K. et al., 1996). To date, no mutations have been identified in patients, although loss of Smad3 expression of tumour samples has been demonstrated (see below) (Levy, L. et al., 2006). Somatic

inactivating mutation of the gene encoding TβRII, occurs in tumours from patients with hereditary non-polyposis colorectal cancer (HNPCC), a hereditary form of colon cancer. These patients have defects in their recombination error repair system, and hence mutations arise in TβRII due to mismatch repair errors resulting in a truncation of the receptor (Kim, S. J. et al., 2000). In addition, mutation of ALK5 has been also been detected in human cancers, with a particularly high level found in ovarian cancers (Wang, D. et al., 2000). More recently, mutations in the gene encoding ALK3 have been found in a subset of JP patients (Howe, J. R. et al., 2001). Interestingly these patients are wildtype for Smad4.

1.7.2 Resistance to tumour suppressor activities of TGF-β

The vast majority of epithelial-derived tumours (>85% of all human cancers) become resistant to the growth inhibitory effects of TGF-β, but remain responsive to the tumour promoting activities of TGF-β (Akhurst, R. J. et al., 2001). Although some of the mechanisms for the loss of the antiproliferative response have been defined by mutations in components of the pathway in tumours, most cancer cells retain normal TGF-β receptors and Smads. As a result, alternative mechanisms for resistance to the antiproliferative effects of TGF-β-induced have been proposed. An emerging theme is a downregulation of components of the pathway, including the receptors, TβRII, TβRII and also Smad3 (Kim, S. J. et al., 2000). The loss of expression of TβRII in association with resistance to the growth inhibitory effect of TGF-β has been reported in various types of cancers, including gastric, colon, breast, and prostate (Levy, L. et al., 2006). Furthermore, decreased Smad3 expression has been reported in gastric cancers, which are refractory to the antiproliferative effects of TGF-β (Han, S. U. et al., 2004). The loss of TGF-β growth inhibitory and apoptotic effects accompanied by this downregulation is often associated with activation of other signaling pathways such as Ras and P13Kinase (Akhurst, R. J. et al., 2001). By lowering the expression level of these TGF-β signaling components, tumour cells escape the growth inhibitory effects of TGF-β but maintain other TGF-β responses. In fact, it has been proposed that tumours which maintain TGF-β signalling correlates with poor prognosis. This has

been demonstrated in patients with HNPCC, whereby individuals with a complete loss of *TβRII* have a better prognosis than patients with sporadic colon caener that retain functional TGF-β receptors (Akhurst, R. J. et al., 2001).

1.7.3 Tumour promoting role of TGF-β

Although the tumour suppressive activities of TGF-β have been lost in cancers, other TGF-β responses prevail, many of which contribute to the spread of metastasis. Tumour metastases arise as a result of a complex series of events that involves cellular migration, tumour vascularisation, interactions with the microenvironment, intravasation into blood or lymphatic vessels, and cell survival at distant sites. TGF-β is involved in several of these processes either by effects of TGF-β on the tumor cells themselves or indirectly through affecting the microenvironment. As previously mentioned, TGF-β signalling in conjunction with Ras induces an epithelial-to-mesenchymal transition (EMT) which results in a more migratory and invasive phenotype. These events lead to the acquisition of metastatic properties *in vivo* (Cui, W. et al., 1996) (See section 1.6.3.4). In addition, many tumours have increased production of TGF-β, which benefits the cancer cells indirectly through production of extracellular matrix, suppression of immune system function, or promotion of angiogenesis (Akhurst, R. J. et al., 2001). For a solid tumour to grow beyond 1-2 mm in diameter, they require nutrients and oxygen, which is often acquired through the formation of a new blood supply (i.e. angiogenesis). As described in Section 1.6.2, TGF-β plays a prominent role in stimulating angiogenesis and many studies implicate the angiogenic-inducing properties of high levels of TGF-β in tumour progression (de Jong, J. S. et al., 1998). Consistent with a role in stimulating angiogenesis, expression of endoglin on endothelial cells is dramatically increased during tumour-induced angiogenesis (Burrows, F. J. et al., 1995). TGF-β also induces the expression of vascular endothelial growth factor (Pertovaara, L. et al., 1994), which then directly promotes angiogenesis. In addition, TGF-β-induced expression of the metalloproteases MMP-2 and MMP-9 and downregulation of the protease inhibitor tissue inhibitor of metalloproteases (TIMP) in both tumour cells and endothelial cells, promotes

degradation of the ECM. By increasing the motility of tumour cells and endothelial cells in a protease rich environment, TGF-β stimulation results in invasive tumour cells, which may represent one of the tumour promoting activities of TGF-β (Akhurst, R. J. et al., 2001). To conclude, it is increasingly evident that genes known to perform critical roles during early embryogenesis, are also expressed during the development of cancer. In this regard, oncogenesis may be considered as the recapitulation of embryogenesis in an inappropriate temporal and spatial manner. As the role of TGF-β is crucial to the developing embryo, it is not surprising that cancer cells exploit the activities of this multifaceted cytokine for the progression and spread of tumours.

1.8 Aims of Thesis

The dual role of TGF-β in cancer has prompted a lot of work in this area. However, investigation into the molecular mechanisms regulating the paradoxical responses of TGF-β signalling during tumour progression has just scraped the surface. How TGF-β functions as a tumour suppressor or a tumour promoter at different stages during tumorigenesis is still a great mystery, although current work is slowly unravelling pieces of the puzzle. The identification of mutations in key components of the pathway or their downregulation by epigenetic mechanisms have revealed ways in which tumour cells exploit the pro-oncogenic activities of TGF-β and have opened the door to exciting new avenues of investigation. The importance of the Smads in both tumour suppressor and pro-oncogenic activities cannot be underestimated and represent a primary target for modulation of TGF-β activities. To this end, the aim of my study was to investigate the molecular mechanisms underlying the different responses of cells to TGF-β with a particular focus on the role of Smad regulation in these processes. Here, I present data detailing my extensive characterisation of TGF-β signalling in a tumour cell model system which uncovers new determinants that could act to modulate TGF-β activities during cancer progression.

2 Materials and Methods

2.1 Molecular Biology

2.1.1 Materials and Solutions

Most chemicals and solvents were obtained from either Merck, Sigma-Aldrich, Roche or BioRad and are of analytical grade. All buffers and solutions were made up using deionised water or DEPC treated water to reduce RNAse contamination. This is a list of general materials and solutions. Details of solutions used specifically for one method are described in the relevant section.

TE buffer

10 mM Tris-HCl (pH 7.5), 1 mM EDTA (pH 8.0)

50 x TAE

2 M Tris-acetate, 50 mM EDTA (pH 8.0)

10 x PCR buffer

500 mM KCl, 100 mM Tris-HCl (pH 8.3), 15 mM $MgCl_2$ and 0.01% (w v) gelatin

10 x dNTPs

2 mM dATP, 2 mM dCTP, 2 mM dGTP, 2 mM dTTP (Amersham Pharmacia Biotech)

6 x DNA Loading Dye

0.25 % (w v) bromophenol blue, 0.25 % (w v) xylene cyanol FF, 30 % (v v) glycerol

Ethidium Bromide

Stock solution made to 10 mg ml in water. Used at 0.5 µg/ml

Ampicillin

Stock solution made to 50 mg ml in water. Used at 50 µg/ml

Luria-Bertani (LB) Medium

1 % w v Bacto-tryptone, 0.5 % w v Bacto-yeast extract, 1 % w v NaCl, pH 7

LB Agar

1.5 % w v Bacto-agar in LB medium

2.1.1.1 List of Plasmids

For plasmids constructed by me for this work see Appendix I. All constructs were sequence verified and checked by restriction digestion and where appropriate gene expression.

Other Plasmids

p-Zome-1-N was a gift from Justin Cross (Cancer Research UK), which was originally obtained from Cell zome (based on pBABE-puro). pcDNA3N was also provided by Justin Cross (Cancer Research UK).

The following plasmids have been previously described; pFTX5 XSmad2Δ3'UTR and pFTX5 HS dpc4 (Howell, M. et al., 1997); EFplink myc hSmad3 and EFplink FLAG-Smad3 (Inman, G. J. et al., 2002a). The human Smad2 cDNA (26-261), human Smad3 cDNA (321-626) and GAPDH cDNA (51-231) cloned into pGEM-T were as previously described (Nicolas, F. J. et al., 2003b). The human γ-actin cDNA (BamHI-HindIII fragment) in pSP64 was previously described (Enoch, T. et al., 1986). The following reporter plasmids were as previously described; $CAGA_{12}$-Luciferase (Dennler, S. et al., 1998), ARE3-Luc (Pierreux, C. E. et al., 2000).) *c-jun* SBR_6-Luciferase (Inman, G. J. et al., 2002a), BRE-luciferase (Korchynskyi, O. et al., 2002), and the EF-LacZ control plasmid (Bardwell, V. J. et al., 1994).

2.1.2 Purification of Plasmid DNA

To prepare plasmid DNA, a single ampicillin-resistant colony was picked and used to inoculate either 3 ml (small-scale preparation – 'miniprep') or 50 ml (large-scale preparation – 'midiprep') of LB containing ampicillin (50 μg/ml). The culture was then shaken overnight at 37°C. For minipreps, the DNA was isolated using QIAprep® spin miniprep kit (Qiagen) according to the Manufacturers' instructions. For midipreps, the DNA was isolated using either a Plasmid Midi Kit (Qiagen) or a NucleoBond Plasmid Midi Kit (Clontech), both according to the Manufacturers' instructions.

2.1.3 Estimation of Nucleic Acid Concentration

Double-stranded DNA, RNA and synthetic oligonucleotides were quantified by spectrophotometer using a Beckman General Purpose Spectrophotometer. A 1/400 dilution in water of DNA solutions was made, and the optical density (OD) determined at a wavelength of 260 nm on a Beckman General Purpose Spectrophotometer. This value was then used to obtain the concentration of the DNA or RNA in μg/ml using the following equation:

$$OD_{260} \times \text{dilution factor} \times \text{Extinction Coefficent} = \text{Concentration in } \mu g/\mu l$$

The extinction coefficients are as follows:

dsDNA: 50

ssRNA: 40

ssDNA: 33

single-stranded oligo: 20

To estimate the purity of the sample, the OD at 280 nm was also measured. A ratio (OD_{260} OD_{280}) of ≥ 1.8 but ≤ 2.0 is an indication of pure DNA.

2.1.4 Subcloning Procedures

Restriction enzyme digestion

Restriction enzyme digestions were performed for 1-2 hr in the appropriate NEB buffers at 37°C unless recommended otherwise in the manufacturer's specification sheet. 10 µl of reaction mixture and 1 unit of enzyme were used per microgram of DNA. Products were analysed by agarose gel electrophoresis.

Klenow

To form blunt end DNA fragments by filling-in 5' overhang, digests were treated with 1 unit DNA Polymerase I Klenow fragment (NEB) per µg DNA supplemented with 2 µl 10 mM dNTPs (10 mM dATP, 10 mM dCTP, 10 mM dGTP and 10 mM dTTP [Amersham Pharmacia Biotech]), and incubated for 15 minutes at room temperature prior to purification.

Phosphatase treatment

Before phosphatase treatment, reactions were ethanol precipitated using sodium acetate. The pellet was resuspended in 50 µl 10 mM Tris-HCl pH 9.5, 1 mM spermidine, 0.1 mM EDTA, 1 mM $MgCl_2$, 0.1 mM $ZnCl_2$ and incubated at 37°C for 1 hr with 1 unit of alkaline phosphatase (Boehringer Mannheim).

Ligation

10 µl ligation reactions were carried out at room temperature using 200 units of T4 DNA ligase in 10 mM $MgCl_2$, 60 mM Tris-HCl pH 7.4, 6 mM DTT, 1 mM ATP and left for a minimum of 3 hr or overnight.

Sequencing

Sequencing was used to verify sequences using the applied Biosystems BigDye® termination protocol. DNA template (500 ng) was mixed with 20 ng of primer and 8 µl BigDye® Terminator v2.0 v3.1 (Applied Biosystems) in a final volume of 20 µl. The sequencing reaction was then carried out in a GeneAmp® PRC System 9700 (Applied Biosystems). Unincorporated dye terminators were removed from sequencing

reactions using DyeEx™ 2.0 Spin Kits (Qiagen) and the pellet was dried. Prior to loading on the sequencing gels, the pellet was resuspended in 3 µl Micro STOP~Red loading buffer (Microzone Limited) and denatured at 95 °C for 5 minutes. All sequencing was performed on ABI PRISM® 377 DNA Sequencers (Applied Biosystems).

2.1.5 Agarose Gel Electrophoresis

Agarose (Invitrogen) gels (1- 2 %) were prepared in 1 x TAE with 0.5 µg/ml ethidium bromide. The molten gel was poured into a sealed gel tray with the appropriate gel comb(s) and allowed to set at room temperature. All gels were run in 1 x TAE with a Lambda DNA-*BstE*II digest DNA ladder (New England Biolabs; NEB) at 120 volts for 15-45 minutes. Visualisation and photography of gels was by ultraviolet illumination using a UVP 2UV Transilluminator at 310 320nm.

2.1.6 Polymerase Chain Reaction (PCR)

Polymerase Chain Reaction (PCR) was used to amplify cDNA for subcloning and for semi-quantitative Reverse Transcriptase (RT-PCR) reactions. Oligonucleotide primers were designed to be 20-25 mers. These were supplied by the in-house Cancer Research UK oligonucleotide synthesis service and laterally Sigma-Aldrich. A list of all oligonucleotides used in this thesis has been included in Appendix II.

PCRs contained template DNA, 100 nM of forward and reverse primers, and 200 µM each of dATP, dTTP, dGTP and dCTP (1 x dNTPs) in a final concentration of 10 mM Tris-HCl (pH 8.3), 50 mM KCl, 1.5 mM $MgCl_2$ and 0.001 % (w/v) gelatin (1 x PCR buffer), with 2.5 units Taq polymerase (Developmental Signalling Laboratory, Cancer Research UK). PCRs were carried out in a GeneAmp® PCR System 9700 (Applied Biosystems).

Standard conditions were as follows:

94°C	3 min	
94°C	30 sec	35 cycles
55°C	30 sec	
72°C	30 sec	
72°C	10 min	
4°C	∞	

2.1.7 RNA preparation from Cells

Total RNA was extracted from EpH4 and EpRas cells using TRIZOL® Reagent (Invitrogen). 15 ml of TRIZOL® was added to each 15 cm dish and pipetted up and down before transfer to a sterile falcon and incubation at RT for 5-10 min. For other dish sizes refer to the table below.

	Area cm2	**Volume TRIZOL®**
6 well plate	10 cm^2	1 ml
6 cm dishes	20 cm^2	2 ml
10 cm dishes	55 cm^2	6 ml
15 cm dishes	150 cm^2	15 ml

This was followed by addition of 0.2 ml of chloroform per ml of TRIZOL added initially. Samples were shaken vigourously for 15 sec and then incubated at RT for 5 min. Phase separation was performed by centrifugation at 3000 rpm at 4 °C for 30 min (Beckman Allegra™ 6KR centrifuge). The upper aqueous phase was then transferred to a fresh tube and 0.5 ml of isopropanol was added per ml of TRIZOL used for the initial homogenization. Samples were incubated for 10 min at room temperature before centrifugation at 3000 rpm for 30 min at 4 °C to precipitate the RNA. RNA was then washed with 75% ethanol and pelleted by centrifugation at 3000 rpm for 10 min. The supernatant was removed and the pellet was left to dry for 5-10 min at RT. The RNA

was resuspended in 480 μl water. The concentration of RNA was determined using 10 μl of RNA in 600 µl of H_2O. To the remaining 470 µl, 50µl of 3 M NaOAc and 500 µl of Isopropanol were added. This RNA slurry was then stable at 80 °C.

Determination of RNA concentration

The concentration of RNA in this slurry is calculated using the equation below. In this case two dilution factors must be taken into account.

OD_{260} × dilution factor × Extinction Coefficent = Concentration in μg/μl

Dilution factor 1: 10 µl 600 µl = 60

Dilution factor 2: 470 µl (470 µl + 50 µl + 500 µl) = 2.17

Extinction coefficient for dsRNA: 40

OD_{260} x (40x60 2.17) = Concentration in μg μl in the slurry

2.1.8 ***RT-PCR***

Reverse transcription

Total RNA prepared from EpH4 and EpRas cells was used for reverse transcription. RNA (5 µg) was reverse transcribed using SuperScript™ II RNase H- Reverse Transcriptase (Invitrogen) Total RNA, dNTPs and Random hexamer were combined (see table) for each RT reaction and heated to 65°C for 5min before being placed on ice. All incubations were carried out in a GeneAmp® PCR System 9700 (Applied Biosystems).

Total RNA	5 µg in 11 µl
50-500ng Random Hexamer (250 ng/µl)	1 µl
dNTP (10mM)	1 µl

4 µl of 5x Buffer and 2 µl of DTT 0.1M (supplied by Invitrogen) was added to the mix and incubated at 25°C for 2min. Finally 1µl of SuperScript™ II RNase H- Reverse Transcriptase was added to each tube and the following incubation programme was used.

25°C	10 min
42°C	50 min
70°C	15 min

PCR reactions

PCR was carried out in the exponential phase (20 to 35 cycles) to allow a semiquantitative comparison of RNA levels. 3 µl of cDNA prepared by reverse transcription was used in each PCR reaction. Specific primers were used for analysis of genes, for which the sequences are given in Appendix II. Grb2 was used as a control. PCR products were analyzed in 1.5% agarose gels. PCR reactions were carried out in a GeneAmp® PCR System 9700 (Applied Biosystems). The standard PCR programme (Section 2.1.6) was used for analysis of the ALK genes.

2.1.9 RNAse Protection Assay

Mouse Smad2, Smad3, GAPDH and actin transcripts were analyzed by quantitative RNase mapping as previously described (Treisman, R., 1985) with singlestranded, uniformly labeled RNA probe synthesized *in vitro* with Sp6/T7 RNA polymerase and [α-^{32}P] rUTP.

2.1.9.1 Probes

All of the probes used for RNase protection were designed against the human sequences but cross-reacted with the mouse sequences (See also section 2.1.1.1).

Smad2

The Smad2 probe protects the region encoding amino acids 9–86 of the human sequence (Nicolas, F. J. et al., 2003b). Linearised with SpeI and transcribed with T7.

Smad3

The Smad3 probe protects the region encoding amino acids 107–208 of the human sequence (Nicolas, F. J. et al., 2003b). Linearised with SpeI and transcribed with T7.

GAPDH

The GAPDH probe protects the region encoding amino acids 18–77 (Nicolas, F. J. et al., 2003b). Linearised with BamH1 and transcribed with Sp6.

γ-actin

The γ-actin was as previously described (Enoch, T. et al., 1986). Linearised with HinfI and transcribed with Sp6.

Linearisation of Plasmids for Probes

10 μg of plasmid was digested with the appropriate enzyme at 37 °C overnight. Linearised plasmid was then extracted using phenol/chloroform, followed by ethanol precipitation resuspension in 5 μl of DEPC-treated water. The concentration of RNA was determined and adjusted to 1 μg μl.

2.1.9.2 Sp6 and T7 RNA Probe Synthesis for RNA Protection Assays

RNA probes were synthesised as previously described using the linearized reporter and reference templates (See section 2.1.9.1) (Melton, D. A. et al., 1984). The 10 μl labelling reactions contained 0.5μl linearised template cDNA (1 μg/μl), 0.5 μl of the appropriate RNA-polymerase (T7, NEB; Sp6 Promega), 2.5 μl ^{32}P-UTP (600Ci mmol), 0.5 μl of each rATP (10 mM), rGTP (10 mM), and rCTP (10 mM), 0.5 μl of RNase inhibitor (Amersham) and 0.25 μl DTT (200 mM). The reactions were incubated at 37°C for 1 hr.

After RNA synthesis, DNA template was digested in 95 μl of 50TE, 0.5 μl of RNase inhibitor, 1.25 μl mixture (10 μl of 1M of $MgCl_2$, 5 μl of 1 M $CaCl_2$, 10 μl of 200 mM DTT), using 0.75 μl of DNase I at 37°C for 30 min. Following addition of 4 μl of 0.5 M EDTA pH 8.0 and 10 μg tRNA as carrier, the reactions were phenol extracted and precipitated with 25 μl 4 M ammonium acetate and 0.3 ml ethanol on

dry ice. Precipitates were spun down at 13000 rpm for 10 min, washed with 80% ethanol. The dried pellet was dissolved in 1 µl of water and 5 µl of formamide loading buffer (see below) and denatured at 95 °C for 3 min. The probes were gel-purified using 6% denaturing acrylamide gel (see below). The gel running was carried out in 0.5 x TBE at 13 W for 1.5 hr. The labelled probes were excised from the gel and eluted in elution buffer for 2 hrs at 50 °C. After phenol extraction, the probes were ethanol precipitated in the presence of carrier tRNA, the pellet was dissolved in 20 µl water and counted in a scintillation counter by Cherencov counting.

Formamide Buffer
0.25% xylene-cyanol
0.25% bromophenol-blue
20 mM EDTA
95% v/v formamide

6% acrylamide gel
6% 40:1 acrylamide:bis acrylamide
7M urea
0.5 x TBE

Elution Buffer
0.5 M NH_4OAc
0.1 % SDS
1 mM EDTA

2.1.9.3 RNA Analysis with Sp6/T7 probes

For probe hybridisation the reactions were carried out in a total volume of 30 µl containing 15 µg total RNA in 30 µl hybridisation buffer and 1 µl labelled probe (2 x 10^5 cpm/sample). Samples were incubated at 85 °C for 5 min to denature RNA and they were hybridised overnight at 45 °C. Digestion of un-hybridised single stranded RNA was carried out by RNAase treatment in 350 µl RNase buffer with 0.4 µl

RNaseT1 (20 U/µl; calbiochem) at 37 °C for 30 min. The RNase was then digested by addition of 5 µl Proteinase K (10 mg/ml, Sigma) and 0.25% SDS at 37°C for 30 min. After phenol/chloroform (1:1) extraction, the double-stranded RNA was precipitated using 1 volume isopropanol and dissolved in 1 µl water and 5 µl formamide loading buffer. The reactions were electrophoresed using 6% denaturing acrylamide gel at 11 W for approximately 1.5 hr. The gel was fixed (10% methanol, 10% acetic acid), dried on Whatman 3MM paper and visualised by autoradiography.

Formamide hybridisation Buffer
400 mM NaCl
40 mM PIPES pH 6.4
1 mM EDTA
80% v/v formamide (deionised)

RNAase Buffer
10 mM Tris HCl, pH 7.5
5 mM EDTA
300 mM NaCl

2.2 Cell Culture

2.2.1 Materials and Solutions

All tissue culture media and solutions were supplied by the in-house Cancer Research UK Cell Services.

Dulbecco's Modified Eagle Media (D-MEM)
6.4 g NaCl, 4.5 g D-Glucose, 10 ml 3:5 Penicillin/Streptomycin solution, 110 µg sodium pyruvate, 3.7 g $NaHCO_3$, 584 µg L-Glutamine, 2 ml 20 % (w/v) KCl, 1 ml 26.5 % (w/v) $CaCl_2$, 1 ml 20 % (w/v) $MgSO_4$, 1 ml 14 % (w/v) NaH_2PO_4, 1 ml 0.01 %

(w/v) $Fe(NO_3)_3$, 1 ml 0.02 % (w/v) antimyotic, 1.5 ml 1 % (w/v) phenol red, 50 ml amino acids and 8 ml vitamins in 1 litre of water. The media was bubbled with CO_2 until pH 7 and filter sterilised. Media was supplemented with 10 % (v/v) foetal bovine serum (Invitrogen) and stored at 4 °C. Prior to use, 10 % D-MEM was heated in a water bath to 37 °C.

5 x Trypsin Versene

2.5 g trypsin, 8 g NaCl, 1.15g Na_2HPO_4, 200 µg KH_2PO_4, 1 g versene (EDTA), 1.5 ml 1 % (w/v) phenol red

2.2.1.1 Growth factors and Inhibitors

TGF-β1 TGF-β3

TGF-β1 TGF-β3 (R&D) was reconstituted in sterile 4 mM HCl containing 1 mg/ml BSA to a stock concentration of 1 µg ml and stored at -80 °C. Stimulation with TGF-β was used at a final concentrations of 2 ng ml.

SB-431542 (ALK5 inhibitor)

SB-431542 (GSK) was resuspended in DMSO to make a stock concentration of 10 mM. Final concentrations were used at 10 µM.

U0126

The MEK1 2 inhibitor, U0126 (Promega), was dissolved in DMSO to make a stock solution of10 mM. final concentration used at 25 µM.

Cycloheximide

Cycloheximide was made up in water to a stock concentration of 10 mg/ml. Used at 20 µg ml final concentration.

2.2.2 General Culture Conditions

Cell lines were all cultured on plastic dishes or flasks of tissue culture grade (Corning Incorporated and BD Falcon™) in an incubator (Sanyo) at 37 °C and 10 % CO_2.

2.2.2.1 Cell lines

Cells were cultured in D-MEM supplemented with foetal bovine serum (Invitrogen) that was warmed to 37 °C before adding to the cells. To remove cells from the flask, the cells were washed once with PBSA and then incubated with trypsin:versene solution for 1-10 minutes, depending on the cell line.

Cell Line	Source	Media	FCS (%)	Supplements
EpH4	Martin Oft, Schering-Plough BioPharma	D-MEM	8 %	10 mM HEPES
EpRas	Ernst Reichmann, University-Children's Hospital, Zurich	D-MEM	8 %	10 mM HEPES +G418 (500mg/ml)
X-tumour	Ernst Reichmann, University-Children's Hospital, Zurich	D-MEM	8 %	10 mM HEPES +G418 (500mg/ml)
HaCaT	Cancer Research UK	D-MEM	10 %	
C2C12	Richard Treisman, Cancer Research UK	D-MEM	10 %	
MDA-MB-468	ATCC	D-MEM	10 %	
AM12	Julian Downward, Cancer Research UK	D-MEM	10 %	
GP+E	Julian Downward, Cancer Research UK	D-MEM	10 %	

2.2.2.2 EpH4 system

EpH4 mouse mammary epithelial cells and their Ras-transformed derivatives EpRas or X-Tumour cells were cultured in DMEM containing 8 % FBS (Invitrogen) and 10 mM HEPES (Invitrogen). EpRas and X-tumour cells were supplemented with G418 (Invitrogen) 500 mg/ml. Subculturing was performed every 2 or 3 days at a ratio of 1: 4 for epithelial cells and 1: 6 for EpRas and XT cells.

2.2.3 Transient Transfections

2.2.3.1 Lipofectamine 2000 Procedure

EpH4, EpRas and HaCaT cells were transfected at a confluency greater than 90% using Lipofectamine™2000 Reagent (Invitrogen) and Opti-MEM® I Reduced Serum Medium (Invitrogen). The DNA, Lipofectamine™ 2000 Reagent (Invitrogen) and Opti-MEM® I Reduced Serum Medium (Invitrogen) were combined (see Table), vortexed and allowed to incubate at room temperature for 15-30 minutes.

Culture Vessel	DNA (μg) and dilution volume	Volume of Lipofectamine 2000 and dilution volume	Volume of Plating Opti-MEM
12-well	1.6 μg in 100 μl	4 μl in 100 μl	200 μl
6 well	4 μg in 250 μl	10 μg in 100 μl	500 μl
6 cm	8 μg in 500 μl	20 μl in 500 μl	1 ml

The cells were washed once with Opti-MEM and the appropriate volume of Opti-MEM was added to each dish (see Table). The transfection mix was added and the cells were incubated for 3-5 hours at 37 °C and 10 % CO_2 before washing and replacing with D-MEM supplemented with 8-10 % foetal bovine serum (Invitrogen). The cells were then incubated overnight or 48 hrs before any inductions with TGF-β were performed.

2.2.3.2 Superfect Procedure

The superfect transfection procedure was used for MDA-MB468 cells only. MDA-MB468 cells (in 12 well plates with 700µl D-MEM supplemented with 10 % foetal bovine serum) were transiently transfected when they were approximately 50-60 % confluent using Superfect transfection reagent (Qiagen). In a sterile eppendorf, 120 µl Opti-MEM® I Reduced Serum Medium (Invitrogen) was combined with 3.5 µl Superfect transfection reagent and allowed to incubate at room temperature for 5 minutes. This transfection mixture was then added dropwise to 1.5 µg DNA and left at room temperature for 10-15 minutes. The transfection mixture was then added to the MDA-MB468 cells and incubated for 3 hours at 37 °C and 10 % CO_2 before washing and replacing with D-MEM supplemented with 10 % foetal bovine serum (Invitrogen). The cells were then incubated overnight before any inductions with TGF-β were performed.

2.2.3.3 The Dharmafect Procedure

5 x 10^4 cells EpH4 and EpRas cells were plated out to achieve 20-30% confluency the following day. siRNA pools (a mix of 4 different siRNA duplexes) and individual siRNA duplexes, obtained from Dharmacon (see table below), were resuspended in 1X siRNA Buffer (Dharmacon) to a stock concentration of 20 µM. siRNA pools or individual duplexes were transfected at a final concentration of 75 nM into EpH4 and or EpRas cells using Dharmafect2 reagent (Dharmacon). Following an overnight incubation, the transfection mix was replaced with fresh media. The next day, the cells were plated for reporter assays or protein preparation.

SMARTpool siRNA reagents were as follows:

SMARTpool siRNA	*Catalogue number*
Smad1	M-055762-00
Smad2	M-040707-00
Smad3	M-040706-00
Smad5	M-057015-00
Smad8	M-046344-00
ALK1	M-043004-00
ALK2	M-042047-00
ALK6	M-051071-00
TβRII	M-040618-00

Individual siRNA duplexes were as follows:

siRNA duplexes	**Catalogue number**
ALK3 (4)	D-040598-04
ALK5 (2)	D-040617-02

siRNA duplexes	**Catalogue number**
RISC-Free siRNA	D-001220-01-05
non-targeting	D-001206-13-05

2.2.3.4 Luciferase and β-Galactosidase assays

All Luciferase and β-Galactosidase assays were performed as previously described (Pierreux, C. E. et al., 2000). EpH4, EpRas and HaCaT cells were plated out in a 12-well plate and transfected with 500 ng reporter construct (either $CAGA_{12}$-Luciferase, *c-jun* SBR_6-Luciferase, ARE_3-Luciferase or BRE-Luciferase), 25-75 ng transcription factor, and 500 ng pEF LacZ as an internal control (Bardwell, V. J. et al., 1994). Cells

were treated ± TGF-β for 8 hours prior to lysis in 100 µl 1 x Reporter Lysis buffer (Promega).

2.2.4 Generation of Stable Cell lines

2.2.4.1 Retroviral Infection

Generation of HaCats expressing the ecotrophic receptor

To generate HaCaT cell lines stably expressing p-Zome, wild-type cells were first infected with an amphotropic retrovirus encoding the ecotrophic receptor (pWZL-Neo-EcoR). Retrovirus stock was obtained from the medium of the packaging cell line, AM12 cells. HaCaT cells were seeded in 10 cm plates so that they reached 40% confluency the following day. Virus supernatant from AM12 cells was diluted 1:10 with fresh media and supplemented with 8 µg/ml Polybrene. After sterile filtering with a 2.2 µM membrane (Roche), 2.5 mls of the retroviral mixture was added to the HaCaT cells and incubated for 3 hrs at 37°C. The next day, pools of cells were selected with 800 µg/ml G418 for 5–6 days. This generated a HaCaT cell line expressing the ecotrophic receptor required for subsequent infections (HaCaT EcoR).

Generation of HaCats expressing TAP-Smads

TAP-Smad2, TAP-Smad3, TAP-Smad4–expressing HaCaT cells were generated by retroviral gene transfer using retroviral vectors of the Smads in p-Zome (Cellzome). p-Zome-Smad constructs were transfected into the packaging cell line, GP+E, (grown in DMEM plus 10% FCS) which were then selected with 2.5 µg/ml puromycin for 3-4 days. Virus supernatants from these transfected GP+E cell lines were then used to infect the HaCaT EcoR cells. These cells were then selected with 5 µg/ml puromycin for 3-4 days. Pools were made from retrovirally infected and drug-selected cell populations. Clones were then isolated by seeding at low density, expansion for 10-14 days and isolation of colonies using sterile cloning rings, dipped in autoclaved silicon grease. The rings were placed over the selected colonies prior to trypsinisation. After the cells had detached they were transferred to selective medium and subsequently cultured as normal.

2.2.4.2 Transfection

EpH4 cells were transfected with the pcDNA3N constructs using the lipofectamine 2000 transfection procedure (Section 2.2.3.1) and incubated overnight. The following day, the cells were trysinised and replated at low density, to make clones and at higher density to produce a pool of cells. These cells were then selected with 5 μg/ml puromycin for 3–4 days. Clones were isolated as described above.

2.2.5 Cell cycle analysis

2.2.5.1 Synchronisation of cell by Contact Inhibition

For G1 S phase progression studies, 5 x 10^5 EpH4, EpRas and X-tumour cells were seeded into 6 cm plates, so that cells were 100% confluent after two days. The cells were arrested in G_0 G_1 by confluency for two days and EDTA released using versene (Gibco, 0.2 g L EDTA) for 30-45 min at 37°C. Cells were then replated at a dilution of either 1:4 (EpH4 cells) or 1:6 (EpRas and X-tumour cells). The majority of cells enter S-phase after 18 hr. Samples for all G1 S profiles shown were collected 22 h after EDTA release. The results were, however, verified extensively throughout a 16-h to 48-h time window.

2.2.5.2 DNA Analysis using Propidium-Iodide

To examine cell cycle distribution, cells were detached from plates by incubation with trypsin, washed in PBS and fixed in 70% ice-cold ethanol for 30 min. After treatment with RNase (100μg ml) for 5 min at room temperature, cells were stained with 50μg ml propidium-iodide (Becton Dickinson) for 5 min. Stained cells were analysed by flow cytometry using 488 nm excitation, carried out by the Cancer Research UK Service. The data profiles were analysed by the Dean-Jett-Fox integration method.

2.2.6 Epithelial-to–Mesenchymal Transtitions (EMT)

2.2.6.1 EMT Assay on Plastic

5 x 10^4 EpRas cells were plated out in 6-well plates and either grown in the presence or absence of TGF-β1 (2 ng/ml). The medium was changed 1 d after seeding and then every other day. TGF-β was added to the cells upon medium change. Three days after plating, the cells were trypsinised and re-plated at equivalent density to day 1. Cells were grown for a total of 10 days, which required two trypsinisations, and then harvested 48 hrs after final TGF-β addition. Cells were processed for immunofluorescence using an anti-E-cadherin antibody (BD), to analyze adherens junctions or an anti-Zona Occludens 1 (Z0-1) antibody (Zymed), to analyze tight junctions. Actin reorganization was visualized with Texas red-conjugated phalloidin, and nuclei were visualized with DAPI.

2.2.6.2 Adaptation of EMT assay for use with siRNA oligonucleotides

5 x 10^4 EpRas cells were plated out in 6-well plates and were transfected with siRNA oligonucleotides (Section 2.2.3.3). After overnight incubation, cells were replated 1:2 and grown in the presence or absence of TGF-β (2 ng/ml). The medium was changed 1 d after seeding and then every other day. TGF-β was added to the cells upon medium change. Three days after plating, the cells were trypsinised and re-plated at equivalent density to day 1. A second siRNA transfection was performed on day 4. One, final replating of cells was carried out on day 7. Cells were grown for a total of 9 days in the presence or absence of TGF-β and then harvested 48 hrs after final TGF-β addition.

2.2.6.3 3-D Collagen gels

Serum-free 3-D collagen gel cultures were prepared as previously described (Oft, M. et al., 1996) with minor modifications. Cells were suspended in standard growth medium to a final density of 1500/100 µl. 500 µl of cells were then mixed with 500 µl of ice-cold rat tail collagen type I solution (BD), achieve a final concentration of 1.5 mg/ml.

Drops (100 µl) were placed into the wells of 17 mm 4-well plates (Nunc). After incubation at RT for 30 min and at 37°C for 4 h the gels were overlaid with 0.5 ml serum-free medium (Mammary Epithelial Basal Medium, Promocell) supplemented with growth factors (see below). Medium changes were performed every other day. For EMT assays, TGF-β1 was added at day 2-3, and then every other day.

Supplements for Feeding Media
Pen/Strep
5ng/ml TGF-α
10µg/ml Insulin
1µM Isoproterenol
1µM Dexamethasone
Bovine Pituatary Extract-15 (BPE-15) 1:250

2.2.7 Immunofluorescence

2.2.7.1 Indirect Immunofluorescence on Plastic

Cells were grown on glass coverslips and fixed either by Formaldehyde or Methanol acetone as previously described (Nicolas, F. J. et al., 2003b).

Formaldehyde fix

Coverslips were placed in a 24-well dish and washed twice with PBS. Fixing was performed using 3.7% Paraformaldehyde (PFA) for 10 minutes at RT. Coverslips were washed again with PBS and then permeabilised for 10 minutes with 0.3 % triton X-100 in PBSA. Blocking was subsequently carried out for 30 minutes at room temperature with a blocking solution (see below) After blocking, coverslips were washed once with PBS before incubation with primary antibody (see table). Antibodies were diluted in blocking solution without milk and incubated for 1 hour at room temperature. The list of antibodies and the concentration used is below. Cells were then washed three times with 1-3 ml of 0.1 % triton X-100 in PBSA and subsequently incubated with secondary antibody diluted in blocking solution without milk for 30 min. After several washes with PBS including a 5 min incubation with dapi and a final wash with water,

coverslips were mounted onto slides using Mioviol (Hoechst) and analysed by confocal microscopy (Section 2.2.7.3).

PFA fix Blocking Solution
0.3% avid BSA
10 % foetal calf serum (Invitrogen),
5 % powdered milk (Marvel)
0.3 % Triton X-100
made up in PBSA

Methanol: Acetone Fix

Coverslips were washed as above in PBS and fixed in methanol: acetone (1:1) at –20°C for 20 min. The fix solution was removed and coverslips were left to dry so any remaining fix evaporated. Coverslips were washed three times with PBS and then left in PBS to rehydrate. Cells were permeabilised for 10 minutes with 0.1 % triton X-100 in PBS for 10 min at RT and then blocked in 2% fish gelatin (Sigma) in PBS for 30 min. Primary antibodies were diluted in fish gelatin blocking solution and added to cells for 1 hr at RT. After the antibody was removed, the cells were washed twice in 0.1 % Trition/PBS and once in PBS and subsequently incubated with secondary antibody also diluted in fish gelatin blocking solution for 30 mintues. Cells were washed, mounted on slides as described above.

Primary Antibodies:

Antibody	Supplier	Species	Concentration	Fixation Method
E-cadherin	BD	Mouse	1:200	Methanol/Acetone
Z0-1	Zymed	Rabbit	1:400	Methanol/Acetone
Vimentin	Sigma	Mouse	1:200	Methanol/Acetone
Smad2/3	BD	Mouse	1:200	PFA
Ki67	Sigma		1:1000	PFA

Phalloidin is a toxin from the toadstool "Death Cap" (*Amanita phalloides*) that binds specifically to F-actin. A fluorescent analog of phalloidin (Phalloidin-AlexaFluor 594, Invitrogen) is used to study F-actin distribution in permeabilised cells (Wulf, E. et al., 1979). It is used at a 1:200 dilution and using a PFA fix.

Secondary Antibodies:

Antibody	Conjugate	Supplier	Species	Concentration
Mouse IgG	AlexaFluor 488	Invitrogen	Goat	1:700
Rabbit IgG	AlexaFluor 488	Invitrogen	Goat	1:700
Mouse IgG	AlexaFluor 594	Invitrogen	Goat	1:700
Rabbit IgG	AlexaFluor 594	Invitrogen	Goat	1:700

2.2.7.2 Indirect Immunofluorescence on Collagen Gel

Collagen gels were fixed with 1% formaldehyde in 250 mM Hepes, pH 7.4, freshly diluted from 16% paraformaldehyde stocks stored at –20°C. After 15 min at room temperature, the gels were washed once each with Tris- and phosphate-buffered saline plus 0.2% Tween 20 (TBST and PBST, respectively) and treated for 1 h at 4°C with blocking solution Gels were incubated with primary antibodies plus DAPI in blocking solution for 1 h at 37°C in a wet chamber, washed three times in PBST for 30 min, and postfixed with 4% PFA in PBST for 15 min at 23°C. After 30-min washes in TBST, PBST, and blocking solution, the gels were incubated with appropriate secondary antibody mixtures made up in blocking solution for at least 1 h or overnight at 4°C. Gels were washed three times in PBS, once in distilled water, and mounted in Mowiol (Hoechst).

Collagen Gel Blocking Solution
PBST
0.1% gelatin
10 µg/ml nonimmune bovine IgG

2.2.7.3 Confocal Microscopy

Immunostained cells were visualised using a Zeiss 520/ Zeiss confocal LSM 510 laser scanning confocal light microscope. Samples were excited at 543 nm and observed with a long-pass filter allowing passage of wavelengths of 600 nm and above.

2.3 Protein Analysis

2.3.1 General Materials and Solutions

10 x TBE

0.9 M Tris-borate, 10 mM EDTA (pH 8.0)

Phosphate buffered saline (PBSA, Cancer Research UK central services)

8 g NaCl, 0.25 g KCl, 1.43 g Na_2HPO_4, 0.25 g KH_2PO_4 in 1 litre of water. pH was adjusted to 7.2

Protease Inhibitors

Complete EDTA-free tablets (Roche) were dissolved directly in 50 ml of the buffer to be used.

DTT

Stock solution made up to 1 M in water. Used at 1 mM

poly dI-dC

Stock solution made in water to make 1 mg/ml. The solution was sonicated on ice for approximately 30 seconds to reduce its average size to below 1 kb

2.3.2 Protein Extract Preparation

2.3.2.1 Whole Cell Extract

Cells were washed twice with ice-cold PBS, ensuring all PBS was removed after the second wash. Extracts were then made essentially as previously described (Marais, R.

et al., 1993). The cells were scraped from the tissue culture dishes into lysis buffer (see below) and sonicated for 10 seconds on ice. Extracts were then centrifuged at 13,000 rpm (Biofuge fresco Heraeus centrifuge) for 5 minutes at 4 °C to remove cell debris and the supernatant transferred to a cold sterile eppendorf. Protein concentration was measured as described. 30 μg of whole cell extract was used for analysis of proteins by Western blotting.

D0.4 Extraction buffer

20 mM HEPES (pH 7.5), 10 % (v/v) glycerol, 0.4 m KCl, 0.4 % (v/v) Triton X-100, 10 mM EGTA, 5 mM EDTA. 1 mM DTT.

RIPA Extraction buffer

150mM NaCl, 50mM Tris pH 8.0, 1% NP-40, 0.5 % deoxycholate, 0.1 % SDS

To each buffer the following was freshly added: 25 mM NaF, 25 mM sodium β-glycerophosphate , 1 mM DTT, and 1 x Complete Protease Inhibitors.

2.3.2.2 Nuclear and Cytoplasmic Extracts of Cells

Nuclear and cytoplasmic extracts were prepared as described previously (Wong, C. et al., 1999) with minor modifications. Cells were washed twice with ice-cold PBS, ensuring all PBS was removed after the second wash. The cells were allowed to swell in ice-cold hypotonic buffer (1 ml for a 15 cm tissue culture dish) for a few minutes before they were scraped into a cold sterile tube. The nuclei were then pelleted by centrifugation at 800 rpm in a swinging-bucket centrifuge (Beckman Allegra™ 6KR centrifuge) for 15 minutes. The supernatant (cytoplasmic fraction) was transferred to a cold sterile eppendorf and protein concentration assayed. The nuclei were washed in hypotonic buffer once and then resuspended in five times the pellet volume of hypertonic buffer. Extracts were rotated for two hours at 4 °C and then centrifuged at 13,000 rpm (Biofuge fresco Heraeus centrifuge) for 5 minutes at 4 °C to remove cell debris. The supernatant (nuclear fraction) was transferred to a cold sterile eppendorf.

Protein concentration was measured as described. Typically, 10 µg of nuclear extract and 30 µg of cytoplasmic extract was used for analysis of proteins by Western blotting.

Hypotonic Solution
20 mM HEPES (pH 7.6)
20 % (v/v) glycerol
10 mM NaCl
1.5 mM $MgCl_2$
0.2 mM EDTA
0.1 % (v/v) Triton X-100

Hypertonic Solution
As for Hypotonic buffer but containing 450 mM NaCl

To each buffer the following was freshly added: 25 mM NaF, 25 mM sodium β-glycerophosphate , 1 mM DTT, and 1 x Complete Protease Inhibitors.

2.3.2.3 Determination of protein concentration

Protein concentrations were determined by the Bradford method using 200 µl of BioRad Protein Assay solution (Biorad). A standard curve was determined using 1-8 µl of a 1 mg/ml BSA solution (NEB). 3 µl of the sample to be determined was used in the assay. The absorbance at 595 nm was measured on a SpectraMax Plus spectrophotometer (Molecular Devices). The protein concentration of the sample was then determined from the BSA standard curve.

2.3.2.4 TCA preciptiation

Final eluates of the dual purification procedure were concentrated before loading on an analytical gel by TCA precipitation (Harlow, E. et al., 1988). One twentieth the total

eluate volume of deoxycholic acid (2mg/ml) was added to the protein sample. The eluates were then adjusted to 10 % TCA with 100% TCA and incubated on ice for 1 hr with periodic vortexing. Eluates were then centrifuged at 13,000 rpm (Biofuge fresco Heraeus centrifuge) for 45 minutes at 4 °C. The supernatant was discarded and the pellet was washed in acetone (-20°C) containing 5 mM HCl. After 5 min centrifugation at 13,000 rpm, the supernatant was discarded again. The pellet was washed a second time in pure acetone (-20°C). The supernatant was removed and the pellet was dried in a speed vaccum. Pellets were resuspended in 4x SDS buffer (10 mM DTT).

2.3.2.5 Alkylation of Proteins

An additional alkylation step was performed to prevent modification of Cysteine residues in the sample protein, which interferes with mass spectrophometric analysis. The protein samples were boiled in 4x SDS sample buffer (DTT). After cooling down to RT, a fresh solution of iodoacetamide in water (0.25 M) was added to give a final concentration of 20 mM. Samples were incubated in the dark at RT for 20 min before loading.

2.3.3 Protein Analysis

2.3.3.1 SDS Polyacrylamide Gel Electrophoresis (SDS-PAGE)

The samples to be analyzed were first boiled in 4x sample buffer to denature the protein structure. Two glass plates (10 cm x 20 cm) were assembled with silicon tubing to form a seal between the plates, and 0.8 mm plastic spacers. Resolving gel mix (15 ml at the appropriate percentage) was then poured between the vertical plates and overlaid with 1 cm of 75 % ethanol to ensure a level, air-free polymerisation interface. The gel was allowed to polymerise for approximately 20 minutes before removal of the surface water. The stacking gel was then poured onto the surface of the resolving gel and a 0.8 mm plastic comb was inserted between the plates to produce the wells.

Once the stacking gel was polymerised, the gel plates were clamped into an electrophoresis apparatus (Cambridge Electrophoresis Ltd), and 1 x SDS Running buffer was added. The comb was removed from the gel and the wells were thoroughly washed out with the Running buffer. Samples were run alongside molecular weight markers that were prepared by Mike Howell (Developmental Signalling Laboratory) (see below for composition). Gels were run for 1 hour 30 minutes at 230 volts and 65 mAmp. Gels were then either stained with Silver stain or Coomassie blue stain or transferred to PVDF membrane and used for Western blotting (see below).

	Resolving Gel		**Stacking Gel**
	15.0 %	20.0 %	
40 % (w/v) acrylamide	5.625 ml	7.5 ml	0.625 ml
2 % (w/v) bisacryamide	0.645 ml	0.495 ml	0.333 ml
1.5 M Tris-HCl (pH 8.8)	3.75 ml	3.75 ml	-
1.0 M Tris-HCl (pH 6.8)	-	-	0.625 ml
Water	4.98 ml	3.255 ml	3.417 ml
20 % (w/v) APS	40 µl	40 µl	15 µl
TEMED	30 µl	30 µl	10 µl

4 x Sample buffer

8 % (w/v) SDS, 320 mM Tris-HCl (pH 6.8), 40 % (v/v) glycerol, 1 % (v/v) 2-mercaptoethanol or 10mM DTT, bromophenol blue

1 x SDS Running buffer

384 mM Glycine

50 mM Tris-HCl

0.1 % (w/v) SDS

Protein Markers

50 µg/ml each of myosin (212 kDa), β-galactosidase (116 kDa), phosphorylase (97.5 kDa), BSA (66.5 kDa), catalase (57.8 kDa), glutamate dehydrogenase (55.5 kDa), GAPDH, ovalbumin (42.7 kDa), carbonic anhydrase (28.9 kDa), SBTI (20 kDa) and RNaseA (13 kDa).

2.3.3.2 Staining of Protein gels

Silver Stain

Silver staining was carried out as previously described (Harlow, E. et al., 1988). Following electrophoresis, gels were fixed for 20 minutes in 5 % acetic acid (v/v) and 50 % methanol (v/v) with gentle rocking. This was followed by washing for 10 minutes in 50 % methanol (v/v) with gentle rocking and further washing in water for 2 hours to overnight. Gels were then sensitised for 1 minute in 0.02 % w/v sodium thiosulphate with gentle rocking and subjected to two 1-minute rinses in water. This was followed by incubation with 0.1 % silver nitrate (w/v) for at least 20 minutes at 4 °C and in the dark. Gels were then rinsed for 1 minute with water and transferred to a fresh gel tray. Finally, development was carried out with 4 % sodium carbonate (w/v) and 0.04% Formalin (v/v) (added directly before use) until protein bands were of an appropriate intensity. The development reaction was terminated with 5 % acetic acid (v/v). The gels were either stored in 1 % acetic acid or dried in cellulose acetate sheets (Promega).

Coomasie Stain

Acrylamide gels were fixed first in 12% glacial acetic acid and 50% methanol for 20 min. A staining solution with 0.125% Coomassie blue R250 was prepared freshly and filtered using 150mm Whatman paper to avoid precipitation. The gel was then stained for 1-2 hr or overnight. Gels were slowly destained in 7.5% acetic acid and 10% methanol for approximately 1 hour to visualise the proteins. Protein gels were then stored at 4°C.

2.3.3.3 Western Blotting

After electrophoresis, SDS gels were soaked in 1 x Semi-Dry Transfer buffer for 15 minutes. Six pieces of Whatman 3 mm paper and a piece of Immobilon™-P PVDF 0.45 μ membrane (Millipore) were cut to the size of the gel. The membrane was pre-wet in methanol, rinsed in water and, along with the Whatman paper, equilibrated in the 1 x Transfer buffer with the gel. Three pieces of Whatman paper, followed by the membrane, the gel and another three pieces of Whatman paper were assembled in the SemiPhor Transfer Unit (Hoefer) and rolled over with a pen to ensure removal of all air bubbles. Proteins were then transferred for 1 hour 30 minutes at 0.8 mAmps/cm^2 of gel.

After transfer, the membrane was stained with Ponceau S solution to visualise the markers. The membrane was then washed briefly in PBS and incubated in 5 % (w/v) milk powder (Marvel)/PBST for an hour at room temperature to block non-specific binding of antibody to filter. Next, the membrane was incubated with the primary antibody in 5 % (w/v) milk/PBST at 4 overnight on a rocking platform. The membrane was then washed 4 times for 15 minutes in 5 % (w/v) milk/PBST prior to incubation with a secondary antibody conjugated to horseradish peroxidase (HRP) in 5 % (w/v) (w/v) milk/PBST for 1 hour. Finally the membrane was washed again 4 times for 15 minutes in 5 % (w/v) milk/PBST, and the HRP was detected with ECL™ Western blotting detection reagents (Amersham Pharmacia Biotech). When the HRP-conjugated primary antibodies (anti-HA-HRP and anti-Flag-HRP), were used, incubation with the secondary antibody was omitted.

10 x Semi-dry Transfer buffer

1.5 M glycine

200 mM Tris-HCl

0.1 % (w/v) SDS

The 1 x solution was made up to contain 20 % (v/v) methanol

Ponceau S solution

2 % (w/v) Ponceau S

30 % (v/v) trichloroacetic acid

2.3.3.4 Antibodies

Primary Antibodies:

Antibody	Supplier	Smad Specificity	Species	Concentration
Smad1	Zymed	Smad1 only	Rabbit	1:1000
Smad1/5 (Madr)	Upstate	Smad1 & 5	Rabbit	1:1000
Smad2/3	BD	Smad2 & 3	Mouse	1:1000
Smad3	Zymed	Smad3 only	Rabbit	1:750
B8	Santa Cruz	Smad4 only	Mouse	1:750
P-Smad1/5/8	Cell Signalling	P-Smad1, 5 & 8	Rabbit	1:500
P-Smad2	Cell Signalling	P-Smad2 only	Rabbit	1:1000
P-Smad3	Cell Signalling	P-Smad1 & 3	Rabbit	1:1000
P-Smad3	Ed Leof (Gift)	P-Smad1 & 3	Rabbit	1:3000
P-T178	Fang Liu (Gift)	Smad2 & 3	Rabbit	1:6000
P-S207	Fang Liu (Gift)	Smad3 only	Rabbit	1:6000
P-ERK	Sigma		Mouse	1:10,000
M2	Sigma		Mouse	1: 1000
FLAG-HRP	Sigma		-----	1:1000
PAI-1	Santa Cruz		mouse	1:500
Id2	Santa Cruz		mouse	1:500
Pan-actin	Sigma		goat	1:1000
Grb2	BD		Mouse	1:1000

Secondary Antibodies

Antibody	Supplier	Conjugate	Species	Concentration
Rabbit IgG	DAKO	HRP	Goat	1/3000
Mouse IgG	DAKO	HRP	Goat	1/3000
Goat IgG	DAKO	HRP	Donkey	1/3000

2.3.4 Protein-DNA Interactions

2.3.4.1 DNA pull-downs

Double-stranded oligonucleotide baits were prepared by annealing 0.5 μg μl^{-1} of each of the appropriate single-stranded oligonucleotides in 1X buffer 2 from New England Biolobs. These annealing reactions were heated at 95 °C for 10 mins and allowed to cool slowly to room temperature over a period of 2 hours.

Probe	Oligonucleotide Sequence
c-Jun SBR wild-type	ggaggtgcgcggagtcaggcagacagacagacacagccagccagccaggtcggca
c-Jun SBR mutant	ggaggtgcgcggagtcaggcatatatatatatacagcatgcatgcatggtcggca

For each DNA pulldown (DNAP), a 10 cm dish of cells (500 μg of extract) and 25 μl oligo-saturated beads was used. Immobilised Neutravadin™ Biotin Binding beads (Perbio) were washed twice in 1 ml cold DNAP Buffer and resuspended in DNAP Buffer to form a 1:1 slurry. The slurry was then incubated with the desired oligo (8μg oligo/ 25μl beads in water) for 1 hour at 4 °C with rotation. Dishes of cells (10 cm) were lysed in 400 μl DNAP Buffer. Lysates were sonicated for 10 seconds on ice and centrifuged at 13,000 rpm (Biofuge fresco Heraeus centrifuge) for 5 minutes at 4 °C. The supernatant was transferred to a sterile pre-chilled eppendorf and the protein concentration assayed. Samples (2 x 30 μg) were retained for use as controls. The oligo-conjugated beads were washed three times in DNAP Buffer, resuspended to give a 1:1 slurry and then incubated with the cell lysates for 1 hour at 4 °C with rotation. After this incubation, the beads were washed three times with DNAP Buffer, resuspended in 4 x Sample buffer and Western blotted to visualise associated proteins.

DNAP Buffer
150 mM NaCl
50 mM Tris
0.1 % Triton
2 mM EDTA

2.3.4.2 Bandshift Assay

Whole cell extracts were prepared as previously described from cells that were uninduced or induced with 2 ng/ml TGF-β for 1 hr (Section 2.3.2.1). Extract (10 μg) was preincubated for 5 minutes of antibody prior to addition of 10 μl probe mix. Final buffer conditions were 210 mM KCl, 5.5 mM $MgCl_2$, 10 % (v/v) glycerol and 0.5 μg poly dI-dC. The samples were then briefly centrifuged in a microcentrifuge and incubated at room temperature for 15 minutes prior to loading on a bandshift gel. Bandshifts were run for 3 hours and 45 minutes. For supershifts, 1 μl of anti-Smad2/3 (BD Biosciences), 1 μl of anti-Smad4 (B8, Santa Cruz) or 1 μl of anti-Flag (m2, Sigma) antibodies were added to extract for 5 minutes before addition of probe.

Probe Mix

1 μl 200 mM KCl
1 μl 110 mM $MgCl_2$
1 μl ARE probe (0.2 ng/μl)
1 μl poly dI-dC
4 μl 50 % (v/v) glycerol
2 μl water

2.3.4.3 Probe Synthesis

Bandshift probes were labelled with [α^{32}P]dATP and [α^{32}P]dCTP by PCR. Probe synthesis reactions contained 1 μl of each oligonucleotide (50 ng/μl), 1 μl 10 x PCR buffer (2.1.1), 1 μl [α^{32}P]dATP, 1 μl [α^{32}P]dCTP, 1 μl dGTP and dTTP mix (0.5 mM), 1 μl dATP and dCTP mix (50 μM), 0.5 μl Taq polymerase (Developmental Signalling Laboratory, Cancer Research UK) and 3.5 μl water.

PCRs were carried out in a GeneAmp® PCR System 9700 (Applied Biosystems). Standard conditions were as follows:

94 °C	3 minutes		
	94 °C	25 seconds	⎫
	37 °C	25 seconds	⎬ x 31 cycles
	72 °C	25 seconds	⎭
	72 °C	3 minutes	
	10 °C	∞	

After synthesis the probes were gel purified on a 5 % (w/v) acrylamide gel, assembled with 0.4 mm spacers and comb. Gels were run for 1 hour at 150 volts and 150 mAmps in 0.5 x TBE. The gels were then exposed on MXB Film (Kodak) for 1 minute. The film was then used to identify the location of the probe band on the gel which was excised with a scalpel, immersed in 350 µl Elution buffer and incubated overnight at 37 °C. Following this incubation, the probe was extracted with 350 µl phenol, centrifuged at 13,000 rpm for 5 minutes (Biofuge pico Heraeus centrifuge) and the aqueous phase removed. The probe was then precipitated with 1 µg tRNA and 700 µl 100 % ethanol at –80 °C for 30 minutes and centrifuged at 13,000 rpm for 20 minutes at 4 °C (Biofuge fresco Heraeus centrifuge). The pelleted probe was washed with 350 µl 70 % ethanol and air dried at room temperature before being resuspended in TE and then quantitated.

Non-denaturaing acyrlamide gel

3.125 ml 40 % (w/v) acrylamide

2.15 ml 2 % (w/v) bisacrylamide

1.25 ml 10 x TBE

Up to 25 ml with deionised water

25 ml gel mix was polymerised with 60 µl 20 % (w/v) APS and 50 µl Temed

2.3.4.4 Probe Quantitation

All probes used in bandshift reactions were at 20 ng/µl. In order to calculate the isotope incorporation and thereby quantitate the probes, 1 µl of the TE-resuspended probe was counted in the scintillation counter (Beckman LS 6500 multi-purpose scintillation counter) along with 1 µl of the original pre-PCR probe mix. The probe was then quantitated as follows:

$$\frac{(\%\ \text{Incorporation}) \times (\text{number moles A+C in probe}) \times \text{probe MWT}}{\text{number labelled A+C in probe}}$$

This equation gives a weight in µg that is then converted into ng. The probe is resuspended in a suitable volume of TE to give a stock solution of probe at a concentration of 0.2 ng µl.

ARE probe:
The % Incorporation is established. 100 % Incorporation is equivalent to 134 ng of probe. The probe is resuspended in a suitable volume of TE to give a stock solution of probe at a concentration of 0.2 ng µl.

2.3.5 Protein-Protein Interactions

2.3.5.1 Co-Immunoprecipitation

Cells in 15 cm dishes were lysed in 1 ml 100 mM Co-IP Lysis buffer. Lysates were sonicated for 10 seconds on ice and centrifuged at 13,000 rpm (Biofuge fresco Heraeus centrifuge) for 5 minutes at 4 °C. Protein concentration was assayed and 3 x 30 µg samples were retained for use as controls. The supernatant was then precleared with pre-equilibrated IgG sepharose for 1 hr at 4 °C with rotation. Extracts were transferred to new eppendorfs and incubated with antibody overnight. The following day, IgG beads, blocked with 1 mg ml BSA, were added to each sample for 2 hrs at 4 °C with rotation. The beads were washed twice with Co-IP Lysis buffer, resuspended in 4 x Sample buffer and Western blotted to visualise associated proteins.

Co-IP Lysis buffer

100 mM NaCl

20 mM Tris-HCl (pH 7.4)

1 mM EDTA

1 mM EGTA

0.1 % (v/v) Triton X-100

5 mM NaF, 10 mM sodium β-glycerophosphate and Complete EDTA-free protease inhibitor tablets were added fresh

2.3.5.2 Covalent crosslinking of anti-HA antibody to protein G-sepharose beads

For two-step affinity purification, the mouse monoclonal anti-HA antibody 12CA5 was covalently conjugated to protein G beads using dimethlypimelimidate (DMPD). The method used is based on that described by Harlow and Lane (Harlow, E. et al., 1988). 500 µl dry beads were washed three times and resuspended in an excess of hypotonic buffer containing 140 mM NaCl. Antibody was then added at a ratio of 0.07 µg antibody per µl bead slurry and this mixture was subjected to gentle agitation at room temperature for 1 hour. Beads were then poured into a Bio-Spin disposable chromatography column (BioRad), washed with 5-7 ml of 0.1 M sodium borate (pH 9.0) and resuspended in 0.1 M sodium borate with 20 mM DMPD. This mixture was subjected to gentle agitation for 30 minutes at room temperature and poured into another disposable column. The beads were then washed with 5-7 ml of 0.2 M ethanolamine, resuspended in this buffer and subjected to gentle agitation for 2 hours at 4 °C. This mixture was then poured into another column, washed with 5-7 ml PBSA and stored in PBSA with 0.1 % sodium azide.

2.3.5.3 Peptide Pulldowns and Peptides

Peptide pulldowns were performed as described (Randall, R. A. et al., 2002). For each peptide pulldown, a 10 cm dish of cells and 40 µl peptide-saturated beads was used. Immobilised Neutravadin™ Biotin Binding beads (Perbio) were washed twice in 1 ml cold Buffer Y (Vastrik, I. et al., 1999) and resuspended in Buffer Y to form a 1:1 slurry. The slurry was then incubated with the desired peptide (at a concentration of 1.5 mg/ml in water) for 1 hour at 4 °C with rotation.

Dishes of cells (10 cm) were lysed in 400 µl Buffer Y. Lysates were sonicated for 10 seconds on ice and centrifuged at 13,000 rpm (Biofuge fresco Heraeus centrifuge) for 5 minutes at 4 °C. The supernatant was transferred to a sterile pre-chilled eppendorf and the protein concentration assayed. Samples (5 x 30 µg) were retained for use as controls. The peptide-conjugated beads were washed three times in Buffer Y, resuspended to give a 1:1 slurry and then incubated with the cell lysates for 1 hour at 4 °C with rotation. After this incubation, the beads were washed three times with Buffer Y, resuspended in 4 x Sample buffer and Western blotted to visualise associated proteins.

Peptide Name	Peptide Sequence
XFoxHI-1 FM WT*[c]	LLSLDLPTSYTKSVAPNVVAPPSVLP
XFoxH1-Scrambled*[c]	YSNLLDSTPLAPLVSVPKTLSPVAVP
XFoxH-1 SIM WT*[d]	PLDLNMLRAMPPNKSVFDVLTSHPGDLV
XFoxH-3 SIM WT*[e]	PEVKNAPKDFPPNKTVFDIPVYTGHPGFLA

All peptides were synthesised by the Cancer Research UK Peptide Synthesis Laboratory.

*All of these peptides were synthesised with an N-terminal biotin group followed by 16 amino acids from helix 3 of Antennapedia prior to the peptide sequence: Biotin.Aminohexanoic acid-RQIKIWFQNRRMKWKK.

[c]These peptides correspond to codons 400-425 of XFast-1. The scrambled peptide corresponds to codons 400-425 of XFast-1 but in a random order.

[d]These peptides correspond to codons 467-495 of XFast-1. The mutant peptide has amino acid substitutions at positions 11 (P-A), 12 (P-A) and 13 (N-A). These peptides are as described (Howell, M. et al., 2002).

[e] These peptides correspond to codons 291-320 of XFast-3. The mutant peptide has amino acid substitutions at positions 11 (P-A), 12 (P-A) and 13 (N-A). These peptides are as described (Howell, M. et al., 2002).

Buffer Y
50 mM Tris-HCl (pH 7.5)
150 mM NaCl
1 mM EDTA
1 % (v/v) NP-40

1 mM DTT and 1 x Complete EDTA-free were added fresh

2.3.6 Tandem Affinity Purification (TAP)

The TAP procedure was based on the methods described (Puig, O. et al., 2001; Rigaut, G. et al., 1999). A brief description with modifications is given below.

TAP Purification Protocol: Conditions used in Figure 3.6.
15 x 150 cm^2 plates of TAP-Smad4 HaCaTs were lysed in 1.5ml Lysis Buffer and sonicated for 10 seconds on ice. Lysates were then centrifuged at 10,000 rpm (Beckman Avnti™ J-20 centrifuge) for 30 minutes at 4 °C. Extracts were rotated for 2 hours at 4 °C with 250 µl of IgG sepharose (Sigma), after which the beads were washed extensively in binding buffer. Washed beads were resuspended in TEV cleavage buffer and transferred to Polyprep® Chromatography Columns (Biorad). 250 units of recombinant TEV protease (in house) was added to the capped column. After rotation for 2 hours at 16°C, the eluate was recovered and stored on ice at 4 °C overnight. The beads were resuspended in additional TEV cleavage buffer and 250 units of recombinant TEV protease was added to the IgG column and left rotating at 4°C overnight. Eluates were pooled and adjusted to the Calmodulin binding conditions: 45 mM Tris pH 8.0, 90 mM NaCl, 0.2 % NP-40, 0.7 mM MgAcetate, 0.7 mM Imidazole, 3.5 mM $CaCl_2$, 10 mM β-ME and rotated with 250 µl of CAM beads (Stratagene) for 5 hours. After extensive washing, the bound proteins were eluted with Calmodulin Elution buffer. Ten elution fractions of 125 µl each were collected. Eluates were pooled and concentrated in Microcon® Centrifugal Filter Devices

(Millipore). Concentrated eluates were loaded onto a 15% SDS-PAGE gel, which was silver stained. Bands were excised and proteins identified by mass spectrometry.

2.3.6.1 TAP Purification Protocol: Conditions used in Figure 3.7.

40 x 150 cm^2 plates of TAP-Smad4 HaCaTs were lysed. Extracts were rotated in batch for 2 hours at 4°C with 600 µl of IgG sepharose. Addition of 600 units of recombinant TEV was used in each cleavage. An equivalent 600 µl of CAM beads were used in the second affinity step. Twenty elution fractions of 200 µl each were collected and were subsequently pooled and concentrated in centricon-20 columns and transferred to Microcon® Centrifugal Filter Devices (Millipore). Samples were loaded onto a 15% SDS-polyacrylamide gel. Proteins were detected by coomassie staining, band were excised and analysed by mass spectrometry.

Lysis Buffer
10 mM Tris pH 8.0
180 mM NaCl
5 % Glycerol
0.2 % NP-40
2 mM EGTA,

TEV Cleavage Buffer
10 mM Tris pH8.0
150 mM NaCl
0.5 mM EDTA
0.1 % Triton
1 mM DTT

CAM Elution Buffer
(10 mM Tris pH 8.0, 90 mM NaCl, 0.1% NP-40, 0.7 mM MgAcetate, 0.7 mM Imidazole, 20 mM EGTA,10 mM β-ME)

2.3.7 Dual Tag Purification

Cell Preparation

Cells were synchronized and released into new media for 18-22hrs. Cells were stimulated with TGF-β for 1 hr prior to harvest. Cells were then washed twice with PBS and subsequently scraped in 5 ml PBS. Cells were pelleted by centrifugation at 1000 rpm (Beckman Allegra™ 6KR centrifuge). Cell pellets were stored at -80 °C until further use. Alternatively cells were lysed directly in lysis buffer on the day of use.

Purification Procedure: Conditions used for Figures 4.11 and 4.12

Cell pellets were lysed in High Salt Lysis Buffer (see below) and douced 3-4 times in a homogeniser before centrifugation at 10, 000 at 4 °C (Beckman Avnti™ J-20 centrifuge) for 20 minutes. Supernatants were then adjusted to 150 mM NaCl with dilution buffer and incubated in batch with 3 µl of pre-equilibrated IgG Sepharose beads per mg of protein for 6-8 hr at 4 °C with rotation. Beads were then pelleted by centrifugation for 5-10 minutes at 1000 rpm (Beckman Allegra™ 6KR centrifuge). Beads were then washed twice with wash Buffer and then subsequently with TEV Protease Buffer and transferred to columns Polyprep® Chromatography Columns (Biorad). 1 ml of TEV cleavage buffer was added per 200 µl of beads. Beads were then incubated with 10 units of AcTEV protease (Invitrogen, 10 U/µl) per ml of TEV cleavage buffer used, for 2 hrs at 14°C. The eluate was recovered and stored on ice at 4 °C overnight. The IgG beads were then resuspended in additional TEV cleavage buffer and incubated with equal units of TEV protease and left rotating at 4°C overnight. The eluates were recovered from the columns and pooled. These eluates were then incubated in re-equilibrated beads beads conjugated with anti-FLAG antibody for 6-8 hrs. Elution was performed with 10 x 200 µl FLAG-peptide (200 µg/ml) per 200 µl of beads. 10 µl of sample were used for Western Blotting analysis. Fractions that were positive for bait protein were pooled, TCA precipitated treated with alkylating agents and loaded onto a 15 % acrylamide gel.

High Salt Lysis Buffer

50 mM Tris pH 8.0

400 mM NaCl

0.1 % Triton

2 mM EGTA

1 mM DTT

Add Fresh

Dilution Buffer

As for High Salt Lysis Buffer but with 0 mM

Wash Buffer

As for High Salt Lysis Buffer but with 150 mM NaCl

TEV Cleavage Buffer

10 mM Tris, pH 8

150 mM NaCl

0.5 mM EDTA

0.1% Triton

To each buffer the following was freshly added: 25 mM NaF, 25 mM sodium β-glycerophosphate , 1 mM DTT, and 1 x Complete Protease Inhibitors.

Purification Procedure: Conditions used for Figures 4.13

The experiment was carried out as described above but with the following modifications. The cells were lysed at with DT Lysis buffer and douced 3-4 times before centrifugation at 18, 000 rpm for 30 minutes at 4°C (Beckman Avnti™ J-20 centrifuge). This centrifugation step was repeated three times. In each case the supernatant was removed and transferred to a new tube. After elution with TEV, lysates were then incubated with fresh IgG Sepharose for 1 hr at 4°C to remove any excess actin. The purification then proceeded as described above.

DT Lysis Buffer

50 mM Tris pH 8.0

150 mM NaCl

0.1 % Triton

2 mM EGTA

0.2 mM EDTA

The following was freshly added: 25 mM NaF, 25 mM sodium β-glycerophosphate , 1 mM DTT, and 1 x Complete Protease Inhibitors.

2.3.7.1 Mass Spectrometry

Mass spectrometry analysis was carried out by the Cancer Research UK Service. Triptic digests were performed. Pepide extracts were fractionated using an LC Packings Integrated nano-LC System. Fractions were analysed with an Applied Biosystems 4700 Proteaomics Analyzer (Foster City, CA). The peptide masses were searched against the National Centre for Biotechnology Information (NCBI) non-redundant database using the Protein Prospector MS-FIT, MS-TAG or Mascot programs.

The mass spectrometry analysis carried out laterally by Ulf Hellman, Ludwig Institute for Cancer Research, Uppsala Sweden. In this case, the data were analysed by database searching using the ProFound search algorithm.

http://129.85.19.192/profound_bin/WebProFound.exe?FORM=1

3 Tandem Affinity Purification

3.1 Introduction

As outlined in Chapter 1, TGF-β regulates many diverse biological processes including proliferation, motility, differentiation and survival. The huge diversity of responses elicited by TGF-β is in sharp contrast to the simple intracellular Smad signalling pathway mediated by Smad2, Smad3 and Smad4. This has raised the question of the mechanism by which signalling specificity and diversity is generated to mediate the wide array of cell-specific responses. The TGF-β signal transduction cascade is controlled at many levels. One important level of regulation, in terms of specific activation and repression of TGF-β target genes, is the interaction of the Smads with various transcription factors. Previous work in our lab has shown that the specific transcription factors that recruit activated Smad complexes determine which specific genes are induced (Germain, S. et al., 2000; Howell, M. et al., 2002). In accordance with this view, a current model of the pathway envisages the Smads interacting with a set of partner proteins that are specific to a particular cell type in a given set of conditions. These partners determine the DNA sequences that the Smad complex will bind, the transcriptional co-activators or co-repressors it will recruit, the other transcription factors it will cooperate with, and how long the response lasts. The repertoire of Smad partners and regulators present in a given cell at the time of TGF-β stimulation would thus decide the outcome of the response and defines in molecular terms, the cellular context. Identifying these partners and regulators is, therefore, critical for understanding TGF-β action. So far, some candidates have been identified, as mentioned in Chapter 1, but although some of these are genuine interactions and have been demonstrated to bind with endogenous Smads *in vivo*, many of the proteins discussed have been identified through overexpression of the partner and/or the Smads. As a consequence, the mechanism by which they function and their physiological relevance is unclear.

My initial aim was to investigate the role of transcription factor partners of the Smads in the context of tumourigenesis. Epithelial cells normally undergo growth arrest and apoptosis in response to TGF-β, whereas tumour cells are resistant to these growth inhibitory effects but frequently maintain responsiveness to the pro-oncogenic activities of TGF-β (Wakefield, L. M. et al., 2002). The main question posed here is whether these different biological responses are governed by the set of transcription factors to which the Smads bind? Consistent with the current model for Smad signalling in a given cell, one could postulate that the differences in TGF-β responses during tumourigenesis may arise as a result of the tumour cell altering its expression pattern of transcription factors and thus diverting the activities of Smads to a different set of target genes. To test this hypothesis, my initial approach was to identify novel Smad-interacting proteins and subsequently determine their involvement in target gene activation and ultimately, in different biological responses.

To identify new interacting partners of the Smads, I made use of a recent innovative purification system developed in the Seraphin lab in EMBL (Rigaut, G. et al., 1999). The tandem affinity purification (TAP) system is a two-step affinity purification scheme, which allows for the purification of endogenous proteins under mild conditions. The TAP tag consists of two IgG binding domains of *Staphylococcus aureus* protein A and a calmodulin binding peptide (CBP) separated by a *Tobacco Etch Virus* (TEV) protease cleavage site (Rigaut, G. et al., 1999). Under native conditions, the fusion protein is first bound to IgG sepharose which binds the protein A (Figure 3.1). The bound protein is released by cleavage with TEV protease and the supernatant is bound to calmodulin-coated beads. The protein is finally eluted in EGTA and protein identification can then be made by mass spectrometry. Epitope-tagged affinity purification has proved to be a valuable tool in purifiying protein complexes. The use of two affinity steps further improves its efficacy by allowing two gentle discriminatory separations under native conditions to retrieve highly purified target proteins. In addition, the process is relatively fast in comparison to the classical biochemical purification methods and results in a high yield of protein complexes. In combination with mass spectrometry, this is an excellent strategy to define interactions with bait proteins.

The application of the TAP method has proved very successful in yeast, however, the transfer of the TAP method for use in mammalian cells had not been

fully established when I first began this project in 2002. My first aim was to adapt the TAP-tag technique to purify Smads in epithelial cells. Once the technique was established, I could then apply it for use in a tumour model system. In this Chapter, I present data on the pilot study of the purification of Smads and interacting proteins using the TAP-tagging system in the TGF-β responsive HaCat cell line. Here I show functional expression of TAP-Smad proteins in stable lines and optimisation of the purification of TAP-Smads.

3.2 Results

3.2.1 Development of the Tandem Affinity Purification System in Mammalian Cells

My first aim was to make N-terminal TAP-tagged constructs of Smad2, Smad3, and Smad4 in the retroviral vector, p-Zome (CellZome) (Figure 3.1). C-terminal tags were not an option in this case due to the location of the phosphorylation sites of Smad2 and Smad3 at the extreme C-terminus.

Since the TAP-tagging system was originally developed in yeast, it was necessary to adapt the system to mammalian cells. The keratinocyte cell line, HaCaTs, was chosen as an appropriate cell line, as the TGF-β/Smad signalling pathway is extremely well characterised in these cells (Nicolas, F. J. et al., 2003a; Pierreux, C. E. et al., 2000). To generate stable cell lines of the TAP-Smads by retroviral gene transfer, it was first necessary to create a HaCat cell line, HaCat-EcoR cells, that expressed an ecotropic receptor, as described in Chapter 2. Subsequently, TAP-Smad2, TAP-Smad3, TAP-Smad4-expressing HaCaT cells were generated by infection of the HaCat-EcoR cells using retroviral vectors of the TAP-Smads. Pools and clones were isolated as described in Chapter 2 and clones whose expression level closely matched endogenous Smad level were chosen. The expression level of endogenous Smads in the clones was examined to ensure homogeneity with the parental line (Figure 3.2). It is clear that TAP-Smad2 and TAP-Smad4 are expressed at a slightly higher level than endogenous Smad2 and Smad4 and TAP-Smad3 is closer to endogenous level.

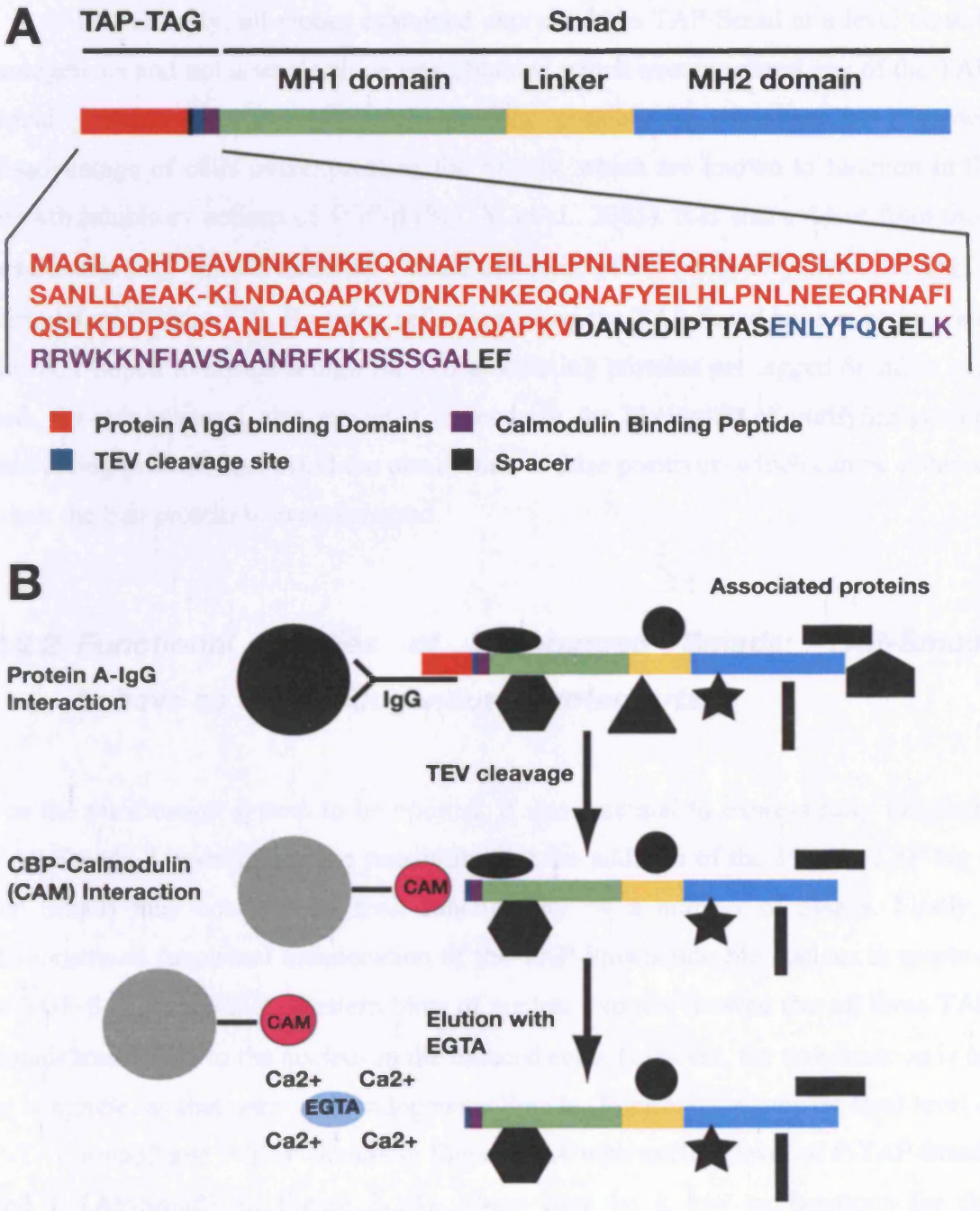

Figure 3.1. The Tandem Affinity Purification (TAP) Procedure

(A) Schematic representation of the N-terminal TAP-tagged Smad constructs. The sequence and structure of the N-terminal tandem tag are illustrated in detail. The TAP tag consists of two tandem Protein A IgG-binding domains, a spacer, a TEV cleavage sequence, and one copy of the Calmodulin Binding Peptide (CBP) sequence.
(B) Overview of the TAP purification strategy. A protein complex containing the TAP-tagged protein is purified sequentially by two independent affinity steps on IgG- and calmodulin-conjugated resins, respectively. The immobilized protein is specifically eluted in the first instance by protease cleavage (TEV) and in the second by lowering the calcium affinity of CBP to calmodulin using EGTA.

Interestingly, all clones examined expressed the TAP-Smad at a level close to endogenous and not a single clone was obtained which overexpressed any of the TAP-Smad proteins (data not shown). This may possibly be explained by a growth disadvantage of cells overexpressing the Smads, which are known to function in the growth inhibitory actions of TGF-β (Shi, Y. et al., 2003). It is also evident from these results that TAP-Smad2 and TAP-Smad3 are successfully phosphorylated after TGF-β stimulation (Figure 3.2). By using cells expressing the TAP-Smad baits at endogenous levels, I hoped to ensure a high ratio of associating proteins per tagged Smad in each cell. By this means I also expected to increase the likelihood of purifying genuine interacting proteins and avoid the occurrence of false positives, which can be observed when the bait protein is overexpressed.

3.2.2 Functional Studies of TAP-tagged Smads: TAP-Smads behave as their endogenous counterparts.

For the purification system to be optimal, it was essential to express fully functional TAP-Smads. I investigated the possibility that the addition of the 19 kDa TAP-tag to the Smads may compromise their functionality by a number of assays. Firstly, I demonstrated functional translocation of the TAP-Smads into the nucleus in response to TGF-β (Figure 3.2B). Western blots of nuclear extracts showed that all three TAP-Smads translocate to the nucleus in the induced cells. However, the translocation is not as complete, as that seen with endogenous Smads (Figure 3.2, Compare total level of P-TAP-Smad2 and P-TAP-Smad3 in Figure 3.2A with nuclear level of P-TAP-Smad2 and P-TAP-Smad3 in Figure 3.2B). There may be a few explanations for this phenomenon: It is possible that the TAP-tag may be masking the nuclear localisation signal in some way or preventing full interaction with the nuclear transport machinery (Reguly, T. et al., 2003). Another possibility is that the tag stabilises the interaction of a naturally occurring Smad retention factor or that a new retention factor is created as a result of the tag, reducing nuclear translocation of a pool of the TAP-Smads (Nicolas, F. J. et al., 2004). In contrast, however, the phosphorylation of TAP-Smad2 and TAP-Smad3 by the TGF-β receptors was not compromised. As a result of this finding, all other functional studies and purifications were performed using whole cell extracts.

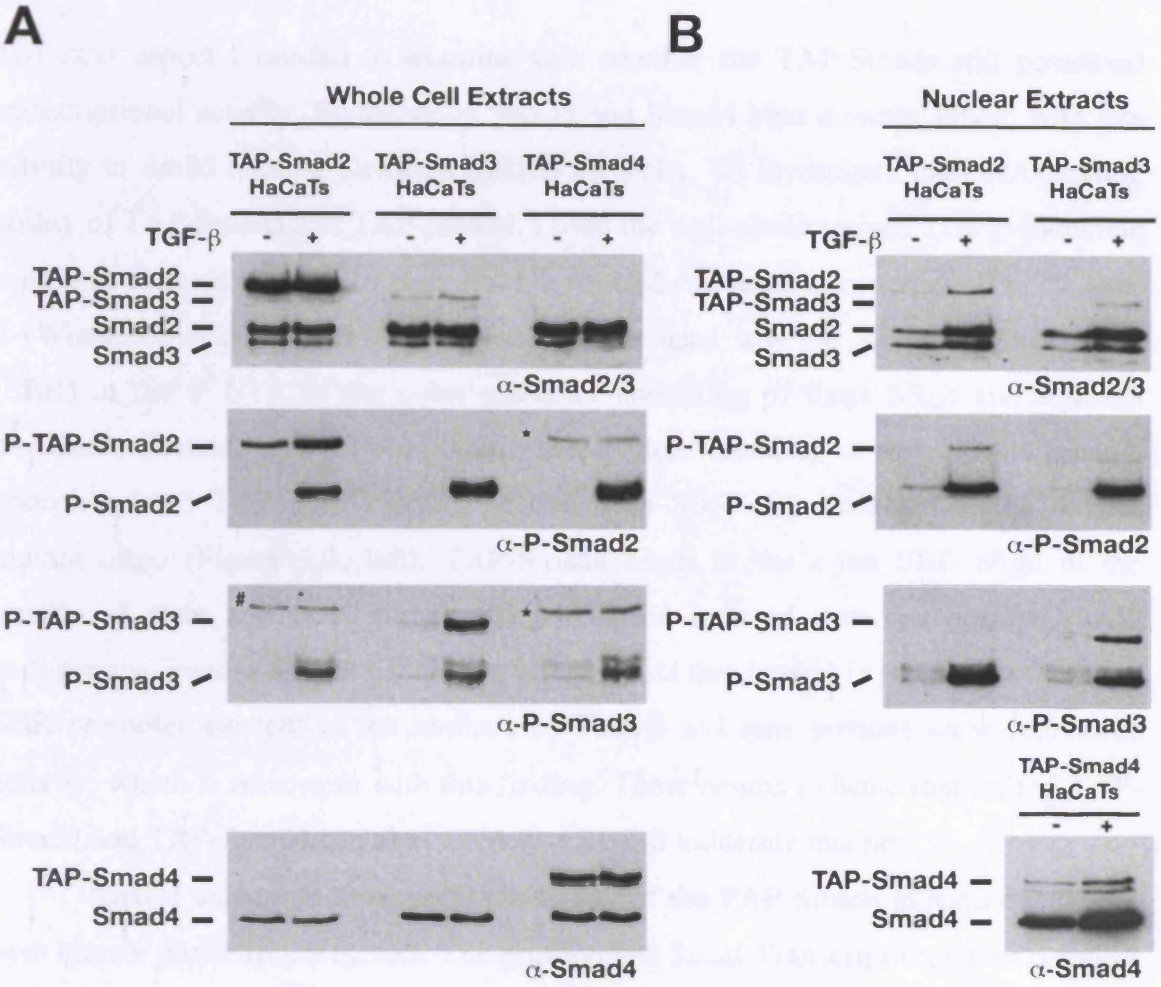

Figure 3.2. TAP-Smads undergo nuclear translocation in a TGF-β-inducible manner

(A) Levels of expression of the TAP-Smads and endogenous Smads in TAP-Smad HaCaT stable cell lines. TAP-Smad2,TAP-Smad3 clones and the TAP-Smad4 pool were either untreated or stimulated with TGF-β1 for 1 hr. Whole cell extracts were prepared and analysed by Western blotting using antibodies against Smad2/3, phosphorylated-Smad2 (P-Smad2), phosphorylated-Smad3 (P-Smad3) and Smad4.

(B) Nuclear extracts of the TAP-Smad HaCaT stable cell lines were prepared and proteins were visualized by western blotting using antibodies against Smad2/3, phosphorylated-Smad2 (P-Smad2), phosphorylated-Smad3 (P-Smad3) and Smad4.

* Indicates the TAP-Smad4 protein, which has been recognised by the α-rabbit secondary antibody via its IgG-binding domains.

# Indicates the TAP-Smad2 protein, which has been recognised in the same manner.

The next aspect I needed to examine was whether the TAP-Smads still possessed transcriptional activity. Endogenous Smad3 and Smad4 bind directly, albeit, with low affinity to Smad binding elements (SBEs) on DNA. To investigate the DNA-binding ability of TAP-Smad3 and TAP-Smad4, I used the well-characterized TGF-β-inducible promotor element of c-*jun* to carry out DNA pulldown assays, as described in Chapter 2 (Wong, C. et al., 1999). The oligonucleotide used was the Smad binding region (SBR) in the 5' UTR of the c-*jun* promoter consisting of three SBEs and adjacent sequences (Inman, G. J. et al., 2002a). In a pattern identical to endogenous Smad3, phosphorylated TAP-Smad3 bound to the c-*jun* SBR oligo and not to the control mutant oligo (Figure 3.3, left). TAP-Smad4 binds to the c-*jun* SBR oligo in the uninduced state and with higher affinity in the induced state, as observed with endogenous Smad4. Recent data in the lab suggests that Smad4 is present on the c-*jun* SBR promoter element in the absence of TGF-β and may possess some repressive activity, which is consistent with this finding. These results indicate that indeed TAP-Smad3 and TAP-Smad4 can bind DNA in a TGF-β inducible manner.

Next, I wanted to investigate the ability of the TAP-Smads to form complexes with known transcription factors. The prototypical Smad-Transcription factor complex is termed ARF1, for Activin Responsive Factor 1. It is composed of Smad2, Smad4 and XFoxH1a, a winged helix/forkhead transcription factor (Chen, X. et al., 1996; Chen, X. et al., 1997). It is responsible for mediating Activin-induced transcription via the Activin-responsive element (ARE) of the *Xenopus Mix.2* promoter. XFoxH1a can recruit the Smad2 Smad4 complex to the ARE through direct interactions between Smad2 and two interaction motifs in XFoxH1a, the Smad Interaction motif (SIM) and the Fast FoxH1 motif (FM) (Randall, R. A. et al., 2004). The SIM is necessary and sufficient to interact with the MH2 domain of either Smad2 or Smad3 and thus recruit active complexes to DNA. The FM differs from the SIM by interacting with only activated complexes of Smad2 and Smad4, or homomeric complexes of Smad2 and not those of Smad3 (Randall, R. A. et al., 2004).

Using SIM and FM peptide pulldowns, as described in Chapter 2, I demonstrated that the SIM peptide bound both unphosphorylated and phosphorylated TAP-Smad2 and the FM bound phosphorylated TAP-Smad2 (Figure 3.4). TAP-Smad4 was detected in SIM and FM pulldowns in the TGF-β induced extracts, through interaction with endogenous Smad2 and Smad3. This pattern exactly mimics the

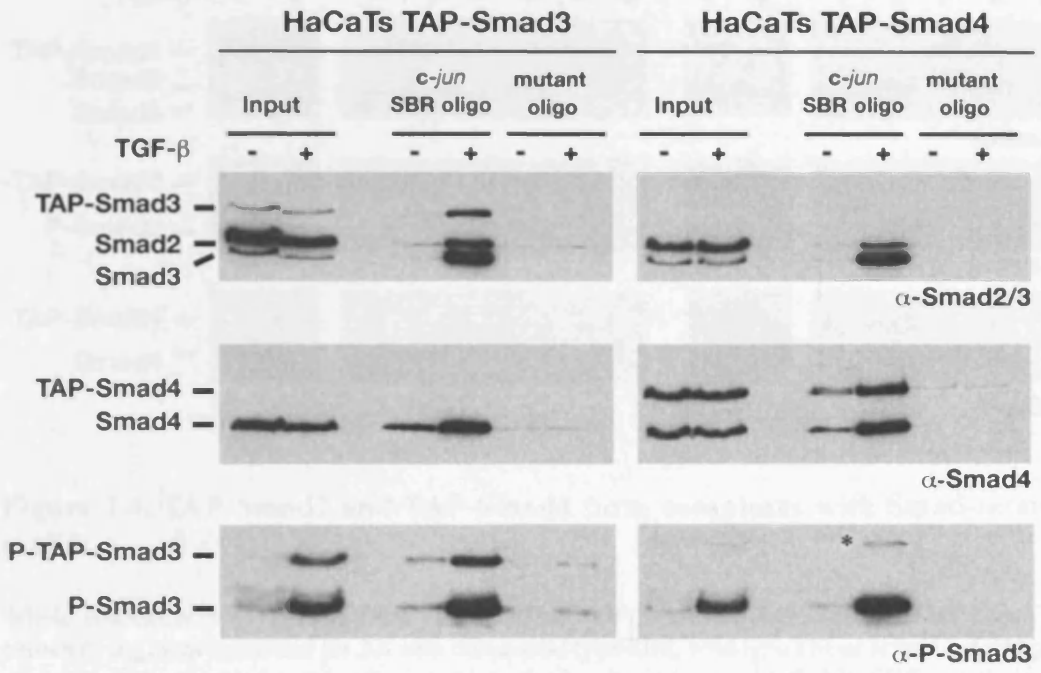

Figure 3.3. TAP-Smad3 and TAP-Smad4 form complexes on DNA

Whole cell extracts were made from uninduced or TGF-β-induced TAP-Smad HaCaT cells. The cell extract was adjusted to 200 mM NaCl and then incubated overnight with either c-*jun* SBR or mutant c-*jun* SBR oligo-conjugated beads as indicated. After washing, the beads were resuspended in SDS sample buffer and associated proteins were analysed by Western blotting using antibodies against phosphorylated-Smad3, Smad3 and Smad4. Ten percent protein input is shown.
* Indicates the TAP-Smad4 protein, which has been recognised by the α-rabbit secondary antibody via its IgG-binding domains.

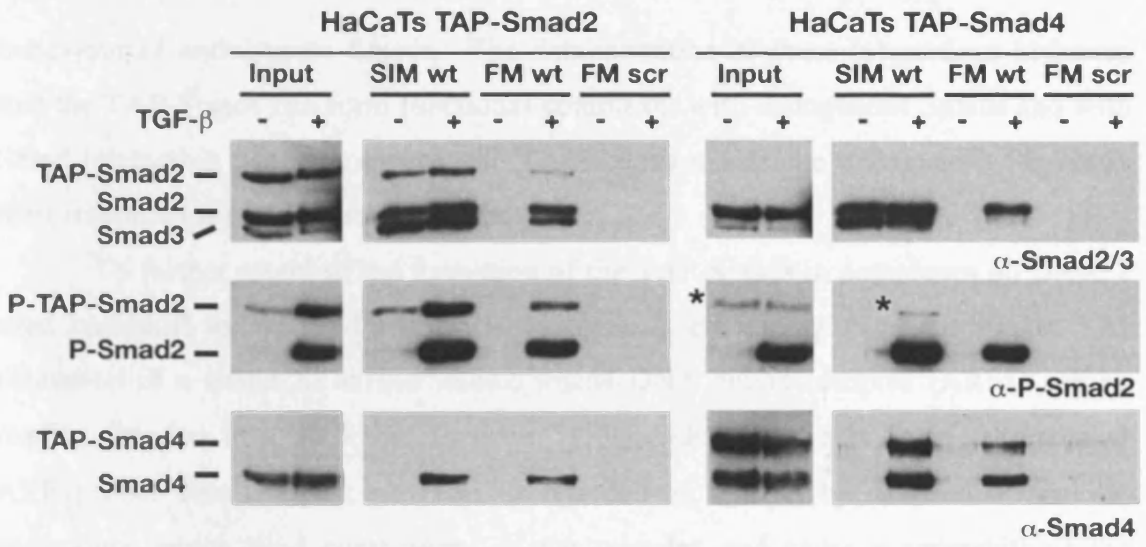

Figure 3.4. TAP-Smad2 and TAP-Smad4 form complexes with Smad-interacting motifs

Whole cell extracts were made from uninduced or TGF-β-induced TAP-Smad HaCaT cells. The cell extract (1 mg) was incubated for 2 h with either wild type SIM, wild type FM or scrambled FM peptide-conjugated beads as indicated. After washing, the beads were resuspended in SDS sample buffer and associated proteins analysed by Western blotting using antibodies against phosphorylated-Smad2, Smad2 and Smad4. 30 μg input protein is also shown.

* Indicates the TAP-Smad4 protein which has been recognised by the α-rabbit secondary antibody via its IgG-binding domains.

behaviour of endogenous Smads. The demonstration of these interactions indicates that the TAP-Smads can form functional complexes with endogenous Smads and with Smad-interacting peptides. Hence, the TAP-Smads mimic the endogenous Smads in their interactions with a partner protein.

To further establish the formation of the TAP-Smads in complexes on DNA, I used bandshift assays to detect ARF1 complexes containing the TAP-Smads. The formation of a stable XFoxH1a/Smad2/Smad4-DNA bound complex (ARF1) can be readily detected in a bandshift assay in TGF-β-induced extracts using radiolabeled ARE probe. This complex can also be retarded on the gel by addition of specific antibodies, which bind components of the complex and cause a supershift of the complex. The ARF1 complex containing TAP-Smad4 was detected by supershift with the anti-Smad4 antibody, seen as a second, slower migrating band above the endogenous Smad complex (Figure 3.5A). Whilst endogenous complexes were formed in the TAP-Smad2 HaCaTs, the fraction of TAP-Smad2 containing complexes could not be identified. This may be due to the inability of the antibody to recognise the TAP-Smad in the DNA-complex, or, more likely the rather low level of TAP-Smad2 compared with endogenous Smad2.

The expression of the TAP-Smads from the weak LTR (long terminal repeats) promoter in transient transfections was not sufficient to compete with endogenous Smads in luciferase reporter assays. However, using MDA-MB468 cells, which are Smad4-null cells, I was able to analyse TAP-Smad4's transcriptional activity (Figure 3.5B). This was not possible for Smad3 as the Smad3-null cells were not available at the time (Piek, E. et al., 2001) . The Smad2-null cells that have been reported in the literature (Piek, E. et al., 2001), have recently been shown to express a truncated form of Smad2, which can form complexes with Smad4 and actively engage in TGF-β-induced transcription, thus eliminating their use as Smad2-null cells (Randall and Hill, unpublished data). To test the ability of TAP-Smad4 to induce transcription, MDA-

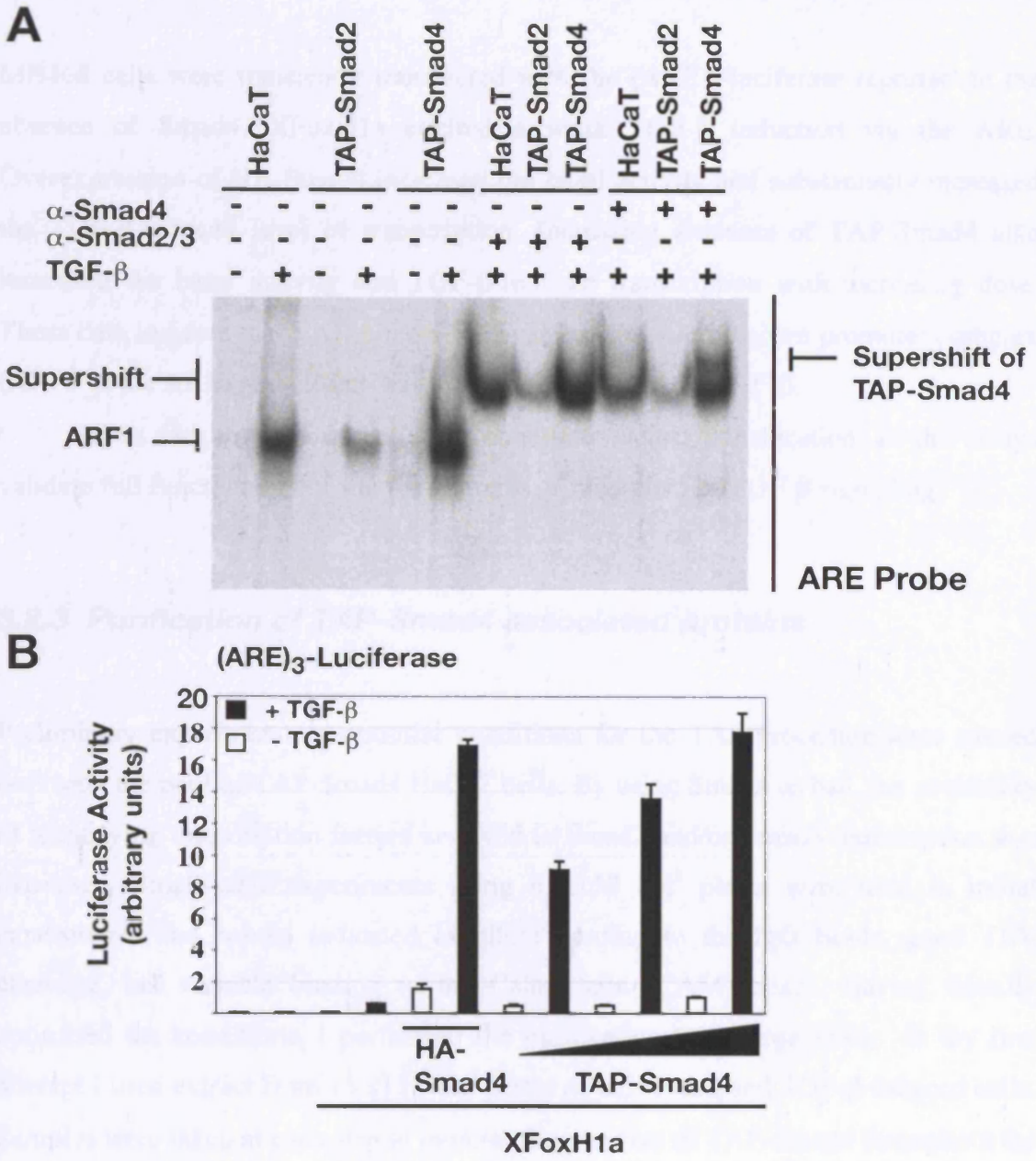

Figure 3.5. TAP-Smad4 forms complexes which are transcritpionally active

(A) TAP-Smad4 forms stable complexes with XFoxH1a and activates endogenous Smad2 on the ARE probe. HaCaTs, TAP-Smad2 HaCaTs and TAP-Smad4 HaCats were transfected with XFoxH1a and were either uninduced or induced with TGF-β1 for 1 hr prior to lysis. Whole cell extracts were analysed by bandshift assay using radioactively labelled ARE probe and in the presence or absence of 1 μl anti-Smad2/3 or anti-Smad4 antibody, as indicated. The Smad-containing complex, Activin Responsive Factor (ARF), is indicated, as is the supershifted complex. When TAP-Smad4 HaCaT cells are supershifted with α-Smad4 antibody, two complexes are seen-one containing endogenous Smad4; the other lower mobility one containing TAP-Smad4 as indicated.

(B) Smad4-null MDA-MB468 cells were transfected with the $(ARE)_3$-luciferase reporter gene together with plasmids expressing XFoxH1a alone or with HA-Smad4 or increasing amounts of TAP-Smad4 as indicated. Cells were lysed in reporter lysis buffer and luciferase assays were performed. Luciferase was quantitated relative to β-galactosidase from the pEFLacZ internal control. The data are means and standard deviations of 3 independent experiments.

MB468 cells were transiently transfected with the $(ARE)_3$-luciferase reporter. In the absence of Smad4, XFoxH1a elicited a weak TGF-β induction via the ARE. Overexpression of HA-Smad4 increased the basal activity and substantially increased the TGF-β-induced level of transcription. Increasing amounts of TAP-Smad4 also increased the basal activity and TGF-β-induced transcription with increasing dose. These data indicate that TAP-Smad4 cells can integrate in a known promoter complex (ARF1 at the ARE) and initiate transcription in response to TGF-β.

Thus far, with the exception of complete nuclear translocation, all the assays validate full functionality of the TAP-Smads as mediators of TGF-β signalling.

3.2.3 Purification of TAP-Smad4 associated proteins

Preliminary experiments to optimise conditions for the TAP procedure were carried out using the pool of TAP-Smad4 HaCaT cells. By using Smad4 as bait, the possibility of identifying transcription factors involved in Smad2 and/or Smad3 transcription was increased. Small-scale experiments using 6 x150 cm^2 plates were used in initial experiments and results indicated excellent binding to the IgG beads, good TEV cleavage, but variable binding to the Calmodulin (CAM) beads. Having initially optimised the conditions, I performed the purification on a large scale. In my first attempt I used extract from 15 x150 cm^2 plates of uninduced and TGF-β-induced cells. Samples were taken at each step to monitor the progress of TAP-Smad4 throughout the purification procedure. Progression through each purification step was successful with a final elution peak at fraction 5 for both samples (Figure 3.6A). Analysis by Western blotting revealed Smad2 in association with Smad4 throughout the whole purification procedure for the extract of induced cells (Figure 3.6A), and not with the extract from uninduced cells, as was expected (data not shown). This acted as an excellent marker for specific interacting proteins co-purifying with the TAP-Smad4 bait. The concentrated fractions of the eluates were then analysed by silver staining (Figure 3.6B). The pattern of bands in both samples was remarkably similar but with the exception of two bands. The first protein was present only in the induced sample and migrated on the SDS-PAGE gel at approximately 66kDa. It was suspected that this

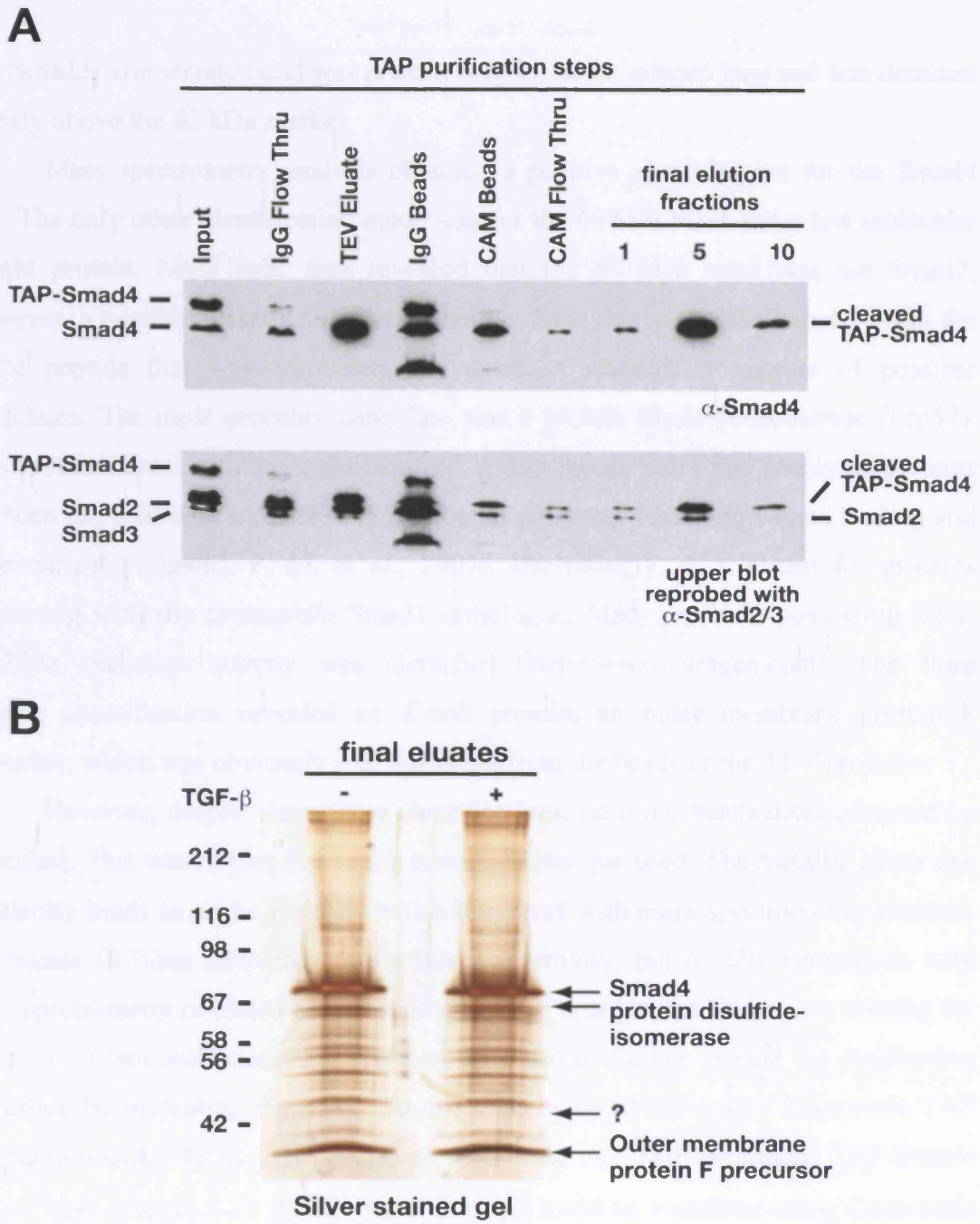

Figure 3.6. Purification of TAP-Smad4 associated proteins

(A) Samples taken from TGF-β-induced TAP-Smad4 HaCaTs at each stage of the purification were analysed by Western blotting. The top blot is probed with an anti-Smad4 antibody. This blot was then reprobed with an anti-Smad2/3 antibody (lower panel). The following proportions of samples were loaded: Input (1/1,300), IgG flow through (1/1,300), TEV eluate (1/60), IgG beads post TEV cleavage (1/8), CAM beads post EGTA elution (1/8), CAM flow through (1/150) and final eluates (1/4).

(B) Silver-stained gel depicting proteins recovered following purification of TAP-Smad4 associated proteins from unstimulated and cells stimulated with TGF-β for 1 hr. The numbers to the left show the positions of molecular size markers (kDa). Proteins identified by mass spectrometry are indicated. Mass spectrometric anlaysis was carried out by the Cancer Research UK Service.

was Smad2. The second band was present only in the uninduced lane and was detected slightly above the 42 kDa marker.

Mass spectrometry analysis obtained a positive identification for the Smad4 bait. The only other identification made was for the 66 kDa band and a low molecular weight protein. Mass Spec data revealed that the 66 kDa band was not Smad2. However, a positive identification could not be made due to limited sample. From the single peptide that was recovered, the database revealed a number of possible candidates. The most probably candidate was a protein disulfide-isomerase (Erp57). This protein contains thioredoxin-like fold and in recent years this family of proteins has been implicated in an increasing number of processes including wound healing and development (Clissold, P. M. et al., 2003). Interestingly, in a screen for proteins interacting with the *Drosophila* Smad1 orthologue, Mad, a protein possessing thiol-disulfide exchange activity was identified (http://www.curagen.com). The third positive identification revealed an *E-coli* protein, an outer membrane protein F precursor, which was obviously a contaminant from the beads or the TEV protease.

However, despite these three identifications, no other bands detected could be identified. This was in part due to the staining technique used. The metallic silver dye covalently binds to acidic residues which interferes with mass spectrometric analysis. Coomassie Brilliant Blue stain has a lower sensitivity, but is fully compatible with mass spectrometry of eluted polypeptide chains. In order to use Coomassie staining for detection of bait and interacting proteins, I needed to further expand the purification procedure by increasing the input. To this end, I carried out a very large scale TAP purification using 40 x15 cm^2 plates of uninduced and TGF-β-induced TAP-Smad4 HaCaT cells (Figure 3.7). At this scale, proteins could be visualised using Coomassie stain. The Western blot and Coomasse stained gel revealed that a high level of Smad4 bait was purified from uninduced cells. Unfortunately, very little bait was recovered from induced cells. This was attributed to the considerable loss of bait during the second step of purification.

A positive identification for human Smad4 was made by mass spectrometry, however, all other identifications made were of *E-coli* proteins. These included Phage λ receptor protein, Ompf Porin (mutant R82c), Phage Lambda receptor protein and Ferrienterobactin receptor precursor. Once again, these proteins were obviously contaminants from the IgG beads, the Calmodulin beads or the TEV protease and were

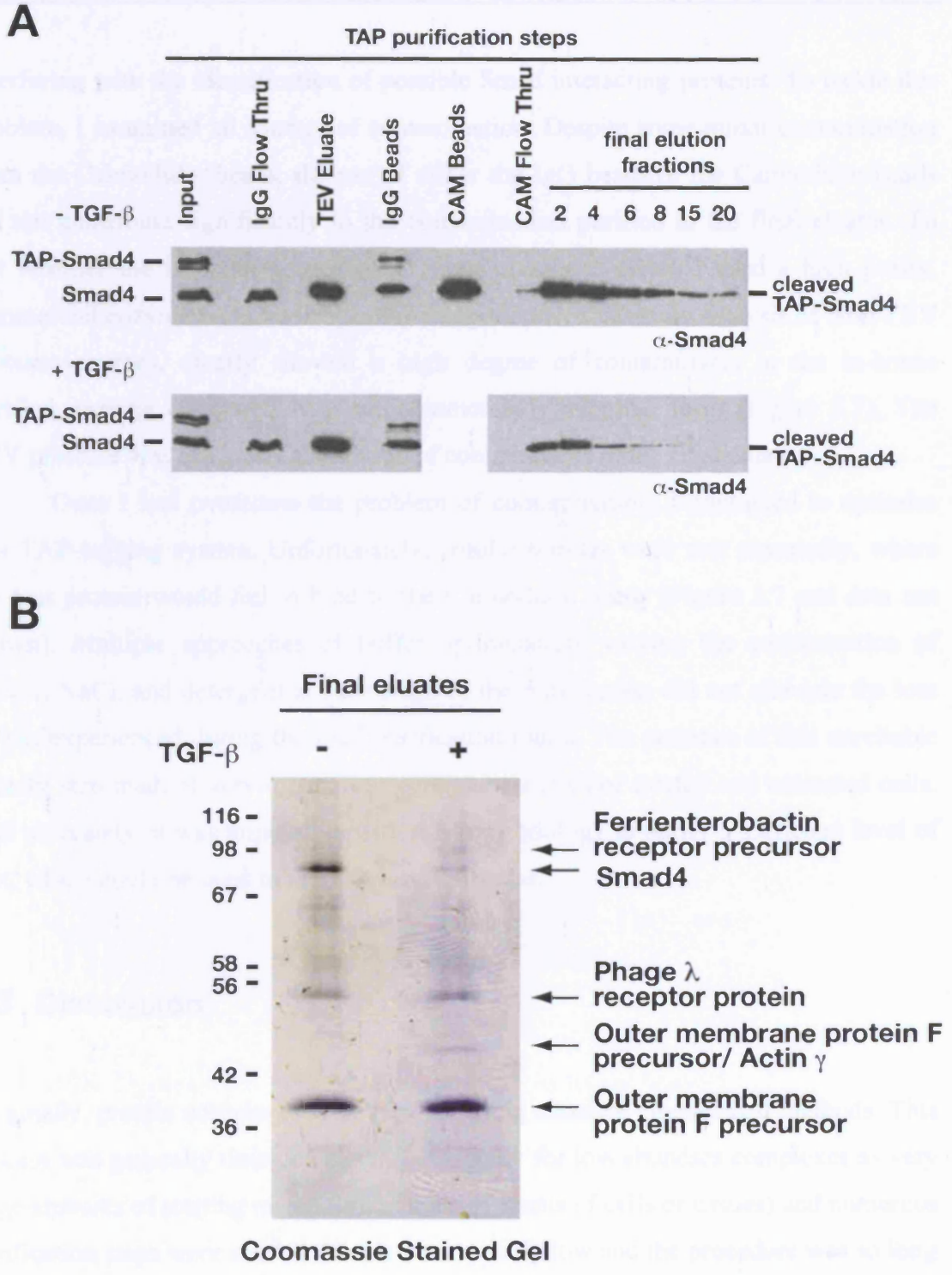

Figure 3.7. Large-scale purification of TAP-Smad4 associated proteins

(A) Samples taken at each step of the purification of both uninduced and TGF-β-induced TAP-Smad4 HaCaTs were analysed by western blotting for Smad4 in each case. The following proportions of samples were loaded: Input (1/2,200), IgG flow through (1/2,200), TEV eluate (1/170), IgG beads post TEV cleavage (1/10), CAM beads post EGTA elution (1/15), CAM flow through (1/800) and final eluates (1/7).

(B) Coomassie-stained gel depicting proteins recovered following purification of TAP-Smad4. The final eluate fractions of the purifications were pooled and concentrated and analysed by SDS-PAGE. Proteins identified by mass spectrometry are indicated.

interfering with the identification of possible Smad interacting-proteins. To tackle this problem, I examined all sources of contamination. Despite some minor contamination from the Calmodulin beads, the use of either the IgG beads or the Calmodulin beads did not contribute significantly to the contamination purified in the final eluates. To test whether the in-house source of TEV protease was clean, I used a high purity, commercial enzyme from invitrogen for comparison. Silver-stain analysis of both TEV protease sources, clearly showed a high degree of contaminants in the in-house purified enzyme compared with the commercially supplied form (Figure 3.7). The TEV protease was obviously the source of contaminants in the final eluate.

Once I had overcome the problem of contamination, I continued to optimise this TAP-tagging system. Unfortunately, similar hurdles were met repeatedly, where the bait protein would fail to bind to the Calmodulin beads (Figure 3.7 and data not shown). Multiple approaches of buffer optimisation, varying the concentration of EGTA, NaCl, and detergent at each stage of the purification did not alleviate the loss of bait experienced during the final purification round. The presence of this unreliable affinity step made it very difficult to compare samples of treated and untreated cells. And ultimately, it was impossible with this methodology to purify a sufficient level of bait, which could be used to identify novel proteins.

3.3 Discussion

Originally, protein complexes were purified using classical biochemical methods. This process was generally time-consuming, especially for low abundant complexes as very large amounts of starting material (hundreds of grams of cells or tissues) and numerous purification steps were needed. Yields were usually low and the procedure was so long that less stable complexes were not preserved. Development of affinity-purification techniques has dramatically improved the purification of protein complexes. In the case of the Tandem Affinity Purification procedure, this system has been used to isolate a wide variety of bait proteins, and moreover, has been applied for use in large scale analysis in yeast (Gavin, A. C. et al., 2002). Given the previous success with this system in yeast, my initial goal was to adapt this procedure to analyse components of the TGF-β pathway in mammalian cells. Indeed, the data presented in this pilot study

Figure 3.8. Comparison of TEV protease from different sources

5µl of Tobacco Etch Virus protease (TEV) from Invitrogen and from an in-house source were analysed by SDS-PAGE and silver stained to visualise contaminants. The invitrogen protein was very pure compared with the in-house version.

shows the development of a purification system for interacting-Smad proteins in HaCat cells. I successfully established stable cell lines expressing exogenous tagged Smad protein, at levels close to endogenous. The expression of the tagged proteins proved non-toxic to the cells. I have confirmed that the presence of a 19kDa tag does not interfere with the ability of the Smads to complex with other proteins. Apart from the slightly compromised nuclear import, the functionality of the TAP-Smads is not hindered.

The initial problem encountered during this pilot study was the presence of contaminants from the purified TEV protease. This resulted in a high level of interference in the process of identification of Smad-interacting proteins. For example, a protein disulfide-isomerase (Erp57) was identified as a possible candidate for a novel Smad partner, but further investigation failed to confirm this interaction (data not shown). Other protein identifications were more obviously classified as contamination due to their bacterial origin (Figure 3.7B). However, this obstacle could be overcome with the use of a highly purified source of TEV protease, as was the case with repeat experiments (Figure 3.8 and data not shown). The major problem, however, was the unreproducible and unreliable two-step purification of the bait Smad4. This is exemplified in Figure 3.7B, which shows the unsuccessful purification of the TGF-β-induced extract, whilst uninduced extract performed well. It was evident from Western blot analysis that substantial loss of the bait protein (TAP-Smad4) occurred during the second step of the purification. In the Coomassie stained gel, background bands were observed in both lanes but Smad4 was only detected in the uninduced lane. This is consistent with the good elution profile of the uninduced sample as confirmed by western blotting (Figure 3.7A).

It was evident from this and many other subsequent experiments that the CAM binding step was the weak point of the purification technique. In some cases, none of the cleaved TAP-Smad bound to the CAM beads. It is important to note that the TAP-Smad protein did not fail to bind the CAM beads because of stimulation with TGF-β. Repeated experiments showed no correlation between the failure of the second step with induction by TGF-β. In fact, despite rigorous testing of purification conditions, there seemed to be no correlation with any of the parameters investigated. This is underscored in the purification of uninduced and induced TAP-Smad4, which were run in parallel under identical conditions, however the efficiency of the bait binding to the

CAM beads differed drastically (Figure 3.7). Purification of both TAP-Smad2 and TAP-Smad3 yielded similar inconsistencies, which indicated that it was not specific to TAP-Smad4.

Interestingly, previous studies have demonstrated that the Smads can interact with CAM (Scherer, A. et al., 2000; Zimmerman, C. M. et al., 1998). Other evidence implicate the Smads as substrates of Calcium/calmodulin-dependent protein kinase II (CamKII) and suggest that phosphorylation of the linker domain by CamKII prevents nuclear translocation of the Smads (Wicks, S. J. et al., 2000). If this is the case, I speculated that this could explain the decreased capacity of the TAP-Smads to translocate to the nucleus and the limited ability of the TAP-Smads to bind to the CAM beads. It was possible that perhaps the presence of the CBP tag increased the amount of endogenous Calmodulin binding to the TAP-Smads. This Calmodulin might recruit CamKII to phosphorylate the TAP-Smads. However, using IgG pulldown assays, it was clear that endogenous Calmodulin did not bind the TAP-Smads during the Protein A-IgG binding step (data not shown). The presence of EGTA in the lysis buffer presumably prevented binding of endogenous Calmodulin to the CBP tag, as intended. Hence, the only other possibility that might explain the poor binding of the TAP-Smads to the CAM beads, is that it is due to a misfolded or denatured CBP in the context of the Smad fusions. This may not happen in all cases, perhaps due to the presence of a chaperone protein in variable amounts in the proteins extract. Furthermore, the TAP-tag was cloned directly upstream of the Smad ATG start site, without the incorporation of a linker sequnce to separate the tag from the Smads. It is possible that this may have increased the steric hindrance of the Tag, in particular upon cleavage of the ProteinA IgG binding domains.

To conclude, it is possible to generate Smad fusion proteins in mammalian cells that are functional with respect to their ability to form complexes with endogenous Smads, bind to DNA and initiate transcription. In addition, the Protein A-IgG binding step together with TEV cleavage of the TAP-Smad, provide a highly discriminating separation step, which allows for the purification of known and unknown interacting partners. Unfortunately, the CAM binding of the TAP-purification procedure proved to be unreliable as a second, final step of purification.

As a result, I investigated the use of an alternative tag, which will be discussed in the next chapter.

4 Chapter 4

4.1 Introduction

As introduced in Chapter 3, the initial aims of my study were to gain insight into the molecular mechanisms governing TGF-β signalling through identification of new components of the pathway. The interactions between Smads and other proteins represent an important determinant of specificity within the TGF-β pathway (ten Dijke, P. et al., 2004). The Smads interact with a wide array of proteins, including cytoskeletal components and nuclear transport machinery which allow access to the nucleus, and a range of discrete and distinct DNA binding cofactors, which give rise to high affinity binding to a specific gene set (ten Dijke, P. et al., 2004). To shed light on new partners of the Smads, I wanted to use the Smad proteins as bait to co-purify associated proteins. It is evident from the pilot study in Chapter 3 that it is feasible to use a two-step purification procedure to search for Smad-interacting partners. The conventional TAP system, however, failed to yield reproducible results due to the unreliability of the Calmodulin binding step. However, the redeeming feature of the TAP system was the efficiency and reproducibility of the Protein A-IgG binding step combined with the TEV cleavage. In this Chapter, I present data on a modified TAP purification scheme, which utilises the Protein A-IgG affinity purification and TEV cleavage steps but with a FLAG-tag as a replacement tag for Calmodulin binding peptide (CBP) for the second purification step.

The TAP system was initially tested in the HaCat keratinocyte cell line in order to establish the feasibility of the purification technique. The HaCat cell line served as an excellent tool in testing the functionality of the TAP-tagged Smads and also in demonstrating a viable multi-step purification procedure. Ultimately though, the aim of this work was to use the purification system to identify novel Smad-interacting transcription factors in a tumour cell model system. A well characterised system developed in Hartmut Beug's laboratory was chosen for this purpose. It is an ideal system to use in this study because the TGF-β responses in the individual cell lines have been investigated in detail. The parental cell line, EpH4 cells, are a non-

transformed clonal epithelial derivative of IM-2 mouse mammary gland epithelial cells, which were originally isolated from mammary tissue of a mid-pregnant mouse (Reichmann, E. et al., 1989). EpH4 cells are non-tumorigenic and undergo growth inhibition and apoptosis in response to TGF-β (Oft, M. et al., 1998; Oft, M. et al., 1996). However, EpH4 cells that have been transformed by stable expression of oncogenic Ras (EpRas cells) undergo an Epithelial-to-Mesenchymal Transition (EMT) in response to TGF-β and form rapidly growing tumours in mice (Oft, M. et al., 1998; Oft, M. et al., 1996). Cells recovered from these mouse tumours give rise to mesenchymal-like cells (X-tumour). These X-tumour cells are characterised by a spindle-like morphology and loss of epithelial markers. The cell lines represent the progression of a tumour from a normal epithelial to an invasive spindle-like cell.

While individual aspects of TGF-β responses have been studied in detail, much less is known about how a cell interprets the TGF-β signal to elicit different responses, such as growth inhibition or EMT. The molecular mechanisms by which TGF-β induces growth arrest in cells has been well documented (Shi, Y. et al., 2003). In epithelial cells, TGF-β induces activation of *p15Ink4b*, which encodes a cyclin-dependent kinase (CDK) inhibitor and also acts to repress c-*myc*, which encodes a potent transcriptional activator of genes required for growth and proliferation (Massague, J. et al., 2000b). The molecular requirements for EMT are more complex but a number of the signalling pathways involved in this process have been elucidated (Huber, M. A. et al., 2005). In the EpH4 system, a cooperative signal via the TGF-β and Ras was found to be essential for progression of EMT (Janda, E. et al., 2002). However, the necessary molecular steps required to achieve EMT versus growth inhibition is yet to be determined. To address this question, I used this tumour model system as a tool to investigate how cells respond differentially to TGF-β. My primary aim was to determine why EpH4 cells respond to TGF-β by growth inhibition compared with the EMT response observed in EpRas cells. The ultimate goal was to unravel a mechanism whereby tumour cells become resistant to the growth suppressive effects of TGF-β, but remain responsive to TGF-β as a tumour promoter.

In this chapter I present data on the use of a tumour model system in combination with an advanced protein purification technique. I begin with results of my initial characterisation of the three different cell lines in the EpH4 tumour model

system and characterisation of the responses of the cell system to TGF-β. I then go on to demonstrate the use of these cells in isolating Smad proteins and their interacting partners.

4.2 Results

4.2.1 Establishing the Tumour Model System

4.2.1.1 Phenotype of EpH4 derivatives

My first task was to set up the EpH4 tumour model system in the lab and demonstrate the different responses to TGF-β of the individual cell lines, as previously observed (Oft, M. et al., 1998; Oft, M. et al., 1996). I began with the morphology of each cell line on plastic. From Figure 4.1A, it is clear that both EpH4 and EpRas cells exhibit a clear epithelial morphology. These cells grow in clusters and form monolayers of cells in close contact, tightly adherent to neighbouring cells and to the plastic substrate. In addition, confluent cultures of EpH4 cells develop hemicysts or domes, which are believed to be due to unidirectional fluid secretion of polarized epithelial cells when cultured on plastic (Lever, J. E., 1979). The X-tumour cells, on the other hand, display a distinct mesenchymal phenotype (Figure 4.1A, right hand panel). This is evident from the elongated cells with a spindle-shaped, fibroblastoid morphology and the lack of contact with neighbouring cells.

4.2.1.2 Characterisation of the EpH4 model system in Collagen Gels

Next, it was important to assess the responses of each cell type to TGF-β. To demonstrate TGF-β-induced EMT in EpRas cells and its absence in EpH4 cells, I set up 3-D collagen gels as previously described (Oft, M. et al., 1998; Oft, M. et al., 1996). Using this technique it is possible to visualize the 3-D structures formed. Previous studies have indicated that both EpH4 and EpRas cells tend to form tubular, branched structures of fully polarized cells. EpRas cells grow faster and mainly form alveolar structures with larger lumina, however the precise structures formed by each cell type can be variable (Oft, M. et al., 1998; Oft, M. et al., 1996). In collaboration with Hartmut Beug's laboratory, experiments were conducted to observe the structures of EpH4 and EpRas cells in 3-D collagen gels. Structures of EpH4 and EpRas cells

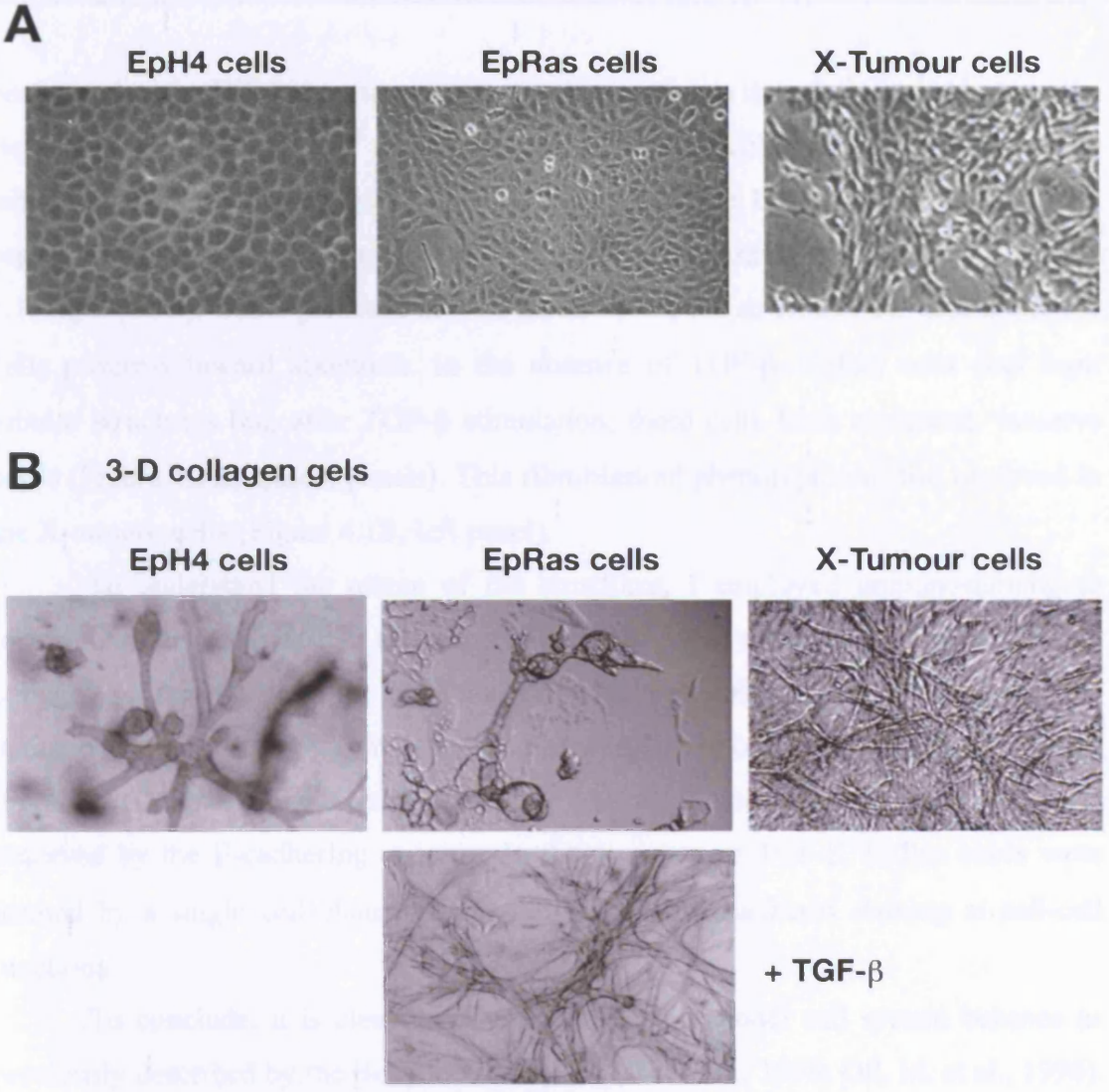
A
EpH4 cells
EpRas cells
X-Tumour cells
B
3-D collagen gels
EpH4 cells
EpRas cells
X-Tumour cells
+ TGF-β
C
E-cadherin
Dapi
Merge
EpRas cells
- TGF-β
EpRas cells
+ TGF-β

performed in the Hill Laboratory were more heterogenous than those carried out in the Beug laboratory. Therefore, experiments conducted in collaboration with the Beug laboratory are shown in Figure 4.1B. In the case of the EpH4 cells, the cells form organ-like ducts similar to those formed by primary mammary epithelial cells (Figure 4.1, right panel). In the presence of TGF-β, however, the structures are absent and the cells progress toward apoptosis. In the absence of TGF-β, EpRas cells also form tubular structures but, after TGF-β stimulation, these cells form elongated, invasive cords (Figure 4.1B, middle panels). This fibroblastoid phenotype was also observed in the X-tumour cells (Figure 4.1B, left panel).

To understand the nature of the structures, I employed immunostaining to identify cell-cell contacts. In this experiment, individual structures of EpRas cells in collagen gels prepared in the Hill laboratory were examined. This revealed that the structures were formed by communication between many cells as seen by dapi staining (Figure 4.1C). Individual cells retained their cell-cell junctions within the structures as observed by the E-cadhering staining. In the presence of TGF-β, EpRas cords were formed by a single cell chain with slightly reduced E-cadherin staining at cell-cell junctions.

To conclude, it is clear that the EpH4 tumour model cell system behaves as previously described by the Beug laboratory (Oft, M. et al., 1998; Oft, M. et al., 1996). EpRas cells undergo an EMT in response to TGF-β in 3-D collagen gels, and the progression to invasive spindle-like cords mimics the phenotype of the X-tumour cells.

4.2.1.3 Effects of TGF-β on the Cell cycle in EpH4 derivatives

Next, I went on to investigate the effect of TGF-β on the growth arrest. EpH4 cells only respond to TGF-β by growth inhibition at specific points in the cell cycle (Petritsch, C. et al., 2000), which does not appear to be the case for other cell lines such as HaCats (Nicolas, F. J. et al., 2003a). Possible explanations for this will be discussed later (Chapter 5 and 7). For an effective response to TGF-β, the cells require synchronisation by contact inhibition (Petritsch, C. et al., 2000) and subsequent release into fresh media in the presence or absence of TGF-β. The effect of TGF-β can be assayed by the ability of the cells to enter S-phase. Using this technique, FACS analysis revealed that all three lines of contact inhibited cells (0 hr) exhibited a

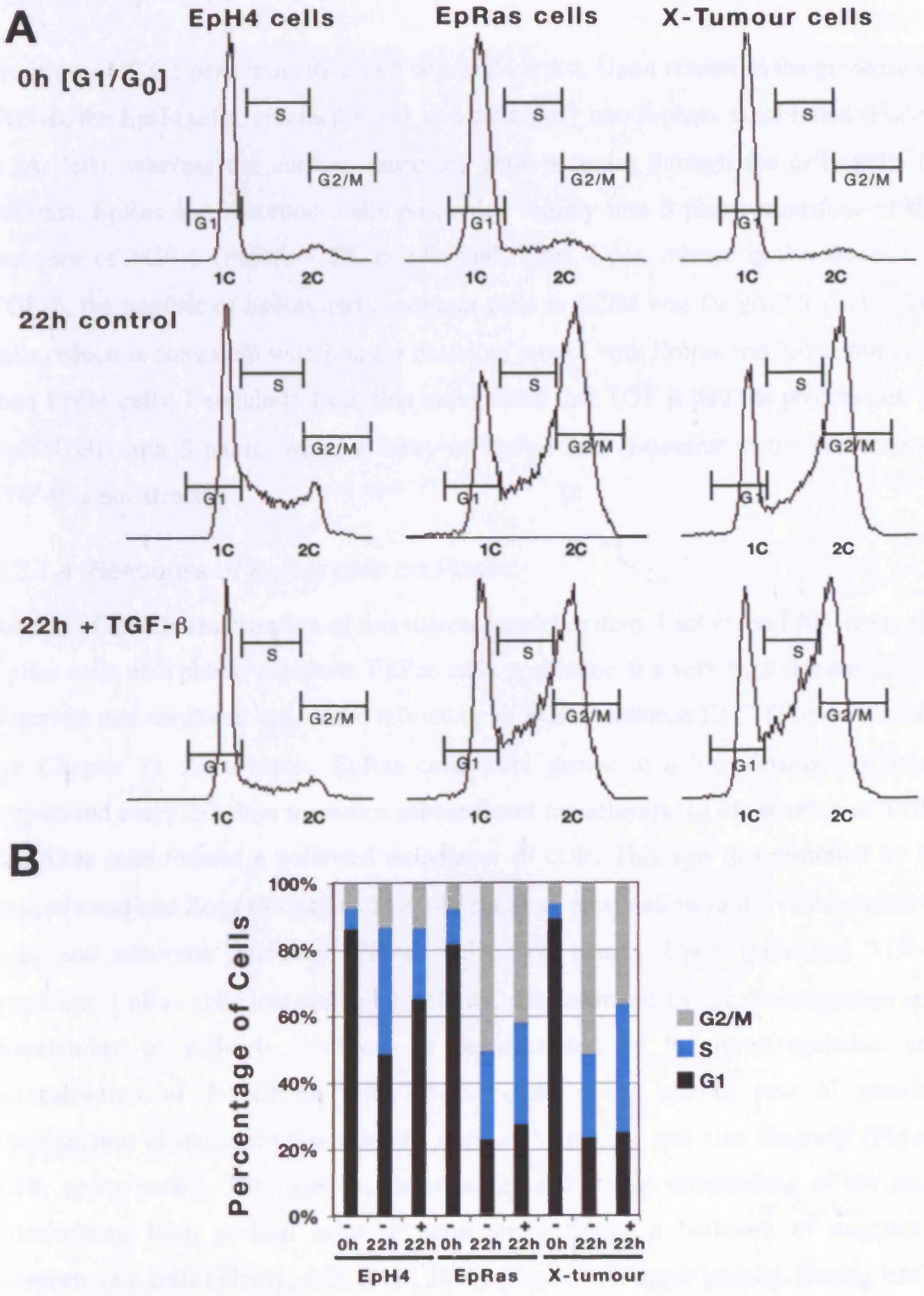

Figure 4.2. EpH4 cells undergo growth arrest in G1 in response to TGF-β, whereas EpRas and X-Tumour cells do not

(A) FACS-DNA profiles of EpH4 cells, EpRas and X-tumour cells. Cells were synchronised in G1 by contact inhibition for 72 hrs. Cells were detached from the plates with 0.2% EDTA and replated in fresh medium and allowed to re-enter the cell cycle for 22 hrs, in the presence or absence of TGF-β1 (2 ng/ml). Cells were harvested and analysed by fluorescence-activated cell sorting (FACS), to determine the number of cells in G1, S and G2/M.
(B) Quantitations of the FACS profiles indicating percentage of cells in each phase of the cell cycle, G1 (black bar), S (blue bar) or G2/M (grey bar).

prominent G0 G1 peak indicative of a cell cycle arrest. Upon release in the presence of TGF-β, the EpH4 cells remained in G1 and their entry into S-phase is inhibited (Figure 4.2A, left), whereas the control, untreated cells progress through the cell cycle. In contrast, EpRas and X-tumour cells proceeded rapidly into S phase regardless of the presence of TGF-β (Figure 4.2B, middle and right). Upon release in the absence of TGF-β, the number of EpRas and X-tumour cells in G2/M was far greater than EpH4 cells, which is consistent with a faster doubling rate of both EpRas and X-tumour cells than EpH4 cells. I conclude from this experiment that TGF-β inhibits progression of EpH4 cells into S-phase, whereas entry of EpRas and X-tumour in the presence of TGF-β is not affected.

4.2.1.4 Response of EpRas cells on Plastic

As part of the characterisation of this tumour model system, I set up an EMT assay for EpRas cells on a plastic substrate. EpRas cells proliferate at a very high rate and it was observed that confluent cells were refractory to TGF-β-induced EMT (For discussion, see Chapter 7). As a result, EpRas cells were grown at a low density and were trypsinised every 2-3 days to ensure subconfluent monolayers. In the absence of TGF-β, EpRas cells formed a polarised monolayer of cells. This was demonstrated by E-cadherin and and Zona Occludens 1 (ZO-1) staining, which allowed the visualisation of tight and adherens junctions (Figure 4.3A, top panel). Upon prolonged TGF-β treatment, EpRas cells lost epithelial polarity, demonstrated by the disintegration and disassembly of cell-cell junctions, as demonstrated by the downregulation and delocalisation of E-cadherin and ZO-1 (Figure 4.3A, second row of panels). Upregulation of mesenchymal markers, such as Vimentin, was also observed (Figure 4.3B, upper panel). This was accompanied by a dramatic remodelling of the actin cytoskeleton from cortical actin to actin stress fibers, a hallmark of migratory, mesenchymal cells (Thiery, J. P. et al., 2006) (Figure 4.4, upper panels). During EMT, an autocrine loop of TGF-β is established and maintains the fibroblastoid phenotype of converted EpRas cells (Oft, M. et al., 1996). To investigate whether a feedback loop had been established, nuclear accumulation of Smad2/3 was investigated. The samples were harvested 48 hrs after addition of TGF-β. In human keratinocytes, phosphorylation of Smad2/3 is terminated approximately 12 hrs after TGF-β addition resulting in the redistribution of Smad2/3 to the cytoplasm (Inman, G. J. et al., 2002c;

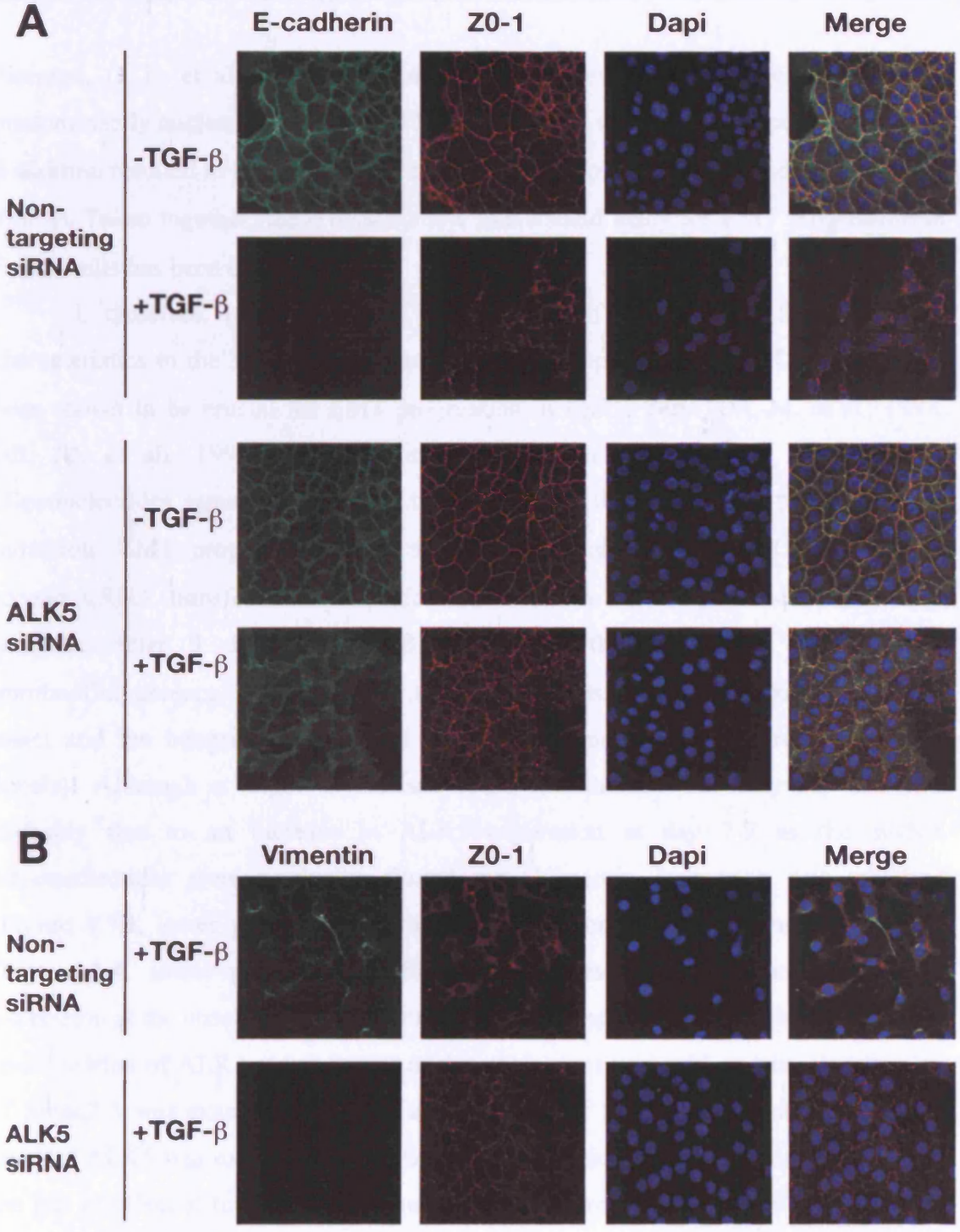

Figure 4.3. Knockdown of ALK5 abolishes TGF-β-induced EMT

(A and B) EpRas cells were transfected at low density with siRNA against ALK5 or a non-targeting oligo. After overnight incubation, cells were replated 1:2 and grown in the presence or absence of TGF-β1 (2 ng/ml). The medium was changed 1 d after seeding and then every other day. TGF-β1 was added to the cells upon medium change. Three days after plating, the cells were trypsinised and re-plated at equivalent density to day 1. A second siRNA transfection was performed on day 4. One, final replating of cells was carried out on day 7. Cells were grown for a total of 9 days in the presence or absence of TGF-β1 and then harvested 48 hrs after final TGF-β addition. Cells were processed for immunofluorescence and examined by confocal laser scanning microscopy. Antibodies against E-cadherin and Zona Occludens 1 (Z0-1) were used to analyze adherens junctions or tight junctions, respectively (A). An anti-vimentin (Vim) antibody was also used to analyze mesenchymal marker expression (B) and nuclei were visualized with DAPI.

Pierreux, C. E. et al., 2000). In EpRas cells, however, Smad2/3 localisation was predominantly nuclear, 48 hours after TGF-β addition, suggesting that prolonged TGF-β addition resulted in the induction of an autocrine loop, which produced high levels of TGF-β. Taken together, these results show that a valid assay for EMT progression in EpRas cells has been established.

I, therefore, tested my EMT assay to see if these cells exhibited similar characteristics to the 3-D gel EMT assay. TGF-β receptor type I (ALK5) activity has been shown to be crucial for EMT progression in EpRas cells (Oft, M. et al., 1998; Oft, M. et al., 1996). As a positive control for inhibition of EMT, siRNA oligonucleotides against ALK5 were transfected into the EpRas cells prior to TGF-β induction. EMT progression requires long-term incubation with TGF-β, hence a second siRNA transfection was performed to ensure continued knockdown of the receptor. After 9 days of TGF-β stimulation, the cells were examined by immunofluorescence. In contrast to the control cells, cell–cell junctions remained intact and the integrity of epithelial polarity was maintained (Figure 4.3A, lower panels). Although a slight delocalisation of E-cadherin was observed, this was probably due to an increase in ALK5 expression at day 7-9 as the siRNA oligonucleotides were gradually diluted out. Vimentin expression was inhibited (Figure 4.3B, lower panel) and the actin cytoskeleton remained virtually unaltered (Figure 4.4, lower panels). This firmly establishes the requirement for ALK5 expression at the onset of TGF-β stimulation for a complete EMT. Further evidence of re-expression of ALK5 at late stages of the experiment was evident when localisation of Smad2/3 was examined. Nuclear accumulation of Smad2/3 suggested that a low level of ALK5 was expressed at the final stages of these cells, which is likely due to the loss of effect of the siRNA oligonucleotides (Figure 4.4, lower set of panels). This gradual re-expression of low levels of ALK5 protein promoted the production of an autocrine loop but which was not sufficient for EMT progression.

These results show that by using a combination of siRNA technology with an established EMT assay, components of the TGF-β pathway involved in EMT progression can be investigated.

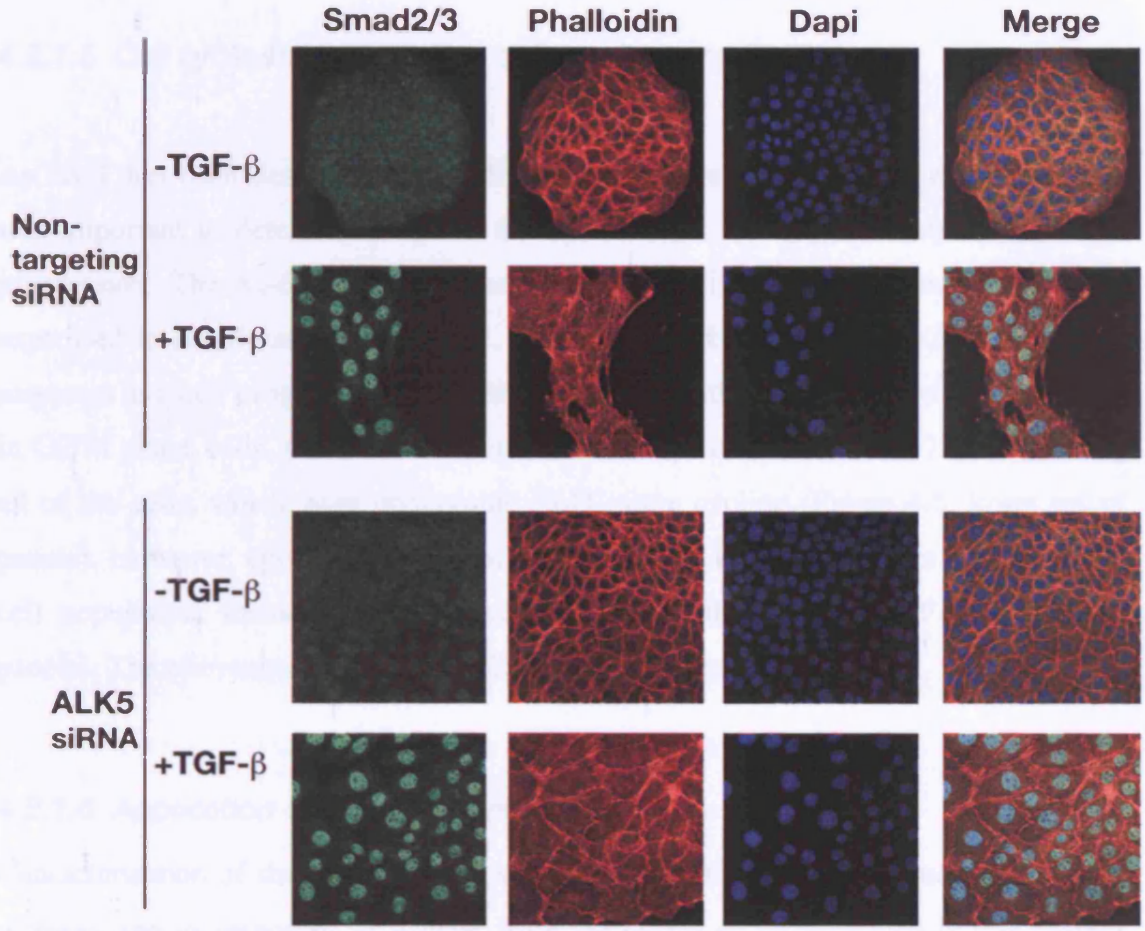

Figure 4.4. An autocrine loop of TGF-β secretion is set up during EMT

EpRas cells were transfected at low density with siRNA against ALK5 or a non-targeting oligo. After overnight incubation, cells were replated 1:2 and grown in the presence or absence of TGF-β1 (2 ng/ml). The medium was changed 1 d after seeding and then every other day. TGF-β1 was added to the cells upon medium change. Three days after plating, the cells were trypsinised and re-plated at equivalent density to day 1. A second siRNA transfection was performed on day 4. One, final replating of cells was carried out on day 7. Cells were grown for a total of 9 days in the presence or absence of TGF-β1 and then harvested 48 hrs after final TGF-β1 addition. Cells were processed for immunofluorescence and examined by confocal laser scanning microscopy. Smad2/3 localisation was determined using anti-Smad2/3. Actin reorganization was visualized with Texas red-conjugated phalloidin, and nuclei were visualized with DAPI. Samples were processed from the same experiment as in Figure 4.3.

4.2.1.5 Cell cycle status of EpRas cells undergoing EMT

As EMT has been described as a dedifferentiation event (Grunert, S. et al., 2003), it was important to determine whether the EpRas cells were proliferating during EMT progression. The Ki-67 antigen is the prototypic cell cycle related nuclear protein, expressed in proliferating cells in G1, S, G2 and M, but not in G0. Ki67 expression increases as a cell progresses through the cell cycle, with highest expression being seen in G2 M phase cells. Cells stained with an antibody recognizing Ki-67, revealed that all of the cells, which were undergoing EMT, were cycling (Figure 4.5, lower set of panels). However, epithelial islands of control EpRas cells revealed an asynchronous cell population, including cells which have exited the cell cycle (Figure 4.5, top panels). The relevance of this will be discussed in Chapter 7.

4.2.1.6 Application of the EpH4 system

Characterisation of the EpH4 system was performed to establish a functional TGF-β pathway and its responses. It is clear from the results so far presented in this chapter that these cells possess an intact TGF-β pathway and elicit biological responses as previously described (Oft, M. et al., 1998; Oft, M. et al., 1996). Further biological characterisation of this system follows in later Chapters (Chapter 5 and 6). Therefore, the EpH4 system is a viable cell system to be used to investigate novel components of the TGF-β pathway by a dual tag purification technique. The application of this method using the EpH4 system will be discussed next.

4.2.2 Dual Tag purification

4.2.2.1 Design of Dual Tags

The main aim of the purification project was to design a dual affinity tag for the Smad proteins, which would facilitate efficient binding during two steps of purification, and thereby result in a reproducibly high yield of Smad associated proteins in the final eluate. The Protein A-IgG binding domains proved to provide an excellent first step in conjunction with TEV cleavage. Previous data has shown that the presence of Protein

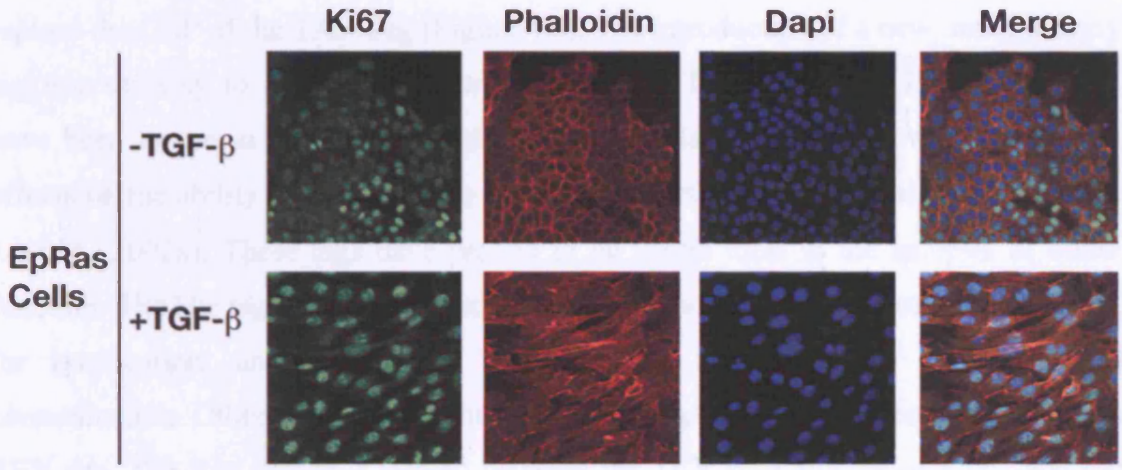

Figure 4.5. EpRas cells undergoing TGF-β-induced EMT are proliferating

Ki67 antigen is expressed in proliferating cells in G1, S, G2, and M, but not in G_0. EpRas cells were plated out at low density and either grown in the presence or absence of TGF-β1 (2 ng/ml). The medium was changed 1 d after seeding and then every other day. TGF-β1 was added to the cells upon medium change. Three days after plating, the cells were trypsinised and re-plated at equivalent density to day 1. Cells were grown for a total of 10 days, which required two trypsinisations, and then harvested 48 hrs after final TGF-β1 addition. Cells were stained with an antibody recognizing the Ki67 antigen and examined by confocal laser scanning microscopy. Actin reorganization was visualized with Texas red-conjugated phalloidin, and nuclei were visualized with DAPI.

A-affinity/TAP tag does not impair the functionality of the Smads in mediating transcriptional responses (Chapter 3). Three alternative affinity tags were chosen to replace the CBP of the TAP-Tag (Figure 4.6). The introduction of a new, small affinity tag was unlikely to cause any further interference. The FLAG and HA epitope-tags have been in use in the lab as N-terminal constructs of the Smads with no adverse effects on the ability of the Smads to act as mediators of TGF-β signalling (Inman, G. J. et al., 2002a). These tags have proved to be useful tools in the analysis of Smad function. The His tag provided a strategy which did not involve the use of an antibody for purification, and offered the possibility of a lower level of background contamination. Other alterations included the introduction of two spacers and a double TEV site. The first spacer is located between the TEV sites and the new tag, and the second between the latter and the Smad of interest (Figure 4.6B). The spacers were added to reduce interference between the tag and the MH1 domain of the Smads, to allow sufficient access of the TEV protease to the cleavage sites and to optimise binding of the new tag post cleavage. The introduction of a second TEV site was to improve the efficiency of cleavage and to reduce residual bait bound to the IgG beads. Thus, the redesign of the affinity tag would, in theory, optimise progress through purification steps. The tagged proteins were assayed to determine which tag was most successful.

4.2.2.2 Trial Purifications using different combinations of the Dual Affinity Tag

To determine the most efficient dual affinity tag combination, it was essential to test the binding capabilities of the individual tags in the cell context that was to be used for the final purification, the EpH4 cells. Each of the affinity tags was fused to Smad3 and constructs expressing these fusion proteins were transiently transfected into EpH4 cells. Purification of the dual tagged Smad3 was carried out under the three different conditions as described in Chapter 2. Samples were taken at each step to monitor the progress of the dual tagged-Smad3 throughout the purification procedure for each case (Figure 4.7A). There was variability in the transfection efficiency due to differences in cell confluency during the transfection. As a result the level of input of the tagged Smad3 was not equal. Nevertheless, a comparison of the different tags was still possible. In each purification procedure, no trace of the dual-tagged Smad3 was

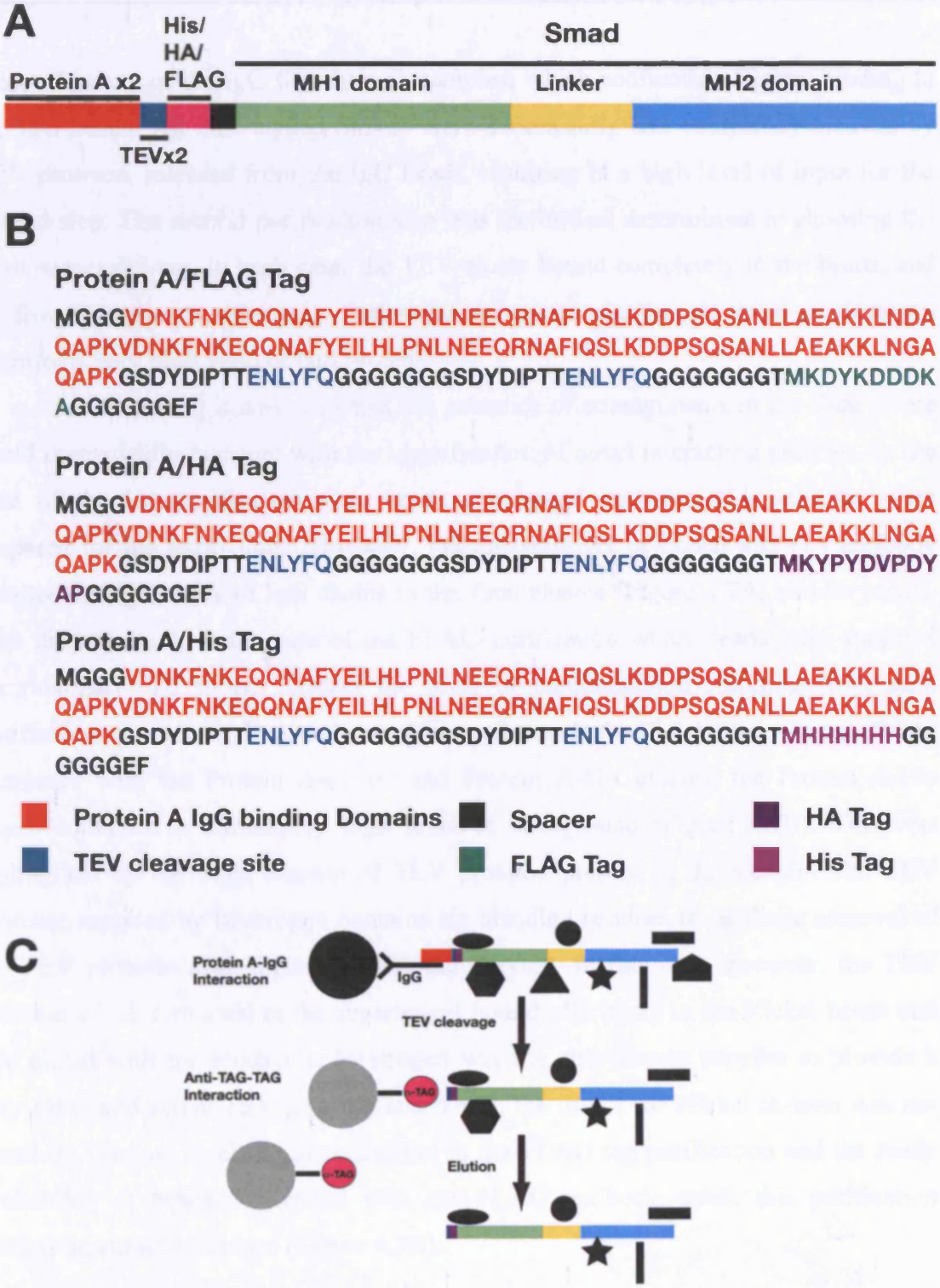

Figure 4.6. Alternative Dual Affinity Tags

(A) Schematic representation of the N-terminal dual-affinity tagged Smad constructs.
(B) The amino-acid structure of three alternative N-terminal dual-affinity tags. The Protein A/FLAG tag consists of two tandem Protein A IgG-binding domains, two TEV cleavage sites, and one copy of the FLAG sequence. The Protein A/HA tag and Protein A/His also contain two tandem Protein A IgG-binding domains and two TEV cleavage sites, but have one copy of the HA sequence or six histidines in place of the FLAG tag, respectively.
(C) Overview of the Dual-affinity Tag purification strategy. A protein complex containing the Dual-tagged protein is purified sequentially by two independent affinity steps. The immobilized protein is specifically eluted in the first instance by protease cleavage (TEV), and by peptide competition or imidazole in the second step.

detected in any of the IgG flowthrough samples, which confirmed efficient binding to the IgG beads. All dual-tagged Smad3 were successfully and completely cleaved by TEV protease, released from the IgG beads, resulting in a high level of input for the second step. The second purification step was the critical determinant in choosing the most successful tag. In each case, the TEV eluate bound completely to the beads, and no flowthrough was detected. Following successful elution, all three purifications revealed a very high yield of bait protein.

In Chapter 3, it was clear that the presence of contaminants in the final eluate could dramatically interfere with the identification of novel interacting proteins. In the case of the HA-purification step, beads conjugated with anti-HA antibody were prepared for the purification. However, leakage/spillover of excess anti-HA antibody resulted in high levels of IgG chains in the final eluates (Figure 4.7A, middle panel). This did not occur in the case of the FLAG purification where beads were supplied commercially. To further inspect the level of contamination resulting from each purification procedure, I carried out silver stain analysis of the final eluates. When compared with the Protein A-FLAG and Protein A-HA eluates, the Protein A-His eluate contained a remarkably high level of background (Figure 4.7B). This was highlighted by the large amount of TEV protease present in the sample. The TEV protease supplied by Invitrogen contains six histidine residues to facilitate removal of the TEV protease after digestion with the enzyme. In this case, however, the TEV protease which remained in the supernatant bound efficiently to the Nickel beads and also eluted with the imidazole. Invitrogen was the only known supplier to provide a very clean and active TEV protease and hence, the use of the Nickel column was not possible. The low level of contamination in the FLAG tag purification and the ready availability of beads conjugated with anti-FLAG antibody, made this purification process an attractive choice (Figure 4.7B).

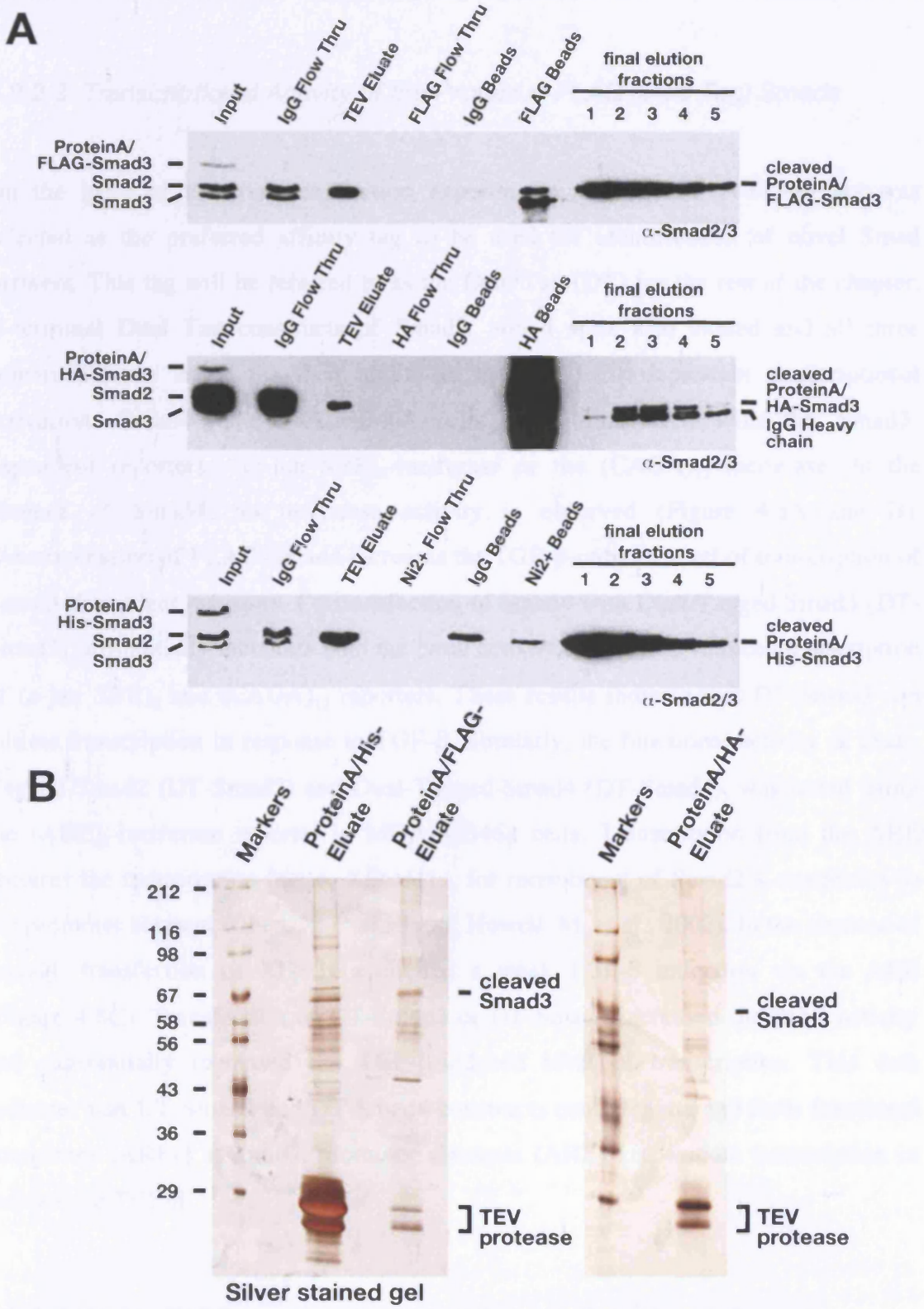

Figure 4.7. A Comparison of Dual Affinity Tag Purification Procedures

(A) EpH4 cells were transfected with the different Dual-tagged Smad3 constructs as indicated. Cells were induced with TGF-β1, harvested, and individual purification procedures were carried out. Samples taken at each stage of the purification were analysed by Western blotting using antibodies against Smad2/3.

(B) Silver-stained gels depicting proteins recovered following purification by the different procedures. The final eluate fractions of the purifications were pooled and concentrated and analysed by SDS-PAGE. The purification protocols for each procedure are given in Chapter 2.

4.2.2.3 Transcriptional Activity of the Protein A-FLAG (Dual Tag) Smads

On the basis of the trial purification experiments, the Protein A-FLAG tag was selected as the preferred affinity tag to be used for identification of novel Smad partners. This tag will be referred to as the Dual Tag (DT) for the rest of the chapter. N-terminal Dual Tag constructs of Smad2, and 4 were also cloned and all three constructs were tested for their ability to induce TGF-β-dependent transcriptional activation. Smad4-null MDA-MB468 cells were transfected with the Smad3-dependent reporters, (c-jun SBR)$_6$-luciferase or the (CAGA)$_{12}$ luciferase. In the absence of Smad4, no luciferase activity is observed (Figure 4.8A and B). Overexpression of FLAG-Smad4 increases the TGF-β-induced level of transcription of Smad3-dependent reporters. Co-transfection of Smad4 with Dual-Tagged Smad3 (DT-Smad3) substantially increases both the basal activity and TGF-β-induced transcription of (c-jun SBR)$_6$ and (CAGA)$_{12}$ reporters. These results indicate that DT-Smad3 can initiate transcription in response to TGF-β. Similarly, the functional activity of Dual-Tagged-Smad2 (DT-Smad2) and Dual-Tagged-Smad4 (DT-Smad4), was tested using the (ARE)$_3$-luciferase reporter in MDA-MB468 cells. Transcription from the ARE requires the transcription factor, XFoxH1a, for recruitment of Smad2/4 complexes to the promoter element (Chen, X. et al., 1996; Howell, M. et al., 2002). In the absence of Smad4, transfection of XFoxH1a elicited a weak TGF-β induction via the ARE (Figure 4.8C). Transfection of DT-Smad2 or DT-Smad4 increased the basal activity and substantially increased the TGF-β-induced level of transcription. This data indicates that DT-Smad2 and DT-Smad4 constructs can integrate and form functional complexes (ARF1) at known promoter elements (ARE) and initiate transcription in response to TGF-β.

4.2.2.4 Stable Cell lines expressing Dual Tagged-Smad3 and -Smad4

The aim of the project was to find different Smad-interacting factors in EpH4 cells versus EpRas cells. To accomplish this, it was necessary to stably express the DT-Smads in both cell lines. To generate stable cell lines, I transfected the cells with plasmids expressing the Dual-Tagged-Smads and selected pools using antibiotics, as

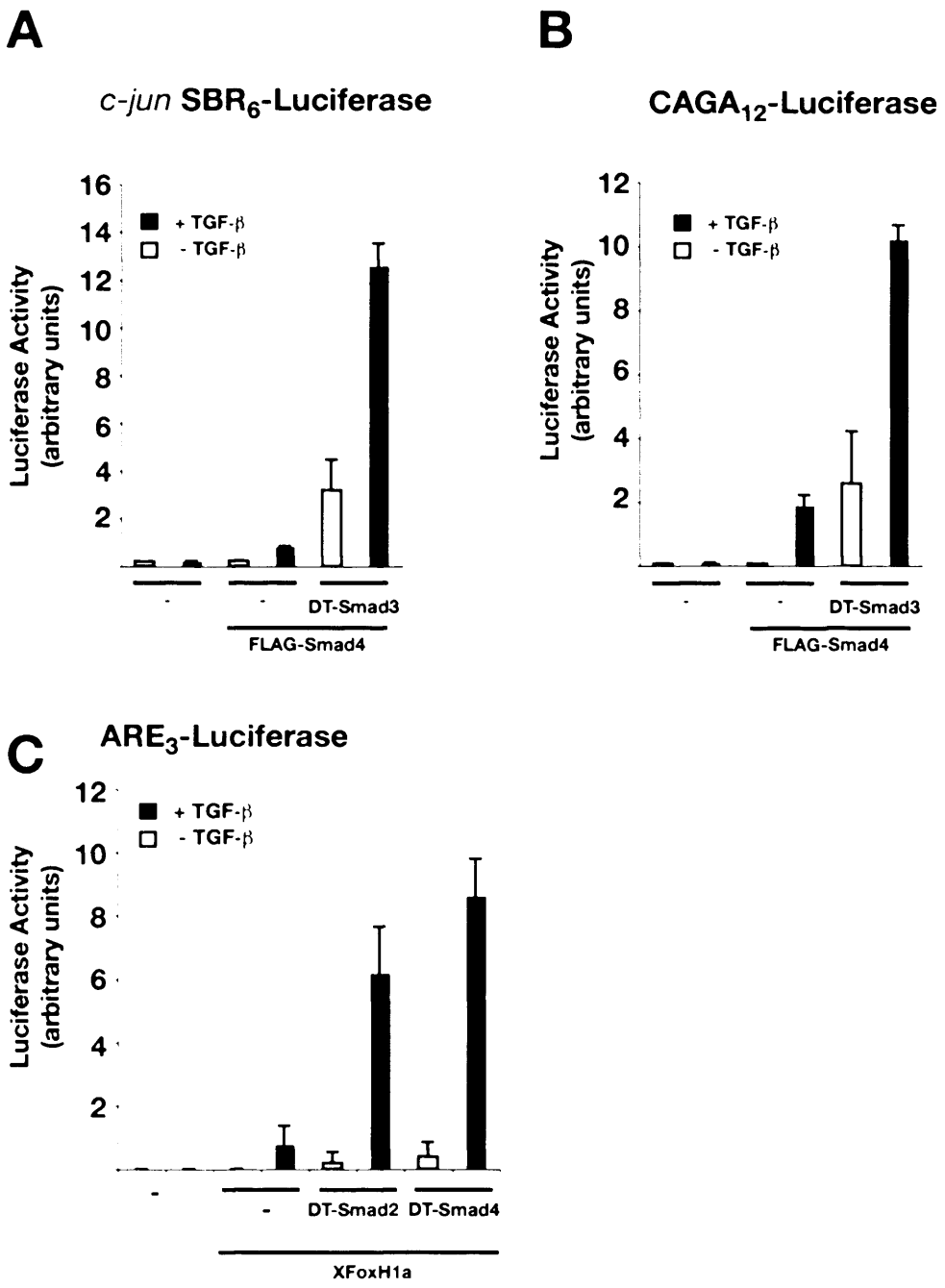

Figure 4.8. Dual tagged-Smad constructs can mediate TGF-β-induced transcriptional activation

Smad4-null MDA-MB468 cells were transfected with the Smad3-dependent reporters, c-jun SBR_6-Luc (A) or $CAGA_{12}$-Luc (B) together with plasmids expressing FLAG-Smad4 either alone or with Dual Tagged (DT) Smad3 as indicated.

(C) Smad4-null MDA-MB468 cells were transfected with the Smad2-dependent reporter, ARE_3-Luc reporter gene, together with plasmids expressing XFoxH1a/XFast-1 alone or with DT-Smad2 or DT-Smad4 as indicated. TGF-β1 was added 8 h before assaying luciferase activity. Luciferase was quantitated relative to β-galactosidase from the pEFLacZ internal control. The data are the means and standard deviations of three independent experiments.

described in Chapter 2. Successful stable expression of Smad proteins had previously been accomplished using this technique (Schmierer, B. et al., 2005). Firstly, I generated EpH4 and EpRas stable lines expressing either DT-Smad3 or DT-Smad4. Smad3 was used in this case because previous studies have implicated a role for Smad3 in both TGF-β-induced growth arrest (Ashcroft, G. S. et al., 1999; Datto, M. B. et al., 1999) and in the progression of TGF-β-dependent EMT (Nicolas, F. J. et al., 2003b; Zavadil, J. et al., 2004). By using Smad3 as bait, transcription factors involved in these processes were more likely to be identified. Smad4 was also selected because it can form complexes with all known R-Smads and therefore, there is a higher potential to discover a wider array of interactions (Zhang, Y. et al., 1997).

Due to the low expression of the Smad proteins in transfected pools, single cell clones were picked to achieve a higher expression of the DT-Smads. Four clones were isolated, which expressed the DT-Smads at levels at or above endogenous. These included EpH4 clones expressing DT-Smad3 (EpH4-DTS3) and DT-Smad4 (EpH4-DTS4) and also EpRas clones expressing DT-Smad3 (EpRas-DTS3) and DT-Smad4 (EpRas-DTS4). Nuclear extracts of the individual clones were analysed to test whether the DT-Smads accumulate in the nucleus upon TGF-β stimulation. Antibodies against the FLAG epitope and anti-rabbit IgGs, which recognises the IgG binding domains of Protein A, were used to detect the DT-Smads (Figure 4.9A) and parental cell lines were used as a negative control. DT-Smad3 was detected in the nucleus, even in the absence of TGF-β, however there was a slight increase in level after 1 hr of TGF-β treatment (Figure 4.9A). DT-Smad4 was also localised in the nucleus in the uninduced state, as is the case for endogenous Smad4, and again nuclear accumulation occurred after TGF-β stimulation. From these results, I conclude that the DT-Smads accumulate in the nucleus upon TGF-β treatment in both EpH4 and EpRas cells.

During the process of analysing the clones, I noticed that the levels of DT-Smads fluctuated relative to endogenous Smads. Although, it is not uncommon to lose expression of a stably expressed protein with increasing passage number, this was not the case here. The expression level of the Smad did not gradually decrease over time but was expressed at high, low and even undetectable levels at different times. The only obvious difference between experiments was the confluency of the culture before lysis and/or the time of harvest after splitting the cells. To investigate whether either of these factors could explain the variation observed, EpH4-DTS3 cells were grown to

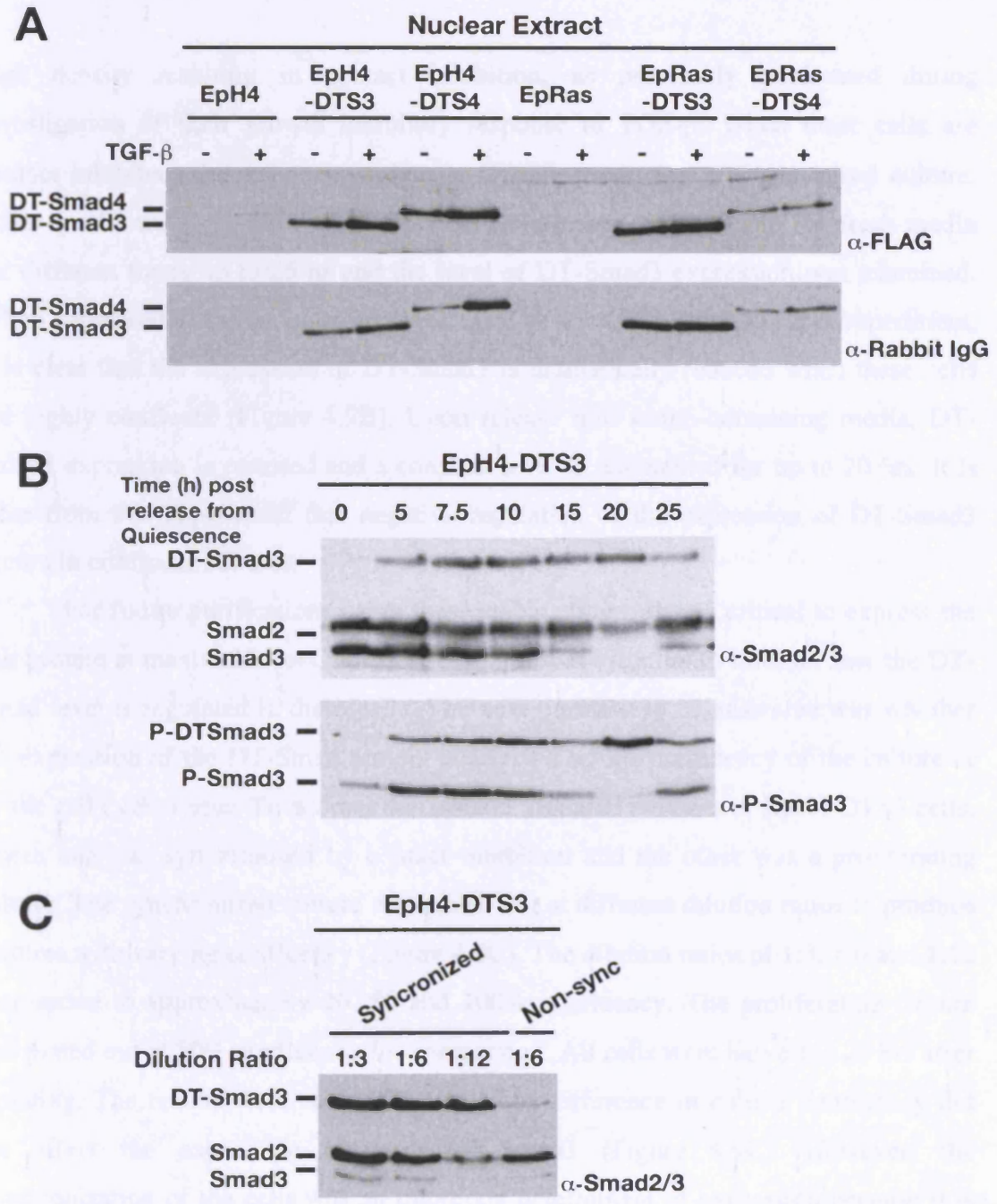

Figure 4.9. Characterisation of stable clones of dual tagged-Smads in EpH4 and EpRas cells

(A) Dual-Tag-Smad3 (DT-Smad3) and Dual-Tag-Smad4 (DT-Smad4) accumulate in the nucleus upon TGF-β stimulation. EpH4, EpRas parental cells and their DT-Smad3 and DT-Smad4 clones were treated with 2 ng/ml TGF-β1 for 1 hr, and equal amounts of nuclear extract were analysed by Western blotting using antibodies against FLAG and rabbit IgG.
(B) Expression of DT-Smad3 is regulated by the confluency of the cells. EpH4-Dual-Tagged-Smad3 (DTS3) cells were synchronized by high density, contact inhibition and released by trypsinisation for the times indicated. Cells were stimulated with TGF-β1 for 1hr prior to harvest. Whole-cell extracts were prepared and analysed by Western blotting using antibodies against Smad2 and Smad3.
(C) Expression of DT-Smad3 is also regulated at the level of the cell cycle. EpH4-DTS3 cells were synchronized by contact inhibition and released by trypsinisation for 20 hrs at different levels of confluency. A second set of cells was released for 20 hrs from a growing culture. Extracts were analysed by Western blotting using antibodies against Smad2/3.

high density resulting in contact inhibition, as previously performed during investigation of their growth inhibitory response to TGF-β. When these cells are contact inhibited, the cells accumulate in G1/G0, producing a synchronised culture. After synchronisation, the EpH4-DTS3 cells were then released into the fresh media for different times up to 25 hr and the level of DT-Smad3 expression was examined. When compared to the endogenous level, used as a loading control in this experiment, it is clear that the expression of DT-Smad3 is dramatically reduced when these cells are highly confluent (Figure 4.9B). Upon release into serum-containing media, DT-Smad3 expression is restored and a constant level is maintained for up to 20 hrs. It is clear from this experiment that negative regulation of the expression of DT-Smad3 occurs in confluent cultures.

For future purifications using these stable clones, it was critical to express the bait protein at maximal levels. For this reason, it was essential to find out how the DT-Smad level is regulated in these cells. The next question to be answered was whether the expression of the DT-Smad protein is affected by the confluency of the culture or by the cell cycle status. To address this issue, I prepared two sets of EpH4-DTS3 cells, where one was synchronised by contact inhibition and the other was a proliferating culture. The synchronized culture was plated out at different dilution ratios to produce cultures with varying confluency (Figure 4.9C). The dilution ratios of 1:3, 1:6 and 1:12 correspond to approximately 20, 50 and 100% confluency. The proliferating culture was plated out at 50% confluency for comparsion. All cells were harvested 20 hrs after replating. The results were strikingly clear. The difference in culture confluency did not affect the expression level of DT-Smad3 (Figure 4.9C). However, the synchronization of the cells was an important determinant of expression because it is clear that an asynchronous culture expresses a very low level of DT-Smad3. This demonstrated that the expression of DT-Smad3 is governed by a specific point in the cell cycle and that the confluency of the culture is not an important determinant. The mechanism of how the expression levels of the DT-Smads were regulated was not investigated, however it was speculated that it was due to promoter activity in these cells. The impact of this finding was great in terms of accumulation of cell mass, but modifications were included to account for this regulation. In all subsequent experiments using the DT-Smad3 and DT-Smad4 clones, cell cultures were sunchronised and released into serum for 20 hrs to to maximise the expression level of

the DT-Smads.

4.2.2.5 Functional Studies of Dual-tagged Smads: DT-Smad3 and DT-Smad4 form compexes on DNA

Further characterisation of the DT-Smads was required to ensure their functionality. Nuclear import in response to TGF-β was confirmed but the next aspect I needed to examine was whether the DT-Smads expressed stably in EpH4 and EpRas cells could bind DNA. To investigate the DNA-binding ability of DT-Smad3 and DT-Smad4, I used DNA pulldown assays with oligonucleotides containing the Smad binding region (SBR) in the 5' UTR of the c-*jun* promoter (Inman, G. J. et al., 2002a). In a pattern identical to endogenous Smad3, phosphorylated DT-Smad3 binds to the c-*jun* SBR oligo and not to the control mutant oligonucleotide in both EpH4 and EpRas cell lines (Figure 4.10). DT-Smad4 binds to the c-*jun* SBR oligo in the uninduced state and with higher affinity in the induced state, as observed with endogenous Smad4. These results indicate that indeed DT-Smad3 and DT-Smad4 can bind DNA and form complexes with endogenous partners on DNA in a TGF-β inducible manner.

4.2.2.6 Preliminary Purification Trials

The EpH4-DTS3 clone was used in preliminary experiments to optimise conditions for the purification. The first small-scale purification procedure was carried out using 30 150 cm^2 plates of mock and DT-Smad3 expressing EpH4 cells each. Silver stain analysis of the final eluates revealed a high level of bait-Smad3 in the eluate from EpH4-DTS3 cells whereas it was absent in the parental line (data not shown). From Chapter 3, it was evident that large amounts of input were required to retrieve a level of bait detectable by Coomassie stain. Coomassie staining was preferrable as it does not interfere with mass spectrometric analysis. Thus I conducted a large-scale experiment using 125 plates of EpH4-DTS3 cells, equivalent to 90 mgs of proteins. An equal amount of input of the parental EpH4 cells (mock) was used as a negative control. Samples were taken at each stage of the mock and trial purification to monitor the progress throughout the purification procedure. Analysis of the mock experiment revealed that equal levels of Smad protein were observed in the IgG flow

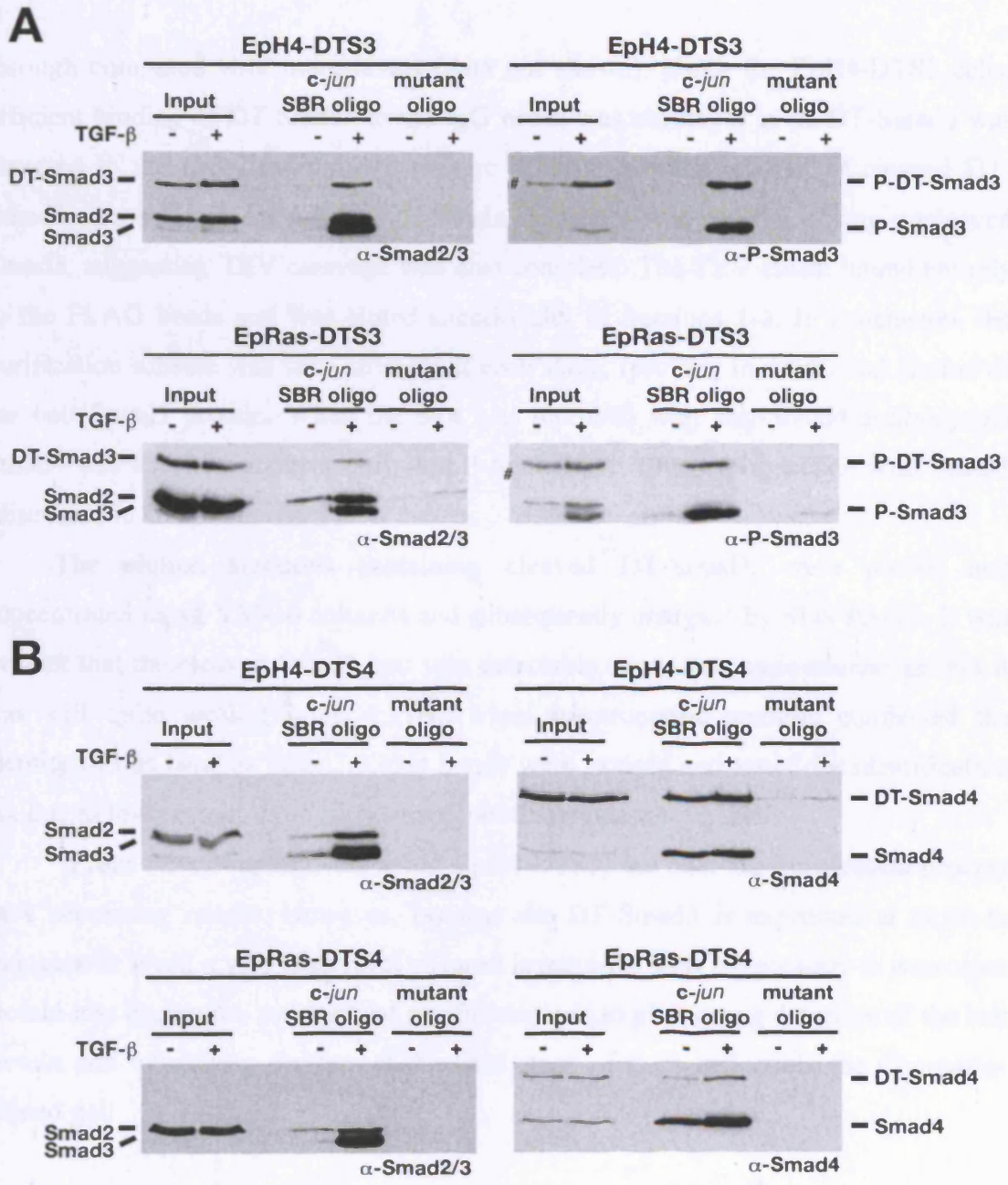

Figure 4.10. DT-Smad3 and DT-Smad4 form complexes on DNA

(A and B) DT-Smad3 (A) and DT-Smad4 clones (B) of EpH4 and EpRas cells were synchronized by contact inhibition and released by trypsinisation for 20 hrs. Whole cell extracts were prepared from uninduced or TGF-β-induced cells and incubated overnight with either c-*jun* SBR or mutant c-*jun* SBR oligo-conjugated beads as indicated. After washing, the beads were resuspended in SDS sample buffer and associated proteins were separated by SDS-PAGE and analysed by Western blotting using antibodies against phosphorylated-Smad3, Smad3 and Smad4. Ten percent protein input is also shown.

# Indicates the DT-Smad3 protein, which has been recognised by the α-rabbit secondary antibody via its IgG-binding domains.

through compared with input levels (data not shown). Using the EpH4-DTS3 cells, efficient binding of DT-Smad3 to the IgG beads was observed, as no DT-Smad3 was detected in the IgG flow through (Figure 4.11A). A small amount of cleaved DT-Smad3 was still present on the IgG beads, but there was no sign of any uncleaved Smad3, suggesting TEV cleavage was also complete. The TEV eluate bound entirely to the FLAG beads and was eluted successfully in fractions 1-4. In conclusion, the purification scheme was very efficient at each stage, resulting in substantial elution of the bait Smad3 protein. When the blot was reprobed with anti-Smad4 antibody, no Smad4 was detected unexpectedly, but P-Smad2 was found to associate with Smad3 (discussed in Chapter 6 and 7).

The elution fractions containing cleaved DT-Smad3, were pooled and concentrated using YM-10 columns and subsequently analysed by SDS-PAGE. It was evident that the cleaved Smad3 bait was detectable on a Coomassie-stained gel but it was still quite weak (Figure 4.11B). Mass spectrometric analysis confirmed the identity of this band as Smad3. Other bands were excised and tested for identification but due to low protein level, no positive identifications were made.

From initial experiments using EpH4-DTS3, the dual-tag purification process gave promising results. However, because the DT-Smad3 is expressed at close to endogenous level, a very high level of input is required. This is necessary to overcome protein loss during the two steps of purification and to give strong detection of the bait protein and interacting partners at the final stage of the purification, the Coomasse-stained gel.

4.2.2.7 Further Scale up of the Purification Scheme

The next experiment carried out was scaled up nearly 4-fold, and 360 mgs of protein extract from EpH4-DTS3 cells was applied to IgG columns. Due to the large scale of the purification, it was not practical to run a mock purification in parallel. The test lysate alone produced a very large volume (600 mls). Due to the high level of protein input, a large volume of beads was required. It is recommended for large-scale purifications to use multiple columns with lower bead volume as the use of large column beds has been shown to increase background contamination (Puig, O. et al., 2001). This theory was applied throughout the purification by employing multiple

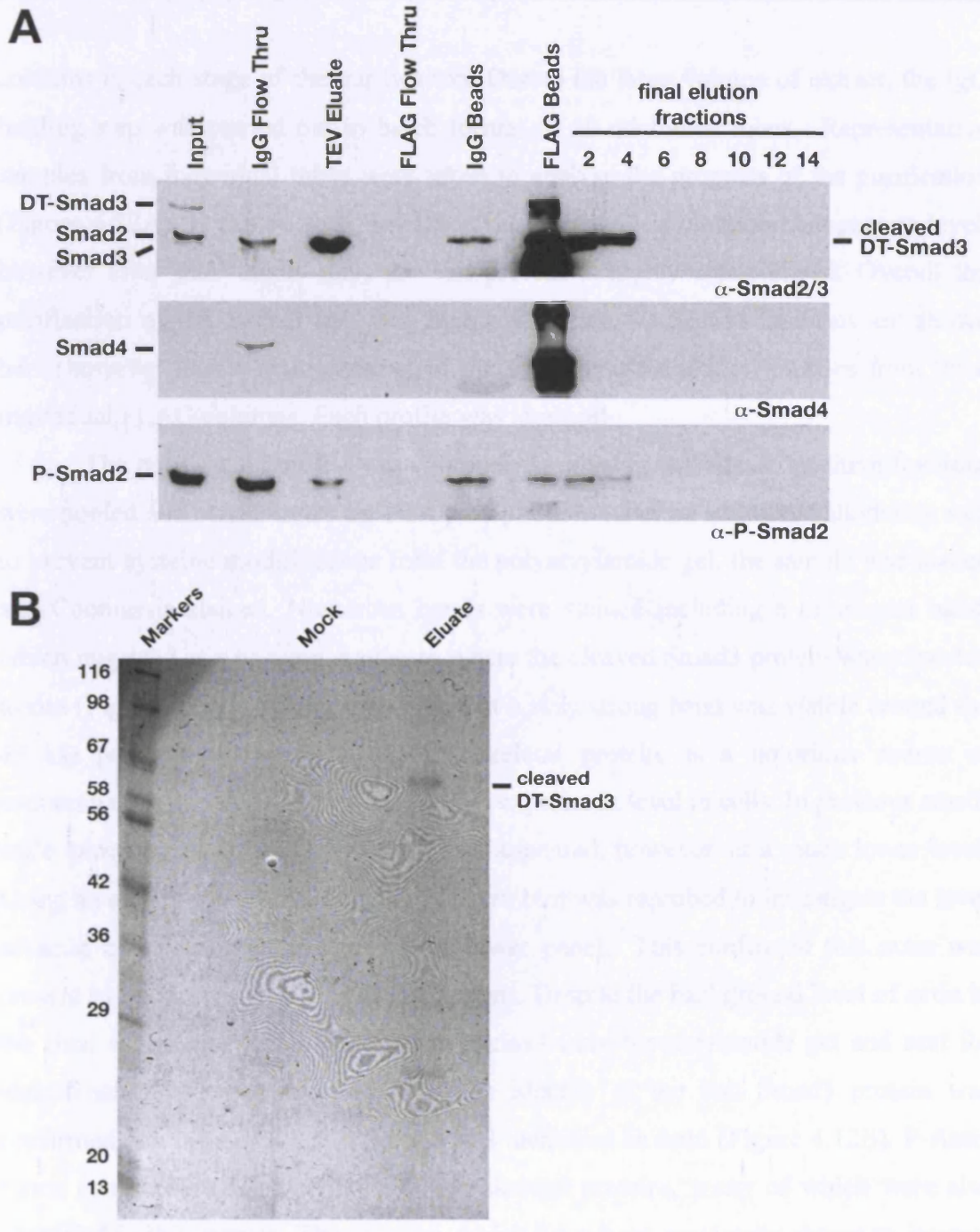

Figure 4.11. Preliminary Dual Tag Purification using DT-Smad3

(A) EpH4-DTS3 cells were synchronized and released into new media for 18-22hrs. Cells were stimulated with TGF-β for 1 hr prior to harvest. 90mgs (x125 15cm plates) EpH4-DTS3 and equivalent input of EpH4 parental cells (mock) was used for the purification. Samples were taken at each stage and analysed by Western blotting using an antibody against Smad2/3. The blot was then stripped and reprobed using antibodies against Smad4 and P-Smad2. The following proportions of samples were loaded: Input (1/10,000), IgG flow through (1/10,000), TEV eluate (1/167), FLAG flow through (1/167) IgG beads (1/6), FLAG beads (1/6), and final eluates (1/20).
(B) Coomassie-stained gels depicting proteins recovered following purification. Smad3 positive fractions and equivalent mock fractions were pooled and concentrated using YM-10 spin columns. Samples were then resuspended in SDS loading buffer and separated by SDS-PAGE and Coomassie stained. The Dual Tag purification protocol is given in Chapter 2. The numbers to the left show the positions of molecular size markers (kilodaltons). Smad3 bait was confirmed by mass spectrometry, which was conducted by Ulf Hellman, Ludwig Institute for Cancer Research, Uppsala, Sweden.

columns at each stage of the purification. Due to the large volume of extract, the IgG binding step was carried out in batch format in 50 ml falcon tubes. Representative samples from individual tubes were taken to analyse the progress of the purification (Figure 4.12A). It can be seen that the level of Smad3 is close to endogenous level, however after TEV eluate step, the bait protein is highly concentrated. Overall the purification of the Smad3 bait was highly efficient. 10 elution fractions are shown here, however this is representative of the three separate elution profiles from three individual FLAG columns. Each profile was identical.

The purification profile was extremely promising. All Smad3 positive fractions were pooled and concentrated by TCA precipitation. After an additional alkylation step to prevent cysteine modifications from the polyacrylamide gel, the sample was loaded and Coomassie stained. Numerous bands were stained including a prominent band, which migrated at a position similar to where the cleaved Smad3 protein was expected to run (Figure 4.12B). It was also clear that a very strong band was visible around the 43 kD position. Actin, a 42 kD cytoskeletal protein, is a notorious source of contamination due to its exceptionally high expression level in cells. In previous small-scale experiments, a 42 kD band had also appeared, however, at a much lower level. Using an anti-pan actin antibody the Western blot was reprobed to investigate the level of actin contamination (Figure 4.12A, lower panel). This confirmed that actin was present in the first couple of elution fractions. Despite the background level of actin in the final eluate, thirty-five bands were excised from the acrylamide gel and sent for identification by mass spectrometry. The identity of the bait Smad3 protein was confirmed and indeed, the 43 kD band was identified as actin (Figure 4.12B). F-Actin forms complexes with a plethora of cytoskeletal proteins, many of which were also identified in this sample. The proteins, which have been previously shown to interact with actin are shown in bold (Figure 4.12B, right). An astonishing twenty-five out of thirty-five proteins were attributed to actin biology. This high percentage of actin partners may reflect the higher level of actin in the final eluate than Smad3.

Despite the presence of multiple cytoskeletal proteins in the final eluate, a handful of new identifications were also made. Where possible, I tried to verify the interactions with Smad3 under similar conditions, for example activation-induced cytidine deaminase (AID). Unfortunately, I did not observe any interactions of Smad3 with these proteins. Some of the identifications were obtained from single polypeptide

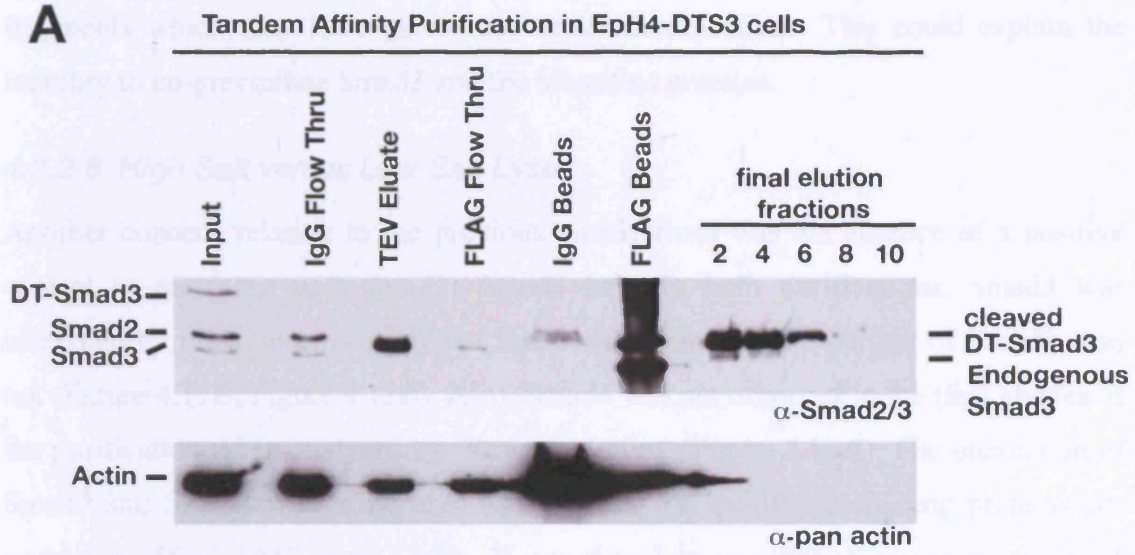
A
Tandem Affinity Purification in EpH4-DTS3 cells
Input
IgG Flow Thru
TEV Eluate
FLAG Flow Thru
IgG Beads
FLAG Beads
final elution fractions
2 4 6 8 10
DT-Smad3
Smad2
Smad3
cleaved DT-Smad3
Endogenous Smad3
α-Smad2/3
Actin
α-pan actin

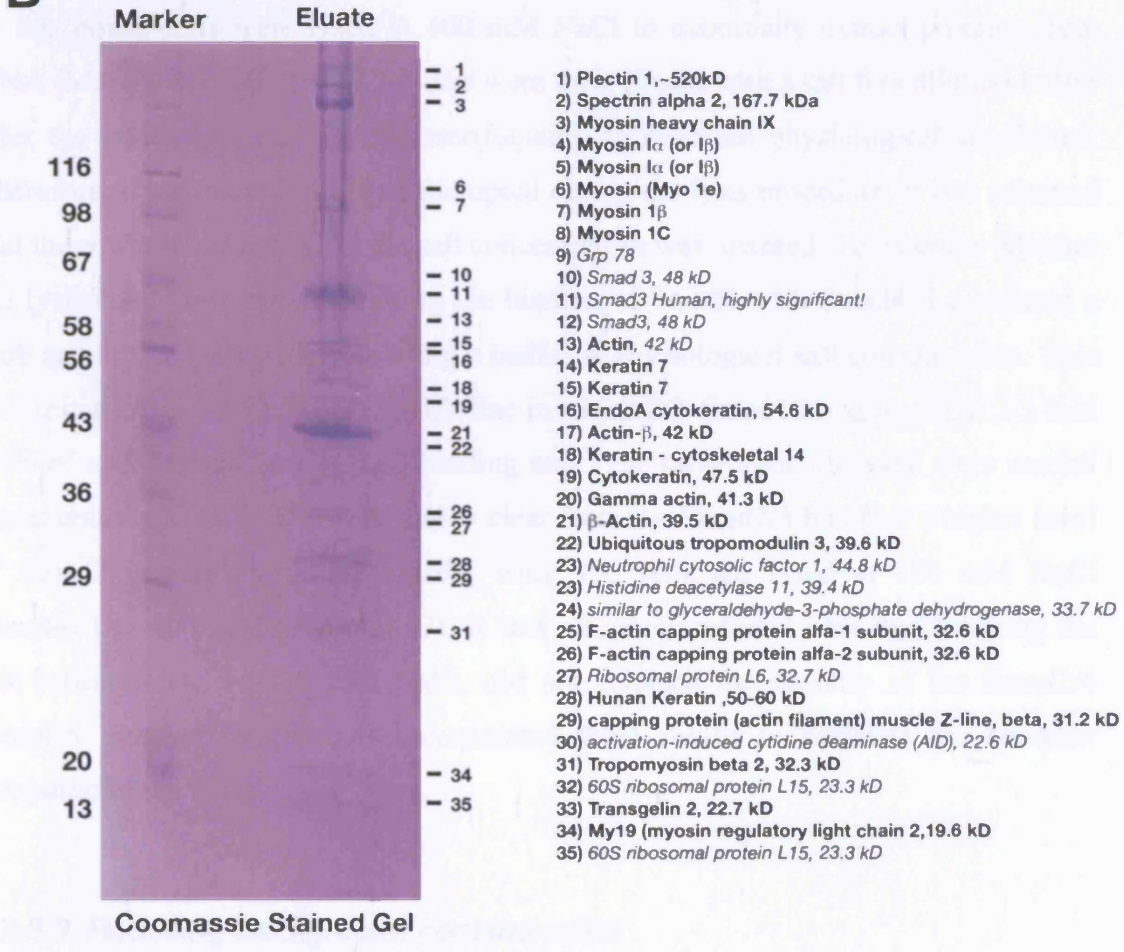
B
Marker
Eluate
116
98
67
58
56
43
36
29
20
13
Coomassie Stained Gel
1) Plectin 1,~520kD
2) Spectrin alpha 2, 167.7 kDa
3) Myosin heavy chain IX
4) Myosin Iα (or Iβ)
5) Myosin Iα (or Iβ)
6) Myosin (Myo 1e)
7) Myosin 1β
8) Myosin 1C
9) Grp 78
10) Smad 3, 48 kD
11) Smad3 Human, highly significant!
12) Smad3, 48 kD
13) Actin, 42 kD
14) Keratin 7
15) Keratin 7
16) EndoA cytokeratin, 54.6 kD
17) Actin-β, 42 kD
18) Keratin - cytoskeletal 14
19) Cytokeratin, 47.5 kD
20) Gamma actin, 41.3 kD
21) β-Actin, 39.5 kD
22) Ubiquitous tropomodulin 3, 39.6 kD
23) Neutrophil cytosolic factor 1, 44.8 kD
23) Histidine deacetylase 11, 39.4 kD
24) similar to glyceraldehyde-3-phosphate dehydrogenase, 33.7 kD
25) F-actin capping protein alfa-1 subunit, 32.6 kD
26) F-actin capping protein alfa-2 subunit, 32.6 kD
27) Ribosomal protein L6, 32.7 kD
28) Hunan Keratin ,50-60 kD
29) capping protein (actin filament) muscle Z-line, beta, 31.2 kD
30) activation-induced cytidine deaminase (AID), 22.6 kD
31) Tropomyosin beta 2, 32.3 kD
32) 60S ribosomal protein L15, 23.3 kD
33) Transgelin 2, 22.7 kD
34) My19 (myosin regulatory light chain 2,19.6 kD
35) 60S ribosomal protein L15, 23.3 kD

fragments which may have given inaccurate identifications. This could explain the inability to co-precipitate Smad3 and the identified proteins.

4.2.2.8 High Salt versus Low Salt Lysis

Another concern relating to the previous purifications was the absence of a positive control co-purifying with the DT-Smad3 bait. In both purifications, Smad3 was identified by mass spectrotmetry but Smad4, the transcription partner of Smad3, was not (Figure 4.11B, Figure 4.12B). Also, Smad4 was not observed in the final eluates of the purification when analysed by Western blotting (Figure 4.11A). The interaction of Smad3 and Smad4 was to be used as a marker for specific interacting proteins co-purifying with the DT-Smad3 bait. It was therefore essential to ensure detection of this complex in the final eluate. As a result, the lysis conditions were investigated. Up to this point, cells were lysed in 400 mM NaCl to maximally extract proteins from DNA (Marais, R. et al., 1993). Lysates were then diluted with a salt free dilution buffer after the lysate was cleared by centrifugation to maintain physiological conditions. Therefore, if any complexes were disrupted during the lysis procedure, it was assumed that these would reform when the salt concentration was lowered. To examine whether the lysis conditions were disrupting the binding of Smad3 with Smad4, I compared a high salt buffer lysis with lysis using a buffer at physiological salt concentration. This was tested using the EpH4-DTS4 cell line in which DT-Smad4 is expressed at 2-3 fold level of endogenous Smad4. IgG binding and TEV proteolytic cleavage were carried out at either 120 or 150 mM. It is very clear from the Smad2/3 blot that a higher level of Smad2 interacts with DT-Smad4, when the cells are lysed at 150 mM NaCl compared to 400 mM (Figure 4.13). It was also demonstrated here that lowering the salt concentration to 120 mM NaCl, did not enhance the stability of the Smad2/4 complex. Further experiments incorporated these results to optimise the complex formation of the Smads.

4.2.2.9 Reducing Background contamination

Actin is one of the most abundant proteins in the cell, and therefore it is not surprising that contamination arises in the final eluates of purified samples. Nevertheless, it was imperative to eliminate this background in order to isolate and identify Smad-

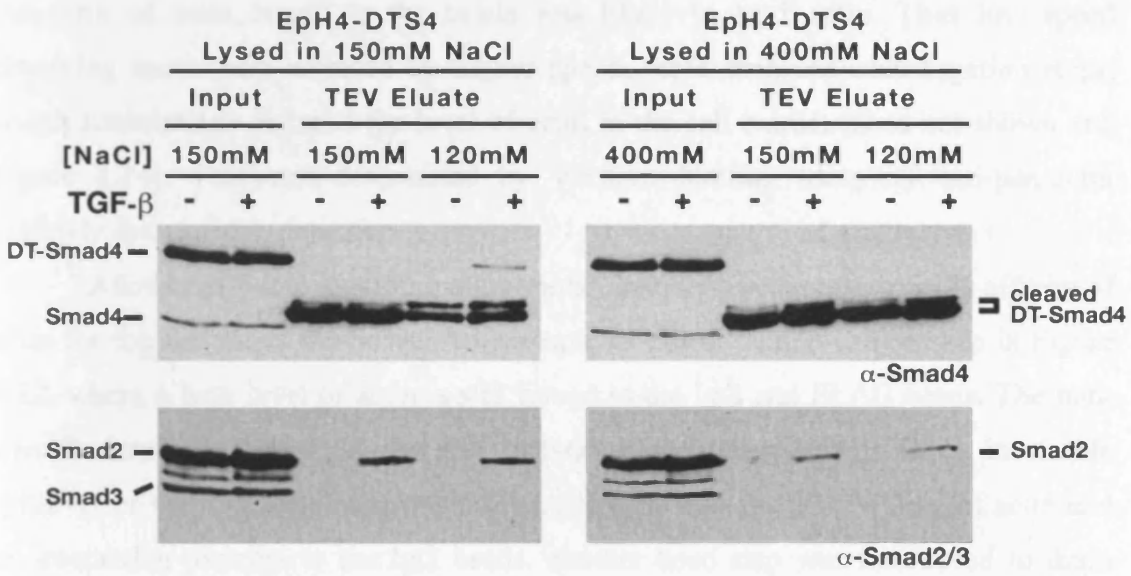

Figure 4.13. Effect of lysis conditions on Smad-Smad interactions

High salt lysis interferes with Smad complex formation. EpH4-DTS4 cells were lysed in buffer with a salt concentration of either 150 mM (left panel) or 400 mM (right panel).The extracts were then adjusted to either 120 mM or 150 mM final salt concentration, as indicated and incubated with IgG beads for 2 hrs at 4 °C. After washing, the beads were incubated with TEV protease at 14 °C for an additional 2 hrs. Supernatants were then fractionated by SDS-PAGE and analysed by Western blotting using antibodies against Smad2/3 and Smad4. Cleaved DT-Smad4 migrates as a doublet. The slower migrating band is likely to contain one of the two TEV cleavage sites due to insufficient cleavage with TEV protease.

interacting partners. A series of trial experiments were carried out to reduce the level of actin throughout the purification procedure. The cytoskeletal components of the cell, including polymerised actin (F-actin), are routinely removed by centrifugation. On the basis of the interacting proteins identified (Figure 4.12), it was concluded that the form of actin bound to the beads was likely to be F-actin. Thus low speed clarifying spins were replaced by higher speed, more stringent centrifugation steps, which substantially reduced the level of actin in the cell extract (Data not shown and Figure 4.14). This was determined by Western blotting using an anti-pan-actin antibody for sensitive detection.

Another problem regarding actin contamination was the non-specific affinity of actin for the surface of the beads. An example of this attraction can be seen in Figure 4.12, where a high level of actin is still bound to the IgG and FLAG beads. The non-specific interaction of actin and the surface of the beads results in an inevitable spillover of actin into the next stage. To exploit the non-specific binding of actin and its interacting partners to the IgG beads, another bead step was introduced to drain excess actin from the lysate. After TEV cleavage, the TEV eluates were transferred to fresh IgG columns before the final affinity anti-FLAG bead column. The bait protein, no longer bound to the IgG beads because the IgG binding domains of protein A had been cleaved. On the other hand, any actin still present bound the IgG beads preferentially, again reducing the total actin in the eluates (data not shown).

4.2.2.10 Purification of DT-Smad4

The next large-scale purification incorporated the new adjustments (4.2.2.8 and 4.2.2.9) to optimise complex formation of Smads and other interacting proteins and also to eliminate high background and contamination with cytoskeletal proteins. In this experiment, the EpH4-DTS4 cells were used as the test cells and EpH4 parental cells were used in a parallel mock experiment to establish the experimental background. As shown in Figure 4.13, a strong interaction exists between DT-S4 and Smad2, which could be used as a marker for true co-purified partners. 500 mgs of protein extract was used as starting material and samples were taken throughout the procedure to monitor the process of the purification. Each step exhibited relatively high efficiency, however there was incomplete TEV cleavage and a small proportion of residual Smad4 found

on each set of beads, resulting in a decrease in the final yield. Most importantly, however, the level of actin present at each stage was dramatically reduced. No trace of actin was detected at the TEV eluate step, indicating that clarifying the extract by centrifugation was successful in pelleting abundant cytoskeletal proteins. P-Smad2 was used as a marker in this final purification. A high proportion of P-Smad2 was lost on the initial IgG binding step, presumably due to its interaction with endogenous Smad3 and Smad4 (Figure 4.14A, bottom panel). Nevertheless, P-Smad2 was bound to DT-Smad4 in the TEV eluate. Subsequently, most of the bound P-Smad2 was lost in the FLAG flow through and only a very low level remained in the final fractions. This indicated that few Smad2-Smad2 complexes survived the purification and suggested a similar case for other partners with equal or lower affinity binding. Indeed, analysis of the final eluates of both the mock and test cells in a Coomassie gel confirmed this result. Apart from a small number of background bands observed in both eluates, the only additional band detected in the test eluate corresponded to the cleaved bait (Figure 4.14B). No other proteins that could be detected at Coomassie stain level had been isolated. From previous experiments, I had learned that if no protein was detectable at Coomassie stain level, it was unlikely that a positive identification could be obtained.

4.3 Discussion

4.3.1 Dual Tag-Purification

4.3.1.1 Purification of Smad proteins in Mammalian Cells

In this chapter, I described the development of a novel dual tag for purification of Smad complexes. Rigorous optimisation of the purification procedure using this tag was carried out to ensure a pure final product. However, although Smad protein was purified to a high degree, this procedure did not recover any co-purifying proteins. The lack of interacting proteins in the final eluate could be attributed to the relatively low amount of Smad protein retrieved from mammalian cells. More importantly it seems that the unstable nature of the Smad protein complexes formed, prevents the preservation of these complexes through two purification steps.

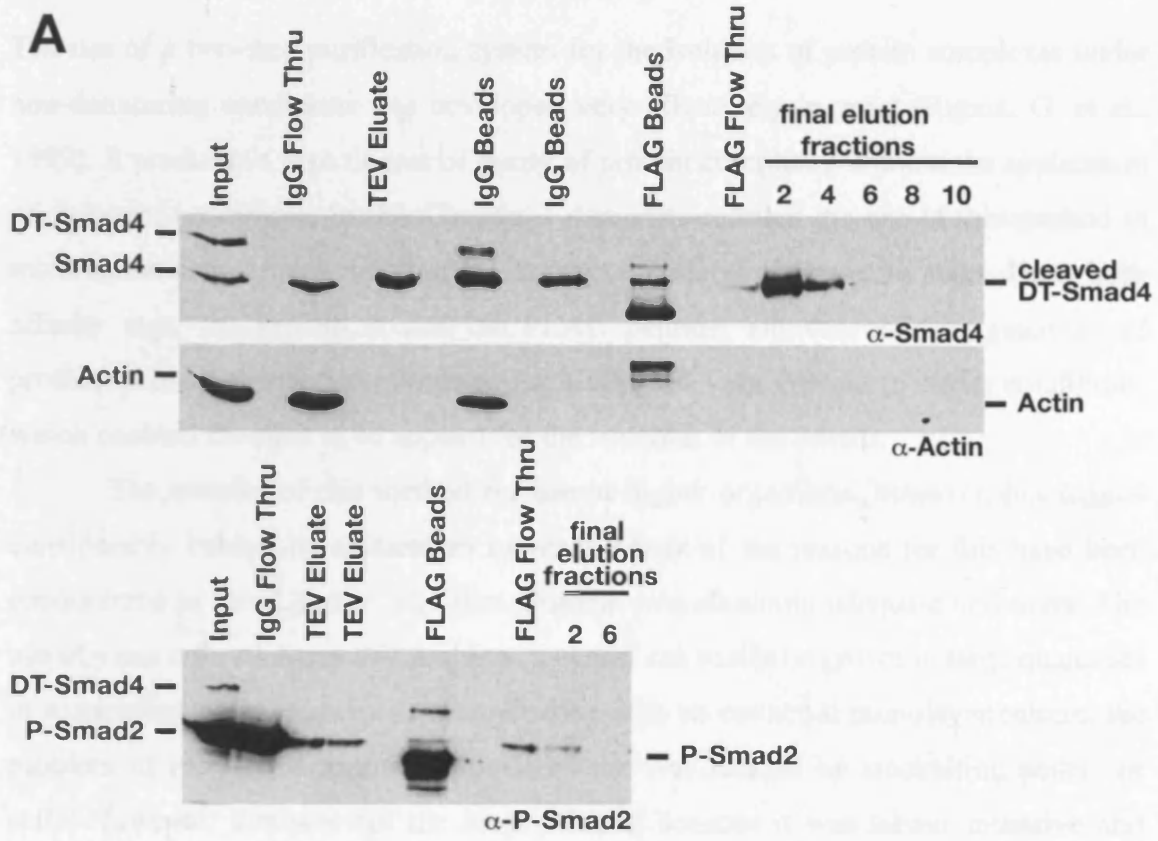
A
Input
IgG Flow Thru
TEV Eluate
IgG Beads
IgG Beads
FLAG Beads
FLAG Flow Thru
final elution fractions
2 4 6 8 10
DT-Smad4
Smad4
cleaved DT-Smad4
α-Smad4
Actin
Actin
α-Actin
Input
IgG Flow Thru
TEV Eluate
TEV Eluate
FLAG Beads
FLAG Flow Thru
final elution fractions
2 6
DT-Smad4
P-Smad2
P-Smad2
α-P-Smad2

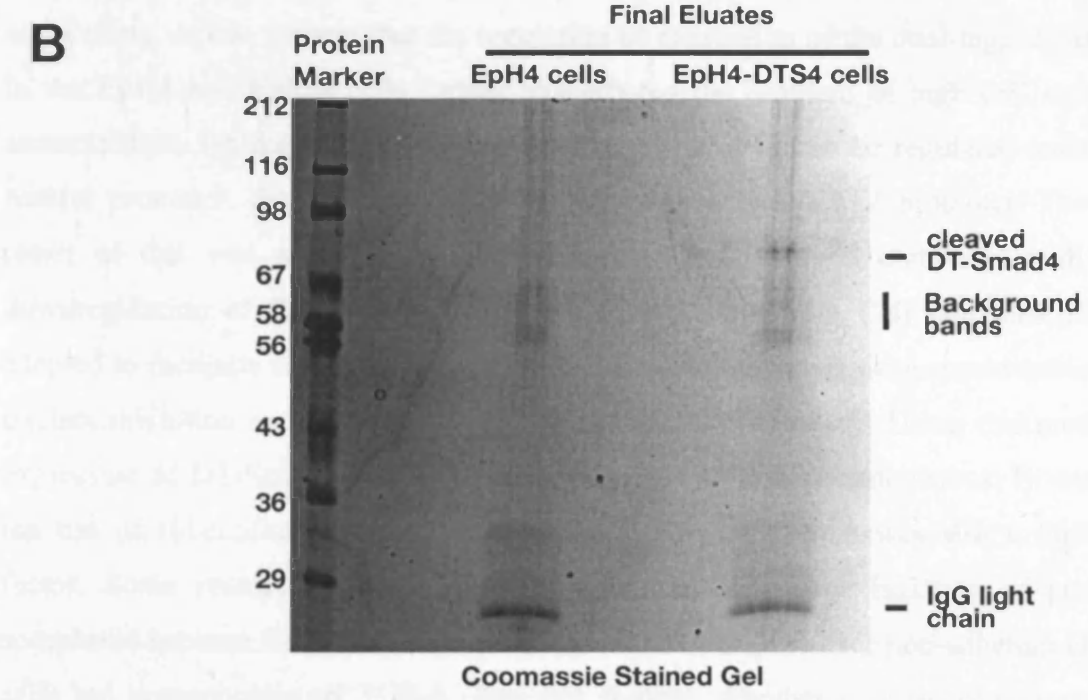
B
Final Eluates
Protein Marker
EpH4 cells
EpH4-DTS4 cells
212
116
98
67
58
56
43
36
29
cleaved DT-Smad4
Background bands
IgG light chain
Coomassie Stained Gel

The use of a two-step purification system for the isolation of protein complexes under non-denaturing conditions was developed very effectively in yeast (Rigaut, G. et al., 1999). It produces a high degree of purity of protein complexes without the application of stringent conditions. In this Chapter, I demonstrated that the use of this method in mammalian cells retains many of the attractive features observed in yeast. Here, both affinity tags, the Protein A and the FLAG peptide, allowed efficient recovery of proteins present at low concentration. Each step was very tolerant to buffer conditions, which enabled changes to be applied for the isolation of the Smads.

The transfer of this method for use in higher organisms, however, has lagged considerably behind its application in yeast. Many of the reasons for this have been encountered in this Chapter. The first obstacle was obtaining adequate cell mass. The use of yeast cells obviates this problem, as yeast can easily be grown in large quantities in suspension flasks. However, when dealing with an epithelial monolayer culture, the problem of recovery became acute. This issue was tackled by stockpiling pellets of cells. However, this was not the ideal solution because it was labour intensive and extremely time consuming. The amount of starting material for purification purposes was dependent on the expression level of the dual-tagged Smad and also by the yield of recovery. It was evident that the regulation of expression of the dual-tagged Smads in the EpH4 and EpRas cells further exacerbated the problem of high cell number accumulation. Unlike yeast cells where the tagged protein can be regulated under its natural promoter, the DT-Smad proteins were driven by a CMV promoter. The net result of this was a cell cycle dependent expression system combined with the downregulation of Smad expression upon contact inhibition. Cell preparation was adapted to facilitate expression of the DT-Smads, whereby cells were synchronised by contact inhibition and replated for 20 hrs at 60-80% confluency. Using this method, expression of DT-Smad3 and DT-Smad4 was close to that of endogenous. However, the use of subconfluent plates with low expression of protein was also a limiting factor. Some researchers have turned to HeLa cells for the isolation of protein complexes because these can be grown in spinner flasks. However non-adherent HeLa cells are unresponsive to TGF-β (data not shown). Another way to overcome this problem of yield was to use overexpressed proteins. However, it has proved difficult to generate a cell line expressing Smads at a high level. Indeed, all of the DT-Smad2 and DT-Smad3 clones tested, expressed DT-Smads at a level close to endogenous. DT-

Smad4 clones were less restricted in that the level of DT-Smad4 protein was 2-3 fold that of endogenous. A similar observation was made in generating the TAP-Smad clones in HaCaT cells (Chapter 3) and has been attributed to a decreased growth advantage of cells expressing high levels of Smad. Furthermore, a very high level of overexpression is not ideal because this can induce its association with non-specific partners or nonnatural partners (heat shock proteins, proteasome) (Puig, O. et al., 2001) resulting in many false positives.

Although the accumulation of cell mass was a problem, it was overcome. The main obstacle encountered using this system was the lack of co-purified partners in the final eluate (Figure 4.14). There are many reasons that may explain this phenomenon. Firstly, the presence of the untagged endogenous Smads may compete for incorporation into multiprotein complexes. This is not the case in yeast because the high efficiency of homologous recombination allows the tagged protein to replace the endogenous, which reduces competition for interacting partners. Furthermore, it has been observed in the Hill laboratory that endogenous Smads are preferentially phosphorylated by the type I receptor over exogenous Smads (data not shown). Consistent with this view, I showed that endogenous Smad3 and Smad4 can integrate much more efficiently into a complex on DNA than their tagged counterparts (Figure 3.3 and Figure 4.10). Therefore, the competition of endogenous Smads is heightened by their higher affinity for partner Smads and most probably other interacting proteins. Despite the high level of input used to overcome such a problem, the purification scheme failed to co-purify interacting proteins.

Other researchers have attempted to circumvent this problem in mammalian cells by developing the iTAP strategy, whereby the TAP-approach is combined with suppression of the corresponding endogenous protein by RNAi (Forler, D. et al., 2003). Depletion of the endogenous protein is implemented to make more partner subunits available for association with the target protein. This alternative strategy was reported to improve the number and level of partners recovered. In this vein, attempts were made to make a stable EpRas line, with inducible siRNA targeted against the Smads. However, this strategy encountered new problems. For the inducible system to function efficiently, it is first necessary to create a cell line that expresses the Tet repressor. In the absence of tetracycline, the tet repressor inhibits the siRNA expression, whereas addition of tetracyclin inhibits the Tet repressor and therefore

induces the expression of the siRNA. However, due to the downregulation of proteins under exogenous promoter control at high confluency of the EpRas cells, the inducibility of the system was lost.

The second setback was a problem common to all purification methods; the copurification of 'contaminating' proteins. In a large-scale analysis of protein complexes in yeast using the TAP system, (Gavin, A. C. et al., 2002) an experimental background was determined. The contaminating proteins were mainly abundant proteins such as cytoskeletal proteins, translation factors (particularly for RNA protein complexes) and molecular chaperones. A sample of such proteins was also identified in the purification of Smad3 (Figure 4.12). It is often difficult to conclude whether these 'contaminants' represent true endogenous partners or artificial asscociations generated by cell lysis. However, due to the substantial level of actin in the final eluate, a level which exceeded the bait Smad3 protein, a pragmatic decision was made to eliminate most of the proteins identified. This conclusion was confirmed by the absence of Smad4 as a co-purifying partner. To overcome this problem, the purification system was adapted to reduce the number of contaminating proteins. This was a necessary action as the abundance of these proteins interfered with the analysis of true partners. Actin and its partners were pelleted efficiently during extensive centrifugation spins (Figure 4.14A). However, such purification steps can also reduce the availability of interacting proteins, such that possible interacting proteins were also lost.

Throughout the optimisation of the purification scheme, the Smad-Smad interaction was always a biochemical consideration. In experiments using EpH4-DTS3, the absence of Smad4 as a co-purifying partner indicated that the purification was too stringent, despite the use of non-denturing, physiological conditions. The salt concentration was adjusted to facilitate this interaction. In the final experiment, however, only a very low level of P-Smad2 was present in the final eluate and it was completely absent from the Coomassie gel (Figure 4.14). This suggested that partners of Smad4 did not proceed to the final stage of purification due to the weak nature of their interactions (Figure 4.12A). Use of a two-step purification has proved successful in identifying proteins interacting in stable complexes as well as more transiently interacting proteins (Puig, O. et al., 2001). In subsequent experiments, co-immunoprecipition of Smad proteins has revealed that a salt concentration of 100mM

allows a more robust and reproducible interaction (Ross, S. et al., 2006) (Chapter 6). In addition, it has been shown that Smad3/Smad4 complexes are stabilised on DNA (Sean Harkin, unpublished data). It may also be the case that interacting partners of the Smads are part of large and easily disrupted complexes. In conclusion, these results show that the weak binding affinities between the Smads and presumably other partners, and hence the destabilisation of complexes during purification, were major limitations for the identification of novel interacting proteins.

Taken together, the purification of Smad protein complexes through a two-step purification is not viable. In addition to the use of two discriminatory purification steps, further measures were required to decrease the level of background contamination. The Smad proteins interact with each other and presumably other proteins with relatively low affinity, and therefore the weak specific interactions of the Smads are not sufficient to overcome non-specific interactions during the purification process. This is in contrast to certain transcription factor complexes with are stable at 500 mM NaCl and thus can be recovered to a high of purity by means of stringent conditions. Unfortunately, this is not the case for Smad-protein interactions.

4.3.1.2 Optimisation strategies for Dual-Tag Purification of Smad complexes

Due to the low affinity interactions of the Smads, a more tailored approach is required to identify partners of the Smads. An example of this is underway in the Hill Laboratory. The purification of the components of the Smad complex on the c-*jun* promoter is being investigated using a combination of immunoprecipitation and DNA pulldown where biotinylated DNA is the second 'affinity hook' for the complex (Sean Harkin, data not shown). Here, HA-Smad3 is affinity purified in the presence of biotinylated DNA that is subsequently captured on a neutravidin-matrix. The protein content of the purified complex is separated by SDS-PAGE and analysed by mass spectrometry. This system is currently being optimised. An example of this has already been applied to the purification of the spliceosome using biotinylated RNA and prefractionation by gel filtration (Neubauer, G. et al., 1998).

Another possibility to stabilise the Smad interactions is to introduce a crosslinking step. This would require further optimisation however and due to time

limitations, the project could not be taken any further. Another method that could be employed would be to use mutated versions of the Smads that might stabilise interactions with partners. The interaction between TGF-β family receptors and R-Smads is transient, but can be visualised using mutant Smads lacking the receptor phosphorylation region (Lo, R. S. et al., 1998). However because of the search for novel, unknown interacting partners, an array of mutated Smads would be required to test this technique. As a result, the purification would be limited to transient transfections. A similar approach using deleted mutants of the Smads would also be feasible, which may unmask contact areas and thus create a stable interaction. Again, time limitations prevented these routes being investigated.

4.3.1.3 Other applications of Dual Tag purification

Although interacting proteins cannot be purified through use of the dual tag purification strategy, a large amount of Smad protein can be isolated to a high degree of purity. Characterisation of purified bait protein is then possible. This allows investigation of post-translational modifications of the Smads, including phosphorylation, acetylation and methylation etc. Employing a 2-D gel approach together with the dual tag purification would increase the sensitivity of the assay. By this means, the effects of growth factors, kinases, phosphatases and inhibitors may be explored. Indeed, the effect of p38 MAPK on purified MEF2A phosphorylation status in mammalian cells was characterised upon purification by tandem affinity purification (Cox, D. M. et al., 2003). Furthermore, the use of this dual tag could also be applied to other proteins of interest, which interact more strongly with their partners. The incorporation of the Protein A and the FLAG peptide, would allow efficient recovery of proteins complexes present at low concentration. This may be especially applicable to proteins that are regulated by Calcium or Calmodulin dependent mechanisms, as it would provide an alternative tag to the Calmodulin Binding Protein (CBP).

4.3.1.4 Other Alternative Tags

An alternative purification system, which is a modified version of the TAP-scheme has been devised, which incorporates the biotin-streptavidin interaction as one of the affinity purification steps (Drakas, R. et al., 2005). Instead of using the CBP as the second affinity tag, a biotinylation tag of 15 amino acids that is specifically biotinylated by the Bir A gene is inserted at the N-terminus. Coexpression of the *Bir* A gene on a separate expression vector, catalyzes the covalent addition of biotin to the ε amino group of the lysine side chain. It was shown that by specifically biotinylating a protein in mammalian cells, the strong biotin-strepavidin interaction can be utilised to dramatically increase the quantity of protein complexes isolated. The system was developed to facilitate the isolation of proteins interacting with IRS-1, which was not feasible through other two-step procedures due to the low yield of bait protein. The strepavidin-biotin interation is among the strongest noncovalent interactions known with a 10^{-15} kd. However, one pitfall of this system is the use of 0.1M glycine, which has a low pH, for elution of the final step. This system would be applicable to increase the level of Smad protein that is purified however, it would not address the problem of the low affinity complexes that are formed.

4.3.1.5 Alternative systems for the identification of Smad-interacting partners

Interestingly, comparison of orthologous complexes purified from various sources has revealed that they share similar subunits (Estevez, A. M. et al., 2001; Gavin, A. C. et al., 2002). In one case, a yeast homologue of a human target protein was purified using the TAP strategy and its partners were identified (Schmitt, C. et al., 1999). Database searches revealed the human homologues of these partners that were shown to associate with the original human target. Thus an alternative strategy based on phylogenetic conservation could possibly be developed. Although TGF-β signalling is absent in yeast, Smad homologues function in *C. elegans* and *Drosophila Melanogaster*. Indeed, the application of tandem affinity purification has also been adapted for isolation of native protein complexes from *C. elegans* (Polanowska, J. et al., 2004). Here large-scale production of nematode transgenic lines are generated in

BioFlo fermenters to produce 60 litres of dense worm culture. The worms are then harvested by centrifuation in 30% sucrose to generate sufficient starting material for purification purposes. This approach was validated by purifying components of the C. elegans BRCA1/BARD1 (CeBcD) complex using a tagged Cebrc-1 protein (Polanowska, J. et al., 2006). The Smad proteins are highly conserved across diverse metazoan phyla. Work in C. elegans revealed three Smads that function in the TGF-β superfamily pathway. By this method, interacting partners of the C.elegans Sma proteins could be identified.

The use of a tandem affinity purification method has also been established as an effective technique for the study of the Drosophila proteome (Veraksa, A. et al., 2005). Here three of the critical features of the TAP method are introduced; the enzymatically cleavable tag-based affinity purification; the use of the native promoter to drive expression of the tagged protein and finally the replacement of the original protein by the tagged version by means of mutant background. Through this technique interacting proteins of *Mad, Medea or dSmad2* could be investigated. Again, this procedure might reduce the problem of mass accumulation, however, as the Smads are highly homologous, presumably the interactions would be of a similar nature and therefore they may not survive the two-step purification. However, the background noise in these systems may be lower and thus allow for less stringent conditions.

4.3.1.6 Genetic Screens to identify novel Smad-interating partners

The protein purification strategy has proved non-productive in yielding novel transcription factor partners of the Smad proteins. Aside from biochemical approaches, genetic based screens have also proved a popular tool in the search for novel partners. An expression system that is based on the detection of protein-protein interaction *in vivo* would potentially overcome the problem of low affinity Smad interactions (Stagljar, I., 2003). The yeast-2-hybrid system (YTH) system is a genetic expression system which provides a means to rapidly screen for binary interactions between proteins in the nucleus of a yeast cell. This approach has also been adapted to perform analysis in mammalian cells, which would make it applicable for use with Smad proteins.

Other genetic strategies designed specifically to dissect interactions among mammalian cells include the Ras recruitment system (RRS) and fluorescence resonance energy transfer (FRET)/bioluminescence resonance energy transfer (BRET)-based assays. The ras recruitment System is based on the complementation of a temperature-sensitive yeast cdc25 mutant, deficient in Ras activity. Ras function requires plasma membrane localisation and this can be achieved through the interaction between two hybrid proteins (Broder, Y. C. et al., 1998). The bait protein can be screened using a cDNA library in which all encoded protens are fused to a myristoylation signal. Interactions are based on the survival of the clones at the restrictive temperature. This system has also been modified to screen for cytoplasmic, phosphorylation-dependent interactions (Nateri, A. S. et al., 2004). The BRET assay is based on a transfer of energy principle. Proteins of interest can be genetically fused to the bioluminescent donor or fluorescent acceptor ('the BRET tags'). When the BRET-tagged proteins come into close proximity, an energy emission can be detected (Pfleger, K. D. et al., 2006). The added advantage of this technique is that it can be monitored in real time, using live cells.

4.3.1.7 Final Conclusion on the Dual Tag purification

Overall the dual purification procedure to find novel Smad-interacting proteins failed to yield any new candidates. Despite great efforts to optimise this technique, the fragile nature of Smad interactions prevented the co-purification of new components of the TGF-β. In conclusion, the generic purification method was not applicable for use by the Smad proteins. A more tailored approach is required to purify Smad partners. This may involve further optimisation of the current system by use of crosslinking or addition of DNA, or an alternative genetic approach.

4.3.2 EpH4 Tumour Cell Model System

The EpH4 tumour model system comprises of three cell lines, which represent the progression of a tumour from a normal epithelial to an invasive spindle-like cells (Oft,

M. et al., 1998; Oft, M. et al., 1996). EpH4 cells are mouse mammary epithelial cells, which are non-tumourigenic and respond to TGF-β by growth inhibition and apoptosis. The parental EpH4 cells, which have been transformed with oncogenic Ras (EpRas), form rapidly growing tumours in mice and have an altered response to TGF-β. EpRas cells no longer growth arrest upon TGF-β stimulation but undergo an EMT, so that they acquire an elongated mesenchymal phenotype. These mesenchymal EpRas cells mimic the phenotype of the X-tumour cells, which have been recovered from tumours formed by injection of EpRas cells into mice (Oft, M. et al., 1998; Oft, M. et al., 1996).

In this Chapter, I demonstrated preliminary work on the characterisation of this system. In my hands, the EpH4 cells exhibited a robust response to the growth inhibitory effects of TGF-β. EpH4 cells, synchronised in G1/G0, were prevented from entry into S-phase in the presence of TGF-β. The EpRas cells and X-tumour cells, however, are resistant to this effect. I have also developed an assay to investigate the contribution of the TGF-β signalling pathway to EMT progression. EpRas cells are grown on a plastic substrate at low density in the presence of TGF-β. After 9-12 days with intermittent trypsinisation, the cells are converted to a mesenchymal phenotype. Unlike the use of 3-D gels, the cell morphology of EpRas cells grown on plastic and undergoing EMT is more obvious and reproducible by visual inspection and EMT markers. This technique also allows easy manipulation of cells for use with siRNA oligonucleotides. This was validated by using siRNA oligonucleotides targeted against ALK5, which was shown to inhibit the downregulation of epithelial markers of EMT.

The main question posed using this model system was whether the different biological responses elicited by EpH4 and EpRas cells are governed by the set of transcription factors to which the Smads bind? To address this question, the Smad purification system was set up using this model system to identify new interacting transcription partners in the individual cell lines. Although the dual tag purification did not yield any novel candidates to be tested, the fundamental question still remains. Why do EpH4 cells growth arrest in response to TGF-β, whereas EpRas cells undergo an EMT? I have demonstrated that the system is robust in its responses to TGF-β, but this question needs to be addressed in a different way. Genetic and biochemical analysis of human tumours has revealed that tumour cells frequently downregulate

components of the TGF-β pathway (Wakefield, L. M. et al., 2002). By this means, the cells overcome the growth inhibitory effects of TGF-β. In light of this evidence, I investigated the levels of the TGF-β pathway components in this tumour model system as an alternative approach. By this means, I have uncovered new insights into the mechanism by which EpRas cells have adapted their response to TGF-β. The evidence for this will be discussed in Chapter 5.

5 The role of Smad3 in tumour progression

5.1 Introduction

Cancer is a multistep process which results in the emergence of tumour cells that have escaped the normal control that governs cell proliferation. At early stages of tumourigenesis, TGF-β signalling is thought to act as a tumour suppressor, as a result of its ability to arrest the growth of epithelial cells (Akhurst, R. J. et al., 2001; Derynck, R. et al., 2001). It is therefore not surprising that many tumour cells downregulate or acquire mutations of components of the TGF-β signalling pathway, resulting in a reduced response or complete abolitian of the antiproliferative effects of TGF-β (Levy, L. et al., 2006). Unlike the other components of the TGF-β pathway, which are mutated in human tumours, such as receptors, Smad2 and Smad4, Smad3 mutations have not been identified. This finding was very surprising as Smad3 has been demonstrated to be a critical mediator of the cytostatic response in response to TGF-β. Smad3 deficient mice show accelerated wound healing due to increased re-epithelialization which can be attributed to impaired TGF-β growth inhibition of keratinocytes and increased recruitment of fibroblasts and macrophages (Ashcroft, G. S. et al., 1999). In addition, a variety of primary cells from Smad3 null mice are partially resistant to the growth inhibitory effects of TGF- β (Datto, M. B. et al., 1999; Yang, X. et al., 1999). Indeed, Smad3 has been shown to suppress liver tumorigenesis by promoting apoptosis in tumor cells (Yang, Y. A. et al., 2006).

Accumulating evidence has now revealed that although Smad3 is not mutated in cancer, Smad3 seems to be inactivated or inhibited by epigenetic factors, resulting in loss or reduction of its expression. For example, Smad3 expression in gastric cancer is dramatically reduced in a significant portion of gastric tumours and gastric cancer cell lines (Han, S. U. et al., 2004). In addition, Smad3 levels decrease during carcinogenesis in some tissues such as the breast, where the nuclear Smad3 level is reduced in high grade breast cancers (Jeruss, J. S. et al., 2003). Interestingly, it has become evident that although there is a strong correlation between reduced expression of Smad3 with cancer progression, the complete loss of Smad3 expression is more rare.

In recent years it has been revealed that the role of TGF-β in cancer progression is more complex than originally anticipated and that during late stages of cancer progression, the activities of TGF-β switch from a tumour suppressor to that of a stimulator of tumour progression, invasion and metastasis (Wakefield, L. M. et al., 2002). Interestingly, the role of Smad3 in TGF-β mediated responses appears to mimic the dual role of TGF-β during tumourigenesis. In addition to its role in TGF-β-induced growth arrest, Smad3 also plays a role in the pro-metastatic activities of TGF-β. Indeed, reduction of Smad3 strongly suppresses lung metastases of aggressive carcinoma cells (Tian, F. et al., 2003).

Furthermore, a critical role for Smad3 in EMT has been firmly established, as highlighted by the inability of TGF-β to induce EMT in response to TGF-β in primary tubular epithelial cells derived from kidneys of Smad3 knockout mice (Zavadil, J. et al., 2005). Taken together, these results would suggest Smad3 is required for both the growth inhibitory and tumour promoting activities of TGF-β and this may help to explain the frequent downregulation of Smad3 expression in human cancers and not a complete deletion of its activity. In line with this hypothesis, MDCK cells undergoing EMT were found to downregulate Smad3 expression, concomitant with a resistance of these cells to TGF-β-induced growth inhibition (Nicolas, F. J. et al., 2003b).

Interestingly a similar observation was discovered when investigating the biological responses to TGF-β in the EpH4 tumour cell model system. In the EpH4 cells, the TGF-β cytostatic response is intact, but EpRas cells are resistant to the antiproliferative effects of TGF-β. While studying the levels of the components of the TGF-β pathways in the EpH4 tumour cell model system, I noticed a remarkable difference in the level of Smad3 in EpRas cells compared with the EpH4 parental cell line. In this Chapter, I describe the details of Smad3 downregulation and provide some insights into the mechanism by which this is regulated. In addition, I provide evidence to suggest that Smad3 levels are important in determining the specificity of the biological responses elicited in response to TGF-β.

5.2 Results

5.2.1 Smad3 is downregulated in EpH4 derivatives

A major aim of my project was to investigate the TGF-β pathway components in the EpH4 tumour model system. Firstly, I analysed the downstream effectors of the TGF-β pathway. Initially I tested the whole cell levels of Smad2, 3 and 4 in confluent cultures of EpH4, EpRas and X-tumour cells. A striking difference was observed in the level of Smad3 protein, whereas both Smad2 and Smad4 expression remained constant. In EpH4 cells, high levels of Smad3 were detected in contrast to the low levels demonstrated in both the EpRas and the X-tumour cell lines (Figure 5.1). Analysis of the TGF-β response in these cells revealed that both Smad2 and Smad3 are phosphorylated in all three cell lines. The P-Smad2 levels were much lower in EpH4 cells compared to both EpRas and X-tumour cells (Figure 5.1, third panel). In this experiment the EpH4 cells were more densely packed than the derivative cell lines, and therefore it is likely that the confluent EpH4 cells had limited access to TGF-β due to the inaccessibility of the receptor, which resulted in low P-Smad2 levels. This may also explain why despite much higher Smad3 protein levels in EpH4 cells, only a slight difference in the level of P-Smad3 was observed (Figure 5.1, fourth panel).

During subsequent investigations of Smad expression, I repeatedly observed that the levels of Smad3 fluctuated relative to Smad2 protein levels. The culture confluency and position in the cell cycle was variable between experiments and I hypothesized that this could be a contributing factor to the differences observed in Smad3 expression levels. As a result I decided to take a systematic approach to analyse the levels of Smad3 through the cell cycle (Figure 5.2). Cells were grown to high density for 3 days, after which they entered a state of quiescence as measured by flow cytometry. A second set of cells was released from a quiescent state into the cell cycle for 24 hr. Analysis of the Smad3 protein levels in these cells revealed that the expression pattern of Smad3 is regulated and dependent on the position of the cells in the cell cycle. This was most apparent in the EpH4 cells, where high levels of Smad3 protein are detected when the cells are quiescent, but Smad3 expression drops dramatically in the proliferating cells (Figure 5.2A, top panel). This is also the case for

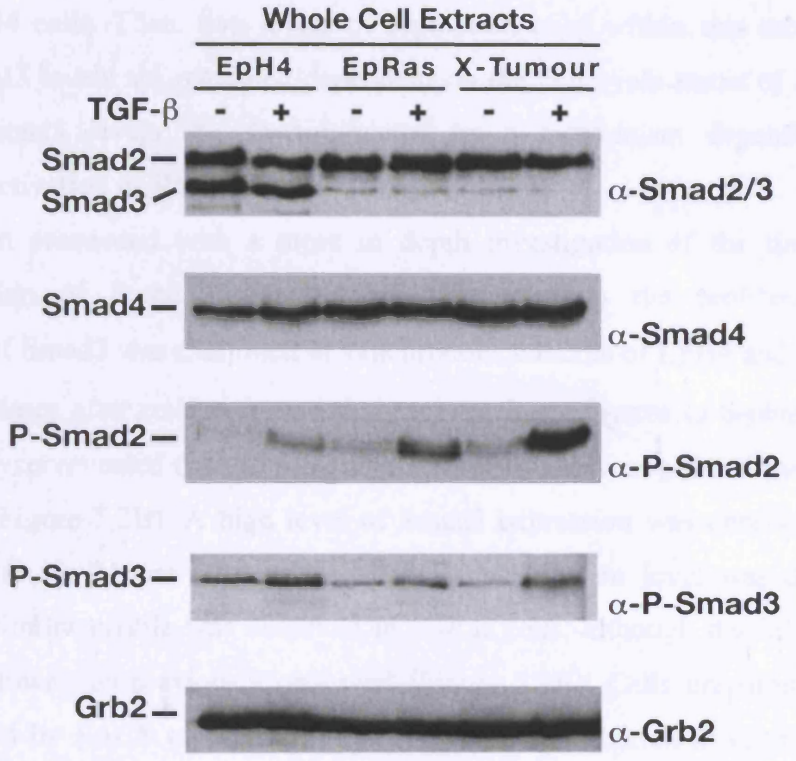

Figure 5.1. Smad3 expression is downregulated in EpRas cells compared with EpH4 cells

EpH4 parental cells and EpRas and X-tumour derivatives were treated with 2 ng/ml TGF-β1 for 1 hr. Whole cell extracts were prepared and equal amounts of protein were analyzed by Western blotting using antibodies against the Smad2, 3 and 4 and phosphorylated Smad2 (P-Smad2) and phosphorylated Smad3 (P-Smad3) and Grb2 as a loading control.

the EpRas cells, however, the levels of Smad3 in quiescent cells are still much lower than in EpH4 cells. Thus, two levels of regulation exist within this model system. Firstly, Smad3 levels are regulated dependent on the cell cycle status of the cell and secondly, Smad3 levels are downregulated by a mechanism dependent on the continuous activation of Ras.

I then proceeded with a more in depth investigation of the timecourse of downregulation of Smad3 protein from quiescence to the proliferative level. Expression of Smad3 was examined in synchronous cultures of EpH4 and EpRas cells at different times after release from quiescence as they progress to S-phase. Western blotting analysis revealed that Smad3 protein level was downregulated over time at a steady rate (Figure 5.2B). A high level of Smad3 expression was observed in EpH4 cells, however by 24 hrs after release, the Smad3 protein level was dramatically reduced. A similar profile was observed in EpRas cells, although the initial level of Smad3 was lower, as previously observed (Figure 5.2B). Cells prepared in parallel were analysed by FACS to determine the cell cycle distribution at each time point. This revealed that in both cell types the drop in Smad3 expression does not correlate with entry into S-phase, but rather it appears to be determined by the time/distance from quiescence. In EpH4 cells, there is a linear rate of Smad3 downregulation, whereas S-phase entry occurs between 16-20 hrs (Figure 5.2B, graphs and data not shown). However in the EpRas cells, there appears to be a more stepwise drop in Smad3 levels but both cell lines exhibit maximal downregulation at the 24 hr timepoint (Figure 5.2B).

In conclusion, Smad3 protein level is high in quiescent cells but upon exit from G0, the Smad3 expression is dramatically reduced. In addition, the EpRas cells have a lower Smad3 protein level than EpH4 cells, in both the quiescent and proliferative state.

5.2.2 Timecourse of signalling and induction of Smad3-depndent genes

The regulation of Smad3 protein levels provided an avenue to pursue regarding the prevailing question of how EpRas cells overcome the growth inhibitory response to TGF-β and undergo an EMT. As discussed in the Chapter 1, Smad3 has been

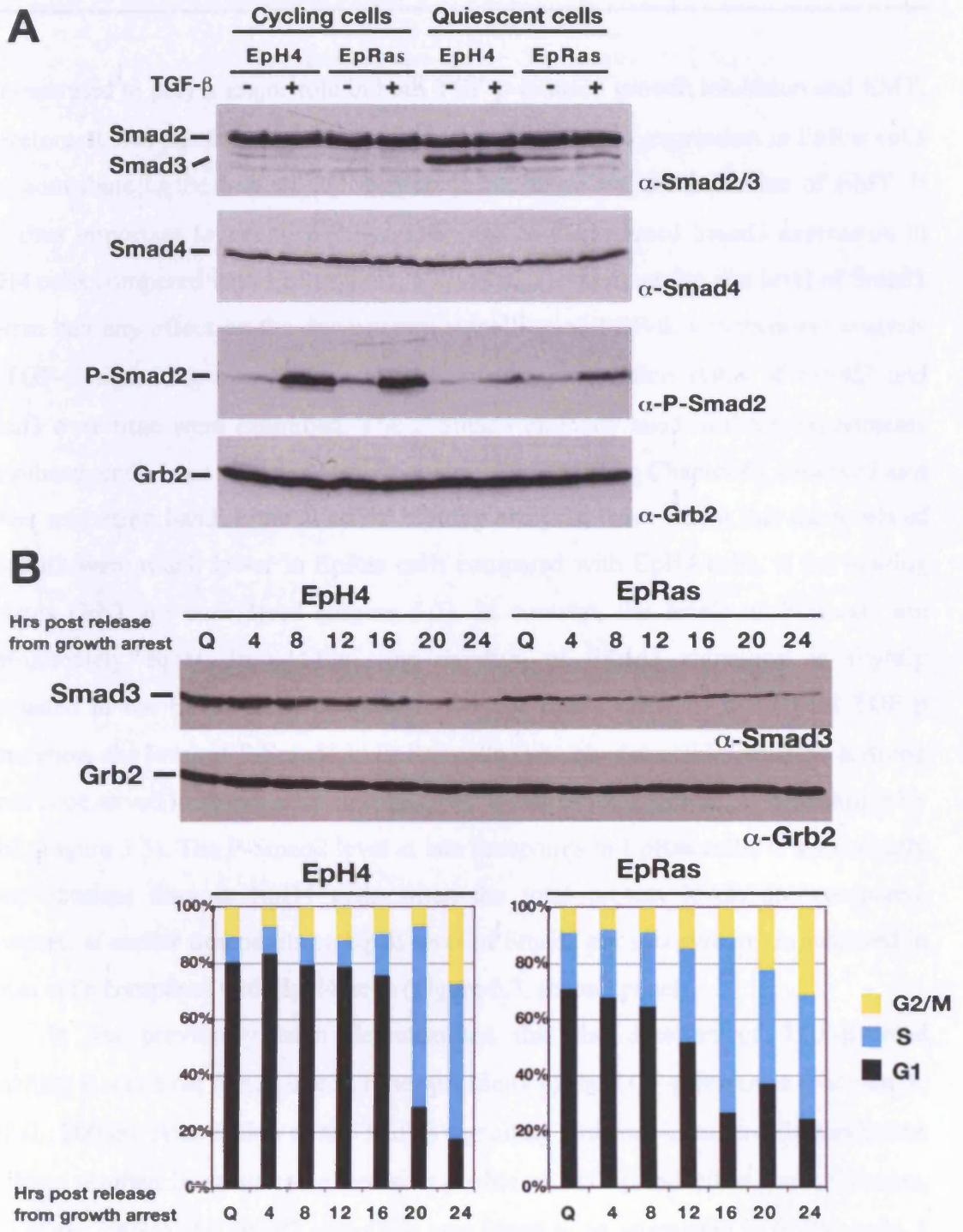

Figure 5.2. The expression pattern of Smad3 is regulated during the cell cycle, with a gradual decrease in Smad3 protein expression upon entry into S-phase

(A) Synchronized, quiescent EpH4 and EpRas cells were prepared by contact inhibition for 72 hrs. Actively cycling low confluency EpH4 and EpRas cells were prepared by synchronizing the cells by contact inhibition and then plating into fresh medium for 24 hrs. Cells were either unstimulated or treated with 2 ng/ml TGF-β1 for 1 hr as indicated. Whole cell extracts were prepared and equal amounts of protein were analyzed by Western blotting using antibodies against Smad2/3 and Smad4 and phosphorylated Smad2 (P-Smad2) and Grb2 as a loading control.

(B) EpH4 and EpRas cells were synchronized by contact inhibition and then plated into fresh medium for the number of hours indicated. Cells were harvested and analysed by fluorescence-activated cell sorting (FACS), to determine the number of cells in G1 (black bar), S (blue bar) or G2/M yellow bar) and by Western blotting, using antibodies against Smad3 and Grb2 as a loading control.

demonstrated to play a major role in both TGF-β-induced growth inhibition and EMT. Therefore, it was possible that the downregulation of Smad3 expression in EpRas cells may contribute to the loss in TGF-β growth inhibition and the induction of EMT. It was thus important to establish the significance of the reduced Smad3 expression in EpH4 cells compared with EpRas cells. To investigate whether the low level of Smad3 protein had any effect on the downstream signalling of TGF-β, a timecourse analysis of TGF-β signalling was performed and the phosphorylation states of Smad2 and Smad3 over time were examined. The P-Smad3 antibody used in these experiments has subsequently been found to also recognise P-Smad1 (See Chapter 6), observed as a slower migrating band. From Western blotting analysis, it is evident that the levels of P-Smad3 were much lower in EpRas cells compared with EpH4 cells, if the loading controls Grb2 are considered (Figure 5.3). In contrast, the levels of P-Smad2 are approximately equal. In addition, the duration of Smad3 signalling is slightly attenuated in the EpRas cells compared with the EpH4 cells. At 6 hrs post TGF-β stimulation, the level of P-Smad3 in EpRas cells is barely detectable, whereas a strong signal is observed in EpH4 cells, despite equal levels of total protein, as determined by Grb2 (Figure 5.3). The P-Smad2 level at late timepoints in EpRas cells, is also slightly more transient than in EpH4 cells when the total protein levels are compared. However, at earlier timepoints an equal level of Smad2 phosphorylation is achieved in EpRas cells compared with EpH4 cells (Figure 5.3, second panel).

It has previously been demonstrated that the duration of TGF-β-Smad signalling is a critical determinant of the specificity of the TGF-β response (Nicolas, F. J. et al., 2003a). Attenuation of the TGF-β signalling pathway in pancreatic carcinoma cell lines resulted in an altered expression profile of TGF-β-inducible genes (Nicolas, F. J. et al., 2003a). As Smad3 signalling was found to be attenuated in EpRas cells, I investigated whether EpRas cells were still responsive to Smad3 signalling. To this end I tested the ability of EpRas cells to induce expression of a well characterized Smad3 dependent gene, Plasminogen Activator Inhibitor-1 (PAI-1) (Dennler, S. et al., 1998; Wong, C. et al., 1999). In EpH4 cells, PAI-1 expression is induced at 4 hours post TGF-β stimulation and its intensity increases gradually until the 8 hr timepoint (Figure 5.3, third panel). Conversely, EpRas cells are unable to induce expression of PAI-1. The inability of EpRas cells to upregulate the Smad3-dependent gene in

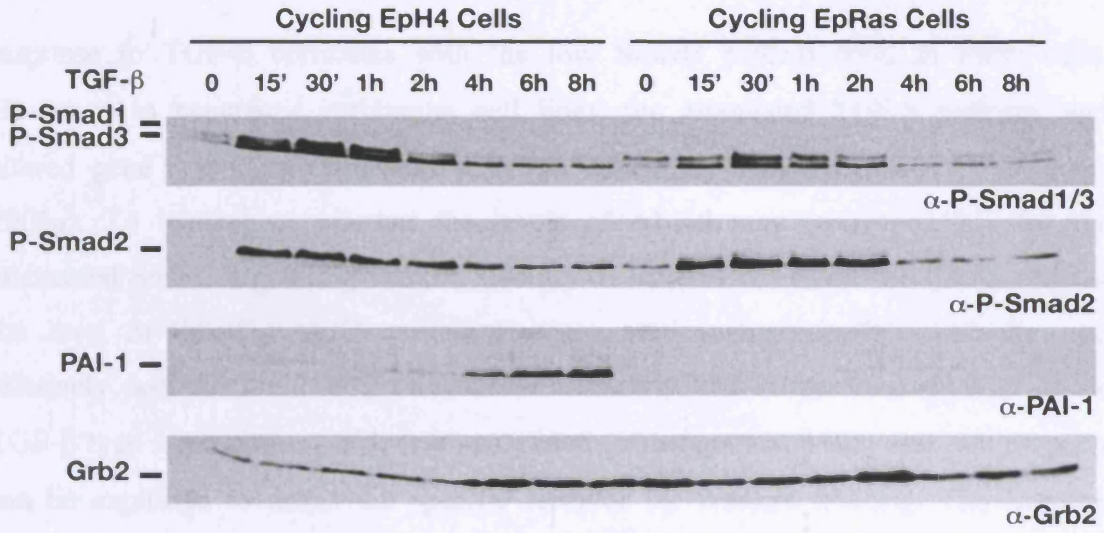

Figure 5.3. TGF-β fails to induce Smad3-dependent target genes in EpRas cells

EpH4 and EpRas cells were synchronized by contact inhibition and released into the cell cycle for 20 hrs before stimulation with TGF-β1 (2 ng/ml) for different time periods. Whole-cell extracts were prepared, and equal amounts of protein were analysed by Western blotting using an antibody against PAI-1 as a representatives of a Smad3-dependent TGF-β target gene, and against P-Smad3 and P-Smad2 to show the level of phosphorylated Smad over time. Grb2 serves as a loading control. The P-Smad3 antibody also detects P-Smad1 (see Chapter 6).

response to TGF-β correlates with the low Smad3 protein level in these cells. However, in pancreatic carcinoma cell lines, the attenuated TGF-β pathway and altered gene responses correlated with low levels of ALK5 (Nicolas, F. J. et al., 2003a). To investigate whether the levels of ALK5 may be responsible for the attenuated Smad3 signalling and the inability of EpRas cells to induce PAI-1 and not the level of Smad3, ALK5 protein levels were investigated. The antibodies are relatively poor for the TGF-β receptors. Fortunately, the extracellular domain of the TGF-β type I receptor, ALK5, is glycosylated (Massague, J., 1998) and this property can be exploited to detect the specific receptor by Western blotting. The enzyme, PNGase F, hydrolyzes nearly all types of N-glycan chains from glycoproteins and therefore upon treatment with this enzyme, there is a shift in the ALK5 band on SDS-PAGE due to the reduced molecular weight. In the absence of PNGaseF ALK5 runs as a smear because of its variable glycosylation state, however treatment with PNGaseF reduces ALK5 to a single band, which is distinguishable from background bands as it is not present in the untreated samples. Comparison of ALK5 levels in EpH4 and EpRas cells in S-phase, revealed that there is no significant variation between EpH4 and EpRas ALK5 levels in cycling cells, which is the cell cycle phase whereby PAI-1 induction was investigated and actually ALK5 levels in quiescent EpRas cells appears to be higher than in EpH4 cells (Figure 5.4). However, although it is conclusive that the receptor protein levels are not affected in cycling cells, this does not rule out the possibility that the activity of ALK5 has been compromised.

In conclusion, it is evident that the TGF-β-Smad3 signalling pathway in EpRas cells is attenuated in comparison with the parental EpH4 cell line. This has resulted in an impaired response to TGF-β induction of Smad3 dependent genes.

5.2.3 Transcriptional regulation of Smad3 contributes to the increased level of Smad3 protein in EpH4 cells.

Although the decreased level of Smad3 in EpRas cells was shown to be biologically significant, it was as yet unclear how these cells regulated the Smad3 levels. The first approach to gain insight into the mechanism involved was to investigate the transcriptional regulation of Smad3 expression. Smad3 mRNA levels were determined

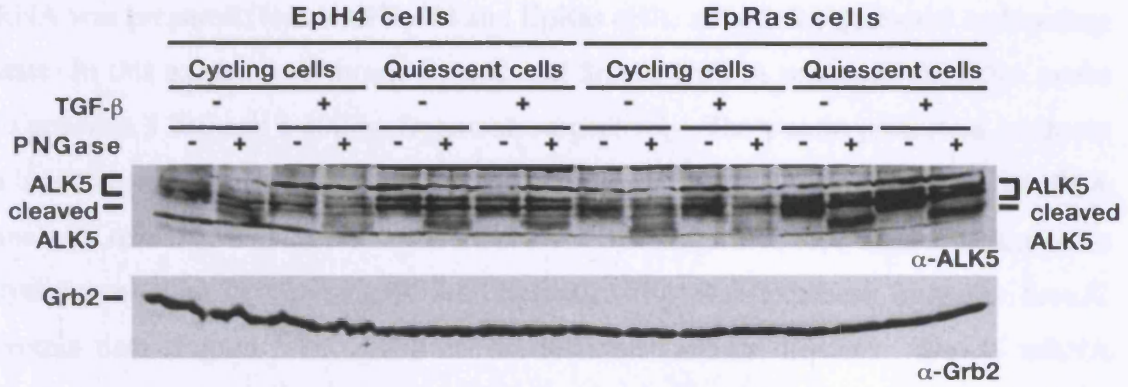

Figure 5.4 ALK5 expression is not donwregulated in EpRas cells

Synchronized, quiescent EpH4 and EpRas cells were prepared by contact inhibition for 72 hrs. Actively cycling low confluency EpH4 and EpRas cells were prepared by synchronizing the cells by contact inhibition and then plating into fresh medium for 24 hrs. Cells were either untreated or stimulated with 2 ng/ml TGF-β1 for 1 hr as indicated. For PNGaseF treated extracts, 30 μg of whole cell extracts from each sample was incubated with PNGase F (0.1 μl; specific activity 1800000 U/mg) for 1 hr at 37°C. Untreated and PNGaseF treated extracts were then analyzed by Western blotting using antibodies against ALK5 and Grb2 as a loading control.

by quantitative RNase mapping, as described in Chapter 2 (Treisman, R., 1985). Total RNA was prepared from both EpH4 and EpRas cells, in both the quiescent and cycling state. In this experiment, mouse Smad2 and Smad3 mRNA protected the RNA probe to generate a 230 and a 300 bp fragment, respectively. The γ-actin protection produces a smaller fragement of 65 bp fragment (Figure 5.5A). The quantitation of RPA analysis revealed that Smad2 mRNA did not vary significantly, from quiescence to cycling cells, or between EpH4 and EpRas, which was expected from the Smad2 protein data (Figure 5.5B, graph on the left). In contrast, however, Smad3 mRNA levels varied substantially, with a 3 fold decrease in Smad3 mRNA in cycling EpH4 cells compared with cells in quiescence (Figure 5.5B, graph on right). The Smad3 transcriptional profile was similar in EpRas cells, however, there was an overall decrease of 2-3 fold in Smad3 mRNA in EpRas cells compared with EpH4 cells. These results exhibited a similar trend as the profiles of the Smad3 protein level, but the differences in protein level were much more pronounced than a 3-fold decrease. Hence, the relatively small decrease in mRNA from quiescence to cycling cells and equally from EpH4 to EpRas cells, was unlikely to account in full for the much more dramatic alteration in Smad3 protein levels.

To conclude, transcriptional regulation of Smad3 mRNA levels contributes in part to the control of expression levels of Smad3 observed during the cell cycle and also the overall decrease Smad3 observed in EpRas cells compared with EpH4 cells. However other mechanisms must play a role in the downregulation of Smad3 in addition to transcriptional regulation.

5.2.4 *Instability of Smad3*

In view of the transcriptional data, it was necessary to further investigate the mechanisms that could account for the significant decrease in Smad3 protein levels. The downregulation of Smad3 observed in both cell types was concomitant with exit from G0. A possible explanation for this was that in addition to decreased transcriptional activation of Smad3 in cycling cells, the changes in cellular environment could affect the stability of Smad3 protein. In order to investigate this hypothesis, I used a well characterized protein synthesis inhibitor, cycloheximide, to prevent translation of newly synthesized Smad3 mRNA. By preventing new protein

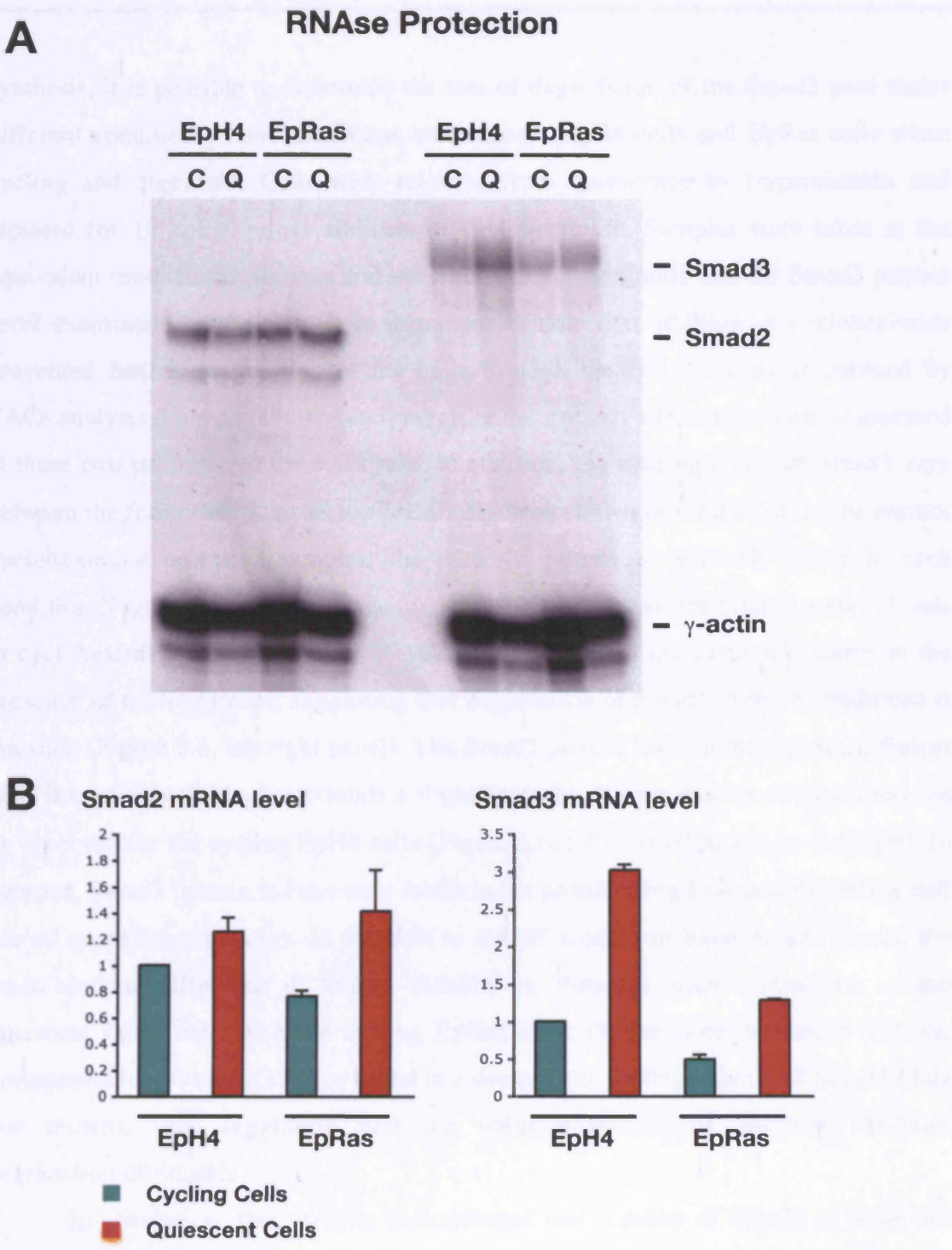

Figure 5.5. Smad3 mRNA levels are elevated in quiescent cells compared with cycling cells and also slightly higher levels of Smad3 mRNA are observed in EpH4 cells compared with EpRas cells

(A) Expression levels of Smad2 and Smad3 was detected by RNase protection. RNA was isolated from both cycling (C) and quiescent (Q) EpH4 and EpRas cells. 20 μg of total RNA were analysed by RNase protection with probes for Smad2 and Smad3. The protected fragments (Smad2 or Smad3) are indicated. γ-actin probe was used as a loading control. Data are representative of two independent experiments.

(B) Quantitation of RNAse protection by phosphorimaging analysis. The data are the means and standard deviations of two separate experiments relative to appropriate controls.

synthesis, it is possible to determine the rate of degradation of the Smad3 pool under different conditions. Four conditions were tested: EpH4 cells and EpRas cells when cycling and quiescent. Cells were released from quiescence by trypsinisation and replated for 15 hours before addition of cycloheximide. Samples were taken at the equivalent times in the absence and presence of cycloheximide and the Smad3 protein level examined (Figure 5.6). It is important to note that addition of cycloheximide prevented further progression of the cells through the cell cycle as determined by FACs analysis (data not shown) and therefore the stability of Smad3 could be assessed at these two positions in the cell cycle. In addition, the starting levels of Smad3 vary between the four conditions, as has previously been shown in Figure 5.2. In the control cycloheximide untreated samples, the level of Smad3 is relatively stable in each condition (Figure 5.6, left set of panels). It is also evident that the Smad3 protein levels in cycloheximide treated samples of quiescent EpH4 cells are extremely stable in the presence of cycloheximde, suggesting that degradation of Smad3 in these conditions is minimal (Figure 5.6, top right panel). The Smad3 protein level in the quiescent EpRas cells is relatively stable, but exhibits a slight degradation over time. A similar trend can be observed for the cycling EpH4 cells (Figure 5.6, third set of panels on the right). In contrast, Smad3 protein is extremely labile in the proliferating EpRas cells, with a half life of approximately 6 hrs. In addition to the differences in basal Smad3 levels, the most obvious difference in Smad3 stability is observed upon comparison of the quiescent EpH4 cells with the cycling EpRas cells. Furthermore, treatment with the proteasome inhibitor, MG132, resulted in a decrease in the degradation of Smad3 (data not shown), thus suggesting that the ubiquitin-proteasome pathway mediates degradation of Smad3.

In conclusion, these results demonstrated that stability of Smad3 in these cell lines appears to contribute to its downregulation during cell proliferation. It was observed that the most stable Smad3 protein exists in the quiescent state in EpH4 cells, whereas the most labile Smad3 protein occurs in cycling EpRas cells.

5.2.5 Regulation of Smad3 Stability

The realization that both the cell cycle state and Ras activity could have an impact on the stability of Smad3 protein was intriguing. Previous studies have already implicated Ras activation through the ERK MAPK pathway in alteration of the activity

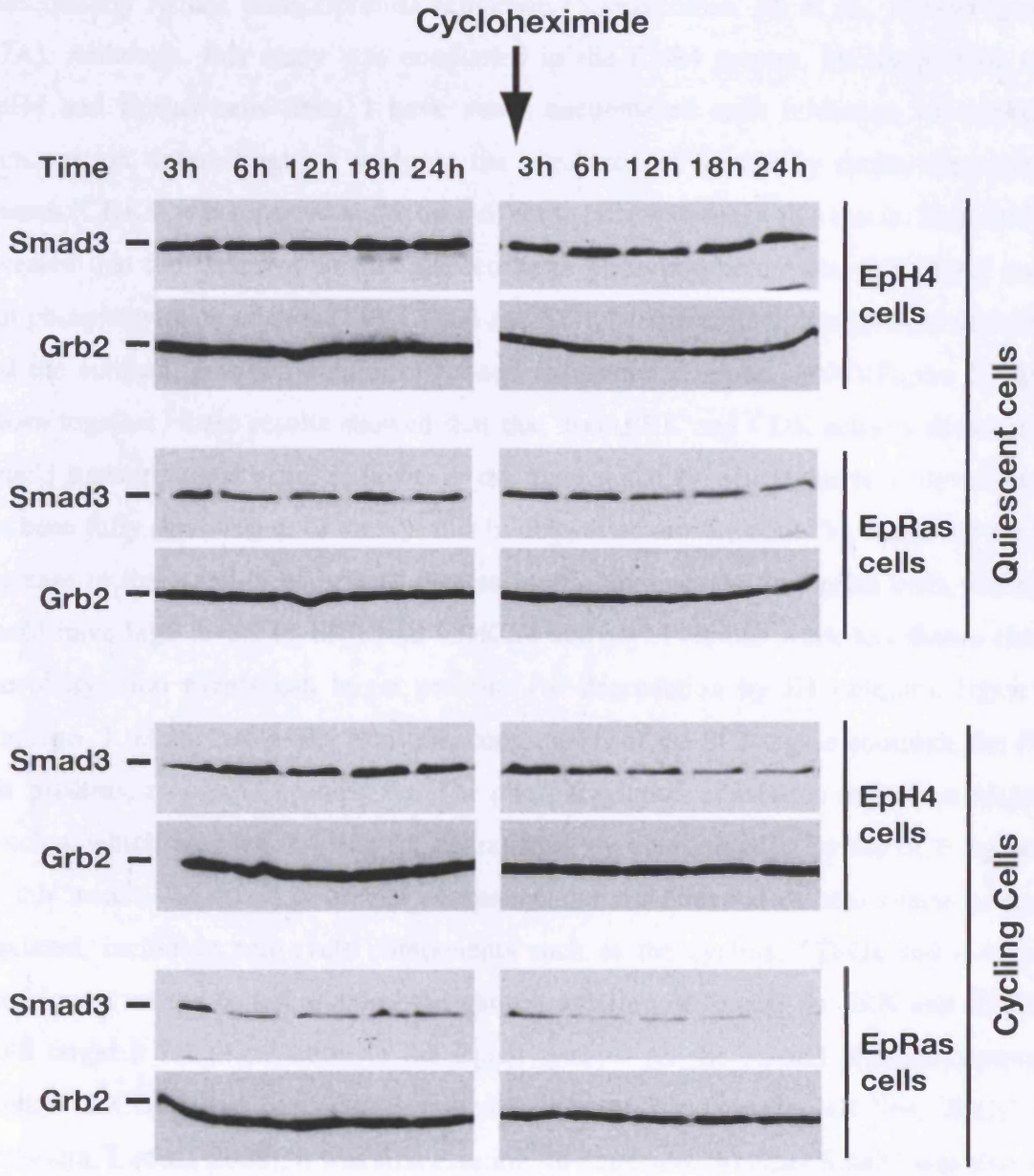

Figure 5.6. Smad3 is less stable in cycling cells than when cells are quiescent

Synchronized, quiescent EpH4 and EpRas cells were prepared by contact inhibition for 72 hrs. Actively cycling, low confluency EpH4 and EpRas cells were prepared by synchronizing the cells by contact inhibition and subsequent release into fresh medium for 15 hrs. EpH4 were either untreated or treated with the protein synthesis inhibitor cyclohexamide (20 μg/ml) for 3 to 24 hrs as indicated. Whole cell extracts were prepared and equal amounts of protein were analysed by Western blotting using antibodies against Smad3 and Grb2 as a loading control.

of Smad3. In this case, phosphorylation on consensus MAPK sites by ERK1/2 in the linker of Smad2 or Smad3 was proposed to inhibit nuclear translocation and consequently reduce transcriptional activation (Kretzschmar, M. et al., 1999)(Figure 5.7A). Although, this study was conducted in the EpH4 system, by comparison of EpH4 and EpRas cells lines, I have never encountered such inhibition of nuclear translocation. Interestingly, a study on the regulation of Smad3 by cyclin dependent kinases (CDKs) was reported at the time of these observations in this thesis. This study revealed that the linker of Smad3 also contains phosphorylation sites for CDKs and that phosphorylation of Smad3 by CDK4 and CDK2 inhibits its transcriptional activity and the antiproliferative function of Smad3 (Matsuura, I. et al., 2004)(Figure 5.7A). Taken together, these results showed that that both ERK and CDK activity decreases Smad3 transcriptional activity, however the mechanism by which this is achieved has not been fully established. In theory, this inhibition of activity could be explained by a decrease in the stability of Smad3 protein levels, as observed in EpRas cells, which would have high levels of ERK and CDK2/4 activity. Previous work has shown that phosphorylation events can target proteins for degradation by E3 ubiquitin ligases (Cardozo, T. et al., 2004). For example, components of the SCF-ligase complex, the F-box proteins, recognize specific Ser/Thr phosphorylation consensus motifs on target proteins, which are then targeted for degradation by ubiquitination by the SCF-ligase. By this means, the levels of crucial components of fundamental cellular functions are regulated, including cell cycle components such as the cyclins, CDKIs and c-myc. Therefore, I set out to test whether the phosphorylation of Smad3 by ERK and CDKs could target it for degradation in the EpH4 system. As the Smad3 phosphorylating activity of CDKs had been demonstrated in human keratinocyte cell line, HaCaTs (Matsuura, I. et al., 2004), it was first essential to determine whether Smad3 was also a physiological target for CDK2 and CDK4 in EpH4 and EpRas cells. Specific antibodies against the phosphorylation sites on Smad3 were generated by Fang Liu and were kindly donated upon request (Matsuura, I. et al., 2004). EpH4 and EpRas cells were released into serum for 24 hrs and analysed by Western blotting with a specific phosphopeptide antibody against a Smad3 ERK phosphorylation site (S207) and with an antibody against a CDK2/4 phosphorylation site (T178) (Matsuura, I. et al., 2004) (Figure 5.7A). Treatment of TGF-β for 1 hr revealed that these phosphorylation sites are rapidly induced by TGF-β (Figure 5.7B). Next, I needed to test the cell cycle

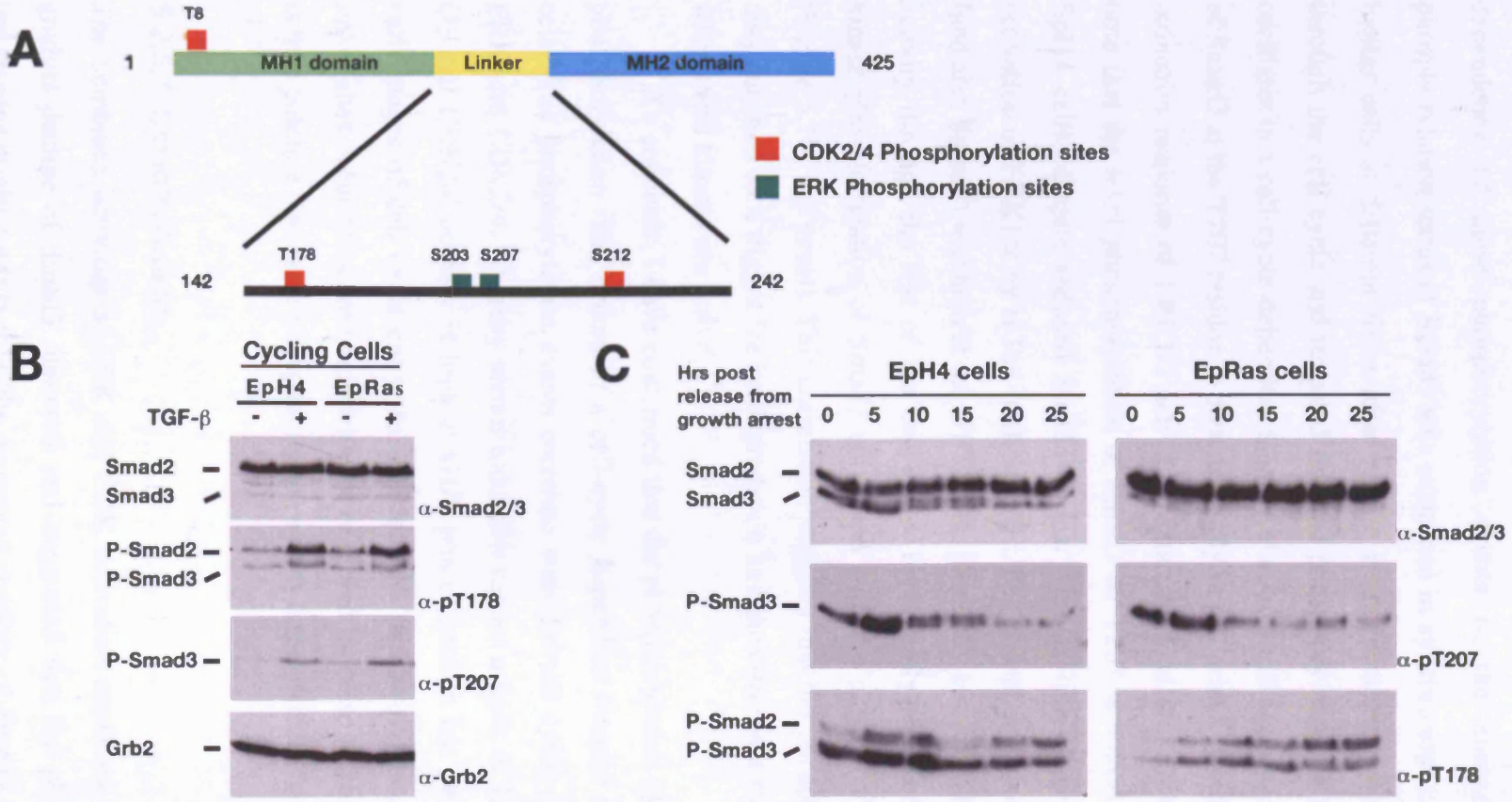

Figure 5.7. Smad3 is phosphorylated at CDK and Erk phosphorylation sites in EpH4 and EpRas cells

(A) Schematic diagram of Smad3 structure, indicating the sites of phosphorylation by ERK and CDK2/4.
(B) Smad3 is phosphorylated at the T178 and T207 sites in the linker. Both T178 and S207 phosphorylation events are rapidly induced by TGF-β. Synchronized, cycling EpH4 and EpRas cells were either untreated or stimulated with TGF-β for 1 hr. Whole cell extracts were fractionated by SDS-PAGE and analysed by Western blotting using phosphopeptide antibodies against T178 and T207 of Smad3.
(C) Endogenous Smad3 is phosphorylated in a cell cycle-dependent manner. EpH4 and EpRas cells were synchronized by contact inhibition and then released into fresh medium. Cells were collected at different time points to analyse the phosphorylation status at each of the sites by Western blotting with the corresponding phosphopeptide antibody. Note that the pT178 antibody also recognises the same site in Smad2.

dependency of these phosphorylation events in the absence of TGF-β. The phosphorylation status of Smad3 was examined in synchronous cultures of EpH4 and EpRas cells at different times after release from quiescence as the cells progressed through the cell cycle and revealed that the phosphorylation of Smad3 at these sites oscillates in a cell-cycle-dependent manner. As shown in Figure 5.7C, phosphorylation of Smad3 at the T207 residue is maximal early in G1, which is consistent with a serum induction response of ERK1/2 activity (Matsuura, I. et al., 2004). It is important to note that the level phosphorylation of Smad3 on T207 is almost equal to that in the EpH4 cells, despite reduced Smad3 levels. This is likely due to the constitutive activation of ERK1/2 by H-Ras in these cells. The phosphorylation of T178 on Smad3 (and also Smad2) was high at the G1/S phase boundary but exhibited a more prolonged activity through the rest of the cell cycle. Importantly, the activity profiles of the kinase phosphorylation of Smad3 correlated with the pattern of Smad3 degradation (Figure 5.7C, top panel). This correlation suggests that the phosphorylation of Smad3 may function as a trigger for its degradation and thus decrease the stability of Smad3 when these kinases are active.

To conclude, I have confirmed that the phosphorylation of Smad3 at the linker phosphorylation sites occurs in a cell-cycle dependent manner in EpH4 and EpRas cells. The phosphorylation events correlate with the cell cycle dependent activity of ERK and CDK2/4, whereby serum induction causes a peak of ERK activity early in G1 and CDK2/4 activity is high at G1/S phase junction but persists throughout the early stages of cell cycle entry. In addition, the phosphorylation of Smad3 at these linker sites occurs concomitantly with the observed increase in Smad3 instability and it is thus possible that these phosphorylation events target Smad3 for degradation.

5.2.5.1 Smad3 Mutants

The combined activities of ERK and CDK activation appeared to correlate with the gradual decline of Smad3 observed and suggested that the phosphorylation of the linker sites might contribute to the decreased stability of Smad3 in cycling EpH4 and EpRas cells. To determine the effect of these phosphorylation events on Smad3 stability, a set of Smad3 mutant constructs were generated by Mike Howell in the Developmental Signalling Laboratory, which included different combinations of S-to-

A mutations of the ERK and CDK phosphorylation sites (Figure 5.8A). By this means, I could test whether the degradation of Smad3 in EpRas cells could be stabilised by inhibition of Smad3 ERK or CDK phosphorylation. Firstly, I needed to test whether these mutant plasmids expressing Smad3 were still responsive to TGF-β. EpRas cells were transiently transfected with each of the plasmids expressing the mutant Smad3 and following immunoprecipitation and Western blotting analysis, the C-terminal phosphorylation status was examined. For each of the mutants tested, the proteins were efficiently phosphorylated following TGF-β stimulation (Figure 5.8B).

I then proceeded to test the effect of these mutants on the stability of the expressed Smad3 protein compared with wild type Smad3 protein. Transient transfections were carried out in EpRas cells, as Smad3 protein was the most labile in these cells. These cells were synchronised by contact inhibition and released into serum containing media to allow them to reenter the cell cycle. The cells were either untreated or treated with cycloheximide for 18 hrs to test for the stability of the Smad3 mutants compared to wild type. In both EpH4 and EpRas cells the wild type FLAG-Smad3 protein was efficiently degraded in the presence of cycloheximide (Figure 5.9, α-FLAG panel). The Smad3 blot serves as an internal control in this experiment, because it demonstrates the stability of endogenous Smad3, which can vary dependent on cell cycle position and culture confluency. The transfection efficiency for the EpH4 cells is relatively weak and thus the contribution of FLAG-Smad3 to the total Smad3 level is generally quite low. In most of the mutants tested, there seemed to be no obvious increased stability compared to the wild type. However, cells expressing Smad3 mutants no 4, 5 and 13, did exhibit some resistance to degradation, which was observed primarily in EpH4 cells (Figure 5.9, right). The endogenous Smad3 levels in each case were also more stable, suggesting that the culture conditions were compromised in these cases. The Smad3 mutant no 13 appeared to be more stable in both cell lines and to further investigate its stability, stable cell lines expressing this mutant were generated. However, when these stable cell lines were investigated, no effect in stability of the mutant was detected (data not shown). These results suggested that phosphorylation of these sites is not involved in targeting Smad3 for degradation. Nevertheless, further investigation is required to determine fully the significance of these phosphorylation events with respect to Smad3 activity.

A

Smad3 Mutant No.	Residue(s) mutated to A
mt1	S203/S207
mt2	S212
mt3	T8/T178
mt4	T8/S212
mt5	T8/S203/S207
mt6	S203/S212
mt7	T178/S212
mt8	T8/T178/S203/S207
mt9	T178/S203/S207
mt10	T8/S203/S212
mt11	T178/S203/S212
mt12	T8/T178/S212
mt13	T8/T178/S203/S212

B

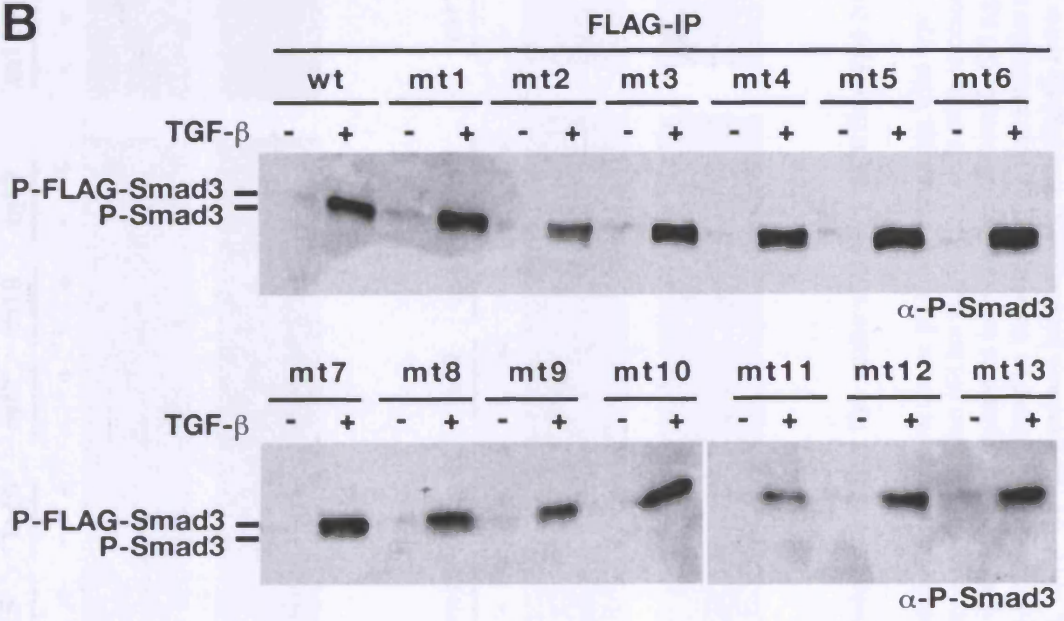

Figure 5.8. The Smad3 mutants are efficiently phosphorylated at the C-terminus

(A) A list of thirteen Smad3 mutants. CDK and ERK phosphorylation sites were mutated to alanine, in various combinations as shown.
(B) EpRas cells were transfected with plasmids expressing wild type FLAG-Smad3 (wt) or each of the FLAG-tagged mutant Smad3s (mt) as indicated. After 48 hrs incubation, cells were either untreated or stimulated with TGF-β1 for 1 hr before lysis. Whole cell extracts were prepared and immuoprecipitated with beads conjugated with anti-FLAG antibody. The immunoprecipation reactions (IPs) were analysed by Western blotting with antibodies against P-Smad3.
Mutant constructs were kindly provided by Mike Howell.

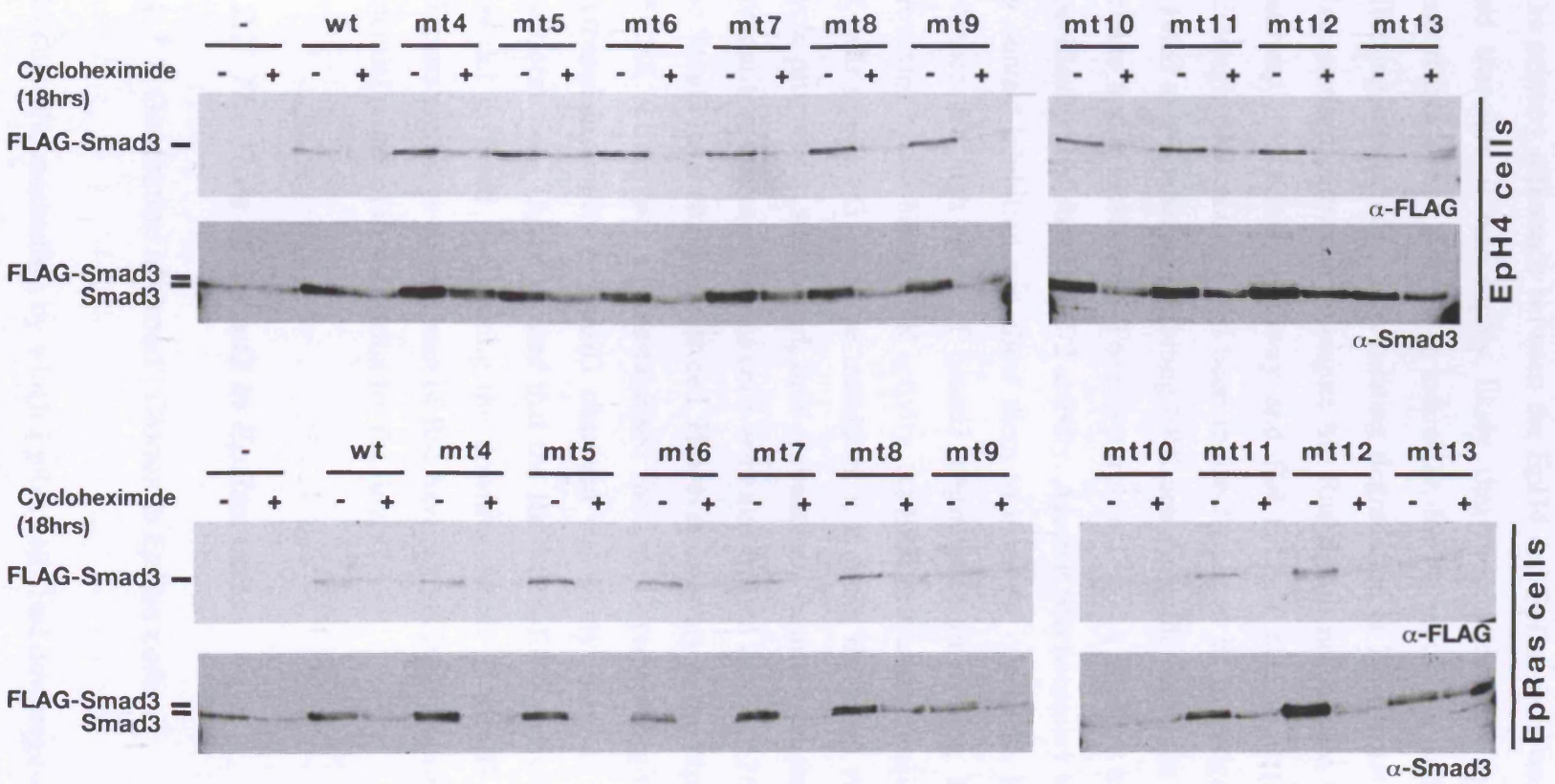

Figure 5.9. Mutant Smad3 proteins exhibit the same stability as wild-type Smad3

EpH4 and EpRas cells were transfected with empty vector, or plasmids expressing wild type (wt) FLAG-Smad3 or each of the mutant (mt) Smad3s as indicated. After contact inhibition (48 hrs incubation), cells were released and replated 1:2 for 15 hrs. Cells were then either untreated or treated with the protein synthesis inhibitor, cyclohexamide (20 μg/ml), for 18hrs to visualise Smad3 degradation. Whole cell extracts were prepared and analysed by Western blotting with antibodies against Smad3 and FLAG. FLAG-Smad3 is observed in the Smad3 blot, where it is detected as a band running with slightly lower mobility compared to endogenous Smad3 (see arrows).

5.2.6 Inhibition of ERK activity

The primary difference between the EpH4 and EpRas cells was the activation of Ras and therefore it was highly likely that the downstream mediators of Ras were responsible, either directly or indirectly, for the regulation of Smad3 levels either by affecting transcription, upregulating degradation or by alternative means. Three well characterised pathways propagate the Ras signal, namely the Raf-ERK MAP kinase pathway, PI3 Kinase pathway and Ral GTPase activation (Downward, J., 1998). Although ERK activity had been indirectly tested by investigation of the mutants, I wanted to test whether inhibiting ERK activity could revert the Smad3 level in EpRas cells to that of EpH4 cells. For this purpose, I used a MEK1/2 inhibitor, U0126, which specifically abolishes ERK1/2 activity. Again it was necessary to synchronise the cells by contact inhibition and allow them to enter the cell cycle. It could then be tested whether the high level of Smad3 degradation in cycling EpRas cells could be prevented by inhibiting ERK activity. As ERK activation is required for the regulation of cells through G1-S phase transition, it is likely that upon addition of U0126, cell cycle progression was halted, thus preventing a further decrease in Smad3 levels. For comparison, quiescent EpRas cells were also treated with U0126, again to test whether the Smad3 level could be restored. However, contrary to the expected result, inhibition of ERK activity actually destabilised the Smad3 protein slightly (Figure 5.10). The increased instability of Smad3 observed was likely to be an indirect result of Ras transformtaion. This suggested that the Raf-MEK-ERK pathway downstream of Ras was not involved in directing the downregulation of Smad3 level. The two other effectors pathways downstream of Ras have not yet been investigated but may provide potential routes of investigation for the future.

5.2.7 The Role of Smad3 in EpRas cells

5.2.7.1 Generation of Smad3 Clones in EpRas cells

Although the mechanism by which EpRas cells had downregulated their Smad3 level not become apparent, the loss of PAI-1 expression in response to TGF-β clearly

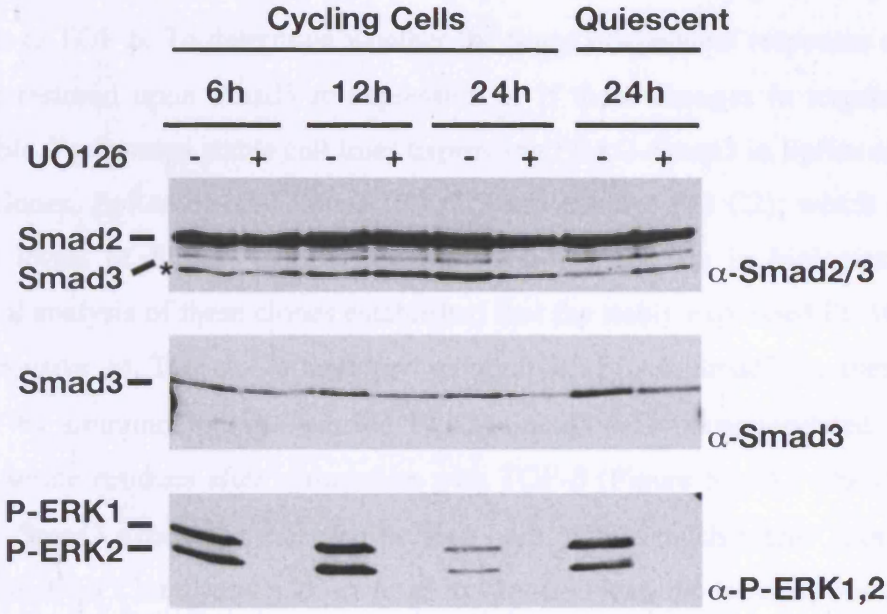

Figure 5.10. MEK activity is not involved in the destabilisation of Smad3

Smad3 protein levels are lower in the presence of U0126. EpRas cells were synchronized by contact inhibition and then released into fresh medium for 15 hrs. Cells were then treated with or without the MEK inhibitor, U0126 (25 μM), for 6, 12 or 24 hrs. Quiescent cells were also treated with the inhibitor for 24 hrs for comparison. Whole cell extracts were prepared and analysed by Western blotting using antibodies against phosphorylated ERK1/2 (P-ERK1 and P-ERK2), Smad2/3.
* indicates a non-specific band recognised by the antibody.

showed that the low level of Smad3 in EpRas cells could significantly alter its responses to TGF-β. To determine whether the Smad3-dependent responses of TGF-β could be restored upon Smad3 re-expression or if these changes in responses were irreversible, I generated stable cell lines expressing FLAG-Smad3 in EpRas cells. Two Smad3 clones, EpRas Smad3 clone1 (S3 C1) and clone 2 (S3 C2), which exhibited different levels of Smad3 expression, were selected for use in biological assays. Functional analysis of these clones established that the stably expressed FLAG-Smad3 was responsive to TGF-β. Immunoprecipitation of FLAG-Smad3 in these clones followed by immunoblotting revealed FLAG-Smad3 was phosphorylated at its C-terminal serine residues after stimulation with TGF-β (Figure 5.11A). The difference in FLAG-Smad3 expression can also be seen here, with a much higher expression of FLAG-Smad3 in Clone1 and a lower level in Clone2. Next, the transcriptional activity of the FLAG-Smad3 expressing clones was compared to the parental EpRas cell line using a Smad3-dependent reporter, $CAGA_{12}$-luciferase. Clones expressing FLAG-Smad3 exhibited both an increase in the basal signalling and slight increase in the induction of $CAGA_{12}$-luciferase activity relative to EpRas cells (Figure 5.11B). Despite large standard deviations within triplicate experiments, there is a trend of increased luciferase activity in EpRas Smad3-expressing clones. Unexpectedly, EpRas S3 Clone2 gave a marginally higher activity compared with EpRas S3 Clone1, despite the lower level of Smad3 present. Further investigation into the levels of Smad3 in these clones, demonstrated that expression of FLAG-Smad3 exhibits a cell cycle dependent regulation as previously observed in the DT-Smad EpRas cell lines (Figure 5.12B). Here the expression of FLAG-Smad3 in quiescent cell clones is very low, however upon release into the cell cycle for 14 hrs, FLAG-Smad3 expression is upregulated. This is more pronounced for the EpRas Clone1, which exhibits a higher expression of FLAG-Smad3. The expression of FLAG-Smad3 in these two clones, however is transient and after 18 hrs after release from quiescence, the expression of FLAG-Smad3 protein is lost.

In conclusion, these results indicate that the FLAG-Smad3 expressed in the EpRas clones is phosphorylated in response to TGF-β and can induce expression of a Smad3-dependent reporter. The short-lived expression of FLAG-Smad3 in these clones accounts for the variable and low induction of expression from this promoter.

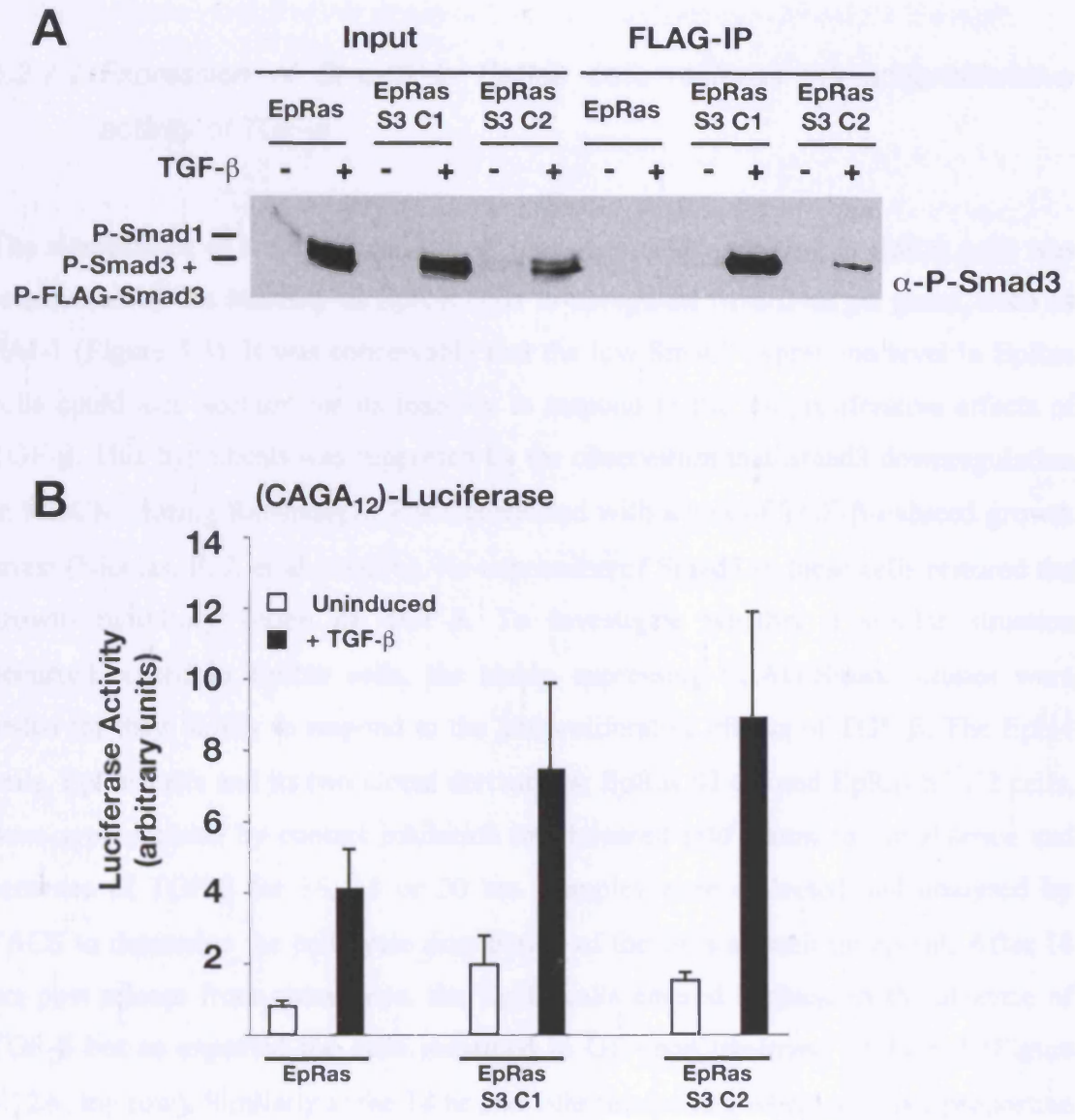

Figure 5.11. Functional analysis of the EpRas Smad3 clones

(A) FLAG-Smad3 is efficiently phosphorylated at the C-terminal in response to TGF-β. EpRas parental cell line, EpRas S3 C1 and EpRas S3 C2 cells were synchronized by contact inhibition and released for 15 hrs. Cells were either untreated or stimulated with TGF-β1 for 1 hr before lysis. Whole cell extracts were prepared and immunoprecipitated with beads conjugated with anti-FLAG antibody. The immunoprecipates (IPs) were analysed by Western blotting with antibodies against P-Smad3. 20% input is shown on the left as a control.

(B) Smad3 transcriptional activity is amplified in EpRas Smad3 clones. EpRas parental cell line and the two FLAG-Smad3 clones (EpRas S3 C1 and EpRas S3 C2) were transfected with the Smad3-dependent reporter $(CAGA)_{12}$-Luc. Following contact inhibition (48h incubation), cells were released into fresh medium for 12 hrs before TGF-β addition for 8 h. Luciferase activity was assayed and quantitated relative to β-galactosidase from the pEFLacZ internal control. The data are the means and standard deviations of three independent experiments.

5.2.7.2 Expression of Smad3 in EpRas cells restores the antiproliferative activity of TGF-β

The significance of the low level and attenuated Smad3 signalling in EpRas cells was established by the inability of EpRas cells to upregulate Smad3-target genes, such as PAI-1 (Figure 5.3). It was conceivable that the low Smad3 expression level in EpRas cells could also account for its inability to respond to the antiproliferative effects of TGF-β. This hypothesis was supported by the observation that Smad3 downregulation in MDCKs during Raf-induced EMT correlated with a loss of TGF-β-induced growth arrest (Nicolas, F. J. et al., 2003b). Re-expression of Smad3 in these cells restored the growth inhibitory action of TGF-β. To investigate whether a similar situation occurred/existed in EpRas cells, the stably expressing FLAG-Smad3 clones were tested for their ability to respond to the antiproliferative effects of TGF-β. The EpH4 cells, EpRas cells and its two clonal derivatives, EpRas S3 C1 and EpRas S3 C2 cells, were synchronized by contact inhibition and released into serum in the absence and presence of TGF-β for 16, 18 or 20 hrs. Samples were collected and analysed by FACS to determine the cell cycle distribution of the cells at each timepoint. After 18 hrs post release from quiescence, the EpH4 cells entered S-phase in the absence of TGF-β but as expected the cells remained in G1 upon treatment of TGF-β (Figure 5.12A, top row). Similarly at the 18 hr and 20hr timepoints, where a higher proportion of EpH4 cells had progressed into S-phase in the absence of TGF-β, this entry was again inhibited when TGF-β was present (Figure 5.12A, top row, on the right). In contrast the EpRas cells, which exhibit a higher proliferation rate, had entered S-phase after 16 hours regardless of the presence of TGF-β (Figure 5.12A, second row, left). At this early timepoint, the EpRas cells were slightly sensitized to TGF-β, however at subsequent timepoints (18 and 20 hr), this sensitivity to TGF-β was lost and the EpRas cells progressed equally well through the cell cycle in the absence or presence of TGF-β. Interestingly, the DNA profiles of the EpRas Smad3-expressing clones more closely matched those of the EpH4 cells. For the EpRas FLAG-Smad3 Clone 1, the percentage of cells in S-phase was reduced compared to the EpRas cells at 16 hr post release, which is indicative of their slower proliferative rate (Figure 5.12A, third row, left). In

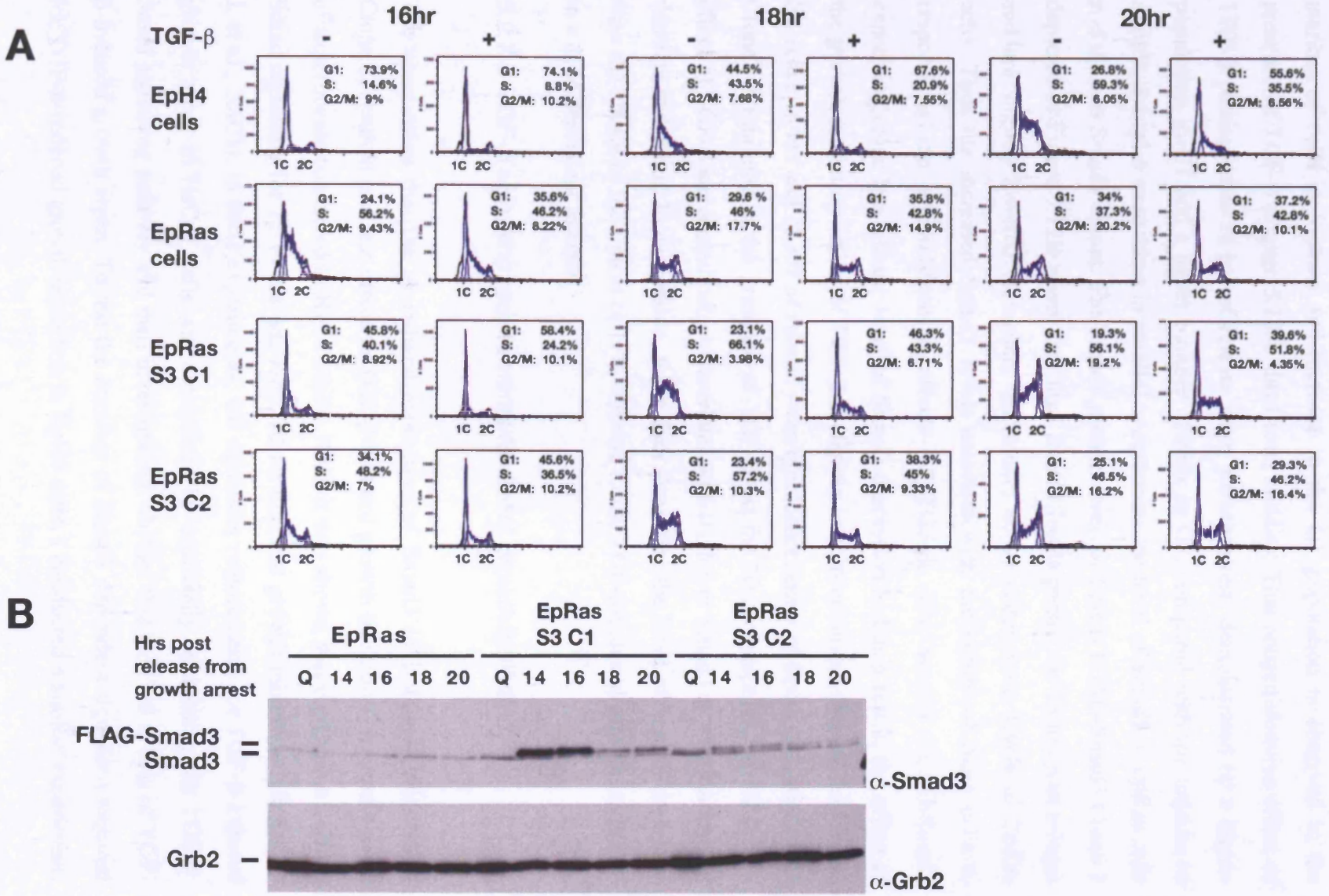
A
16hr
18hr
20hr
TGF-β
-
+
EpH4 cells
EpRas cells
EpRas S3 C1
EpRas S3 C2
1C 2C
B
Hrs post release from growth arrest
EpRas
EpRas S3 C1
EpRas S3 C2
Q 14 16 18 20
FLAG-Smad3
Smad3
α-Smad3
Grb2
α-Grb2

addition, the entry of these cells into S-phase was inhibited in the presence of TGF-β. This is even more evident at the 18 hr timepoint, where a substantial reduction in the number of cells in S-phase and increase in the G1 population is observed in the presence of TGF-β (Figure 5.12A, third row, middle). This antiproliferative effect of TGF-β persists after 20 hrs of release from growth arrest, demonstrated by a higher population in G1 and a lower number of cells in G2, compared with the uninduced sample. Samples were taken in parallel to determine the level of Smad3 in EpRas cells and the two Smad3 clones. The Smad3 protein levels of EpRas FLAG-Smad3 Clone 1 depicted in Figure 5.12B reveal that high Smad3 levels persist for 16 hrs post release and are slightly lowered thereafter, but remain above endogenous levels of EpRas cells. Thus the increased Smad3 levels correlate with the ability of these cells to respond to the antiproliferative effects of TGF-β. The second FLAG-Smad3 expressing clone has a lower level of Smad3 expression and as a result, the effect of the growth inhibitory action of TGF-β is slightly less prounounced (Figure 5.12A and B). After 16 hrs and 18 hrs of release from quiescence, entry of EpRas FLAG-Smad3 Clone2 is inhibited in the presence of TGF-β. At the 20 hr timepoint, the inhibitory effect of TGF-β has abated, which correlates with the lower Smad3 expression level at this late timepoint. In conclusion, these data show that the level of Smad3 correlates with the ability of the EpRas cells to respond to the TGF-β-induced growth inhibition in a dose dependent manner.

5.2.7.3 TGF-β signalling requirements for EpH4 growth inhibition

The observation that the short-lived expression of Smad3 in EpRas FLAG-Smad3 Clone 2, resulted in a less effective TGF-β-induced growth inhibition was reminiscent of experiments conducted in HaCaT cells. Here, it was shown that continuous TGF-β-Smad signalling for 12-14 hrs was required for efficient growth inhibition(Nicolas, F. J. et al., 2003a). In these experiments, the signalling requirements for TGF-β-induced growth arrest in HaCaT cells was determined by artificially attenuating the TGF-β-Smad signalling pathway and then investigating whether this then led to loss of TGF-β-induced growth arrest. To test the duration of Smad3 dependent signalling required for TGF-β-induced growth inhibition in EpH4 cells, I conducted a similar experiment.

The TGF-β signalling pathway was therefore terminated at different times after TGF-β stimulation, and the effect of this on the ability of TGF-β to prevent entry into the cell cycle was investigated. Termination of the signal was achieved by treatment with the ALK5 inhibitor, SB-431542. It has previously been demonstrated that the SB-431542 inhibitor is a potent and selective inhibitor of ALK4, ALK5 and ALK7 and acts almost immediately to inhibit receptor kinase activity, thus preventing Smad2 and Smad3 phosphorylation (Inman, G. J. et al., 2002b). As shown in Figure 5.13, continuous stimulation of EpH4 cells with TGF-β resulted in inhibition of S-phase entry, indicated by the high number of cells still in G1. Treatment of the cells with SB-431542 at the same time as TGF-β inhibited the effect of TGF-β, as expected (Figure 5.13). Allowing TGF-β signalling for 4, 8 or 12 hrs was not sufficient to inhibit S-phase entry, however, receptor signalling for 16 hr was sufficient to inhibit cell cycle entry (Figure 5.13). This demonstrates that continuous Smad signalling for between 12 and 16 hr is required for the antiproliferative effect of TGF-β and that attenuated Smad signalling in these cells would confer resistance to these effects. Interestingly, the short-lived expression of Smad3 in EpRas Smad3-expressing Clone2 results in a partial growth inhibitory response. Taken together, this suggests that high levels of Smad3 signalling for 12-16 hours is required for TGF-β-induced growth inhibition in EpH4 or EpRas cells.

5.2.7.4 Effect of Smad3 stable expression on TGF-β-induced EMT

Strong evidence exists for an essential role for Smad3 in EMT, however the levels of Smad3 required for this response have not been investigated (Sato, M. et al., 2003; Zavadil, J. et al., 2004). Smad3 levels in MDCK are gradually downregulated during Raf-induced EMT and re-expression of Smad3 in MDCK cells that have undergone an EMT did not reverse the EMT as these cells still maintained a mesenchymal phenotype (Nicolas, F. J. et al., 2003b). It was important to determine whether the increased Smad3 levels could interfere with the progression of EpRas cells through EMT. The clones were assayed for their ability to undergo an EMT in response to TGF-β by the assay described in Chapter 4. The EpRas parental line and its two clonal derivatives were plated out at low density on plastic and stimulated with TGF-β over the course of

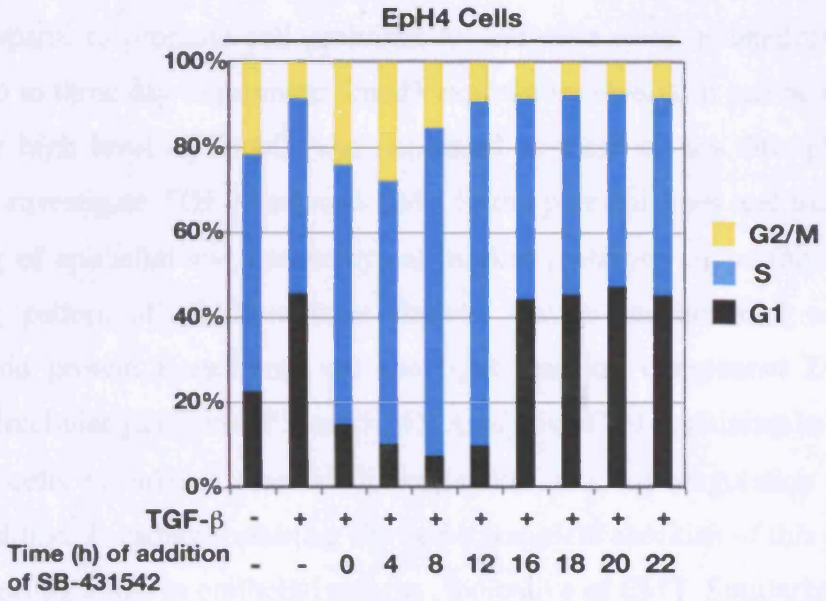

Figure 5.13. Continuous TGF-β signaling for 12–16 h is required for TGF-β-induced growth arrest in EpH4 cells

The ALK5 inhibitor, SB-431542, inhibits activation of Smad2/3 and their translocation to the nucleus when added simultaneously with TGF-β. EpH4 were synchronized by contact inhibition and then plated into fresh medium. EpH4 cells were either untreated or treated with 2 ng/ml TGF-β1, then treated with10 μM SB-431542 at the same time as TGF-β1 (0 time point), or at the times shown after TGF-β addition. After 22 h, cells were harvested and analysed by FACS to determine the number of cells in G1 (black bar), S (blue bar) or G2/M (yellow bar).

10 days. It is noteworthy that the expression of Smad3 in the clonal lines exhibits variability in a cell cycle dependent manner, however, the culture confluency of these cells was kept sparse to promote cell proliferation and cells were replated into fresh media every two to three day to promote Smad3 expression. Overall it can be assumed that a relatively high level of Smad3 was expressed in these clones throughout the EMT assay. To investigate TGF-β-induced EMT in the parental lines and the clones, immunostaining of epithelial and mesenchymal marker proteins was performed. The immunostaining pattern of all three lines showed that in unstimulated cells, the adherens junction protein E-cadherin and the tight junction component ZO-1 are localized to intercellular junctions (Figure 5.14). Analysis of Z0-1 staining in TGF-β-induced EpRas cells revealed a marked delocalisation and downregulation of tight junctions. In addition, E-cadherin staining showed a complete abolitian of this junction component, revealing a loss in epithelial polarity, indicative of EMT. Similarly the two EpRas FLAG-Smad3 expressing clones revealed an identical phenotype, with loss of E-cadherin and downregulation of Z0-1, suggesting that Smad3 expression in these cells does not interfere with the progression of EMT. In addition, cells were also stained with phalloidin to visualise actin organisation within the cell. In the absence of TGF-β, cortical actin can be seen at the cell periphery in all three cell lines (Figure 5.15). However, in the presence of TGF-β the actin organisaton has undergone a dramatic remodelling resulting in actin stress fibers, typical of migratory, mesenchymal cells (Thiery, J. P. et al., 2006). These cells were also stained with an antibody recognising Smad2 and Smad3. What is quite clear from these images, is the higher level of nuclear Smad2/3 in both EpRas Smad3 clones compared with EpRas cells (Figure 5.15, left panel). This suggests that basal TGF-β signalling in these cells results in a higher level of nuclear Smad3. However, this does not affect the epithelial integrity of these Smad3 expressing cells.

In conclusion these results establish that Smad3 does not interfere with progression of TGF-β induced EMT in EpRas cells. In addition, although Smad3 levels are sufficient for TGF-β-induced EMT, higher levels of Smad3 do not inhibit it as shown by the dramatic decrease in epithelial markers and remodelling of the actin cytokeleton in Smad3 expressing cells.

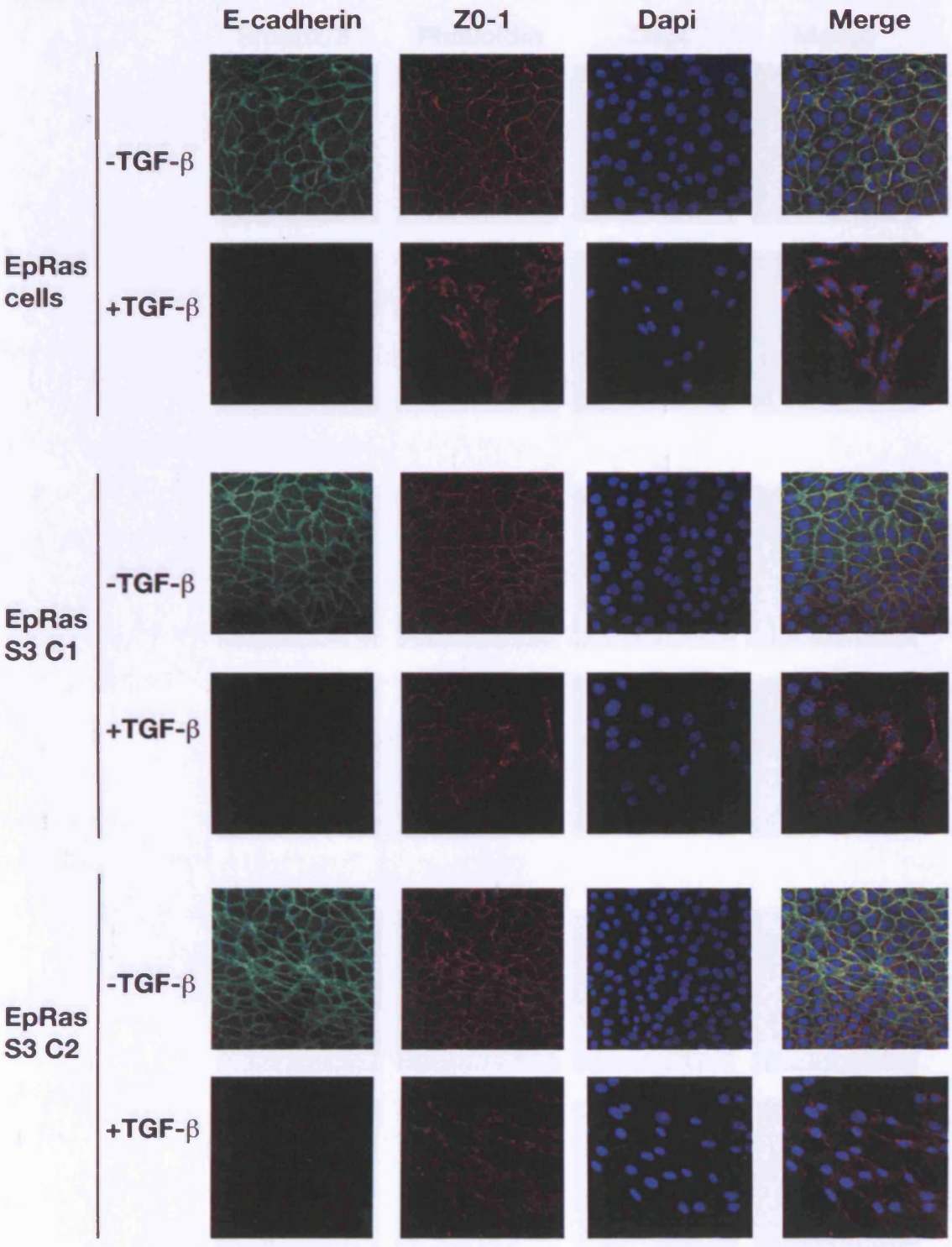

Figure 5.14. Stable expression of Smad3 does not inhibit TGF-β-induced EMT in EpRas cells

Downregulation of E-cadherin and Z0-1 occurs in EpRas cells and EpRas Smad3 clones. EpRas, EpRas S3 C1 and EpRas S3 C2 cells were plated out at low density and either grown in the presence or absence of TGF-β (2 ng/ml). The medium was changed 1 d after seeding and then every other day. TGF-βwas added to the cells upon medium change. Three days after plating, the cells were trypsinised and re-plated at equivalent density to day 1. Cells were grown for a total of 10 days, which required two trypsinisations, and then harvested 48 hrs after final TGF-β addition. Cells were processed for immunofluorescence using an anti-E-cadherin antibody, to analyze adherens junctions or an anti-Zona Occludens 1 (Z0-1) antibody, to analyze tight junctions. Nuclei were visualized with DAPI.

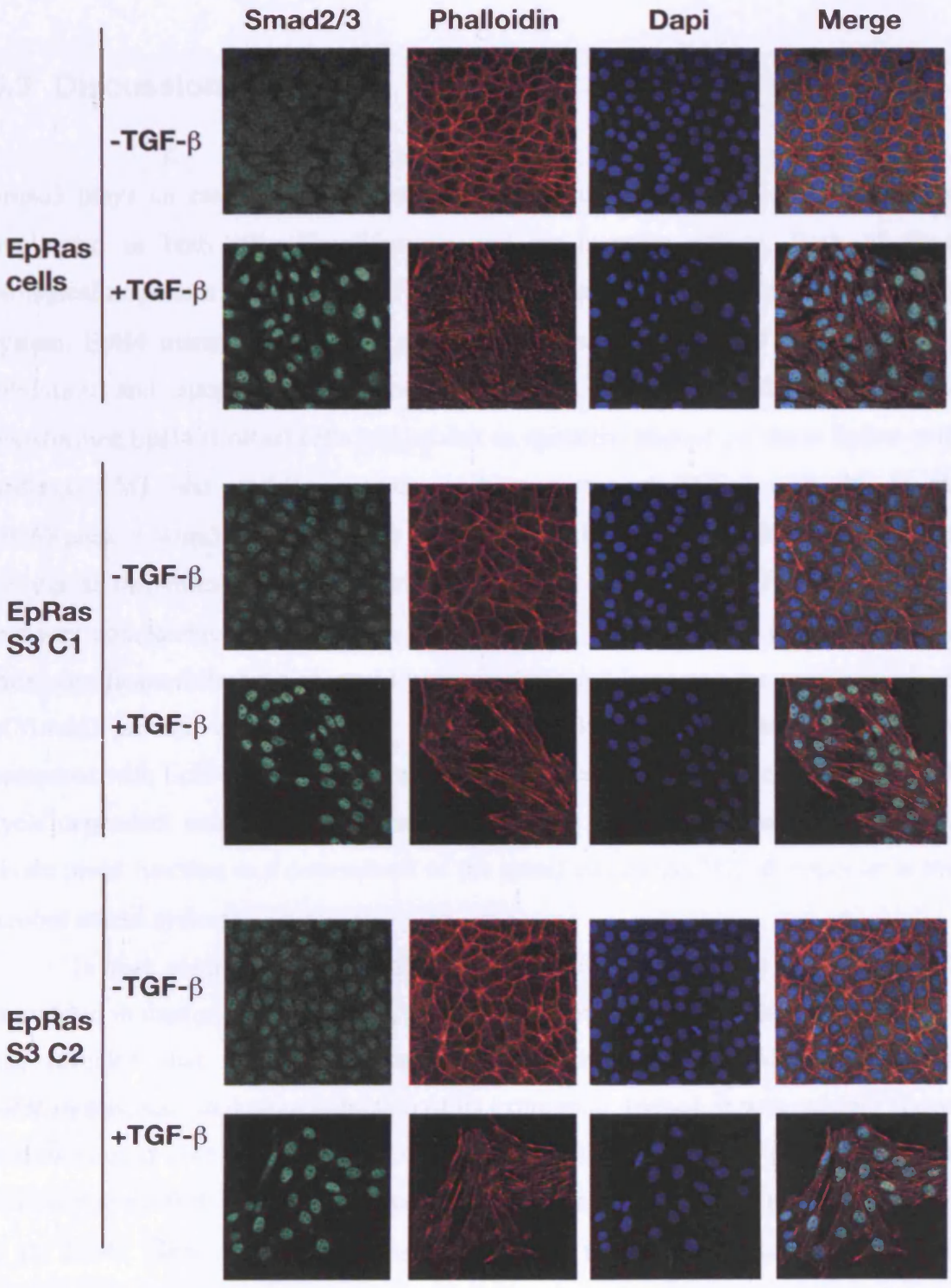

Figure 5.15. EpRas Smad3 clones exhibit higher level of nuclear Smad3 in the uninduced state.

EpRas, EpRas S3 C1 and EpRas S3 C2 cells were treated as in Figure 5.14. Cells were then processed for immunofluorescence using antibodies against Smad2/3 . Actin reorganization was visualized with Texas red-conjugated phalloidin, and nuclei were visualized with DAPI. Note images are taken from the same experiment as analysed in Figure 5.14.

5.3 Discussion

Smad3 plays an essential role in mediating the responses of TGF-β and has been implicated in both its antiproliferative and pro-invasive effects. Both of these biological responses induced by TGF-β are functional in the EpH4 tumour cell model system. EpH4 mammary epithelial cells, are non-tumourigenic and undergo growth inhibition and apoptosis in response to TGF-β. However, although the Ras-transformed EpH4 (EpRas) cells still exhibit an epithelial phenotype, these EpRas cells undergo EMT and invasive growth in the presence of TGF-β (Oft, M. et al., 1996)(present work). To dissect the molecular mechanisms governing these distinct biological responses, I began by investigating the levels of the TGF-β signalling pathway components in these cells. Data presented in this chapter revealed that the most significant difference observed between these cell lines was the expression level of Smad3 protein, whereby Smad3 was dramatically downregulated in EpRas cells compared with EpH4 cells. In addition, Smad3 expression levels is regulated in a cell-cycle dependent manner. I also present evidence to demonstrate that Smad3 protein levels could function as a determinant of the specificity of the TGF-β response in this tumour model system.

In stark contrast to Smad2 and Smad4, there is no evidence to date that Smad3 is mutated in cancer (Levy, L. et al., 2006). On the other hand, accumulating evidence has revealed that Smad3 expression is more likely controlled by epigenetic mechanisms, such as loss or reduction of its expression. Indeed, it was recently shown that two out of nine gastric cancer cell lines are deficient in Smad3 protein level that have lost some TGF-β responsiveness, with concomitant low mRNA levels (Han, S. U. et al., 2004). However, the mechanisms controlling the epigenetic factors responsible for Smad3 loss of expression have not yet been uncovered. In this chapter, investigations were carried out to determine the downregulation of Smad3 expression in the EpH4 tumour cell model system and additionally, the significance of Smad3 in this system was determined.

5.3.1 Mechanisms of Smad3 Downregulation

I have established that within the EpH4 system two levels of regulation are in place to determine expression of Smad3 protein. At one level, Smad3 expression is regulated by the cell cycle in both EpH4 and EpRas cells and results in a maximal level of Smad3 expression in quiescent cells and a gradual decrease of Smad3 upon entry into the cell cycle. A second level appears to overlay the cell cycle regulation of Smad3, whereby EpRas cells exhibit a much reduced expression of Smad3 protein compared with EpH4 cells, and this is possibly the result of the constitutive activation of oncogenic Ras. One question that has arisen from this study is whether these two levels of Smad3 expression are regulated by similar mechanims or do the EpRas cells exhibit an exaggeration of the cell cycle dependency? One reason to suggest that the mechanisms are the same is that activation of Ras activity appears to be a common factor (see below).

5.3.1.1 Transcriptional Regulation

My results reveal that two mechanisms play a role in controlling the expression of Smad3. The first of these is the transcriptional regulation of Smad3. On average a threefold decrease in Smad3 mRNA was observed from quiescent to cycling cells in both cell types, and additionally an approximate two fold reduction in the levels of Smad3 mRNA was observed in EpRas cells compared with EpH4 cells (Figure 5.5). Consistent with the protein expression, the highest level of Smad3 mRNA was observed in quiescent EpH4 cells, whereas the lowest level was observed in EpRas cycling cells (Figure 5.2 and Figure 5.5). This seems to suggest that a fluctuation in Smad3 transcripts affects both levels of Smad3 expression and supports a role for transcriptional regulation in the cell cycle dependent- and Ras induced- Smad3 expression. The transcriptional fluctuation during the cell cycle is by no means a novel phenomenon, as this has been recorded for hundreds of genes in human fibroblasts (Cho, R. J. et al., 2001). Furthermore, it has been revealed through studies in model organisms that one in every five genes may be subject to cell cycle regulated transcription (Breeden, L. L., 2003). How this regulation is achieved, however, is

much less well understood. To date, no information on regulatory elements located in the Smad3 promoter exists. However, in depth promoter analysis of upstream sequences of the Smad3 gene is required to identify cell cycle-dependent regulatory elements. The preliminary work performed on Smad3 transcriptional regulation does not distinguish at which phase of the cell cycle Smad3 is regulated. It will be important to gain a valid transcriptional profile for Smad3 across the cell cycle. This could be achieved by taking a high number of samples per cell cycle and multiple measurements at each time point. Transcriptional regulation of genes often associates with the function of the gene product in that particular phase of the cell cycle and this future analysis may reveal additional functions of Smad3 in cell cycle control.

5.3.1.2 Stability

The second mechanism by which Smad3 expression is regulated is through alterations in the rate of degradation of Smad3 protein. The maximal difference in stability of Smad3 protein is observed when comparing quiescent EpH4 cells to cycling EpRas cells, which is again consistent with the protein levels of Smad3. The observation that both the instability of Smad3 in addition to decreased transcriptional regulation of Smad3 is more exaggerated in the EpRas cells, lends support to the idea that Smad3 protein level in EpRas cells is regulated in a similar manner to the cell-cycle dependent regulation observed in EpH4 cells. However, the two contributing mechanisms are more pronounced in EpRas cells, which is mostly likely due to the increased Ras activity. The effect of Ras activity on Smad3 in EpRas cells can be monitored by the phosphorylation of ERK1/2 phosphorylation sites in the linker region of Smad3. The level of Ras activity peaks early in G1 in the cell cycle, in response to growth factors. This is evident in Figure 5.7C, where phosphorylation at T203 in both EpH4 and EpRas cells is maximal upon release into the cell cycle. Moreover, the level of Smad3 phosphorylation on this residue in EpRas cells is much higher than in EpH4 cells, relative to Smad3 protein levels. The existence of this Smad3 phosphorylated state in EpRas cells persists throughout S-phase, despite the undetectable Smad3 level with the Smad2/3 antibody. This is a measure of constitutive Ras activation though ERK1/2 activity in these cells.

As Ras and CDK activity correlated with the timing of Smad3 degradation, it was reasonable to propose that the phosphorylation of Smad3 by these kinases was a trigger to target Smad3 for ubiquitin-mediated degradation. For example, the F-box proteins, Fbw1 and Fbw7, have been proposed to recognize phosphorylation motifs on target proteins generated by GSK-3β. This results in SCF-ligase-mediated degradation of target proteins including Myc, jun and cyclin E (Cardozo, T. et al., 2004; Wei, W. et al., 2005). Furthermore the activity of GSK-3β is regulated by Ras through the PI3 Kinase pathway, which contributes to the cell-cycle dependency of these proteins (Cardozo, T. et al., 2004). In spite of these similarities, initial investigations have not supported a role for ERK1/2 and CDK activity in the increased instability of Smad3 in EpH4 and EpRas cells. Smad3 mutants lacking these phosphorylation sites did not appear to protect these proteins from degradation in cycling EpRas cells (Figure 5.9). In addition, the phosphorylation of the linker sites of Smad3 by ERK1/2 and CDKs in human keratinocytes did not lead to Smad3 degradation in these cells (Matsuura, I. et al., 2004). However, this could also be explained by expression of a cell-type specific ubiquitin ligase complex, which is not present in keratinocytes.

Activated Ras propagates downstream signals through activation of three well known pathways including the Raf- MEK-ERK pathway, PI3 Kinase pathway and the Ral pathway (Downward, J., 1998). As the ERK1/2 activity has been ruled out, further investigation into the other effector pathways is required to determine the mechanism of Smad3 degradation. EpH4 derivative cell lines have also been generated using two well characterized Ras mutants, which selectively signal along the ERK MAPK pathway, S35-V12–Ras (S35-Ras), or the PI3K pathway, C40-V12–Ras (C40-Ras), due to specific amino acid changes in the effector loop of the Ras protein (Downward, J., 1998). These cell lines have now been acquired and I will investigate the Smad3 levels in each line, which will hopefully shed some light on the pathway involved in Smad3 degradation. The PI3 Kinase pathway is also a likely candidate for this role as it has been previously implicated in abrogating Smad3 signalling in TGF-β-induced apoptosis (Conery, A. R. et al., 2004; Remy, I. et al., 2004; Yang, Y. A. et al., 2006). Hence, it is possible that in EpRas cells, the PI3 Kinase pathway could act to lower Smad3 levels, which would desensitise these cells to an apoptotic response upon TGF-β stimulation. Recent studies have demonstrated a direct physical interaction between Akt and Smad3 in some epithelial and hematopoietic cell lines (Conery, A. R. et al.,

2004; Remy, I. et al., 2004). It has been proposed that through binding of Smad3, Akt acts to sequester it at the plasma membrane, thus preventing nuclear accumulation and transcriptional activity and ultimately, protection from TGF-β induced apoptosis. Therefore a balance between Akt activity and Smad3 level are thought to determine the sensitivity of a cell to TGF-β-induced apoptosis. Furthermore, a recent publication has revealed that Smad3 protein has been found to protect hepatocarcinoma cells from TGF-β-induced apoptosis by repressing the anti-apoptotic regulator, Bcl-2 (Yang, Y. A. et al., 2006). Consistently, studies in EpRas cells and in EpH4 cell lines expressing Ras mutants, PI3Kinase was also found to protect these cells from TGF-β-induced apoptosis (Janda, E. et al., 2002). Future work will focus on investigating the role of PI3 Kinase pathway in regulating Smad3 stability.

To date, evidence already exists for the degradation of basal Smad3. Two mechanisms have been proposed, involving the Skp1—Cul1-F-box-protein (SCF) and U-box E3 ligases. The F-box protein, Fbw1 (βTrCP1), has been shown to weakly interact with Smad3, however the RING-containing component Rbx/Roc1 of the SCF-Fbw1 complex binds to Smad3, which then targets it for degradation (Fukuchi, M. et al., 2001). In addition, an independent study demonstrated an interaction of Smad3 with another F-box protein, βTrCP2 (Ray, D. et al., 2005). However, it is unclear whether these interactions between Smad3 and Rbx1 or the F-box proteins are biologically significant as the determinants of specificity in both cases have not been demonstrated. CHIP (Carboxy of Hsc70 interating protein), a newly recognized E3 ubiquitin ligase, has also been implicated in the basal level of Smad3 through a ubiquitin-dependent degradation pathway (Xin, H. et al., 2005). However, the specificity of this degradation is questionable as Smads 1, 2 and 4 were also found to bind directly to CHIP (Li, L. et al., 2004).

As ubiquitin-mediated proteolysis is integral to the TGF-β signaling pathway, with an important role in Smad3 signalling, it is important to determine the E3 ubiquitin ligases that function in this pathway. To this end a screen for ubiquitin modifiers in the TGF-β-Smad3 pathway is being carried out in the Developmental Signalling Laboratory. By employing a siRNA library for ubiquitin ligases with a Smad3 dependent readout, it is hoped that the ubiquitin modifiers involved in Smad3 regulation will be identified.

5.3.1.3 Other mechanism for regulation of Smad3 expression

One final route of investigation is the regulation of Smad3 stability by microRNAs (miRNAs). miRNAs are small, non-coding RNAs that modulate the expression of target mRNA. Many of the miRNAs that have been studied, act to reduce steady state protein levels for the targeted gene(s) without impacting the corresponding levels of mRNA (Olsen, P. H. et al., 1999). Although the mechanism by which miRNAs reduce protein level is not fully understood, it has been proposed that translational elongation, termination or protein stability are likely to be influenced by miRNA (Hutvagner, G. et al., 2002; Olsen, P. H. et al., 1999). Many miRNAs are known to be up- or downregulated in a variety of cancers, suggesting a role for miRNAs in tumorigenesis (Lee, Y. S. et al., 2006). Hence it is possible that through activation of Ras, a miRNA targeting Smad3 is upregulated and hence decreases the level of Smad3 protein by translational inhibition.

5.3.1.4 Smad3 versus Smad2

It is important to account for the selective degradation of Smad3 over the highly homologous (98% sequence identity) Smad2. The linker region is the most divergent sequence among Smads and is an ideal region for selective regulation of Smad3. In addition, the configuration of phosphorylation sites in the linker region of Smad2 and Smad3 are slightly different. The Smad2 linker contains one PXTP (Thr-220) followed by three XXSP sequences (Ser-245, Ser-250, Ser-255), whereas Smad3 contains two classical MAPK sites (Ser-203, Ser-207) and two XXSP sites (Kretzschmar, M. et al., 1999). As demonstrated, these sequences can serve as phosphorylation sites for proline-directed protein kinases including ERK. If these phosphorylation sites were involved in regulating Smad3 stability by kinases other than ERK or CDK, it is likely that the intervening sequences could determine the specificity of a binding site for a ubiquitin ligase. Regulation of Smad3 at the transcriptional or translational level would alleviate this problem of specificity as there is much greater variation at the level of the promoters of these genes.

5.3.2 Smad3 downregulation and the implications for cancer progression

5.3.2.1 Growth Inhibition

From my work it has been revealed that a minimum threshold level of Smad3 expression is required for the growth inhibitory responses of TGF-β. In the EpRas cells, the decrease is Smad3 levels is sufficient to abrogate the responsiveness of these cells to TGF-β-mediated growth inhibition. Furthermore, ectopic expression of Smad3 in these cells sensitises them to this response in a dose dependent manner (Figure 5.12). This is consistent with work in other cell systems. A gradual down-regulation of Smad3 during the process of Raf-induced EMT in MDCK cells results in a concomitant resistance to the antiproliferative effects of TGF-β (Nicolas, F. J. et al., 2003b). Responsiveness is restored upon re-expression of Smad3 to previous levels of expression. In addition, introduction of Smad3 into Smad3 deficient gastric cancer cell lines restores TGF-β-mediated p15 and p21 induction as well as growth inhibition. Moreover, these Smad3 expressing cells showed dramatically reduced tumourigenicity *in vivo*, providing strong evidence that Smad3 has an important tumour suppressive function in the early stages of gastric carcinogenesis (Han, S. U. et al., 2004). Taken together, these results suggest that Smad3 plays a critical role in the control of cell proliferation by TGF-β and that lowering the level of Smad3 in these cells compromises their antiproliferative response to TGF-β.

5.3.2.2 EMT

In contrast to the effects on growth arrest, the levels of Smad3 do not appear to be critical for the progression of TGF-β-mediated EMT. Expression of Smad3 in EpRas clones did not interfere with the progression of EMT. Similar results were found in MDCK cells where re-introducing Smad3 did not revert the mesenchymal phenotype induced by TGF-β (Nicolas, F. J. et al., 2003b). However this may be cell-type specific as introduction of Smad3 into Smad3 deficient gastric cell lines revealed that these Smad3 expressing cells showed dramatically reduced tumourigenicity, which was accompanied by re-expression of E-cadherin (Han, S. U. et al., 2004).

To conclude, the work presented in this chapter reveals that the activity of Smad3 mimics the dual role of TGF-β in tumourigenesis. By its manipulation through a complex integration of signals, the level of Smad3, and therefore its activity is altered. The high level of Smad3 is attributed to the antiproliferative effects of TGF-β, whereas a lower, less critical level performs the migratory and invasive properties associated with TGF-β.

6 Smad1 phosphorylation in response to TGF-β

6.1 Introduction

As explained in Chapter 1, the myriad of responses elicited by TGF-β highlights the requirement for tight regulation of the downstream signalling pathway. Regulation can be achieved through numerous strategies to achieve specificity of the response. As discussed in Chapter 5, alteration of the expression levels of the Smad proteins is one example of the how the TGF-β pathway is modulated to determine alternative responses. The diversity of gene targets of TGF-β, however, is thought to arise from the DNA binding cofactors, to which the Smad complexes bind (Massague, J. et al., 2005). Current models of TGF-β action envision that activated Smad proteins move into the nucleus, recruit transcriptional coactivators and associate with a host of DNA binding cofactors, generating a range of discrete and distinct transcriptional complexes, each with high affinity and specificity toward a particular gene or set of genes. The work presented in this Chapter suggests a novel mode of activation in response to TGF-β, which may result in an even broader range of gene targets.

To date, two main branches exist within the superfamily, defined by the Smads that are phosphorylated in response to ligand binding. Smads 2 and 3 are phosphorylated by the TGF-β and Activin class of ligand receptors, and Smads 1, 5, and 8 signal from the BMP and GDF class of ligand receptors. The two classes of R-Smads initiate distinct transcriptional programs specific to the signal to which they respond (Graff, J. M. et al., 1996). The first evidence to suggest that there was overlap of the two branches was observed specifically in endothelial cells (Goumans, M. J. et al., 2002). In this cell context, TGF-β also signals through a heteromeric receptor complex consisting of TβRII, ALK5 and ALK1. The activation of both ALK1 and ALK5 in these cells results in the phosphorylation of Smad2 and Smad3 as well as Smad1 and Smad5. Furthermore, signalling via the ALK1-ALK5 receptor complex was shown to mediate a BMP-like response, demonstrated by induction of a BMP specific reporter. Thus, it was proposed that TGF-β stimulation results in the activation

of both classes of Smad proteins, eliciting BMP-like and TGF-β like responses (Goumans, M. J. et al., 2003b; Goumans, M. J. et al., 2002).

During my investigation of the signalling pathways downstream of TGF-β in EpH4 and EpRas cells, I made another striking observation. In addition to the prototypic Smad2 and Smad3 phosphorylation, Smad1 was also phosphorylated in response to TGF-β in these cells. In this Chapter, I have investigated Smad1 signalling in more detail and analysed the role of phosphorylated Smad1 in EpH4 and EpRas cells. As a result, I discovered a new branch of signalling in epithelial cells, whereby Smad1 can form complexes with Smads 2 and 3, which are likely to regulate a unique set transcriptional gene targets.

6.2 Results

6.2.1 Smad1 and Smad5 are phosphorylated by TGF-β

While investigating the levels and the phosphorylation states of Smad3 (Chapter 5), an unusual observation was made. When synchronous cultures of EpH4 and EpRas cells were prepared and analysed by Western blotting using an antibody against the phosphorylated form of Smad3 (anti-P-Smad3 antibody), two bands of equal intensity appeared in the lanes where cells have been stimulated with TGF-β (Figure 6.1, third panel). Interestingly, the upper, slower migrating band was only observed in cycling cells and not in quiescent cells, yet the lower band was observed under both conditions. The lower band migrates at the position where Smad3 is expected to run, but the higher band migrates at a position similar to Smad2. The increase in intensity of the upper band upon TGF-β treatment was an indication that it was a direct target of TGF-β signalling. In view of this, there was a high possibility that the P-Smad antibodies could cross-react with other Smads as the phospho-antobodies are raised against the peptide containing either the phosphorylation motif SSpMSp for Smad2 or SSpVSp for Smad1, Smad3 and Smad5. Smad2 was eliminated as a candidate because its pattern of phosphorylation did not match that of the upper band. Further investigation suggested the possibility that the P-Smad3 antibody could cross-react with the phosphorylated form of Smad1. This was not surprising as the C-terminal

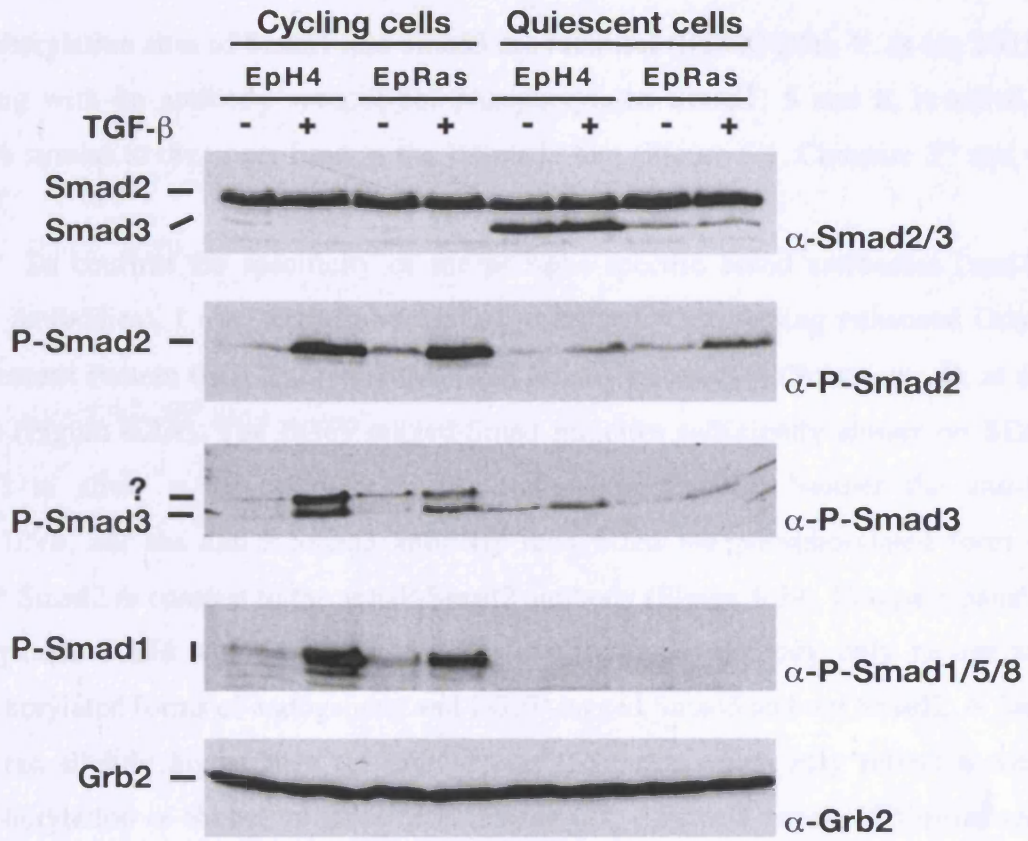

Figure 6.1. Smad1 is phosphorylated in response to TGF-β

Synchronized, quiescent EpH4 and EpRas cells were prepared by contact inhibition for 72 hrs. Actively cycling, low confluency EpH4 and EpRas cells were prepared by synchronizing the cells by contact inhibition and then plating into fresh medium for 24 hrs. Cells were either uninduced or induced with 2 ng/ml TGF-β1 for 1 hr as indicated. Whole cell extracts were prepared and equal amounts of protein were analysed by Western blotting using antibodies against Smad2/3, phosphorylated Smad1 (P-Smad1), P-Smad2, P-Smad3 and Grb2 as a loading control.

phosphorylation sites of Smad1 and Smad3 are identical (SSVS) (Shi, Y. et al., 2003). Probing with an antibody specific for phosphorylated Smad1, 5 and 8, revealed a pattern similar to the upper band in the P-Smad3 blot (Figure 6.1, Compare 3rd and 4th panel).

To confirm the specificity of the phospho-specific Smad antibodies (anti-P-Smad antibodies), I used extracts of HaCaT cells stably expressing enhanced Green Fluorescent Protein (EGFP)-Smad2 and GFP-Smad3 as controls (Schmierer, B. et al., 2005) (Figure 6.2A). The EGFP-tagged-Smad migrates sufficiently slower on SDS-PAGE to allow a separation from the endogenous Smads. Neither the anti-P-Smad1/5/8, nor the anti-P-Smad3 antibody recognized the phosphorylated form of EGFP-Smad2 in contrast to the anti-P-Smad2 antibody (Figure 6.2A, Compare panel 2 with panels 3 and 4). It is clear that the anti-P-Smad3 antibody only recognized phosphorylated forms of endogenous and EGFP-tagged Smad3 and not Smad2. A faint band ran slightly higher than the endogenous P-Smad3, which may reflect a weak phosphorylation of Smad1 in these cells (Figure 6.2, P-Smad3 panel, TGF-β-induced lanes). Since, P-Smad1/5/8 cross-reactivity with either P-Smad2 or P-Smad3 has been eliminated from the results of this experiment, I conclude that Smad1, 5 or 8 is phosphorylated upon TGF-β stimulation in EpH4 and EpRas cells.

To determine which of the BMP-Smads, Smad1, 5 or 8 were phosphorylated in response to TGF-β, I made use of small interfering RNA (siRNA) oligonucleotides against the individual R-Smads (Figure 6.2B, top panel). EpH4 and EpRas cells are also responsive to BMP treatment and BMP induction was used as a positive control for P-Smad1 events in this experiment. In cells transfected with non-targeting oligonucleotide, it is clear that upon BMP treatment, Smad1/5/8 is phosphorylated to the same extent as stimulation with TGF-β (Figure 6.2B, top panel, non-targeting oligo lanes). However, when cells have been depleted of Smad1, both the TGF-β and the BMP inductions of Smad phosphorylation were abrogated. (Figure 6.2B, top panel, Smad1 siRNA panels). This clearly showed the Smad1 was the primary target for these activations. Knockdown of Smad5 also slightly reduced the Smad phosphorylation observed using the anti-P-Smad1/5/8 antibody but transfection with siRNA against Smad8 had no effect (Figure 6.2B, top panel, right). In addition, no differences were observed using siRNA oligonucleotides against Smad2 and Smad3, as expected. This

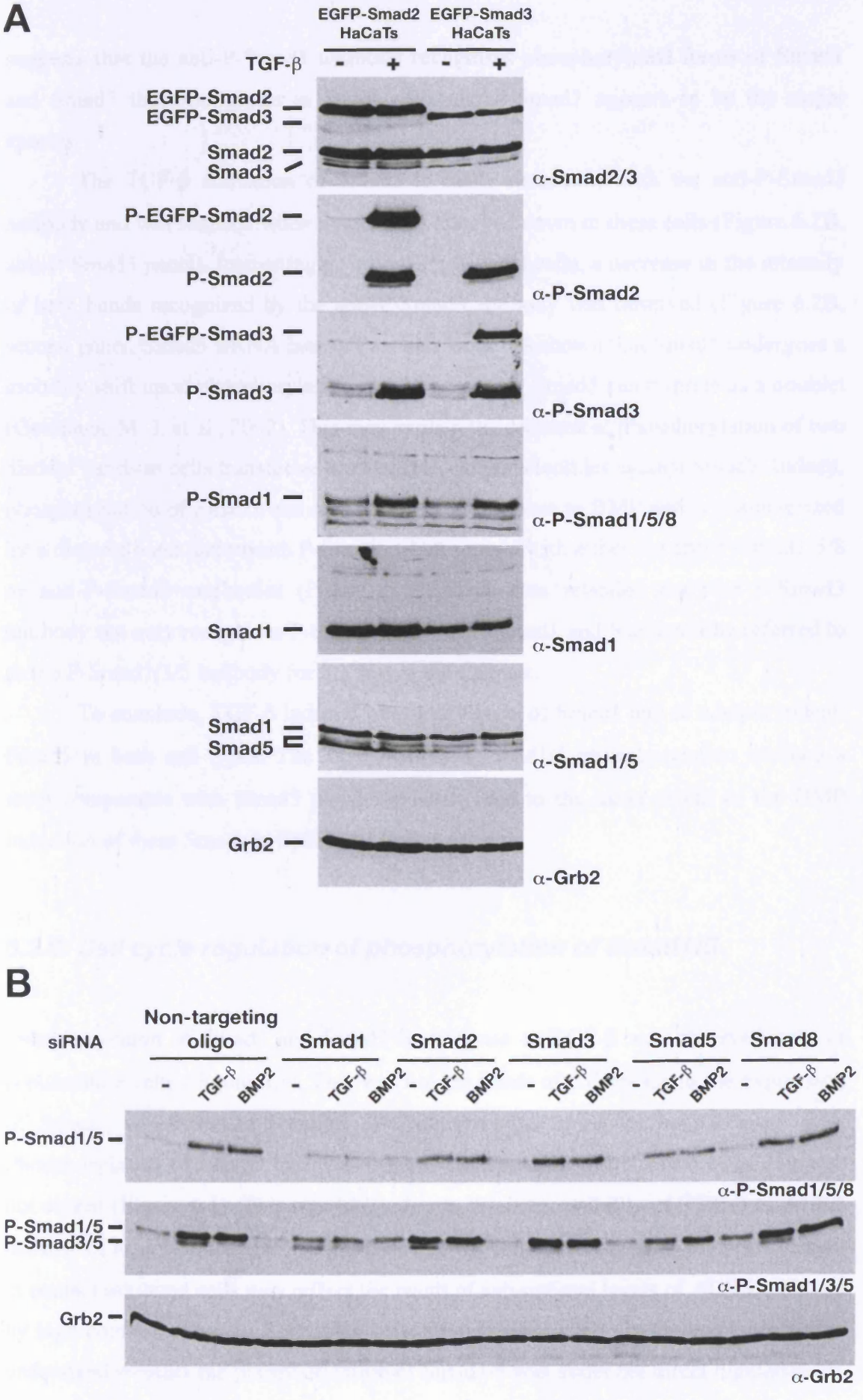
A
EGFP-Smad2 HaCaTs
EGFP-Smad3 HaCaTs
TGF-β
- + - +
EGFP-Smad2
EGFP-Smad3
Smad2
Smad3
α-Smad2/3
P-EGFP-Smad2
P-Smad2
α-P-Smad2
P-EGFP-Smad3
P-Smad3
α-P-Smad3
P-Smad1
α-P-Smad1/5/8
Smad1
α-Smad1
Smad1
Smad5
α-Smad1/5
Grb2
α-Grb2
B
siRNA
Non-targeting oligo
Smad1
Smad2
Smad3
Smad5
Smad8
- TGF-β BMP2
P-Smad1/5
α-P-Smad1/5/8
P-Smad1/5
P-Smad3/5
α-P-Smad1/3/5
Grb2
α-Grb2

suggests that the anti-P-Smad1 antibody recognises phosphorylated forms of Smad1 and Smad5 that comigrates in EpH4 cells and P-Smad1 appears to be the major species.

The TGF-β activation of Smad3 is easily detectable with the anti-P-Smad3 antibody and was reduced when Smad3 was knocked down in these cells (Figure 6.2B, anti-P-Smad3 panel). Interestingly, in Smad5 depleted cells, a decrease in the intensity of both bands recognized by the anti-P-Smad3 antibody was observed (Figure 6.2B, second panel, Smad5 siRNA lanes). Previous work has shown that Smad5 undergoes a mobility shift upon phosphorylation and consequently Smad5 can migrate as a doublet (Goumans, M. J. et al., 2002). This may explain the decrease in phosphorylation of two distinct bands in cells transfected with siRNA oligonucleotides against Smad5. Indeed, phosphorylation of Smad5 was also observed in response to BMP and is characterized by a discrete band underneath P-Smad1 when probed with either the anti-P-Smad1/5/8 or anti-P-Smad3 antibodies (Figure 6.10). This data revealed that the P-Smad3 antibody not only recognizes P-Smad3, but also P-Smad1 and 5 and will be referred to as the P-Smad1/3/5 antibody for the rest of the Chapter.

To conclude, TGF-β induced phosphorylation of Smad1 and to a lesser extent, Smad5 in both cell types. The TGF-β-induced Smad1/5 phosphorylation attained a level comparable with Smad3 phosphorylation, and to the same extent as the BMP induction of these Smads in EpH4 and EpRas cells.

6.2.2 Cell cycle regulation of phosphorylation of Smad1/5

Phosphorylation of Smad1 and Smad5 in response to TGF-β was observed only in proliferating cells (Figure 6.1). This was not the result of a decrease in the expression of Smad1, which stayed constant in cycling versus quiescent cells (Figure 6.3). Phosphorylation of Smad2 and 3 is reduced substantially in quiescent cells, but was not absent (Figure 6.1). This was likely due to the inaccessibility of TGF-β to ALK5 because of high cell density. The absence of TGF-β-induced Smad1/5 phosphorylation in contact inhibited cells may reflect the result of sub-optimal levels of ALK5 achieved by high confluency or the exit of the cells from the cell cycle. In an attempt to better understand whether the phosphorylation of Smad1/5 was under the direct regulation of

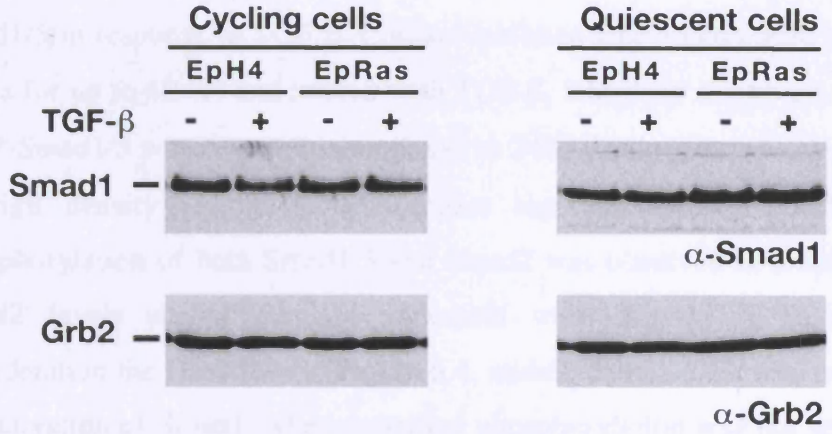

Figure 6.3. Smad1 expression is level thoughout the cell cycle.

Synchronized, quiescent EpH4 and EpRas cells were prepared by contact inhibition for 72 hrs. Actively cycling, low confluency EpH4 and EpRas cells were prepared by synchronizing the cells by contact inhibition and then plating into fresh medium for 24 hrs. Cells were either uninduced or induced with 2 ng/ml TGF-β1 for 1 hr as indicated. Whole cell extracts were prepared and equal amounts of protein were analysed by Western blotting using antibodies against Smad1 and Grb2 as a loading control.

cell cycle components or whether it was affected by a decrease in the availability of ALK5, I tested the effect of cell cycle status on the ability of the cells to phosphorylate Smad1/5 in response to TGF-β. Contact inhibited EpH4 cells were released into fresh media for up to 40 hrs and treated with TGF-β, 1 hr prior to harvest. Neither P-Smad2 nor P-Smad1/5 was detected in response to TGF-β in quiescent cells, presumably due to high density (Figure 6.4, Compare top and middle panels, 0 timepoint). Phosphorylation of both Smad1/5 and Smad2 was observed at 5 hrs after release. P-Smad2 levels stayed relatively constant over the 40 hr release, taking into consideration the Grb2 levels (Figure 6.4, middle panel). This was in sharp contrast to the activation of Smad1, where maximal phosphorylation was not attained until 15-20 hrs. The most obvious difference in the intensity of P-Smad1/5 was observed between 5 hrs and 15 hrs, whereas the P-Smad2 levels were equal at both timepoints (Figure 6.4, top panel).

Cell cycle analysis has revealed that the G0-S phase interval of EpH4 cells under these conditions is ~ 18 hr (Figure 5.2, Figure 6.4 and data not shown), yet significant detection of P-Smad1/5 in response to TGF-β was observed at around 15 hrs. This was not the case for phosphorylation of Smad2. This suggests that maximal phosphorylation of Smad1/5 preceded entry into S-phase with a time lag of about 15 hrs after exit from growth arrest. The absence of phosphorylation of Smad1/5 during quiescence and early G1 suggests the downregulation or deactivation of critical components for this receptor/Smad pathway. The time lag before maximal phosphorylation of Smad1/5 may reflect the requirement of synthesis or activation of key components for this pathway. On the other hand, the expression levels of Smad1 and ALK5 did not alter from cycling to quiescent cells (Figure 5.4 and Figure 6.3) and also the activity of ALK5 was not compromised in early G1, as shown by phosphorylation of Smad2 (Figure 6.4).

From these results, I conclude the requirement of additional components for high levels of phosphorylation of Smad1/5. The expression of these components, for example specific TGF-β receptors, is likely to be dependent on cell cycle status and thus, gives rise to variation in the level of Smad1/5 phosphorylation.

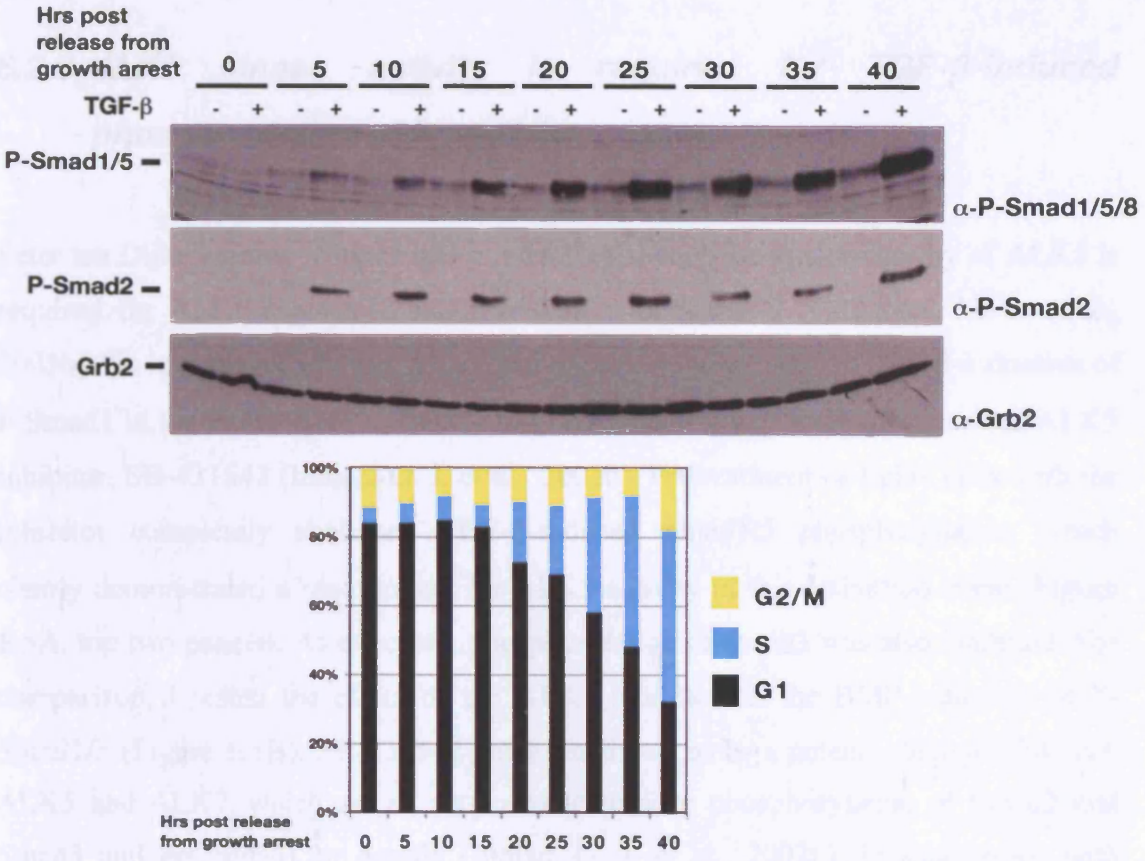

Figure 6.4. Phosphorylation of Smad1/5 is regulated at the level of the cell cycle, where Smad1/5 can only be phosphorylated in cycling cells and not in quiescent cells.

EpH4 were synchronized by contact inhibition and then plated into fresh medium for the number of hours indicated. Cells were either uninduced or induced with 2 ng/ml TGF-β1 for 45 min prior to harvest and then analysed by Western blotting, using antibodies against P-Smad1, P-Smad2 and Grb2 as a loading control. Cells were also analysed by FACS to determine the number of cells in G1 (black bar), S (blue bar) or G2/M (yellow bar).

6.2.3 ALK5 kinase activity is required for TGF-β-induced phosphorylation of Smad1/5

Peter ten Dijke's group showed that in endothelial cells the kinase activity of ALK5 is required for ALK1-dependent phosphorylation of Smad1/5 (Goumans, M. J. et al., 2003b). To investigate whether ALK5 activity was involved in the TGF-β-induction of P-Smad1 in the EpH4 system, I made use of a selective and well characterised ALK5 inhibitor, SB-431542 (Inman, G. J. et al., 2002b). Pretreatment of EpH4 cells with the inhibitor completely abolished TGF-β-induced Smad1/5 phosphorylation, which clearly demonstrated a requirement for ALK5 activity in this activation event (Figure 6.5A, top two panels). As expected, phosphorylation of Smad3 was also inhibited. For comparison, I tested the effect of the ALK5 inhibitor on the BMP-induction of P-Smad1/5 (Figure 6.5B). SB-431542 has been shown to be a potent inhibitor of ALK4, ALK5 and ALK7, which are all proposed to mediate phosphorylation of Smad2 and Smad3 and not Smad1 or Smad5 (Inman, G. J. et al., 2002b). In accordance with previous studies, BMP-induced phosphorylation of Smad1/5 was unaffected by treatment with the inhibitor (Inman, G. J. et al., 2002b). I also examined the nature of the BMP response, to see whether the BMP-induced P-Smad1/5 also exhibited similar cell cycle regulation. A high level of basal BMP-Smad1 signalling was evident in cycling cells but was no longer observed in quiescent cells (Figure 6.5B, top panel). The lack of basal BMP signalling in quiescent cells may reflect the low accessibility of secreted BMP ligand to cell surface receptors in these densely packed cells. BMP induction of P-Smad1/5 was strong in cycling cells and weaker in quiescent cells but was still present, in a similar fashion to P-Smad2 (Figure 6.5B, second panel). Similarly, the reduced level of P-Smad1/5 in quiescent cells was indicative of low accessibility of receptors. However, the ability of these cells to induce Smad1/5 in response to BMP under these conditions, suggests that the components of the BMP signalling receptor complex are functional in quiescent cells, which is sharp contrast to TGF-β-dependent Smad1/5 signalling .

Taken together, these results suggest that a separate receptor complex is involved in the BMP and TGF-β-dependent Smad1/5 phosphorylation.

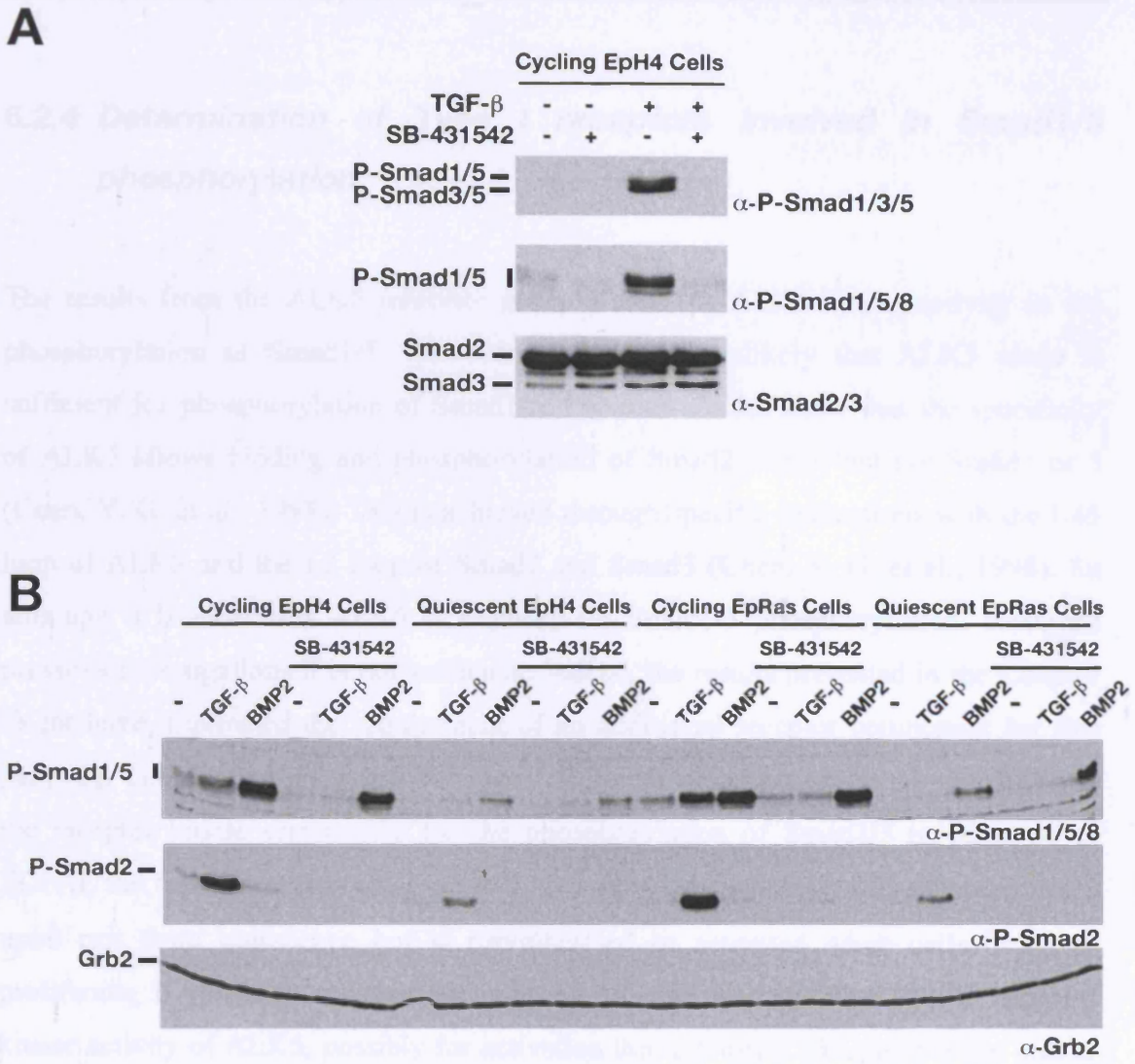

Figure 6.5. ALK5 kinase activity is required for the phosphorylation of Smad1/5 by TGF-β

(A) Inhibition of ALK5 activity by SB-431542 abolishes TGF-β-induced Smad1/5 phosphorylation. EpH4 cells were synchronized by contact inhibition and then plated into fresh medium for 20 hrs. Cells were either untreated or treated with SB-431542 (10 μM) 15 min prior to stimulation with TGF-β1 for 1 hr. Whole cell extracts were prepared and equal amounts of protein were analysed by Western blotting using antibodies against Smad2/3, phosphorylated Smad1/3 (P-Smad1/3), P-Smad1/5/8.
(B) SB-431542 does not inhibit Smad1/5/8 phosphorylation by BMP-2. Synchronized, quiescent EpH4 and EpRas cells were prepared by contact inhibition for 72 hrs. Actively cycling, low confluency EpH4 and EpRas cells were prepared by synchronizing the cells by contact inhibition and then plating into fresh medium for 20 hrs. Cells were either untreated or treated with SB-431542 (10 μM) 15 min prior to stimulation with TGF-β1 or BMP2 for 1 hr as indicated. Whole cell extracts were prepared and equal amounts of protein were analyzed by Western blotting using antibodies against P-Smad1/5/8, P-Smad2 and Grb2 as a loading control.

6.2.4 Determination of Type I receptors involved in Smad1/5 phosphorylation

The results from the ALK5 inhibitor imply a role for ALK5 kinase activity in the phosphorylation of Smad1/5. However, it is highly unlikely that ALK5 alone is sufficient for phosphorylation of Smad1/5. Previous studies show that the specificity of ALK5 allows binding and phosphorylation of Smad2 and 3, but not Smad1 or 5 (Chen, Y. G. et al., 1998). This is achieved through specific interactions with the L45 loop of ALK5 and the L3 loop of Smad2 and Smad3 (Chen, Y. G. et al., 1998). So although it is clear that ALK5 is required for Smad1/5 phosphorylation, based on previous investigations it is not sufficient. Indeed, the results presented in the Chapter so far have implicated the requirement of an additional receptor component for this pathway. The accumulating data have provided some specifications to the regulation of the receptor kinase responsible for the phosphorylation of Smad1/5 in response to TGF-β; the type I receptor can bind and phosphorylate Smad1/5; it is downregulated upon exit from quiescence but is resynthesised or activated when cells begin to proliferate; it works in cooperation with ALK5, and is dependent on the receptor kinase activity of ALK5, possibly for activation through direct phosphorylation and/or recruitment into the TGF-β receptor complex.

With these specifications in mind, I sought to identify the additional component of the functional receptor complex. Firstly, I analysed the expression of all seven TGF-β superfamily type I receptors (ALKs 1-7) by RT-PCR to determine the repertoire of receptors expressed in both EpH4 and EpRas cells (Figure 6.6). Both cell lines express *ALK3* and *ALK5* mRNA. This correlates with their ability to transduce signals via BMP and TGF-β, respectively. They also express equivalent levels of *ALK4* mRNA, which would suggest that they are responsive to Activin. However, ALK4 has the same specificity for Smads as ALK5 and has not been shown to phosphorylate Smad1/5. ALK6, is not expressed, which implies that ALK3 alone is responsible for the BMP signalling in these cells. This is consistent with the restricted ALK6 expression profile in that it is only found in brain and lung (ten Dijke, P. et al., 1994b). ALK1 is not present in EpH4 cells, however, EpRas cells express detectable levels of *ALK1* mRNA in cycling cells and this is upregulated in quiescent cells

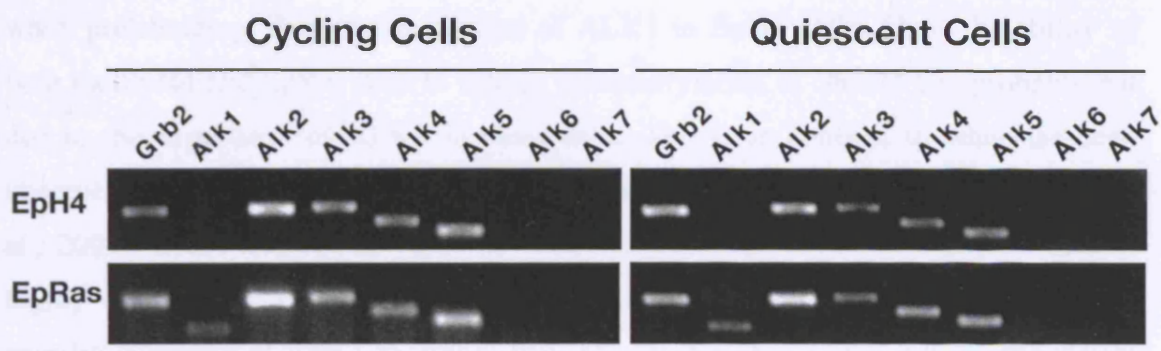

Figure 6.6. Expression of TGF-β type I receptors

The expression of genes encoding the ALK receptors was analysed by reverse-transcription polymerase chain reaction (RT-PCR). RNA was isolated from EpH4 and EpRas cells, both cycling and quiescent cells, and RT-PCR was performed using primers specific for ALKs 1-7 and Grb2 as a control. The amplified product is indicated on the top of the panel. Expression of ALKs 2-5 is observed in both cell lines under the two conditions. ALK1 expression is observed in EpRas cells only. The expression pattern of the receptors in both cycling and quiescent cells is identical in the individual cell lines.

(Figure 6.6). EpH4 and EpRas cells both have an equal ability to phosphorylate Smad1 when proliferating, despite the absence of ALK1 in EpH4 cells. Thus, the ability of both the EpH4 and EpRas cells to induce phosphorylation of Smad1/5 is probably not due to the expression of ALK1 in these cells. This is in contrast to what has been observed in endothelial cells, where expression of ALK1 is high (Goumans, M. J. et al., 2002). EpH4 and EpRas cells, however, express high levels of ALK2, which is highly homologous to ALK1 (Figure 6.6). ALK1 and ALK2 are classified into a specific subgroup of type I receptors that interact with the TβRII but phosphorylate Smad1/5 instead of Smad2/3 (Chen, Y. G. et al., 1999). Furthermore, the highly homologous ALK1 has been shown to form complexes with ALK5, and so it is possible that ALK2 behaves similarly. Thus, ALK2 is a possible candidate for the hetero-dimer complex of type I receptors involved in the phosphorylation of Smad1/5 in EpH4 and EpRas cells.

If downregulation of the receptor kinase is responsible for the cell cycle regulation of the TGF-β-induced P-Smad1/5, a change in the pattern of expression of these type I receptors between cycling and quiescent cells might give an indication of the receptor involved. Unfortunately, apart from an overall decrease in expression levels, no obvious decrease in the mRNA levels of an individual receptor was observed in quiescent cells (Figure 6.6). The expression pattern of the receptors in cycling EpH4 cells is identical to the pattern in quiescent cells, as is also the case for EpRas cells.

Next, I wanted to confirm the contribution of the individual receptors to the Smad1/5 induction in response to TGF-β. This was achieved by depletion of the individual receptors in EpH4 cells by siRNA and by assaying for phosphorylated Smad1/5 in response to TGF-β and to BMP (Figure 6.7A). When antibodies permitted, knockdown of siRNA was verified (data not shown). ALK1, 2 and 6 siRNA oligonucleotides had no effect on the ability of Smad1/5 to be phosphorylated in response to either TGF-β or BMP or on the basal level of P-Smad1/5 (Figure 6.7A). This result disagreed with the idea of ALK2 as a possible candidate for the receptor kinase responsible for Smad1/5 phosphorylation. Depletion of ALK2 could not be verified, however, by analysis of protein knockdown due to lack of specific antibodies. To overcome this hurdle, more attempts were made to ensure knockdown of ALK2 by use of oligonucleotides from another supplier. Regardless of this, similar results were

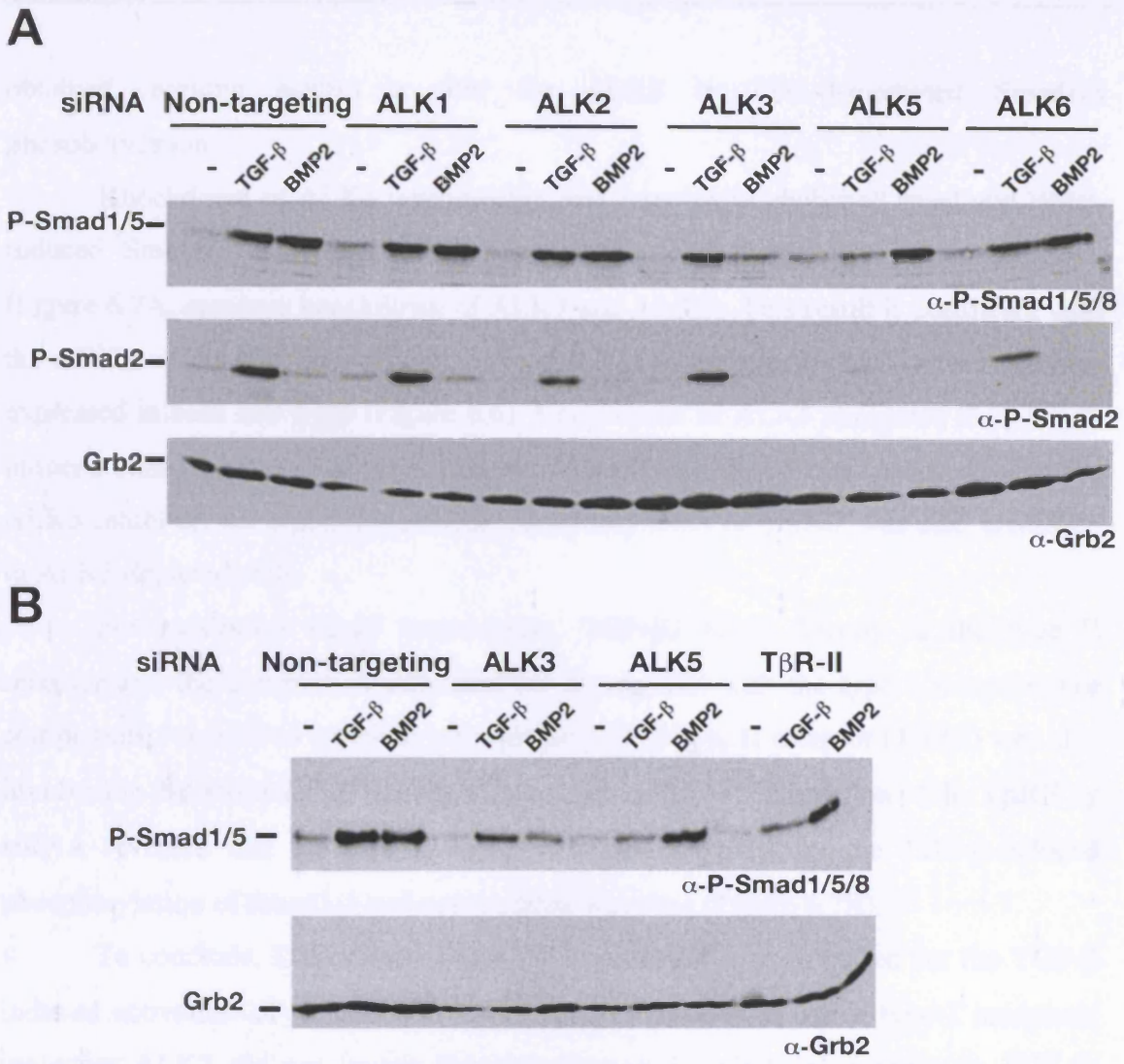

Figure 6.7. ALK5 is required for TGF-β-induced Smad1/5 phosphorylation, whereas ALK3 is responsible for basal and BMP induced Smad1/5 phosphorylation

(A) ALK1, ALK2, ALK3 and ALK6 are not involved in TGF-β-induced Smad1/5 phosphorylation. Low-density EpH4 cells were transfected with siRNA oligos against the ALKs or a non-targeting oligo. After 48 hrs of incubation, cells were trypsinised and plated out into fresh medium for 20 hrs. Cells were either uninduced or stimulated with TGF-β1 or BMP2 for 45 min as indicated. Whole cell extracts were prepared, fractionated by SDS-PAGE and analysed by Western blotting using antibodies against P-Smad1/5/8, P-Smad2 and Grb2 as a control for protein loading.
(B) TβRII is also required for TGF-β-induced Smad1/5 phosphorylation. Low-density EpRas cells were transfected with siRNA oligos against the ALK3, ALK5 and TβRII or a non-targeting oligo. Cells were harvested as in (A) and analysed by Western blotting using antibodies against P-Smad1/5/8 and Grb2 as a loading control.

obtained, arguing against a role for ALK2 in TFG-β-mediated Smad1/5 phosphorylation.

Knockdown of ALK3 reproducibly and completely abolished basal and BMP-induced Smad1/5 phosphorylation, whereas the TGF-β response was unchanged (Figure 6.7A, compare knockdown of ALK3 and ALK6). This result is consistent with the mRNA expression data, which shows that ALK3 is the only BMP type I receptor expressed in both cell types (Figure 6.6). Knockdown of ALK5 abrogated the TGF-β-induced phosphorylation of Smad1/5, which confirmed the results obtained using the ALK5 inhibitor. As a positive control, phosphorylation of Smad2 was also abolished in ALK5 depleted cells.

For successful signal transduction, TGF-β1 binds directly to the type II receptor and the complex is stabilized by interactions with the type I receptor. For completion, I wanted to establish whether the TGF-β type II receptor (TβRII) was also involved in the activation of Smad1/5 in response to TGF-β. Depletion of the TβRII by siRNA revealed that the type II receptor is also required for the TGF-β-induced phosphorylation of Smad1/5 and not the BMP response (Figure 6.7B).

To conclude, I have shown that TβRII and ALK5 are required for the TGF-β induced activation of Smad1/5 in EpH4 cells. Depletion of other type I receptors, including ALK2 did not impair the activation of Smad1/5 in response to TGF-β. However, as ALK5 alone is unable to phosphorylate BMP-Smads (Chen, Y. G. et al., 1998), it is unlikely that it is the sole component of the TGF-β-Smad1/5 signalling complex. Therefore, I hypothesise the involvement of an additional receptor kinase. In addition, ALK3 is required for the basal level and BMP-induction of P-Smad1/5.

6.2.5 High Doses of TGF-β are required for phosphorylation of Smad1/5

Next, I went on to further analyse the possibility of a heteromeric type I receptor complex containing ALK5 with another type I receptor and this complex being responsible for TGF-β-induced P-Smad1/5. I tested this hypothesis biochemically, by investigating the induction of phosphorylated Smad1/5 and comparing it with the

induction of phosphorylated Smad3. Firstly, I examined the effect of different doses on TGF-β-induced Smad3 versus Smad1/5 phosphorylation in both EpH4 and EpRas cells (Figure 6.8A). TGF-β induced considerable Smad3 phosphorylation at 0.2 ng/ml and reached a maximum at 1.6 ng/ml, which remained at this level at all higher doses of TGF-β in both cell types. The requirement for high concentrations of TGF-β1 was made more apparent when the basal BMP signalling was reduced by siRNA knockdown of ALK3 (Figure 6.8B, right hand side). Here, phosphorylation of Smad3 is observed even at 0.1 ng/ml, whereas Smad1/5 is only induced when stimulated with a dose of 1.6 ng/ml or higher. The requirement of an 8-10 fold higher concentration of ligand has also been shown for ALK1 phosphorylation of Smad1 compared with phosphorylation of Smad2 via ALK5 in response to TGF-β in primary endothelial cells (Goumans, M. J. et al., 2002). The difference in dose response in this latter case was attributed to the different affinities of ALK1 and ALK5 for TGF-β ligand (Goumans, M. J. et al., 2002; ten Dijke, P. et al., 1994a).

I also compared the dose responses of TGF-β1 with TGF-β3, whose activities have been shown to exhibit different physiological responses *in vivo* (Brunet, C. L. et al., 1995). The dose response profile of TGF-β3 was similar to the TGF-β1 profile in that Smad1/5 required a higher concentration of this isoform for maximal phosphorylation. However, differences were also observed, in that TGF-β3 phosphorylated both Smad1/5 and Smad3 at lower concentrations than TGF-β1 (Figure 6.9). This difference may reflect a higher binding affinity of TGF-β3 to both homomeric and heteromeric type I complexes and may have significant consequences *in vivo*.

From these results, I conclude that the activation of Smad1/5 requires higher concentrations of ligand than is required for phosphorylation of Smad3. This has been shown for two of the TGF-β isoforms, TGF-β1 and TGF-β3. This suggests that the phosphorylation of Smad1/5 in response to TGF-β is dependent on a lower affinity receptor complex than phosphorylation of Smad3. Moreover, this evidence supports the hypothesis whereby a lower affinity ALK5/type I heteromeric receptor complex activates Smad1/5 whereas the ALK5 homomeric complex induces Smad2/3 activation in response to TGF-β.

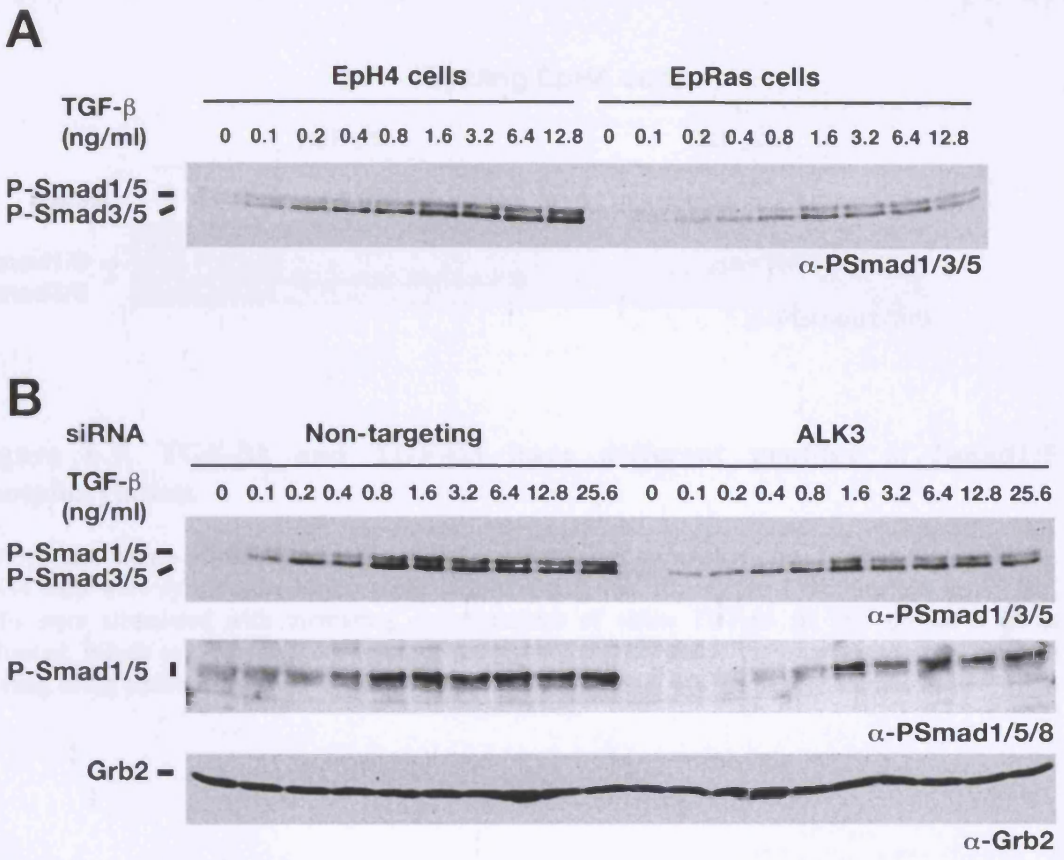

Figure 6.8. High doses of ligand are required for TGF-β-induced Smad1/5/8 phosphorylation

(A) EpH4 and EpRas cells were synchronized by contact inhibition and then plated into fresh medium for 20 hrs. Cells were stimulated with increasing concentrations of TGF-β1 for 1 hr at 37°C before lysis. Whole cell extracts were prepared and equal amounts of protein were analyzed by Western blotting using antibodies against P-Smad1/3/5.

(B) Reduction of ALK3 basal Smad1/5 phosphorylation accentuates the high dose requirement of TGF-β1. SiRNA oligos against ALK3 or a non-targeting oligo were transfected into low density EpH4 cells. After 48 hrs of incubation, cells were trypsinised and plated out into fresh medium for 20 hrs. Cells were stimulated with increasing concentrations of TGF-β1 for 1 hr at 37°C as indicated. Whole cell extracts were prepared and analysed by Western blotting using antibodies against P-Smad1/5/8, P-Smad1/3/5 and Grb2 as a loading control. The blot probed with α-P-Smad1/3/5 antibodywas stripped and reprobed with α-P-Smad1/5/8 antibody.

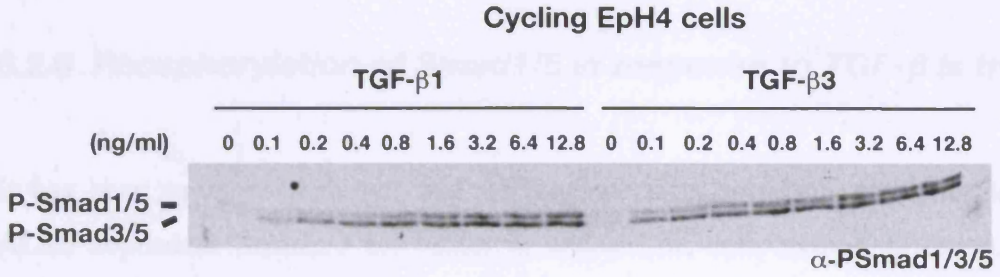

Figure 6.9. TGF-β1 and TGF-β3 have different profiles of Smad1/5 phosphorylation.

TGF-β3 can induce Smad1/5 phosphorylation at much lower concentrations of ligand than TGF-β1. EpH4 cells were synchronized by contact inhibition and then plated into fresh medium for 20 hrs. Cells were stimulated with increasing concentrations of either TGF-β1 or TGF-β3 for 1 hr as indicated. Whole cell extracts were prepared and equal amounts of protein were analysed by Western blotting using antibodies against P-Smad1/3/5.

6.2.6 Phosphorylation of Smad1/5 in response to TGF-β is transient

It has been previously shown that ALK1-dependent Smad1/5 phosphorylation and ALK5-dependent Smad2/3 activation in endothelial cells exhibit differences in the kinetics of Smad phosphorylation. To investigate whether the different receptor signalling complexes in the EpH4 and EpRas cells exhibited similar differences, I determined the kinetics of TGF-β-induced Smad1/5 versus Smad3 phosphorylation (Figure 6.10A). After 15 min of continuous TGF-β stimulation, Smad1/5 and Smad3 are efficiently phosphorylated and the levels of P-Smad1/5 and P-Smad3 peak at approximately 30 min after TGF-β stimulation. P-Smad3 declined after 4 hr but did not decrease to zero even after 8 hr. Note that the lower band of the anti-P-Smad3/5 blot comprises mainly of P-Smad3 (Figure 6.2). These results are consistent with the duration of signalling observed in the human keratinocyte cell line HaCaT (Inman, G. J. et al., 2002c). In contrast, however, TGF-β-induced Smad1/5 phosphorylation is dramatically reduced by 2 hr and absent 4 hr after stimulation, as determined by the anti-P-Smad1/5/8 antibody, which does not recognize any P-Smad3. The same behaviour is observed for the upper band of the P-Smad1/3/5 blot, which comprises P-Smad1/5. Conversely, BMP-induced Smad1/5 remained phosphorylated after 8 hr of ligand stimulation (Figure 6.10B). The disparity in signalling duration of the individual Smad pathways strongly suggests the existence of a receptor kinase in addition to ALK5, which may be differentially regulated and exhibits distinct properties.

To further analyse the mechanism underlying the transient P-Smad1/5 phosphorylation, I treated the cells with the protein synthesis inhibitor, cycloheximide. Valdomarsdottir and colleagues previously investigated the temporal activation of the ALK1-induced Smad1/5 phosphorylation in endothelial cells and discovered it was affected by *de novo* protein synthesis (Valdimarsdottir, G. et al., 2006). Indeed, compared to control EpH4 cells, the TGF-β-induced Smad1/5 phosphorylation in cyclohexamide-treated cells was more sustained and lasted at least 8 h (Figure 6.11A). These results suggest that TGF-β-induced Smad1/5 signalling is attenuated by newly synthesized proteins, whereby the activity of the receptor kinase responsible for the phosphorylation is compromised.

In BMP-treated cells a different scenario is evident. In cells not treated with cycloheximide, there is a slow trailing off of the P-Smad1/5 signal after 2 hr of

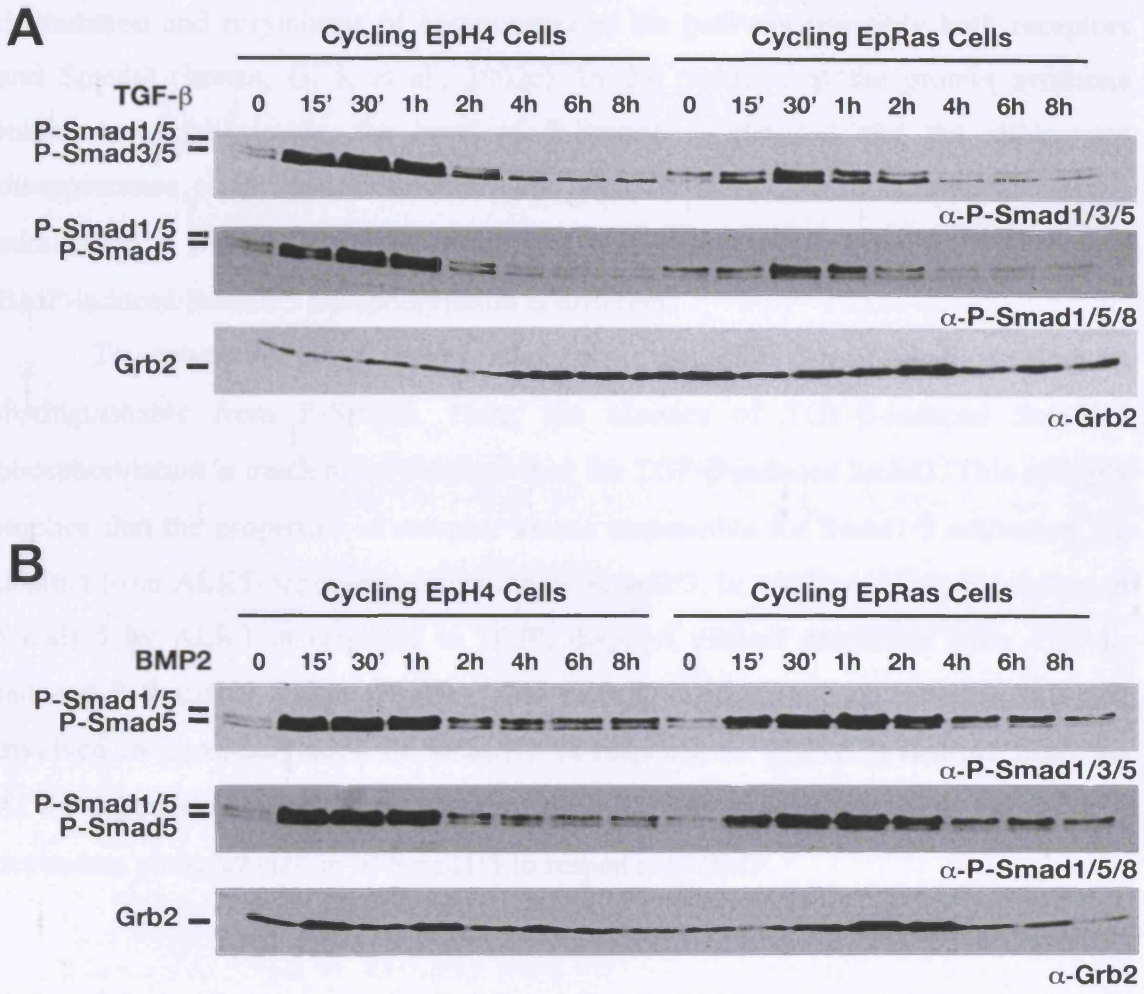

Figure 6.10. TGF-β-induced Smad1/5 phosphorylation occurs transiently

(A) TGF-β-induced Smad1/5 phosphorylation is transient and absent 4 h after stimulation. EpH4 and EpRas cells were synchronized by contact inhibition and released into the cell cycle for 20 hrs before stimulation with TGF-β1 (2 ng/ml) for different time periods. Whole cell lysates were fractionated by SDS-PAGE and analysed by Western blotting with antibodies against P-Smad1/3/5, P-Smad1/5/8 and Grb2 as a control for protein loading.To note, this is the same experiment that was used for Figure 5.3 (B) BMP-induced Smad1/5 phosphorylation is stable for at least 8 hrs. Synchronized, cycling EpH4 and EpRas cells were stimulated with BMP2 (40 ng/ml) for different time periods at 37°C before lysis. Whole cell extracts were prepared and analysed by Western blotting as in (A). The blots probed with α-P-Smad1/5/8 antibody in (A) and (B) were stripped and reprobed with α-P-Smad1/3/5 antibody.

continuous stimulation (Figure 6.11B). This is likely due to a combination of degradation and resynthesis of components of the pathway (possibly both receptors and Smads) (Inman, G. J. et al., 2002c). In the presence of the protein synthesis inhibitor, cycloheximide, the level of P-Smad1 is elevated and the subsequent disappearance of P-Smad1/5 occurs more abruptly after 2 hr of continuous TGF-β stimulation. It is clear from these results that the negative regulation of the TGF-β- and BMP-induced Smad1/5 phosphorylation is different.

To conclude, these results show that the TGF-β-induced P-Smad1/5 is distinguishable from P-Smad3. Here, the kinetics of TGF-β-induced Smad1/5 phosphorylation is much more transient than the TGF-β-induced Smad3. This strongly implies that the properties of receptor kinase responsible for Smad1/5 activation are distinct from ALK5-dependent activation of Smad2/3. In addition, phosphorylation of Smad1/5 by ALK3 in response to BMP, displays distinct properties from TGF-β-induced P-Smad1/5. Taken together, this stongly implies that the receptor complex involved in phosphorylation of Smad1/5 in response to TGF-β is distinct from the ALK5-dependent Smad2/3 activation upon TGF-β stimulation and the ALK3-dependent phosphorylation of Smad1/5 in response to BMP.

6.2.7 Distinct downstream targets of BMP- and TGF-β-induced Smad1

Cell cycle dependence, receptor requirement and kinetics of activation in response to ligand have revealed obvious differences in the regulation of BMP- and TGF-β-induced P-Smad1/5. I wanted to investigate further the extent to which these responses varied, in the hope that this may shed some light on the origin of the TGF-β-induced Smad1/5 phosphorylation. First, I assayed the transcriptional response of TGF-β- and BMP-induced EpH4 and EpRas cells using a BMP-specific transcriptional reporter, the (BRE)-luc. The BRE-luc consists of two repeats of a BMP response element (BRE) from the Id1 promoter, and is used as a transcriptional readout for BMP-Smad1/5 signalling (Korchynskyi, O. et al., 2002). In endothelial cells, stimulation with TGF-β induced weak BRE-luc activity (~3 fold) and therefore, activation of ALK1 in

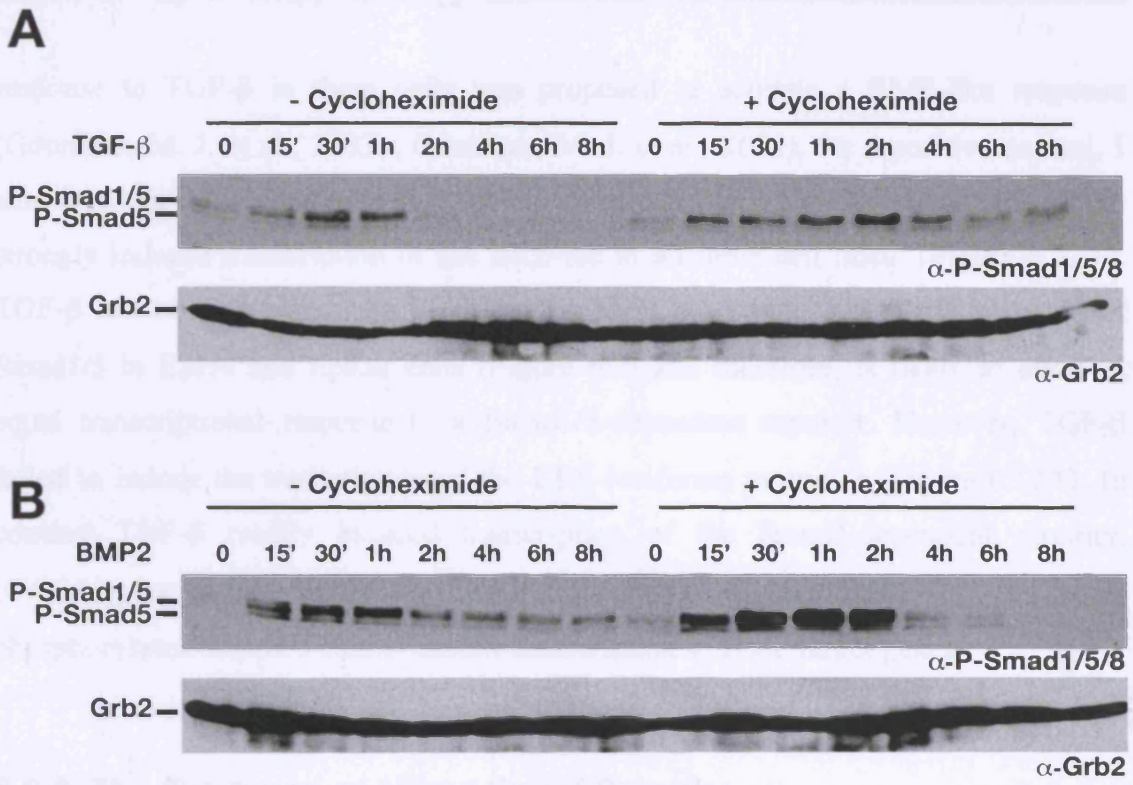

Figure 6.11. TGF-β– and BMP-induced Smad1/5 phosphorylation is regulated by *de novo* protein synthesis

(A) TGF-β-induced Smad1/5 phosphorylation is more sustained in the absence of protein synthesis. Synchronized, cycling EpH4 were either untreated or treated with the protein synthesis inhibitor, cyclohexamide (20 μg/ml), 15 minutes before they were stimulated with TGF-β1 (2 ng/ml) for different time periods, as indicated. Whole cell lysates were fractionated by SDS-PAGE and analysed by Western blotting with antibodies against P-Smad1/5/8 and Grb2 as a control for protein loading.

(B) Sustained BMP-induced Smad1/5 phosphorylation requires *de novo* protein synthesis. Synchronized, cycling EpH4 were either untreated or treated with the protein synthesis inhibitor, cyclohexamide (20 μg/ml), 15 minutes before they were stimulated with BMP2 (40 ng/ml) for different time periods at 37°C before lysis. Whole cell extracts were prepared and analysed by Western blotting as in (A).

response to TGF-β in these cells was proposed to activate a BMP-like response (Goumans, M. J. et al., 2003b; Goumans, M. J. et al., 2002). As a positive control, I stimulated EpH4, EpRas cells also the myoblast cell line, C2C12, with BMP2, which strongly induced transcription of the BRE-luc in all three cell lines (Figure 6.12A). TGF-β has been shown to be as potent as BMP in stimulating phosphorylation of Smad1/5 in EpH4 and EpRas cells (Figure 6.2) and therefore, is likely to elicit an equal transcriptional response to a Smad1/5-dependent reporter. However, TGF-β failed to induce the transcription of the BRE-luciferase promoter (Figure 6.12A). In contrast TGF-β readily induced transcription of the Smad3-dependent reporter, $(CAGA)_{12}$-luc in both EpH4 and EpRas cells (Figure 6.12B). Thus, TGF-β-induced phosphorylated Smad1/5 cannot initiate transcription of BMP target genes.

6.2.8 The Existence of Mixed Smad Complexes

The inability of TGF-β to induce a BMP responsive, Smad1/5-dependent reporter raised many questions. From previous studies it has been shown that BMP stimulation results in the phosphorylation of the BMP R-Smads, Smad1, Smad5 or Smad8, which then form complexes with Smad4 and accumulate in the nucleus (ten Dijke, P. et al., 2003). BMP R-Smad-Smad4 complexes then engage in specific DNA binding and recruitment of transcription cofactors to regulate transcription. If Smad1/5 do not form complexes with Smad4 in response to TGF-β, this might explain the failure to induce BMP-responsive elements. To investigate if Smad1 can still form complexes with Smad4 in these cells, I analysed the ability of Smad1 to form complexes with other Smads in response to TGF-β and BMP2. EpH4 whole cell extracts were used to immunoprecipitate endogenous Smads using antibodies specific to Smads1, 2, 3 and 4. As previously reported, Smad2 and Smad3 co-precipitated Smad4 in response to TGF-β specifically and not BMP2 (Figure 6.13A, compare lanes 11 and 14 with lanes 12 and 15). Smad4 could interact with P-Smad2 and P-Smad1, in response to TGF-β and BMP2, respectively (Figure 6.13A, lanes 17 and 18). This interaction was weak in both cases. Interestingly, Smad1 co-immunoprecipitated Smad4 only after stimulation with BMP, and not TGF-β (Figure 6.13A, compare lanes 8 and 9). Also Smad2, and

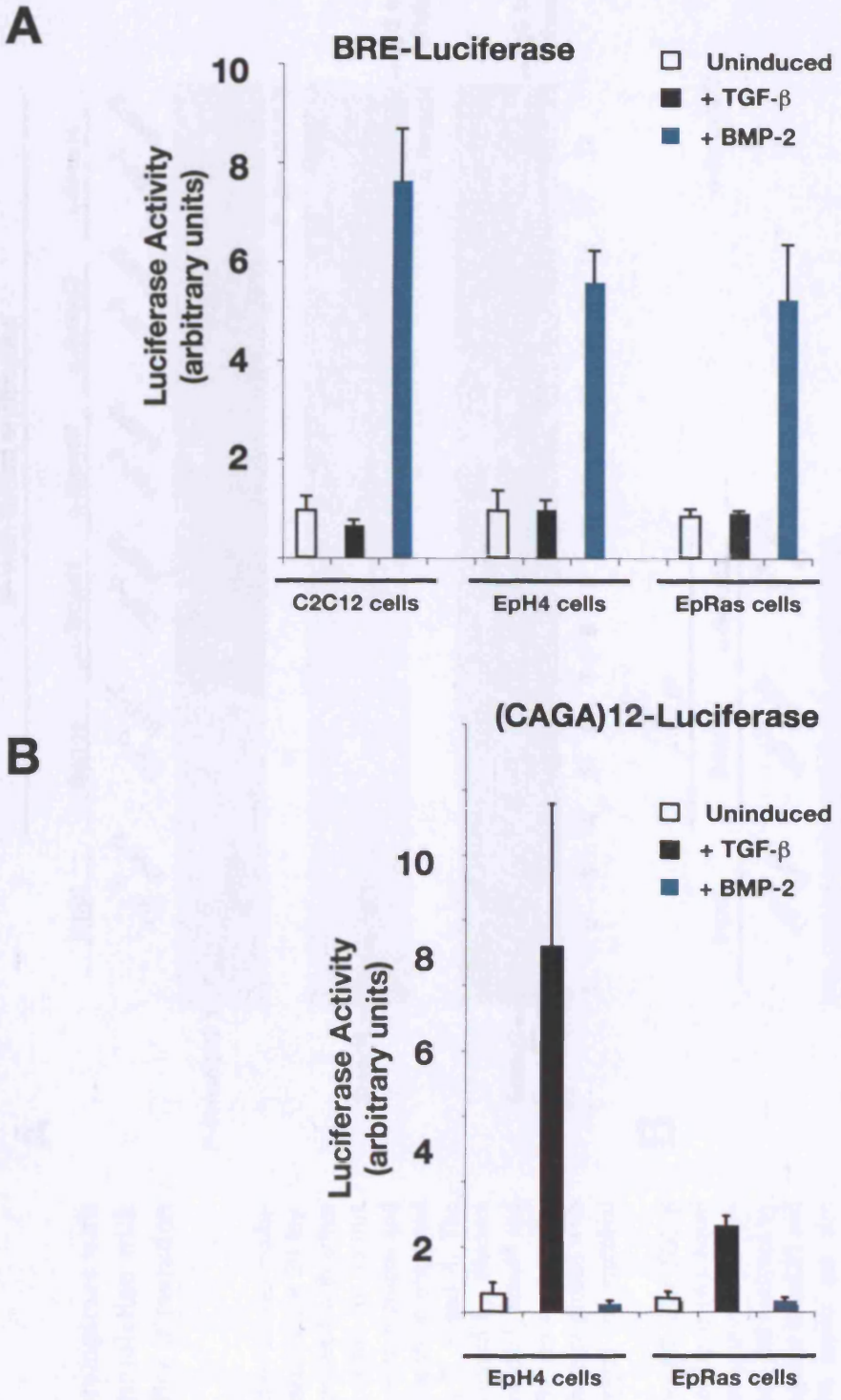

Figure 6.12. BMP-induced Smad1/5 phosphorylation induces transcription from a BMP-responsive element, wheras TGF-β-induced Smad1/5 phosphorylation fails to activate transcription from this promoter

BMP-induced BRE-luc transcriptional activation in EpH4 and EpRas cells is comparable with the BMP-response of the myoblast cell line, C2C12. TGF-β-induced Smad1/5 phosphorylation has no transcriptional activity from this Smad1-dependent reporter. C2C12, EpH4 and EpRas cells were transfected with the BRE-luciferase reporter. After overnight incubation, the cells were replated into fresh medium for 16 hrs before induction with TGF-β for 8 hrs. Luciferase activity was assayed and quantitated relative to β-galactosidase from the pEFLacZ internal control. The data are the means and standard deviations of three independent experiments.

Figure 6.13. Smad1 forms complexes with Smad2 and Smad3 after stimulation with TGF-β, and with Smad4 after stimulation with BMP

(A) EpH4 cells were synchronized by contact inhibition and then plated into fresh medium for 20 hrs. Cells were either untreated or stimulated with either TGF-β1 (2 ng/ml) or BMP2 (40 ng/ml) for 45 min before lysis. Whole cell extracts were prepared and equal amounts of protein were immuoprecipitated with antibodies against Smads1, 2, 3 and 4. The immunoprecipates (IPs) were analysed by Western blotting with antibodies against Smad2/3, Smad4 and P-Smad1/5/8. As a control, 20% inputs are also shown on the left of the panel. The blot probed with α-P-Smad1/5/8 antibody was stripped and reprobed with α-Smad2/3 antibody.

(B) Smad1 immunoprecipitates Smad2 after TGF-β induction. EpH4 cells were prepared as in (A). Equal amounts of whole cell extract were immuoprecipitated with antibodies against Smad1 and analysed by Western blotting with antibodies against Smad2/3 and P-Smad1/5/8. As a control, 10% inputs are also shown. the asterisk indicates an aspecific band recognised by the antibody.

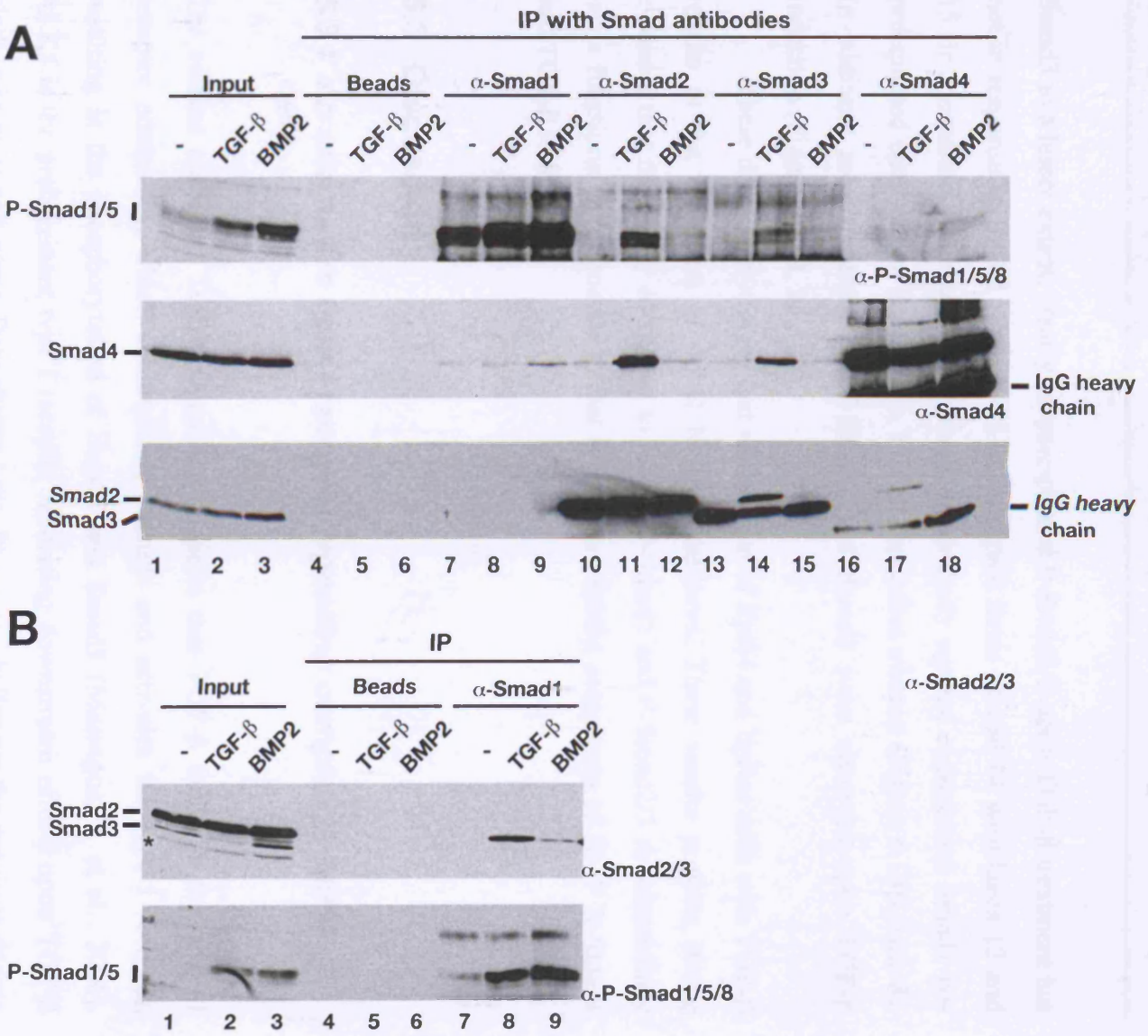

Smad3 to a lesser extent, clearly co-precipitated P-Smad1/5 upon TGF-β treatment but not in response to BMP2 (Figure 6.13A, compare lanes 11 and 14 with lanes 12 and 15. In a separate, reciprocal experiment, an antibody against endogenous Smad1 co-precipitated endogenous Smad2 in a TGF-β dependent manner (Figure 6.13B, lane 8). In addition, mixed complexes of Smad2 and Smad3 were observed upon TGF-β induction (Figure 6.13B, lane 14).

These data clearly reveal that stimulation of EpH4 and EpRas cells with TGF-β results in the formation of novel Smad complexes. These results provide strong evidence that the ability of TGF-β to induce P-Smad1 and P-Smad2/3 simultaneously has a functional consequence in that it produces mixed complexes of BMP R-Smads and TGF-β R-Smads.

6.3 Discussion

6.3.1 An alternative type I receptor signalling complex in EpH4 cells

The current model of TGF-β signalling suggests that TGF-β binds to the type II receptor complexes, which subsequently recruits and activates the type I receptor, resulting in the phosphorylation of Smad2 and Smad3 (Massague, J. et al., 2006). ALK5 is the predominant type I receptor mediating downstream effects upon TGF-β binding in most cell types. Data shown here, however, challenges the previous dogma regarding receptor complexes and signal transduction schemes. I propose a novel paradigm for TGF-β signalling in mammary epithelial cells, in which the same ligand can activate two different classes of Smad through a heteromeric type I receptor complex, comprising of ALK5 and as yet, an unidentified receptor kinase. This dual activation results in the formation of novel heteromeric complexes containing R-Smads from two distinct Smad pathways. These 'mixed' complexes fail to induce transcription from defined promoter elements, but most likely induce transcription of a unique set of genes.

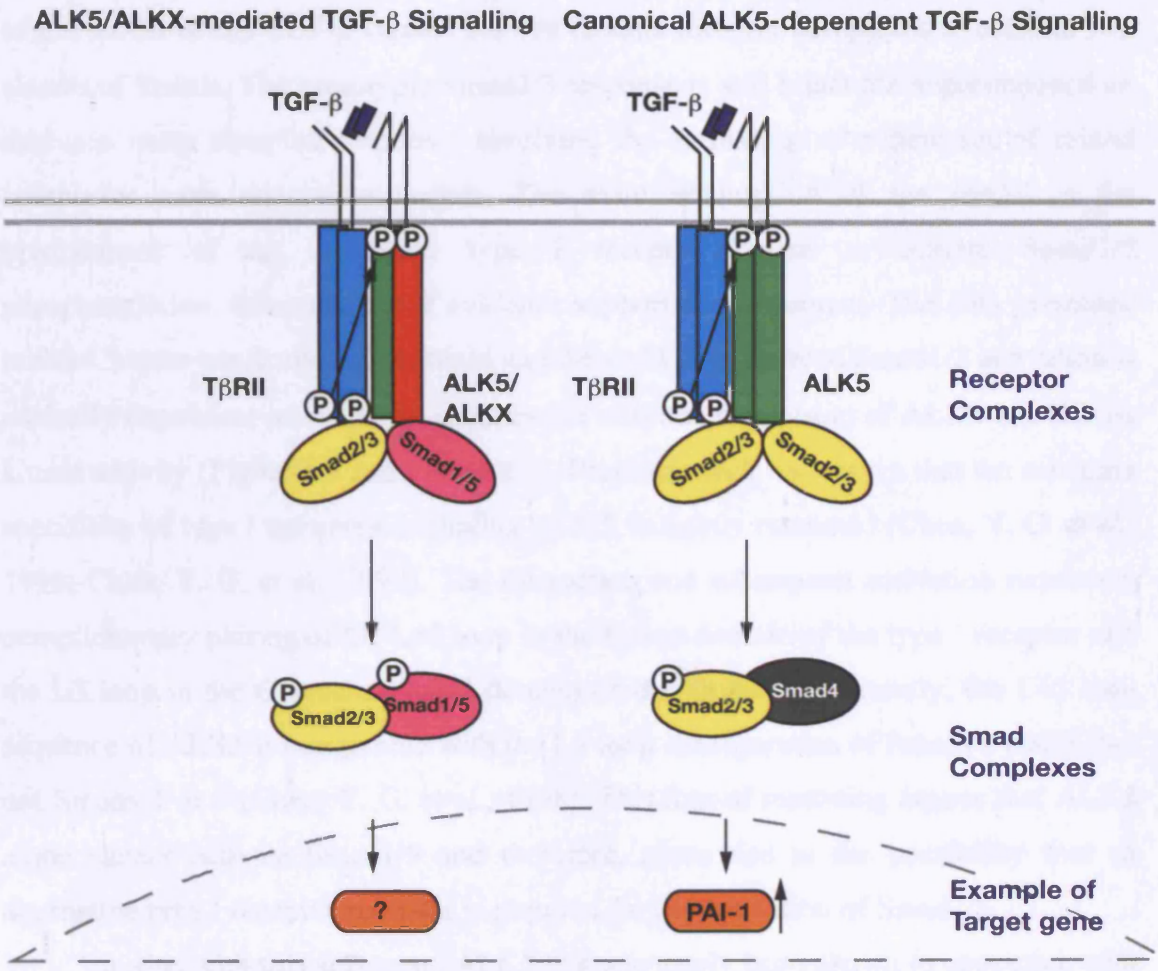

Figure 6.14 Two pathways signal downstream of TGF-β in EpH4 and EpRas cells

Schematic illustration of the signalling events downstream of TGF-β binding in mouse mammary epithelial cells. See text for discussion. For simplicity, Smad complexes are portrayed as dimers.

A model is shown in Figure 6.14 to depict the dual signalling pathways. The essence of the model is that TGF-β signals via two distinct receptor complexes to activate two classes of Smads. The prototypic Smad2/3 response is still intact but superimposed on this is a more complex response, involving the formation of a new set of mixed complexes with alternative targets. The main assumption of the model is the involvement of an additional type I receptor kinase to initiate Smad1/5 phosphorylation. Several lines of evidence support this argument. The data presented in this Chapter confirms that the rapid and direct TGF-β-induced Smad1/5 activation is critically dependent on ALK5. It requires not only the expression of ALK5 but also its kinase activity (Figure 6.5 and Figure 6.7). Previous work has shown that the substrate specificity of type I receptors, including ALK5, is tightly restricted (Chen, Y. G. et al., 1998; Chen, Y. G. et al., 1999). The interaction and subsequent activation requires a complimentary pairing of the L45 loop in the kinase domain of the type I receptor and the L3 loop in the C-terminal MH2 domain of the Smad. Importantly, the L45 loop sequence of ALK5 is compatible with the L3 loop configuration of Smads 2 and 3, but not Smads 1 or 5 (Chen, Y. G. et al., 1998). This line of reasoning argues that ALK5 alone cannot activate Smad1/5 and therefore, gives rise to the possibility that an alternative type I receptor complex is required for the activation of Smad1/5.

In line with this argument, ALK5 has previously been shown to cooperate with another type I receptor, ALK1, to induce phosphorylation of Smad1/5 (Goumans, M. J. et al., 2003a). Goumans *et al.* showed that in endothelial cells, ALK5 can recruit ALK1 to form a heteromeric type I complex which can then induce phosphorylation of Smad1/5 in a TGF-β dependent manner. In this study they showed that TGF-β binding results in the complex formation of a heterodimer of ALK1 and ALK5, together with a TβRII homodimer, and that Smad1/5 phosphorylation requires active kinase domains of all three receptor types.

The evidence revealed in this Chapter supports the role of an alternative receptor kinase in the TGF-β-induced Smad1/5 phosphorylation. The first piece of data that alluded to the possibility of an additional signalling component, was the observation that quiescent cells are unable to induce Smad1/5 phosphorylation in response to TGF-β but Smad2 is activated in response to TGF-β in quiescent cells (Figure 6.1). This immediately suggested that the activity of the receptor responsible for this phosphorylation event was compromised in quiescent cells. This may be due to

downregulation of the receptor or an inactive form of the receptor under these conditions. This observation does not appear to be explained through the regulation of ALK5 in this case as both protein levels and activity of ALK5 do not alter between cycling and quiescent cells. mRNA levels of ALK5 were not dramatically reduced in quiescent cells (Figure 6.6), and as shown in Chapter 5, the level of ALK5 protein does not alter significantly between cycling cells and quiescence. In support of this argument, I showed the requirement of 10 to 15 hrs post release from growth arrest to restore optimal activation of Smad1/5, whereas Smad2 phosphorylation is restored immediately. This distinction highlights the requirement for an additional component for Smad1/5 phosphorylation. The time lag may reflect the time taken for new protein synthesis and accumulation of receptor or possibly a co-receptor as the cells re-enter the cell cycle.

Type I receptors bind with different affinities to their ligands. The apparent affinity of TGF-β for ALK5 was found to be higher than for ALK1 (ten Dijke, P. et al., 1994a). As a result, the heterodimeric ALK1/ALK5 type I complex exhibited differential dose responses to TGF-β than ALK5 homodimers (Goumans, M. J. et al., 2002). Consistent with the hypothesis that ALK5 heterodimers also signal via Smad1/5 in EpH4 cells, about a ten-fold higher concentration of ligand was required for Smad1/5 phosphorylation compared with the ALK5-induced Smad3 phosphorylation (Figure 6.8). This suggests that TGF-β also has a lower affinity for the receptor kinase involved in Smad1/5 phosphorylation than for ALK5. It is possible that this difference in affinity may function to regulate the balance of the two pathways downstream of TGF-β *in vivo*.

The duration of the TGF-β signal is dependent on the lifetime of active receptor as Smads continuously cycle between the nucleus and the cytoplasm, enabling them to sense receptor activity (Inman, G. J. et al., 2002c). Negative regulation is exerted on type I receptors to extinguish the signal via dephosphorylation, inactivation and/or degradation of the receptors (Ebisawa, T. et al., 2001; Kavsak, P. et al., 2000; Shi, W. et al., 2004; Valdimarsdottir, G. et al., 2006). Here I show a clear distinction between the regulation of ALK5 kinase activity and that of the heteromeric complex responsible for P-Smad1/5 by direct comparison of signal duration. Whereas, P-Smad3 is still present at 8 hrs after TGF-β stimulation, P-Smad1/5 is much more transient and is completely absent after 4 hrs of induction (Figure 6.10). Once again, these

differences in the Smad2/3 and the Smad1/5 pathway downstream of TGF-β suggest the existence of an alternative ALK5 containing receptor complex. It is also important to note that the duration of the BMP-induced P-Smad1/5 has a completely distinct profile from the P-Smad1/5 phosphorylation in response to TGF-β. This is consistent with the data that suggests ALK3 is responsible for BMP-induced P-Smad1/5, whereas an ALK5 heteromeric receptor complex mediates phosphorylation of Smad1/5 in response to TGF-β.

The ALK1-induced phosphorylation of Smad1/5 in endothelial cells was also observed to be short lived, which was later shown to be due to dephosphorylation and inactivation of ALK1 by PPIα, which required *de novo* protein synthesis (Valdimarsdottir, G. et al., 2006). In EpH4 cells, a similar result was observed, in that when protein synthesis was inhibited, P-Smad1/5 levels were sustained until at least 8 hrs after stimulation with TGF-β (Figure 6.11). However, previous studies on the duration of Smad2 signalling in HaCats shows that the disappearance of P-Smad2 occurs more abruptly in the presence of cycloheximide, approximately 2 hr after continuous TGF-β stimulation (Inman, G. J. et al., 2002c). This is similar to the observed effect on BMP-induced Smad1/5 phosphorylation in the presence of cycloheximide. The effect of prolonged TGF-β-induced Smad1/5 phosphorylation when protein synthesis is blocked suggests that the receptor kinase is regulated negatively, independently of ALK5 but dependent on protein synthesis, similar to ALK1. Perhaps a similar mechanism exists for the termination of the Smad1/5 signal in epithelial cells. Taken together, these results give strength to the argument of a heteromeric type I receptor complex, responsible for the phosphorylation of Smad1/5 in response to TGF-β.

Although ALK1 was not expressed in EpH4 and EpRas cells, ALK2 was an attractive candidate for the kinase involved in Smad1 phosphorylation. ALK1 and ALK2 can be classified into a specific subgroup of type I receptors that interact with the TβRII and/or activin type II receptors, but phosphorylate Smad1 and 5 instead of Smad2 and 3 (Chen, Y. G. et al., 1999; Macias-Silva, M. et al., 1998). The data using siRNA oligonucleotides against ALK2 did not support this idea (Figure 6.7A). However, the lack of good antibodies to ALK2 interfered with assessing the depletion

of ALK2 from the cells and I cannot entirely rule out this possibility. Future work will focus on testing this idea, and looking for other candidates (Chapter 7).

6.3.2 Bifurcation of the TGF-β response

Several parallels have been made between the TGF-β-induced Smad1/5 phosphorylation in endothelial cells and epithelial cells. However, when investigating the TGF-β signalling responses in EpH4 and EpRas cells, an important distinction was made when compared to the responses in endothelial cells. This difference was characterised by the lack of BRE-luciferase activity upon TGF-β stimulation (Figure 6.12). Equal levels of Smad1/5 phosphorylation were obtained upon either TGF-β or BMP stimulation, however, the transcriptional readout from the different ligands was far from similiar. One could argue that this may be due to the transient nature of TGF-β-induced P-Smad1/5. However, previous work has shown that continuous TGF-β signalling for 1-2 hrs is sufficient for a significant and measurable induction in the transcriptional readout, whereas 2-4 hrs is required for maximal transcriptional activity (Inman, G. J. et al., 2002c). A more convincing argument to explain these results is the evidence of mixed Smad complexes. Upon TGF-β treatment, Smad1 is phosphorylated and forms complexes with Smad2 and 3 (Figure 6.13). Hence, the inability of TGF-β-induced P-Smad1/5 to initiate transcription of the BRE-luc is likely due to the fact that it is not in a complex with Smad4 and therefore cannot bind to the DNA elements in a similar fashion to P-Smad1/5-Smad4 complexes formed upon BMP signalling.

This result is in sharp contrast to the response observed in endothelial cells, where Smad1/5 phosphorylation resulted in an increase in BRE-luciferase activity. This has been interpreted as a BMP-like response, whereby Smad1/5 forms complexes with Smad4 to initiate transcription of BRE-responsive elements. However, similarly to my work, evidence for the formation mixed complexes was also detected in endothelial cells. Goumans and colleagues have observed that ALK1 activity antagonises the ALK5 activity as measured by $(CAGA)_{12}$-luciferase, and therefore they have speculated that these complexes could only be inhibitory. They suggest that the interactions with different Smads may interfere with specific DNA binding and/or recruitment of cofactors (Goumans, M. J. et al., 2003b; Goumans, M. J. et al., 2002).

In contrast to this proposed inhibitory role for mixed complexes, I found that knockdown of Smad1, 5 and 8 did not significantly affect the transcriptional activation of the $(CAGA)_{12}$-luciferase promoter (data not shown). Furthermore, the transcriptional responses of downstream targets of TGF-β supported this view. TGF-β signals through ALK5 via Smad3/4 complexes to induce transcription of PAI-1. Despite the presence of P-Smad1/5 signalling, PAI-1 is efficiently upregulated in EpH4 cells (Figure 5.3). Taken together, this evidence suggests that these complexes are not inhibitory. However, the activity of the mixed complexes cannot be measured because the DNA element to which they bind has not yet been determined.

The model in Figure 6.14 also challenges the established role of Smad4 as a common Smad partner and suggests that Smad4 is in fact dispensable for some TGF-β responses. Recent evidence supports this idea and proposes TGF-β-induced regulation of a subset of genes in a Smad4-independent manner (Levy, L. et al., 2005). Interestingly, the knockdown of Smad4 results in a loss of the tumour-suppressor functions of TGF-β, for example growth arrest, but it has no effect on the tumour-promoting function of TGF-β. Smad4 is not required for EMT in that study and the data suggest that loss of Smad4 may predispose a cell to the tumour promoting activities of TGF-β, resulting in a more aggressive phenotype. This is consistent with the fact that Smad4 expression is frequently lost or decreased in pancreatic and colon cancer. Further investigation of the role of mixed complexes in regulating TGF-β responsive Smad4 independent genes is required.

The work presented in this Chapter has uncovered a novel mechanism by which specificity of the signalling pathway downstream of TGF-β can be achieved. A new level of complexity is added to the pathway, whereby the ligand can induce different responses depending on the nature of the activated receptor complex. In addition, the TGF-β pathway is bifurcated as both classes of R-Smads are employed, each exhibiting different dose requirements and kinetics. Through this action alone, critical determinants of specificity have been met. Yet, this investigation has yielded now many more questions. Does cooperation exist between the two signalling pathways? Is the main function of P-Smad1/5 to upregulate cofactors required for the transcription of a defined gene set? One could imagine that the transient Smad1/5 signalling could then feed into the Smad2/3 pathway by upregulating transcription

factors which then mediate a specific transcription programme. The presence of alternative 'mixed' Smad complexes also raises many questions. Do they have the same affinity for previously characterised response elements? (Chapter 7) What are the downstream targets? It will also be important to establish the role of P-Smad1/5 in mediating TGF-β-induced growth arrest and EMT. However, the identification of the receptor required for phosphorylation of Smad1/5 in response to TGF-β is needed to determine this role (Chapter 7).

In conclusion, TGF-β signalling via both Smad1/5 and Smad2/3 allows regulation of a wide spectrum of genes, which may reflect its plethora of biological responses. Much work is required to establish the role of P-Smad1/5 signalling in the TGF-β pathway.

7 Discussion

TGF-β plays a complex, biphasic role in the progression of cancer. In the early stages of tumourigenesis, TGF-β acts as a tumor suppressor through its ability to inhibit proliferation in epithelial cells from which the majority of human tumors are derived. However, pro-metastatic effects of TGF-β occur in later stages of carcinogenesis, thus implicating TGF-β as a tumour promoter (Akhurst, R. J. et al., 2001; Wakefield, L. M. et al., 2002). It has frequently been found that tumor cells become resistant to TGF-β-induced growth inhibition, however remain responsive to the tumour promoting activities of the cytokine. The EpH4/EpRas system developed in Hartmut Beug's laboratory provided the means to investigate the dual activities of TGF-β observed in tumourigenesis in a model cell culture system. The cell lines in the EpH4 system represent the stages of tumourigenesis, whereby a normal epithelial cell develops into an invasive spindle-like cell. The EpH4 cells are mammary epithelial cells which exhibit sensitivity to the antiproliferative effects of TGF-β, whereas the EpRas cells are resistant to growth inhibition but remain responsive to the pro-metastatic responses of TGF-β (Oft, M. et al., 1998; Oft, M. et al., 1996). The EpRas cells undergo an EMT upon stimulation with TGF-β, which involves epithelial plasticity changes towards a migratory, fibroblastoid phenotype. This transition to an invasive, mesenchymal phenotype during EMT is a hallmark of carcinoma progression and metastasis (Thiery, J. P., 2002). The main aim of my thesis project was to investigate the mechanisms that determine the outcome of the TGF-β response, whether it is growth inhibition or a dramatic morphological alteration. To this end, this thesis represents an in-depth study of the determinants of specificity governing the different biological responses of TGF-β in this model system.

7.1 Regulation of TGF-β-Smad signalling in the EpH4 system

During the characterisation of these cells, a common overriding theme in Smad regulation was the effect of the cell cycle. Both the phosphorylation of Smad1 and protein expression level of Smad3 are cell cycle regulated. So in essence, the position

of the cells in the cell cycle sets the scene for the outcome of the response to TGF-β in this model system. In quiescent cells, a high level of Smad3 is achieved, whereas the phosphorylation of Smad1 is inhibited (Figure 7.1). High Smad3 levels correlates with the ability of TGF-β to induce growth inhibition upon exit from quiescence. The abolition of Smad1 phosphorylation upon cell cycle exit into a quiescent state suggests that responses through activated Smad1 are restricted to the proliferative state (Chapter 6). Conversely, in cycling cells Smad3 levels are low and these cells can now strongly phosphorylate Smad1 in response to TGF-β (see below).

7.1.1 The relevance of Smad3 levels in EpRas cells

The low Smad3 level observed is consistent with data from both tumour samples and tumour cell lines. In addition, a downregulation of Smad3 has been observed during progression of EMT concomitant with a loss in growth inhibition, suggesting that this low Smad3 is sufficient to promote transdifferentiation, but not growth arrest. My data together with other observations point to a model whereby the high levels of Smad3 protect cells from tumour progression by inducing growth arrest and apoptosis, whereas these responses in cells expressing lower levels are compromised (Figure 7.1). In this model, the low levels of Smad3 would be sufficient to induce and maintain the invasive phenotype observed in cells undergoing EMT or metastasis. The epigenetic mechanisms governing the loss of Smad3 expression have to date not been uncovered. From my work it seems that multiple modes of action could affect the level of Smad3 in the cell, including transcriptional regulation and protein stability. Downregulation of Smad3 in MDCK cells was attributed to methylation due to the slow timing of this event. Indeed, the Smad3 promoter has CpG islands, which could be targeted by methylation. Other mechanisms could also act to downregulate Smad3, for example the activity of microRNAs.

7.1.2 The role of Smad1 in Endothelial Cells

The phosphorylation of Smad1 upon stimulation of TGF-β in these cells represents a major novel finding. Up until now, TGF-β induction of P-Smad1 has only been

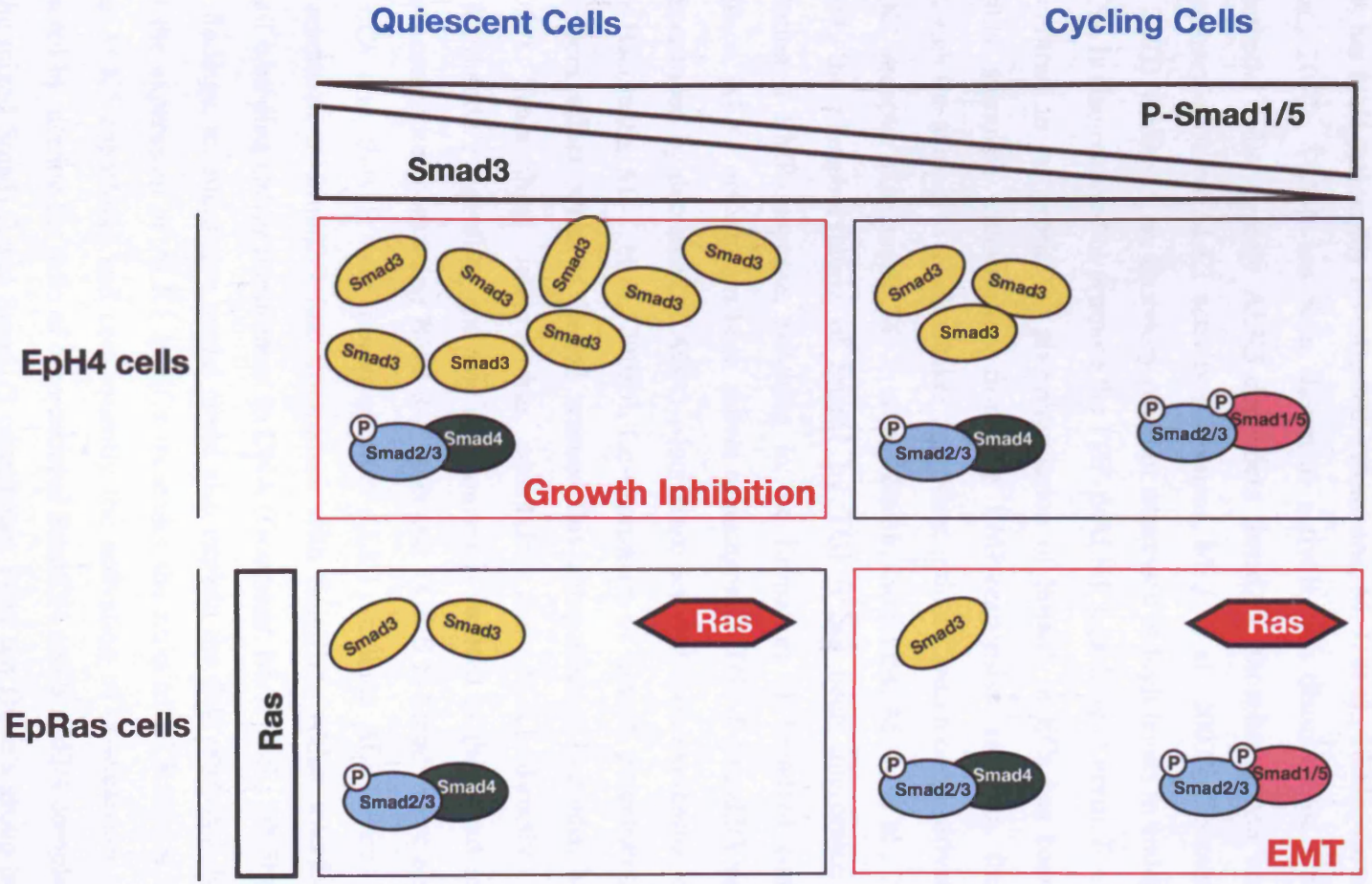

Figure 7.1. Cell cycle control of TGF-β signalling in EpH4 and EpRas cells

Schematic model for the regulation of the components of the TGF-β pathway in mouse mammary epithelial cells. For discussion, see text. Smad complexes are displayed as dimers for simplicity.

documented specifically in endothelial cells (ECs) (Goumans, M. J. et al., 2003b; Goumans, M. J. et al., 2002) and in some breast carcinoma cell lines (Inman, G. personal communication). The mechanism underlying this observation in endothelial cells has been thoroughly investigated (Goumans, M. J. et al., 2003b; Goumans, M. J. et al., 2002). TGF-β has been shown to activate two distinct type I receptors in endothelial cells; namely ALK5-dependent Smad2/3 phosphorylation and Smad1/5 phosphorylation by ALK1 activity (Goumans, M. J. et al., 2003b; Goumans, M. J. et al., 2002). Endoglin, an accessory receptor expressed at high levels in endothelial cells (ECs), is also required to promote the TGF-β/ALK1 signalling (Lebrin, F. et al., 2004). In contrast to my work, the phosphorylation of Smad1 in ECs has been shown to weakly stimulate transcription from the BMP-responsive reporter, the BRE-luc, although the activity is much weaker than when induced with a constitutively activated ALK1 receptor (Goumans, M. J. et al., 2003b; Goumans, M. J. et al., 2002). As a result, the phosphorylation of Smad1 by TGF-β has been interpreted as TGF-β inducing a BMP response, resulting in the formation of Smad1/4 complexes. In addition, ALK1 activity has been shown to antagonise TGF-β-Smad2/3 signalling, as demonstrated by decreased $(CAGA)_{12}$-luciferase activity upon expression of ALK1 in ECs (Goumans, M. J. et al., 2003b). Co-expression of Smad5 potentiated the ALK1 inhibitory effect, whereas Smad3 rescued this antagonism (Goumans, M. J. et al., 2003b). From these data, it was concluded that ALK1 directly antagonizes ALK5/Smad2/3 signalling and this antagonism is exerted at the Smad level. Mixed Smad complexes containing BMP R-Smads and TGF-β R-Smads were also observed in ECs and thus it was proposed that ALK1 inhibits ALK5 activity through sequestration of Smad2/3 into complexes with Smad1/5, which interfere with the specific binding and/or recruitment to DNA (Goumans, M. J. et al., 2003b). In light of my findings, an alternative model could also explain the data observed. It is possible that the expression of ALK1 in ECs increases the ratio of ALK1/ALK5 complexes over ALK5 complexes and consequently the activation of downstream signalling is affected by altering the ratio of conventional Smad2/4 and Smad3/4 complexes relative to the mixed Smad1/2 and Smad1/3 complexes. Peter ten Dijke's group has proposed that these mixed complexes are inhibitory because they do not induce $CAGA_{12}$-luc or BRE-luc activity. However it is more likely that these complexes are active at distinct but as yet unidentified promoter sites, recruiting new factors and performing new

tricks. My work is currently focusing on identifying the targets of these mixed complexes.

7.1.3 The role of mixed complexes in EpH4 and EpRas cells

My results suggest that similar to ECs, TGF-β signals via two receptor complexes in EpH4 and EpRas cells, which results in activation of BMP-type R- Smads and TGF-β R-Smads (Figure 7.2). ALK1 expression is highly specific to endothelail cells and therefore it is not involved in the activation of Smad1 in this system. The simultaneous activation of ALK5 and an alternative receptor, results in the formation of 'mixed' complexes containing both TGF-β and BMP-type R-Smads. However, in contrast to TGF-β signalling in ECs, there is no BMP-like response observed in EpH4 or EpRas cells. The biological relevance of these mixed Smad complexes has yet to be elucidated, however it is envisioned that these Smad complexes behave very differently to the conventional complexes defined by different DNA specificity and recruitment of a specific set of transcription factors. Strong evidence for endogenous complexes of both Smad1/2 and Smad1/3 has been demonstrated, however, the exact stoichiometry and combinations of the mixed Smad complexes have not been determined The presence of Smad4 in these complexes has not been shown, however, this possibility cannot be excluded, particularly regarding the weak binding of Smad1 with Smad4 complex and the poor quality of the antibody. In the case of Smad1 replacing a Smad2 monomer, Smad1 would confer DNA binding ability and this is likely to confer some functional differences between Smad2/4 and Smad1/2 complexes. However it is likely that Smad1 could replace Smad4 in a Smad2/4 homotrimer and this alone is likely to direct these complexes to alternative DNA site, such as GC rich sequences as opposed to an SBE.

Furthermore, these mixed complexes are likely to recruit either novel transcription factors or unique combinations compared with a conventional BMP or TGF-β response. In the case of Smad1/4 complexes, *Drosophila* and mammalian Schnurri has been proposed to act as a scaffolding protein for the recruitment of transcriptional coactivators and corepressors (Yao, L. C. et al., 2006). The promoter elements which recruit Schnurri are highly conserved, with a GC-rich binding site for

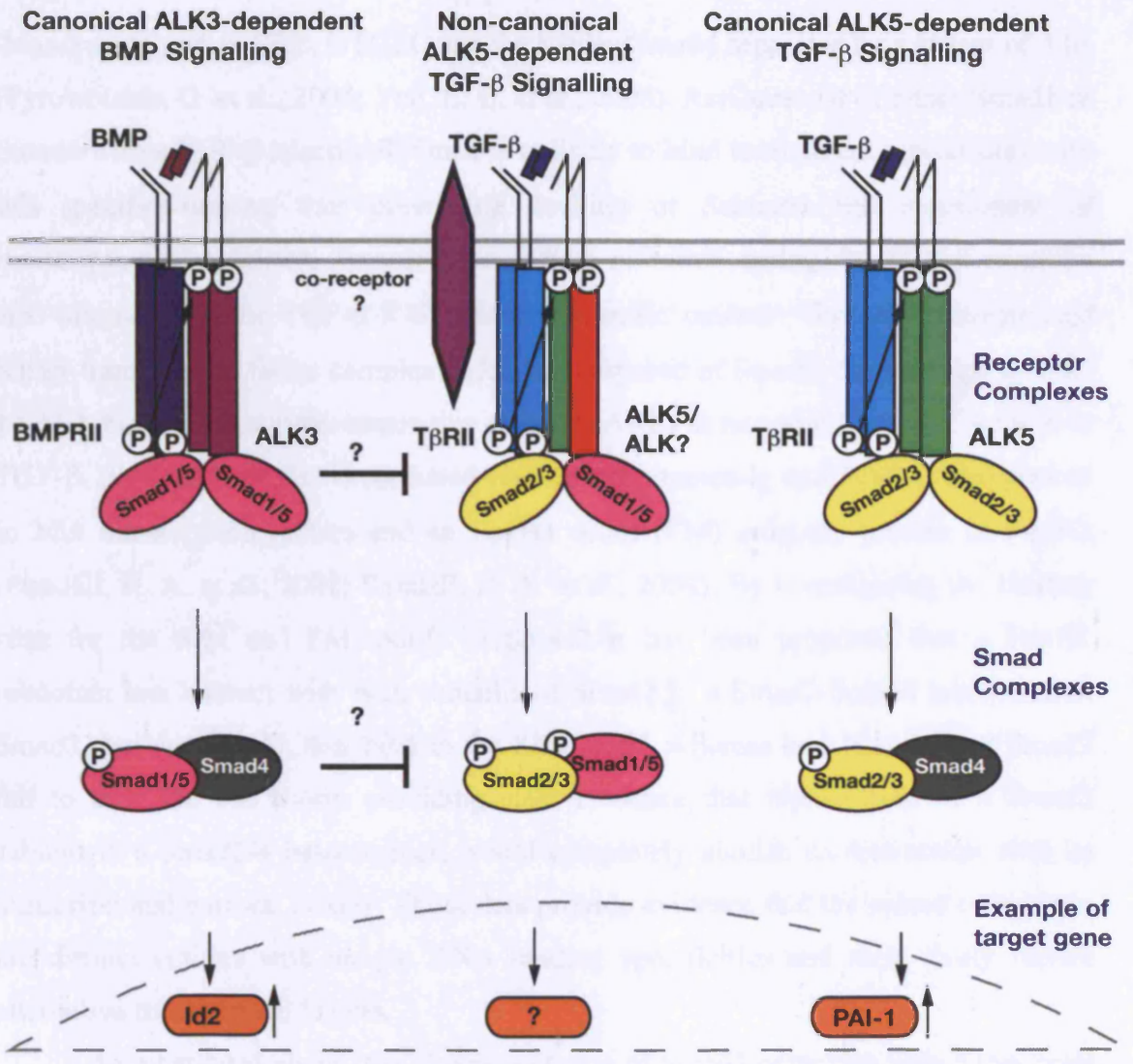

Figure 7.2. TGF-β superfamily signalling in EpH4 and EpRas cells

Three pathways are known to act downstream of TGF-β superfamily ligands in the EpH4 and the EpRas cells. Different sets of receptor complexes are formed to phosphorylate the R-Smads, which then form complexes in a variety of combinations. The complexes then accumulate in the nucleus, where they are involved in transcriptional activation and repression of a plethora of gene promoters. For simplicity, complexes are portrayed as dimers.

Mad/Smad1 and an SBE, GTCTG site for Medea/Smad4 separated by a spacer of 5 bp (Pyrowolakis, G. et al., 2004; Yao, L. C. et al., 2006). Replacement of either Smad1 or Smad4 with a TGF-β specific R-Smad is unlikely to bind to these conserved sites with this specific spacing thus preventing docking of Schnurri and recruitment of transcriptional mediators. Transcription factors recruited during the TGF-β response also interact with the TGF-β R-Smads in a specific manner. The well characterised Smad–transcription factor complex, ARF, is composed of Smad2, Smad4 and XFoxH-1 which binds to an activin-responsive element (ARE) in response to Nodal, Activin or TGF-β. Binding of FoxH1 is mediated via a Smad-interacting motif (SIM) also present in Mix transcription factors and an FoxH1 motif (FM) uniquely present in FoxH1 (Randall, R. A. et al., 2002; Randall, R. A. et al., 2004). By investigating the binding sites for the SIM and FM motifs in Smad2 it has been proposed that a FoxH1 monomer can interact with both subunits of Smad2 in a Smad2-Smad4 heterotrimer. Smad3, but not Smad1, can bind to the SIM motif, whereas both Smad1 and Smad3 fail to bind the FM motif, providing clear evidence that replacement of a Smad2 subunit in a Smad2/4 heterotrimer, would completely abolish its interaction with its transcriptional partner, FoxH1. These data provide evidence that the mixed complexes are distinct entities with unique DNA binding specificities and most likely recruit alternative transcription factors.

As mentioned above, the phosphorylation of Smad1 coincides with a low level of Smad3. In co-immunoprecipitation experiments, Smad1 was found to be predominantly complexed to Smad2, with a much lower proportion in complex with Smad3. This raises the question as to whether the downregulation of Smad3 influences the specific ratio of Smad1/2 complexes and Smad1/3 complexes. In addition to the mixed classes of Smad complexes, there is also evidence to suggest that TGF-β can induce Smad2/3 complexes. Therefore, the competition between Smad1 and Smad3 for Smad2 binding would be reduced when Smad3 levels are lowered. Further work is required to establish the stochiometry of these mixed complexes, their reletive abundance and biological effects.

7.1.4 Receptor regulation during the cell cycle

It has been established that the Smad3 downregulation upon entry into the cell cycle is mediated through a combination of protein stability and transcriptional regulation. However, the mechanism by which Smad1 is activated specifically in proliferating cells, has not yet been established. Data in Chapter 6 indicates the requirement of an alternative receptor that is either inactive or downregulated in quiescent cells. The main piece of evidence which points to this is the observed delay in Smad1 activation upon release from quiescence, which suggests the requirement of protein synthesis or activation of a latent form of the receptor for maximal phosphorylation of Smad1 (Chapter 6). Cell cycle mediated downregulation could be achieved either by transcriptional repression or increased protein degradation in the quiescent state, whereas activation of the receptor may be dependent on the activity of a cell cycle regulated protein. Unfortunately, this receptor has not yet been identified. ALK1 is primarily expressed in ECs so is not a candidate in this case. However, ALK2 is a highly related receptor with similar signalling specificities and is expressed EpH4 cells. As ALK1 has been demonstrated to form heteromeric complexes with ALK5, it was reasonable to propose that ALK2 may also function in this manner. However, initial evidence has not supported this hypothesis, and knockdown of this receptor does not impair phosphorylation of Smad1. In addition, ALK2 transcripts did not vary significantly between the proliferative and quiescent state. However, it is possible that downregulation of the receptor is mediated at the translational or posttranslational level. ALK4 is also expressed in these cells but its specificity is identical to ALK5, in that it phosphorylates Smad2 and Smad3 only (Chen, Y. G. et al., 1998). The specific interaction between the L45 loop of the receptor and L3 loop in the R-Smads does not allow crossover of activation and therefore ALK4 or indeed ALK5, cannot mediate the phosphorylation of Smad1. ALK3, on the other hand, efficiently phosphorylates Smad1/5, but this receptor mediates BMP signals only, as was convincingly demonstrated in Chapter 6. Work is now underway to uncover the receptor responsible for this signalling event, including a search for an as yet unidentified ALK.

Alternatively, it is equally possible that a co-receptor essential for Smad1 phosphorylation could be downregulated during quiescence. Endoglin, an accessory TGF-β receptor has been shown to be absolutely required for Smad1 phosphorylation

in ECs (Lebrin, F. et al., 2004). A co-receptor may function similarly in EpH4 cells, and potentially it could be targeted for cell cycle regulated degradation during quiescence. Betaglycan has been shown to facilitate the binding of TGF-β isoforms to its type II receptor, and is absolutely required for efficient TGF-β2 binding (Lopez-Casillas, F. et al., 1993). These results reveal that co-receptors are required for facilitating the binding of low affinity interactions. It has also been shown that the receptor responsible for Smad1 activation in EpH4 and EpRas cells has a lower affinity for TGF-β1 and 3 than ALK5 (Chapter 6). Thus it is likely that a co-receptor is required for efficient binding in this instance. It is also clear that high levels of ALK5 are required for the activation of Smad1 in response to TGF-β. Incomplete depletion of ALK5 completely abolishes phosphorylation of Smad1, whereas Smad2 and Smad3 phosphorylation is only partially affected (data not shown). It is possible that ALK5 preferentially forms homomeric complexes to signal via Smad2 and Smad3, whereas excess ALK5 allows the lower affinity complex formation with the alternative ALK.

7.1.5 The relevance of Smad1/5 activation in proliferating cells

The inhibition of Smad1/5 activation in quiescent cells is intriguing. Whereas the downregulation of Smad3 upon entry is compatible with its role in mediating a cytostatic response, the relevance for Smad1 phosphorylation only in cycling cells is a mystery. It is noteworthy that there appears to be a reciprocal relationship regarding the regulation of Smad3 and the proposed regulation of the receptor required for Smad1 phosphorylation. In short, when Smad3 expression is repressed, activity of the receptor is upregulated. What is the significance of this? Are these processes coupled? The answers to these questions have not been established but this observation prompted investigation into whether high Smad3 levels exerted an inhibitory effect on the phosphorylation of Smad1. However, there is no apparent difference in P-smad1 levels between EpH4 and EpRas, despite a significant variation in Smad3 levels, when the proliferation rate of EpRas cells is taken into consideration. In addition, stable expression of high levels of Smad3 in the EpRas Smad3 clone1, did not compromise phosphorylation of Smad1 in response to TGF-β (data not shown).

An important question remains, what is the relevance of P-Smad1 activation in proliferating cells? A role for Smad1 in antiproliferative effects of TGF-β is unlikely, as high levels of P-Smad1 are not present until 15 hours after release from quiescence and it was shown that 12-16 hours of signalling is required to prevent entry of EpH4 cells into the cell cycle (Chapter 6). This led us to ask whether it is involved in the other response of TGF-β, such as EMT. In my attempts to study TGF-β induced EMT in EpRas cells, it was continuously observed that the EMT induced by TGF-β is more pronounced in subconfluent cells, where confluent cultures are more refractory to morphological changes induced by TGF-β. This has also been observed in tubular epithelial cells, where cell cultures at lower density exhibited more dramatic epithelial plasticity than higher density cultures (Strutz, F. et al., 2002). Evidence from Ki67 staining shows cells undergoing EMT and those that have reached EMT are proliferating. These results indicate that the ability of EpRas cells to undergo EMT correlates with their capacity to induce P-Smad1. Numerous studies have implicated TGF-β type R-Smads and not BMP specific R-Smads as playing a role in EMT, however this has been shown through the expression of either type of R-Smad alone (Valcourt, U. et al., 2005). In the EpH4 model system, both types of R-Smads are activated by TGF-β in the presence of each other, and can form heteromeric complexes which are likely to mediate different signalling responses.

Further support for a role for Smad1/5 in EMT comes from the findings that ALK2, which specifically phosphorylates Smad1, 5 and 8, can mediate EMT. A role for ALK2 has also been implicated in MIS-induced EMT of coelomic epithelium during Mullerian duct regression. It was recently revealed that siRNA knockdown of ALK2 resulted in inhibition of coelomic EMT and Mullerian duct regression in organ culture (Zhan, Y. et al., 2006). Inhibition of Smad5 mimicked this response, however knockdown of Smad8 accelerated the response. These data support a role for BMP-Smad activation in the progression of EMT. Furthermore, ALK2 has been shown to be sufficient to mediate EMT in endocardial chick cells (Desgrosellier, J. S. et al., 2005). In addition, ALK2 has been proposed to mediate EMT in response to TGF-β in cultured mammary epithelial cells (Miettinen, P. J. et al., 1994). However, efforts to confirm this observation have been unsuccessful (Piek, E. et al., 1999; Valcourt, U. et al., 2005). In studies using overexpressed constitutively active (ca) ALK receptors in NMuMG cells, it was concluded that only ALK5 can mediate EMT (Valcourt, U. et

al., 2005). In light of the data presented in this thesis, these results are by no means complete. These experiments were conducted by overexpressing caALKs individually which may not recapitulate the *in vivo* conditions (Valcourt, U. et al., 2005). The phosphorylation of Smad1/5 in EpH4/EpRas cells requires not only the expression, but also the kinase activity of ALK5. Therefore, by overexpressing a constitutively active form of this unidentified receptor, the response would not be replicated. So to take into account signalling through heteromeric type I receptor complexes, combinations of caALKs need to be investigated and could prove critical for the investigation of the mediators of the response.

Again, parallels can be drawn from the TGF-β signalling in endothelial cell and the EpH4 system. In ECs, ALK1 is thought to induce cell proliferation and ALK5 signalling has been implicated in the differentiation phase. I have proposed a similar model for TGF-β signalling in the EpH4 system, whereby canonical ALK5 signalling predominantly mediates the antiproliferative effects of TGF-β, whereas the phosphorylation of Smad1/5 promotes cell-cycle progression and EMT (Figure 7.1). The regulation of the alternative receptor signalling is achieved at the level of the cell cycle, through the upregulation of a receptor/co-receptor and the downregulation of Smad3. This model proposes that in cycling cells, TGF-β signalling activates both the canonical and alternative signalling pathways in EpH4 and EpRas cells, and in the case of EpRas cells both pathways cooperate to promote the progression of EMT. In quiescent cells, however, Smad2/3 signalling is dominant and can lead to the growth inhibitory effect of TGF-β upon stimulation of ligand in EpH4 cells.

7.1.6 BMP signalling in the EpH4 cell system

During development, TGF-β superfamily members are all working in concert. The ultimate result of this is a fine tuned response. In the case of the EpH4 cell system, TGF-β responses have a background of basal BMP signalling. Depletion of ALK3 in both EpH4 and EpRas cells substantially reduced basal P-Smad1 levels, suggesting that this receptor mediates the BMP response in these cells (Chapter 6). Three type I receptors have been found to mediate signals via BMP2 or BMP4, namely ALK2, ALK3 and ALK6 (Macias-Silva, M. et al., 1998). ALK6 expression is tightly restricted

and is only found in brain and lung, and as such is not expressed in EpH4 cells, as confirmed by RT-PCR (ten Dijke, P. et al., 1994b). ALK2 knockdown by siRNA did not affect induction of P-Smad1 by BMP, whereas depletion of ALK3 completely abolished the phosphorylation of Smad1 in response to BMP2/4 (Chapter 6). Therefore, ALK3 alone mediates the BMP response in EpH4 and EpRas cells.

As Smad1 and 5 are common components to both the TGF-β and BMP pathways, it is possible that the two pathways are integrated by some means. Goumans et al., showed that knockdown of ALK1 potentiated the Smad2/3 response of TGF-β as measured by an increase in $CAGA_{12}$-luciferase activity (Goumans, M. J. et al., 2003b; Goumans, M. J. et al., 2002). In the EpH4 cells, an antagonistic effect on Smad2/3 signalling could not be investigated because, without the identification of the receptor, it is impossible to selectively knockdown the non-canonical signalling pathway. However, knockdown of ALK3 revealed that the basal BMP signalling is largely antagonistic to canonical Smad2/3 signalling, as measured using $CAGA_{12}$-luciferase (data not shown). This cannot be explained by simple competition, because addition of excess Smad4 does not relieve this antagonism and suggests that this antagonism may act at the level of the receptors. In addition, preliminary data suggests that knocking down ALK3 sensitises EpRas cells to TGF-β-induced EMT. Abrogation of BMP signalling liberates both Smad1 and Smad4 from complexes which could potentially complex with Smad2 and Smad3 to elicit cellular responses. The release of both of these components may contribute to TGF-β-induced EMT. Conversely, BMP signalling has been implicated in developmental EMT such as neural crest formation. However, the level of BMP signal is crucial to theses events, such that high levels of BMP signalling in the ectoderm and low levels in the neural plate, inhibit neural crest formation (Tucker, R. P., 2004). Moreover, BMP is thought to play a more important role in the specification of the neural crest cells, whereas its role in maintaining the invasive and migratory phenotype associated with these cells is under debate (Barembaum, M. et al., 2005). An increasing number of studies report an antagonistic effect of BMP in EMT, which is consistent with my observations. BMPs have been shown to revert mesechymal cells produced by the activity of TGF-βs to epithelial cells (MET). BMP7 has been shown to reverse TGF-β-induced EMT in a mouse model of renal injury (Zeisberg, M. et al., 2003b). An esophageal cell line was induced with

TGF-β, which resulted in morphological changes and molecular changes similar to EMT. These changes could be reversed by addition of BMP7 or siRNA with Smad4 (Rees, J. R. et al., 2006). Consistently, BMP-7 has been identified as a key regulator during MET in kidney ontogenesis (Dudley, A. T. et al., 1995). The mechanism underlying this inhibition has not been established. However, if the phosphorylation of Smad1 in response to TGF-β is required for EMT, then BMP signalling could act to sequester P-Smad1 away from Smad2 and Smad3 to form canonical complexes with Smad4 and therefore inhibit EMT (Figure 7.2).

7.2 Future Perspectives

Many questions have been raised by this work and require further investigation. Downregulation of Smad3 has been observed in some human cancers and my work further supports a role for Smad3 as tumour suppressor. A systematic analysis of expression levels of Smad3 in relation to Ras activity in human cancers would give an indication of the prevalence of this event. Given my identification of the import of Smad3 levels, it was possible to make another correlation. It has been repeatedly observed that low Smad3 protein levels correlate with the ability of cells to be transformed by oncogenic Ras. In two cases, both MDCK cells and EpRas cells, transformation with oncogenic raf or ras, respectively, was concomitant with a downregulation of Smad3. Many epithelial cell lines, for example, the human keratinocyte HaCat cell line, however, which have high levels of Smad3, senesce in response to these agents, which could possibly be attributed to their inability to downregulate Smad3. Transformation of primary cells by *ras* requires either a cooperating oncogene or the inactivation of tumor suppressors such as p53 or p16 (Serrano, M. et al., 1997). Inactivation of either p53 or p16 overcomes *ras*-induced senescence in rodent cells, whereas E1A achieves a similar effect in human cells (Serrano, M. et al., 1997). I would also like to propose that overcoming *ras* induced senescence may be achieved by inactivation or downregulation of the tumour suppressor Smad3. This is supported by data that revealed that defects in TGF-β signalling can overcome ras-induced senescence in mouse kertinocytes (Tremain, R. et al., 2000). This resistance is associated with low expression of p15ink4b and p16ink4a,

constitutive Rb phosphorylation and high levels of cdk4 and cdk2 kinase activity (Tremain, R. et al., 2000). Furthermore, it is also possible that the differential sensitivity between human and rodent cells to downregulate Smad3 levels may contribute to the well-known difficulty in establishing and transforming human cell lines in culture. Using a HaCat cell line with constitutive expression of shRNA against Smad3, I hope to test whether these cells can at least proliferate in the presence of oncogenic Ras. Preliminary evidence suggests that this may be the case. Following on from this, I hope to investigate a possible link between the deownregulation Smad3 and TERT expression. Telomerase reverse transcriptase (TERT) is required to regulate the structures of chromosomal ends (telomeres) for continuous cell division during embryonic development, stem cell renewal and proliferation, and cancer cell immortalization. Recent work has revealed that Smad3 binds to the TERT gene promoter to repress gene expression (Li, H. et al., 2006). Furthermore it has been shown that autocrine TGF-β signaling in human cancer cells, suppresses telomerase activity by repression of TERT (Yang, H. et al., 2001). It would be interesting to determine whether Smad3 downregulation increases the basal expression level of TERT and contributes to the cancer cell immortalisation. Furthermore, I would like to investigate the mechanism governing the downregulation of Smad3 in the EpH4/EpRas model system and test whether this is a general mechanism during tumour progression.

The phosphorylation of Smad1 in response to TGF-β also requires further investigation. The main question I would like to address is which receptor is responsible for this phosphorylation event. We know that ALK5 is required, however, previous work from the literature suggests that it, alone, is not sufficient. I would like to identify the receptor using a two-pronged approach, through more rigorous analysis of the characterised ALKs and bioinformatic investigation for novel ALKs. Additional investigations of co-receptors of the pathway by siRNA depletion of these proteins in EpH4 cells will also be pursued. Once the receptor and/or co-receptor has been identified, gene targets of the new Smad1 complexes may be explored and the biological role of phosphorylated-Smad1 may be addressed. Moreover, this study, together with the work from Peter Ten Dijke's laboratory, has opened up a new realm of investigation. It is not known whether only ALK5 can form a heteromeric type I

receptor complex or whether this may also apply to ALK4 and ALK7. Can these receptors also engage in recruiment of ALK1, ALK 2 or an as yet unidentified ALK and mediate phosphorylation of Smad1/5 in respsonse to Activin and Nodal? This question may easily be addressed in EpH4 cells, which also express ALK4, but not ALK7. It would be interesting to investigate whether these are responsive to Activin, and if so, what are the downstream targets of this ligand stimulation? This may provide an alternative route to assess the contribution of receptors to the phosphorylation of Smad1 in this system. Another question is whether ALK1-like type I receptors can also form heteromeric receptor complexes with ALK3 and ALK6 and thereby modulate the pattern of activation of Smads1, 5 and 8? This investigation has the potential to uncover an added level of complexity which would allow a fine-tuning of the transcriptional response downstream of the TGF-β superfamily. Ultimately, it is hoped that these investigations will lead to a better understanding of the dual role of TGF-β signalling in Cancer.

References

Affolter, M., Marty, T., Vigano, M. A., and Jazwinska, A. (2001). Nuclear interpretation of Dpp signaling in Drosophila. EMBO J *20*, 3298-3305.

Ahmed, F., Wyckoff, J., Lin, E. Y., Wang, W., Wang, Y., Hennighausen, L., Miyazaki, J., Jones, J., Pollard, J. W., Condeelis, J. S., and Segall, J. E. (2002). GFP expression in the mammary gland for imaging of mammary tumor cells in transgenic mice. Cancer Res *62*, 7166-7169.

Akhurst, R. J., and Derynck, R. (2001). TGF-β signaling in cancer--a double-edged sword. Trends Cell Biol *11*, S44-51.

Akhurst, R. J., Lehnert, S. A., Gatherer, D., and Duffie, E. (1990). The role of TGF β in mouse development. Ann N Y Acad Sci *593*, 259-271.

Annes, J. P., Munger, J. S., and Rifkin, D. B. (2003). Making sense of latent TGFβ activation. J Cell Sci *116*, 217-224.

Armes, N. A., and Smith, J. C. (1997). The ALK-2 and ALK-4 activin receptors transduce distinct mesoderm-inducing signals during early Xenopus development but do not co-operate to establish thresholds. Development *124*, 3797-3804.

Arsura, M., Panta, G. R., Bilyeu, J. D., Cavin, L. G., Sovak, M. A., Oliver, A. A., Factor, V., Heuchel, R., Mercurio, F., Thorgeirsson, S. S., and Sonenshein, G. E. (2003). Transient activation of NF-kappaB through a TAK1/IKK kinase pathway by TGF-β1 inhibits AP-1/SMAD signaling and apoptosis: implications in liver tumor formation. Oncogene *22*, 412-425.

Arthur, H. M., Ure, J., Smith, A. J., Renforth, G., Wilson, D. I., Torsney, E., Charlton, R., Parums, D. V., Jowett, T., Marchuk, D. A., *et al.* (2000). Endoglin, an ancillary TGFβ receptor, is required for extraembryonic angiogenesis and plays a key role in heart development. Dev Biol *217*, 42-53.

Ashcroft, G. S., Yang, X., Glick, A. B., Weinstein, M., Letterio, J. L., Mizel, D. E., Anzano, M., Greenwell-Wild, T., Wahl, S. M., Deng, C., and Roberts, A. B. (1999). Mice lacking Smad3 show accelerated wound healing and an impaired local inflammatory response. Nature Cell Biol. *1*, 260-266.

Attisano, L., Carcamo, J., Ventura, F., Weis, F. M., Massague, J., and Wrana, J. L. (1993). Identification of human activin and TGF β type I receptors that form heteromeric kinase complexes with type II receptors. Cell *75*, 671-680.

Attisano, L., Wrana, J. L., Cheifetz, S., and Massague, J. (1992). Novel activin receptors: distinct genes and alternative mRNA splicing generate a repertoire of serine/threonine kinase receptors. Cell *68*, 97-108.

Attisano, L., Wrana, J. L., Montalvo, E., and Massague, J. (1996). Activation of signalling by the activin receptor complex. Mol Cell Biol *16*, 1066-1073.

Aybar, M. J., Nieto, M. A., and Mayor, R. (2003). Snail precedes slug in the genetic cascade required for the specification and migration of the Xenopus neural crest. Development *130*, 483-494.

Azhar, M., Schultz Jel, J., Grupp, I., Dorn, G. W., 2nd, Meneton, P., Molin, D. G., Gittenberger-de Groot, A. C., and Doetschman, T. (2003). Transforming growth factor β in cardiovascular development and function. Cytokine Growth Factor Rev *14*, 391-407.

Bachelder, R. E., Yoon, S. O., Franci, C., de Herreros, A. G., and Mercurio, A. M. (2005). Glycogen synthase kinase-3 is an endogenous inhibitor of Snail transcription: implications for the epithelial-mesenchymal transition. J Cell Biol *168*, 29-33.

Baker, J. C., and Harland, R. M. (1996). A novel mesoderm inducer, Madr2, functions in the activin signal transduction pathway. Genes Dev *10*, 1880-1889.

Bakin, A. V., Rinehart, C., Tomlinson, A. K., and Arteaga, C. L. (2002). p38 mitogen-activated protein kinase is required for TGFβ-mediated fibroblastic transdifferentiation and cell migration. J Cell Sci *115*, 3193-3206.

Bakin, A. V., Tomlinson, A. K., Bhowmick, N. A., Moses, H. L., and Arteaga, C. L. (2000). Phosphatidylinositol 3-kinase function is required for transforming growth factor β-mediated epithelial to mesenchymal transition and cell migration. J Biol Chem *275*, 36803-36810.

Bang, A. G., Papalopulu, N., Kintner, C., and Goulding, M. D. (1997). Expression of Pax-3 is initiated in the early neural plate by posteriorizing signals produced by the organizer and by posterior non-axial mesoderm. Development *124*, 2075-2085.

Barbara, N. P., Wrana, J. L., and Letarte, M. (1999). Endoglin is an accessory protein that interacts with the signaling receptor complex of multiple members of the transforming growth factor-β superfamily. J Biol Chem *274*, 584-594.

Bardwell, V. J., and Treisman, R. (1994). The POZ domain: a conserved protein-protein interaction motif. Genes Dev *8*, 1664-1677.

Barembaum, M., and Bronner-Fraser, M. (2005). Early steps in neural crest specification. Semin Cell Dev Biol *16*, 642-646.

Barrallo-Gimeno, A., and Nieto, M. A. (2005). The Snail genes as inducers of cell movement and survival: implications in development and cancer. Development *132*, 3151-3161.

Batlle, E., Sancho, E., Franci, C., Dominguez, D., Monfar, M., Baulida, J., and Garcia De Herreros, A. (2000). The transcription factor snail is a repressor of E-cadherin gene expression in epithelial tumour cells. Nat Cell Biol *2*, 84-89.

Benanti, J. A., and Galloway, D. A. (2004). The normal response to RAS: senescence or transformation? Cell Cycle *3*, 715-717.

Benchabane, H., and Wrana, J. L. (2003). GATA- and Smad1-dependent enhancers in the Smad7 gene differentially interpret bone morphogenetic protein concentrations. Mol Cell Biol *23*, 6646-6661.

Bhowmick, N. A., Ghiassi, M., Bakin, A., Aakre, M., Lundquist, C. A., Engel, M. E., Arteaga, C. L., and Moses, H. L. (2001). Transforming growth factor-β1 mediates epithelial to mesenchymal transdifferentiation through a RhoA-dependent mechanism. Mol Biol Cell *12*, 27-36.

Bianco, C., Adkins, H. B., Wechselberger, C., Seno, M., Normanno, N., De Luca, A., Sun, Y., Khan, N., Kenney, N., Ebert, A., *et al.* (2002). Cripto-1 activates nodal- and ALK4-dependent and -independent signaling pathways in mammary epithelial Cells. Mol Cell Biol *22*, 2586-2597.

Bienz, M., and Clevers, H. (2000). Linking colorectal cancer to Wnt signaling. Cell *103*, 311-320.

Blagosklonny, M. V., and Pardee, A. B. (2002). The restriction point of the cell cycle. Cell Cycle *1*, 103-110.

Blanco, M. J., Moreno-Bueno, G., Sarrio, D., Locascio, A., Cano, A., Palacios, J., and Nieto, M. A. (2002). Correlation of Snail expression with histological grade and lymph node status in breast carcinomas. Oncogene *21*, 3241-3246.

Blavier, L., Lazaryev, A., Groffen, J., Heisterkamp, N., DeClerck, Y. A., and Kaartinen, V. (2001). TGF-β3-induced palatogenesis requires matrix metalloproteinases. Mol Biol Cell *12*, 1457-1466.

Boesen, C. C., Radaev, S., Motyka, S. A., Patamawenu, A., and Sun, P. D. (2002). The 1.1 A crystal structure of human TGF-β type II receptor ligand binding domain. Structure *10*, 913-919.

Bohnsack, B. L., and Hirschi, K. K. (2004). Red light, green light: signals that control endothelial cell proliferation during embryonic vascular development. Cell Cycle *3*, 1506-1511.

Bolos, V., Peinado, H., Perez-Moreno, M. A., Fraga, M. F., Esteller, M., and Cano, A. (2003). The transcription factor Slug represses E-cadherin expression and induces epithelial to mesenchymal transitions: a comparison with Snail and E47 repressors. J Cell Sci *116*, 499-511.

Bottinger, E. P., Jakubczak, J. L., Haines, D. C., Bagnall, K., and Wakefield, L. M. (1997). Transgenic mice overexpressing a dominant-negative mutant type II transforming growth factor β receptor show enhanced tumorigenesis in the mammary gland and lung in response to the carcinogen 7,12-dimethylbenz-[a]-anthracene. Cancer Res *57*, 5564-5570.

Boyd, F. T., and Massague, J. (1989). Transforming growth factor-β inhibition of epithelial cell proliferation linked to the expression of a 53-kDa membrane receptor. J Biol Chem *264*, 2272-2278.

Boyer, A. S., Ayerinskas, II, Vincent, E. B., McKinney, L. A., Weeks, D. L., and Runyan, R. B. (1999). TGFβ2 and TGFβ3 have separate and sequential activities during epithelial-mesenchymal cell transformation in the embryonic heart. Dev Biol *208*, 530-545.

Breeden, L. L. (2003). Periodic transcription: a cycle within a cycle. Curr Biol *13*, R31-38.

Broder, Y. C., Katz, S., and Aronheim, A. (1998). The ras recruitment system, a novel approach to the study of protein-protein interactions. Curr Biol *8*, 1121-1124.

Brown, C. B., Boyer, A. S., Runyan, R. B., and Barnett, J. V. (1996). Antibodies to the Type II TGFβ receptor block cell activation and migration during atrioventricular cushion transformation in the heart. Dev Biol *174*, 248-257.

Brown, C. B., Boyer, A. S., Runyan, R. B., and Barnett, J. V. (1999). Requirement of type III TGF-β receptor for endocardial cell transformation in the heart. Science *283*, 2080-2082.

Brummel, T. J., Twombly, V., Marques, G., Wrana, J. L., Newfeld, S. J., Attisano, L., Massague, J., O'Connor, M. B., and Gelbart, W. M. (1994). Characterization and relationship of Dpp receptors encoded by the saxophone and thick veins genes in Drosophila. Cell *78*, 251-261.

Brunet, C. L., Sharpe, P. M., and Ferguson, M. W. (1995). Inhibition of TGF-β 3 (but not TGF-β 1 or TGF-β 2) activity prevents normal mouse embryonic palate fusion. Int J Dev Biol *39*, 345-355.

Buchmann, A., Ruggeri, B., Klein-Szanto, A. J., and Balmain, A. (1991). Progression of squamous carcinoma cells to spindle carcinomas of mouse skin is associated with an imbalance of H-ras alleles on chromosome 7. Cancer Res *51*, 4097-4101.

Burrows, F. J., Derbyshire, E. J., Tazzari, P. L., Amlot, P., Gazdar, A. F., King, S. W., Letarte, M., Vitetta, E. S., and Thorpe, P. E. (1995). Up-regulation of endoglin on vascular endothelial cells in human solid tumors: implications for diagnosis and therapy. Clin Cancer Res *1*, 1623-1634.

Burstyn-Cohen, T., and Kalcheim, C. (2002). Association between the cell cycle and neural crest delamination through specific regulation of G1/S transition. Dev Cell *3*, 383-395.

Burstyn-Cohen, T., Stanleigh, J., Sela-Donenfeld, D., and Kalcheim, C. (2004). Canonical Wnt activity regulates trunk neural crest delamination linking BMP/noggin signaling with G1/S transition. Development *131*, 5327-5339.

Byfield, S. D., and Roberts, A. B. (2004). Lateral signaling enhances TGF-β response complexity. Trends Cell Biol *14*, 107-111.

Camenisch, T. D., Molin, D. G., Person, A., Runyan, R. B., Gittenberger-de Groot, A. C., McDonald, J. A., and Klewer, S. E. (2002). Temporal and distinct TGFβ ligand requirements during mouse and avian endocardial cushion morphogenesis. Dev Biol *248*, 170-181.

Cano, A., Perez-Moreno, M. A., Rodrigo, I., Locascio, A., Blanco, M. J., del Barrio, M. G., Portillo, F., and Nieto, M. A. (2000). The transcription factor snail controls epithelial-mesenchymal transitions by repressing E-cadherin expression. Nat Cell Biol *2*, 76-83.

Carcamo, J., Weis, F. M., Ventura, F., Wieser, R., Wrana, J. L., Attisano, L., and Massague, J. (1994). Type I receptors specify growth-inhibitory and transcriptional responses to transforming growth factor β and activin. Mol Cell Biol *14*, 3810-3821.

Cardozo, T., and Pagano, M. (2004). The SCF ubiquitin ligase: insights into a molecular machine. Nat Rev Mol Cell Biol *5*, 739-751.

Carette, M. J., and Ferguson, M. W. (1992). The fate of medial edge epithelial cells during palatal fusion in vitro: an analysis by DiI labelling and confocal microscopy. Development *114*, 379-388.

Carver, E. A., Jiang, R., Lan, Y., Oram, K. F., and Gridley, T. (2001). The mouse snail gene encodes a key regulator of the epithelial-mesenchymal transition. Mol Cell Biol *21*, 8184-8188.

Chacko, B. M., Qin, B. Y., Tiwari, A., Shi, G., Lam, S., Hayward, L. J., De Caestecker, M., and Lin, K. (2004). Structural basis of heteromeric smad protein assembly in TGF-β signaling. Mol Cell *15*, 813-823.

Cheifetz, S., Bellon, T., Cales, C., Vera, S., Bernabeu, C., Massague, J., and Letarte, M. (1992). Endoglin is a component of the transforming growth factor-β receptor system in human endothelial cells. J Biol Chem *267*, 19027-19030.

Cheifetz, S., Hernandez, H., Laiho, M., ten Dijke, P., Iwata, K. K., and Massague, J. (1990). Distinct transforming growth factor-β (TGF-β) receptor subsets as determinants of cellular responsiveness to three TGF-β isoforms. J Biol Chem *265*, 20533-20538.

Cheifetz, S., Weatherbee, J. A., Tsang, M. L., Anderson, J. K., Mole, J. E., Lucas, R., and Massague, J. (1987). The transforming growth factor-β system, a complex pattern of cross-reactive ligands and receptors. Cell *48*, 409-415.

Chen, C. R., Kang, Y., Siegel, P. M., and Massague, J. (2002). E2F4/5 and p107 as Smad cofactors linking the TGFβ receptor to c-myc repression. Cell *110*, 19-32.

Chen, D., Ji, X., Harris, M. A., Feng, J. Q., Karsenty, G., Celeste, A. J., Rosen, V., Mundy, G. R., and Harris, S. E. (1998). Differential roles for bone morphogenetic protein (BMP) receptor type IB and IA in differentiation and specification of mesenchymal precursor cells to osteoblast and adipocyte lineages. J Cell Biol *142*, 295-305.

Chen, F., and Weinberg, R. A. (1995). Biochemical evidence for the autophosphorylation and transphosphorylation of transforming growth factor β receptor kinases. Proc Natl Acad Sci U S A *92*, 1565-1569.

Chen, H. B., Rud, J. G., Lin, K., and Xu, L. (2005). Nuclear targeting of transforming growth factor-β-activated Smad complexes. J Biol Chem *280*, 21329-21336.

Chen, H. B., Shen, J., Ip, Y. T., and Xu, L. (2006). Identification of phosphatases for Smad in the BMP/DPP pathway. Genes Dev *20*, 648-653.

Chen, R. H., Moses, H. L., Maruoka, E. M., Derynck, R., and Kawabata, M. (1995). Phosphorylation-dependent interaction of the cytoplasmic domains of the type I and type II transforming growth factor-β receptors. J Biol Chem *270*, 12235-12241.

Chen, X., Rubock, M. J., and Whitman, M. (1996). A transcriptional partner for MAD proteins in TGF-β signalling. Nature *383*, 691-696.

Chen, X., Weisberg, E., Fridmacher, V., Watanabe, M., Naco, G., and Whitman, M. (1997). Smad4 and FAST-1 in the assembly of activin-responsive factor. Nature *389*, 85-89.

Chen, Y. G., Hata, A., Lo, R. S., Wotton, D., Shi, Y., Pavletich, N., and Massagué, J. (1998). Determinants of specificity in TGF-β signal transduction. Genes Dev *12*, 2144-2152.

Chen, Y. G., Liu, F., and Massague, J. (1997). Mechanism of TGFβ receptor inhibition by FKBP12. EMBO J *16*, 3866-3876.

Chen, Y. G., and Massague, J. (1999). Smad1 recognition and activation by the ALK1 group of transforming growth factor-β family receptors. J Biol Chem *274*, 3672-3677.

Cheng, S. K., Olale, F., Bennett, J. T., Brivanlou, A. H., and Schier, A. F. (2003). EGF-CFC proteins are essential coreceptors for the TGF-β signals Vg1 and GDF1. Genes Dev *17*, 31-36.

Cho, R. J., Huang, M., Campbell, M. J., Dong, H., Steinmetz, L., Sapinoso, L., Hampton, G., Elledge, S. J., Davis, R. W., and Lockhart, D. J. (2001). Transcriptional regulation and function during the human cell cycle. Nat Genet *27*, 48-54.

Claassen, G. F., and Hann, S. R. (2000). A role for transcriptional repression of p21CIP1 by c-Myc in overcoming transforming growth factor β -induced cell-cycle arrest. Proc Natl Acad Sci U S A *97*, 9498-9503.

Clissold, P. M., and Bicknell, R. (2003). The thioredoxin-like fold: hidden domains in protein disulfide isomerases and other chaperone proteins. Bioessays *25*, 603-611.

Cobrinik, D. (2005). Pocket proteins and cell cycle control. Oncogene *24*, 2796-2809.

Coleman, M. L., Marshall, C. J., and Olson, M. F. (2004). RAS and RHO GTPases in G1-phase cell-cycle regulation. Nat Rev Mol Cell Biol *5*, 355-366.

Comijn, J., Berx, G., Vermassen, P., Verschueren, K., van Grunsven, L., Bruyneel, E., Mareel, M., Huylebroeck, D., and van Roy, F. (2001). The two-handed E box binding zinc finger protein SIP1 downregulates E-cadherin and induces invasion. Mol Cell *7*, 1267-1278.

Conery, A. R., Cao, Y., Thompson, E. A., Townsend, C. M., Jr., Ko, T. C., and Luo, K. (2004). Akt interacts directly with Smad3 to regulate the sensitivity to TGF-β induced apoptosis. Nat Cell Biol *6*, 366-372.

Cox, D. M., Du, M., Marback, M., Yang, E. C., Chan, J., Siu, K. W., and McDermott, J. C. (2003). Phosphorylation motifs regulating the stability and function of myocyte enhancer factor 2A. J Biol Chem *278*, 15297-15303.

Crawford, S. E., Stellmach, V., Murphy-Ullrich, J. E., Ribeiro, S. M., Lawler, J., Hynes, R. O., Boivin, G. P., and Bouck, N. (1998). Thrombospondin-1 is a major activator of TGF-β1 in vivo. Cell *93*, 1159-1170.

Cuervo, R., and Covarrubias, L. (2004). Death is the major fate of medial edge epithelial cells and the cause of basal lamina degradation during palatogenesis. Development *131*, 15-24.

Cuervo, R., Valencia, C., Chandraratna, R. A., and Covarrubias, L. (2002). Programmed cell death is required for palate shelf fusion and is regulated by retinoic acid. Dev Biol *245*, 145-156.

Cui, W., Fowlis, D. J., Bryson, S., Duffie, E., Ireland, H., Balmain, A., and Akhurst, R. J. (1996). TGFβ1 inhibits the formation of benign skin tumors, but enhances progression to invasive spindle carcinomas in transgenic mice. Cell *86*, 531-542.

Cui, X. M., Chai, Y., Chen, J., Yamamoto, T., Ito, Y., Bringas, P., and Shuler, C. F. (2003). TGF-β3-dependent SMAD2 phosphorylation and inhibition of MEE proliferation during palatal fusion. Dev Dyn *227*, 387-394.

Dai, H., Hogan, C., Gopalakrishnan, B., Torres-Vazquez, J., Nguyen, M., Park, S., Raftery, L. A., Warrior, R., and Arora, K. (2000). The zinc finger protein schnurri acts as a Smad partner in mediating the transcriptional response to decapentaplegic. Dev Biol *227*, 373-387.

Datto, M. B., Frederick, J. P., Pan, L., Borton, A. J., Zhuang, Y., and Wang, X. F. (1999). Targeted disruption of Smad3 reveals an essential role in transforming growth factor β-mediated signal transduction. Mol Cell Biol *19*, 2495-2504.

de Caestecker, M. (2004). The transforming growth factor-β superfamily of receptors. Cytokine Growth Factor Rev *15*, 1-11.

De Crescenzo, G., Hinck, C. S., Shu, Z., Zuniga, J., Yang, J., Tang, Y., Baardsnes, J., Mendoza, V., Sun, L., Lopez-Casillas, F., *et al.* (2006). Three key residues underlie the differential affinity of the TGFβ isoforms for the TGFβ type II receptor. J Mol Biol *355*, 47-62.

de Jong, J. S., van Diest, P. J., van der Valk, P., and Baak, J. P. (1998). Expression of growth factors, growth-inhibiting factors, and their receptors in invasive breast cancer. II: Correlations with proliferation and angiogenesis. J Pathol *184*, 53-57.

Deckers, M., van Dinther, M., Buijs, J., Que, I., Lowik, C., van der Pluijm, G., and ten Dijke, P. (2006). The tumor suppressor Smad4 is required for transforming growth factor β-induced epithelial to mesenchymal transition and bone metastasis of breast cancer cells. Cancer Res *66*, 2202-2209.

Degen, W. G., Weterman, M. A., van Groningen, J. J., Cornelissen, I. M., Lemmers, J. P., Agterbos, M. A., Geurts van Kessel, A., Swart, G. W., and Bloemers, H. P. (1996). Expression of nma, a novel gene, inversely correlates with the metastatic potential of human melanoma cell lines and xenografts. Int J Cancer *65*, 460-465.

del Barrio, M. G., and Nieto, M. A. (2002). Overexpression of Snail family members highlights their ability to promote chick neural crest formation. Development *129*, 1583-1593.

Delaune, E., Lemaire, P., and Kodjabachian, L. (2005). Neural induction in Xenopus requires early FGF signalling in addition to BMP inhibition. Development *132*, 299-310.

Dennler, S., Itoh, S., Vivien, D., ten Dijke, P., Huet, S., and Gauthier, J. M. (1998). Direct binding of Smad3 and Smad4 to critical TGF β-inducible elements in the promoter of human plasminogen activator inhibitor-type 1 gene. EMBO J *17*, 3091-3100.

Derynck, R., Akhurst, R. J., and Balmain, A. (2001). TGF-β signaling in tumor suppression and cancer progression. Nat Genet *29*, 117-129.

Derynck, R., Gelbart, W. M., Harland, R. M., Heldin, C. H., Kern, S. E., Massague, J., Melton, D. A., Mlodzik, M., Padgett, R. W., Roberts, A. B., *et al.* (1996). Nomenclature: vertebrate mediators of TGFβ family signals [letter]. Cell *87*, 0092-8674.

Derynck, R., and Zhang, Y. E. (2003). Smad-dependent and Smad-independent pathways in TGF-β family signalling. Nature *425*, 577-584.

Desgrosellier, J. S., Mundell, N. A., McDonnell, M. A., Moses, H. L., and Barnett, J. V. (2005). Activin receptor-like kinase 2 and Smad6 regulate epithelial-mesenchymal transformation during cardiac valve formation. Dev Biol *280*, 201-210.

Di Guglielmo, G. M., Le Roy, C., Goodfellow, A. F., and Wrana, J. L. (2003). Distinct endocytic pathways regulate TGF-β receptor signalling and turnover. Nat Cell Biol *5*, 410-421.

Dickson, M. C., Slager, H. G., Duffie, E., Mummery, C. L., and Akhurst, R. J. (1993). RNA and protein localisations of TGF β 2 in the early mouse embryo suggest an involvement in cardiac development. Development *117*, 625-639.

Diehl, J. A., Cheng, M., Roussel, M. F., and Sherr, C. J. (1998). Glycogen synthase kinase-3β regulates cyclin D1 proteolysis and subcellular localization. Genes Dev *12*, 3499-3511.

Diehl, J. A., Zindy, F., and Sherr, C. J. (1997). Inhibition of cyclin D1 phosphorylation on threonine-286 prevents its rapid degradation via the ubiquitin-proteasome pathway. Genes Dev *11*, 957-972.

Dono, R., Scalera, L., Pacifico, F., Acampora, D., Persico, M. G., and Simeone, A. (1993). The murine cripto gene: expression during mesoderm induction and early heart morphogenesis. Development *118*, 1157-1168.

Dorey, K., and Hill, C. S. (2006). A novel Cripto-related protein reveals an essential role for EGF-CFCs in Nodal signalling in Xenopus embryos. Dev Biol *292*, 303-316.

Dottori, M., Gross, M. K., Labosky, P., and Goulding, M. (2001). The winged-helix transcription factor Foxd3 suppresses interneuron differentiation and promotes neural crest cell fate. Development *128*, 4127-4138.

Downward, J. (1998). Ras signalling and apoptosis. Curr Opin Genet Dev *8*, 49-54.

Drakas, R., Prisco, M., and Baserga, R. (2005). A modified tandem affinity purification tag technique for the purification of protein complexes in mammalian cells. Proteomics *5*, 132-137.

Dubois, C. M., Laprise, M. H., Blanchette, F., Gentry, L. E., and Leduc, R. (1995). Processing of transforming growth factor β 1 precursor by human furin convertase. J Biol Chem *270*, 10618-10624.

Dudas, M., Kim, J., Li, W. Y., Nagy, A., Larsson, J., Karlsson, S., Chai, Y., and Kaartinen, V. (2006). Epithelial and ectomesenchymal role of the type I TGF-β receptor ALK5 during facial morphogenesis and palatal fusion. Dev Biol *296*, 298-314.

Dudas, M., Nagy, A., Laping, N. J., Moustakas, A., and Kaartinen, V. (2004). Tgf-β3-induced palatal fusion is mediated by Alk-5/Smad pathway. Dev Biol *266*, 96-108.

Dudley, A. T., Lyons, K. M., and Robertson, E. J. (1995). A requirement for bone morphogenetic protein-7 during development of the mammalian kidney and eye. Genes Dev *9*, 2795-2807.

Dunn, N. R., Vincent, S. D., Oxburgh, L., Robertson, E. J., and Bikoff, E. K. (2004). Combinatorial activities of Smad2 and Smad3 regulate mesoderm formation and patterning in the mouse embryo. Development *131*, 1717-1728.

Ebisawa, T., Fukuchi, M., Murakami, G., Chiba, T., Tanaka, K., Imamura, T., and Miyazono, K. (2001). Smurf1 interacts with transforming growth factor-β type I receptor through Smad7 and induces receptor degradation. J Biol Chem *276*, 12477-12480.

Ebner, R., Chen, R. H., Shum, L., Lawler, S., Zioncheck, T. F., Lee, A., Lopez, A. R., and Derynck, R. (1993). Cloning of a type I TGF-β receptor and its effect on TGF-β binding to the type II receptor. Science *260*, 1344-1348.

Eger, A., Aigner, K., Sonderegger, S., Dampier, B., Oehler, S., Schreiber, M., Berx, G., Cano, A., Beug, H., and Foisner, R. (2005). DeltaEF1 is a transcriptional repressor of E-cadherin and regulates epithelial plasticity in breast cancer cells. Oncogene *24*, 2375-2385.

Eger, A., Stockinger, A., Park, J., Langkopf, E., Mikula, M., Gotzmann, J., Mikulits, W., Beug, H., and Foisner, R. (2004). β-Catenin and TGFβ signalling cooperate to maintain a mesenchymal phenotype after FosER-induced epithelial to mesenchymal transition. Oncogene *23*, 2672-2680.

Eger, A., Stockinger, A., Schaffhauser, B., Beug, H., and Foisner, R. (2000). Epithelial mesenchymal transition by c-Fos estrogen receptor activation involves nuclear translocation of β-catenin and upregulation of β-catenin/lymphoid enhancer binding factor-1 transcriptional activity. J Cell Biol *148*, 173-188.

Eisenberg, L. M., and Markwald, R. R. (1995). Molecular regulation of atrioventricular valvuloseptal morphogenesis. Circ Res *77*, 1-6.

el Ghouzzi, V., Le Merrer, M., Perrin-Schmitt, F., Lajeunie, E., Benit, P., Renier, D., Bourgeois, P., Bolcato-Bellemin, A. L., Munnich, A., and Bonaventure, J. (1997). Mutations of the TWIST gene in the Saethre-Chotzen syndrome. Nat Genet *15*, 42-46.

Enoch, T., Zinn, K., and Maniatis, T. (1986). Activation of the human β-interferon gene requires an interferon-inducible factor. Mol Cell Biol *6*, 801-810.

Eppert, K., Scherer, S. W., Ozcelik, H., Pirone, R., Hoodless, P., Kim, H., Tsui, L. C., Bapat, B., Gallinger, S., Andrulis, I. L., *et al.* (1996). MADR2 maps to 18q21 and encodes a TGFβ-regulated MAD-related protein that is functionally mutated in colorectal carcinoma. Cell *86*, 543-552.

Erlacher, L., McCartney, J., Piek, E., ten Dijke, P., Yanagishita, M., Oppermann, H., and Luyten, F. P. (1998). Cartilage-derived morphogenetic proteins and osteogenic protein-1 differentially regulate osteogenesis. J Bone Miner Res *13*, 383-392.

Estevez, A. M., Kempf, T., and Clayton, C. (2001). The exosome of Trypanosoma brucei. EMBO J *20*, 3831-3839.

Estevez, M., Attisano, L., Wrana, J. L., Albert, P. S., Massague, J., and Riddle, D. L. (1993). The daf-4 gene encodes a bone morphogenetic protein receptor controlling C. elegans dauer larva development. Nature *365*, 644-649.

Felici, A., Wurthner, J. U., Parks, W. T., Giam, L. R., Reiss, M., Karpova, T. S., McNally, J. G., and Roberts, A. B. (2003). TLP, a novel modulator of TGF-β signaling, has opposite effects on Smad2- and Smad3-dependent signaling. EMBO J *22*, 4465-4477.

Feng, X. H., and Derynck, R. (1997). A kinase subdomain of transforming growth factor-β (TGF-β) type I receptor determines the TGF-β intracellular signaling specificity. EMBO J *16*, 3912-3923.

Feng, X. H., and Derynck, R. (2005). Specificity and versatility in tgf-β signaling through Smads. Annu Rev Cell Dev Biol *21*, 659-693.

Feng, X. H., Liang, Y. Y., Liang, M., Zhai, W., and Lin, X. (2002). Direct interaction of c-Myc with Smad2 and Smad3 to inhibit TGF-β-mediated induction of the CDK inhibitor p15(Ink4B). Mol Cell *9*, 133-143.

Ferguson, M. W. (1988). Palate development. Development *103 Suppl*, 41-60.

Forler, D., Kocher, T., Rode, M., Gentzel, M., Izaurralde, E., and Wilm, M. (2003). An efficient protein complex purification method for functional proteomics in higher eukaryotes. Nat Biotechnol *21*, 89-92.

Franzen, P., Heldin, C. H., and Miyazono, K. (1995). The GS domain of the transforming growth factor-β type I receptor is important in signal transduction. Biochem Biophys Res Commun *207*, 682-689.

Franzen, P., ten Dijke, P., Ichijo, H., Yamashita, H., Schulz, P., Heldin, C. H., and Miyazono, K. (1993). Cloning of a TGF β type I receptor that forms a heteromeric complex with the TGF β type II receptor. Cell *75*, 681-692.

Fukuchi, M., Imamura, T., Chiba, T., Ebisawa, T., Kawabata, M., Tanaka, K., and Miyazono, K. (2001). Ligand-dependent degradation of Smad3 by a ubiquitin ligase complex of ROC1 and associated proteins. Mol Biol Cell *12*, 1431-1443.

Gaddy-Kurten, D., Tsuchida, K., and Vale, W. (1995). Activins and the receptor serine kinase superfamily. Recent Prog Horm Res *50*, 109-129.

Galvin, K. M., Donovan, M. J., Lynch, C. A., Meyer, R. I., Paul, R. J., Lorenz, J. N., Fairchild-Huntress, V., Dixon, K. L., Dunmore, J. H., Gimbrone, M. A., Jr., *et al.* (2000). A role for smad6 in development and homeostasis of the cardiovascular system. Nat Genet *24*, 171-174.

Garamszegi, N., Dore, J. J., Jr., Penheiter, S. G., Edens, M., Yao, D., and Leof, E. B. w. (2001). Transforming growth factor β receptor signaling and endocytosis are linked through a COOH terminal activation motif in the type I receptor. Mol Biol Cell *12*, 2881-2893.

Gato, A., Martinez, M. L., Tudela, C., Alonso, I., Moro, J. A., Formoso, M. A., Ferguson, M. W., and Martinez-Alvarez, C. (2002). TGF-β(3)-induced chondroitin sulphate proteoglycan mediates palatal shelf adhesion. Dev Biol *250*, 393-405.

Gaussin, V., Van de Putte, T., Mishina, Y., Hanks, M. C., Zwijsen, A., Huylebroeck, D., Behringer, R. R., and Schneider, M. D. (2002). Endocardial cushion and myocardial defects after cardiac myocyte-specific conditional deletion of the bone morphogenetic protein receptor ALK3. Proc Natl Acad Sci U S A *99*, 2878-2883.

Gavin, A. C., Bosche, M., Krause, R., Grandi, P., Marzioch, M., Bauer, A., Schultz, J., Rick, J. M., Michon, A. M., Cruciat, C. M., *et al.* (2002). Functional organization of the yeast proteome by systematic analysis of protein complexes. Nature *415*, 141-147.

Germain, S., Howell, M., Esslemont, G. M., and Hill, C. S. (2000). Homeodomain and winged-helix transcription factors recruit activated Smads to distinct promoter elements via a common Smad interaction motif. Genes Dev *14*, 435-451.

Getsios, S., Amargo, E. V., Dusek, R. L., Ishii, K., Sheu, L., Godsel, L. M., and Green, K. J. (2004). Coordinated expression of desmoglein 1 and desmocollin 1 regulates intercellular adhesion. Differentiation *72*, 419-433.

Gilboa, L., Wells, R. G., Lodish, H. F., and Henis, Y. I. (1998). Oligomeric structure of type I and type II transforming growth factor β receptors: homodimers form in the ER and persist at the plasma membrane. J Cell Biol *140*, 767-777.

Gomperts, B. D., Kramer, I. M., and Tatham, P. E. R. (2003). Signal Transduction, 3rd Edition edn: Elsevier Academic Press).

Gotzmann, J., Huber, H., Thallinger, C., Wolschek, M., Jansen, B., Schulte-Hermann, R., Beug, H., and Mikulits, W. (2002). Hepatocytes convert to a fibroblastoid phenotype through the cooperation of TGF-β1 and Ha-Ras: steps towards invasiveness. J Cell Sci *115*, 1189-1202.

Gougos, A., and Letarte, M. (1988). Identification of a human endothelial cell antigen with monoclonal antibody 44G4 produced against a pre-B leukemic cell line. J Immunol *141*, 1925-1933.

Gougos, A., and Letarte, M. (1990). Primary structure of endoglin, an RGD-containing glycoprotein of human endothelial cells. J Biol Chem *265*, 8361-8364.

Gougos, A., St Jacques, S., Greaves, A., O'Connell, P. J., d'Apice, A. J., Buhring, H. J., Bernabeu, C., van Mourik, J. A., and Letarte, M. (1992). Identification of distinct epitopes of endoglin, an RGD-containing glycoprotein of endothelial cells, leukemic cells, and syncytiotrophoblasts. Int Immunol *4*, 83-92.

Goumans, M. J., Lebrin, F., and Valdimarsdottir, G. (2003a). Controlling the angiogenic switch: a balance between two distinct TGF-β receptor signaling pathways. Trends Cardiovasc Med *13*, 301-307.

Goumans, M. J., and Mummery, C. (2000). Functional analysis of the TGFβ receptor/Smad pathway through gene ablation in mice. Int J Dev Biol *44*, 253-265.

Goumans, M. J., Valdimarsdottir, G., Itoh, S., Lebrin, F., Larsson, J., Mummery, C., Karlsson, S., and ten Dijke, P. (2003b). Activin receptor-like kinase (ALK)1 is an antagonistic mediator of lateral TGFβ/ALK5 signaling. Mol Cell *12*, 817-828.

Goumans, M. J., Valdimarsdottir, G., Itoh, S., Rosendahl, A., Sideras, P., and ten Dijke, P. (2002). Balancing the activation state of the endothelium via two distinct TGF-β type I receptors. EMBO J *21*, 1743-1753.

Graff, J. M., Bansal, A., and Melton, D. A. (1996). *Xenopus* Mad proteins transduce distinct subsets of signals for the TGF-β superfamily. Cell *85*, 479-487.

Gray, P. C., Bilezikjian, L. M., and Vale, W. (2002). Antagonism of activin by inhibin and inhibin receptors: a functional role for βglycan. Mol Cell Endocrinol *188*, 254-260.

Greenwald, J., Fischer, W. H., Vale, W. W., and Choe, S. (1999). Three-finger toxin fold for the extracellular ligand-binding domain of the type II activin receptor serine kinase. Nat Struct Biol *6*, 18-22.

Greenwald, J., Groppe, J., Gray, P., Wiater, E., Kwiatkowski, W., Vale, W., and Choe, S. (2003). The BMP7/ActRII extracellular domain complex provides new insights into the cooperative nature of receptor assembly. Mol Cell *11*, 605-617.

Greenwald, J., Vega, M. E., Allendorph, G. P., Fischer, W. H., Vale, W., and Choe, S. (2004). A flexible activin explains the membrane-dependent cooperative assembly of TGF-β family receptors. Mol Cell *15*, 485-489.

Grimm, O. H., and Gurdon, J. B. (2002). Nuclear exclusion of Smad2 is a mechanism leading to loss of competence. Nat Cell Biol *4*, 519-522.

Gritsman, K., Zhang, J., Cheng, S., Heckscher, E., Talbot, W. S., and Schier, A. F. (1999). The EGF-CFC protein one-eyed pinhead is essential for nodal signaling. Cell *97*, 121-132.

Grunert, S., Jechlinger, M., and Beug, H. (2003). Diverse cellular and molecular mechanisms contribute to epithelial plasticity and metastasis. Nat Rev Mol Cell Biol *4*, 657-665.

Gu, Z., Reynolds, E. M., Song, J., Lei, H., Feijen, A., Yu, L., He, W., MacLaughlin, D. T., van den Eijnden-van Raaij, J., Donahoe, P. K., and Li, E. (1999). The type I serine/threonine kinase receptor ActRIA (ALK2) is required for gastrulation of the mouse embryo. Development *126*, 2551-2561.

Guerrero-Esteo, M., Sanchez-Elsner, T., Letamendia, A., and Bernabeu, C. (2002). Extracellular and cytoplasmic domains of endoglin interact with the transforming growth factor-β receptors I and II. J Biol Chem *277*, 29197-29209.

Hahn, S. A., Schutte, M., Hoque, A. T., Moskaluk, C. A., da Costa, L. T., Rozenblum, E., Weinstein, C. L., Fischer, A., Yeo, C. J., Hruban, R. H., and Kern, S. E. (1996). DPC4, a candidate tumor suppressor gene at human chromosome 18q21.1. Science *271*, 350-353.

Hajra, K. M., Chen, D. Y., and Fearon, E. R. (2002). The SLUG zinc-finger protein represses E-cadherin in breast cancer. Cancer Res *62*, 1613-1618.

Han, S. U., Kim, H. T., Seong do, H., Kim, Y. S., Park, Y. S., Bang, Y. J., Yang, H. K., and Kim, S. J. (2004). Loss of the Smad3 expression increases susceptibility to tumorigenicity in human gastric cancer. Oncogene *23*, 1333-1341.

Hanks, S. K., and Hunter, T. (1995). Protein kinases 6. The eukaryotic protein kinase superfamily: kinase (catalytic) domain structure and classification. Faseb J *9*, 576-596.

Harlow, E., and Lane, D. (1988). Antibodies, a Laboratory Manual.: Cold Spring Harbour Laborator Press.).

Hart, P. J., Deep, S., Taylor, A. B., Shu, Z., Hinck, C. S., and Hinck, A. P. (2002). Crystal structure of the human TβR2 ectodomain--TGF-β3 complex. Nat Struct Biol *9*, 203-208.

Hata, A., Lagna, G., Massague, J., and Hemmati-Brivanlou, A. (1998). Smad6 inhibits BMP/Smad1 signaling by specifically competing with the Smad4 tumor suppressor. Genes Dev *12*, 186-197.

Hata, A., Lo, R. S., Wotton, D., Lagna, G., and Massague, J. (1997). Mutations increasing autoinhibition inactivate tumour suppressors Smad2 and Smad4. Nature *388*, 82-87.

Hata, A., Seoane, J., Lagna, G., Montalvo, E., Hemmati-Brivanlou, A., and Massague, J. (2000). OAZ uses distinct DNA- and protein-binding zinc fingers in separate BMP-Smad and Olf signaling pathways. Cell *100*, 229-240.

Hay, E. D. (2005). The mesenchymal cell, its role in the embryo, and the remarkable signaling mechanisms that create it. Dev Dyn *233*, 706-720.

Henis, Y. I., Moustakas, A., Lin, H. Y., and Lodish, H. F. (1994). The types II and III transforming growth factor-β receptors form homo-oligomers. J Cell Biol *126*, 139-154.

Hoodless, P. A., Haerry, T., Abdollah, S., Stapleton, M., O'Connor, M. B., Attisano, L., and Wrana, J. L. (1996). MADR1, a MAD-related protein that functions in BMP2 signaling pathways. Cell *85*, 489-500.

Howe, J. R., Bair, J. L., Sayed, M. G., Anderson, M. E., Mitros, F. A., Petersen, G. M., Velculescu, V. E., Traverso, G., and Vogelstein, B. (2001). Germline mutations of the gene encoding bone morphogenetic protein receptor 1A in juvenile polyposis. Nat Genet *28*, 184-187.

Howe, J. R., Roth, S., Ringold, J. C., Summers, R. W., Jarvinen, H. J., Sistonen, P., Tomlinson, I. P., Houlston, R. S., Bevan, S., Mitros, F. A., *et al.* (1998). Mutations in the SMAD4/DPC4 gene in juvenile polyposis. Science *280*, 1086-1088.

Howell, M., and Hill, C. S. (1997). XSmad2 directly activates the activin-inducible, dorsal mesoderm gene XFKH1 in Xenopus embryos. EMBO J *16*, 7411-7421.

Howell, M., Inman, G. J., and Hill, C. S. (2002). A novel Xenopus Smad-interacting forkhead transcription factor (XFast-3) cooperates with XFast-1 in regulating gastrulation movements. Development *129*, 2823-2834.

Howell, M., Itoh, F., Pierreux, C. E., Valgeirsdottir, S., Itoh, S., ten Dijke, P., and Hill, C. S. (1999). *Xenopus* Smad4β is the co-Smad component of developmentally-regulated transcription factor complexes responsible for induction of early mesodermal genes. Dev Biol *214*, 354-369.

Huber, M. A., Azoitei, N., Baumann, B., Grunert, S., Sommer, A., Pehamberger, H., Kraut, N., Beug, H., and Wirth, T. (2004a). NF-kappaB is essential for epithelial-mesenchymal transition and metastasis in a model of breast cancer progression. J Clin Invest *114*, 569-581.

Huber, M. A., Beug, H., and Wirth, T. (2004b). Epithelial-mesenchymal transition: NF-kappaB takes center stage. Cell Cycle *3*, 1477-1480.

Huber, M. A., Kraut, N., and Beug, H. (2005). Molecular requirements for epithelial-mesenchymal transition during tumor progression. Curr Opin Cell Biol *17*, 548-558.

Huse, M., Chen, Y. G., Massague, J., and Kuriyan, J. (1999). Crystal structure of the cytoplasmic domain of the type I TGF β receptor in complex with FKBP12. Cell *96*, 425-436.

Huse, M., Muir, T. W., Xu, L., Chen, Y. G., Kuriyan, J., and Massague, J. (2001). The TGF β receptor activation process: an inhibitor- to substrate-binding switch. Mol Cell *8*, 671-682.

Hutvagner, G., and Zamore, P. D. (2002). A microRNA in a multiple-turnover RNAi enzyme complex. Science *297*, 2056-2060.

Imamura, T., Takase, M., Nishihara, A., Oeda, E., Hanai, J., Kawabata, M., and Miyazono, K. (1997). Smad6 inhibits signalling by the TGF-β superfamily. Nature *389*, 622-626.

Inman, G. J., and C.S., H. (2002a). Stoichiometry of active Smad-transcription factor complexes on DNA. J. Blol. Chem. *277*, 51008-51016.

Inman, G. J., Nicolas, F. J., Callahan, J. F., Harling, J. D., Gaster, L. M., Reith, A. D., Laping, N. J., and Hill, C. S. (2002b). SB-431542 is a potent and specific inhibitor of transforming growth factor-β superfamily type I activin receptor-like kinase (ALK) receptors ALK4, ALK5, and ALK7. Mol Pharmacol *62*, 65-74.

Inman, G. J., Nicolas, F. J., and Hill, C. S. (2002c). Nucleocytoplasmic shuttling of Smads 2, 3, and 4 permits sensing of TGF-β receptor activity. Mol Cell *10*, 283-294.

Ishida, W., Hamamoto, T., Kusanagi, K., Yagi, K., Kawabata, M., Takehara, K., Sampath, T. K., Kato, M., and Miyazono, K. (2000). Smad6 is a Smad1/5-induced smad inhibitor. Characterization of bone morphogenetic protein-responsive element in the mouse Smad6 promoter. J Biol Chem *275*, 6075-6079.

Ito, Y., Yeo, J. Y., Chytil, A., Han, J., Bringas, P., Jr., Nakajima, A., Shuler, C. F., Moses, H. L., and Chai, Y. (2003). Conditional inactivation of Tgfbr2 in cranial neural crest causes cleft palate and calvaria defects. Development *130*, 5269-5280.

Izzi, L., and Attisano, L. (2004). Regulation of the TGFβ signalling pathway by ubiquitin-mediated degradation. Oncogene *23*, 2071-2078.

Janda, E., Lehmann, K., Killisch, I., Jechlinger, M., Herzig, M., Downward, J., Beug, H., and Grunert, S. (2002). Ras and TGFβ cooperatively regulate epithelial cell plasticity and metastasis: dissection of Ras signaling pathways. J Cell Biol *156*, 299-313.

Javelaud, D., and Mauviel, A. (2005). Crosstalk mechanisms between the mitogen-activated protein kinase pathways and Smad signaling downstream of TGF-β: implications for carcinogenesis. Oncogene *24*, 5742-5750.

Jayaraman, L., and Massague, J. (2000). Distinct oligomeric states of SMAD proteins in the transforming growth factor-β pathway. J Biol Chem *275*, 40710-40717.

Jechlinger, M., Grunert, S., Tamir, I. H., Janda, E., Ludemann, S., Waerner, T., Seither, P., Weith, A., Beug, H., and Kraut, N. (2003). Expression profiling of epithelial plasticity in tumor progression. Oncogene *22*, 7155-7169.

Jeruss, J. S., Santiago, J. Y., and Woodruff, T. K. (2003). Localization of activin and inhibin subunits, receptors and SMADs in the mouse mammary gland. Mol Cell Endocrinol *203*, 185-196.

Jin, J. Z., and Ding, J. (2006). Analysis of cell migration, transdifferentiation and apoptosis during mouse secondary palate fusion. Development *133*, 3341-3347.

Johnson, D. W., Berg, J. N., Baldwin, M. A., Gallione, C. J., Marondel, I., Yoon, S. J., Stenzel, T. T., Speer, M., Pericak-Vance, M. A., Diamond, A., *et al.* (1996). Mutations in the activin receptor-like kinase 1 gene in hereditary haemorrhagic telangiectasia type 2. Nat Genet *13*, 189-195.

Johnson, L. N., Noble, M. E., and Owen, D. J. (1996). Active and inactive protein kinases: structural basis for regulation. Cell *85*, 149-158.

Jonk, L. J., Itoh, S., Heldin, C. H., ten Dijke, P., and Kruijer, W. (1998). Identification and functional characterization of a Smad binding element (SBE) in the JunB promoter that acts as a transforming growth factor-β, activin, and bone morphogenetic protein-inducible enhancer. J Biol Chem *273*, 21145-21152.

Ju, W., Ogawa, A., Heyer, J., Nierhof, D., Yu, L., Kucherlapati, R., Shafritz, D. A., and Bottinger, E. P. (2006). Deletion of Smad2 in mouse liver reveals novel functions in hepatocyte growth and differentiation. Mol Cell Biol *26*, 654-667.

Kaartinen, V., Cui, X. M., Heisterkamp, N., Groffen, J., and Shuler, C. F. (1997). Transforming growth factor-β3 regulates transdifferentiation of medial edge epithelium during palatal fusion and associated degradation of the basement membrane. Dev Dyn *209*, 255-260.

Kaartinen, V., Voncken, J. W., Shuler, C., Warburton, D., Bu, D., Heisterkamp, N., and Groffen, J. (1995). Abnormal lung development and cleft palate in mice lacking TGF-β 3 indicates defects of epithelial-mesenchymal interaction. Nat Genet *11*, 415-421.

Kang, Y., Chen, C. R., and Massague, J. (2003). A self-enabling TGFβ response coupled to stress signaling: Smad engages stress response factor ATF3 for Id1 repression in epithelial cells. Mol Cell *11*, 915-926.

Karin, M., and Hunter, T. (1995). Transcriptional control by protein phosphorylation: signal transmission from the cell surface to the nucleus. Curr Biol *5*, 747-757.

Kavsak, P., Rasmussen, R. K., Causing, C. G., Bonni, S., Zhu, H., Thomsen, G. H., and Wrana, J. L. (2000). Smad7 binds to Smurf2 to form an E3 ubiquitin ligase that targets the TGF β receptor for degradation. Mol Cell *6*, 1365-1375.

Kawabata, M., Inoue, H., Hanyu, A., Imamura, T., and Miyazono, K. (1998). Smad proteins exist as monomers in vivo and undergo homo- and hetero-oligomerization upon activation by serine/threonine kinase receptors. EMBO J *17*, 4056-4065.

Keller, S., Nickel, J., Zhang, J. L., Sebald, W., and Mueller, T. D. (2004). Molecular recognition of BMP-2 and BMP receptor IA. Nat Struct Mol Biol *11*, 481-488.

Kim, J., Johnson, K., Chen, H. J., Carroll, S., and Laughon, A. (1997). Drosophila Mad binds to DNA and directly mediates activation of vestigial by Decapentaplegic. Nature *388*, 304-308.

Kim, S. G., Kim, H. A., Jong, H. S., Park, J. H., Kim, N. K., Hong, S. H., Kim, T. Y., and Bang, Y. J. (2005). The endogenous ratio of Smad2 and Smad3 influences the cytostatic function of Smad3. Mol Biol Cell *16*, 4672-4683.

Kim, S. J., Im, Y. H., Markowitz, S. D., and Bang, Y. J. (2000). Molecular mechanisms of inactivation of TGF-β receptors during carcinogenesis. Cytokine Growth Factor Rev *11*, 159-168.

Kinoshita, K., and Asashima, M. (1995). Effect of activin and lithium on isolated Xenopus animal blastomeres and response alteration at the midblastula transition. Development *121*, 1581-1589.

Kirsch, T., Sebald, W., and Dreyer, M. K. (2000). Crystal structure of the BMP-2-BRIA ectodomain complex. Nat Struct Biol *7*, 492-496.

Kluppel, M., and Wrana, J. L. (2005). Turning it up a Notch: cross-talk between TGF β and Notch signaling. Bioessays *27*, 115-118.

Knockaert, M., Sapkota, G., Alarcon, C., Massague, J., and Brivanlou, A. H. (2006). Unique players in the BMP pathway: small C-terminal domain phosphatases dephosphorylate Smad1 to attenuate BMP signaling. Proc Natl Acad Sci U S A *103*, 11940-11945.

Koleva, R. I., Conley, B. A., Romero, D., Riley, K. S., Marto, J. A., Lux, A., and Vary, C. P. (2006). Endoglin Structure and Function: Determinants of endoglin phosphorylation by transforming growth factor-β receptors. J Biol Chem *281*, 25110-25123.

Kondo, M., Cubillo, E., Tobiume, K., Shirakihara, T., Fukuda, N., Suzuki, H., Shimizu, K., Takehara, K., Cano, A., Saitoh, M., and Miyazono, K. (2004). A role for Id in the regulation of TGF-β-induced epithelial-mesenchymal transdifferentiation. Cell Death Differ *11*, 1092-1101.

Korchynskyi, O., and ten Dijke, P. (2002). Identification and functional characterization of distinct critically important bone morphogenetic protein-specific response elements in the Id1 promoter. J Biol Chem *277*, 4883-4891.

Kowanetz, M., Valcourt, U., Bergstrom, R., Heldin, C. H., and Moustakas, A. (2004). Id2 and Id3 define the potency of cell proliferation and differentiation responses to transforming growth factor β and bone morphogenetic protein. Mol Cell Biol *24*, 4241-4254.

Kretzschmar, M., Doody, J., and Massague, J. (1997). Opposing BMP and EGF signalling pathways converge on the TGF-β family mediator Smad1. Nature *389*, 618-622.

Kretzschmar, M., Doody, J., Timokhina, I., and Massague, J. (1999). A mechanism of repression of TGFβ/ Smad signaling by oncogenic Ras. Genes Dev *13*, 804-816.

Kurisaki, A., Kose, S., Yoneda, Y., Heldin, C. H., and Moustakas, A. (2001). Transforming growth factor-β induces nuclear import of Smad3 in an importin-β1 and Ran-dependent manner. Mol Biol Cell *12*, 1079-1091.

Kuroda, H., Fuentealba, L., Ikeda, A., Reversade, B., and De Robertis, E. M. (2005). Default neural induction: neuralization of dissociated Xenopus cells is mediated by Ras/MAPK activation. Genes Dev *19*, 1022-1027.

Labbe, E., Letamendia, A., and Attisano, L. (2000). Association of Smads with lymphoid enhancer binding factor 1/T cell-specific factor mediates cooperative signaling by the transforming growth factor-β and wnt pathways. Proc Natl Acad Sci U S A *97*, 8358-8363.

Lai, Y. T., Beason, K. B., Brames, G. P., Desgrosellier, J. S., Cleggett, M. C., Shaw, M. V., Brown, C. B., and Barnett, J. V. (2000). Activin receptor-like kinase 2 can mediate atrioventricular cushion transformation. Dev Biol *222*, 1-11.

Laiho, M., Weis, M. B., and Massague, J. (1990). Concomitant loss of transforming growth factor (TGF)-β receptor types I and II in TGF-β-resistant cell mutants implicates both receptor types in signal transduction. J Biol Chem *265*, 18518-18524.

Lamouille, S., Mallet, C., Feige, J. J., and Bailly, S. (2002). Activin receptor-like kinase 1 is implicated in the maturation phase of angiogenesis. Blood *100*, 4495-4501.

Lan, H. Y., Mu, W., Tomita, N., Huang, X. R., Li, J. H., Zhu, H. J., Morishita, R., and Johnson, R. J. (2003). Inhibition of renal fibrosis by gene transfer of inducible Smad7 using ultrasound-microbubble system in rat UUO model. J Am Soc Nephrol *14*, 1535-1548.

Larsson, J., Goumans, M. J., Sjostrand, L. J., van Rooijen, M. A., Ward, D., Leveen, P., Xu, X., ten Dijke, P., Mummery, C. L., and Karlsson, S. (2001). Abnormal angiogenesis but intact hematopoietic potential in TGF-β type I receptor-deficient mice. EMBO J *20*, 1663-1673.

Lastres, P., Bellon, T., Cabanas, C., Sanchez-Madrid, F., Acevedo, A., Gougos, A., Letarte, M., and Bernabeu, C. (1992). Regulated expression on human macrophages of endoglin, an Arg-Gly-Asp-containing surface antigen. Eur J Immunol *22*, 393-397.

Lawler, S., Feng, X. H., Chen, R. H., Maruoka, E. M., Turck, C. W., Griswold-Prenner, I., and Derynck, R. (1997). The type II transforming growth factor-β receptor autophosphorylates not only on serine and threonine but also on tyrosine residues. J Biol Chem *272*, 14850-14859.

Lebrin, F., Goumans, M. J., Jonker, L., Carvalho, R. L., Valdimarsdottir, G., Thorikay, M., Mummery, C., Arthur, H. M., and ten Dijke, P. (2004). Endoglin promotes endothelial cell proliferation and TGF-β/ALK1 signal transduction. EMBO J *23*, 4018-4028.

Lebrun, J. J., and Vale, W. W. (1997). Activin and inhibin have antagonistic effects on ligand-dependent heteromerization of the type I and type II activin receptors and human erythroid differentiation. Mol Cell Biol *17*, 1682-1691.

Lee, Y. S., and Dutta, A. (2006). MicroRNAs: small but potent oncogenes or tumor suppressors. Curr Opin Investig Drugs *7*, 560-564.

Lehmann, K., Janda, E., Pierreux, C. E., Rytomaa, M., Schulze, A., McMahon, M., Hill, C. S., Beug, H., and Downward, J. (2000). Raf induces TGFβ production while blocking its apoptotic but not invasive responses: a mechanism leading to increased malignancy in epithelial cells. Genes Dev *14*, 2610-2622.

Letamendia, A., Lastres, P., Almendro, N., Raab, U., Buhring, H. J., Kumar, S., and Bernabeu, C. (1998a). Endoglin, a component of the TGF-β receptor system, is a differentiation marker of human choriocarcinoma cells. Int J Cancer *76*, 541-546.

Letamendia, A., Lastres, P., Botella, L. M., Raab, U., Langa, C., Velasco, B., Attisano, L., and Bernabeu, C. (1998b). Role of endoglin in cellular responses to transforming growth factor-β. A comparative study with βglycan. J Biol Chem *273*, 33011-33019.

Lever, J. E. (1979). Regulation of dome formation in differentiated epithelial cell cultures. J Supramol Struct *12*, 259-272.

Levy, L., and Hill, C. S. (2005). Smad4 dependency defines two classes of transforming growth factor β (TGF-β) target genes and distinguishes TGF-β-induced epithelial-mesenchymal transition from its anti-proliferative and migratory responses. Mol. Cell. Biol. *18*, 8108-8125.

Levy, L., and Hill, C. S. (2006). Alterations in components of the TGF-β superfamily signaling pathways in human cancer. Cytokine Growth Factor Rev *17*, 41-58.

Lewis, K. A., Gray, P. C., Blount, A. L., MacConell, L. A., Wiater, E., Bilezikjian, L. M., and Vale, W. (2000). Bglycan binds inhibin and can mediate functional antagonism of activin signalling. Nature *404*, 411-414.

Li, C., Hampson, I. N., Hampson, L., Kumar, P., Bernabeu, C., and Kumar, S. (2000). CD105 antagonizes the inhibitory signaling of transforming growth factor β1 on human vascular endothelial cells. Faseb J *14*, 55-64.

Li, D. Y., Sorensen, L. K., Brooke, B. S., Urness, L. D., Davis, E. C., Taylor, D. G., Boak, B. B., and Wendel, D. P. (1999). Defective angiogenesis in mice lacking endoglin. Science *284*, 1534-1537.

Li, H., Xu, D., Toh, B. H., and Liu, J. P. (2006). TGF-β and cancer: is Smad3 a repressor of hTERT gene? Cell Res *16*, 169-173.

Li, L., Xin, H., Xu, X., Huang, M., Zhang, X., Chen, Y., Zhang, S., Fu, X. Y., and Chang, Z. (2004). CHIP mediates degradation of Smad proteins and potentially regulates Smad-induced transcription. Mol Cell Biol *24*, 856-864.

Liebner, S., Cattelino, A., Gallini, R., Rudini, N., Iurlaro, M., Piccolo, S., and Dejana, E. (2004). B-catenin is required for endothelial-mesenchymal transformation during heart cushion development in the mouse. J Cell Biol *166*, 359-367.

Lin, X., Duan, X., Liang, Y. Y., Su, Y., Wrighton, K. H., Long, J., Hu, M., Davis, C. M., Wang, J., Brunicardi, F. C., *et al.* (2006). PPM1A functions as a Smad phosphatase to terminate TGFβ signaling. Cell *125*, 915-928.

Linker, C., and Stern, C. D. (2004). Neural induction requires BMP inhibition only as a late step, and involves signals other than FGF and Wnt antagonists. Development *131*, 5671-5681.

Liu, F., Hata, A., Baker, J. C., Doody, J., Carcamo, J., Harland, R. M., and Massague, J. (1996). A human Mad protein acting as a BMP-regulated transcriptional activator. Nature *381*, 620-623.

Liu, F., and Matsuura, I. (2005). Inhibition of Smad antiproliferative function by CDK phosphorylation. Cell Cycle *4*, 63-66.

Liu, F., Ventura, F., Doody, J., and Massague, J. (1995). Human type II receptor for bone morphogenic proteins (BMPs): extension of the two-kinase receptor model to the BMPs. Mol Cell Biol *15*, 3479-3486.

Lloyd, A. C. (1998). Ras versus cyclin-dependent kinase inhibitors. Curr Opin Genet Dev *8*, 43-48.

Lo, R. S., Chen, Y. G., Shi, Y., Pavletich, N. P., and Massague, J. (1998). The L3 loop: a structural motif determining specific interactions between SMAD proteins and TGF-β receptors. EMBO J *17*, 996-1005.

Lo, R. S., and Massague, J. (1999). Ubiquitin-dependent degradation of TGF-β-activated smad2. Nat Cell Biol *1*, 472-478.

Lopez-Casillas, F., Cheifetz, S., Doody, J., Andres, J. L., Lane, W. S., and Massague, J. (1991). Structure and expression of the membrane proteoglycan βglycan, a component of the TGF-β receptor system. Cell *67*, 785-795.

Lopez-Casillas, F., Payne, H. M., Andres, J. L., and Massague, J. (1994). Bglycan can act as a dual modulator of TGF-β access to signaling receptors: mapping of ligand binding and GAG attachment sites. J Cell Biol *124*, 557-568.

Lopez-Casillas, F., Wrana, J. L., and Massague, J. (1993). Bglycan presents ligand to the TGF β signaling receptor. Cell *73*, 1435-1444.

Louvi, A., and Artavanis-Tsakonas, S. (2006). Notch signalling in vertebrate neural development. Nat Rev Neurosci *7*, 93-102.

Luo, G., Hofmann, C., Bronckers, A. L., Sohocki, M., Bradley, A., and Karsenty, G. (1995). BMP-7 is an inducer of nephrogenesis, and is also required for eye development and skeletal patterning. Genes Dev *9*, 2808-2820.

Luo, K., and Lodish, H. F. (1996). Signaling by chimeric erythropoietin-TGF-β receptors: homodimerization of the cytoplasmic domain of the type I TGF-β receptor and heterodimerization with the type II receptor are both required for intracellular signal transduction. EMBO J *15*, 4485-4496.

Luo, K., and Lodish, H. F. (1997). Positive and negative regulation of type II TGF-β receptor signal transduction by autophosphorylation on multiple serine residues. EMBO J *16*, 1970-1981.

Lutz, M., and Knaus, P. (2002). Integration of the TGF-β pathway into the cellular signalling network. Cell Signal *14*, 977-988.

Lux, A., Attisano, L., and Marchuk, D. A. (1999). Assignment of Transforming Growth Factor β1 and β3 and a Third New Ligand to the Type I Receptor ALK-1. J Biol Chem *274*, 9984-9992.

Lyons, R. M., Keski-Oja, J., and Moses, H. L. (1988). Proteolytic activation of latent transforming growth factor-β from fibroblast-conditioned medium. J Cell Biol *106*, 1659-1665.

Ma, L., Lu, M. F., Schwartz, R. J., and Martin, J. F. (2005). Bmp2 is essential for cardiac cushion epithelial-mesenchymal transition and myocardial patterning. Development *132*, 5601-5611.

Macias-Silva, M., Abdollah, S., Hoodless, P. A., Pirone, R., Attisano, L., and Wrana, J. L. (1996). MADR2 is a substrate of the TGFβ receptor and its phosphorylation is required for nuclear accumulation and signaling. Cell *87*, 1215-1224.

Macias-Silva, M., Hoodless, P. A., Tang, S. J., Buchwald, M., and Wrana, J. L. (1998). Specific activation of Smad1 signaling pathways by the BMP7 type I receptor, ALK2. J Biol Chem *273*, 25628-25636.

Malumbres, M., and Pellicer, A. (1998). RAS pathways to cell cycle control and cell transformation. Front Biosci *3*, d887-912.

Manning, G., Whyte, D. B., Martinez, R., Hunter, T., and Sudarsanam, S. (2002). The protein kinase complement of the human genome. Science *298*, 1912-1934.

Marais, R., Wynne, J., and Treisman, R. (1993). The SRF accessory protein Elk-1 contains a growth factor-regulated transcriptional activation domain. Cell *73*, 381-393.

Martinez-Alvarez, C., Blanco, M. J., Perez, R., Rabadan, M. A., Aparicio, M., Resel, E., Martinez, T., and Nieto, M. A. (2004). Snail family members and cell survival in physiological and pathological cleft palates. Dev Biol *265*, 207-218.

Massague, J. (1998). TGF-β signal transduction. Annu Rev Biochem *67*, 753-791.

Massague, J. (2000). How cells read TGF-β signals. Nat Rev Mol Cell Biol *1*, 169-178.

Massague, J. (2004). G1 cell-cycle control and cancer. Nature *432*, 298-306.

Massague, J., Blain, S. W., and Lo, R. S. (2000a). TGFβ signaling in growth control, cancer, and heritable disorders. Cell *103*, 295-309.

Massague, J., and Gomis, R. R. (2006). The logic of TGFβ signaling. FEBS Lett *580*, 2811-2820.

Massague, J., Seoane, J., and Wotton, D. (2005). Smad transcription factors. Genes Dev *19*, 2783-2810.

Massague, J., and Wotton, D. (2000b). Transcriptional control by the TGF-β/Smad signaling system. EMBO J *19*, 1745-1754.

Massagué, J. (1998). TGF-β signal transduction. Ann. Rev. Biochem. *67*, 753-791.

Matsuura, I., Denissova, N. G., Wang, G., He, D., Long, J., and Liu, F. (2004). Cyclin-dependent kinases regulate the antiproliferative function of Smads. Nature *430*, 226-231.

Maurice, D., Pierreux, C. E., Howell, M., Wilentz, R. E., Owen, M. J., and Hill, C. S. (2001). Loss of Smad4 function in pancreatic tumors: C-terminal truncation leads to decreased stability. J Biol Chem *276*, 43175-43181.

McAllister, K. A., Grogg, K. M., Johnson, D. W., Gallione, C. J., Baldwin, M. A., Jackson, C. E., Helmbold, E. A., Markel, D. S., McKinnon, W. C., Murrell, J., and et al. (1994). Endoglin, a TGF-β binding protein of endothelial cells, is the gene for hereditary haemorrhagic telangiectasia type 1. Nat Genet *8*, 345-351.

Mehler, M. F., Mabie, P. C., Zhang, D., and Kessler, J. A. (1997). Bone morphogenetic proteins in the nervous system. Trends Neurosci *20*, 309-317.

Melton, D. A., Krieg, P. A., Rebagliati, M. R., Maniatis, T., Zinn, K., and Green, M. R. (1984). Efficient in vitro synthesis of biologically active RNA and RNA hybridization probes from plasmids containing a bacteriophage SP6 promoter. Nucleic Acids Res *12*, 7035-7056.

Meulemans, D., and Bronner-Fraser, M. (2004). Gene-regulatory interactions in neural crest evolution and development. Dev Cell *7*, 291-299.

Miettinen, P. J., Ebner, R., Lopez, A. R., and Derynck, R. (1994). TGF-β induced transdifferentiation of mammary epithelial cells to mesenchymal cells: involvement of type I receptors. J Cell Biol *127*, 2021-2036.

Millan, F. A., Denhez, F., Kondaiah, P., and Akhurst, R. J. (1991). Embryonic gene expression patterns of TGF β 1, β 2 and β 3 suggest different developmental functions in vivo. Development *111*, 131-143.

Minchiotti, G., Parisi, S., Liguori, G., Signore, M., Lania, G., Adamson, E. D., Lago, C. T., and Persico, M. G. (2000). Membrane-anchorage of Cripto protein by glycosylphosphatidylinositol and its distribution during early mouse development. Mech Dev *90*, 133-142.

Mittl, P. R., Priestle, J. P., Cox, D. A., McMaster, G., Cerletti, N., and Grutter, M. G. (1996). The crystal structure of TGF-β 3 and comparison to TGF-β 2: implications for receptor binding. Protein Sci *5*, 1261-1271.

Mittnacht, S. (1998). Control of pRB phosphorylation. Curr Opin Genet Dev *8*, 21-27.

Mittnacht, S., Paterson, H., Olson, M. F., and Marshall, C. J. (1997). Ras signalling is required for inactivation of the tumour suppressor pRb cell-cycle control protein. Curr Biol *7*, 219-221.

Miura, S., Takeshita, T., Asao, H., Kimura, Y., Murata, K., Sasaki, Y., Hanai, J. I., Beppu, H., Tsukazaki, T., Wrana, J. L., *et al.* (2000). Hgs (Hrs), a FYVE domain protein, is involved in Smad signaling through cooperation with SARA. Mol Cell Biol *20*, 9346-9355.

Miyazono, K., Kusanagi, K., and Inoue, H. (2001). Divergence and convergence of TGF-β/BMP signaling. J Cell Physiol *187*, 265-276.

Monsoro-Burq, A. H., Fletcher, R. B., and Harland, R. M. (2003). Neural crest induction by paraxial mesoderm in Xenopus embryos requires FGF signals. Development *130*, 3111-3124.

Moody, S. E., Perez, D., Pan, T. C., Sarkisian, C. J., Portocarrero, C. P., Sterner, C. J., Notorfrancesco, K. L., Cardiff, R. D., and Chodosh, L. A. (2005). The transcriptional repressor Snail promotes mammary tumor recurrence. Cancer Cell *8*, 197-209.

Moore, R. K., Otsuka, F., and Shimasaki, S. (2003). Molecular basis of bone morphogenetic protein-15 signaling in granulosa cells. J Biol Chem *278*, 304-310.

Morales, A. V., Barbas, J. A., and Nieto, M. A. (2005). How to become neural crest: from segregation to delamination. Semin Cell Dev Biol *16*, 655-662.

Moustakas, A., Lin, H. Y., Henis, Y. I., Plamondon, J., O'Connor-McCourt, M. D., and Lodish, H. F. (1993). The transforming growth factor β receptors types I, II, and III form hetero-oligomeric complexes in the presence of ligand. J Biol Chem *268*, 22215-22218.

Moustakas, A., Souchelnytskyi, S., and Heldin, C. H. (2001). Smad regulation in TGF-β signal transduction. J Cell Sci *114*, 4359-4369.

Mulcahy, L. S., Smith, M. R., and Stacey, D. W. (1985). Requirement for ras proto-oncogene function during serum-stimulated growth of NIH 3T3 cells. Nature *313*, 241-243.

Muller, B., Hartmann, B., Pyrowolakis, G., Affolter, M., and Basler, K. (2003). Conversion of an extracellular Dpp/BMP morphogen gradient into an inverse transcriptional gradient. Cell *113*, 221-233.

Muraoka, R. S., Dumont, N., Ritter, C. A., Dugger, T. C., Brantley, D. M., Chen, J., Easterly, E., Roebuck, L. R., Ryan, S., Gotwals, P. J., *et al.* (2002). Blockade of TGF-β inhibits mammary tumor cell viability, migration, and metastases. J Clin Invest *109*, 1551-1559.

Nakamura, T., Nishizawa, T., Hagiya, M., Seki, T., Shimonishi, M., Sugimura, A., Tashiro, K., and Shimizu, S. (1989). Molecular cloning and expression of human hepatocyte growth factor. Nature *342*, 440-443.

Nakao, A., Afrakhte, M., Moren, A., Nakayama, T., Christian, J. L., Heuchel, R., Itoh, S., Kawabata, M., Heldin, N. E., Heldin, C. H., and ten Dijke, P. (1997). Identification of Smad7, a TGFβ-inducible antagonist of TGF-β signalling. Nature *389*, 631-635.

Nakashima, K., Yanagisawa, M., Arakawa, H., Kimura, N., Hisatsune, T., Kawabata, M., Miyazono, K., and Taga, T. (1999). Synergistic signaling in fetal brain by STAT3-Smad1 complex bridged by p300. Science *284*, 479-482.

Naldini, L., Weidner, K. M., Vigna, E., Gaudino, G., Bardelli, A., Ponzetto, C., Narsimhan, R. P., Hartmann, G., Zarnegar, R., Michalopoulos, G. K., and et al. (1991). Scatter factor and hepatocyte growth factor are indistinguishable ligands for the MET receptor. EMBO J *10*, 2867-2878.

Nateri, A. S., Riera-Sans, L., Da Costa, C., and Behrens, A. (2004). The ubiquitin ligase SCFFbw7 antagonizes apoptotic JNK signaling. Science *303*, 1374-1378.

Nawshad, A., and Hay, E. D. (2003). TGFβ3 signaling activates transcription of the LEF1 gene to induce epithelial mesenchymal transformation during mouse palate development. J Cell Biol *163*, 1291-1301.

Nawshad, A., LaGamba, D., and Hay, E. D. (2004). Transforming growth factor β (TGFβ) signalling in palatal growth, apoptosis and epithelial mesenchymal transformation (EMT). Arch Oral Biol *49*, 675-689.

Nawshad, A., Lagamba, D., Polad, A., and Hay, E. D. (2005). Transforming growth factor-β signaling during epithelial-mesenchymal transformation: implications for embryogenesis and tumor metastasis. Cells Tissues Organs *179*, 11-23.

Neubauer, G., King, A., Rappsilber, J., Calvio, C., Watson, M., Ajuh, P., Sleeman, J., Lamond, A., and Mann, M. (1998). Mass spectrometry and EST-database searching allows characterization of the multi-protein spliceosome complex. Nat Genet *20*, 46-50.

Newfeld, S. J., Wisotzkey, R. G., and Kumar, S. (1999). Molecular evolution of a developmental pathway: phylogenetic analyses of transforming growth factor-β family ligands, receptors and Smad signal transducers. Genetics *152*, 783-795.

Nicolas, F. J., De Bosscher, K., Schmierer, B., and Hill, C. S. (2004). Analysis of Smad nucleocytoplasmic shuttling in living cells. J Cell Sci *117*, 4113-4125.

Nicolas, F. J., Hill, C. S., Lehmann, K., Warne, P. H., Downward, J., Inman, G. J., Callahan, J. F., Harling, J. D., Gaster, L. M., Reith, A. D., and Laping, N. J. (2003a). Attenuation of the TGF-β-Smad signaling pathway in pancreatic tumor cells confers resistance to TGF-β-induced growth arrest. Oncogene *22*, 3698-3711.

Nicolas, F. J., Lehmann, K., Warne, P. H., Hill, C. S., and Downward, J. (2003b). Epithelial to mesenchymal transition in Madin-Darby canine kidney cells is accompanied by down-regulation of Smad3 expression, leading to resistance to transforming growth factor-β-induced growth arrest. J Biol Chem *278*, 3251-3256.

Nieto, M. A. (2002). The snail superfamily of zinc-finger transcription factors. Nat Rev Mol Cell Biol *3*, 155-166.

Nieto, M. A., Sargent, M. G., Wilkinson, D. G., and Cooke, J. (1994). Control of cell behavior during vertebrate development by Slug, a zinc finger gene. Science *264*, 835-839.

Nishita, M., Hashimoto, M. K., Ogata, S., Laurent, M. N., Ueno, N., Shibuya, H., and Cho, K. W. (2000). Interaction between Wnt and TGF-β signalling pathways during formation of Spemann's organizer. Nature *403*, 781-785.

Nishitoh, H., Ichijo, H., Kimura, M., Matsumoto, T., Makishima, F., Yamaguchi, A., Yamashita, H., Enomoto, S., and Miyazono, K. (1996). Identification of type I and type II serine/threonine kinase receptors for growth/differentiation factor-5. J Biol Chem *271*, 21345-21352.

Nomura, M., and Li, E. (1998). Smad2 role in mesoderm formation, left-right patterning and craniofacial development [see comments]. Nature *393*, 786-790.

Oft, M., Akhurst, R. J., and Balmain, A. (2002). Metastasis is driven by sequential elevation of H-ras and Smad2 levels. Nat Cell Biol *4*, 487-494.

Oft, M., Heider, K. H., and Beug, H. (1998). TGFβ signaling is necessary for carcinoma cell invasiveness and metastasis. Curr Biol *8*, 1243-1252.

Oft, M., Peli, J., Rudaz, C., Schwarz, H., Beug, H., and Reichmann, E. (1996). TGF-β1 and Ha-Ras collaborate in modulating the phenotypic plasticity and invasiveness of epithelial tumor cells. Genes Dev *10*, 2462-2477.

Oh, S. P., Seki, T., Goss, K. A., Imamura, T., Yi, Y., Donahoe, P. K., Li, L., Miyazono, K., ten Dijke, P., Kim, S., and Li, E. (2000). Activin receptor-like kinase 1 modulates transforming growth factor-β 1 signaling in the regulation of angiogenesis. Proc Natl Acad Sci U S A *97*, 2626-2631.

Okadome, T., Oeda, E., Saitoh, M., Ichijo, H., Moses, H. L., Miyazono, K., and Kawabata, M. (1996). Characterization of the interaction of FKBP12 with the transforming growth factor-β type I receptor in vivo. J Biol Chem *271*, 21687-21690.

Olsen, P. H., and Ambros, V. (1999). The lin-4 regulatory RNA controls developmental timing in Caenorhabditis elegans by blocking LIN-14 protein synthesis after the initiation of translation. Dev Biol *216*, 671-680.

Onichtchouk, D., Chen, Y. G., Dosch, R., Gawantka, V., Delius, H., Massague, J., and Niehrs, C. (1999). Silencing of TGF-β signalling by the pseudoreceptor BAMBI. Nature *401*, 480-485.

Ota, T., Fujii, M., Sugizaki, T., Ishii, M., Miyazawa, K., Aburatani, H., and Miyazono, K. (2002). Targets of transcriptional regulation by two distinct type I receptors for transforming growth factor-β in human umbilical vein endothelial cells. J Cell Physiol *193*, 299-318.

Ozdamar, B., Bose, R., Barrios-Rodiles, M., Wang, H. R., Zhang, Y., and Wrana, J. L. (2005). Regulation of the polarity protein Par6 by TGFβ receptors controls epithelial cell plasticity. Science *307*, 1603-1609.

Padgett, R. W., St Johnston, R. D., and Gelbart, W. M. (1987). A transcript from a Drosophila pattern gene predicts a protein homologous to the transforming growth factor-β family. Nature *325*, 81-84.

Patterson, G. I., and Padgett, R. W. (2000). TGF β-related pathways. Roles in Caenorhabditis elegans development. Trends Genet *16*, 27-33.

Peeper, D. S., Upton, T. M., Ladha, M. H., Neuman, E., Zalvide, J., Bernards, R., DeCaprio, J. A., and Ewen, M. E. (1997). Ras signalling linked to the cell-cycle machinery by the retinoblastoma protein. Nature *386*, 177-181.

Peifer, M., and Polakis, P. (2000). Wnt signaling in oncogenesis and embryogenesis--a look outside the nucleus. Science *287*, 1606-1609.

Peinado, H., Portillo, F., and Cano, A. (2004). Transcriptional regulation of cadherins during development and carcinogenesis. Int J Dev Biol *48*, 365-375.

Peinado, H., Quintanilla, M., and Cano, A. (2003). Transforming growth factor β-1 induces snail transcription factor in epithelial cell lines: mechanisms for epithelial mesenchymal transitions. J Biol Chem *278*, 21113-21123.

Pepper, M. S. (1997). Transforming growth factor-β: vasculogenesis, angiogenesis, and vessel wall integrity. Cytokine Growth Factor Rev *8*, 21-43.

Perez-Moreno, M. A., Locascio, A., Rodrigo, I., Dhondt, G., Portillo, F., Nieto, M. A., and Cano, A. (2001). A new role for E12/E47 in the repression of E-cadherin expression and epithelial-mesenchymal transitions. J Biol Chem *276*, 27424-27431.

Perk, J., Iavarone, A., and Benezra, R. (2005). Id family of helix-loop-helix proteins in cancer. Nat Rev Cancer *5*, 603-614.

Pertovaara, L., Kaipainen, A., Mustonen, T., Orpana, A., Ferrara, N., Saksela, O., and Alitalo, K. (1994). Vascular endothelial growth factor is induced in response to transforming growth factor-β in fibroblastic and epithelial cells. J Biol Chem *269*, 6271-6274.

Petritsch, C., Beug, H., Balmain, A., and Oft, M. (2000). TGF-β inhibits p70 S6 kinase via protein phosphatase 2A to induce G(1) arrest. Genes Dev *14*, 3093-3101.

Pfleger, K. D., and Eidne, K. A. (2006). Illuminating insights into protein-protein interactions using bioluminescence resonance energy transfer (BRET). Nat Methods *3*, 165-174.

Piek, E., Moustakas, A., Kurisaki, A., Heldin, C. H., and ten Dijke, P. (1999). TGF-(β) type I receptor/ALK-5 and Smad proteins mediate epithelial to mesenchymal transdifferentiation in NMuMG breast epithelial cells. J Cell Sci *112 (Pt 24)*, 4557-4568.

Piek, E., Ju WJ, Heyer J, Escalante-Alcalde D, Stewart CL, Weinstein M, Deng C., Kucherlapati R, Bottinger EP, Roberts AB (2001). Functional characterization of transforming growth factor beta signaling in Smad2- and Smad3-deficient fibroblasts. J Biol Chem, *8*, 19945-19953.

Pierreux, C. E., Nicolás, F. J., and Hill, C. S. (2000). Transforming growth factor β-independent shuttling of Smad4 between the cytoplasm and nucleus. Mol. Cell. Biol. *20*, 9041-9054.

Polanowska, J., Martin, J. S., Fisher, R., Scopa, T., Rae, I., and Boulton, S. J. (2004). Tandem immunoaffinity purification of protein complexes from Caenorhabditis elegans. Biotechniques *36*, 778-780, 782.

Polanowska, J., Martin, J. S., Garcia-Muse, T., Petalcorin, M. I., and Boulton, S. J. (2006). A conserved pathway to activate BRCA1-dependent ubiquitylation at DNA damage sites. EMBO J *25*, 2178-2188.

Polyak, K. (1996). Negative regulation of cell growth by TGF β. Biochim Biophys Acta *1242*. 185-199.

Portella, G., Cumming, S. A., Liddell, J., Cui, W., Ireland, H., Akhurst, R. J., and Balmain, A. (1998). Transforming growth factor β is essential for spindle cell conversion of mouse skin carcinoma in vivo: implications for tumor invasion. Cell Growth Differ *9*, 393-404.

Potts, J. D., Vincent, E. B., Runyan, R. B., and Weeks, D. L. (1992). Sense and antisense TGF β 3 mRNA levels correlate with cardiac valve induction. Dev Dyn *193*, 340-345.

Proetzel, G., Pawlowski, S. A., Wiles, M. V., Yin, M., Boivin, G. P., Howles, P. N., Ding, J., Ferguson, M. W., and Doetschman, T. (1995). Transforming growth factor-β 3 is required for secondary palate fusion. Nat Genet *11*, 409-414.

Pruitt, K., and Der, C. J. (2001). Ras and Rho regulation of the cell cycle and oncogenesis. Cancer Lett *171*, 1-10.

Puig, O., Caspary, F., Rigaut, G., Rutz, B., Bouveret, E., Bragado-Nilsson, E., Wilm, M., and Seraphin, B. (2001). The tandem affinity purification (TAP) method: a general procedure of protein complex purification. Methods *24*, 218-229.

Pyrowolakis, G., Hartmann, B., Muller, B., Basler, K., and Affolter, M. (2004). A simple molecular complex mediates widespread BMP-induced repression during Drosophila development. Dev Cell *7*, 229-240.

Qin, B. Y., Chacko, B. M., Lam, S. S., de Caestecker, M. P., Correia, J. J., and Lin, K. (2001). Structural basis of Smad1 activation by receptor kinase phosphorylation. Mol Cell *8*, 1303-1312.

Qin, B. Y., Lam, S. S., Correia, J. J., and Lin, K. (2002). Smad3 allostery links TGF-β receptor kinase activation to transcriptional control. Genes Dev *16*, 1950-1963.

Qin, B. Y., Liu, C., Lam, S. S., Srinath, H., Delston, R., Correia, J. J., Derynck, R., and Lin, K. (2003). Crystal structure of IRF-3 reveals mechanism of autoinhibition and virus-induced phosphoactivation. Nat Struct Biol *10*, 913-921.

Raftery, L. A., and Sutherland, D. J. (1999). TGF-β family signal transduction in Drosophila development: from Mad to Smads. Dev Biol *210*, 251-268.

Raftery, L. A., Twombly, V., Wharton, K., and Gelbart, W. M. (1995). Genetic screens to identify elements of the decapentaplegic signaling pathway in Drosophila. Genetics *139*, 241-254.

Randall, R. A., Germain, S., Inman, G. J., Bates, P. A., and Hill, C. S. (2002). Different Smad2 partners bind a common hydrophobic pocket in Smad2 via a defined proline-rich motif. EMBO J *21*, 145-156.

Randall, R. A., Howell, M., Page, C. S., Daly, A., Bates, P. A., and Hill, C. S. (2004). Recognition of phosphorylated-Smad2-containing complexes by a novel Smad interaction motif. Mol Cell Biol *24*, 1106-1121.

Ray, D., Terao, Y., Nimbalkar, D., Chu, L. H., Donzelli, M., Tsutsui, T., Zou, X., Ghosh, A. K., Varga, J., Draetta, G. F., and Kiyokawa, H. (2005). Transforming growth factor β facilitates β-TrCP-mediated degradation of Cdc25A in a Smad3-dependent manner. Mol Cell Biol *25*, 3338-3347.

Rees, J. R., Onwuegbusi, B. A., Save, V. E., Alderson, D., and Fitzgerald, R. C. (2006). In vivo and In vitro Evidence for Transforming Growth Factor-{β}1-Mediated Epithelial to Mesenchymal Transition in Esophageal Adenocarcinoma. Cancer Res *66*, 9583-9590.

Reguly, T., and Wrana, J. L. (2003). In or out? The dynamics of Smad nucleocytoplasmic shuttling. Trends Cell Biol *13*, 216-220.

Reichmann, E., Ball, R., Groner, B., and Friis, R. R. (1989). New mammary epithelial and fibroblastic cell clones in coculture form structures competent to differentiate functionally. J Cell Biol *108*, 1127-1138.

Reichmann, E., Schwarz, H., Deiner, E. M., Leitner, I., Eilers, M., Berger, J., Busslinger, M., and Beug, H. (1992). Activation of an inducible c-FosER fusion protein causes loss of epithelial polarity and triggers epithelial-fibroblastoid cell conversion. Cell *71*, 1103-1116.

Remy, I., Montmarquette, A., and Michnick, S. W. (2004). PKB/Akt modulates TGF-β signalling through a direct interaction with Smad3. Nat Cell Biol *6*, 358-365.

Reynisdottir, I., and Massague, J. (1997). The subcellular locations of p15(Ink4b) and p27(Kip1) coordinate their inhibitory interactions with cdk4 and cdk2. Genes Dev *11*, 492-503.

Reynisdottir, I., Polyak, K., Iavarone, A., and Massagué, J. (1995). Kip/Cip and Ink4 Cdk inhibitors cooperate to induce cell cycle arrest in response to TGF-β. Genes Dev *9*, 1831-1845.

Rigaut, G., Shevchenko, A., Rutz, B., Wilm, M., Mann, M., and Seraphin, B. (1999). A generic protein purification method for protein complex characterization and proteome exploration. Nat Biotechnol *17*, 1030-1032.

Roberts, A. B., Anzano, M. A., Lamb, L. C., Smith, J. M., and Sporn, M. B. (1981). New class of transforming growth factors potentiated by epidermal growth factor: isolation from non-neoplastic tissues. Proc Natl Acad Sci U S A *78*, 5339-5343.

Roberts, A. B., and Wakefield, L. M. (2003). The two faces of transforming growth factor β in carcinogenesis. Proc Natl Acad Sci U S A *100*, 8621-8623.

Roelen, B. A., van Rooijen, M. A., and Mummery, C. L. (1997). Expression of ALK-1, a type 1 serine/threonine kinase receptor, coincides with sites of vasculogenesis and angiogenesis in early mouse development. Dev Dyn *209*, 418-430.

Romano, L. A., and Runyan, R. B. (2000). Slug is an essential target of TGFβ2 signaling in the developing chicken heart. Dev Biol *223*, 91-102.

Ross, S., Cheung, E., Petrakis, T. G., Howell, M., Kraus, W. L., and Hill, C. S. (2006). Smads orchestrate specific histone modifications and chromatin remodeling to activate transcription. EMBO J *25*, 4490-4502.

Rotzer, D., Roth, M., Lutz, M., Lindemann, D., Sebald, W., and Knaus, P. (2001). Type III TGF-β receptor-independent signalling of TGF-β2 via TβRII-B, an alternatively spliced TGF-β type II receptor. EMBO J *20*, 480-490.

Runyan, R. B., and Markwald, R. R. (1983). Invasion of mesenchyme into three-dimensional collagen gels: a regional and temporal analysis of interaction in embryonic heart tissue. Dev Biol *95*, 108-114.

Saika, S., Ikeda, K., Yamanaka, O., Sato, M., Muragaki, Y., Ohnishi, Y., Ooshima, A., Nakajima, Y., Namikawa, K., Kiyama, H., *et al.* (2004a). Transient adenoviral gene transfer of Smad7 prevents injury-induced epithelial-mesenchymal transition of lens epithelium in mice. Lab Invest *84*, 1259-1270.

Saika, S., Kono-Saika, S., Ohnishi, Y., Sato, M., Muragaki, Y., Ooshima, A., Flanders, K. C., Yoo, J., Anzano, M., Liu, C. Y., *et al.* (2004b). Smad3 signaling is required for epithelial-mesenchymal transition of lens epithelium after injury. Am J Pathol *164*, 651-663.

Saika, S., Kono-Saika, S., Tanaka, T., Yamanaka, O., Ohnishi, Y., Sato, M., Muragaki, Y., Ooshima, A., Yoo, J., Flanders, K. C., and Roberts, A. B. (2004c). Smad3 is required for dedifferentiation of retinal pigment epithelium following retinal detachment in mice. Lab Invest *84*, 1245-1258.

Saitoh, M., Nishitoh, H., Amagasa, T., Miyazono, K., Takagi, M., and Ichijo, H. (1996). Identification of important regions in the cytoplasmic juxtamembrane domain of type I receptor that separate signaling pathways of transforming growth factor-β. J Biol Chem *271*, 2769-2775.

Sampath, T. K., Rashka, K. E., Doctor, J. S., Tucker, R. F., and Hoffmann, F. M. (1993). Drosophila transforming growth factor β superfamily proteins induce endochondral bone formation in mammals. Proc Natl Acad Sci U S A *90*, 6004-6008.

Sanford, L. P., Ormsby, I., Gittenberger-de Groot, A. C., Sariola, H., Friedman, R., Boivin, G. P., Cardell, E. L., and Doetschman, T. (1997). TGFβ2 knockout mice have multiple developmental defects that are non-overlapping with other TGFβ knockout phenotypes. Development *124*, 2659-2670.

Sato, M., Muragaki, Y., Saika, S., Roberts, A. B., and Ooshima, A. (2003). Targeted disruption of TGF-β1/Smad3 signaling protects against renal tubulointerstitial fibrosis induced by unilateral ureteral obstruction. J Clin Invest *112*, 1486-1494.

Savage, C., Das, P., Finelli, A. L., Townsend, S. R., Sun, C.-Y., Baird, S. E., and Padgett, R. W. (1996). *Caenorhabditis elegans* genes *sma-2, sma-3*, and *sma-4* define a conserved family of transforming growth factor β pathway components. Proc. Natl. Acad. Sci. USA *93*, 790-794.

Scherer, A., and Graff, J. M. (2000). Calmodulin differentially modulates Smad1 and Smad2 signaling. J Biol Chem *275*, 41430-41438.

Schlessinger, J. (2000). Cell signaling by receptor tyrosine kinases. Cell *103*, 211-225.

Schmierer, B., and Hill, C. S. (2005). Kinetic analysis of Smad nucleocytoplasmic shuttling reveals a mechanism for transforming growth factor β-dependent nuclear accumulation of Smads. Mol Cell Biol *25*, 9845-9858.

Schmitt, C., von Kobbe, C., Bachi, A., Pante, N., Rodrigues, J. P., Boscheron, C., Rigaut, G., Wilm, M., Seraphin, B., Carmo-Fonseca, M., and Izaurralde, E. (1999). Dbp5, a DEAD-box protein required for mRNA export, is recruited to the cytoplasmic fibrils of nuclear pore complex via a conserved interaction with CAN/Nup159p. EMBO J *18*, 4332-4347.

Schock, F., and Perrimon, N. (2002). Molecular mechanisms of epithelial morphogenesis. Annu Rev Cell Dev Biol *18*, 463-493.

Schohl, A., and Fagotto, F. (2002). B-catenin, MAPK and Smad signaling during early Xenopus development. Development *129*, 37-52.

Schreiber, S. L. (1991). Chemistry and biology of the immunophilins and their immunosuppressive ligands. Science *251*, 283-287.

Sebald, W., and Mueller, T. D. (2003). The interaction of BMP-7 and ActRII implicates a new mode of receptor assembly. Trends Biochem Sci *28*, 518-521.

Sefton, M., Sanchez, S., and Nieto, M. A. (1998). Conserved and divergent roles for members of the Snail family of transcription factors in the chick and mouse embryo. Development *125*, 3111-3121.

Sekelsky, J. J., Newfeld, S. J., Raftery, L. A., Chartoff, E. H., and Gelbart, W. M. (1995). Genetic characterization and cloning of mothers against dpp, a gene required for decapentaplegic function in Drosophila melanogaster. Genetics *139*, 1347-1358.

Sekiya, T., Adachi, S., Kohu, K., Yamada, T., Higuchi, O., Furukawa, Y., Nakamura, Y., Nakamura, T., Tashiro, K., Kuhara, S., *et al.* (2004a). Identification of BMP and activin membrane-bound inhibitor (BAMBI), an inhibitor of transforming growth factor-β signaling, as a target of the β-catenin pathway in colorectal tumor cells. J Biol Chem *279*, 6840-6846.

Sekiya, T., Oda, T., Matsuura, K., and Akiyama, T. (2004b). Transcriptional regulation of the TGF-β pseudoreceptor BAMBI by TGF-β signaling. Biochem Biophys Res Commun *320*, 680-684.

Selleck, M. A., Garcia-Castro, M. I., Artinger, K. B., and Bronner-Fraser, M. (1998). Effects of Shh and Noggin on neural crest formation demonstrate that BMP is required in the neural tube but not ectoderm. Development *125*, 4919-4930.

Serrano, M., Lin, A. W., McCurrach, M. E., Beach, D., and Lowe, S. W. (1997). Oncogenic ras provokes premature cell senescence associated with accumulation of p53 and p16INK4a. Cell *88*, 593-602.

Sheaff, R. J., Groudine, M., Gordon, M., Roberts, J. M., and Clurman, B. E. (1997). Cyclin E-CDK2 is a regulator of p27Kip1. Genes Dev *11*, 1464-1478.

Sherr, C. J., and Roberts, J. M. (1995). Inhibitors of mammalian G1 cyclin-dependent kinases. Genes Dev *9*, 1149-1163.

Sherr, C. J., and Roberts, J. M. (1999). CDK inhibitors: positive and negative regulators of G1-phase progression. Genes Dev *13*, 1501-1512.

Shi, W., Sun, C., He, B., Xiong, W., Shi, X., Yao, D., and Cao, X. (2004). GADD34-PP1c recruited by Smad7 dephosphorylates TGF{β} type I receptor. J Cell Biol *164*, 291-300.

Shi, Y., Hata, A., Lo, R. S., Massague, J., and Pavletich, N. P. (1997). A structural basis for mutational inactivation of the tumour suppressor Smad4. Nature *388*, 87-93.

Shi, Y., and Massague, J. (2003). Mechanisms of TGF-β signaling from cell membrane to the nucleus. Cell *113*, 685-700.

Shi, Y., Wang, Y. F., Jayaraman, L., Yang, H., Massague, J., and Pavletich, N. P. (1998). Crystal structure of a Smad MH1 domain bound to DNA: insights on DNA binding in TGF-β signaling. Cell *94*, 585-594.

Shou, W., Aghdasi, B., Armstrong, D. L., Guo, Q., Bao, S., Charng, M. J., Mathews, L. M., Schneider, M. D., Hamilton, S. L., and Matzuk, M. M. (1998). Cardiac defects and altered ryanodine receptor function in mice lacking FKBP12. Nature *391*, 489-492.

Shuler, C. F., Halpern, D. E., Guo, Y., and Sank, A. C. (1992). Medial edge epithelium fate traced by cell lineage analysis during epithelial-mesenchymal transformation in vivo. Dev Biol *154*, 318-330.

Solnica-Krezel, L. (2003). Vertebrate development: taming the nodal waves. Curr Biol *13*, R7-9.

Soos, T. J., Kiyokawa, H., Yan, J. S., Rubin, M. S., Giordano, A., DeBlasio, A., Bottega, S., Wong, B., Mendelsohn, J., and Koff, A. (1996). Formation of p27-CDK complexes during the human mitotic cell cycle. Cell Growth Differ *7*, 135-146.

Sosic, D., Richardson, J. A., Yu, K., Ornitz, D. M., and Olson, E. N. (2003). Twist regulates cytokine gene expression through a negative feedback loop that represses NF-kappaB activity. Cell *112*, 169-180.

Souchelnytskyi, S., ten Dijke, P., Miyazono, K., and Heldin, C. H. (1996). Phosphorylation of Ser165 in TGF-β type I receptor modulates TGF-β1-induced cellular responses. EMBO J *15*, 6231-6240.

Sporn, M. B. (1996). The war on cancer. Lancet *347*, 1377-1381.

Stacey, D. W., Roudebush, M., Day, R., Mosser, S. D., Gibbs, J. B., and Feig, L. A. (1991). Dominant inhibitory Ras mutants demonstrate the requirement for Ras activity in the action of tyrosine kinase oncogenes. Oncogene *6*, 2297-2304.

Stagljar, I. (2003). Finding partners: emerging protein interaction technologies applied to signaling networks. Sci STKE *2003*, pe56.

Stenvers, K. L., Tursky, M. L., Harder, K. W., Kountouri, N., Amatayakul-Chantler, S., Grail, D., Small, C., Weinberg, R. A., Sizeland, A. M., and Zhu, H. J. (2003). Heart and liver defects and reduced transforming growth factor β2 sensitivity in transforming growth factor β type III receptor-deficient embryos. Mol Cell Biol *23*, 4371-4385.

Stevaux, O., and Dyson, N. J. (2002). A revised picture of the E2F transcriptional network and RB function. Curr Opin Cell Biol *14*, 684-691.

Stockwell, B. R., and Schreiber, S. L. (1998). TGF-β-signaling with small molecule FKBP12 antagonists that bind myristoylated FKBP12-TGF-β type I receptor fusion proteins. Chem Biol *5*, 385-395.

Stoker, M., and Perryman, M. (1985). An epithelial scatter factor released by embryo fibroblasts. J Cell Sci *77*, 209-223.

Strizzi, L., Bianco, C., Normanno, N., and Salomon, D. (2005). Cripto-1: a multifunctional modulator during embryogenesis and oncogenesis. Oncogene *24*, 5731-5741.

Strutz, F., Zeisberg, M., Ziyadeh, F. N., Yang, C. Q., Kalluri, R., Muller, G. A., and Neilson, E. G. (2002). Role of basic fibroblast growth factor-2 in epithelial-mesenchymal transformation. Kidney Int *61*, 1714-1728.

Sugi, Y., Yamamura, H., Okagawa, H., and Markwald, R. R. (2004). Bone morphogenetic protein-2 can mediate myocardial regulation of atrioventricular cushion mesenchymal cell formation in mice. Dev Biol *269*, 505-518.

Sun, D., Vanderburg, C. R., Odierna, G. S., and Hay, E. D. (1998). TGFβ3 promotes transformation of chicken palate medial edge epithelium to mesenchyme in vitro. Development *125*, 95-105.

Suzuki, A., Chang, C., Yingling, J. M., Wang, X. F., and Hemmati-Brivanlou, A. (1997). Smad5 induces ventral fates in Xenopus embryo. Dev Biol *184*, 402-405.

Suzuki, C., Murakami, G., Fukuchi, M., Shimanuki, T., Shikauchi, Y., Imamura, T., and Miyazono, K. (2002). Smurf1 regulates the inhibitory activity of Smad7 by targeting Smad7 to the plasma membrane. J Biol Chem *277*, 39919-39925.

Szuts, D., Eresh, S., and Bienz, M. (1998). Functional intertwining of Dpp and EGFR signaling during Drosophila endoderm induction. Genes Dev *12*, 2022-2035.

Tajima, Y., Goto, K., Yoshida, M., Shinomiya, K., Sekimoto, T., Yoneda, Y., Miyazono, K., and Imamura, T. (2003). Chromosomal region maintenance 1 (CRM1)-dependent nuclear export of Smad ubiquitin regulatory factor 1 (Smurf1) is essential for negative regulation of transforming growth factor-β signaling by Smad7. J Biol Chem *278*, 10716-10721.

Tang, B., Bottinger, E. P., Jakowlew, S. B., Bagnall, K. M., Mariano, J., Anver, M. R., Letterio, J. J., and Wakefield, L. M. (1998). Transforming growth factor-β1 is a new form of tumor suppressor with true haploid insufficiency. Nat Med *4*, 802-807.

Tavares, A. L., Mercado-Pimentel, M. E., Runyan, R. B., and Kitten, G. T. (2006). TGFβ-mediated RhoA expression is necessary for epithelial-mesenchymal transition in the embryonic chick heart. Dev Dyn *235*, 1589-1598.

Taya, Y., O'Kane, S., and Ferguson, M. W. (1999). Pathogenesis of cleft palate in TGF-β3 knockout mice. Development *126*, 3869-3879.

ten Dijke, P., and Heldin, C. H. (2006). Smad Signal Transduction. Smads in Proliferation, Differentiation and Disease, Vol 5: Springer.

ten Dijke, P., and Hill, C. S. (2004). New insights into TGF-β-Smad signalling. Trends Biochem Sci *29*, 265-273.

ten Dijke, P., Ichijo, H., Franzen, P., Schulz, P., Saras, J., Toyoshima, H., Heldin, C. H., and Miyazono, K. (1993). Activin receptor-like kinases: a novel subclass of cell-surface receptors with predicted serine/threonine kinase activity. Oncogene *8*, 2879-2887.

ten Dijke, P., Korchynskyi, O., Valdimarsdottir, G., and Goumans, M. J. (2003). Controlling cell fate by bone morphogenetic protein receptors. Mol Cell Endocrinol *211*, 105-113.

ten Dijke, P., Yamashita, H., Ichijo, H., Franzen, P., Laiho, M., Miyazono, K., and Heldin, C. H. (1994a). Characterization of type I receptors for transforming growth factor-β and activin. Science *264*, 101-104.

ten Dijke, P., Yamashita, H., Sampath, T. K., Reddi, A. H., Estevez, M., Riddle, D. L., Ichijo, H., Heldin, C. H., and Miyazono, K. (1994b). Identification of type I receptors for osteogenic protein-1 and bone morphogenetic protein-4. J Biol Chem *269*, 16985-16988.

Thiery, J. P. (2002). Epithelial-mesenchymal transitions in tumour progression. Nat Rev Cancer *2*, 442-454.

Thiery, J. P. (2003). Epithelial-mesenchymal transitions in development and pathologies. Curr Opin Cell Biol *15*, 740-746.

Thiery, J. P., and Sleeman, J. P. (2006). Complex networks orchestrate epithelial-mesenchymal transitions. Nat Rev Mol Cell Biol *7*, 131-142.

Thompson, T. B., Woodruff, T. K., and Jardetzky, T. S. (2003). Structures of an ActRIIB:activin A complex reveal a novel binding mode for TGF-β ligand:receptor interactions. EMBO J *22*, 1555-1566.

Tian, F., DaCosta Byfield, S., Parks, W. T., Yoo, S., Felici, A., Tang, B., Piek, E., Wakefield, L. M., and Roberts, A. B. (2003). Reduction in Smad2/3 signaling enhances tumorigenesis but suppresses metastasis of breast cancer cell lines. Cancer Res *63*, 8284-8292.

Timmerman, L. A., Grego-Bessa, J., Raya, A., Bertran, E., Perez-Pomares, J. M., Diez, J., Aranda, S., Palomo, S., McCormick, F., Izpisua-Belmonte, J. C., and de la Pompa, J. L. (2004). Notch promotes epithelial-mesenchymal transition during cardiac development and oncogenic transformation. Genes Dev *18*, 99-115.

Treisman, R. (1985). Transient accumulation of c-fos RNA following serum stimulation requires a conserved 5' element and c-fos 3' sequences. Cell *42*, 889-902.

Tremain, R., Marko, M., Kinnimulki, V., Ueno, H., Bottinger, E., and Glick, A. (2000). Defects in TGF-β signaling overcome senescence of mouse keratinocytes expressing v-Ha-ras. Oncogene *19*, 1698-1709.

Tsang, M., Kim, R., de Caestecker, M. P., Kudoh, T., Roberts, A. B., and Dawid, I. B. (2000). Zebrafish nma is involved in TGFβ family signaling. Genesis *28*, 47-57.

Tsukazaki, T., Chiang, T. A., Davison, A. F., Attisano, L., and Wrana, J. L. (1998). SARA, a FYVE domain protein that recruits Smad2 to the TGFβ receptor. Cell *95*, 779-791.

Tsushima, H., Kawata, S., Tamura, S., Ito, N., Shirai, Y., Kiso, S., Imai, Y., Shimomukai, H., Nomura, Y., Matsuda, Y., and Matsuzawa, Y. (1996). High levels of transforming growth factor β 1 in patients with colorectal cancer: association with disease progression. Gastroenterology *110*, 375-382.

Tucker, R. P. (2004). Neural crest cells: a model for invasive behavior. Int J Biochem Cell Biol *36*, 173-177.

Uchida, K., Nagatake, M., Osada, H., Yatabe, Y., Kondo, M., Mitsudomi, T., Masuda, A., Takahashi, T., and Takahashi, T. (1996). Somatic in vivo alterations of the JV18-1 gene at 18q21 in human lung cancers. Cancer Res *56*, 5583-5585.

Udagawa, Y., Hanai, J., Tada, K., Grieder, N. C., Momoeda, M., Taketani, Y., Affolter, M., Kawabata, M., and Miyazono, K. (2000). Schnurri interacts with Mad in a Dpp-dependent manner. Genes Cells *5*, 359-369.

Ulloa, L., Doody, J., and Massague, J. (1999). Inhibition of transforming growth factor-β/SMAD signalling by the interferon-gamma/STAT pathway. Nature *397*, 710-713.

Urness, L. D., Sorensen, L. K., and Li, D. Y. (2000). Arteriovenous malformations in mice lacking activin receptor-like kinase-1. Nat Genet *26*, 328-331.

Valcourt, U., Kowanetz, M., Niimi, H., Heldin, C. H., and Moustakas, A. (2005). TGF-β and the Smad signaling pathway support transcriptomic reprogramming during epithelial-mesenchymal cell transition. Mol Biol Cell *16*, 1987-2002.

Valdimarsdottir, G., Goumans, M. J., Itoh, F., Itoh, S., Heldin, C. H., and ten Dijke, P. (2006). Smad7 and protein phosphatase 1alpha are critical determinants in the duration of TGF-β/ALK1 signaling in endothelial cells. BMC Cell Biol *7*, 16.

van den Driesche, S., Mummery, C. L., and Westermann, C. J. (2003). Hereditary hemorrhagic telangiectasia: an update on transforming growth factor β signaling in vasculogenesis and angiogenesis. Cardiovasc Res *58*, 20-31.

Vastrik, I., Eickholt, B. J., Walsh, F. S., Ridley, A., and Doherty, P. (1999). Sema3A-induced growth-cone collapse is mediated by Rac1 amino acids 17-32. Curr Biol *9*, 991-998.

Vega, S., Morales, A. V., Ocana, O. H., Valdes, F., Fabregat, I., and Nieto, M. A. (2004). Snail blocks the cell cycle and confers resistance to cell death. Genes Dev *18*, 1131-1143.

Veraksa, A., Bauer, A., and Artavanis-Tsakonas, S. (2005). Analyzing protein complexes in Drosophila with tandem affinity purification-mass spectrometry. Dev Dyn *232*, 827-834.

Verschueren, K., Remacle, J. E., Collart, C., Kraft, H., Baker, B. S., Tylzanowski, P., Nelles, L., Wuytens, G., Su, M. T., Bodmer, R., *et al.* (1999). SIP1, a novel zinc finger/homeodomain repressor, interacts with Smad proteins and binds to 5'-CACCT sequences in candidate target genes. J Biol Chem *274*, 20489-20498.

Vinals, F., and Pouyssegur, J. (2001). Transforming growth factor β1 (TGF-β1) promotes endothelial cell survival during in vitro angiogenesis via an autocrine mechanism implicating TGF-alpha signaling. Mol Cell Biol *21*, 7218-7230.

Vivien, D., and Wrana, J. L. (1995). Ligand-induced recruitment and phosphorylation of reduced TGF-β type I receptor. Exp Cell Res *221*, 60-65.

Waerner, T., Alacakaptan, M., Tamir, I., Oberauer, R., Gal, A., Brabletz, T., Schreiber, M., Jechlinger, M., and Beug, H. (2006). ILEI: A cytokine essential for EMT, tumor formation, and late events in metastasis in epithelial cells. Cancer Cell *10*, 227-239.

Wakefield, L. M., and Roberts, A. B. (2002). TGF-β signaling: positive and negative effects on tumorigenesis. Curr Opin Genet Dev *12*, 22-29.

Wang, D., Kanuma, T., Mizunuma, H., Takama, F., Ibuki, Y., Wake, N., Mogi, A., Shitara, Y., and Takenoshita, S. (2000). Analysis of specific gene mutations in the transforming growth factor-β signal transduction pathway in human ovarian cancer. Cancer Res *60*, 4507-4512.

Wang, J., Sridurongrit, S., Dudas, M., Thomas, P., Nagy, A., Schneider, M. D., Epstein, J. A., and Kaartinen, V. (2005). Atrioventricular cushion transformation is mediated by ALK2 in the developing mouse heart. Dev Biol *286*, 299-310.

Wang, T., Donahoe, P. K., and Zervos, A. S. (1994). Specific interaction of type I receptors of the TGF-β family with the immunophilin FKBP-12. Science *265*, 674-676.

Wang, T., Li, B. Y., Danielson, P. D., Shah, P. C., Rockwell, S., Lechleider, R. J., Martin, J., Manganaro, T., and Donahoe, P. K. (1996). The immunophilin FKBP12 functions as a common inhibitor of the TGF β family type I receptors. Cell *86*, 435-444.

Wang, X. F., Lin, H. Y., Ng-Eaton, E., Downward, J., Lodish, H. F., and Weinberg, R. A. (1991). Expression cloning and characterization of the TGF-β type III receptor. Cell *67*, 797-805.

Waskiewicz, A. J., and Cooper, J. A. (1995). Mitogen and stress response pathways: MAP kinase cascades and phosphatase regulation in mammals and yeast. Curr Opin Cell Biol *7*, 798-805.

Watanabe, M., Masuyama, N., Fukuda, M., and Nishida, E. (2000). Regulation of intracellular dynamics of Smad4 by its leucine-rich nuclear export signal. EMBO Rep *1*, 176-182.

Wei, W., Jin, J., Schlisio, S., Harper, J. W., and Kaelin, W. G., Jr. (2005). The v-Jun point mutation allows c-Jun to escape GSK3-dependent recognition and destruction by the Fbw7 ubiquitin ligase. Cancer Cell *8*, 25-33.

Weis-Garcia, F., and Massagué, J. (1996). Complementation between kinase-defective and activation defective TGF-β receptors reveals a novel form of receptor cooperativity essential for signaling. EMBO J *15*, 276-289.

Wells, R. G., Gilboa, L., Sun, Y., Liu, X., Henis, Y. I., and Lodish, H. F. (1999). Transforming growth factor-β induces formation of a dithiothreitol-resistant type I/Type II receptor complex in live cells. J Biol Chem *274*, 5716-5722.

Whitman, M. (1998). Smads and early developmental signaling by the TGFβ superfamily. Genes Dev *12*, 2445-2462.

Whitman, M. (2001). Nodal signaling in early vertebrate embryos: themes and variations. Dev Cell *1*, 605-617.

Wiater, E., and Vale, W. (2003). Inhibin is an antagonist of bone morphogenetic protein signaling. J Biol Chem *278*, 7934-7941.

Wicks, S. J., Lui, S., Abdel-Wahab, N., Mason, R. M., and Chantry, A. (2000). Inactivation of smad-transforming growth factor β signaling by Ca(2+)-calmodulin-dependent protein kinase II. Mol Cell Biol *20*, 8103-8111.

Wieser, R., Wrana, J. L., and Massagué, J. (1995). GS domain mutations that constitutively activate TβR-I, the downstream signaling component in the TGF-β receptor complex. EMBO J *14*, 2199-2208.

Wikstrom, P., Stattin, P., Franck-Lissbrant, I., Damber, J. E., and Bergh, A. (1998). Transforming growth factor β1 is associated with angiogenesis, metastasis, and poor clinical outcome in prostate cancer. Prostate *37*, 19-29.

Wilkes, M. C., Murphy, S. J., Garamszegi, N., and Leof, E. B. (2003). Cell-type-specific activation of PAK2 by transforming growth factor β independent of Smad2 and Smad3. Mol Cell Biol *23*, 8878-8889.

Willis, S. A., Zimmerman, C. M., Li, L. I., and Mathews, L. S. (1996). Formation and activation by phosphorylation of activin receptor complexes. Mol Endocrinol *10*, 367-379.

Wong, C., Rougier-Chapman, E. M., Frederick, J. P., Datto, M. B., Liberati, N. T., Li, J. M., and Wang, X. F. (1999). Smad3-Smad4 and AP-1 complexes synergize in transcriptional activation of the c-Jun promoter by transforming growth factor β. Mol Cell Biol *19*, 1821-1830.

Wozney, J. M., Rosen, V., Celeste, A. J., Mitsock, L. M., Whitters, M. J., Kriz, R. W., Hewick, R. M., and Wang, E. A. (1988). Novel regulators of bone formation: molecular clones and activities. Science *242*, 1528-1534.

Wrana, J. L., Attisano, L., Carcamo, J., Zentella, A., Doody, J., Laiho, M., Wang, X. F., and Massague, J. (1992a). TGF β signals through a heteromeric protein kinase receptor complex. Cell *71*, 1003-1014.

Wrana, J. L., Carcamo, J., Attisano, L., Cheifetz, S., Zentella, A., Lopez-Casillas, F., and Massague, J. (1992b). The type II TGF-β receptor signals diverse responses in cooperation with the type I receptor. Cold Spring Harb Symp Quant Biol *57*, 81-86.

Wrana, J. L., Tran, H., Attisano, L., Arora, K., Childs, S. R., Massague, J., and O'Connor, M. B. (1994). Two distinct transmembrane serine/threonine kinases from Drosophila melanogaster form an activin receptor complex. Mol Cell Biol *14*, 944-950.

Wu, G., Chen, Y. G., Ozdamar, B., Gyuricza, C. A., Chong, P. A., Wrana, J. L., Massague, J., and Shi, Y. (2000). Structural basis of Smad2 recognition by the Smad anchor for receptor activation. Science *287*, 92-97.

Wu, J. W., Fairman, R., Penry, J., and Shi, Y. (2001a). Formation of a stable heterodimer between Smad2 and Smad4. J Biol Chem *276*, 20688-20694.

Wu, J. W., Hu, M., Chai, J., Seoane, J., Huse, M., Li, C., Rigotti, D. J., Kyin, S., Muir, T. W., Fairman, R., *et al.* (2001b). Crystal structure of a phosphorylated Smad2. Recognition of phosphoserine by the MH2 domain and insights on Smad function in TGF-β signaling. Mol Cell *8*, 1277-1289.

Wulf, E., Deboben, A., Bautz, F. A., Faulstich, H., and Wieland, T. (1979). Fluorescent phallotoxin, a tool for the visualization of cellular actin. Proc Natl Acad Sci U S A *76*, 4498-4502.

Xiao, Z., Brownawell, A. M., Macara, I. G., and Lodish, H. F. (2003a). A novel nuclear export signal in Smad1 is essential for its signaling activity. J Biol Chem *278*, 34245-34252.

Xiao, Z., Latek, R., and Lodish, H. F. (2003b). An extended bipartite nuclear localization signal in Smad4 is required for its nuclear import and transcriptional activity. Oncogene *22*, 1057-1069.

Xiao, Z., Watson, N., Rodriguez, C., and Lodish, H. F. (2001). Nucleocytoplasmic shuttling of Smad1 conferred by its nuclear localization and nuclear export signals. J Biol Chem *276*, 39404-39410.

Xie, L., Law, B. K., Aakre, M. E., Edgerton, M., Shyr, Y., Bhowmick, N. A., and Moses, H. L. (2003). Transforming growth factor β-regulated gene expression in a mouse mammary gland epithelial cell line. Breast Cancer Res *5*, R187-198.

Xin, H., Xu, X., Li, L., Ning, H., Rong, Y., Shang, Y., Wang, Y., Fu, X. Y., and Chang, Z. (2005). CHIP controls the sensitivity of transforming growth factor-β signaling by modulating the basal level of Smad3 through ubiquitin-mediated degradation. J Biol Chem *280*, 20842-20850.

Xu, L., Alarcon, C., Col, S., and Massague, J. (2003). Distinct domain utilization by Smad3 and Smad4 for nucleoporin interaction and nuclear import. J Biol Chem *278*, 42569-42577.

Xu, L., Chen, Y. G., and Massague, J. (2000). The nuclear import function of Smad2 is masked by SARA and unmasked by TGFβ-dependent phosphorylation. Nat Cell Biol *2*, 559-562.

Xu, L., Kang, Y., Col, S., and Massague, J. (2002). Smad2 nucleocytoplasmic shuttling by nucleoporins CAN/Nup214 and Nup153 feeds TGFβ signaling complexes in the cytoplasm and nucleus. Mol Cell *10*, 271-282.

Xu, X., Han, J., Ito, Y., Bringas, P., Jr., Urata, M. M., and Chai, Y. (2006). Cell autonomous requirement for Tgfbr2 in the disappearance of medial edge epithelium during palatal fusion. Dev Biol *297*, 238-248.

Xu, X., Yin, Z., Hudson, J. B., Ferguson, E. L., and Frasch, M. (1998). Smad proteins act in combination with synergistic and antagonistic regulators to target Dpp responses to the Drosophila mesoderm. Genes Dev *12*, 2354-2370.

Yagi, K., Furuhashi, M., Aoki, H., Goto, D., Kuwano, H., Sugamura, K., Miyazono, K., and Kato, M. (2002). c-myc is a downstream target of the Smad pathway. J Biol Chem *277*, 854-861.

Yagi, K., Goto, D., Hamamoto, T., Takenoshita, S., Kato, M., and Miyazono, K. (1999). Alternatively spliced variant of Smad2 lacking exon 3. Comparison with wild-type Smad2 and Smad3. J Biol Chem *274*, 703-709.

Yamada, M., Szendro, P. I., Prokscha, A., Schwartz, R. J., and Eichele, G. (1999). Evidence for a role of Smad6 in chick cardiac development. Dev Biol *215*, 48-61.

Yamashita, H., ten Dijke, P., Franzen, P., Miyazono, K., and Heldin, C. H. (1994). Formation of hetero-oligomeric complexes of type I and type II receptors for transforming growth factor-β. J Biol Chem *269*, 20172-20178.

Yamashita, H., ten Dijke, P., Huylebroeck, D., Sampath, T. K., Andries, M., Smith, J. C., Heldin, C. H., and Miyazono, K. (1995). Osteogenic protein-1 binds to activin type II receptors and induces certain activin-like effects. J Cell Biol *130*, 217-226.

Yan, Y. T., Gritsman, K., Ding, J., Burdine, R. D., Corrales, J. D., Price, S. M., Talbot, W. S., Schier, A. F., and Shen, M. M. (1999). Conserved requirement for EGF-CFC genes in vertebrate left-right axis formation. Genes Dev *13*, 2527-2537.

Yang, H., Kyo, S., Takatura, M., and Sun, L. (2001). Autocrine transforming growth factor β suppresses telomerase activity and transcription of human telomerase reverse transcriptase in human cancer cells. Cell Growth Differ *12*, 119-127.

Yang, J., Mani, S. A., Donaher, J. L., Ramaswamy, S., Itzykson, R. A., Come, C., Savagner, P., Gitelman, I., Richardson, A., and Weinberg, R. A. (2004). Twist, a master regulator of morphogenesis, plays an essential role in tumor metastasis. Cell *117*, 927-939.

Yang, X., Letterio, J. J., Lechleider, R. J., Chen, L., Hayman, R., Gu, H., Roberts, A. B., and Deng, C. (1999). Targeted disruption of SMAD3 results in impaired mucosal immunity and diminished T cell responsiveness to TGF-β. EMBO J *18*, 1280-1291.

Yang, Y. A., Dukhanina, O., Tang, B., Mamura, M., Letterio, J. J., MacGregor, J., Patel, S. C., Khozin, S., Liu, Z. Y., Green, J., *et al.* (2002). Lifetime exposure to a soluble TGF-β antagonist protects mice against metastasis without adverse side effects. J Clin Invest *109*, 1607-1615.

Yang, Y. A., Zhang, G. M., Feigenbaum, L., and Zhang, Y. E. (2006). Smad3 reduces susceptibility to hepatocarcinoma by sensitizing hepatocytes to apoptosis through downregulation of Bcl-2. Cancer Cell *9*, 445-457.

Yao, L. C., Blitz, I. L., Peiffer, D. A., Phin, S., Wang, Y., Ogata, S., Cho, K. W., Arora, K., and Warrior, R. (2006). Schnurri transcription factors from Drosophila and vertebrates can mediate Bmp signaling through a phylogenetically conserved mechanism. Development *133*, 4025-4034.

Yeo, C., and Whitman, M. (2001). Nodal signals to Smads through Cripto-dependent and Cripto-independent mechanisms. Mol Cell *7*, 949-957.

Yingling, J. M., Datto, M. B., Wong, C., Frederick, J. P., Liberati, N. T., and Wang, X. F. (1997). Tumor suppressor Smad4 is a transforming growth factor β-inducible DNA binding protein. Mol Cell Biol *17*, 7019-7028.

Yokoyama, K., Kamata, N., Hayashi, E., Hoteiya, T., Ueda, N., Fujimoto, R., and Nagayama, M. (2001). Reverse correlation of E-cadherin and snail expression in oral squamous cell carcinoma cells in vitro. Oral Oncol *37*, 65-71.

Yu, L., Hebert, M. C., and Zhang, Y. E. (2002). TGF-β receptor-activated p38 MAP kinase mediates Smad-independent TGF-β responses. EMBO J *21*, 3749-3759.

Yue, J., and Mulder, K. M. (2000). Requirement of Ras/MAPK pathway activation by transforming growth factor β for transforming growth factor β 1 production in a smad-dependent pathway. J Biol Chem *275*, 35656.

Zavadil, J., Bitzer, M., Liang, D., Yang, Y. C., Massimi, A., Kneitz, S., Piek, E., and Bottinger, E. P. (2001). Genetic programs of epithelial cell plasticity directed by transforming growth factor-β. Proc Natl Acad Sci U S A *98*, 6686-6691.

Zavadil, J., and Bottinger, E. P. (2005). TGF-β and epithelial-to-mesenchymal transitions. Oncogene *24*, 5764-5774.

Zavadil, J., Cermak, L., Soto-Nieves, N., and Bottinger, E. P. (2004). Integration of TGF-β/Smad and Jagged1/Notch signalling in epithelial-to-mesenchymal transition. EMBO J *23*, 1155-1165.

Zawel, L., Dai, J. L., Buckhaults, P., Zhou, S., Kinzler, K. W., Vogelstein, B., and Kern, S. E. (1998). Human Smad3 and Smad4 are sequence-specific transcription activators. Mol Cell *1*, 611-617.

Zeisberg, M., Bottiglio, C., Kumar, N., Maeshima, Y., Strutz, F., Muller, G. A., and Kalluri, R. (2003a). Bone morphogenic protein-7 inhibits progression of chronic renal fibrosis associated with two genetic mouse models. Am J Physiol Renal Physiol *285*, F1060-1067.

Zeisberg, M., Hanai, J., Sugimoto, H., Mammoto, T., Charytan, D., Strutz, F., and Kalluri, R. (2003b). BMP-7 counteracts TGF-β1-induced epithelial-to-mesenchymal transition and reverses chronic renal injury. Nat Med *9*, 964-968.

Zhan, Y., Fujino, A., MacLaughlin, D. T., Manganaro, T. F., Szotek, P. P., Arango, N. A., Teixeira, J., and Donahoe, P. K. (2006). Mullerian inhibiting substance regulates its receptor/SMAD signaling and causes mesenchymal transition of the coelomic epithelial cells early in Mullerian duct regression. Development *133*, 2359-2369.

Zhang, H., and Bradley, A. (1996). Mice deficient for BMP2 are nonviable and have defects in amnion/chorion and cardiac development. Development *122*, 2977-2986.

Zhang, J., Talbot, W. S., and Schier, A. F. (1998). Positional cloning identifies zebrafish one-eyed pinhead as a permissive EGF-related ligand required during gastrulation. Cell *92*, 241-251.

Zhang, Y., Musci, T., and Derynck, R. (1997). The tumor suppressor Smad4/DPC 4 as a central mediator of Smad function. Curr Biol *7*, 270-276.

Zhou, B. P., Deng, J., Xia, W., Xu, J., Li, Y. M., Gunduz, M., and Hung, M. C. (2004). Dual regulation of Snail by GSK-3β-mediated phosphorylation in control of epithelial-mesenchymal transition. Nat Cell Biol *6*, 931-940.

Zhu, Y., Richardson, J. A., Parada, L. F., and Graff, J. M. (1998). Smad3 mutant mice develop metastatic colorectal cancer. Cell *94*, 703-714.

Zimmerman, C. M., Kariapper, M. S., and Mathews, L. S. (1998). Smad proteins physically interact with calmodulin. J Biol Chem *273*, 677-680.

Appendix I

List of Constructs:

Construct	Details of Construct	Construction Details
pcDNA3N-Smad2	ProteinA-CBP Smad2 fusion used for expression in stable lines	Cloned by PCR with using CH1123 and CHRSRF2 pFTX5 Xmad2Δ3'UTR as a template. PCR product cut with EcoRI/SeI and ligated into pcDNA3N cut with EcoRI/XbaI.
pcDNA3N-Smad3	ProteinA-CBP Smad2 fusion used in stable lines	EFplink myc hSmad3 EcoRI/XbaI fragment ligated into pcDNA3N EcoRI/XbaI
p-Zome-Smad 2	ProteinA-CBP Smad2 fusion used for retroviral infection	Cloned by PCR with using CH1123 and CH1225 pFTX5 Xmad2Δ3'UTR as a template. PCR product cut with EcoRI and ligated into p-Zome-1-N cut with EcoRI.
p-Zome-Smad 3	ProteinA-CBP Smad3 fusion used for retroviral infection	Cloned by PCR with CH1123(T7) and CH1226 using EFplink myc hSmad3 as a template. PCR product cut with EcoRI and ligated into p-Zome-1-N cut with EcoRI.
p-Zome-Smad 4	ProteinA-CBP Smad4 fusion used for retroviral infection	Cloned by PCR with CH74 and CH1144 using pFTX5 HS dpc4 as a template. PCR product cut with EcoRI and ligated into p-Zome-1-N cut with EcoRI.

pcDNA3NHis2	ProteinA-His Tag	Linker created using CH1604 and CH1605 and inserted into pcDNA3N cut with EcoRI and BamHI.
pcDNA3NHis2-Smad3	ProteinA-His Smad3 fusion used for expression in stable lines	Linker created using CH1604 and CH1605 and inserted into pcDNA3N-Smad3 cut with EcoRI and BamHI.
pcDNA3NHA2	ProteinA-HA Tag	Linker created using using CH1619 and CH1620 and inserted into pcDNA3N cut with EcoRI and BamHI.
pcDNA3NHA2-Smad3	ProteinA-HA Smad3 fusion used for expression in stable lines	Linker created using CH1619 and CH1620 and inserted into pcDNA3N-Smad3 cut with EcoRI and BamHI.
pcDNA3NFLAG2	ProteinA-FLAG Tag	Linker created using CH1602 and CH1603 and inserted into pcDNA3N cut with EcoRI and BamHI.
pcDNA3NFLAG2-Smad2	ProteinA-FLAG Smad2 fusion used for expression in stable lines	p-Zome Smad2 EcoRI fragment was ligated into pcDNA3NFLAG2 EcoRI.
pcDNA3NFLAG2-Smad3	ProteinA-FLAG Smad3 fusion used for expression in stable lines	Linker created using CH1602 and CH1603 and inserted into pcDNA3N-Smad3cut with EcoRI and BamHI.
pcDNA3NFLAG2-Smad4	ProteinA-FLAG Smad4 fusion used for expression in stable lines	p-Zome Smad4 EcoRI fragment was ligated into pcDNA3NFLAG2 EcoRI.

Appendix II

List of Oligonucleotides:

ID	Description	Oligonucleotide Sequence
CH1123	XSmad2Forward	aacatcatgcactggacagg
CHRSRF2	XSmad2 Reverse	cctggagggaggtggggtc
CH1225	XSmad2 ECORI reverse	Gccgaattcttaggacatgcttgagcagc cgaattcttaggacatgcttgagca
CH243	β-Globin/HSmad3 Forward	tgcttacatttgcttctg
CH1142	HSmad3 ECOR1 REV	gccgaattcctaagacacactggaaca
CH74	T7 PRIMER	tgcttacatttgcttctg
CH1144	HSmad4 ECOR1 REV	gccgaattcctagtctaaaggttgtgggtc

ID	Description	Oligonucleotide Sequence
CH1602	pcDNA3N-Flag for	gggagatctgattatgatattccaactactgagaatttgtattt tcagggtggaggtggaggtggaggtaccatgaaggactacaagg
CH1603	pcDNA3N-Flag rev	cccgaattcacctccacctccacctccggccttgtcatcgtcgt ccttgtagtccttcatggtacctccacctccacctccaccctg
CH1604	pcDNA3N-His for	gggagatctgattatgatattccaactactgagaatttgtattt tcagggtggaggtggaggtggaggtaccatgcatcatc
CH1605	pcDNA3N-His rev	cccgaattcacctccacctccacctccatgatgatgatgatgat gcatggtacctccacctccacctccaccctgaaaatac
Ch1619	pcDNA3N-HA for	Gggggtaccatgaagtacccttacgatgtgcccgattac gccccccggtggaggtggaggtggagaattcggg
CH1620	pcDNA3N-HA rev	Cccgaattctccacctccacctccaccgggggcgtaatcggg cacatcgtaagggtacttcatggtaccccc

Oligonuclotides used in RT-PCR:

ID	Description	Oligonucleotide Sequence
CH2030	ALK1F1	gcagtgttgcattgcagacc
CH2031	ALK1 R1	gcactctctcatcatctgg
CH2036	ALK2 F2	gacagcactctagcggaactac
CH2037	ALK2 R2	gactgccaggcccaaatctgc
CH2319	ALK3 F1	gccacctccacacagaaatt
CH2320	ALK3 R1	ttacatcctgggattcaacc
CH2324	ALK4 F1	ctcctccttcttccccttg
CH2325	ALK4 R1	ctccatgtccaacctctggc
Ch2330	ALK5 F1	cctttcatttcagagggcac
CH2331	ALK5 R1	ccacttgctgtggacagagc
CH2334	ALK6 F2	caccaagcgctatatgcctc
Ch2335	ALK6 R2	ctctcttccaggaaagtctg
CH2336	ALK7 F1	catctattcggtggggctgg
CH2337	ALK7 R1	cgggaaggaaagctgtgagc
CH2637	Grb2	gatcaacatccgtgtccagg
CH2638	Grb2	aacatcatgcactggacagg

Bold letters indicate bases that have been used to introduce a whole or partial restriction site for cloning purposes.

MOLECULAR AND CELLULAR BIOLOGY, Feb. 2004, p. 1106–1121 Vol. 24, No. 3
0270-7306/04/$08.00+0 DOI: 10.1128/MCB.24.3.1106–1121.2004

Recognition of Phosphorylated-Smad2-Containing Complexes by a Novel Smad Interaction Motif

Rebecca A. Randall,[1] Michael Howell,[1] Christopher S. Page,[2] Amanda Daly,[1] Paul A. Bates,[2] and Caroline S. Hill[1]*